EUR 11.037

Radioactive Waste Management Series

Natural Analogues in Radioactive Waste Disposal

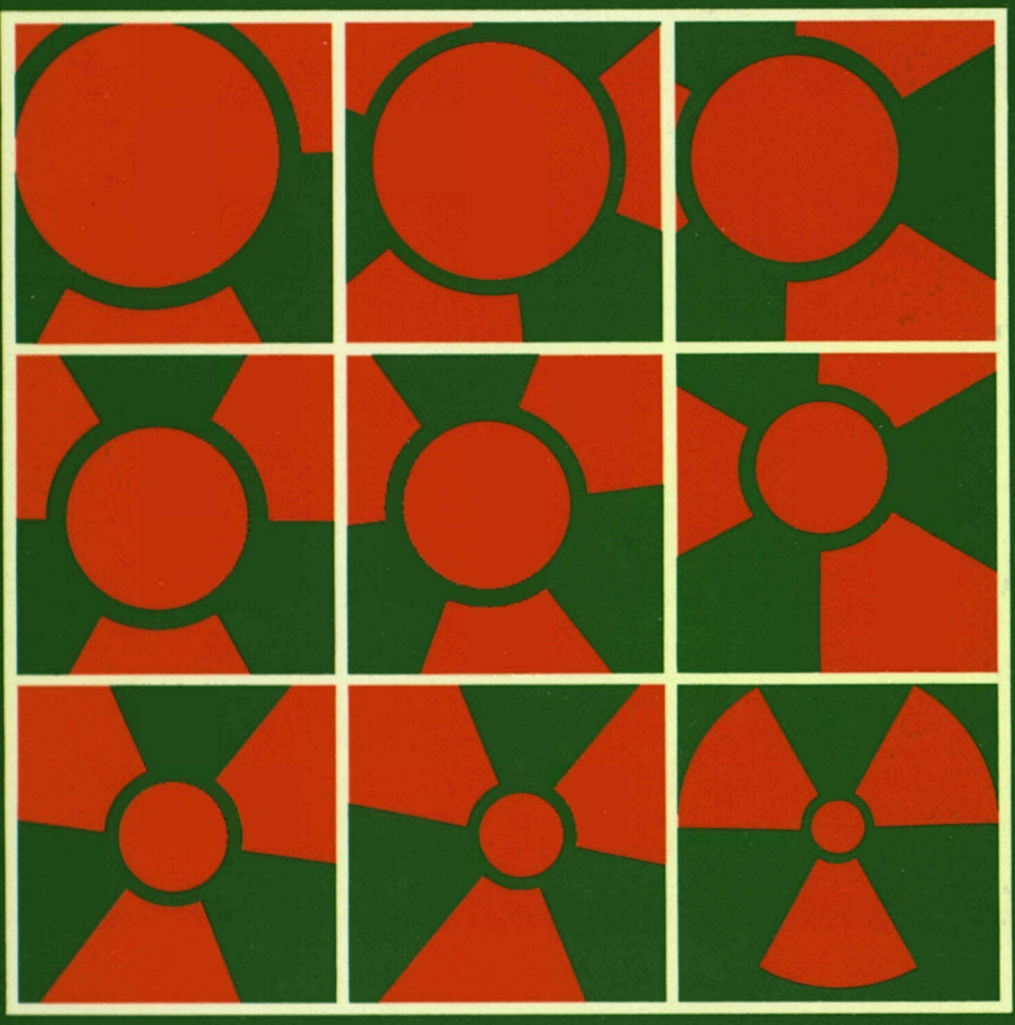

edited by
B. Côme and N.A. Chapman

Published by GRAHAM & TROTMAN
for the Commission of the European Communities

THE COMMISSION OF THE EUROPEAN COMMUNITIES

Natural Analogues in Radioactive Waste Disposal

Proceedings of a Symposium organised by the Commission of the European Communities under the Programme on Radioactive Waste Management (Directorate-General Science, Research and Development) and held in Brussels on 28-30 April 1987.

Scientific Secretariat

B. CÔME
Commission of the European Communities
Rue de la Loi 200
B – 1049 BRUSSELS

N.A. CHAPMAN
British Geological Survey
Nicker Hill, Keyworth
UK – NOTTINGHAM NG12 5GG

Programme Committee

M. D'ALESSANDRO	CEC-JRC, Ispra
P. AIREY	IAEA, Vienna
D. BROOKINS	University of New Mexico, Albuquerque (USA)
S. CARLYLE	OECD-NEA, Paris
G. DE MARSILY	Ecole des Mines, Fontainebleau (F)
I. McKINLEY	EIR, Würenlingen (CH)
I. NERETNIEKS	Royal Institute of Technology, Stockholm (S)
F.P. SARGENT	AECL, Pinawa (CANADA)
B. SKYTTE-JENSEN	Risø NL, Roskilde (DK)

S

Radioactive Waste Management Series

NATURAL ANALOGUES IN RADIOACTIVE WASTE DISPOSAL

edited by

B. Côme

Commission of the European Communities
and

N.A. Chapman

British Geological Survey

PARL. EUROP. Biblioth.
N.C./EUR 11.037
CL

published by
Graham & Trotman
for the Commission of the European Communities

Published in 1987 by

Graham & Trotman Ltd
Sterling House
66 Wilton Road
London SW1V 1DE
UK

Graham & Trotman
Kluwer Academic Publishers Group
101 Philip Drive
Assinippi Park
Norwell, MA 02061
USA

For the Commission of the European Communities
Directorate-General Telecommunications, Information
Industries and Innovation, Luxembourg

EUR 11037 EN

© ECSC, EEC, EAEC, Brussels and Luxembourg, 1987

ISBN 1-85333-105-8 (volume)
ISBN 0-86010-929-1 (series)

British Library and Library of Congress Cataloguing
in Publication Data are available

Legal Notice
Neither the Commission of the European Communities, its contractors nor any person acting on their behalf, make any warranty or representation, express or implied, with respect to the accuracy, completeness or usefulness of the information contained in this document, or that the use of any information, apparatus, methods or process disclosed in this document may not infringe privately owned rights; or assume liability with respect to the use of, or for damages resulting from the use of any information, apparatus, method or process disclosed in this document.

All rights reserved. No part of this publication may be reproduced, stored in a retrieval system, or transmitted in any form or by any means, electronic, mechanical, photocopying, recording or otherwise, without the prior permission of the publishers.

Printed in Great Britain at the Alden Press, Oxford

TABLE OF CONTENTS

PREFACE

In order to validate predictive models of the very long-term processes which affect the performance of radioactive waste repositories, there has been an increased interest in the information and understanding which can be obtained from studying similar mechanisms in natural systems. These "natural analogues", as they are known in the jargon of waste management, have been studied sporadically for many years, but there has been a considerable rejuvenation of interest in the last four years, possibly owing to the fact that performance assessment methodology is gradually maturing to the point where it needs the kind of support which analogues can offer.

Since 1982, the Commission of the European Communities has been involved in specific work on natural analogues in the framework of its activities on radioactive waste management, principally within the MIRAGE project which concerns migration of radionuclides in the geosphere. As a consequence, the Commission took the initiative, in 1985, of establishing a Natural Analogue Working Group (NAWG) whose members can benefit from the overall expertise available for managing their own natural analogue research programmes. In this group, modeller's requirements and the results of field research are exchanged at regular intervals. A number of wide-ranging investigation programmes, both on national and international scales, are currently underway or being initiated, and several of these have been discussed recently at the NAWG. Owing to the considerable upsurge in interest in the topic, not least from the regulatory bodies, the time seemed very appropriate to present the results of these many research programmes to a wider audience.

This present Symposium is in fact the first wide-ranging conference to be held on natural analogues, and follows on naturally from the Lake Geneva workshop of October 1984 (Chemical Geology, 55, 1986). The meeting was attended by more than 100 specialists from all round the world, who heard five oral sessions and viewed poster displays which included background on some of the major international analogue programmes.

The conclusions of the three days of lectures and discussion were brought together in a panel session on the final day. Perhaps the main conclusion was that the next phase of analogue studies should be aimed at determining how the information and the knowledge which they impart can actually be incorporated into the presentation of the results of safety assessments. This is likely to form the central theme for future activities of the CEC Natural Analogue Working Group.

Bernard Côme, CEC, Brussels
Neil Chapman, BGS, Keyworth
July 1987

OPENING ADDRESS

by S. ORLOWSKI, Head, Nuclear Fuel Cycle Division, CEC

Ladies and Gentlemen,

I have the pleasure and honour of welcoming you all on behalf of the Commission of the European Communities, the organiser of this Symposium.

The size of this meeting, the variety of your home countries, the presence of distinguished representatives of the IAEA and the OECD-NEA, all show - if it were needed - the increasing worldwide interest caused by natural analogues.

The concept of natural analogues originated in the mists of time: Icarus drew his inspiration to try the first human flight from the bird's wings. I shall not put too much emphasis on this, first because it is an old story, and second because I wish you better success ! This anecdote shows, however, that it is not so easy to know what will be a "good" analogue, and be aware of its limitations and capabilities.

Let us now turn back to radioactive waste. In assessing the long-term performance and safety of a repository, the main issue is to be able to predict, with sufficient confidence, the nature and effects of the processes and geological events involved. These predictions must extend over timescales which will depend upon the wastes and the repository designs involved, ranging from centuries up to hundreds of thousands of years.

The principal processes of concern are those involved in the various aspects of radionuclide mobilization from the disposed waste forms, and their subsequent transport by groundwaters. Fortunately, Mother Nature offers us the possibility of observing many similar processes in the natural environment, that is to say, assessing the effect of these processes over very long times. Here, I shall only mention one of the first, and probably the most famous, of such examples to be studied: the fossil reactors at OKLO in Gabon, details of which will be given in the course of this Symposium.

Our own interest, at the CEC, became focused in 1982, when we introduced, as part of the MIRAGE Project (Migration of Radionuclides in the Geosphere) of the Community R & D Programme, a research topic, which at that time was called "natural geological migration systems". Within this topic, we have participated in, among others, the British studies at LOCH LOMOND, the Italian research at ORTE, the French investigations in the mineralized zones at LANGENBERG (Vosges) and LA TELHAIE (Brittany). The work gave interesting, albeit preliminary, results, which were reported at the plenary meetings of the MIRAGE project (1984 and 1985) as well as the second Luxembourg conference in 1985.

In parallel to these first activities, deeper consideration was being given to the application of natural analogues in the field of radioactive waste disposal. In 1984, a report commissioned by SKB (S) and NAGRA (CH), was prepared on this topic by N.A. CHAPMAN, I. Mc KINLEY and J. SMELLIE. I would like here to summarize the "five commandments" which figured in this report, and which should be used for the selection of a "good analogue":

- The process involved should be clear-cut. Other processes which may have been involved in the geochemical system should be identifiable and amenable to quantitative assessment as well, so that their effects can be "subtracted";

- The chemical analogy should be good. It is not always possible to study the behaviour of a mineral system, chemical element or isotope identical to that whose behaviour requires assessing. The limitations of this should be fully understood;

- The magnitude of the various physico-chemical parameters involved (P, T, pH, Eh, concentration, etc.) should be determinable, preferably by independant means and should not differ greatly from those envisaged in the disposal system;

- The boundaries of the system should be identifiable (whether it is open or closed, and consequently how much material has been involved in the process being studied);

- The timescale of the process must be measurable, since this factor is of the greatest significance (the raison d'être) for a natural analogue.

In October of the same year, our colleagues at SKB and US-DOE organized a workshop at Lake Geneva, near Chicago, to consider natural analogues, mainly those concerning crystalline rock environments. The concept of an international working group on the natural analogue theme emerged as a step beyond the technical discussions.

In April 1985, SKB, US-DOE and NAGRA (and subsequently UK-DOE) were discussing the launching of an international research programme at the Poços de Caldas site (Minas Gerais, Brazil). The idea of a working group concerned with ongoing projects came more and more to the foreground. Many natural analogue programmes were, in fact, being initiated at this time:

- the Poços de Caldas project (mentioned above);
- the vast project at Alligator Rivers, Australia (AAEC - US-DOE - UK-DOE - Japan);
- several programmes in the USA, e.g. the MARYSVALE crystalline rock system;
- the new Community-sponsored research projects in Europe, particularly in the United Kingdom.

Considering this blossoming of ideas, projects, and initiatives of various natures, the Commission proposed, in June 1985, to enlarge the nucleus of specialists which had been active in natural analogue studies for the Community project MIRAGE since 1982, to include all those who had developed or were planning projects in the field. The Commission in fact thought that such a proposal offered a twofold advantage:

- in meeting the need for an international discussion forum which would be wider than the Community nucleus;

- by starting from a pre-existing structure.

This was the origin of the Natural Analogue Working Group (NAWG).

It was conceived as a very flexible structure, in which the Commission should play the rôle of "animateur".

The first meeting of this Group was held in Brussels in November 1985, and I must say that its success exceeded all expectations. All the countries involved in programmes on this theme had sent representatives; apart from our Member-States, these included Canada, Sweden, Switzerland, the USA (with which we have cooperation agreements), Australia, the OECD-NEA, and the IAEA.

This meeting allowed, for the first time, the needs of the "modellers" (involved in disposal safety assessments) to be set against the present capabilities of "experimentalists", with a view to improved efficiency of research. The exchanges of views led to the drafting of a "statement" by the Group which, for instance, presented the four means of application of natural analogues in disposal studies. Once again, I would like to summarize them briefly. The use of a natural analogue can be envisaged as one of the following:

1. As natural experiments which replicate a process, or a group of processes, which are being considered in a model. This is probably the most quantitative application of analogues, which allows confident constraints to be placed on, for example, extrapolations of laboratory experiments to larger time or space scales.

2. For determining the bounds of specific parameter values. This application would be most useful at the stage where a modeller needs limiting values on a parameter, but can obtain these from any or many geological systems. The origins of the data are not particularly important, and need not be linked to the process being modelled. Diverse sources may be used and a statistical approach adopted. An example of this is thermodynamic or kinetic data which could be obtained from any system.

3. As simple "signposts" indicating which phenomena can occur in the system being modelled by reference to a parallel natural system. This is a purely qualitative application which gives "yes-no" answers, or indicates the "direction" of long-term processes. It would be the first means of application used when carrying out scoping exercises.

4. In an empirical sense to integrate the results of many processes at one site, over long time periods. Not all of the processes involved may be evident, nor may the manner in which they have been linked. Only the end result is important, and in this sense this application is the most directly useful to a safety assessment (as distinguished from the individual models which comprise it). An example might be to determine whether there is any surface radiological manifestation of a deeply buried uranium ore body.

This latter application should in no way be disdained. For example, as pointed out to me in a letter by J. HAMSTRA in 1986, it seems of paramount importance to be able to show, through natural analogues considered as global systems, that annual radioactivity release rates predicted by repository performance assessments are not at all remarkable. Without any "pro-nuclear" bias, one can demonstrate that these rates can actually be found in Nature. An example is given by the natural system of MORRO DO FERRO (Brazil), the subject of presentations in this Symposium.

The potential of natural analogues, as evoked above, points to the desirability of an international consensus on their application, with respect to the safety assessment of radioactive waste disposal. This is, by the way, one of the conclusions drawn by the second meeting of the NAWG, which was hosted by NAGRA at Interlaken, in June 1986. The formation of an "Advisory Group" by the IAEA, scheduled for November this year, on this theme of a consensus on the rôle and application of analogues is therefore particularly welcome. Members of the NAWG, and the European Community, will participate.

I am now pleased to take this opportunity to emphasize the excellent level of co-operation which exists in this field between the various international organizations attending this Symposium. In particular, the work of the CEC and the IAEA will complement each other very well. The OECD-NEA is also active under the aegis of its Performance Assessment Advisory Group (PAAG). It will be the task of those in charge of these activities in the international organizations involved - and your own task as well - to ensure that the present complementarity and focusing of work does not result in proliferation and competition.

Today, we have all come together in the wide framework of this Symposium organized by the CEC. For us, it constitutes an important step, that of a state-of-the-art survey after several years of our own research programmes. We are pleased to be able to do this in your company, and to broaden the scope to the whole community of countries who are active in this field. It will also be necessary for you to discuss the direction of future activities, for much remains to be done.

The programme you received is actually built with this idea in mind, since it encompasses three themes:

- What do we expect from natural analogues ?
- What is the present state of research ?
- Are results matching expectations, and what remains to be done ?

The first two themes will be covered by oral presentations and also by numerous displays of photographs which, one hopes, will bring a lighter "exotic" touch to the more serious scientific proceedings. They may enable you to sit and dream about a trip "around the world in 80 days" through the numerous sites of interest which are scattered over our entire planet. For the third theme, the conclusions of this meeting, we have organized a final panel session, in which each of you is encouraged to participate.

On behalf of the Commission, I wish you all a successful meeting.

SESSION 1 :

WHY NATURAL ANALOGUES

(RATIONALE AND KEY AREAS OF NEED)

Chairman : N.A. CHAPMAN (BGS, UK)

Co-Chairman : M. d'ALESSANDRO (JRC Ispra)

NATURAL ANALOGUES AND PERFORMANCE ASSESSMENTS
A point of view based on the PAGIS experience

N. CADELLI
Directorate-General Science, Research and Development
Commission of the European Communities

Summary

In the light of the methodologies set up and implemented in Performance Assessment (PA) studies, with particular reference to the presently available results from the PAGIS exercise, the paper reviews briefly the two broad areas in which Natural Analogues (NA) might represent a support to PA studies.

The first area covers global approaches from which only indirect support to PA methodologies can be expected by building up confidence, essentially among the members of the public.

The second area, more quantitative, may provide the necessary elements for validating, in the long term, and at the appropriate scale, models and codes representing single phenomena as used in PA studies.

Indications are given about the priorities as resulting from the PAGIS studies among the fields of investigation already selected in the previous meetings of the NA working group. The paper also makes suggestions about other fields or other NA which may contribute to the validation in the long term (but also in the medium term) of particular phenomena.

1. INTRODUCTION

The implementation of Performance Assessment (PA) methodologies for evaluating the long term impact of underground radwaste repositories necessarily implies the use of predictive models describing the behaviour of the whole disposal system and hence the capabilities of the various natural and engineered barriers to retain or delay the migration of the radionuclides once they are released from their original embedding materials.

Hence one of the major tasks which the PA teams are facing, together with the modelers, concerns the confirmation of the assumed release and migration processes, and the validation of the corresponding models and eventually of the PA calculation tool as a whole. Validation is an essential aspect since it represents the basis for the credibility that both the scientific community and the members of the public will accord to the results of the calculations obtained in PA's and to the related conclusions.

The models used and the corresponding parameters are based on laboratory and field experiments, which increasingly reflect the real conditions of the medium in which the repository could be located. It is questionable, however, if these models can be considered satisfactorily validated, particularly with reference to the long term and the scale involved in the various phenomena. Certainly, following the experience gained in the PAGIS exercise (Performance Assessment of Geological Isolation Systems applied to deep underground repositories for HLW from reprocessing facilities) (1),(2), even with the necessary safety margins incorporated in the evaluations, the computed peak values of dose and risk are shown to be extremely low, at least considering the less improbable scenarios. The large uncertainties still affecting many parameters need, however, to be accounted for in the calculations through Sensitivity and Uncertainty Analyses (SA and UA). The dispersion of the doses and risks obtained and the high degree of sophistication in the calculation methods and procedures may introduce some doubts about the significance of the results, particularly among the members of the general public who may not correctly interpret the complex calculations needed and even such technical words as "uncertainties" currently used in PA are sometimes misunderstood.

Properly selected case studies of Natural Analogues (NA) may be a relevant support to PA since they would provide understandable evidences of phenomena covering long periods of time in environments of highly variable characteristics.

2. PA METHODOLOGIES

Before trying to identify areas where NA would be particularly useful, a short description of the main characteristics of PA

methodologies seems appropriate, with particular reference to the PAGIS exercise (1).

- In general, an executive code steers the evaluations calling for the appropriate sub-routines as required by the calculation scheme. This implies that there are two levels for which a support from NA could be expected: in a global approach involving, in some way, the significance and validity of the results obtained by the executive code as a whole; specifically through the validation of the single sub-routines describing the radioelements release and migration processes through each subsequent barrier.
- In PAGIS the PA is obtained through two parallel approaches for each of the release scenarios selected. The first is intended for determining the so-called "best estimate" values of doses and makes use of the best available models and parameter values, chosen realistically but which still are thought to incorporate some degree of safety margins. Sophisticated models may be used, where available, since the calculations are performed deterministically, with one or few computer runs per case.
- The second approach, which is increasingly considered in PA studies, is probabilistic in nature and implements statistical sampling techniques for selecting parameter values within an assumed range of variability. This approach is used in SA and UA. The result of SA is a ranking of the most important factors; if the appropriate uncertainty ranges due to the model and the values for the scenario probabilities are duly incorporated, results of UA are the expectation values of the dose, and the risk, or at least the conditional doses and risks. Due to the numerous runs needed for such statistical analyses, in many cases simplified models are used as sub-routines which need, therefore, to be adapted to specific conditions corresponding to the selected sites, the repository designs and the various release scenarios.
- Finally, and as already mentioned this is the most challenging aspect, PA are to be extended over time spans beyond hundreds of thousand of years, if the peak values of dose and risk have to be put into evidence, as it is the case in PAGIS. This implies such extrapolation from laboratory experiments (conducted only for a few years) which necessarily imply a fundamental uncertainty in the computed results.

But this remains also true if a time cut-off, for instance at 10.000 years would be accepted for PA studies, although if, in this case, some of the uncertainties, for instance those related to geological events, would be drastically reduced.

3. NA SUPPORT TO PA

From the remarks made above the kind of support which can be expected from NA is evident. But, in order to simplify the picture, it can be useful to discuss separately two levels at which NA may provide in principle a direct or indirect support to PA studies: (a) globally, that means considering the whole retention or retardation effect of host rocks, essentially on a qualitative basis; (b) specifically and possibly quantitatively on single processes and models.

I would like to recall that during the last meetings of the NA Working Group an excellent summary has been made of the areas where NA would effectively contribute to providing confidence in radwaste disposal safety (3),(4).

3.1 The global approach

The global approach will help in establishing or improving the dialogue with the members of the public by providing evidence of the effective confinement capabilities of the rocks. The approach is essentially qualitative but it will contribute in putting into the right perspective the question of the retention of most chemical species by geological media.

Interesting from this point of view are uranium deposits such as, for instance the Cigar Lake, where no significant radioactivity could be detected at the ground level or in the surface waters, despite the very high uranium concentration in the ore body; or the Alligator Rivers ores where very slow movements of U have been measured: Two examples among many others.

Of course, it may be very tempting to make a step further with a more quantitative approach and apply PA methodologies, in particular to such situations where evidences of radionuclide migration did take place. By

tracing the geohistory of events that occurred since the formation of the ore, one would expect validation of both the models and the PA codes as a whole. To some extent that can be useful since it may contribute to building up confidence among the scientific community on the methodologies used. However, the effort needed for characterising the host rock and to assess the parameters of past events, the boundary conditions and the processes involved, might easily go beyond the expected benefit of such a global validation exercise.

Indeed, due to the complexity of the release and transport phenomena, most of the codes in use include, as already said, a number of assumptions and model simplifications which only are valid when applied to specific sites and event sequences. The results would prove the capability of a code to reproduce certain given situations and this is already an important achievement but it does not necessarily imply its ability to predict the evolution of a repository under other circumstances.

This is particularly true for codes allowing a statistical approach where simplification of the models would be particularly severe, so that with such an exercise one would only displace the uncertainty. Moreover, due to the complexity, variety and variability of the possible phenomena, the exercise would not necessarily provide the assurance that all essential processes are appropriately accounted for in PA studies applied to particular sites and conditions.

3.2 The approach through specific phenomena

Apart from this global approach, NA will prove more directly useful for validating in the long term, (but in some cases also in the medium term) and at an appropriate scale, single models for single chemical species or compounds, in individual components of the system.

It can be anticipated, however, that the best benefit to PA would be assured if the selection of NA studies would be made keeping in mind specific disposal projects.

- It does not seem that the experience gained in PAGIS has yet indicated many other applications than those listed in the final reports of the Natural Analogue Working Groups (3),(4). But certainly different emphasis shall be given to the various items, depending on various aspects, starting with the nature of host rock wherein the repository is

located. For instance, near-field processes (e.g. solubility limits or leaching are important essentially for cristalline rocks but have almost no influence for deep repositories in clay, at least assuming the most probable scenarios.

- In respect of scenarios, PAGIS 2 has shown that the risks associated with altered evolution scenarios, in many cases, are at least as large as those associated with the natural evolution. Hence, the most relevant benefit from NA would come from work focused on situations related to altered evolutions. Typical examples are the repositories in salt, or the case of water wells over a clay host rock and, more generally, situations with faulted rocks.
- Concerning the radionuclides to be investigated, an extremely wide range of possibilities have been mentioned.

  A situation as that presented by the Oklo deposit appears extremely interesting since it could provide valuable data for the migration properties of a number of nuclides, otherwise not found in nature. Of course, apart from the case of uranium species, techniques are available to detect certain nuclides also in more normal uranium deposits.

  In order to cover the wide spectrum of radionuclides present in the waste, however, also natural deposits of other minerals need to be taken into consideration, in view of demonstrating their behaviour and the possible retention within different host rocks.

  Moreover, not only the same naturally occurring elements as those conditioned in the waste (such as Zr and Th), but also chemical or geochemical analogues can be studied. For instance, deposits containing REE (particularly Nd) or Cs and Hf associated with acid and alcaline magmatism respectively, as well as Th can be used as analogues, as it has been proposed by various authors (5),(6).

  I would also like to add industrial discharges of chemical analogues which might provide indications of the migration properties of selected elements. The number of possibilities for such punctual atudies is almost unlimited, and perhaps some attention could be given to such NA applications in the future. Although not as spectacular as the studies on large ore deposits, they may contribute to the understanding of particular migration phenomena of particular elements.
- As far as the radioactive elements are concerned which have been shown in PAGIS to be predominant for the doses to man from deep HLW

repositories, the following may be mentioned: Se, Zr, Tc, Sn, Sb, Cs, Pb, Ra, Th, U, Np, Pu, Am and Cm. Their relative importance depends, however, upon the option, the site and scenario considered and vary with the time. For example, in the salt dome option and the water intrusion scenario, Cs 135, Np 237 and Se 79, are, in this order, the most significant contributors to the maximum individual doses, whereas Np 237, Cs 135 and Tc 99 predominate in all scenarios of a clay option, Np 237 being, in the long term, also the major contributor to doses from repositories in granite and in the sub-seabed in the normal evolution scenario.

- Due to complexity of the repository system and its barriers, it would be extremely difficult to find a good near field analogue. However, specific natural or man induced phenomena occurred not far from the earth surface may give interesting elements for understanding and interpreting (in the long or in the medium term) particular mechanisms affecting the near field; and in many cases this would not imply heavy and costly researches into deep ore deposits.

  I am thinking of the behaviour of bitumen deposits and the state of the rocks around their boundary; the behaviour of bitumen is not only significant in view of its use as waste matrix for certain waste types, but also as sealing material for the repository shafts and seals (or the sealing dams in the salt option). A similar analysis could be useful on glassy rocks from old magmatic activities or on more recent cementitious products.

  Thermally induced processes with permanent modification of the rock properties may be important for predicting the retention capabilities of the near-field barriers; I am thinking of the buffer materials, of course, but also, more generally, of the clay layers surrounding a repository. Other examples as those analysed at Orciatico (7), should be used in order to confirm model predictions or provide new data on the changes in the geochemical properties of the rock.

  May I also recall disaffected salt mines where the results of the essential phenomenon of rock salt convergence, after decades, could be measured and compared with the existing models. The Asse mine in Germany where the process is studied is only one example.

- For all scenarios, sorption phenomena together with colloid formation and behaviour are the items which in PA still constitute the largest

contributors to uncertainties ranges in UA, together with all aspects connected with the hydrology in fractured media, particularly in granite.

It is worth remembering, for instance that almost no data can still be used for the colloids and that Kd values are assumed which are linear and reverarible, thus taking into account retardation but no final retention, whereas NA can provide evidences of important mass accumulation of materials confined within the host rock over extremely long periods of time.

The hydrology and the radionuclides migration, for instance in clay faults, is still poorly modeled; the variation of the permeability and the areas of pertubations around the faults deserve further investigation.

It is important to stress that unlike research models obtained through small acale and short time experiments, those developed for simulating particular phenomena as observed in NA are expected to be representative of the far field, particularly in clay, and thus of immediate application in PA.

- Turning to medium or short term analogues, an area where useful work could be done concerns the behaviour of underground water where fresh and salt waters are conflicting. The phenomena occurring at the possibly moving interface, if any, between the two could be studied at coastal sites and provide data for improving or validating the present models, where the often assumed existence of a well defined salt water front may prove to be inadequate. Similarly, models of the variations of the water characteristics in the aquifers surrounding salt formations still deserve validation.
- Finally, I would like to draw the attention of the participants to this meeting to the fact that most of the NA activity of the group has been devoted so far to near-field and far-field phenomena. It is worthwhile remembering the use of data on natural occurring radionuclides, stable elements and analogues in developing and validating biosphere models.

4. CONCLUSIONS

There are numerous and wide areas where NA can provide a valid, and for some aspect, indispensable support to PA studies. The possibility of demonstrating the reality of a geological confinement, under certain

conditions, and the support in validating models of specific phenomena in the near and far field and in the biosphere are NA objectives of primary interest to PA.

During the past meetings the Working Group already identified the essential research areas, although the results from PA evaluations, as for example from PAGIS, show that priorities may be different depending on the type of host rock and on the scenarios considered. In this respect, a permanent dialogue between the groups in charge of NA and PA studies including the modellers can only improve the mutual understanding and the usefulness of the results, by focusing the research studies on NA situations corresponding to well defined disposal projects.

5. REFERENCES

(1) PAGIS - Summary Report of phase 1 - EUR 9220,
(2) " - Summary Report of phase 2 and Comprehensive Reports for the options clay, salt, granite and the sub-seabed - to be issued,
(3) NAWG - I meeting - EUR 10315,
(4) NAWG - II meeting - to be issued as EUR 10671,
(5) Devenir à long terme des stockages de déchets radioactifs - to be issued as EUR 10839,
(6) The potential of natural analogues - NAGRA Technical Report 84-41
(7) Effetti del riscaldamento naturale sulle formazioni argillose - EUR 10200

The role of natural analogues in safety assessment and acceptability

by Tönis Papp

Swedish Nuclear Fuel and Waste Management Co.

ABSTRACT

The safety assessment must evaluate the level of safety for a repository, the confidence that can be placed on the assessment and how well the repository can meet the acceptance criteria of the society.

Many of the processes and phenomena that govern the long term performance of a deep geologic repository for radioactive waste also take place in nature. To investigate these natural analogues and try to validate the models on which the safety assessments are based is a main task in the effort to build of confidence in the safety assessments.

The assessment of the safety of a repository can, however, not only be based on good models. The possible role of natural analogues or natural evidence in other parts of the safety assessment is discussed. Specially with regard to

- the need to demonstrate that all relevant processes have been taken into account, and that the important ones have been validated to an acceptable level for relevant parameter spans,
- the definition and analysis of external scenarios for the safety assessment and for the claim that all reasonable scenarios have been addressed,
- the public confidence in the long-term relevance of the acceptance criteria.

1 Introduction

Many aspects of the use of and need for natural analogues in the design and approval of a final repository for high level radioactive waste will be presented during this symposium. This presentation will focus on the requirements posed by the safety assessment process. Since the safety assessment to a high degree is influenced by the given criteria for acceptable safety, this area will also be touched upon.

Although the structure of a safety assessment is to a great extent generic, some parts are strongly influenced by the host medium and by the conceptual design of the repository system. The ideas and thinking in this paper are of course influenced by the fact that the Swedish work is focused on disposal concepts in crystalline rock and, with regard to high-level waste, concentrated on the direct disposal of unreprocessed spent nuclear fuel.

The concept "natural analogue" is here used in a quite general way. A natural analogue is any system in a natural setting giving information on processes of importance to the repository performance. In essence, it gives information on interactions in systems with two kinds of qualities. First - systems with environmental interfaces that are natural, and not selected in order to facilitate an easy interpretation of the results. Secondly - systems that exhibit time scales outside of what can be achieved in laboratories and controlled experiments.

The first type of systems, irrespective of whether they are natural or caused by man, can provide a check on our ability to identify and model those processes in a complex system that are relevant to the long time safety of the repository system. The second type of systems gives us the only tool for evaluating the possible effects of processes which, due to e.g. slow kinetics are difficult to measure, but may have an influence on repository behaviors over long times.

2. Requirements on the Assessment.

The primary objective for the safety assessment is to evaluate the repository performance over time, and to express its effects on man and his environment in terms that are compatible with the society's criteria for acceptability.

The safety assessment must be characterized by a number of quality requirements to enhance the confidence in the process and results. This means in practice that it must be shown to the satisfaction of the competent authorities:

- That the selected site has natural properties of a quality consistent with those assumed in the safety assessment.
- That engineered components in the repository can be constructed as required, and that the quality of them can be proven to the level assumed in the evaluations.
- That the relevant processes of interaction in the repository system have been identified, their relative importance has been evaluated, and that the dominating processes can be modelled in an acceptable way.
- That the data on the materials and processes apply to the parameter intervals that are relevant, and are site and system specific.
- That all external circumstances (scenarios) for which the repository shall exhibit the required safety are identified and can be described.
- That the performance evaluation is made with due regard to the very long times over which the potential toxicity of the waste constitutes a significant hazard to man.

The assessment process must be presented in such a way that the assumptions and judgments made are clearly identified, and it must be shown that the resulting quantities are meaningful with regard to the uncertainties of the assessment. This also includes that all relevant processes and external circumstances are covered.

3. The Safety Assessment Structure

When talking about safety assessment in this paper the structure in Figure 1 is meant.

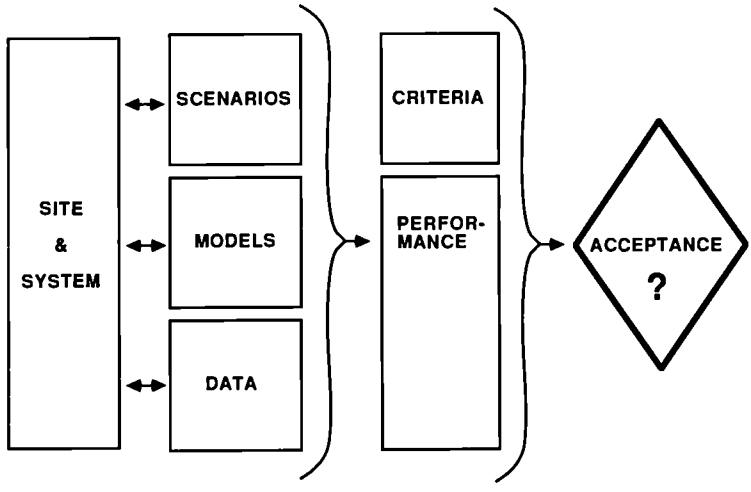

Figure 1.

Schematic structure of the safety assessment process

With the objective to get a safe repository, a site has been selected and a system for handling, conditioning and emplacement of the waste has been designed for it. The system also includes engineered safety barriers against the release and dispersion of radionuclides. A quality assurance program will be used to ensure that the required qualities are achieved.

To predict the long term performance of the repository the interactions of the various components in the repository and of the geological setting have to be described by relevant models and a set of corresponding data. Scenarios must be defined to cover the external circumstances that are considered realistic or important enough to be taken into account in the safety evaluation. There must be a correspondence between the scenarios, the models and the data-sets used, and the models must express the results in terms that are relevant for the acceptance criteria given by the society.

The decision to consider the repository as safe or not safe enough with regard to the criteria is the final result of the safety assessment.

In practice this sequence of design, scenario definition, modelling and data collection has been done in many iterations during the concept development and site selection phase as well as during the performance evaluation and optimization of the repository. At an early stage the assessments are made as simplified screening exercises, at a later stage they turn into more and more complete assessments. During these iterations the design is adapted not only to the requirements of the acceptance criteria, but also to the restrictions caused by lack of validated models or by problems in evaluating scenarios.The final design also reflects the balance reached between the various man made and natural safety barriers in a multibarrier concept with regard to safety allocation and required redundancy.

In the following sections the role of natural analogues and natural evidence in safety assessment will be discussed along the same structure as given for the assessment in Figure 1.

4. Natural Analogues in Safety Assessment.

4.1 Models and Data.

The most important use of natural analogues is for development and for validation of models that are relevant for the safety of the repository. This has been discussed by many groups at many occasions, and a number of priority lists have been published (see e.g. ref 1-3). Basically there will not be much difference between those lists and a priority list based on the KBS 3 assessments. A recent summary of experiments, in situ tests and natural analogues in the SKB program that have or can be used for validation exercises, was presented at the Geoval symposium in April 1987 in Stockholm (ref 4). As many other papers at this meeting will deal with the use of natural analogues in model development, the subject will only be touched upon to highlight three main questions. They do also represent three different types of qualities sought for in the safety assessment procedure.

The first is connected with the canister - for many concepts the first barrier against release of radionuclides from the isolation in the repository. It is selected to highlight the requirement for the safety assessment to be as realistic as possible.

When evaluating upper boundaries to the possible consequences phenomena which are supposed to have an overall beneficial effect on the safety are often disregarded if their effects are difficult to assure under all circumstances. However leaving such phenomena out of the assessment can sometime affect the safety case in such a way that the possibility of comparing various systems is lost.

One such a phenomena that we do have very little information on is how the corrosion product layer around canisters of eg copper or iron will be built up and function. In both cases the corrosion products have low

solubilities and will be formed in a rather special environment with regard to pressure. It will be influenced by hydrostatic and geostatic pressures as well as a pressure from the bentonite buffer. At the same time a swelling is caused by the fact that the corrosion products have a lower density than the original canister material. How will these factors influence the structure of the corrosion layer, its porosity, its sorption characteristics or its diffusivity for agents causing more corrosion or for radionuclides? How will the build up of the corrosion layer affect the rock-stress situation in the surrounding rock mass?

Experiments in the laboratory might give some of the answers, but the possibilities that the environment will have an influence on the slow re-crystallization of less stable phases and thereby modify the near field migration situation can probably only be addressed by natural analogues.

The second quality concerns the availability of models and their validity, and is exemplified with the innermost barrier - the waste matrix.

Although many groups around the world are working on the release mechanisms of the radionuclides (see e.g. ref 5 and 6), we are still today a long way from having a working model of the processes governing the release of radionuclides from the waste matrix, be it the vitrified waste or the spent fuel.

Up to now limiting factors like solubilities in the far field etc. have been used in safety assessments. Still, the process of release of the radionuclides from the waste matrix is such a primary process in the consequence calculations that a major effort seems to be appropriate. To clarify the release process studies are underway on how the various nuclides are distributed in the matrix, and how they are released over time to various leachants. These studies will give some of the picture, but further investigations are needed on:

- Possible solubility limiting phases in the vicinity of the waste.
- The solid solubility of the various nuclides in the precipitate of eg UO_2 in a recrystallization process or a redox front.
- The availability of reducing species in the near field and the surrounding hostrock.

Both the identification of possible solubility-limiting phases under natural conditions in repository-like environments, and examples of how much fission products or actinides (or analogue substances to them) can be found in uranium mineralizations (e.g. at a redox front) are geologic evidence that constitutes important factors in the theoretical models. Otherwise a substantial uncertainty would remain on the validity of the assumption that the important phenomena influencing the leaching have been identified.

The third area I would like to highlight is within the geosphere, and adresses the fact that also well validated models often have a rather limited parameter space within which the validity of the model is tested.

A major area of discussion today concerns water transport in fissured crystalline rock in different rock types or in different scales. Can it be

treated as flow in a porous medium, or as flow in a set of intersecting fissure planes or a bundle of splitting and merging flow channels. The different flow-systems will also require different ways to take account of the retardation and dispersion mechanisms that affect the nuclide transport. Since the barrier function of the geosphere often is the only one where the long-time function can be assured, the understanding of the limitations in the parameter domains for which the ground water models are valid is important to the assessment.

In geohydrology a lot of activity is going on already, but probably many years of collection of detailed basic data on the flow regimes coupled with validation tests in different scales are needed to clarify this issue.

4.2 Scenarios

Scenarios are sets of data that define phenomena that could initiate and/or influence the release and transport of radionuclides from a repository to man or his environment. A scenario defines the probabilities, interactions and external restrictions that might influence the repository performance.

Scenarios can be selected on a theoretical basis by analyzing the parameter span within which a used set of models are valid. If there is a substantial possibility that the repository state is not always within that span, new scenarios will have to be defined. This method is often used to define concept-specific bounding scenarios by assuming extreme values of parameters or disregarding beneficial phenomena when data have large uncertainties or when phenomena are difficult to model. The validation of so called conservative models used in bounding scenarios will require special methodology depending on how the conservatism is built into the model. The use of conservative models in a sensitivity analysis is another area where great care must be taken.

A special kind of scenarios are those with large or special consequences. They often have to be analysed extensively just to show that the decision not to take them into account is well founded, an example is criticality in a repository for spent fuel.

Scenarios can also be selected on the basis of the occurrence of natural phenomena registered as geologic or historic evidence, like meteoric impacts or changes in climate. In principle, naturally occurring scenarios that are well understood would constitute a better base for a safety assessment than a set of theoretical bounding scenarios because of the internal consistency, given to the parameter set in an interacting natural system.

Quality requirements for a set of scenarios are that they should cover all the situations that might occur, and that the scenarios should be realistic with regard to the expected environment. Information from nature is essential both to identify the phenomena that can occur and to describe a consistent set of parameters as an input to the performance evaluation of the repository.

PARLEMENT EUROPÉEN BIBLIOTHÈQUE

For disposal concepts deep in geologic media two scenarios have more often than others been discussed as essential but problematic. It is difficult both to calculate their probabilities and to analyze their consequences on safety. One is the faulting scenario, the other is the glaciation. In both cases the global phenomena that can influence them have just recently been identified and theories for how they develope are far from quantified. Probabilities of those scenarios are often only inferred from an extrapolation of geologic evidence of past occurrences.

In the old crystalline shield areas large-scale fault systems have developed due to various stress regimes caused by plate tectonics, near-by orogenesis, glaciations etc. These fault systems constitute weaker lines in the rock mass allowing movements between various blocks which will relieve the stresses. A well sited and designed repository could then be protected by surrounding faults and the importance of the scenario would be reduced. To have a better understanding of the safety value of such a siting restriction, it would be of great interest to evaluate the probability for how often a future fault will cut corners or take shortcuts through earlier unaffected rock. Another thing of interest would be to know where in a fault-zone the main waterbearing fissures will occur, and the rate at which the water transport capacity in a recent fault is affected by interaction with ground water.

A study with these intentions has recently been started by SKB in northern Sweden (ref 7). A neotectonic fault probably caused by pressure relief due to the deglaciation will be investigated. Similar investigations focusing on faults caused by other mechanisms and at different time periods would be of interest for comparison.

The ice age is another scenario very difficult to evaluate. Yet the consequences and possible duration of a glaciation plays an important role in the discussions on whether it is meaningful to talk about individual doses as measure for acceptability when the doses might only occur very far in the future.

Assuming that a glaciation will have a duration somewhere around 100,000 years, man - if still existing - will most probably be living in an environment completely different from the one existing now, invalidating our biosphere transfer models and perhaps also the conversion factors translating intake of radionuclides to dose. But will we have an ice age? Or will the ongoing heat pollution or the greenhouse effect change the old patterns? It might even be that ice ages can have rather short durations, perhaps only ten thousand years. Do we then have to assess the consequences of such a mini-glaciation?

There is especially one phenomena that is of importance when evaluating the consequences of an ice age on the repository, will the contact-zone between the ice and the bedrock be frozen? or rather, during what phases of a glaciation can great hydrostatic pressures from the glacier affect the normal groundwater gradients? Such and many other nature related questions need to be answered in order for the safety assessors to be able to know what importance should be given to the various scenarios in a safety assessment.

Since many scenarios are common to all deep repositories, the need for an international cooperation in this field has been recognised by many groups. The Performance Assessment Advisory Group to the Radioactive Waste Management Committee in OECD/NEA, PAAG, has recently initiated a effort to compile and evaluate the work done in the OECD countries up to now. The intention is to try to create a common basis for how scenarios are selected, how they should be defined and categorized, when they could be disregarded and what the requirements are for accepting a set of scenarios as complete. The availability of natural evidence for scenario evaluation will be an important aspect of that work.

4.3 Site and System Selection

Especially during the design phase of a repository problems are encountered when trying to quantify the repository performance. A process might be unsatisfactorily known or the long term aspects of it might be impossible to quantify. One often used way out is to redesign the repository in such a way that the importance of the less known processes are reduced (e.g. site the repository in such a way that fault-zones protect the repository against new faulting, or reduce the importance of the quality of the plugging of the shafts by siting the repository under a guaranteed inflow area). Many of the impulses for such design changes come intuitively during the conceptional design phase, based on a general awareness of "how nature works", or the state of the science in various fields.

To be able to use natural analogues for a formal validation of a model one must know the dominating parameters of the natural system as they exist today and also how the system has changed over time. But the problems encountered are often so big that validations efforts are limited to one or a few processes that happen to be possible to define in an acceptable way. The value of validation of models for limited processes can not be disputed. It must be recognised, however, that a safety assessment based on a full set of formally validated models will probably never be achieved, and acceptability decisions will often have to be made on the basis of a general confidence in the analysis and the results.

There are two ways to reach this confidence - either through some sort of sensitivity analysis or, in a more qualitative way, through "scientific judgement". Scientific judgement can be exercised in many forms from detailed peer reviews by expert groups, over second opinions and comparisons all the way to intuitive processes.

To build up a capacity for good scientific understanding and judgment more interest should be given to the big integrated repository analogues like Oklo and Morro do Ferro. They may contain a number of possibilities for validating various processes, but they will also provide an example of integration of a number of naturally occurring phenomena some of which we may not even be aware of. They may constitute signposts for possible neglected phenomena. The evaluations should not only look on the phenomena that are beneficial for the containment of the hazardous substances, but also try to answer questions like: Why have we not found more of these old reactors? and What are the limits for the various parameters at which we do no longer think the nuclides would stay confined to the original area?

To further enhance the applicability of natural evidence on the repository performance a repository should be designed in a way that changes the environmental parameters as little as possible.

4.4 Acceptance Criteria and Acceptability

The final input to the safety assessment comes from the systematic set of acceptance criteria given by society. The requirement of a systematics approach is intentionally stressed because the criteria set has to address not only limits for doses or for risk of detriment to individuals but also address a number of qualities not easily compared, like uncertainty, the level of optimization and the relevance of very small doses or very long time spans. The level (components - total system) at which the criteria are set must be reflecting the allocation of responsibility in the society.

The development of repository criteria lies often with the national authorities and must of course be based on a balanced view of all risks for man and the resources of the society for reducing them. When talking of time spans over hundreds of years it must be recognised, however, that neither our understanding of detriment nor our resources to reduce them will be the same. It is then essential that the criteria system also is founded on something more stable than the present risk - benefit balance.

One possibility explored is to couple the acceptance of the effects that a repository has on its environment to the level of radioactivity that normally exists in the area (eg in the bedrock or in the surface waters). If it can be shown that normal levels are not significantly changed by the existence of the repository, the siting and system would be acceptable. From a philosophical standpoint this is a good criterion - it is based on a very stable and measurable entity which is relevant to the detriment from the repository. Furthermore, irrespective of how we look upon the effects of low-dose exposures, the repository will not radiologically change the existing framework for natural evolution in the repository environment, nor limit mans future use of it. Another suggested criterion of a similar kind would be to limit the release to be below the span of variation in the natural radiation levels in the nearby region.

The coupling of acceptance criteria to the natural radiation levels should however be supported by a detailed analysis of the how the radioactivity exists and is transported in the natural system. Efforts should be made to model the natural levels of eg uranium and thorium and their daughters in the environment by using the same kinds of models that are used for evaluating the release of nuclides from the repository. This is an especially interresting exercise in granitic areas, where the naturally existing radionuclides above a deep geologic repository sometime exceed the amount of radionuclides in the waste.

A main quality requirement on acceptance criteria is that they should be accepted not only by the experts but also by the public in general. When discussing these questions, sometimes it is felt that some of the fear for the long-term safety of final disposal of radioactive wastes might be caused by the belief that the requirements posed by a repository

on the quality of the site and its environmental characteristics are so high and the time spans involved so long that they are in some way "unnatural" for nature. Every opportunity should therefore be taken to enhance the visibility of how natural analogues and geological evidence are used in safety assessments.

5. Concluding Comments

The safety assessment must evaluate the level of safety for a repository, the confidence that can be placed on the assessment and how well the repository can meet the acceptance criteria of the society.

The long term potential toxicity of high-level radioactive waste requires that the protective barriers of a final repository perform their role over equally long times. To prove this long term function, natural evidence must support man made tests and experiments.

A main task today is to validate the models for the governing processes affecting the radionuclide confinement or release, and to provide a confidence for the judgement that all the important processes have been identified. To exploit the evidence provided by natural analogues to the maximum the protection principles used in the repository should be based on processes that can be evaluated in natural settings. This might enhance the possibility to prove the safety level of the repository in an acceptable way.

Some processes or phenomena will not easily be validated in a formal and complete way and scientific judgement, e.g. in the form of a peer review process, will continue to play an important role when evaluating the quality of data, models and scenarios. A continued analysis of available "total repository analogues" is needed to test our understanding of how the processes will interact in various scenarios.

In a setting where the repository design, the external scenarios and the relevant data and models are all supported by natural evidence, the acceptance of the safety of the repository system could also be enhanced if the criteria system was shown to be well balanced to the natural and unavoidable release of radionuclides from the geosphere to mans environment.

6. References

1. CHAPMAN, N. A., McKINLEY, I.G. and SMELLIE, J. A. T. (1984). The potential of natural analogues in assessing systems fo deep disposal of high-level radioactive waste. SKB TR 84-16 and NAGRA, NTB 84-41.

2. SMELLIE, J. A. T. (Editor) (1984). Natural analogues to the conditions around a final repository for high-level radioactive waste. Proceedings of the natural analogue workshop held at Lake Geneva, Wisconsin, USA (october 1-3, 1984). SKB TR 84-i8, Swedish Geological Company Uppsala, Sweden.

3. COME, B. and CHAPMAN, N. (Editors) (1985). Natural Analogue Working Group, Final Meeting Report from First Meeting, November 5-7, 1985. CEC report No EUR 10315.

4. KARLSSON, F. and BÄCKBLOM, G. (1987). Validation of radionuclide migration models within the SKB research program on nuclear waste management. Presented at the GEOVAL meeting, April 7-9, 1987, Stockholm Sweden.

5. WERME, L. (Editor) (1984). Proceedings of the third spent fuel workshop. SKBF/KBS TR 83-76, Stockholm Sweden.

6. JSS-Project (1985). JSS-Project Phase II, Final Report of Work performed at Studsvik Energiteknik AB and at Swiss Federal Institute for Reactor Research. JSS-Project Technical Report 85-1.

7. SKB (1986). R&D programme 86. Handling and final disposal of nuclear waste. Programme for research, development and other measures. SKB, Stockholm, Sweden.

NATURAL ANALOGUES AND RADIONUCLIDE TRANSPORT MODEL VALIDATION

D.A. LEVER
Theoretical Physics Division
Harwell Laboratory
Oxon, U.K.

Summary

In this paper, some possible roles for natural analogues are discussed from the point of view of those involved both with the development of mathematical models for radionuclide transport and with the use of these models in repository safety assessments. The characteristic features of a safety assessment are outlined in order to address the questions of where natural analogues can be used to improve our understanding of the processes involved and where they can assist in validating the models that are used. Natural analogues have the potential to provide useful information about some critical processes, especially long-term chemical processes and migration rates. There is likely to be considerable uncertainty and ambiguity associated with the interpretation of natural analogues, and thus it is their general features which should be emphasized, and models with appropriate levels of sophistication should be used. Experience gained in modelling the Koongarra uranium deposit in the Alligator Rivers region of Northern Australia is drawn upon.

1. Introduction

Radionuclides will move very slowly from the deep geological repositories that have been proposed as a possible option for their long-term disposal. Laboratory and field experiments can be devised to investigate the important physical and chemical processes, however these only yield information on relatively short time-scales (up to 1 year). Natural geological systems have been developing over far longer time-scales, and so potentially they can provide important insight into the behaviour of radionuclides over times that are relevant to repository safety assessments. So in recent years they have been receiving increased attention in many countries (1-3).

In this paper, we present some ideas about the potential usefulness of natural analogues in validating models used in assessing the safety of radioactive waste disposal. It is based on recent experience with developing (4-6) and using mathematical models for performing such safety

assessments and for analysing laboratory (7,8) and field (9,10) migration experiments and natural analogues (11). We start, in section 2, by discussing the process of model validation and some of the experience that has been gained to date. Then in the next two sections, we outline the important aspects of a safety assessment for a cementitious repository and we examine some ways in which natural analogues can be helpful. Finally, in section 5 we draw on experience gained in modelling the Koongarra uranium deposit in the Alligator Rivers region of northern Australia.

2. Model validation

The IAEA definition of validation is:

> "A conceptual model and the computer code derived from it are 'validated' when it is confirmed that the conceptual model and the derived computer code provide a good representation of the actual processes occurring in the real system. Validation is thus carried out by comparison of calculations with field observations and experimental measurements." (12)

There are three complementary types of investigation that can be used in model validation: laboratory experiments, field experiments and natural analogues.

In laboratory experiments, the initial and boundary conditions and the geometry will probably be well defined. In addition, they can be designed so that a very small number of processes are important. However, there are severe restrictions on the size of experiments ($\lesssim$ 1m) and on the duration ($\lesssim$1 yr).

With field experiments, substantially longer transport distances can be examined (up to about 100m), but again there are similar time constraints to those in laboratory experiments. Boundary conditions may not be as well defined as with laboratory experiments, and there may be considerable uncertainty in the geometry (e.g. fracture networks and channelling).

The great advantage of natural geochemical systems is that they provide information relevant to the time and space scales required for repository safety assessments. However, the corollary is that hydrogeochemical conditions may be poorly characterized. For example, the initial extent and duration of a geochemical anomaly cannot be known with anything like the certainty of the source term in a field experiment. There may also have unknown variations in conditions such as water flow over the intervening time. Although it may be possible to find analogues for single processes, frequently a number of processes will be coupled together, making analysis more difficult.

So all three types of study have advantages and disadvantages, and none is the perfect validation tool. However, if they are used together, they can build confidence in the models that are used in safety assessments.

The international collaboration exercises INTRACOIN and HYDROCOIN have provided valuable experience over the past few years. These dealt respectively with transport by groundwater and with groundwater flow. The INTRACOIN study was carried out at three levels (13, 14): (1) code verification (i.e. checking codes solve equations correctly), (2) model validation and (3) uncertainty analysis. In Level 2, two experiments were studied by participants - a single hole injection/withdrawal

experiment in a sandy aquifer in Canada and a dual hole tracer experiment in granitic bedrock in Sweden. In the latter, tracers were passively injected into one hole and water was pumped out of the second, creating a radially inward flow field. There were difficulties with the interpretation of both experiments. These arose from a shortage of data, with a choice of processes that could be included and with inconsistencies with laboratory data on parameter values. So, whilst the verification part of the study was successful, the validation part pointed to a need for further work.

As a result, the Swedish Nuclear Power Inspectorate have recently suggested that a further international project should take place, called INTRAVAL, which will focus upon the validation of geosphere transport models (15,16). It is hoped that this will get underway in Autumn 1987, and a number of test cases based upon laboratory and field experiments and natural analogues will be studied. Interactions between experiments and modellers will be a vital part of this study.

3. Safety assessments

As an example to help us examine the ways in which analogues can be useful in model validation, we outline the important aspects of the safety assessment of a cementitious repository, suitable for either LLW or ILW. This is summarized in Table I, where the important barriers in the near and far field are shown for pathways other than intrusion and disruptive events. In addition, the key quantities in the inventory that need to be known are given. These include not only the radionuclides but also substances such as metals and organics, which may affect the repository performance. It is important to know what the barriers are, and also to be aware of how significant a role they each play in the overall assessment. Different barriers may prevent different radionuclides returning to the surface and reaching Man. Obviously, there are uncertainties with regard to various quantities and processes, and some unresolved questions are listed in the table. Analogues may help in answering some of these.

4. Role of analogues

In the final columns of Table I, we identify some processes where either historical or natural analogues could potentially be useful if appropriate ones exist. Broadly these fall into a number of categories:

(i) They can provide evidence that the migration mechanisms included in models are valid during relevant time-scales, and that the models can be used to describe the migration that naturally occurring radionuclides have undergone.

(ii) They can provide evidence that laboratory measurements of, for example, sorption found from short-term experiments are relevant to long-term migration.

(iii) Even though the source term and hydrogeological environment are likely to be poorly defined, it should be possible to obtain specific information on the relative migration rates of different species on the migration rates of individual species.

(iv) They can indicate important mechanisms which are not included in the models. Laboratory and field experiments can then be used to provide quantitative information on the identified phenomena.

(v) They may provide guidance as to whether long term changes in climatic and hydrogeological conditions can significantly affect migration, in which case they should be considered in repository safety assessments.

As there is likely to be considerable uncertainty and ambiguity associated with the interpretation of natural analogues, it is their general features which should be emphasized, and models with appropriate levels of sophistication should be used.

In the study of analogues, as with other validation exercises, the interaction between experimentalists and modellers is important, so that experimental data are not collected without being put into context nor are models generated which do not take full account of all available evidence. In addition, the results and conclusions should not only be expressed for the benefit of the scientists involved, but also in relatively straightforward ways to give confidence to the wider public that nature helps us understand the migration of long-lived radionuclides.

5. The Koongarra ore body

Finally, we close this paper by briefly summarizing some modelling work, reported earlier (11), on the uranium ore body at Koongarra in the Alligator Rivers Region of the Northern Territory of Australia. This is a particularly promising natural analogue, and details of the experimental programme appear elsewhere in these proceedings. The upper 30m of the No. 1 ore body has been weathered and the uranium mobilized. There is a strong groundwater flow within the weathered zone, which has created a tongue-like fan of secondary mineralization extending down slope for about 50m. This fan has been the subject of the substantial experimental investigation.

The data that are available include the concentrations on rock samples at various depths down boreholes of the long-lived parent ^{238}U, $^{234}U/^{238}U$ and $^{230}Th/^{234}U$ activity ratios on the same samples, ^{238}U concentrations in borehole water and laboratory estimates of uranium sorption. Estimates of the groundwater flow have also been made.

These data have been interpreted using a very simple one-dimensional groundwater transport model, which includes the effects of transport by flowing groundwater, linear equilibrium sorption and radioactive decay. Although very simplified, this model contains many of the essential features of transport models that are used in safety assessments of radioactive waste burial. Two independent estimates of the migration time have been developed. The first is based on laboratory and field estimates of the distribution coefficients of ^{238}U, numerical estimates of the groundwater velocity, and the migration distance. The second is based upon the disequilibria between ^{230}Th, ^{234}U and ^{238}U activities on rock samples, the migration distance and the spatial gradient of ^{238}U activity on rock samples. Details are given in reference (11). Although the second estimate is based on very limited data, the two approaches give a consistent picture if the migration time is between 10^6 and $3\ 10^6$ yr. This is very much a preliminary interpretation and there is considerable potential for further data to be collected and more sophisticated models to be developed. Nevertheless, it shows that there is scope for the investigation of the migration of naturally occurring long-lived

radionuclides using the type of transport model used in repository safety assessments.

Acknowledgements

The work described in the last section was undertaken whilst the author was a Visiting Scientist at the Lucas Heights Research Laboratories of the Australian Atomic Energy Commission. The visit was funded by the United States Nuclear Regulatory Commission project "Radionuclide migration around uranium ore bodies - analogue of radioactive waste repositories", contract number NRC-04-81-172.

The author's continued interest in natural analogues is funded by the U.K. Department of the Environment, as part of its radioactive waste research programme, under the Verification and Validation of Models contract (PECD-7/9/230-86/84). The results will be used in the formulation of Government policy, but at this stage do not necessarily represent Government policy.

REFERENCES

1. CHAPMAN, N.A. and SMELLIE, J.A.T. (ed.)(1986). Natural analogues to the conditions around a final repository for high-level radioactive waste, Chem. Geol. 55 (3/4).
2. COME, B. and CHAPMAN, N. (ed.)(1986). Natural analogue working group, First meeting, Brussels, November 1985. CEC Report EUR 10315 EN-FR.
3. COME, B. and CHAPMAN, N. (ed.)(1987). Natural analogue working group, Second meeting, Interlaken, June 1986. CEC Report EUR 10671.
4. HERBERT, A.W., HODGKINSON, D.P., LEVER, D.A., RAE, J. and ROBINSON, P.C. (1986). Mathematical modelling of radionuclide movement underground. Q.J. Eng. Geol. 19, 109-120.
5. ROBINSON, P.C., HODGKINSON, D.P., TASKER, P.W., LEVER, D.A., WINDSOR, M.E., GRIME, P.W. and HERBERT, A.W. (1987). A solubility-limited source-term model for the geological disposal of cemented intermediate-level waste. UK Atomic Energy Authority Report, AERE-R.11854.
6. HODGKINSON, D.P. and MAUL, P.R. (1985). One-dimensional modelling of radionuclide migration through permeable and fractured rock for arbitrary length decay chains using numerical inversion of Laplace transforms. UK Atomic Energy Authority Report, AERE-R.11880.
7. BRADBURY, M.H., LEVER, D.A. and KINSEY, D.V. (1982). Aqueous phase diffusion in crystalline rock. Scientific Basis for Waste Management V (ed. W. Lutze), 568-578, Elsevier.
8. BRADBURY, M.H., GREEN, A., LEVER, D.A. and STEPHEN, I.G. (1986). Diffusion and permeability based sorption measurements in sandstone, anhydrite and upper magnesian limestone samples. UK Atomic Energy Report, AERE-R.11995.
9. HODGKINSON, D.P. and LEVER, D.A. (1983). Interpretation of a field experiment on the transport of sorbed and non-sorbed tracers through a fracture in crystalline rock. Radioact. Waste Manage. Nucl. Fuel Cycle 4, 129-158.
10. NOVAKOWSKI, K., EVANS, G.V., LEVER, D.A. and RAVEN, K.G. (1985). A field example of measuring hydrodynamic dispersion in a single fracture, Water Resour. Res. 21, 1165-1174.

11. LEVER, D.A. (1987). Modelling radionuclide transport at the Koongarra uranium deposit. In reference (3).
12. Radioactive waste management glossary (1982). IAEA Report IAEA-TECDOC-264.
13. INTRACOIN (1984). Final report Level 1. Swedish Nuclear Power Inspectorate Report SKI 84:3.
14. INTRACOIN (1986). Final report Levels 2 and 3. Swedish Nuclear Power Inspectorate Report SKI 86:2.
15. INTRAVAL (1987). Project proposal. Swedish Nuclear Power Inspectorate Report SKI 87:3 (Draft).
16. INTRAVAL (1987). Geosphere model validation: A status report. Swedish Nuclear Power Inspectorate Report SKI 87:4 (Draft).

Table I The role of analogues in safety assessments

	Impact on dose to man	Queries and complications	Role for historical analogue	Role for natural analogue
Inventory				
Radionuclides				
Stable isotopes	Isotopic dilution			
Metals		H_2 generation by corrosion	*	
Cellulosics and other organics		CO_2, CH_4 generation by degradation		
		Organic complexation	*	
Near-field barriers				
Physical containment by metal canisters	Negligible release whilst short-lived nuclides decay	Canister life short compared to half-life of long-lived nuclides		
		Different types of corrosion - uniform and localised, external and internal	*	
Containment by low permeability concrete	Low flow through repository reduces flux to geosphere	Longevity of repository integrity	*	
		Impact of gas generation on repository integrity	*	
Near-field chemical environment	Low concentrations in high pH/low Eh environment arising from sorption and solubility limits	Variability in estimates of solubility limits		
		Confidence in techniques for measuring sorption		
		Appropriateness of linear equilibrium sorption model		
		Effects of organics and colloids	*	
		Evolution of near-field environment		

Table I - continued

	Impact on dose to man	Queries and complications	Role for historical analogue	Role for natural analogue
Geosphere				
Groundwater flow		Porous vs fractured flow		
		Short Circuits		
		Impact of gas release from near-field		*
		Transport by colloids or organics	*	*
Sorption	Retarded release to biosphere	Confidence in techniques for measuring sorption		*
		Appropriateness of linear equilibrium sorption model		*
		Sensitivity to sorption of long-lived parent		
		Disturbed zone - excavation of repository, clay/concrete interface	*	*
		Sensitivity of sorption to redox potential		*
	Dose from short-lived daughters	Different distributions between rock and porewater of parent and short-lived daughters, arising from different sorption properties		*
		Multi-phase effects		*
Diffusion		Importance of surface diffusion of sorbed nuclides		*
		Importance of coupled processes, e.g. osmosis in clay		*

Table I - continued

	Impact on dose to man	Queries and complications	Role for historical analogue	Role for natural analogue
Geosphere - cont.				
Longitudinal dispersion	Earlier arrival Reduction in maximum concentration with sufficiently long migration paths	Confidence in dispersion models		*
Transverse dispersion	Reduction in maximum concentration with sufficiently long migration paths	May still enter the same biosphere compartment		
Diffusion into fractured rocks	Delay arrival of peak Reduction in maximum concentration	Sensitivity to diffusion (and sorption) parameters Validity of estimates of in situ values		*
Biosphere				
Transfer from deep soil to various compartments	Sometimes diluting (surface waters), sometimes concentrating, possibly delaying (allowing reequilibrium of short-lived daughters)	Understand transfer processes (including sorption) Uncertainty in site specific data Evolution of the environment (human influence, climatological changes)	* *	* *
Ingestion	Food and drink			
Inhalation	Radioactive gas generated Radon from long-lived nuclides Toxic gases			*

Application of Natural Analogue Studies to the Long-Term Prediction of Far Field Migration at Repository Sites

by

P. L. Airey

International Atomic Energy Agency

A B S T R A C T

Evidence of compliance of proposed repositories with long-term performance criteria will inevitably be based on computer modelling. Natural analogue studies based on uranium ore bodies are being directed towards verification of codes for radionuclide migration in the far-field. The residence time of secondary uranium in the weathered zone at the Koongarra deposit has been calculated using a transport equation. It agrees to a factor of 10 with other independent estimates despite experimental evidence for colloid transport and for a significant kinetic component of sorption coefficients over the time scales days to years. The application of open system uranium modelling to support elements of rock matrix diffusion calculations related to natural analogue studies is discussed.

1. INTRODUCTION

Natural analogue studies are designed to contribute to the processes of (a) assessing compliance of proposed high level radioactive waste (HLW) repositories with national standards, and (b) convincing the public of the acceptability of repositories complying with such standards. The use which can be made of analogues will depend on the standards adopted and the nature of the evidence accepted by licencing authorities as demonstrating compliance.

This paper will be concerned principally with uranium ore bodies as analogues of the transport of leached actinides and fission products in the far field[1-3]. Such analogues provide direct information on the cumulative effect on the transport of uranium series nuclides over time scales commensurate with the half-lives of nuclides and are of potential value in identifying processes leading to radionuclide mobility, and in verifying mathematical procedures for calculating transport rates over long periods. They are particularly relevant to the concept fovoured by Kocher [4] that the long-term risk to the public from unmined uranium ore is, in principle, a satisfactory basis for defining acceptable risk in a high-level waste standard[5]. With state of the art technology, the analogues may be extended to include actinides and fission products[6][7]. However, analogues appear of little use in assessing risks associated with very low probability, high consequence events.

2. VERIFICATION OF PREDICTIVE MODELS

There is general acceptance that evidence of compliance with long-term repository performance criteria will be based on computer modelling[8]. A number of codes have been subject to systematic intercomparison through the INTRACOIN and HYDROCOIN programmes [9-11] co-ordinated by the Swedish Nuclear Power Inspectorate (SKI). Neither programme was designed to address two questions fundamental to long-term prediction viz

(a) Are significant changes in the hydrogeology over the next 100,000 years likely?

(b) Are the generating equations which are the basis for the codes adequate for long-term prediction.

The probability of significant perturbations to the hydrogeology as a result of climatic and geomorphological changes has been discussed by Szoreen and Kocher[12]. Such effects may be neglected if there is consistency between water transit times calculated from hydraulic models (reflecting current hydrology) and those calculated from carbon - 14 or chlorine - 36 dating techniques (reflecting the cumulative effect of transport over thousands or hundreds of thousands of years respectively).

Crucial to the second question are such issues as:

(a) Do transport mechanisms (e.g. colloidal or biological) exist which cannot be satisfactorily incorporated within a composite sorption coefficient? These will be designated non-linear mechanisms.

(b) Is it necessary to include a kinetic term into sorption coefficients for long-term prediction i.e. is the parameter time dependent?

These issues will be discussed under three headings: (a) Is there experimental evidence for non-linear transport parameters at analogue sites. (b) If so, is a quantitative assessment possible at repository sites. (c) Will any non-linear effects significantly alter long-term radio-nuclide transit time predictions in the far-field?

2.1 Experimental evidence for non-classical transport parameters.

(a) Colloid transport. Laboratory and field evidence for actinide transport by natural colloids has been extensively reviewed[13-14].

(b) Variation of sorption coefficient (radium) with residence time. Using the procedures of Krishnaswami et al[15], in situ estimates were made of the relative sorption coefficients for ^{223}Ra, ^{224}Ra and ^{226}Ra with half lives of 11d, 3.6d and 1620y respectively. Sorption coefficients were found to increase with residence time over factors ranging from 2 to 10[16].

(c) Effect of α recoil on sorption coefficients. Recoil from surface adsorbed parent nuclei can have a dramatic effect on the distribution of the daughters in the substrates. Isotopic discrimitation factors exceeding 100 were observed in dilute kaolinite suspensions between ^{224}Ra (formed by recoil from surface adsorbed ^{228}Th) and ^{226}Ra adsorbed from solution. Interpreted as sorption coefficients, K (^{224}Ra)/K (^{226}Ra) varied from 1.0 on montmorillonite to 3.7 on kaolinite [16].

(d) Geochemical redistribution of radio nuclides

Gray [17] identified a geochemical mechanism for the separation of uranium and thorium in lateritic profiles. Ferrihydrite adsorbs both uranium and thorium from solution. UO_2^+ is trapped in the hematite formed on aggregation of the ferrihydrite and is located in disordered phases. Thorium, on the other hand is sulestituted in the goethite and/or hematite phases. The significance for our discussion is that the dynamic processes associated with the aggregation and crystalization of ferrihydrite may lead to a kinetic component of the effective sorption coefficient.

2.2 Measurement of transport parameters at repository sites.

Confirmation of whether the phenomena (a) to (d) Section 2.1 are significant at respository sites can, in principle, the readily established because (a) uranium series elements are ubiquitous and can be

measured at ambient levels and (b) all measurements are based on individual samples and are not dependent on the spatial distribution of uranium and groundwater flow.

2.3 Will the non-linear effects significantly perturb radionuclide transit time predictions?

With the possible exception of colloid transport, all effects thus far identified in the weathered zone of the Alligator Rivers Uranium region lead to an increase in radionuclide retardation factors with increase residence time. Thus correctly interpreted sorption coefficients established over a short time scale lead to an under estimate of radionuclide retardation in the long-term.

Evidence that transport codes form a satisfactory basis for predicting the long-term migration rates has recently been reported by Lever[18-19]. He showed that the residence times of secondary uranium within the Koongarra deposit obtained, on the one hand from the basic one dimension transport equation (simplified to neglect dispersion), and on the other from independent estimates of groundwater transit times and sorption coefficients led to agreement within a factor of 10. Those with regulatory responsibility will determine what level of agreement constitutes a verification of the generating equations of codes to be used for long-term prediction.

3. APPLICATION OF URANIUM SERIES TO MIGRATION STUDIES IN CRYSTALLINE ROCKS

The efficiency of crystalline rock as a barrier to radionuclide migration depends on many factors including (a) the extent to which groundwater diffuses into the bulk rock through microcracks and fissures, (b) the mineralogy of accessible surfaces and (c) the efficiency of colloid migration through fractures Although the general

features of solute transport in crystalline rock and well understood, it is frequently not possible to distinguish between such mechanisms as[20]

Advection - despersion - surface adorption
Advection - despersion - matrix diffusion
Advection - channelling - matrix diffusion

Evidence for the mobility of radium in unweathered schists from the Jabiluka Two uranium deposit in the Allegator Rivers region of the Northern Territory of Australia has been obtained. The activity ratios $^{226}Ra/^{238}U$ increase regularly with decreasing uranium concentrations from values close to 1 (secular equilibrium) at high concentrations to values exceeding 5 at background level (<20 g/g)[21]. It appears that radium can disperse appreciable distances within the schist in time scales of thousands of years.

More definitive experiments have commenced involving the mapping the densities of fission track (reflecting uranium) and α- tracks (biassed towards radium levels) and correlating the ratios with mineralogy[23]. Initial results using high level uranium indicated little uranium/radium separation. The technique will be extended to low level samples and to the mapping of a suite of elements using the PIXE/PIGME techniques.

Attempts have been made to quantify the cumulative effects of uranium series transport in crystalline rock by correlating calculated rates of uranium leacbing (or deposition) with the uranium concentration gradient in the vicinity of pre existing fractures. The method has been made possible by the development of a generalized open system model which can be used to calculate uranium leaching (or deposition rates) from $^{234}U/^{238}U$ and $^{230}Th/^{234}U$ activity ratios on individual samples. Uranium migration patterns are developed measuring leaching (or deposition) rates on suites of samples.

It was shown in ref. (21) that small fractional uranium gradients (say 1.5x10-3) over long periods 10^5y or greater) are sufficient to induce readily estimated rates of redistribution. If a correlation of uranium leaching rates with concentration gradient is found, an effective diffusion coefficient can be calculated from Fick's diffusion law

$$\frac{\partial U}{\partial t} = K \frac{\partial U}{\partial x}$$

This value, relevant to processess which have occurred over timescales of the order 10^4 to 10^5 year can be used in RMD computations.

4. CONCLUSIONS

1. Natural analogue studies are of potential value in identifying processes leading to radionuclide mobility and in verifying mathematical procedures for calculating transport rates over long periods.

2. Evidence suggests that, in weathered schists, generating equations forming the basis of many common transport codes are satisfactory for long-term prediction of uranium migration.

3. With the possible exception of colloid transport, all effects identified through tbe Alligator Rivers analogue study lead to an underestimate of long-term retardation when sorption coefficients measured over short time scales are used.

4. The systematic study of uranium series disequilibrium the vicinity of pre-existing cracks and fissures in crystalline rock can in principle be used to calculate effective diffusion coefficients associated with the long-term redistribution of uranium.

5. In general natural analogues are not appropriate for assessing the long-term risks associated with low probability/high consequence events.

REFERENCES

1. M.A. Chapman, I.G. Mc Kinley and J.A.T. Smellie (1984), The potential of natural analogues in assessing systems for deep disposal of high level radioactive waste. NAGRA, NTB 84-41; KBS

2. P.L. Airey and M. Ivanovich (1986), Geochemical analogues of high level radioactive waste repositories, Chem Geol 55, 203-213

3. P.L. Airey, P. Duerden et al, (1986) Radionuclide migration around uranium ore bodies - Analogue of radioactive waste repositories. Annual Report 1984-1985, AAEC/C55

4. Kocher, D.E., (1984), On the development of environmental radiation standards for geological disposal of high level radioactive wastes NUREG, CR-3714 ORNL- 6006

5. M.M. Maxie, L.I. Moss, B.C. Musgraru and G.B. Watkins, (1980), General criteria for radioactive waste disposal, Scientific Basis for Nuclear Waste Management ed C.J.M. Northrup Inc. (Plenum Press NY 1980)

6. J.T. Fabryka-Martin (1986), In site migration of ^{129}I in uranium ore deposits ref. (3), chap 5.

7. J.T. Fabryka-Martin, D. Roman, P.L. Airey, D. Elmore, P.W. Kubik, (1987), Redistribution of natural I-129 among mineral phases and groundwater in the Koongarra Uramium ore deposit N.T. Australia - this proceedings.

8. K. Kuehn (1986), Are we ready to construct and operate an underground repository? Proc IAEA Symp. "Siting, Design and construction of Underground Repositories for Underground Waste, 3-7 March 1986 Hannover pp 1-8 (IAEA, Vienna 1986).

9. Swedish Nuclear Power Inspectorate, INTRACOIN Final Report, Level I code verification, Technical Report 84.3 SKI Stockholm 1984

10. Swedish Nuclear Power Inspectorate, INTRACOIN Final Report, Levels 2 and 3, SKI Stockholm

11. Swedish Nuclear Power Inspectorate, HYDRACOIN Progress Report Nos 1-3, SKI Stockholm, 1985

12. A.L. Szoreen and D.C. Kocher (1984), Uncertainties in long-term repository performance due to the effects of future geologic processes. Oak Ridge National Laboratory Report ORNL-6049, NUREG/CR-3832

13. M. Ivanoviah and C.J. Hardy (1986), Identification and measurement of colloids in groundwater. Proc. Natural Analogue Working Group Meeting Interlaken (CH), 17-19 June 1986, EUR 10671

14. J.I. Kim, Investigations about natural colloids,

15. S. Krishnaswami, W.C. Graustein, K.K. Turikian and J.F. Dowd (1982), Radium, thorium and radioactive lead isotopes in groundwater: Application to the insite delimination of adsorption rate constants and retardation factors. Water Resources Research, 18, 1633-1675

16. P.L. Airey, D. Roman, C. Golian, S. Short, T. Nightingale, T. Payne, R.T. Lourson and P. Duerden (1985). Radionuclide migration around uranium ore bodies-analogues of radioactive waste repositories. USNRC Contract NRC-04-81-172, Annual Report 1983-4 AAEC Report C45.

17. D. Gray (1986). The geochemistry of uranium and thorium during weathering: PhD Thesis (University of Sydney) Chapter 5.

18. D. Lever (1986). Ref. 3 Chapter 11

19. P.L. Airey, C. Golian and D.A. Lever (1986), an approach to mathematical modelling of the uranium series redistribution within ore bodies. Topical Report AAEC/C49.

20. H. Alielin, I. Neretnieks, S. Tunlirant, L. Moreno (1985) Final report on the migration in a single fracture - experimental results and evaluation. Stripa Project 85-03

21. ref. 3, chapter 6 page 101

22. ref. 17, chapter 5 page 199

NATURAL AND ARCHEOLOGICAL ANALOGUES: A REVIEW

DOUGLAS G. BROOKINS
Department of Geology
University of New Mexico
Albuquerque, New Mexico, USA 87131

ABSTRACT

There are numerous natural analogues for the many facets of radioactive waste disposal in geomedia. Certainly the best of these is the Oklo Natural Reactor, Gabon, where a naturally occurring uranium deposit formed some 2 Ga ago sustained a fission nuclear reaction for roughly 0.5 Ma. During this period copious quantities of fission products were produced, along with transuranics. Oklo allows a semi-quantitative to quantitative evaluation of the fate of fission products and actinides in rocks, and it is noteworthy that evidently most of these radionuclides either stayed in the host pitchblende or migrated only locally.

There are other analogues as well. Igneous contact zones provide an opportunity to study the fate of fission product and actinide analogue elements in rocks intruded by magma. This very high temperature heat source is the analogue for the heat generating radwaste canister, and the migration of elements in the intruded and intrusive rocks can be assessed by geochronologic, stable isotopic, and chemical means. Examples studied so far include the Eldora-Bryan stock and Alamosa River Stock in Colorado, USA, and other sites in Utah and South Dakota. Conditions for both convective and conductive cooling are known from stable O isotopic studies, and this allows evaluation of elemental migration/retardation under these conditions. Form most elements, migration is restricted to within a few meters of the igneous contact, even in the presence of very high thermal and chemical gradients. Rock fracturing plays an important role in the ability of elements to migrate under igneous contact conditions. At least one lamprophyre dike intrusive into bedded salts (near the WIPP site, USA) has also been studied, again with no evidence for any widespread elemental migration. In the Cerillos, New Mexico, USA area, there has been a pronounced recrystallization of clay minerals in shales intruded by syenitic to quartz monzonitic magma, and resetting of K-Ar ages yield thermal information consistent with this crystallization. In some cases, it is possible to estimate the time-temperature-distance parameters for very long periods of geologic time (i.e. 2 Ma in some cases), and, from this information, it may be possible to estimate leach rates of certain radionuclides under these conditions and then make comparisons to the very short laboratory leaching experiments.

Waste form materials have many analogues as well. Naturally occurring obsidians and other glasses are, under many terrestrial conditions, very stable for up to tens of Ma, while under other conditions dehydration-devitrification is rapid. The minerals that make up the natural counterparts of SYNROC are, for the most part, extremely stable, as are most other ceramic materials. Stability of metals such as copper, platinoids, etc. indicate remarkable stability under natural conditions.

Sandstone uranium deposits (discussed in detail elsewhere in this symposium) are good analogues for uranium oxide or silicate

waste forms, and provide many data on behavior of fission product elements as well. Engineered barriers and metal containers can be assessed by analogues as well. How various clay minerals behave in response to hydrothermal conditions similar to those expected in a radwaste repository is known under a wide variety of conditions, and there exists a large literature on the use of clay minerals to retain or retard many elements under chemical waste and other disposal systems in which the analogue elements for radionuclides are present.

Archeological studies show that very ancient glasses, ceramics and metals have, in many instances, ben very well preserved even under rather adverse chemical conditions. So, too, have clay minerals in materials used in ancient graves, linings, and other purposes. In cases where the overall conditions are reducing and the water/rock (or radwaste analogue material) is now low, the degree of preservation is excellent in most cases. These archeological studies confirm that the analogue can be resistant for periods of time up to thousands of years. Coupled with the information of natural analogues, stability for much greater times is indicated.

Finally, very useful information for analogue purposes is obtained from rock and mineral dating by standard geochronologic methods. Rocks and minerals as old as the earth have been dated successfully by Rb-Sr, K-Ar, U-Pb, Th-Pb, Sm-Nd, Lu-Hf, K-Ca methods. For rocks where data for these methods exist, the chemical and isotopic integrity of alkali, alkaline earth, rare earth, actinide, and actinide daughter elements can be assessed. Where ages have been re-set by some process, the rate and mechanism of loss can be addressed. Rock and mineral dating is a powerful analogue tool.

In many instances natural analogues applied to radwaste studies involve trans-scientific reasoning. While it may not be possible to quantitatively assess and evaluate all aspects of buried radwaste, the natural and archeological analogues nevertheless provide invaluable information about the fate of fission product, actinide and other elements, as well as information about the ability of waters to move through, and interact with, various geomedia.

1. Introduction: Analogs and Radwaste

When dealing with the disposal of radioactive wastes in geomedia, it is often stated that man is working with an experimental system for which there is no precedent. Yet this is not, in the strictest sense, true. There exist analogs for virtually all parts of the radwaste package in natural settings, and for the surrounding media, artificial barriers, and the interaction of water with each in the presence of radwaste radionuclides.

Man's intent is to confine the radioactive wastes by a series of redundant barriers, starting with the waste form. In the USA this waste form may consist of poured radionuclide-enriched borosilicate glass (for Savannah River Defense Waste and commercial, partly reprocessed waste from West Valley, New York) or spent fuel rods (either intact with cladding, or disassembled in part). Both will be encased in a steel container. The sleeves around the drill holes into which the canisters will be placed will also be lined with these steels, with or without an inner sleeve of alumina depending on more testing. In some scenarios, there may also be

an engineered barrier of clay minerals around the canister as well. The host rock then surrounds this waste package. The temperatures of the stored wastes will vary at canister edge from near 450°C for the glasses to 350°C for the spent fuel rods at the time of emplacement, and steadily decrease as the short lived radionuclides decay.

Analogs representative of parts (or all?) of this complex system are actually widespread. The ultimate concern of the radwaste disposal is the retention of the radionuclides until they have decayed into harmless levels or, alternately, their retardation so that they do not reach the near- or surface-environment in levels that would cause an adverse health effect. In nature, the most obvious analog is the Oklo natural reactor, Gabon. This is the site of an economic uranium deposit in sandstone-shale formed some two billion years ago and which sustained fission and other nuclear reactions for about 100,000 to 800,000 years very shortly after ore formation. Oklo is the subject of many separate reports (IAEA, 1976, 1978; Brookins, 1984). Suffice it to say here that of the hundreds of tons of fission products produced in the uraninite ores, most can be accounted for within the ore, in aureoles immediately adjacent to the ore, and out to a few meters, and, in some instances, at slightly further distances. Oklo presents strong testimony to the ability of rocks to retard and retain radionuclides.

Yet there are other analogs of importance. For convenience I break these down into the following types:

1.1 Geochronology. The fact that radiometric means can be used to successfully determine radiometric ages of rocks and minerals attests to the suitability of such media to remain closed systems to elements such as U. Th, Pb, Rb, Sr, K, Ar, Sm, Nd. In this group are actinides, an actinide daughter, alkali and alkaline earth elements, an inert gas, and rare earths; all of which are analogs to fission products or fuel elements.

1.2 Intrusive contact zones. Here the intrusive body is analog, on an immense to small scale, for a heat generating body intruded into various rocks. By studying the type of cooling (conductive versus convective), response of sensitive indicators to P,T conditions accompanying intrusions in the host rocks, and elemental migration in response to the intrusion, it is possible to apply these results qualitatively to predict behavior of radionuclides in geomedia. The hydrothermal activity accompanying igneous intrusions is analogous to the near field hypothetical behavior of a radwaste package breached by water. These analogs include active hot springs systems, more deep seated geothermal systems, and fossil systems such as many ore deposits.

1.3 Special mineral or rock occurrences. This includes natural glasses, natural metals, natural ores of interest such as uranium ores, and others. Study of these occurrences allows an understanding of how these materials formed, and how and why (or if) they are preserved in nature. This information can then be applied to the proper parts of the waste package.

1.4 Anthropogenic analogs. Man has been making and storing or discarding useful radwaste analogs for up to thousands of years. Study of these artifacts and other sources can be very useful in observing first hand how these materials have stood up to natural weathering and other factors under widely differing climatic conditions.

1.5 Others. Other useful, and/or potentially useful analogs include such things as study of weapons generated fallout radionuclides such as ^{137}Cs and ^{239}Pu (and other isotopes), accumulation of various elements under different weathering conditions (laterites, playas, etc.), behavior of certain elements in brines and other natural aqueous fluids, and a careful

consideration of elements that are analogs for fission products or actinides or actinide daughters (i.e. Re for Tc, etc.).

2. Geochronology and Radwaste

Absolute age determination based on radioactive decay of parent isotopes to stable daughter isotopes is an accepted tool for geologic research. Rocks as old as the age of the earth (i.e., meteorites and some lunar samples) have been successfully dated, and the time scale for the earth has been rigorously worked out by a combination of several geochronologic methods.

It is important to point out that the standard geochronologic methods involve an understanding of the geochemistry of U. Th. the actinide daughters, and Rb, Sr, K, Ar, Sm, Nd, Re, Os, Lu, Hf, and others, and that isotopes of many of these elements are either products of fission in man-made reactors or are some of the heavy metals encountered in radwaste. The importance of this relationship will be addressed below. As examples, repository rocks can be dated in order to test their chemical and isotopic integrity, and their radiometric ages are valuable tools for investigation of natural analogs as well.

The importance of the various major methods for radiometric age determinations lies in the diversity of the parent, intermediate, radioactive daughters, and stable daughters involved. If a rock has been dated by all methods, then one knows a great deal about the daughters with moderate to short half-lives (^{234}U, ^{230}Th, ^{226}Ra, ^{222}Rn, ^{210}Pb, ^{210}Po, etc.), nonradioactive, mutagenic isotopes (Pb), alkali elements (Rb, K), alkaline earths (Sr), and an inert gas (Ar). Further, advances in studies of samarium-neodymium dating (i.e. ^{147}Sm-^{143}Nd) show that both Sm and Nd are retained in rocks datable by other major methods, hence indirect inferences can be made concerning lanthanide element retention as well.

In considering elements and their isotopes present in HLW one is concerned with actinides (including transuranics), intermediate, radioactive daughters (primarily Ra), some Pb, alkali elements (^{137}Cs), alkali earths (^{90}Sr, Ba), lanthanides, and inert gases (Kr, Xe). In radioactive waste, we are also concerned with several other elements (I, Br, chalcophile and lithophile elements), but, if it can be demonstrated that the Rb, Sr, K, U, Th, Pb and Ar (and Sm and Nd) of a rock have not migrated, then this suite is diverse enough to strongly suggest that other elements in the rock should not migrate as well.

3. Igneous Contacts an Analogs for Buried Radwaste

The disposal of HLW calls for implacement at depth of the waste package in geologic media such as tuff, basalt, evaporites, granites and possible other rocks (see Brookins, 1984). The HLW package will be heat producing due to radioactive decay, but the temperature is a few to several hundred degrees celsius below crystallization temperatures of typical igneous rocks. Further, the dimensions of typical waste canisters is on the orders of 0.3 m diameter and 3 m length, many orders of magnitude less than the dimension of an igneous pluton of moderate size. It is further presumed that the waste package can only be breached and radionuclides released by events requiring the presence of water. When first buried and sealed, the waste package will be encased in a low temperature dry medium This environment will possess low oxidation potential by design except for the Yucca Mountain, Nevada site. Consequently the media are saturated with respect to water, and the 'dry' surrounding to the HLW package will be subjected to encroachment of some

water some time after emplacement.

Ideally one would like a laboratory study that would allow consideration of waste package - medium interaction at low temperature and over several tens to possibly a few thousands of years. Since this is not practical, then laboratory studies must be conducted under possibly atypical conditions in order to carry out such experiments in the shortest time which will give reasonable results. Typical leaching experiments, for example, commonly run from days to months and sometimes longer. After a few days to months the fraction leached is asymptotic to the time axis, and extrapolations to much greater times are based on this fact. While this approach is certainly necessary in order to conduct the experimentation, it is also questionable in that such things as phase changes, now complexes in solution, etc. may form at a considerable time under a natural setting. This would be missed in the experiments due to the short time factor. Hence one must look at natural analogs to attempt to address this and other time-temperature-fluid parameters.

Igneous rocks as analogs for the waste package are obvious choices. The suite of fission product, actinide and actinide daughter elements is present in most igneous rocks, and this is especially true for rocks of granitic compositions, in which elements such as Cs, Rb, REE, Ba, U, Th, Zr, Mo, Pb may be significantly enriched. If the intruded rock is compositionally more basic in compositions, then a favorable chemical gradient between intrusive and intruded rock exists, and potential for elemental migration thus exists.

The use of igneous rocks as analogs for buried HLW packages is, however, exceedingly complex. In addition to the problem of extreme differences in temperature and dimensions, many smaller igneous bodies (i.e. narrow dikes) will cool rapidly while the HLW package will cool more slowly. Further, the naturally occurring igneous rocks may be impermeable, or else permeable, with the intrusive rock either impermeable or more or less or equal in permeability to the intrusive. These differences will, of course, be of most importance if the cooling of the intrusive body is by convection rather than conduction, although both conditions must be examined. Even in the absence of large scale convective systems about an intrusive body, the anhydrous nature of the contact zone in the intruded rock attests to some transport of water. In some cases (see discussion later in this report) these results of migration of intruded rock water into the igneous rock, often with concomitant transfer of some elements as well. In the case of a radwaste container, this can be interpreted to mean that the HLW package may act as a heat sink which might promote transfer of water (and possible other constituents) from the intruded rock to the package.

The point to be stressed here is the transfer of elements from one place to another in the contact zones of igneous rocks. Where such transfer occurs, and where it does not, will provide information on elemental behavior in natural rock systems. Further, in some cases it may be possible to place time-temperature values on long-time elemental transfer, and then to compare such information with the extrapolations of laboratory results.

Most studies conducted in contact zone aureoles are aimed at a precise mineralogic phase rule interpretation, with careful estimation of temperature, compositional changes in minerals, and related items. Only somewhat infrequently to investigators look into the problem of possible elemental transfer from intrusive to intruded rock or vice versa. Yet the author has identified from the literature more than one hundred such examples (Brookins, ms. in preparation), a few of which will be summarized

below. In most of these cases, traverses have been made across the intrusive contacts, but commonly only one or two traverses per occurrence was conducted. This is unfortunate for reasons to be outlined later. In the cases discussed herein, no attempt is made to explain the chemical trends in terms of rock permeability, fracture patterns, thermal characteristics, thermal diffusivities, and related parameters. Such studies must be conducted for specific sites with the analog question in mind.

Case 1: Lamprophyre Dike intrusive into bedded evaporite

Brookins (1981) has reported on trace elements studies of a lamprophyre dike intrusive into the Salado formation halite of the WIPP site area. This dike was emplaced at a temperature of about 850°C at 34 Ma (Brookins, 1981). Loehr (1979) made a study of recrystallization of clay minerals in the halite as a function of distance from the contact. She found that within 3 meters of the contact, the normal clay mineral sequence was observed, and isochemical recrystallization occurred inward toward the dike. Only in the immediate contact zone of a few centimeters were there any pronounced effects; i.e. partial melting of halite with new salts formed. A new generation of polyhalite formed in the contact zone, which is of interest as this mineral contains two structurally bonded water molecules. The source of this water is unknown, but must have originated from within that zone as fluid inclusions less than two meters away give normal crystallization temperatures. No large scale migration of fluids toward the dike is evident, and no apparent transfer of elements from the dike into the evaporite is observed (Brookins, 1981), including U, Th, REE, Rb, Sr, Cr, Ni.

Case 2: Eldora Stock intrusive into Idaho Springs Formation, Colorado

The 60 Ma. Eldora stock, a quartz monzonite, intrudes the Precambrian schists and gneisses and pegmatites of the Idaho Spring Formation near Nederland, Colorado. This area is the subject of the classic work of Hart (1964) for mobility of $^{*40}Ar$ and $^{*87}Sr$ from mineral systems due to heat of intrusion, and was chosen for analog work because of the preliminary control. The studies of elemental migration are summarized by Brookins et al. (1981, 1982). Cooling of the stock was by conduction, and no elemental transfer from stock into intruded rock was suggested past the immediate 0-2 contact zones where there is evident some apophyses of stock into the metamorphic rocks. Even in the cases where $^{*40}Ar$ and $^{*87}Sr$ were lost from minerals, the $^{*87}Sr$ was retained in the whole rock samples, indicating movement of $^{*87}Sr$ only on a scale of microns to millimeters. Since the cooling time is estimated (Hart, 1964) to be between 10^5 and possibly 10^6 y., this attests to the fact that elemental transport in the absence of a convective fluid medium is minimal. This is important because at the time of intrusion (approximately 60 Ma.) it is safe to assume that the Idaho Springs rocks were saturated with water, but, due to its low permeability and porosity, even such a drastic event as the intrusion of the Eldora stock was insufficient to set up flow of this water.

Case 3: Alamosa Rive Stock intrusive in to Tuffs and Andesites

The Alamosa Rive stock, a monzonite, intrudes tuffaceous and andesitic volcanic rocks of the Platoro Caldera complex, Colorado. This site was chosen for analog study because the work of Williams (1981) had shown the presence of a large convencive system around the stock, based on oxygen isotopic studies, and some preliminary K-Ar data which indicated

that a 0.5 to 1.5 Ma. time of hydrothermal constraint could be placed on the rocks as well (see Brookins et al., 1983). Detailed study of two traverses from well within the stock into the tuffaceous rocks were conducted. Significantly, elemental migration is again indicated only in the few cm. to m. closest to the contact. Hence even the presence of the very long hydrothermal event was possibly insufficient to cause widespresd migration.

It should be possible to obtain more fine detail information from this site for elements showing the limited migration noted. Hence it may be possible to quantify the amount of elemental migration over a time-temperature framework of 10^5-10^6 y.:500° - 800°C and then extrapolate to t=0 and compare with laboratory measured leach rate information. Despite many apparent pitfalls, this site has the potential for obtaining long time, high temperature data which are badly needed in assessing radwaste analogs and long-term radwaste behavior in rocks.

Case 4: Notch Peak Pluton, Utah

The Notch Peak quartz monzonite (Laramide age) intrudes Cambrian limestone, argillaceous limestone, and siltstone in western Utah. Laul and Papike (1981) have investigated the effect on the intruded rocks in terms of trace elements behavior, including V, Cr, La, Sc, Pb, As, Sb, Rb, Sc, K, U, Th and others. Samples were taken in a traverse from the contact zone out to 40 meters, and a reference point established at 1 kilometer for presumed background control. Temperatures in the immediate contact zone are from 550°C (calcite, dolomite, diopside, forsterite, tremolite) to 450°C (calcite, dolomite, quartz, talc, tremolite). The rocks grade from very argillaceous limestone-siltstone near the contact to argillaceous-poor rocks at 40 meters from the contact.

Laul and Papike (1981) note that V. Cr, La, Sc, when ratioed to Al, form linesr relationships between high- and low-argillaceous rocks, indicative of sedimentary end member mixing and not elemental redistribution due to the intrusive contact. For other elements, however, there is some evidence for elemental mobility. They propose that Cs has migrated up to 5 m from the contact based on analysis of Rb/Cs ratios, and that Rb has also migrated to nearly the same extent based on K/Rb ratios. These data are not terribly convincing without better mineralogic control, and chemical analyses on constituent minerals. In nature the K/Cs, K/Rb, and Cs/Rb ratios can vary widely in argillaceous rocks, and without knowing the amount of this variation, so-called anomalies may or may not be real in intruded rocks such as reported by Laul and Papike (1981).

These authors also argue that Ba and Sr have also migrated to some degree, with Ba more mobile than Sr. This is not consistent with the well known geochemical observations that Sr is usually more mobile than Ba, and with Ba-Sr data from other analog sites (i.e. Oklo, others).

Laul and Papike (1981) argue for some Pb migration up to 40 m, but although this can easily be tested isotopically, no such isotopic variation is noted. It is probably that some Pb migration has occurred based on similar studies, which include isotopic data, made elsewhere (see Brookins, et al. 1981), but the extent is unknown. Similarly, As and Sb data suggest limited migration of these elements in response to the intrusion.

The Notch Peak area is of interest in that different sedimentary rocks have been intruded by the quartz monzonite, and the area certainly offers a good opportunity to additional chemical and isotopic data to be gathered.

Case 5: Santa Rosa Range, Nevada

The the Santa Rosa Range, Nevada, a series of Upper Triassic metapelites, metasiltstones, quartzites, limestone and dolomite has been regionally metamorphosed followed by intrusion of gradodiorites in the Late Cretaceous - Early Tertiary. Wodzicki (1971) has conducted extensive analyses of trace elements in the intruded rocks in an attempt to quantitatively assess the amount of elemental migration in the contact zones. His study was concerned with commenting on formation and movement of ore fluids, but his data are directly applicable to radwaste analog studies (see Brookins, 1986). His data (figs. 2-4; Wodzicki, 1971) show that there has been no apparent migration of Mn, Cr, V, Ni or Ti in response to the intrusions, regardless of the intruded rock, and that Sn, Li, B. Pb show a linear decrease in concentration from the outer edge of the contact zone to the edge of the intruaive bodies. Wodzicki (1971) interprets the Sn, Li, B, Pb data to indicate migration into the magmatic rocks. Further, H_2O has apparently migrated into the magmatic body as well, which is supported by the O isotopic studies of Shieh and Taylor (1969). Two elements, Cu and Zn, show evidence for irregular distribution in the contact zones, with local enrichment in both elements in metapelites which mirror depletions in siltstones. In all cases the migration is restricted to distances of or less than one half intrusive body diameter.

Case 6: Monzonite intrusive into Mancos Shale, Cerillos, New Mexico

Near Cerillos, New Mexico a aeries of monzonite plugs intrude Cretaceous sedimentary rocks, including the Mancos Shale. Aronson and Lee (1986) have reported findings from their studies of the intrusive contact zone. Howard and White (1981) used this zone to test for clay mineral recrystallization in conjunction with their studies on argillaceous materials for engineered backfill. They note that the degree of illitization of mixed layer smectite-illite increase in a regular fashion toward the contact.Aronson and Lee (1986) further confirmed the earlier work of Howard and WHite (1981) and, further, showed that radiogenic ^{40}Ar was lost form some, but not all, samples due to the intrusion. Their work showed remarkable retention of ^{40}Ar in some samples containing detrital illites even in the immediate contact with the monzonite. Their data further support the ability of mineral structures to retain key radionuclides even under high temperature (i.e. the monzonite intrusive temperature is given as 750°C; Aronson and Lee, 1986). Study of elemental migration in these samples has not yet been carried out.

Case(s) 7: Miscellaneous Studies For Intrusive Contacts

Numerous studies of chemical variations across intrusive contacts into various intruded rocks are documented in the literature. Most of these are interesting in terms of elemental migration and mineralogy, but rarely include time-temperature, stable isotopic or other data important for applying the chemical variations to problems associated with the breaching of a hypothetical radwaste canister in crystalline rocks. Some early studies (Dennen, 1951; Brookins and Dennen, 1965) involved major and trace elementa variations for many igneous rocks and their intruded country rocks. Data for the major elements are questionable in some instances and minor element data are more appropriate. Elements studied include Co, Cu, Zr, Mn, Tr, Ni. The following systems were investigated (Table 1):

Intrusive rock	Intruded rock	Comments
basalt	granite	migration of Ti, Zr into granite for 2 cm.
basalt	granodiorite	Ti, Zr, Ni, Mn (±) migration into granodiorite for 1 cm.
granite	Shale	Assimilation of some elements from shale (Cu, Mn, Co, Ni) within 3 cm (1.5 cm on either side of contact).
basalt	rhyolite	Possibly migration of Ti, Zr, Mn, Ni, Co into rhyolite to 0.5 cm.
diabase	rhyolite	Ti, Zr, Mn, Ni (±) migration into rhyolite to 0.5 cm.
diabase	arkose	Redistribution of Ti, Zr, Ni, Co, Cu in 1 cm contact zone on either side of contact.
basalt	diorite	Essentially no elemental transfer across contact.
granite	siltstone	Mn, Zr, Ti, Ni, Cu redistribution in 3 cm contact zone; no clear evidence for migration.

In these traverses the possible transfer of elements from intrusive into intruded rock is noted in several cases, although the apparent distance for such transfer is on the order of centimeters only. The redistribution due to formation of simple mineralogic zones (commonly monomineralic zones or 2- to 3-phase zones) at the contact causes elemental redistribution which can be mistaken for transfer if caution is not used in interpretation.

4. Special Mineral Occurrences

There are numerous special mineral occurrences useful as radwaste analogs. Various kinds of uranium deposits are perhaps the most obvious of these, but these will not be covered here as they are given treatment in much greater detail in these symposium proceedings (see articles by Brookins; Airey, Shea; this volume). In addition, the Oklo deposit is a uranium deposit.

There are many others, however. The Morro do Ferro rare earth - thorium deposit in Brazil has been extensively studied, but it, too, is covered elsewhere in these proceedings (see Linsalata et al.) and so will be omitted here.

Occurrences of special minerals are useful in discussing radwaste analogs. Naturally occurring corundum is remarkably stable in the weathering environment of the earth, and attests to this minerals ability to withstand mild to severe oxidizing conditions. The sleeves that have been proposed to encase steel canisters may be made out of alumina. Some

proposed sleeves are native copper, and it, too, is stable over a wide range of natural Eh-pH. The Eh-pH diagram shows a wide field for native copper even above the sulfide-sulfate boundary (Brookins, in press), and even at surface Eh native copper has remarkable stability. Native iron is rare in nature, yet is found in Disko Island near Greenland. The iron has withstood millions of years of weathering without failing. In both this case and for some copper, films of alteration products that form on the surface may effectively armor the metals from rapid chemical attack. The constituent minerals of the artificial radwaste form SYNROC (including sub-varieties) in nature are mostly resistant to chemical attack. Naturally occurring zirconolite has been shown to be resistant to both chemical weathering and radiation damage (see discussion in Brookins, 1984), and resistance to chemical weathering by natural perovskite and monazites is also well known (Brookins, ibid.). Nepheline is a constituent of Na-bearing SYNROC. While metastable under surface oxidizing conditions, under the low Eh of the canister emplacement, it, too, should be very long lived. Still further, the special phosphate glasses being pursued such as NZP (sodium zirconim phosphate) are analogous to natural phosphates, such as apatite, which are common in resistate fractions of sediments.

Natural glasses have received a great deal of attention for radwaste analogs (Ewing, 1979; Brookins, 1984). Natural glasses are metastable on the earth's surface, but the time it takes to devitrify them is very lengthy. Glasses as old as 35 Ma are known, and possible older. Release of certain elements during the devitrification is commonly observed (see Brookins, 1984). Basically, natural glasses show that glass can be preserved at the earth's surface for long periods of geologic time; and, secondly, their rate of devitrification takes place over times sufficient to severly restrict the release of radionuclides (i.e. much less than the 10^{-5} release rate advocated in the USA).

Certain rock formations have been proposed as analogs as well. Brookins (1982) has shown that the Dakota Formation (Cretaceous) of the San Juan Basin, USA, which is a bentonitic sandstone, is similar in chemistry to the Swedish proposed engineered barrier of quartz sand plus bentonite. Further, the uranium mineralization of the Dakota is fracture controlled, with essentially no penetration of the unfractured rock. Argillaceous rocks in general are often used to evaluate the ability of clay minerals to serve as getters for radionuclides (see discussion in Brookins, 1984). Discussion of some of these is covered in other papers in this symposium.

The study of uranium bearing minerals for the effects of radiation damage is also of great interest. Many natural minerals have been subjected to radiation doses over considerable periods of geologic time. The degree of damage, or metamictization, varies as a function of crystal structure, chemistry, and the chemistry and physics of the surroundings. Study of naturally occurring minerals as analogs to disposed actinides shows, so far, extreme retention of uranium (see discussion in Brookins, 1984).

Laterites, too, have potential as radwaste analogs. The Morro do Ferro occurrence in Brazil (see Linsalata et al., this volume) is a good exampled of how surface laterization over ultramafic rocks has enriched the REE and Th in the surface rocks. Elsewhere, the fixation of elements such as Fe, Co, Ni, Y, Ree, Th and even U is well documented.

5. Anthropogenic Analogs

Man has been using earth materials, and altering the earth's surface in many ways, for possibly two million years. Without meaning to, man has left behind numerous materials that can serve as radwaste analogs. The whole concept of anthropogenic analogs is essentially transscience; i.e. the problem is of scientific interest but not likely to be solved by scientific methods; or, we can infer, but not necessarily prove in a quantitative fashion, what these analogs mean. This is, in general, true for most of the analogs of all types referred to in this paper.

Anthropogenic analogs of use to radwaste disposal in the unsaturated zone (i.e. Yucca Mountain site, Nevada) have been discussed in great detail by Winograd (in press), and the immediate material to follow is modified from his work. Winograd notes, for example, that there are several ways of using archeological science for purposes of radwaste disposal: the general applicability of unsaturated zones for isolating radwaste from the surface, the use of manmade (or natural), durable objects suitable for encapsulation of radwaste for use as markers, and the possibility of future human intrusion. Here I will be concerned primarily with the second of these, but will summarize Winograd's ideas on the first. Late Paleolithic man (40,000 to 10,000 BCE) left an impressive record of events in caves and rock shelters while Neolithic to Iron Age Man (8,000 to 1,000 BCE) left his record in manmade structures. Durable objects, both rugged and delicate, have been preserved from both. Ice cave art, ivory animal statues, clay bison figures from 35,000 to 15,000 years old, all remarkably well preserved, have found, even under oxidizing conditions and high humidity. Winograd proposes that the caves were well drained with a near constant humidity and annual temperature. In additions, well preserved horsebean (6,000 years old) heaps have been found in Israel, and marvelously preserved leather, food (beans) hair, frescoes, etc. from Masada (70 CE). Preserved fabric, feathers, paintings, etc. have been found at sites from 1000 to several thousand years old sites in Egypt, China and elsewhere. Winograd is careful to point out, that because of a lack of precise knowledge on climatic change, etc. over the period of time between age of site and the present, the use of such sites as analogs is tricky.

The durable objects cited by Winograd include a wide variety of glasses, natural and manmade, that have been studied. Natural glasses have received a great deal of study (see section 3) but manmade glasses much less. Kaplan (1980) has studied glasses from climates of many different ages, and 7500 year old mortars and plasters have also been studied. Under arid climates many of the glasses are remarkably well preserved, even when exposed to humid climates.

In addition to the treatment by Winograd, there are numerous other examples of well preserved manmade objects. Statues of bronze, copper, iron, dating back to several thousand years are known. Even in cases where such statues have been buried on the sea floor for many hundreds of years, they have often remained very little damaged. Clearly there is a real need for detailed work on such objects with the goal being use of these analogs to radwaste canister materials. What is needed is a systematic study of such materials, including detailed petrography, elemental studies, site studies, and so on (Winograd, in press).

6. Others

Considerable knowledge about radionuclide behavior in the surface environment has resulted by studying nuclear weapon fallout. Two radionuclides commonly studied are ^{137}Cs and ^{239}Pu. Brookins (1984) has discussed behavior of these isotopes briefly, and key references to more

detailed work is given therein.

Playa environments are extremely interesting from the poisoned land concept. This concept recognizes that there exist large areas of land that have been poisoned by accumulation of toxic and carcinogenic elements, often to the point where both plant and animal life are not readily supported. This poisoning can result from natural causes or from anthropogenic causes. In the USA these poisoned lands include playas in the western and southwestern USA, abandoned iron mine waste areas in the southeastern and Great Lakes areas, gypsum spoils in Florida swamps, certain coal wastelands, and others (Brookins and Vogler, 1983). The playas in the USA are of special potential. Many of these are in closed hydrologic basins, with the only water lost by evaporation; and the rate of evaporation to recharge is very high, ranging from a factor of 5 to much higher (see Brookins and Vogler, 1983). Many are also naturally poisoned by gradual accumulation of As and other toxic elements. In the case where such playas are removed from urban centers (i.e. much of Nevada fills this requirement), and in which there are no valuable resources, then these may be candidates for radwaste disposal. They also serve as analogs to desert sites for HLW disposal, the argument being that should HLW radionuclides reach the surface, they would be transported to the playa and remain there over the isolation times required by the USA licensing agencies.

Another analog approach is the use of geochemically similar elements to radionuclides for purposes of predicting radionuclide behavior in rocks. Use is made of crystal chemical characteristics, solubilities, activity diagrams, Eh-pH diagrams and other factors. Thus the following pairs or groups have been advocated: REE for actinides, U for other actinides, Th for reduced U(IV), Re for Tc, Mo or Mn for Tc, Ni-Co-Fe and/or Pt-Ir-Os for Pd-Rh-Ru, Re for Ru, Cu for Ag, Zn for Cd, As for Sb,Bi, Se for Te, Cl for I, Ar for XE,Kr, Sr for Bs, Br for Cs, Ba for Ra, Sc for Y, Ti for Zr, Ta for Nb, Ge for Sn, and others. Admittedly this approach is qualitative, yet in some cases (i.e. Re for Tc) the control is very good (Brookins, 1986).

7. Conclusions

In the preceding pages many different types of natural analogues for radioactive waste disposal are listed, yet this list is far from complete. Behavior of the different components of the radwaste package can be investigated by use of native metals, ceramic analog minerals, clay minerals, and other natural materials. Examination of igneous contact zones gives insight into how radionuclides may behave in response to a breached radwaste container. Special mineral occurrences address different parts of the problem. Anthropogenic analogues, including glass, metal, and other materials, are of extreme value in assessing preservation of parts of the radwaste package under different weathering conditions. Rock dating provides information on behavior of radionuclides in different media. Collectively, the analogues discussed here are important for two main reasons: (1) All parts of the radwaste package are covered. (2) The studies to date indicate very limited movement of radionuclide analogues under very adverse conditions. Future work must include ways to make the studies more quantitative for modeling and other purposes.

References

1. ARONSON, J.L., and LEE, M. (1986). K/Ar systematics of bentonite and shale in a contact metamorphic zone, Cerillos, New Mexico: Clays and

Clay Mins., v. 34, p. 483-487.
2. BROOKINS, D.G. (1981). Geochemical study of a lamprophyre dike near the WIPP site: in Sci. Basis Nuc. Wste. Mngt., v. III (J.G. Moore, Ed.), p. 307-314.
3. BROOKINS, D.G. (1982). Geochemistry of the Dakota Formation of northwestern New Mexico: relevance to radioactive waste studies: Nuc. Tech., v. 59, p. 420-428.
4. BROOKINS, D.G. (1984). Geochemical aspects of radioactive waste disposal: Springer-Verlag Pubs., New York, 347 p.
5. BROOKINS, D.G. (1986). Rhenium as analog for fissiogenic technetium: Eh-pH diagram (25°C, 1 bar) constraints: Jour. Appd. Geoch., v. 1, p. 513-517.
6. BROOKINS, S.G., and DENNEN, W.H. (1964). Trace element variations across some igneous contacts: Trans. Ks. Acad. Sci., v. 67, p. 70-91.
7. BROOKINS, D.G., and VOGLER, H.A. (1983). Playas for the siting of low level radioactive waste: studies in the Estancia Valley, New Mexico: Amer. Nuc. Soc. Trans., v. 44, p. 64-65.
8. BROOKINS, D.G., COHEN, L.H., WOLLENBERG, H.A., and ABASHIAN, M.S. (1981). The Bryan-Eldora stock, Colorado: application to the disposal of radioactive waste in crystalline rocks: Int. Atomic Energy Agency Sym. 257, p. 775-782.
9. BROOKINS, D.G., ABASHIAN, M.S., COHEN, L.H. and WOLLENBERG, H.A. (1982). A natural analogue for storage of radwaste in crystalline rocks: Sci. Basis Nuc. Wste. Mgt. IV (S.V. Topp, Ed.), p. 231-238.
10. BROOKINS, D.G., ABASHIAN, M.S., COHEN, L.H., WILLIAMS, A.E., WOLLENBERG, H.A. and FLEXSER, S. (1983). Natural analogues: Alamosa River Stock mononite intrusive into tuffaceous and andesitic rocks: Sci. Basis Nuc. Wste. Mngt. VI (D.G. Brookins, Ed.,), p. 299-306.
11. BROOKINS, D.G., MURPHY, M.T., WOLLENBERG, H.A. and FLEXSER, S. (1984). Geochemical studies of Columbia River basalts: Sci. Basis Nuc. Wste. Mngt. (G.L. McVay, Ed.), p. 917-926.
12. DENNEN, W.H. (1951). Variations in chemical compositions across some igneous contacts: Bull. Geol. Soc. Amer., v. 62, p. 547-558.
13. EWING, R.C. (1979). Natural glasses: analogues for radioactive waste forms: Sci. Basis Nuc. Wste. Mngt. I, (G.J. McCarthy, Ed.), p. 57-68.
14. HART, S.R. (1964). The petrology and isotopic mineral age relations of a contact zone in the Front Range, Colorado: Jour. Geol., v. 72, p. 493-525.
15. HOWARD, J.D., and WHITE, W.B. (1981). Clay metamorphism: a natural analog for argillaceous backfill material: Battelle Columbus - Office Nuc. Wste. Isolation Rpt for 1981, Section II-K, p. 247-251.
16. KAPLAN, M.F. (1980). Characterization of weathered glass by analyzing ancient artifacts: Sci. Basis Nuc. Wste. Mngt. II, (C.J. Northrup, Ed.), p. 85-92.
17. LAUL, J.C. and PAPIKE, J.J. (1981). Chemical migration by contact metamorphism between granite and silt/carbonate systems: Int. Atomic Energy Agency, Sym. 257, p. 603-614.
18. LOEHR, C.A. (1979). Mineralogical and geochemical effects of basaltic dike intrusion into evaporite sequences near Carlsbad, New Mexico: Unpub. M.S. Thesis, N.M. Inst. Min. Tech., 70 p.
19. SHIEH, Y.N. and TAYLOR, H.P. (1969). Oxygen and hydrogen isotope studies of contact metamorphism in the Santa Rosa Range, Nevada, and other areas: Contr. Min. Petrol., v. 20, p. 306-356.

20. WILLIAMS, A.E. (1981). Investigation of oxygen-18 depletion of igneous rocks and ancient hydrothermal-meteoric circulation in the Alamosa River Stock region, Colorado: Unpub. Ph.D. Thesis, Brown Univ., 355 p.
21. WODZICKI, A. (1971). Migration of trace elements during contact metamorphism in the Santa Rosa Range, Nevada, and its bearing on the origin of ore deposits associated with granitic intrusions: Miner. Deposita, v. 6, p. 49-64.
22. WINOGRAD, I.J., in press: Archeology and public perception of a transscientific problem - disposal of toxic wastes in the unsaturated zone: U.S. Geol. Surv. Circ. 990.

SESSION 2 :

ANALOGUE SITE STUDIES

Chairman : I. McKINLEY (EIR, CH)

Co-Chairman : S. CARLYLE (OECD-NEA)

NEAR-FIELD ANALOG FEATURES FROM THE CIGAR LAKE URANIUM DEPOSIT

J.J. Cramer, P. Vilks and J.P.A. Larocque
Atomic Energy of Canada Limited
Whiteshell Nuclear Research Establishment
Pinawa, Manitoba, Canada, ROE 1LO

Summary

The Proterozoic Cigar Lake uranium deposit in northern Saskatchevan is being studied as a natural analog system that includes many features similar to those of a conceptual disposal vault for used fuel. The more than one billion year old deposit has survived without significant secondary dispersion and, at present, without any direct indications at surface as to its presence at a depth of about 450 m. This paper gives a description of the deposit and its analog features, including uranium mineralogy, clay mineralogy and host rock alteration, radionuclide migration, groundvater compostion, colloids and radiolysis.

1 Introduction

Since 1982 Atomic Energy of Canada Limited (AECL) has conducted natural analog studies as part of the research program to assess the concept of underground disposal of nuclear fuel waste in plutonic rock. A major component of this natural analog program is the study of rich uranium ore deposits in sandstone host rocks. Although there is no geological system that is an exact analog to a used fuel disposal vault, the high-grade uranium ore deposits in the Athabasca Sandstone Formation of northern Saskatchevan (Figure 1) provide opportunities to study analogs to certain components of a disposal vault. These deposits are very important because of their analogous characteristics such as the composition of the ore minerals compared with that of used fuel, the survival of the uranium ore in vater-rich systems for periods of up to 1 billion years and, for the deeper deposits, the lack of surface indicators. It is important to determine the parameters controlling the long-term stability of the uranium minerals in these deposits, which are open, water-saturated, systems unlike the "closed" system of the disposal vault concept. An understanding of the role of the various components of these deposits, such as the groundvater, the host rock and the non-uranium minerals in the ore, and of the fixation and survival of the uranium minerals and their radioactive decay products could add confidence to the predictions of the performance of a diposal vault.

For the past 3 years, the analog studies have been concentrated on the Cigar Lake deposit because of its unique features. This deposit, at a depth of about 430 m, has not been significantly affected by surface-controlled processes, such as remobilization by oxidizing recharge waters, compared with other shallover deposits at, for instance, Rabbit Lake, Cluff Lake and

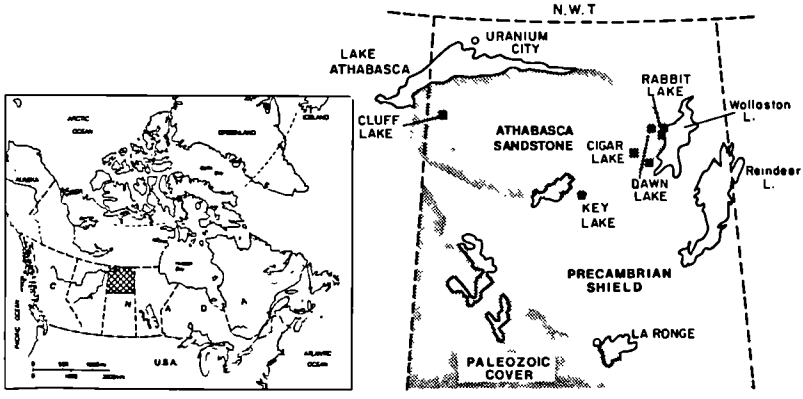

Figure 1 Location map showing the Cigar Lake uranium deposit in the Athabasca Sandstone Formation in northern Saskatchewan.

Key Lake. The Proterozoic Cigar Lake deposit and its alteration halo in the overlying sandstone are separated from the surface by an additional 150 m of unaltered sandstone and overburden. This deposit is very valuable for analog study because of the depth of the mineralization, its composition of mainly uraninite, its total content of uranium and the content and geometry of surrounding clay-rich zones in the host rock. In addition, the timing of the mine-development program for the deposit is favorable because it allows the study of both the undisturbed system and the dynamically disturbed system during the mine-development phase. A considerable amount of data and information on the Cigar Lake deposit has already been collected, including detailed chemical, physical and hydrological databases, data from an environmental impact study, as well as about 85 km of core from 200 drill holes.

The survival of the 1.3 billion year old Cigar Lake deposit and the absence of any direct physical or chemical signatures of the mineralization at the surface are mainly due to the composition and conditions in the centre of the deposit. The ore zone and the surrounding alteration zone is similar to the near-field of a disposal vault. This paper deals with the analog features of this near-field system.

2 Description of the Cigar Lake Deposit

The Cigar Lake uranium deposit is located in northern Saskatchewan (Figure 1) at the southwestern tip of Waterbury Lake. The geology and characteristics of this deposit have been described in detail previously (1-3) and are summarized here. The mineralization occurs in the basal unit of the Athabasca Sandstone Formation in the Athabasca Basin and it is the first major occurrence found at great depth. The Athabasca Basin is host to several major U-deposits of the so-called "unconformity type". The Cigar

Lake mineralization is located in the sandstone at the unconformity contact of the sandstone formation and the underlying high-grade metamorphic rocks of the basement. In most of the shallow deposits, such as Cluff Lake, Rabbit Lake and Key Lake, the ore occurs both in the sandstone and below the unconformity in the underlying basement rocks. The Cigar Lake deposit was discovered by Cogema Canada Ltd. in 1981 and has been extensively drilled to demonstrate the presence of sufficient ore to justify building a mine. The Cigar Lake Mining Corporation was formed in 1985 to determine the mining techniques and to develop the deposit for underground mining.

The ore body occurs as an irregular shaped, east-west trending lens (~2100 m long by 25 to 100 m wide by 1 to 20 m high) inside a 5 to 30 m thick clay-rich halo in the sandstone (Figure 2). This clay-rich halo forms the inner part of an extensive alteration halo (up to 300 m wide) in the sandstone host rock surrounding the deposit. The primary uranium mineralization consists of uranium oxides (uraninite and pitchblende) and uranium silicate (coffinite), and has been dated at 1.3 billion years using U-Pb isotope analyses (4). Sulphide, arsenide and sulpho-arsenide minerals containing nickel, cobalt, iron, copper, molybdenum and radiogenic lead are associated with the uranium ore. Three stages of hydrothermal mineralization are recognized (2): the first stage includes euhedral uraninite and pitchblende associated with primary As-S-minerals of nickel, cobalt and iron; the second stage includes pitchblende associated with secondary As-S-minerals as well as copper, molybdenum and lead sulphides; and the third stage includes pitchblende and coffinite associated with iron oxides and hydroxides. The first stage of uraninite plus pitchblende mineralization constitutes the bulk of the ore deposit. Some mobilization of the primary ore constituents is observed in so-called perched mineralization and basement mineralization. In both cases mobilization is very localized and of very limited importance and is found along isolated fractures above (perched) and below (basement) the main ore zone.

An iron oxide/hydroxide-rich zone forms the contact between the high-grade ore and the overlying clay-rich halo. The thickness of this zone varies from less than 1 m to a maximum of 10 m. Within this zone, the intensity of the iron-red colouration of the clay matrix decreases with distance from the contact with the ore. The clay-rich halo consists of illite plus kaolinite (from ~30 to ~80 vol.%) and quartz with zircon, anatase, leucoxene, rutile, apatite and monazite as accessory phases. In the altered sandstone zone beyond the clay-rich halo (Figure 2), the clay content decreases gradually to that of the unaltered sandstone beyond the quartz-cemented cap. The altered sandstone is characterized by its white colour and the presence of iron sulphide (pyrite) instead of iron oxide (hematite) in the unaltered reddish sandstone. In the ore zone, kaolinite is the dominant clay mineral in addition to illite, chlorite and iron- and magnesium carbonate (siderite and dolomite).

The ore body contains an extremely high-grade mineralization, particularly in the "main pod", which comprises the eastern one third of the ore body. The average grade of the main pod is 14 wt.% U_3O_8 with U concentrations of more than 40 wt.% occurring over several metres. The maximum concentrations found range from 60 to 65 wt.% U_3O_8. The present ore reserve is calculated at 1.5×10^5 Mg U, which is approximately equivalent to the expected U inventory of used fuel in a fully loaded disposal vault.

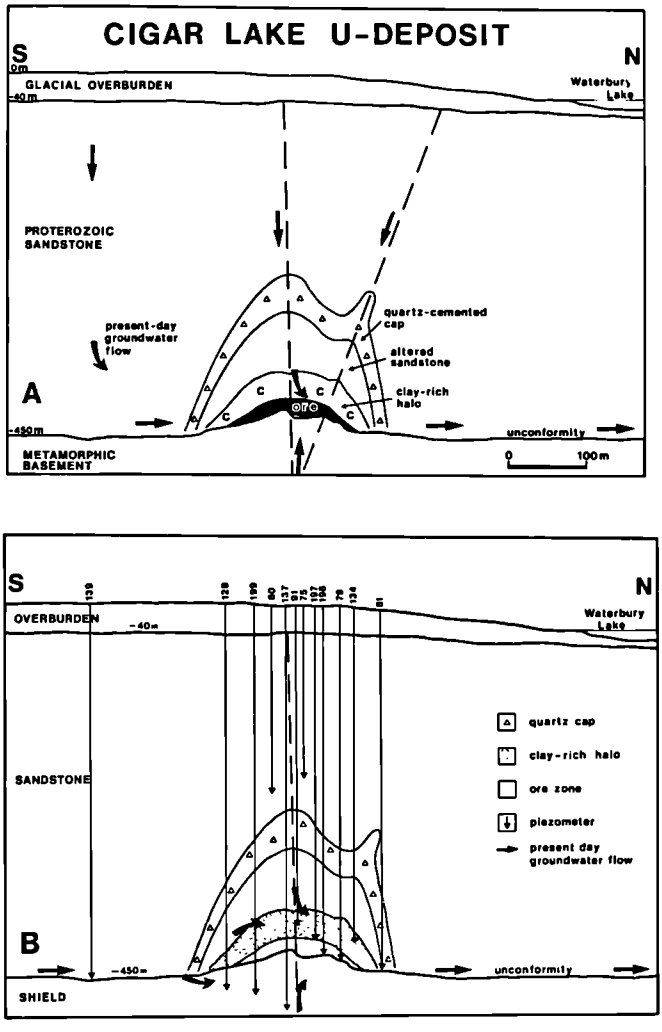

Figure 2 A: Schematic cross section through the Cigar Lake uranium deposit showing the different rock units of the deposit, major fracture orientation (dashed lines) and the present-day groundwater flow regime. B: Same section as in A showing the location of piezometers used for groundwater sampling.

Groundwater is present in large amounts throughout the deposit and the sandstone host rock. The basal sandstone member, particularly the conglomeratic unit directly overlying the unconformity, and the altered sandstone overlying the ore zone have hydraulic conductivities about two orders of magnitude higher ($\sim 10^{-6}$ m.s^{-1}) than those for the upper sandstone members and the basement. Although the ore zone and the clay-rich halo have measured hydraulic conductivities similar to that of the basement, abundant groundwater has been observed and sampled from piezometers in the ore zone and the clay-rich halo. As indicated in Figure 2, the regional groundwater flow direction through the deposit is from south to north. Additional but minor groundwater inflow to the deposit comes from recharge along fractures and from discharge from the basement. The hydraulic conductivity of the different zones in the deposit is also due to the extensive fracturing of the rocks. The main structural control of the deposit (2) is formed by a ridge in the unconformity contact that resulted from block faulting along vertical and sub-vertical fractures. These fractures are original lineaments in the Precambrian basement that were reactivated after deposition of the sandstone sediments and they have been and still are pathways for groundwater flow.

Hydrothermal fluids, which were responsible for the alteration of the sandstone host rock and the U mineralization, were discharged from the basement into the sandstone along these fracture conduits. Alteration of the host rock is characterized by changes in the colour and the clay content of the sandstone. The unaltered hematite-rich sandstone changes in colour from brick red to grey white due to the dissolution of the hematite. The clay content of the altered sandstone, particularly inside the quartz cap, increases towards the ore zone as a result of dissolution of the quartz from the rock matrix. Quartz, dissolved from the rock matrix by the hydrothermal fluids upon their discharge into the sandstone, migrated down the thermal gradient and precipitated in cooler, less altered rock. This alteration process and the resultant quartz cap are typical of the unconformity-type deposits in the Athabasca Basin (5,6).

3 Analog Features

There are many features of the Cigar Lake deposit that are analogous to components of a used fuel disposal vault. Unlike the 2 billion year old U deposit at Oklo in Gabon, the younger deposit at Cigar Lake never went critical and has not produced radioactive fission products. Nevertheless, the Cigar Lake deposit is of particular interest for several reasons, including its U content, setting (size, geometry, depth), geological history and the absence of surface indicators. The different features are investigated in two types of studies : I) studies on the groundwater now present in the deposit, and II) studies on the rocks and minerals in the ore and host rock. In addition, data on the deposit are used in the modelling of various analog aspects. Initial modelling has been conducted on the simulation of element migration in the deposit and the overlying rocks (7).

The observation that the deposit at Cigar Lake is saturated with groundwater is very important with respect to predictions on the performance of a disposal vault over long periods of time. In fact, the deposit has probably been a water-saturated system since its formation. Sediment waters and hydrothermal solutions interacted to produce the

mineralization and the alteration of the host rocks (8) and, subsequently, the porous and permeable sandstone likely remained a water-conducting formation. In addition, the fractures intersecting the deposit and the unconformity provided pathways for water access to the ore zone. Further evidence for the interaction of groundwater with the uranium mineralization comes from lead isotope data. A compilation of U-Pb isotopic ages for the uranium deposits associated with the Athabasca Sandstone Formation (9) shows that several common isotope fractionation events occurred since ore formation. This fractionation resulted from mobilization of Pb and possibly some U, and indicates water interaction with the ores. Despite the long history of water-ore interaction, which is common to all the large deposits and must also apply to the deposit at Cigar Lake, secondary uranium mobilization has been very limited and appears to be restricted to migration along fractures (2). This occurrence of uranium in certain fractures can be distinguished from the primary dispersion of uranium during initial hydrothermal ore formation because the latter is more uniform in the rock matrix and follows the contours of hydrothermal alteration (3). It is thus evident that, in the past, and at present, the fixation of uranium in the ore zone in contact with water is controlled by the parameters and composition of the water-ore-host rock system.

At present, the studies on the groundwater found in the Cigar Lake deposit are aimed at identifying the processes and parameters controlling the uranium fixation. This includes the characterization of the undisturbed system prior to the onset of mining related activities and, subsequently, the effects of mining on the composition of this system. The studies involve the determination of groundwater compositions, its constituents and parameters, to gain information on 1) solution and redox chemistry, 2) colloid chemistry and 3) organic chemistry and microbial activity. This information is used to analyze the dissolution of the natural uranium minerals as an analog to fuel dissolution, the effect of colloids on the migration of radionuclides and trace elements, the effect of organics and microorganisms on both ore dissolution and radionuclide migration, the effect of radiolysis in the ore, and the buffering capacity of the original steady-state system with respect to changes resulting from major disturbances.

The studies on the rocks and minerals of the Cigar Lake deposit are also aimed at understanding their role in the preservation of the uranium mineralization and its associated elements. The analyses of the minerals in both the mineralization and the surrounding envelope of altered rock give information about their history of formation and stability. The hydrothermal conditions during ore formation were similar to, or more extreme than, the conditions expected to exist in the near-field of a disposal vault during the thermal transient from used fuel (5). The clay minerals and quartz in the clay-rich halo around the mineralization have thus been subjected to analogous conditions of elevated temperature, of high salinity solutions and of a long period of time. A detailed study is in progress on the mineralogy and chemistry of the clay minerals in this deposit, and on the role of these minerals in retardating radionuclide migration. Of particular interest in this respect is the red ferric-iron zone in the clay-rich halo that forms the contact with the mineralization. The quartz dissolution and cementation that took place during ore formation is another analog to the predicted stability of quartz in the buffer and backfill during the hydrothermal conditions in a disposal vault. Aspects of this analog for quartz include the effect of quartz dissolution and

cementation on the physical properties of the clay-rich zone and host rock, and modelling of the kinetics of quartz dissolution under similar conditions.

An important analog is found in the iron phases present in the deposit. The solid iron phases, consisting of oxides and oxyhydroxides, carbonates and sulphides, are found in the deposit and, where coexisting, indicate a metastable or dynamic system in terms of the redox conditions. The role of the Fe^{2+}/Fe^{3+} redox couple in the redox chemistry of the ore zone is important because of the fast kinetics of the iron oxidation reaction compared with the oxidation of uranium. The close spatial association of ferric-iron phases with the uranium ore minerals is also found in other types of uranium deposits and is evidence of the coupling of iron oxidation with uranium reduction in the redox chemistry. The predominantly amorphous nature of the ferric-iron phases, compared with the crystalline ferrous-iron phases, indicates the dynamic nature of the redox system for iron. Recycling of the iron from the amorphous ferric oxides and hydroxides must occur on a shorter time scale than that required for conversion of the amorphous phases to crystalline minerals. The formation and stability of the iron oxides and hydroxides are also crucial to radionuclide migration, since these phases are known for their fixation potential for dissolved radionuclides. The Cigar Lake deposit is thus an important analog for studying the role of the iron chemistry in the near field for both redox control and the retardation of radionuclides onto ferric-iron phases.

Other analog aspects that are being studied include the paleo-dispersion of elements from the mineralization and the distribution of nuclides from the natural fission occurring in the high-grade ore. Only some of the radionuclides in the uranium decay series are suitable for indicating secondary dispersion through groundwater interaction. Depending on parameters such as solubility, flow rate of the water, sorption and half-life of the nuclide, only the isotopes of uranium, thorium and lead are useful to determine paleo-dispersion (7). Of the fission products, the isotopes ^{129}I and ^{99}Tc are of particular interest because of their chemical mobility. A study on ^{99}Tc and ^{239}Pu in the high-grade ore from the main pod has been initiated whereas a study on ^{129}I is planned for the near future.

4 Field methods

Field studies at Cigar Lake are an integral part of the natural analog study on this U deposit. The numerous drill holes on the site provide the only access to the deposit at depth. In addition to information collected by the exploration company from logging both the drill holes and the cores, specific information and samples of both rock and water are collected. Systematic sampling of profiles through the deposit has been carried out for a variety of studies, including clay mineralogy and chemistry, U mineralogy, element dispersion, fluid inclusion work and isotope analyses. A large component of the field studies is devoted to characterization of the parameters of rock-water interaction. The determination of groundwater compositions is thus an important aspect, requiring systematic and dedicated sampling methods.

The diagram in Figure 2B shows the location of some of the piezometers installed in drill holes on the deposit. These are the main piezometers used for characterization of the groundwater composition. Additional piezo-

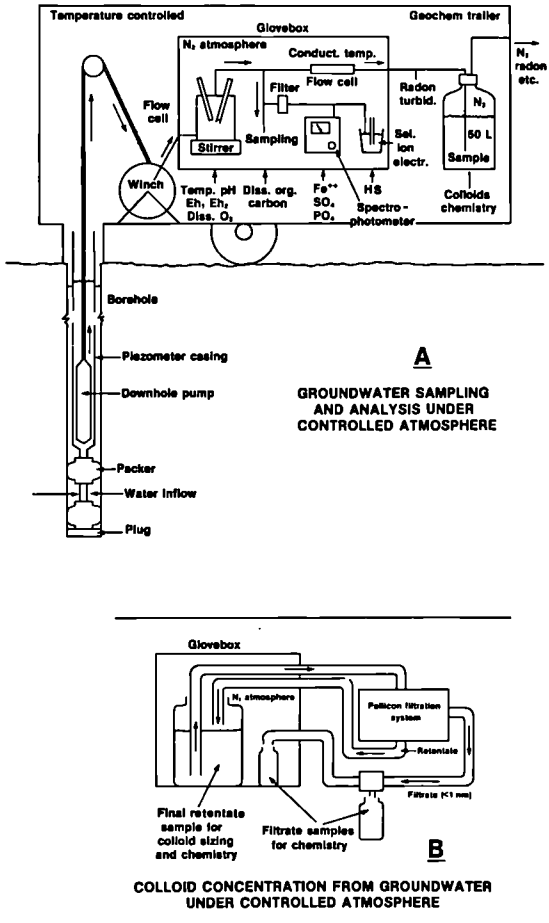

Figure 3 A: Schematic diagram showing set up used for groundwater sampling and analysis under controlled atmosphere. B: Schematic diagram showing set up used for groundwater filtration under controlled atmosphere.

meters have been installed across the deposit for hydrogeological work. Half of the piezometers in Figure 2B use stainless steel packers to isolate the desired sampling interval; the other piezometers contain bentonite seals separated by a sand column across the sampling interval. The piezometers have been located so that samples of groundwater can be

collected from different parts of the deposit representing the various components of the flow regime.

Two different systems are used for collection of groundwater samples. One system collects samples of water under the ambient pressure at depth inside the piezometer using a system of stainless steel pressure vessels equipped with remote-controlled valves. This system is used primarily to collect samples for the analysis of dissolved gases and of bacteria. The second system collects samples of the deep groundwater at surface by means of a stainless steel squeeze pump located at the bottom of the piezometer. This system (Figure 3A) is used to sample large volumes of groundwater combined with on-line monitoring and analysis of critical parameters. The on-line monitoring and analysis are done inside a glovebox under a controlled nitrogen atmosphere in order to prevent oxidation from exposure to air. This controlled atmosphere is very important since the groundwaters are very reducing and their oxidation would affect both the solution and colloid chemistry. The large volume samples collected with this system are used for colloid filtration which is also carried out under controlled atmosphere in a second glovebox (Figure 3B).

The measurement and analysis of critical parameters and sensitive constituents is carried out in the field. On-line measurements of temperature, conductivity, turbidity, pH, Eh and dissolved oxygen, as well as analysis of sulphide, sulphate, phosphate and ferrous-iron are carried out during sampling with the downhole pump. In addition, the collected samples are analyzed in the field for uranium, radium and radon using fluorometry, α-spectrometry and scintillometry, respectively. Filtration of the samples is carried out with a flow-through plate filtration system to concentrate particles with a size greater than 10,000 molecular weight or nominal 1 nanometre. Following filtration, particle-sizing of the colloid concentrate is carried out in the glovebox. The precautions taken to minimize atmospheric contamination during sampling and filtration are needed to prevent changes in the groundwater composition, particularly the oxidation of iron and the resulting formation of iron colloids.

5 Results and discussion

Results of the various analytical programs have been summarized in a recent paper (3) and will be briefly discussed and updated here. The following discussion will deal with the uranium mineralogy, the clay-rich halo, the groundwater composition, the colloids and the organics and microbial activity.

The main uranium minerals in the ore zone are uraninite-pitchblende and coffinite, often found as prismatic uraninite surrounded by pitchblende and interstitial coffinite. Results from an X-ray Photoelectron Spectrometry (XPS) study (10) on five ore samples from Cigar Lake indicate that the oxidation state of uranium in the minerals is equal to or lower than that in U_3O_7. Values for the ratio of U^{6+}/U^{4+} range from 0.24 to 0.57, suggesting a reducing environment in the mineralized zone. It is known from experimental work on the oxidation of UO_2 that the dissolution rate of uranium oxide does not become significant until its oxidation has proceeded beyond the U_3O_7 stage. Recent detailed X-ray Diffraction studies on the same samples analyzed by XPS (11) show the presence of α-U_3O_7. These results support the observation of a strongly reducing environment in the

water-ore interaction as seen in the groundwater compositions, and explain, at least for the present-day system, the lack of uranium dispersion.

A detailed study on the clay-rich halo surrounding the ore zone is focussed on the origin of the clay minerals, their composition and trace element content and their role in the preservation of the mineralization. The study is partly undertaken by Carleton University in Ottawa on contract to AECL. Although the clay minerals in the halo are not smectites, which are proposed for buffer material, the mainly illitic clays above and the mainly chloritic clays below the ore appear to have acted as important first barriers to dissolved radionuclides. The first few metres into the clay zone from the contact with the ore are enriched in uranium, thorium, radium, lead, lanthanides and several other trace elemnts. Part of this enrichment is due to a higher concentration of accessory minerals such as zircon, apatite and monazite. However the exponential decay of the element enrichment away from the clay-ore contact indicates that the source of the elements is the mineralization. Hence an important part of the work is on the mode of fixation of uranium and other elements in the clay-rich rock. It is important to determine whether this fixation is of primary (during ore formation) or of secondary origin and, in the latter case, what retardation process is involved. Preliminary results of selective extraction experiments (J.B.Percival, Carleton University) indicate that the amorphous ferric-iron phases in this clay contact are strongly enriched in uranium. The coprecipitation and sorption of uranium upon ferric oxihydroxides and the filtration or sorption of these ferric colloids onto the clay minerals is the most likely interpretation of these observations. Further detailed work is being carried out on the role of the iron chemistry and mineralogy in the clay contact.

Data on the groundwater composition (3) show the distinct nature of the water in different parts of the deposit. The low uranium concentrations in the groundwater correspond to the reducing environment found in this deposit as indicated by the redox chemistry of iron, sulphur and dissolved gases and the mineralogy in the ore and host rock. Recent information on groundwater from hole 139 (Figure 2B) shows that the regional groundwater flowing toward the deposit is oxidizing in nature. This implies that the deposit must have an important buffering capacity to maintain the reducing conditions, if this oxidizing water is flowing through the deposit as indicated by the hydrological information. An indication of the time scale involved in the water-rock interaction may be obtained from stable isotope data for the groundwater. The diagram in Figure 4 shows data for deuterium and oxygen-18 isotopes. There is a significant enrichment in both light isotopes as well as a clustering of values for the groundwaters from the deposit proper compared with the values for the regional meteoric water from hole 139 (point on meteoric water line). These isotope data indicate that mixing of the groundwater in the deposit with meteoric water is relatively slow because the isotopes in the deposit waters still retain a signature of fractionation under cold temperature conditions most likely during the last glaciation in this area. This evidence on both the time scale and nature of groundwater mixing is a good analog to mixing of groundwaters to be considered in a waste disposal concept.

The control of the redox conditions in the deposit involves several processes, both inorganic and organic. In addition to the above mentioned inorganic redox couples, there is evidence that other processes may be involved in maintaining a reducing environment. There is mounting evidence

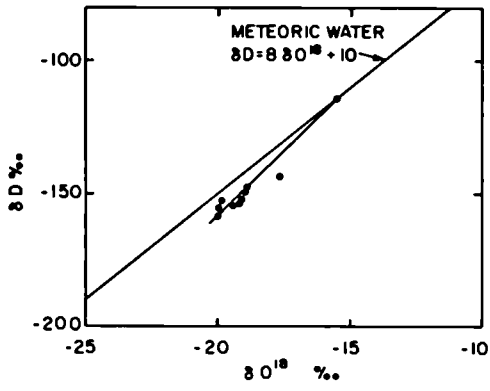

Figure 4 Plot of values of δD and $\delta^{18}O$ for groundwater sample from the Cigar Lake deposit. The point on the meteoric water line is for groundwater from hole 139.

that radiolysis of groundwater in contact with the high-grade ore may play a role in the redox chemistry (3). The evidence comes from data on the iron and sulphur redox chemistry, mineralogy and dissolved-gas composition, suggesting a complex interaction of electrochemical processes. An important parameter here is the fast reaction rate of iron oxidation relative to that of uranium oxidation, where iron acts as a scavenger for the oxidizing species produced by radiolysis. An indication of the reaction rate of iron oxidation is illustrated in Table 1.

Table I presents two sets of iron data on the same samples that were filtered through the plate filtration system under controlled atmosphere. An aliquot of the filtrate (<1 nm) was immediately analyzed for ferrous iron in the glovebox in the field. A separate aliquot of the same filtrate was acidified and later analyzed for total iron, resulting, after correction for ferrous iron, in the ferric iron value (2nd column). By comparison, using the total iron values for the filtrate (under "Pellicon" in Table I), the values for ferrous iron are higher than those reported under "Field". This indicates that ferrous iron in the filtrate oxidizes very rapidly on a time scale of minutes, assuming that the 1 nm filter separates dissolved ferrous and suspended ferric iron.

The presence of bacterial activity and the role of bacteria in the redox chemistry is being investigated by D. Champ at AECL's Chalk River Nuclear Laboratories. The association of the uranium mineralization with high concentrations of graphite in the underlying basement rocks corresponds to a high concentration of dissolved organic carbon in the waters in different parts of the deposit. Concentrations of up to 29 mg/L in the basement waters and of up to 13 mg/L in the ore zone waters provide good feedstocks for bacterial activity. The presence of sulphate-reducing bacteria has been identified in water samples collected from the ore zone and preliminary results indicate also the potential presence of methano-

Table I
IRON REDOX CHEMISTRY IN GROUNDWATER FROM CIGAR LAKE U DEPOSIT

Hole #	FIELD Fe^{2+} mg/L <1 nm	FIELD Fe^{3+} mg/L <1 nm	PELLICON Fe^{2+} mg/L <1 nm	PELLICON Fe^{3+} mg/L >1 nm
79	0.02	0.69	0.71	3.11
80	0.01	<0.01	<0.01	0.04
83	1.29	4.41	5.70	0.17
128	1.36	5.54	6.90	1.41
134	0.04	1.51	1.55	0.16
137	0.01	<0.01	<0.01	0.19
139	0.01	<0.01	<0.01	0.10
197	0.01	<0.01	<0.01	0.10
198	0.02	<0.01	<0.01	0.26
199	0.02	0.25	0.27	3.19

genic bacteria in some samples. This information shows that, in addition to potential involvement of anaerobic bacteria in controlling the redox conditions, bacteria are found and are active in the high radiation field of the uranium ore.

The concentration, composition and trace element content of colloids in the groundwaters from the deposit are being determined. Colloid concentrations in the sampled groundwaters range from 0.6 to 261 mg/L, with the majority of samples containing less than 10 mg/L. A large percentage of particles filtered from the retentate (>1 nm) is larger than 400 nm. Particles appearing in SEM micrographs are not larger than 10 microns, with the exception of some organic needle-shaped particles. Particles within the 1 to 5 micron size range are very common. The SEM and XRD results indicate a colloidal particle mineralogy consisting of clay minerals (illite, chlorite and kaolinite), Fe-Si oxides, quartz and organic particles. The exact mineralogy of the Fe-Si oxides has not been determined because they are X-ray amorphous. Filtration of groundwater in the glovebox on site indicates the presence of Fe-Si oxides in the water at depth. When groundwater samples were left exposed to the atmosphere for several hours, additional Fe-Si oxide formation was noted. The association of radionuclides with colloids is determined by comparing concentrations in the colloid enriched retentate with those in the filtrate. Results for uranium and radium are illustrated in Figure 5. Data for both uranium and thorium show that the fractions of these elements in the groundwater associated with colloidal particles vary from 5 to 100 %. The fraction of colloid-associated radium ranges from 0 to 70 %. These results indicate that an important component of radionuclide migration in groundwater under reducing conditions may occur in colloidal form depending on such physical parameters as flow rate and filtration.

6 Conclusions

Information on the Cigar Lake uranium deposit shows that, in an open water-saturated system, the large high-grade mineralization survived for

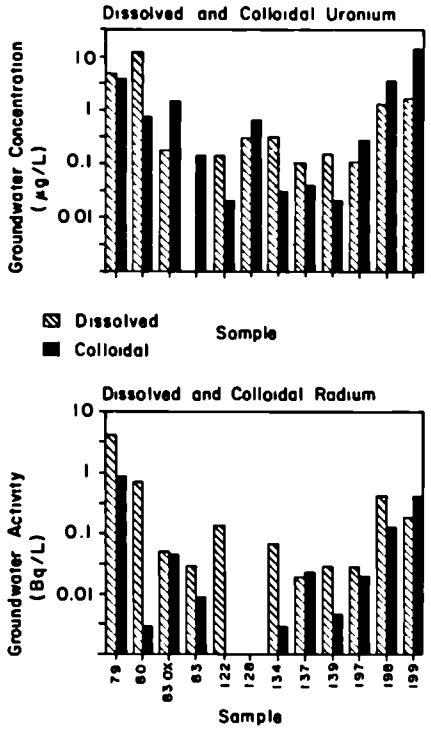

Figure 5 Diagrams showing the concentrations of uranium and radium for both the dissolved and colloidal fractions of groundwater samples.

about 1 billion years without significant secondary dispersion of the ore elements. The deposit provides an excellent opportunity to study a number of processes and systems analogous to aspects of the concept being studied in Canada for the disposal of used fuel. The absence of any surface indicators for this ore body is mainly due to the composition of each component in the water-ore-host rock system. The mobility of uranium in the ore zone, and thereby the preservation of the deposit, is controlled by the redox conditions. The deposit has an important redox buffering capacity in a dynamic system that includes bacteria, radiolysis and iron as the main components.

7 Acknowledgements

The authors like to thank the Cigar Lake Mining Corporation and Cogema Canada Ltd. for their generous support to this work.

References

1. FOUQUES, J.P., FOWLER, M., KNIPPING, H.D. and SCHIMANN, K. (1986). The Cigar Lake uranium deposit - Discovery and general characteristics. Can. Inst. Mining Bulletin, Vol. 79, pp 70-82.

2. BRUNETON, P. (1986). Geology of the Cigar Lake uranium deposit (Saskatchewan, Canada). In: Conference on economic minerals in Saskatchewan, Sask. Geol. Soc., Regina, November 17-18, 1986.

3. CRAMER, J.J. (1986). A natural analog for a fuel waste disposal vault. 2nd Int. Conf. Radioactive Waste Management, Can. Nuclear Soc., September 7-11, 1986, Proc. pp 697-702.

4. RUDZICKA, V. and LECHEMINANT, G.M. (1986). Developments in uranium geology in Canada, 1985. In: Current research, Part A. Geol. Survey Canada, Paper 86-1A, pp 531-540.

5. CRAMER, J.J. (1986). Sandstone-hosted uranium deposits in northern Saskatchewan as natural analogs to nuclear fuel waste disposal vaults. Chem. Geol., Vol. 55, pp 269-279.

6. HOEVE, J. (1984). Host rock alteration and its application as an ore guide at the Midwest Lake uranium deposit, northern Saskatchewan. Can. Inst. Mining Bulletin, Vol. 77, pp 63-72.

7. McCONNELL, D.B. and CRAMER, J.J. (1987). Simulating the movement of radium and lead away from the Cigar Lake uranium deposit. In: CEC Symposium on Natural Analogues in Radioactive Waste Disposal. Brussels, April 28-30, 1987.

8. HOEVE, J., SIBBALD, T.I.I., RAMAEKERS, P. and LEWRY, J.F. (1980). Athabasca Basin unconformity-type uranium deposits: a special class of sandstone-type deposits? In: Uranium in the Pine Creek Geosyncline. Proc. Int. Uranium Symp., Int. At. Energy Agency, Vienna, pp 575-594.

9. PAGEL, M. (1983). Datations des minéralisations uranifères liées aux discordances protérozoiques. In: Géologie et géochimie de l'uranium. CREGU (Cent. Rech. Études Géol. Uranium), Vandoeuvre-lès-Nancy, Mém., No. 1, pp 333-349.

10. SUNDER, S., CRAMER, J.J. and DOERN, F.E. (1986). XPS studies of uranium minerals. 69th Can. Chem. Conf., Saskatoon, Abstract p 81.

11. SUNDER, S., CRAMER, J.J., TAYLOR, P. and DOERN, F.E. (in preparation). XPS and XRD study of uranium ore minerals from the Cigar Lake deposit in northern Saskatchewan.

SANDSTONE URANIUM DEPOSITS : ANALOGUES FOR SURF DISPOSAL IN SOME SEDIMENTARY ROCKS

D.G. BROOKINS
Department of Geology
University of New Mexico
Albuquerque, New Mexico 87131

Summary

Sandstone uranium deposits are well suited as analogs for SURF. These deposits typically occur as tabular or lensoid masses of uraniferous sandstone, commonly where the argillaceous mineral and organic content is high. Primary minerals consist of pitchblende and/or coffinite, with possibly some urano-organic phases as well. The ore is usually associated with authigenic ferromagnesian clay minerals, such as chlorite and/or authigenic illite and/or mixed layer smectite-illite; and with pyrite $\pm$ jordisite $\pm$ seleniferous species $\pm$ calcite. Organic matter is usually associated with the ore. The clay minerals in the ore zones are commonly vanadiferous.

The genesis of the sandstone uranium deposits is now fairly well understood and allows semi-quantitative estimates to be placed on behavior of analog-elements for many constituents of SURF (or HLW). Prior to mineralization, oxidized species of U, V, Se, Mo, As are carried together as oxyanions; these species precipitate in a restricted range of Eh-pH when reducing conditions are met. Concomitant with removal of these species, due to formation of reduced, insoluble species, several other elements of interest are concentrated in the ore zones as well. Chalcophile elements, such as Cu, Co, Mn, Zn, Cd, Sb, and others are fixed in authigenic sulfide phases, and the alkalis Rb, K, and Cs are fixed in the authigenic illite and illitic mixed layer clays. The alkaline earth elements Sr and Ba are commonly fixed in sulfate-rich rock. The rare earth elements (REE) are incorporated into authigenic clay minerals or into oxy-hydroxide phases.

1. Introduction

The ore, accessory and gangue minerals of sandstone uranium deposits contain most of the elements found in spent unreprocessed uranium fuel (SURF). The actinides present include U and some Th, and even small amounts of Pu have been calculated to be present. (1) Further, a good data base exists for Rb behavior in these deposits. Analog elements for SURF fission products include Rb, Sr, Zr, Mo, Nb, Cd, Ag, Y, Sb, Cs, Ba, and the REE (La-Lu). Some data also exist for Br and I. Data are few for the valley elements Rh, Pd, Ru, Cd, Sn, and Te, but a combined Eh-pH diagram: sulfide phase study allows assessment of the mobility of these elements to be made as well. Further, information concerning Tc can be obtained from use of Mo or Re as analog and from theoretical considerations. (2,3)

The fission product and actinide analog elements in sandstone uranium deposits are distributed among several different phases, whereas these same elements are contained within the UO_2 of the SURF. In a sense, then, the

uranium deposit is like a spent fuel rod in which the elements of interest have already migrated to the surface of the rod. Further, since (as will be shown later) the accessory and gangue uranium deposit minerals are in most instances as susceptible to alteration and leaching as the ore minerals, then the uranium deposit assemblage is a worst case scenario for the SURF. Stated another way, should the analog elements of interest be retained in the uranium ore, then the same fission and actinide elements of SURF should be even more firmly fixed in a similar natural setting.

2.1 Formation of Sandstone Uranium Deposits

The processes by which sandstone uranium deposits form are fairly well known. (4,5) In brief, solutions containing dissolved oxyions of uranium, along with oxyions of V, Se, Mo, and As, penetrate into permeable rocks such as sandstone and, when chemically reducing conditions are encountered, reduction of the high valence U(VI), Mo(VI), V(V), Se(VI), As(V) in oxyions occurs with resultant precipitation of U(IV), Mo(IV), Se(0,-II), V(III,IV) and AS(III) species. The zone of reduction is marked in sandstone by transition from Fe(III) oxy-hydroxide-bearing, organic carbon-free, sulfate-carbonate cemented sandstone of the oxidized zone to pyritiferous, organic carbon-rich, calcite cemented sandstone of the reduced zone.

Certain clay mineral assemblages are also commonly characteristic of the sandstone uranium deposits. In the oxidized rocks, kaolinite is commonly the dominant phase, with some detrital chlorite and re-worked smectites. In the reduced rocks, smectites, illites, authigenic chlorite, and mixed layer varieties are common. In the mineralized rocks, rosette chlorite with a high vanadium content is typical, although vanadiferous illite or smectite sometimes occur instead of chlorite. (5)

The uranium mineralization usually occurs as cryptocrystalline U(IV) minerals such as coffinite ($USiO_4$) and/or pitchblende, commonly in close association with organic carbonaceous matter (OCM). While urano-organic phases have often been proposed as responsible for mineralization, it is more likely that the coffinite or pitchblende are admixed with the OCM. (4) The OCM-rich parts of the sandstone occur with increased clay mineral content of the sandstones, and both act together as an effective trapping site for penetrating uraniferous solutions.

The V, Mo, Se, and As are removed in large part in U-poor minerals. The V is commonly incorporated into vanadiferous chlorite (or other ferromagnesian clay minerals) and less often into V-oxides. The Mo is removed in jordisite (MoS_2), in Mo-rich pyrite, or in other sulfides. Most selenium is removed in ferroselite ($FeSe_2$) or as seleniferous pyrite, but native selenium (both primary and secondary) is also fairly common. Most As is removed in sulfide minerals.

Thus although the elements U, V, Mo, Se, and As are carried in solution as a group, they are precipitated largely into different phases, all of which are commonly intergrown. A typical uranium ore in sandstone may broadly be described as a mixture of coffinite or pitchblende with vanadiferous clay mineral(s) plus pyrite $\pm$ jordisite $\pm$ selenium species $\pm$ calcite, all with OCM, and the entire mixture surrounded by somewhat argillaceous sandstone.

2.2 Sandstone Uranium Deposits in the United States

In the United States most sandstone U deposits are found in the San Juan Basin of New Mexico-Colorado-Utah, the sedimentary basins of Wyoming, and the basins in the Gulf Coastal area of Texas. The writer has conducted extensive research on the uranium deposits of the San Juan Basin, and especially in the well known Grants Mineral Belt (GMB). The GMB runs east-southeast from near Gallup, New Mexico to near Laguna, New Mexico,

and most ore is found in the Late Jurassic Morrison Formation sandstones (Westwater Canyon and Jackpile sandstones). Some ore is thought to be Late Jurassic in age (Ambrosia Lake district) while some is mid-Cretaceous (?) (Laguna district), and some uranium has been remobilized very recently (10 Ma). (4)

The deposits of the GMB have accounted for over 60 percent of total U production in the United States, and may contain 20-25 percent of total world reserves. Extensive underground and open pit mining of the deposits have taken place over the last thirty years, and the writer was able to visit many active (and some inactive) mines for sampling of ore, near ore and barren rock removed from ore zones. Most of this sampling took place between 1974 and 1982, but continues to the present time.

3.1 Behavior of Specific Elements in Grants Mineral Belt Ores

Extensive data for Grants Mineral Belt sandstone uranium ores have been compiled by the writer and his students. (4,6)(7,8,9) For several hundred samples each of barren sandstone (i.e., non-uraniferous), near-ore sandstone (i.e., uraniferous but below ore grade) and ore sandstone (i.e., on most cases with total U_3O_8 above 0.05%); large samples were taken so that clay mineral could be separated from them. The data reported (see references above) are, in most instances, for whole rock (i.e., aliquot of untreated sandstone) and minus-two micron aliquot (i.e., clay mineral rich). Data were obtained by instrumental neutron activation analysis for thirty-four elements, and U and Th contents were obtained by delayed neutron activation analysis. Stable isotope studies and Rb-Sr geochronologic studies were carried out on numerous -2 (size fraction less than two microns). (10) Many of the chemical data have been discussed previously, but not in the context of application to radwaste disposal studies. The elements discussed below are chosen because of a good data base, except where indicated.

3.2 Alkali and Alkaline Earth Elements: Rb, Sr, Cs, Ba

Most Rb is contained in clay minerals, especially the illites and mixed layer illite-smectite (or chlorite) species. (5) From the geochronologic work by Lee and Lee and Brookins, (8,10) it is shown that the clay minerals formed penecontemporaneously with the ore at about 140 Ma (millions of years before the present) have retained their isotopic and chemical integrity since that time for primary ores in the Ambrosia Lake sub-district, very early (i.e., near 140 Ma) ore was mobilized due to extreme mid-Cretaceous tectonism, and redeposited at about 110-120 Ma, with the mobilization thought to be on the order of no more than some tens of meters. The Rb-Sr studies also document the retention of Sr in these same clay minerals.

Strontium is not only contained in the clay minerals, but is also a common constituent of gangue calcite in reduced rocks, and of anhydrite or gypsum in oxidized rocks. While these minerals cannot be dated by conventional means, the calcite contains stable isotopic signatures suggesting formation with U mineralization (i.e., near 140 Ma). (5) No evidence for Sr remobilization is noted.

Data for Cs are not as abundant as for Rb, but K/Cs and Rb/Cs ratios fall well within the normal range for argillaceous rocks for all samples studied. (4) There is some enrichment of Cs relative to K and Rb in authigenic clay minerals, which is consistent with theoretical considerations. (11) Since the Rb-Cs ratios for samples which show isochemical Rb-Sr geochronologic behavior vary only within narrow limits, no mobilization of Cs is likely.

The Ba behavior in the samples is moderately well known. The Ba is contained in accessory barite (and locally, other sulfates) in oxidized rocks and in calcite and partly in clay minerals in the ore zones. Some of the barite is rich in Ra and referred to as radiobarite. It is speculated that as Ba is released from detrital phases (mainly plagioclase) during alteration, it is incorporated into sulfate or carbonate phases. Since Ba is less mobile than Sr under most crustal conditions, then the fact that the Rb-Sr studies argue for Sr retention can be used indirectly to argue for Ba retention as well.

3.3 Y, Zr, Nb, Mo, Tc, Ru, Rh, Pd, Cd, Ag, In, Sb, Sn, Te

These elements are discussed together as a matter of convenience. Data are abundant for Y, Zr, Nb, Mo, and Sb only.

The Y is largely contained in detrital phases, although some local Y accumulations occur when phases like magnetite are destroyed by alteration, in which case secondary oxide coating contain the Y. No evidence for Y migration is noted, consistent with findings elsewhere. (1,4)

The Zr and Nb are also largely contained in detrital phases, and no abnormal abundance of these elements are noted.

Data for Mo are abundant; see summary in Brookins. (4) In ore zones Mo is fixed in gangue minerals (see discussion elsewhere in this report) such as jordisite or pyrite, or when these minerals are subjected to mildly oxidizing waters, as ilsemannite (Mo_3O_8). The behavior of Mo is readily explainable in terms of Eh-pH diagrams. (12) Mo can be readily mobile under strongly oxidizing conditions. Under reducing to mildly oxidizing conditions, and in the pH range from about 6-9, sulfide-phases may be destroyed but the Mo incorporated into a new oxide (ilsemannite). U/Mo ratios in the sandstone deposits can be quite variable, due in part to the fact that both elements can be mobile under different Eh-pH conditions. However, most data suggest that Mo is less mobile than U in the deposits. (1,4)

Data for Ru and Tc are not available. Ru is present in such low crustal amounts as to not be readily determinable by INAA and Tc consists only of radioactive isotopes. Theoretical considerations argue that both Ru and Tc should be less mobile than Mo and U. (1,2,12) Consequently, since the migration of Mo and U is limited, Ru and Tc should be even more highly retained in the sandstone ores.

The Eh-pH diagram for Rh shows that the greater part of the stability field of water is covered by fields for solids (Rh, Rh_2O_3), (12) hence no migration is likely. This is consistent with studies of Oklo. (1)

There are limited data for Cd and Ag for sandstone U deposits, but no Pd data. Theoretical considerations, Eh-pH diagrams mainly, argue for either complete retention of Pd and Ag and some limited migration of Cd. (See discussion in 1, 2, and 12.) The Pd, Cd and Ag are contained in sulfide phases. When the sulfides are altered, Pd and Ag will remain immobile as native Pd and Ag while Cd may either be incorporated into new calcite (Ca, Cd) CO_3 or an oxhydroxide phase in most of the pH range 6-9, whereas at lower pH it will be quite mobile. At higher temperatures, Cd mobility will increase, however. (1,2)

Data for Sb show this element to be fixed in sulfides in reduced rocks and in oxyhydroxide phases in near-ore oxidized rocks. The Eh-pH diagram shows a field of $Sb(OH)_3$ occupying that part of the central pH range over the sulfide field. (3) Sb haloes in oxidized rocks can also be occasionally used for localizing remobilized U. (4) Sb does not appear to be mobile in the environment of the sandstone U deposits.

Data for Sn and Te are few. Theoretical considerations again argue for retention of both elements in the environment of the sandstone U deposits. (See discussion in 1, 2, 12)

3.4 Iodine

Data are virtually non-existent for I and other halides, although there are some Cl data from fluid inclusion work. (4) It is thus not possible to comment on I mobility or retention, although elsewhere the author has commented on the possibility of I fixation on sulfide phases. (1)

3.5 The Rare Earth Elements (REE)

The data base for the REE is extensive. (4,9) There are some data which suggest mobilization of the REE with U during formation of the sandstone U deposits, (13) but no data to suggest mobilization after the ore are formed. The REE patterns are typical of argillaceous rocks in general, although the total REE in the ore zone clay minerals correlate positively with both Th and U. A slight negative Eu anomaly is present in all cases. The REE are fixed in clay minerals, but they are not mobile under natural conditions in the Grants Mineral Belt.

3.6 The Actinides

Data are available only for U and Th for the Grants samples. The Th is fixed in detrital phases for the most part, although some is present in ore zone oxyhydroxide phases, presumably derived by release of alteration of detrital phases. The U/Th ratios, of course, in the deposits are extremely high since U is strongly mobile under surface oxidizing conditions and Th is extremely insoluble over all Eh-pH space above pH of 2 or so. There are abundant U data, most of which suggest limited mobility of U under reducing conditions. The author suggests that U can only be successfully remobilized under dynamic, highly oxidizing conditions, at least in the pH range of 6-9 or so. (4) Most U is fixed in the U(IV)-bearing species coffinite and pitchblende.

Data for the transuranics are, of course, non-existent, although attempts have been made to estimate the amounts of naturally occuring Pu and Np in some U ores. (1) From a theoretical viewpoint, Pu, Np, and Am should be less mobile than U, hence if U mobility is restricted to near-ore environments, then the mobility of Pu, Np and Am should be even less.

3.7 Actinide Daughters: 234-U, Ra, Pb

There is commonly a disequilibrium between 234-U and 238-U noted in sandstone ores, resulting from the fact that 234-Pa formed from 238-U is present as a hexavalent species, and beta decay to 234-U results in U(VI) formation. Since U(VI) is much more mobile than U(IV), then there is local migration of 234-U from some samples, adjoining samples possess excess 234-U; hence the overall migration is extremely local.

Radium is a large ion (1.4 A) with charge of +2, and, as such, is highly metastable in either coffinite or pitchblende. Consequently, Ra is lost from the structures of these minerals, but usually fixed in the gangue and accessory minerals adjacent to the ore. Ra is taken into newly formed sulfates (e.g., radiobarite) or carbonates, and some is fixed on clay minerals. (1) The argument is again used that Ra should be less mobile than either Sr and Ba, and where, for example, Rb-Sr studies show Sr retention, then Ra, too, should be retained.

Lead is common in sandstone U deposits, with most found in pyrite or in small amounts of galena. Radiogenic lead formed in U minerals is easily lost from these minerals, and found in sulfates, carbonates, and some clay minerals associated with the ores. Data do not support widespread migration of Pb under the natural conditions in the U deposits. (1)

PARLEMENT EUROPÉEN BIBLIOTHÈQUE

4. Discussion

The distribution of elements in SURF is moderately well known. It is probable that many of the fission products, actinides and actinide daughters will be present as the simple ions with common valences found in natural media. Diffusion of these elements in the SURF is difficult to assess. The radiation damage to the UO_2 will cause structural damage which will promote diffusion of those elements already incompatible in the UO_2 structure (i.e., Ra, Pb, Cs, Ba, etc.). Yet despite this difference, the total alpha radiation dose in the natural uranium deposit may be as high if not higher than that in SURF; (1) certainly the coffinite and/or pitchblende have often been extensively damaged by natural radiation. In the case of the naturally occurring U deposits, many of the fission product analog elements are contained in minerals intimately mixed with the U minerals. Some of these minerals are more resistant to alteration (clay minerals) than others (sulfides) under mildly oxidizing conditions, and this makes them useful to comment on possibly SURF behavior in the rocks.

The earliest U deposits of the Grants Mineral Belt are Late Jurassic, and ores of the Ambrosia Lake and Smith Lake districts have not been, for the most part, remobilized since. In the Laguna district, however, uplift caused arching, fracturing, and opening of conduits into the mineralized rocks. Oxidizing solutions invaded the mineralized rocks, causing destruction and remobilization of the U ores. This event probably took place in the mid-Cretaceous as evidenced by Rb-Sr dates on the newly formed clay minerals formed with the reprecipitated U ores. These ores now possess high U/V ratios since the first formed V minerals were clay minerals which, while subjected to oxidation, retained the V in their structure; i.e., V(III, IV) was oxidized to V(V) which is still compatible in the lattice. In addition, the ores also possess high U/Se since some of the first formed Se was removed as native Se (probably due to oxidations of Se(-II) from ferroselite or seleniferous pyrite). Even some Mo was segregated from U during this major event due to U in solution while some Mo was removed as ilsemannite. Evidence for this event is seen in part in barren sandstones near the present Laguna district ores with high V and locally high Se, Mo contents. (4) The destruction of the Late Jurassic ores may have taken place over five to ten million years, (4) but interestingly, the remobilization is thought to have been on the order of tens to perhaps low hundreds of meters from where the ore was first formed. This is due in turn to the fact that the penetrating oxidizing solutions were favored along fractures in otherwise chemically reducing rocks. This can be used to argue that, in the case of SURF, while nearfield events will likely be oxidizing, at depths of several hundred meters the overall medium will probably be a chemically reducing environment. In the case of the Laguna ores, the haloes of several trace elements useful elsewhere for prospecting guides (e.g., Sb, Mn, Cu, Ta, REE) are not present around the newly formed ores (mid-Cretaceous) since they were largely removed and retained where the earliest, Late Jurassic ores formed. This is also of interest for SURF considerations as it indicates that one suite of elements, Y, REE, Zr, Nb, Sb, (and, in theory, Ru, Pd, Rh, Te, Sn) would be essentially fixed in the near field or rock immediately surrounding it. Further, Mo data argue for possibly less migration than U, also suggesting limited Tc mobility under identical conditions. The Ba present in the Laguna ores is more difficult to assess due to locally high background values, (4) yet it apparently was fixed as barite in the environment of the earliest ores. Similarly, the Sr content of the barren rocks at the site of the first ore is higher than that at the present site, (4) yet the radiogenic Sr of the earliest clay minerals has not been perturbed. (1,4) Limited Cs data argue for near

constant Rb/Cs in the two sites as well.

Elsewhere in the Grants Mineral Belt there exists evidence for the mid-Cretaceous event that affected the Laguna ores, and also evidence for Tertiary disturbances. (9) In the last case, local uplifting at about 40-50 Ma also allowed oxidizing solutions to penetrate the rocks causing remobilization of the U ores and a new generation of 40-50 Ma ores to form. (1,9) Again, the new ore is somewhat depleted in V, Mo and Se and more depleted in the REE, Sb, etc., relative to the Late Jurassic ores.

The data base for the GMB is adequate to investigate most of the fission product, actinide and actinide daughter elements common to SURF, and the reader is referred to Brookins, Riese, Lee, and Della Valle for details. (4, 6; 7, 8, 9) The opportunity for quantitative statements concerning behavior of the elements of interest, based on the study of these U deposits, exists, however.

The probable locations of analog elements in the GMB ores are given in Table I. A summary of the retention or migration potential of radionuclides in the GMB ores is given in Table II.

5. Conclusions

The use of sandstone U deposits as anslog for SURG disposal leades to the following conclusions:

1. The formation of the deposits can be used to comment on the behavior of fissiogenic and actinide elements of SURF.
2. Some of the key elements of concern, Sr, Cs, Sb, U can be stated to be relatively immobile in argillaceous sandstone.
3. This in turn suggests that argillaceous rocks in general, whether as main repository medium or as backfill, will be effective as a radionuclide retainer in the multibarrier system.
4. While no data are possible for Tc, and only rare data available for Ru, a combination of data for Mo and Mn, with theoretical Eh-pH diagrams, strongly suggests that Tc and Ru are quite immobile in the sandstone U deposit environment.
5. There exists a widespread occurrence of sandstone U deposits, including some cut by dikes, etc., all of which can be used for future analog purposes.

References Cited

(1) Brookins, D.G., 1984, Geochemical Aspects of Radioactive Waste Disposal: Springer-Verlag, New York, 345 p.

(2) Brookins, D.G., 1983, Migration and retention of elements at the Oklo Natural Reactor: Environ. Geol. 4, p. 201-208.

(3) Brookins, D.G., 1986, Geochemical behavior of antimony, arsenic, cadmium and thallium: Eh-pH diagrams for 25°C, 1 bar pressure: Chem. Geol., 54, p. 271-278.

(4) Brookins, D.G., 1979, Uranium deposits of the Grants, New Mexico Mineral Belt (II): U.S. Dept. Energy Rept. BFEC 76-029E, 411 p.

(5) Brookins, D.G., 1982, Geochemistry of clay minerals for ursnium exploration in the Grants Mineral Belt, New Mexico: Mineral. Deposita 17, p. 37-53.

(6) Brookins, D.G., 1976, Uranium deposits of the Grants, New Mexico Mineral Belt, U.S. Energy & Research Development Administration: Final Report GJO-1636-1, 120 p.

(7) Riese, W.C., 1980, The Mount Taylor uranium deposit, San Mateo, New Mexico: Unpub. Ph.D. Diss., University of New Mexico, 648 p.

(8) Lee, M.J., 1976, Geochemistry of the sedimentary uranium deposits of the Grants Mineral Belt, southern San Juan Basin, New Mexico: Unpub. Ph.D. Diss., University of New Mexico, 241 p.

(9) Della Valle, R.S., 1981, Geochemical studies of the Grants Mineral Belt, New Mexico: Unpub. Ph.D. Diss., University of New Mexico, 648p.
(10) Lee, M.J., and Brookins, D.G., 1978, Rubidium-strontium minimum ages of sedimentation, uranium mineralization, and provenance, Morrison Formation (Upper Jurassic), Grants Mineral Belt, New Mexico: Amer. Assoc. Petrol. Geol. Bull. 62, No. 9, p. 1673-1683.
(11) Kharaka, Y., and Berry, R.A.F., 1973, Simultaneous flow of water and solutes through geological membranes - I. Experimental investigation: Geochim. Cosmochim. Acta 37, p. 2577-2603.
(12) Brookins, D.G., 1978, Eh-pH diagrams for elements from Z = 40 to Z = 52: Application to the Oklo natural reactor: Chem. Geol., 23, p. 324-342.
(13) Della Valle, R.S., and Brookins, D.G., 1983, Geochemical studies of the Grants Mineral Belt, New Mexico: in The Significance of Trace Elements in Solving Petrogenetic Problems and Controversies: (S.S. Augustithis, Ed.), Theophrastus Pub., Athens, p. 793-818.

Table I Location of Analog Elements in Grants Mineral Belt Ores*

Elements	Host Mineral(s)
Rb, Cs	Clay minerals: illite, chorite, smectite
Sr	Clay minerals (*Sr), carbonates, sulfates
Ba	Barite, calcite
Nb, Zr, Th	In resistate minerals mainly
Y, REE	Clay minerals (ore zones), oxyhydroxide phases, resistates
Mo, Tc, Ru	Sulfides (mainly pyrite)
Rh, Pd, Ag, Cd, In, Sb, Sn, Te	Sulfides (mainly pyrite)
I	Unknown

*Based on data from Brookins (1982).

Table II Retention or Migration of Grants Mineral Belt Analog Elements*

Element	Retention	Migration	Comment (on migration)
Rb	XXX		Many data
Sr	XXX		Many data
Zr	XXX		Several data
Nb	XXX		Several data
Y	XXX		Many data
Mo	XX	XX	Limited; local oxidation
Tc	XX ?		Theoretical basis
Ru	XX		Theoretical basis
Rh	XX		Theoretical basis
Pd	XX		Theoretical basis
Ag	XX		Theoretical basis; some data
Cd	X	XX	Theoretical basis
In	XX		Theoretical basis
Sn	XX		Theoretical basis
Sb	XXX	X	Many data; minor migration
Te	XX		Theoretical basis
I		XX ?	Speculation
Cs	XXX		Several data
Ba	XXX		Many data
REE	XXX		Many data
U	XXX	X	Many data; limited migration
Th	XXX		Several data
Np,Pu,Am	XX ?		Theoretical basis
Pb	XX		Several data
Ra	XX	X	Local migration only

*Based on data from Brookins (1979) and Della Valle (1981), and theoretical Eh-pH, activity, and other diagrams (See Brookins, 1979; 1982; 1984; 1986).

ALLIGATOR RIVERS ANALOGUE PROJECT

REVIEW OF RESEARCH AND ITS IMPLICATIONS FOR MODEL VALIDATION

P Duerden, C Golian, C J Hardy, T Nightingale and T Payne
Australian Atomic Energy Commission

Summary

A comprehensive study of the uranium ore bodies in the Alligator Rivers Region of the Northern Territory of Australia has been carried out during the past six years. The principal aims of the project have been

(a) to collect field data from several uranium deposits, particularly the secondary mineralization dispersion fan at Koongarra, to enable radionuclide transport model codes to be developed and evaluated; and

(b) to identify and quantify processes which occur on both short and geological timescales and which may be significant in the transport or retardation of radionuclides in the geosphere - examples are the behaviour of colloids, time-dependent adsorption and crystallization, and matrix diffusion.

This paper presents some early conclusions from the overall program, provides details of the more recent work and recommends topics for further study.

1.1 Introduction

Analogue studies in the Alligator Rivers region of the Northern Territory of Australia commenced in 1981. The progress of the work was reported at the 1st and 2nd Natural Analogue Working Group Meetings (1,2) and detailed descriptions of the work have been included in Annual Reports to the United States Nuclear Regulatory Commission (USNRC) (3,4,5), which has been the principal sponsor of the project.

The work that has been carried out can be divided into four broad categories:

- radionuclide distribution in rock samples and rock fractures,
- the role of groundwater and colloids in radionuclide transport,
- the production and dispersion of fission products and transuranics, and
- development of modelling codes and evaluation of the Koongarra site for modelling studies.

A number of papers included in the proceedings of this conference describe particular research tasks in detail. In this paper, an outline is given of the total program, recent progress is discussed, conclusions presented and topics for further study are recommended.

In addition to the involvement of Australian Atomic Energy Commission (AAEC) staff, the project has involved collaborators from numerous organisations, within and outside Australia, including the Universities of Sydney and New England, the Commonwealth Scientific and Industrial Research Organisation (CSIRO), the Water Resources Division of the Northern Territory Department of Mines and Energy, Los Alamos National Laboratory (LANL), the Universities of Arizona and Rochester, the United Kingdom Atomic Energy Research Establishment (UKAERE) Harwell, and the Japan Atomic Energy Research Institute (JAERI). Additional financial support for collaborative research has been provided by the United Kingdom Department of the Environment (UKDOE) and JAERI.

2.1 The Alligator Rivers Region Ore Bodies

Although the four major uranium deposits in the Alligator Rivers Province of the Pine Creek Geosyncline, namely Jabiluka, Ranger, Koongarra and Nabarlek, have been studied in the investigation, the present studies are concerned primarily with the Koongarra system.

The primary mineralization in the Koongarra deposit contains uraninite veins within a zone of steeply-dipping sheared quartz-chlorite schists of the lower member of the Cahill Formation, which is adjacent to a steeply-dipping reverse fault that brings the schists into contact with the Kombolgie sandstone (6,7). In the No. 1 ore body which is the subject of this investigation, secondary mineralization is present in the weathered schists almost from the surface down to the base of weathering at a depth of 25 m to 30 m. The secondary mineralization in the weathered schists forms a tongue-like fan of ore grade material extending down-slope for about 80 m.

The groundwater hydrology in the Koongarra area has been interpreted by Snelling (7) to recharge along a major fault line and flow in a generally southerly direction away from the escarpment.

Core from 71 drill holes through the ore body was surveyed during the uranium exploration program. In addition, there are many vertical drill holes available for water sampling, approximately 40 of which are in the zone of the proposed pit area. The drill core material is stored at the site and is available for examination, and extensive mineralogical, hydrological and geochemical information has been made available by Denison Australia Pty Ltd.

3.1 Radionuclide Distribution in Rock Samples and Fractures

The main objective of the considerable work carried out during the past six years at the four deposits was to measure the distribution of uranium and thorium series nuclides in the region of the uranium ore bodies, to study the role of iron minerals in the transport of radionuclides, and to study other processes which affect the long-term uptake of uranium and thorium series nuclides by clay minerals in the oxidized zones.

The studies were broad ranging and included such aspects as the development of selective phase separation techniques, X-ray diffraction (XRD) measurements to identify the separated mineral phases, adsorption experiments on crushed ore samples, an evaluation of the rock α-recoil and the distribution of uranium series nuclides and associated elements in the vicinity of fractures. This has provided an extensive radionuclide data base for the ore bodies.

Much of this research has been described elsewhere (3,4,5), so only a summary is given below:

(a) Based upon the systematic variations $^{230}Th/^{234}U$ activity ratios (ARs) and mineralogical descriptions, the upper sequences of the Ranger No. 1,

Jabiluka No. 1 and Nabarlek ore bodies were classified into four zones. This model was then used to calculate leaching/deposition rates and the rate of advance of the weathering front.

(b) A detailed study of drill core $^{234}U/^{238}U$ and $^{230}Th/^{234}U$ ARs in sections through the Koongarra ore body has been made (Figure 1A). An example of this work is shown in Figure 1B. Interpretation of these data (see Section 6) has identified regions of depletion and deposition within the secondary mineralization and indicated that ^{234}U migrates more slowly than ^{238}U in the Koongarra system.

(c) Selective extraction techniques were developed and used to selectively dissolve identifiable phases within the ore. Three phases were identified as significant in a weathered sample from Ranger core samples: (1) amorphous minerals of Fe, Al, Si and secondary U minerals, and ferrihydrite, (2) crystalline iron minerals, and (3) clay/quartz resistate phases of iron oxides. Distribution measurements of uranium and thorium in the three phases showed that these were concentrated principally in the iron oxide phases, even though Fe comprises only between 1% and 4% of the weathered ore. High gradient magnetic separation was also used to concentrate iron oxides in clay fractions of Nabarlek soil profiles (5). This work suggested that uranium and thorium in the first phase were not primarily associated with ferrihydrate but could originate from aluminium oxides allophane-imogolite or specifically surface adsorbed species. The uranium and thorium in the second phase were however shown to be associated with goethite and hematite.

(d) Laboratory studies of the distribution of uranium between a synthetic groundwater and mineral surfaces have been carried out. An aqueous phase containing ^{236}U was equilibrated with crushed ore samples from the Ranger and Koongarra ore bodies, and the amounts of ^{236}U adsorbed from the groundwater by the solid for PHs in the range 4 to 8.5 were determined. Figure 2 shows the results for the Ranger sample with uranium sorption reaching a maximum at pH 6 to 8 (the maximum distribution ratio (Rd) of 15,000 mL/g being found at pH 6.7). The amount of accessible natural uranium in the samples was then determined by a sequential extraction procedure. The $^{238}U/^{236}U$ ratio of the initial extracted phases was the same as the isotope ratio in the synthetic groundwater which suggests that this 'accessible' uranium was exchangeable with uranium in solution over the timescale of the experiment. The accessible fraction was found to comprise of the urania associated with amorphous mineral phases of the ore samples.

(e) The effect of α-recoil and displacement of daughter nuclei was tested by a laboratory experiment where ^{228}Th and ^{226}Ra were added to suspensions of kaolinite, illite and montmorillonite (sodium form). Radium-224 was formed by decay of ^{228}Th on the clay and the proportion of ^{224}Ra to ^{226}Ra was found to increase as the surface was repeatedly etched away by progressively harsher reagents. This was interpreted to indicate that ^{224}Ra was emplaced deep into the minerals by α-recoil, whereas the ^{226}Ra could only adsorb and then diffuse into the surface layers.

(f) The distribution of uranium series nuclides in the vicinity of fractures in unweathered rock has been measured so that possible diffusion mechanisms into the bulk rock via microscopic fissures can be assessed. An example of this is shown in Figure 3. The Jabiluka sample is predominantly quartz-chlorite schist with the fracture-filling material being mainly dolomite. Powdery material was scraped from the fracture surface, then seven 2.5 mm wide sections were sawn off parallel to the fracture. The samples were analysed for ^{238}U, ^{234}U, ^{230}Th and ^{226}Ra, lead isotopes and the isotopes of several other elements. Although the $^{234}U/^{238}U$ AR in the

fracture was close to unity, it fell to an unusually low value of 0.63 before rising to marginally above unity in the innermost section. Leaching of the fracture sections with a mild extraction reagent removed a uranium fraction which was markedly enriched in ^{234}U relative to the bulk sample; this suggests that ^{234}U is more mobile than ^{238}U in the rock.

(g) The microdistribution of uranium and other associated elements in the vicinity of fractures is also being studied. Thin sections of Koongarra drill core, which includes both unweathered and weathered material, have been prepared. The sections will be studied with an extensive range of techniques including electron microscopy and proton induced X-ray and gamma-ray emission (PIXE/PIGME) analysis. A facility is available which provides a 50 μm diameter collimated proton beam and allows for X-Y movement so that a 25 x 50 mm area of the target can be analysed. Element concentrations for a large suite of major and trace elements can be measured by the PIXE-PIGME technique. It is intended that a map of element distributions will be correlated with the sample mineralogy and with fission track and α-recoil track analyses of the uranium and uranium series nuclide distributions in the thin core sections.

4.1 The Role of Groundwater and Colloids in Radionuclide Transport

The potential importance of colloids in the groundwater transport of such radionuclides as Th and Pu was identified in the early stages of work in the Alligator Rivers region. If colloidal transport is shown to be significant, one of the implications would be that particular attention needs to be given to modelling the transfer of nuclides between groundwater, colloid and rock.

Four factors which are believed to be important in the formation and transport of colloids have been selected for investigation:

(a) The proportions of uranium and thorium series nuclides associated with the colloids as a function of particle size.
(b) The relative rate of transport of 'dissolved' and 'colloidal' radionuclides.
(c) The state of equilibrium between solute and colloidal radionuclides.
(d) The conditions that promote or enhance transport of radionuclides by colloids.

Techniques have been developed to concentrate the colloid fraction of groundwater samples so that the colloid can be characterized and the fraction of uranium and thorium series radionuclides on the colloid measured.

Previous field sampling programs were undertaken for radionuclide and element concentration measurements only. The most recent field work, described in detail by Ivanovich et al. in these Proceedings and carried out in an AAEC/UKAERE Harwell collaborative project funded by the UKDOE, was planned to extend this work by fractionating the colloidal particles into specified size groups and then preserving them unchanged for subsequent laboratory examinations.

Investigations included particle size analysis by photon correlation spectroscopy and transmission electronmicroscopy and associated energy dispersive spectroscopy (EDS) and electron energy loss spectrometry (EELS) analysis as well as radionuclide, element composition, cation, anion and total organic carbon analyses.

5.1 The Production and Transport of Fission Products and Tranuranics
5.2 Iodine-129

Although natural levels of ^{129}I are extremely low, they are of sufficient magnitude within a uranium ore body for their production and

dispersion to be studied. A major study has been under-way on ^{129}I in the Alligator Rivers analogue project for the last three years (J Fabryka-Martin, these Proceedings). During this time, sampling and iodine extraction procedures have been developed, and ^{129}I production has been modelled. Samples were collected from the Ranger and Koongarra ore bodies and $^{129}I/I$ ratios were measured on the tandem accelerator mass spectrometry facility at the University of Rochester. Results on rock samples were compared with calculated ^{129}I production and the mobilization of the ^{129}I under groundwater flow was studied by measuring ^{129}I in groundwater samples. Their are a number of possible sources of error in the ^{129}I production model such as the in situ neutron fluence and measurements of the in-ground neutron flux and fission rate are now under way.

In Figure 4, preliminary measurements of ^{129}I in a suite of ore samples are shown as a function of uranium content, where they can be related to the predicted values with different rates of loss. Samples from the top of the Koongarra primary ore body at the base of weathering are considerably depleted in ^{129}I compared to the model prediction, whereas measurements within the primary ore are in agreement.

The results indicate that ^{129}I is preferentially leached from the ore relative to U during weathering of the primary ore body. Down-gradient of the deposit, ^{129}I is scavenged from solution by sorption onto clays or Fe oxides, as evidenced by the enriched ^{129}I content of the ore and near-background ^{129}I concentrations in the groundwater.

More recent sampling of ore and groundwater has been directed to measurements through the Koongarra dispersion fan. Samples of surface and near-surface material have also been collected so that the effect of the bomb pulse contribution to the subsurface yield can be evaluated.

5.3 Technetium-99

Procedures for isolating technetium from rock samples and measuring technetium isotopes by positive ion mass spectrometry analysis have been developed at LANL by David Curtis (these Proceedings) and Don Rokop in a United States Department of Energy (USDOE) sponsored project. The technetium preparation techniques have since been adapted by June Fabryka-Martin (University of Arizona) to groundwater sampling where, in a manner similar to that used for iodine collection, pumped water was passed through a bed of strongly basic anion-exchange resins.

Measurements for one ore and one groundwater sample from Koongarra have been reported by David Curtis and June Fabryka-Martin respectively (these Proceedings). The molar ratio of ^{99}Tc to U in the groundwater sample was 2.8×10^{-11} which was a factor of 2-17 times greater than predicted for equilibrium conditions, implying that ^{99}Tc has a much higher mobility than U.

5.4 Plutonium-239

The study of the production and dispersion of ^{239}Pu through a geological system has been another major sub-project of the analogue study. Techniques to measure qualitatively plutonium-239 levels down to 10^{-14} g using isotope dilution mass spectrometry have been developed by Curtis, Perrin and Cappis (these Proceedings) at LANL. These should allow the abundance of ^{239}Pu in rock to be measured along the hydrological gradient in both the oxidized and reduced zones at Koongarra. They may also permit measurements of the Pu abundance of a groundwater sample from the centre of the uranium ore, with the contained colloidal fraction concentrated by a factor of approximately 100.

An initial measurement for a homogenized rock sample from just below the highly altered weathered zone has been discussed by Curtis (these

Proceedings). The measured ^{239}Pu abundance was corrected for measurement of $^{240}Pu/^{239}Pu$ contamination and was 3.5-3.9 x 10^{-13} g ^{239}Pu/g U, a molar ratio of 1.4-1.6 x 10^{-12} ^{239}Pu/U.

The abundances of ^{239}Pu, ^{129}I and ^{99}Tc in rock samples from Koongarra will be measured and compared so that calculations of their production and models of their dispersion through the secondary mineralization can be evaluated. The uncertainties resulting from the lack of knowledge of in situ neutron fluence in the production models are then expected to be reduced and the effects of isotope migration in the overall system more clearly understood.

6.1 Development of Modelling Codes and Evaluation of the Koongarra Site for Modelling Studies

Preliminary modelling studies have been undertaken to evaluate the potential of the Koongarra ore body for use in transport model validation. Two procedures were used to study the formation of the secondary mineralization and estimate the timescale of the process.

In the first, David Lever (Harwell) (9) used the typical formalism of hydrodynamic modelling. In one of his approaches, a one-dimensional model, based on the spatial gradient of ^{238}U, retardation factors (R) and ^{238}U, ^{234}U and ^{230}Th disequilibria, was used with various relative magnitudes of R_{238}, R_{234} and R_{230} to calculate $^{234}U/^{238}U$ and $^{230}Th/^{234}U$ activity ratios. These were then compared with measured drill core samples through a section of the ore body. The best fit to the data was obtained for the case where ^{230}Th is considered to be the least mobile (large R_{230}), with $R_{238} < R_{234}$. The timescale of the uranium migration was estimated to be 1-3 My.

An alternative approach was developed by Airey and Golian (8). They described the decay of the uranium series radionuclides in an open system, where leaching and deposition are included as first order processes (i.e. they are proportional to the concentration of the accessible uranium in rock and in water; other case-specific constraints were also included.

An example of this approach for a data set consisting of $^{234}U/^{238}U$ and $^{230}Th/^{234}U$ ARs for samples through the same section of the secondary mineralization provided the deposition/leaching rate solution shown in Figure 5 as a function of sample position. The age of the mobilization process by this approach was estimated to be at least 700 ky and as extensive as several My, which is consistent with the value estimated by the hydrodynamic modelling (see Golian and Duerden, these Proceedings).

Koongarra groundwater monitoring measurements made during 1972-80 have recently been reviewed (10). Additional hydrogeologic work was identified as being necessary before final interpretation of possible paths of hydrologic transport can be determined and incorporated in future transport model studies. Even though a large amount of geologic information is available for the site, additional hydrologic tests in the bedrock aquifers are needed. Two most critical questions must be answered:

1) Is groundwater flow primarily along fractures even in the highly weathered zone? If not, at what depth does the transition occur between matrix flow and fracture flow?
2) What are the connections, if any, between groundwater in the bedrock and groundwater in the surficial deposits?

7.1 Conclusions

A substantial body of information has been collected during the past six years which has allowed preliminary investigation of radionuclide transport through the Alligator Rivers ore bodies.

Results have been obtained on

- the migration of uranium, thorium and radium isotopes,
- the role of specific minerals in retarding migration,
- the importance of colloidal material, in the migration of thorium, and
- the behaviour of naturally occurring levels of selected fission products and transuranium nuclides, e.g. technetium-99, iodine-129 and plutonium-239.

It is proposed that further work should be carried out at the Koongarra deposit as part of an international collaborative study, and invitations to participants in the project have been given to national agencies and organisations within member countries of the OECD Nuclear Energy Agency.

8.1 Acknowledgements

The work in the Alligator Rivers region was supported by the USNRC from 1981-1987, the UKDOE from 1986-1987 and JAERI from 1987.

The continued support of the Northern Territory Department of Mines, Water Resources Division, and Mr Carlos Sorentino and Dr Andrew Snelling of Denison Australia Pty Ltd is gratefully acknowledged.

9.1 References

1. Natural Analogue Working Group, Commission of the European Communities, First Meeting, Brussels, 5-7 November 1985. Ed B Come and N Chapman. EUR 10315 EN-FR.
2. Natural Analogue Working Group, Commission of the European Communities, Second Meeting, Interlaken, 17-19 June 1986. To be published as EUR 10671.
3. AIREY, P.L., ROMAN, D., GOLIAN, C., SHORT, S., NIGHTINGALE, T., LOWSON, R.T. and CALF, G.E.. Radionuclide Migration around Uranium Ore Bodies - Analogues of Radioactive Waste Repositories, USNRC Contract NRC-04-81-172, Annual Report 1982-83, AAEC Report C40, 1984 (NUREG/CR-3941, Vol. 1).
4. AIREY, P.L., ROMAN, D., GOLIAN, C., SHORT, S., NIGHTINGALE, T., PAYNE, T., LOWSON, R. and DUERDEN, P. Radionuclide Migration around Uranium Ore Bodies - Analogues of Radioactive Waste Repositories, USNRC Contract NRC-04-81-172, Annual Report 1983-84, AAEC Report C45, 1985.
5. AIREY, P.L., DUERDEN, P., ROMAN, D., GOLIAN, C., NIGHTINGALE, T. and PAYNE, T. Radionuclide Migration around Uranium Ore Bodies - Analogues of Radioactive Waste Repositories, USNRC Contract NRC-04-81-172, Annual Report 1984-85, AAEC Report C55, 1986.
6. SNELLING, A.A. and DICKSON, B.L. Uranium/Daughter Disequilibrium in the Koongarra Uranium Deposit, Australia. Mineral. Deposita (Berl.) 14, 109-118 (1979).
7. SNELLING, A.A. Uraninite and its Alteration Products, Koongarra Uranium Deposit, p.487, in Proceedings of IAEA International Symposium Uranium in the Pine Creek Geosyncline, Sydney, 4-8 June 1979, Ed J. Ferguson and A.B. Goleby (IAEA, Vienna, 1980).
8. AIREY, P.L., GOLIAN, C. and LEVER, D.A. An Approach to the Mathematical Modelling of Uranium Series Redistribution within Ore Bodies, USNRC Contract NRC-04-81-172, Topical Report, AAEC Report C49, June 1986.
9. LEVER, D.A. A Preliminary Theoretical Interpretation of the Evolution of Secondary Mineralization at the Koongarra Uranium Deposit. To be submitted to J. Geophys. Res. (B), 1986.
10. DAVIS, S.N. University of Arizona, private communication.

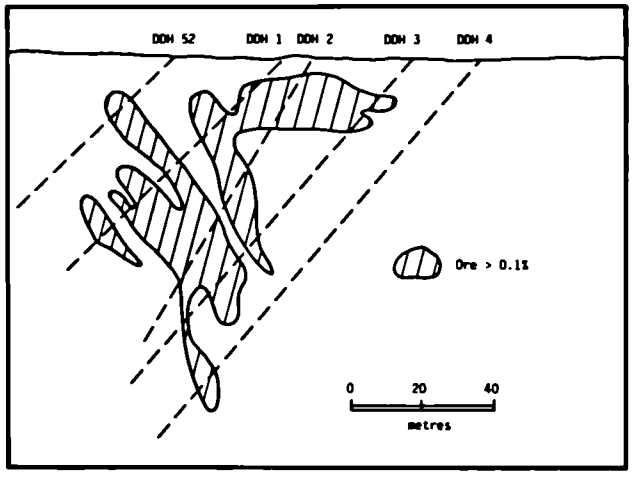

Figure 1A Section through the Koongarra ore body showing location of drill holes.

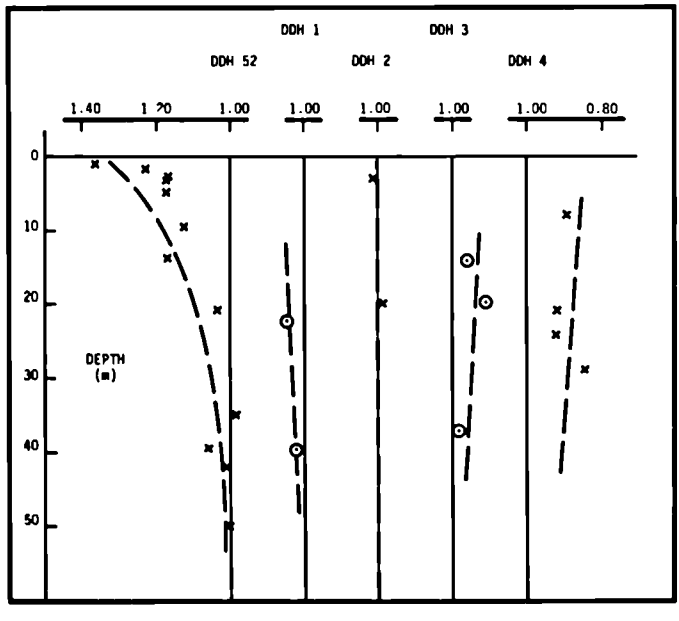

Figure 1B Measurements of the activity ratio $^{234}U/^{238}U$ versus depth for drill core samples from Koongarra section shown in Figure 1A.

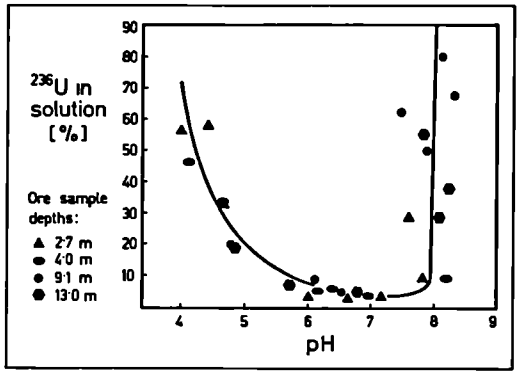

Figure 2 Percentage ^{236}U in solution as a function of pH.

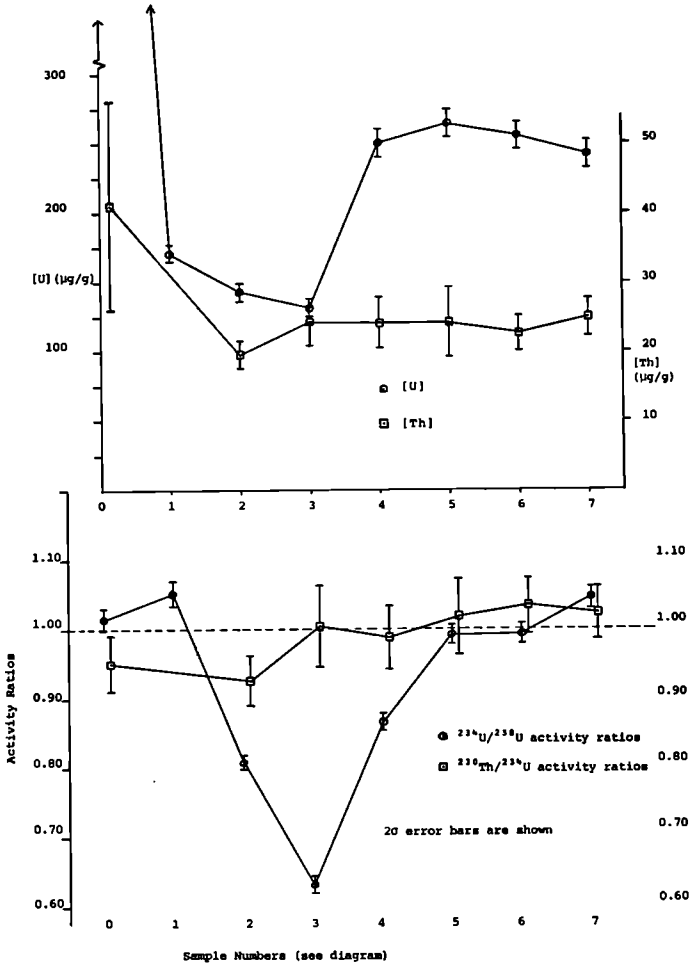

Figure 3 [U], [Th], ^{234}U/^{236}U and ^{230}Th/^{234}U activity ratios in Jabiluka fracture.

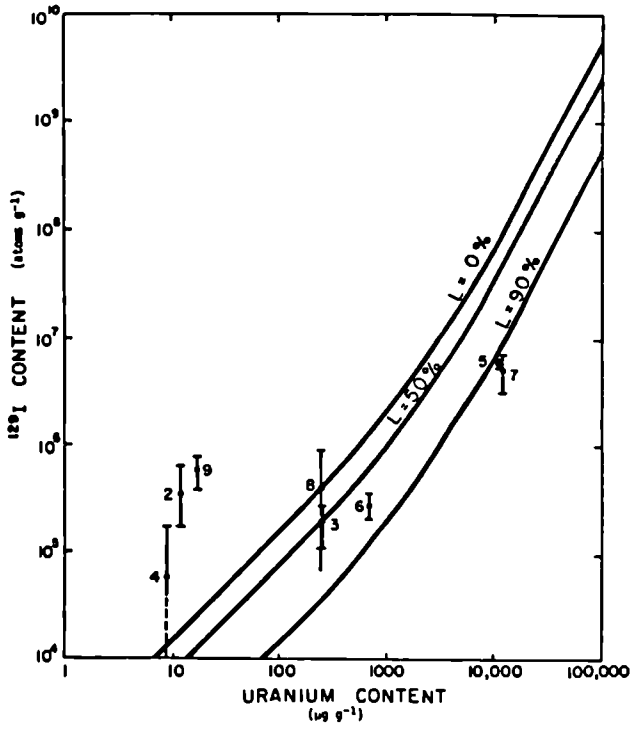

Figure 4 Measured iodine-129 contents of uranium ore relative to predicted content for different rates of loss.

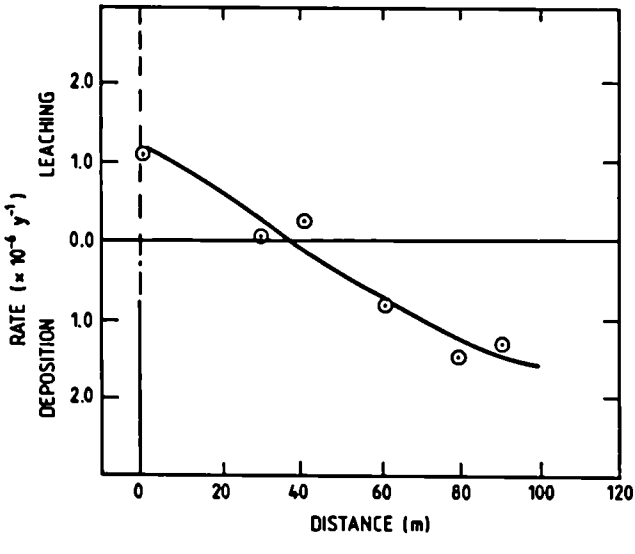

Figure 5 Modelling of Koongarra 'dispersion fan' formation. Average uranium transport rates versus distance of the original distance.

URANIUM IN SELECTED ENDORHEIC BASINS AS PARTIAL ANALOGUE FOR SPENT FUEL BEHAVIOR IN SALT

A. E. VAN LUIK
Performance Assessment Scientific Support Program
Waste Technology Center
Pacific Northwest Laboratory

Summary

If uranium (U) behavior with respect to the components of certain endorheic (closed) basin subsurface, playa, or terminal lake brines were quantitatively understood, the ability to predict the long-term redistribution of emplaced U among analogous components of salt formations may be enhanced. Tests that determine the nature of U interactions with pure mineral and organic matter surfaces are important, but studying the natural systems available could give indications of long-term stabilities of processes, and of preferential processes. For example, some metals present in trace quantities, such as U, may be coprecipitated in the oxidized zone with an evaporite mineral that may afterward undergo diagenesis, especially if conditions become more reducing. During diagenesis, the trace metal may be remobilized, but scavenged by sulfides or organic particulates, leaving the evaporite mineral depleted of its trace metal content. A survey of the literature shows some trace metal behavior in closed basins has been studied. However, information on U consists of only a few abundance determinations for some evaporite systems. Obtaining and interpreting natural analogue data for the U and Th decay series in selected endorheic basin environments is suggested.

1.0 Introduction

1.1 Naturally occurring uranium as a natural analogue

The geochemistry of uranium (U) has been studied in depth, especially its mineralization. The geochemistry of U and other naturally occurring elements has been discussed in terms of implications for the probable performance of nuclear waste repositories. The meeting reports of the Commission of the European Communities' Natural Analogue Working Group (1,2) give overviews of this work. In the first working group meeting report, however, Glasbergen (3) notes that few natural analogues address processes related to the expected performance of a repository for nuclear waste in salt. This paper proposes that the characterization of selected endorheic basin environments may provide natural analogue data concerning processes that may be operative in or adjacent to the waste package emplaced in salt. The endorheic basins of interest would have playa or terminal lakes with brine compositions chemically analogous to those expected to contact the waste form, and have sediments that contain halite

as well as clays and organics analogous of the salt-repository host rock and its principal impurities (4).

1.2 The need for data on U behavior in brine-salt systems

U is an element for which much geochemical data exists. To date, however, only estimates of maximum U concentrations in brines have been available for use in salt repository performance analyses. These estimates range from 0.001 (5) to 20 mg U/kg (6). If flow of brine occurs, U is expected to be minimally retarded with respect to the velocity of the brine. Estimates of this retardation from reversible interactions between U and solid-phase surfaces contacted by the brine are generally described in terms of unitless retardation coefficient values on the order of 10 or 20 (7). This lack of definitive data is a constraint on the geochemical modelling that can currently be done in support of salt repository performance assessments. Perhaps natural analogue data can be useful in meeting some specific data needs or in helping define important operative geochemical processes.

1.3 Natural analogues for processes related to repositories in salt

A study by Wollenberg et al. (8) gives examples of analogue studies in which salt has been intruded by crystalline rocks. They cite preliminary evidence that suggests U and Th have not migrated appreciably into surrounding rock salt from intrusives after tens to hundreds of millions of years. For the hypothetical case where spent nuclear fuel comes in contact with brine, however, these results would have little analogue value.

In 1984, results of a study of radionuclides in alkaline lake environments were reported by Simpson et al. (9). Solution levels of radionuclides as well as distribution coefficients between solution and sediment were reported, with the objective of providing analogue data for the far-field where radionuclides would be traveling in briney aquifers. This work was part of a series of natural analogue studies sponsored by the U.S. Nuclear Regulatory Commission (10). The needs for near-field analogue data, focused on the behavior of radionuclides in a brine-salt environment, with some carbonate, sulfate, clay, and organic impurities, were not specifically addressed by Simpson et al. (9). The work suggested in this paper would be an extension of this previous effort, focusing on endorheic basin environments more germane to the processes operating immediately adjacent to the waste package.

1.4 Endorheic basins as possible locations for U/salt natural analogues

In an endorheic basin playa and/or terminal lake with evaporitic sediments, U is generally found in the terrigenous clastics rather than associated with the evaporite minerals precipitating from the playa or terminal lake brines (11). Additionally, clays and organic matter scavenge U from the brine, leaving evaporites relatively, but not entirely, depleted of U. The presence of organic and terrigenous mineral surfaces that sorb U compete with the reported enhancement of U solubility through the formation of carbonate and phosphate complex ions. As the precipitation of carbonate minerals occurs, carbonate concentrations in an evaporating solution are lowered, which suggests some likelihood of U coprecipitation. Some closed-basin brines are low-carbonate systems, even though their inflow waters may be carbonaceous. Finding U in the carbonate rings around the evaporite deposits, as well as on terrigenous

clastics and organic matter of these brines, seems likely. On the other hand, high-carbonate content waters and brines may keep U in solution even under mildly reducing conditions (9,11,12).

If U behavior with respect to the competing components of halite-saturated playa and terminal lakes were quantitatively understood, the ability to predict the distribution of U among analogous components of salt formations after long time periods may be enhanced. Tests that determine the sorption of U onto pure mineral and organic matter surfaces are important. However, studying the natural systems available could give indications of long-term stabilities of processes, and of preferential processes over long time periods. For example, some trace metals, such as U, may be coprecipitated in the oxidized zone with an evaporite mineral. In turn, that precipitated evaporite mineral may undergo diagenesis at the bottom of the lake, where conditions may be more reducing. During diagenesis, the trace metal may be remobilized but scavenged by sulfides or organic particulates, leaving the evaporite mineral depleted in comparison to its original, short-term, trace metal content.

This scenario of U coprecipitation and subsequent remobilization, transport, and fixation could be reproduced over a very long time period in a hypothetical bedded salt repository where sufficient brine exists to erode metal barriers and expose UO_2. With a well-engineered waste package system, this penetration by brines should not take place until many thousands of years after emplacement, when gamma-radiation and thermal outputs from the waste have become minimal. Under expected conditions, brine penetration to the spent fuel matrix may not occur at all because of limited amounts of available brine in salt formations (5). For our hypothetical case, however, sufficient alpha radiation may occur to induce oxidizing conditions at the UO_2-brine interface, especially since the solution would contain considerable ferrous iron (13). At some distance, the brines in contact with ferrous-iron corrosion-products would be reduced (14).

The migration of brine in such a system is unlikely, but even in a no-flow system, the brine is in dynamic equilibrium with the solid-phase evaporite minerals that are present (11). Thus, coprecipitation, resolubilization, and diffusion are likely operative processes that will directly affect the U distribution in this system over time.

2.0 Uranium behavior in endorheic basin brine/evaporite systems

2.1 Closed basins of interest

Endorheic basins of interest may include those having sufficiently slow interior drainage so that evaporite deposits and/or highly concentrated brines occur on or below the surface. Of particular interest, however, are the closed basins in which internal drainage is sufficiently slow to allow the playa and terminal lake environments that occur to have brines from which evaporites precipitate. Finding a location where active formation of substantial evaporite deposits is occurring is not likely. This phenomenon seems to have been largely Devonian and Permian, with only minor and localized depositions currently taking place (15).

Toward the end of summer, somewhat idealized playa environments may be found, where halite occurs predominantly in the lower part of the playa lake basin surrounded by a sulfate-dominated evaporite ring, which is in turn surrounded by a carbonate-dominated evaporite ring (Figure I) (16). Also promising are closed basins with terminal lakes that are

saturated with respect to halite in at least some of their reaches, and which have definable zones of carbonate and detrital sediments around the areas where halite may seasonally or more permanently be deposited (Figure II).

The nature of the brine types that could be encountered in a salt repository is dependent on the nature of the salt and the source of the brine. For example, in the Palo Duro Basin, Texas, brines that may migrate thermally are expected to be high-magnesium, high-potassium brines,

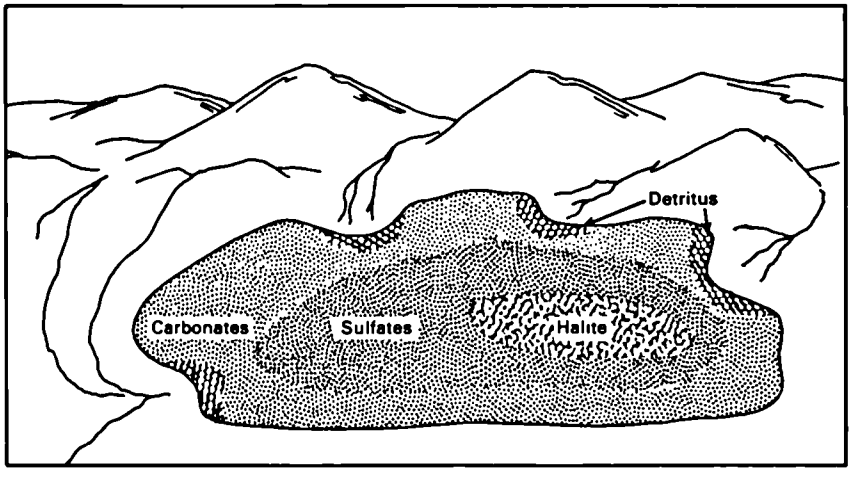

Figure I: Idealized Playa Evaporites Pattern [Modified from (16)].

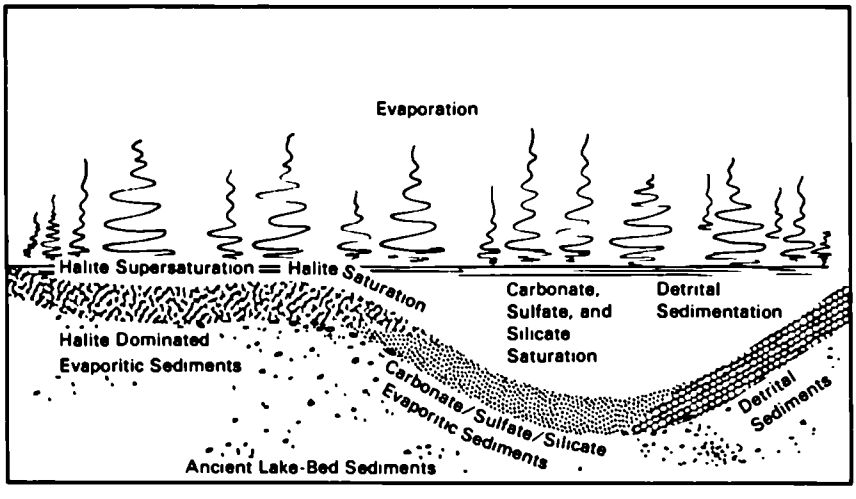

Figure II: Idealized Terminal Salt Lake Brines and Sediments.

while dissolution brines are expected to be high-sodium brines (5). The chemical makeup of known playa and terminal lake brines encompasses this range. Many playa and terminal lake inflow waters are carbonate-rich and result in either salt or alkali lakes. Salt lakes produce halite as a primary evaporite as it becomes highly concentrated, and alkali lakes produce trona as evaporation proceeds. It is possible that some playa lakes may change their character as evaporation to dryness proceeds, precipitating trona after halite precipitation has run its course. Alkali lakes are also known as trona lakes or soda lakes. Natural bittern, or high-magnesium brine lakes also occur; the best-known example is the Dead Sea in Israel (17).

2.2 Literature pertinent to U behavior in endorheic basin brine/evaporite systems

A number of studies are concerned with trace metals in brine-evaporite systems (9,11,18,19,20,21,22), but few include U. Notable exceptions are Bell (22), Thurber (21) and Simpson et al. (9). Bell cites work that shows evaporites generally have very low levels of U even though the terranes from which they were derived may have more than average amounts of U. Thurber reports determinations of isotopes of U, Th, and Ra for waters from 11 streams and 5 lakes in the Great Basin. Thurber's water analyses show a positive correlation between U and carbonate concentrations, but shed little light on the subject of U-brine-evaporite-sediment interactions. The work by Simpson et al. also shows elevated U-levels in carbonate-rich brines in alkali lakes. U levels for Mono Lake, for example, were two orders of magnitude greater than found in sea water. Brine-sediment competition for U was also measured; distribution coefficient results between 10 and 200 were found, although the usefulness of these numbers is diminished by the limited amount of sediment characterization reported. The Simpson et al. study also included data for Am, Pu, Pa, Th, Ac, Ra, Po, Pb, Cs, and Sr isotopes; of the studies reviewed, this far-field oriented natural analogue study most closely represents the type of work and data collection being suggested here as still being needed for brine-evaporite systems.

The geochemistry of carnotite occurrences in calcareous desert drainages (23,24,25) partly describes U behavior in actual playa/terminal lake environments. Australian occurrences were detailed by Mann and Deutscher (25); more recent work on these occurrences has been reported by Briot (26,27). The Australian occurrences are numerous, but the carnotite location of greatest interest to this study is the apparent result of the decomplexing of the uranyl carbonate anionic complex as a groundwater drainage meets the higher salinity ground waters of a salt lake. Carnotite precipitation, with the formation of an ore body, was the apparent result. Whether the geochemistry responsible for the formation of this ore body is of interest as a repository analogue depends on the amount of vanadium in the repository brines and the prevailing redox conditions.

A somewhat similar occurrence in New Mexico, dating from the Jurassic, has been described by Rawson (28). The primary ore here, however, is uraninite, not carnotite, making this occurrence of particular interest in terms of U behavior in systems without the proper vanadium/redox conditions necessary to precipitate carnotite. The postulated ore-forming mechanism was the retreat of an ancient lake, leaving a large, shallow flat of gypsum and algal limestone. Evaporative pumping moved U-bearing ground water from the underlying sandstone aquifer upward into the re-

duced, algae-rich, porous limestone sediments, where U(VI) was reduced to U(IV) and precipitated as uraninite. Because limestones lithify and lose their permeability, the time during which U-bearing ground waters could migrate through this sediment was limited. Age dating has suggested that the primary uraninite ore mineralized during the sediment diagenesis. Secondary mineralizations along fractures occurred later.

2.3 Geochemistry of U, with emphasis on highly saline environments

To understand U behavior in endorheic brine-evaporite systems, the general literature on U geochemistry may also be consulted for studies in systems that may be partial analogues, such as briney aquifers or other high-salinity environments. These studies represent analogues twice removed, however, hence their value is restricted.

Recent natural analogue work specific to salt repositories has included ongoing work on the behavior of U, Th, and Ra in briney aquifers by Pacific Northwest Laboratory on behalf of the Salt Repository Project operated by the U.S. Department of Energy. A series of papers have been written describing this work; the most recently published overview is by Laul, Smith, and Hubbard (29). Some of the experimental aspects of these studies of U behavior in subsurface brine-salt systems should be directly applicable to studies of natural U behavior in playa or terminal lake brine-evaporite systems.

Descriptions of the geochemistry of U, including the ground-water transport of U(VI) as the uranyl ion, its reduction to U(IV), and subsequent immobilization as uraninite, $UO_2(c)$, appear in Duffy and Ogard (30) and Osmond (31). Duffy and Ogard suggest this redox-dependent transport-immobilization behavior should be applicable to some expected repository environments. This applicability would also appear to hold for U in a salt repository, because the spent nuclear fuel matrix that may eventually be contacted by brine is 95% uranium dioxide, UO_2 (32). Without reducing conditions, however, the uranyl cation may be immobilized in the presence of phosphate or vanadate ions by precipitating as secondary minerals such as autunite, $Ca(UO_2)_2(PO_4)_2.12H_2O$, carnotite, $K_2(UO_2)_2(VO_4)_2.nH_2O$ (33), or tyuyamunite, $Ca(UO_2)_2(VO_4)_2.nH_2O$ (12).

Additionally, from thermodynamic arguments, Muller and Duda (34) have suggested that $UO_2(c)$, $UO_2(am)$, $UO_2SO_4(c)$, $CaUO_4(c)$, $U_3O_8(c)$, and $U_4O_9(c)$ may be the solid phases that control the solubility of U in a salt-repository brine over the expected pH and Eh range. On the other hand, the presence of vanadate, or elevated levels of silicate or phosphate, may make potassium or calcium uranyl vanadates or a uranyl silicate the solubility-controlling solid phase under proper redox conditions (12,15,33).

Oil-field and oceanographic geochemistry researchers have made observations concerning the behavior of U in brine-rock or brine-sediment systems that need further evaluation before they can be applied to our understanding of the expected behavior of U in brine-evaporite systems. For example, Collins (35) cites work related to petroleum exploration in which U was found to be either absent or only present in very low concentrations in bicarbonate-sodium type oil-field waters. The U in solution was reportedly in the tetravalent tricarbonate complex-anion form.

Oceanographic research reviewed by Richards (36) raises questions concerning the U(VI)/U(IV) redox couple. Apparently, a direct correlation exists between the depth of the water column over Black Sea sediments and their U content, suggesting that the more reduced, deeper-lying sediments have accumulated more U. This condition suggests a U(VI)

to U(IV) change at a given depth in the Black Sea, perhaps where the Eh falls below the calculated Eh of about -0.2 V for the U(VI) to U(IV) reaction. Measurements at various depths in the Black Sea suggest the U(VI) state prevails throughout, and that U remains in solution in the uranyl tricarbonate anionic complex. This may in turn suggest that U reduction takes place within the sediment. Goldberg (37) reviewed oceanographic literature and observed that U reduction probably occurs in the sediment, because, at the pH of anoxic sea water, the Eh needed to convert U(VI) to U(IV) in the water column is probably -0.4 to -0.5 V. Goldberg also cites work suggesting that U is removed from solution at the peripheries of stagnant basins where the sapropels and their overlying waters contain H_2S, and not in the more reducing centers of these basins. In marine apatite deposits off the coast of southern California, from half to three-fourths of the associated U was in the U(IV) state, and had substituted for calcium in the apatite. The remaining U(VI) associated with the apatite was in the form of adsorbed uranyl ions. The reduction of U(VI) in the sediments under only mildly reducing conditions is suggested by this data. A study by Robbins (38) included the accumulation of U in an overview of metal deposition in rift lakes. This study also pointed to the role of anoxic H_2S-bearing bottom waters and sediments.

The geochemistry of U in sedimentary rocks may also give information about the behavior of U in brine-evaporite systems. Kelepertsis (39), who studied the geochemistry of U in carboniferous sedimentary rocks, found that the U was primarily associated with the high-organic-carbon shales; minor amounts were found associated with clays. Kelepertsis found evidence of U(VI) reduction by Fe(II) oxidation, which could occur in biogenic sapropels. Borovec, Kribec, and Tolar (40) found that humic acid sorption of uranyl ions may also remove U(VI) from solution, as the uranyl divalent cation, without prior reduction to U(IV). Borovec (41) has also demonstrated uranyl sorption on finely divided clay mineral surfaces.

The sodium-chloride brines of salt lakes, in contrast with the brines of soda or alkali lakes, tend to be depleted in carbonate. For example, typical inflows to the Great Salt Lake, Utah, carry 100 mg/kg carbonate, while the lake brines typically have less than 0.1 mg/kg (42). High carbonate lakes precipitate trona as evaporation concentrates the brines. For example, Harney Lake in southern Oregon has had water analyses that indicated carbonate levels of 2.7 and 4.4 g/kg at two widely separated times (42). This type of system may be of interest for the opportunity to study the behavior of U-carbonate complex ions in an environment where solid carbonates are present, whether earlier in the evaporation cycle as aragonite, or later as trona.

Morse et al. (43) reviewed the literature on U-carbonate mineral interactions. They investigated the behavior of U, as the uranyl ion, in dilute and sea water solutions in the presence of calcium carbonate minerals. Some of the literature reviewed by Morse et al. reported probable coprecipitation of U with calcium carbonate in sea water and a partition coefficient that approached 1 for the uranyl cation with respect to sea water and aragonite.

The experimental work by Morse et al. (43) was undertaken in part to study these reported results. Calcite, aragonite, coral, magnesium calcite, and a sediment were used for sorption-desorption studies. Typical results showed little sorption at very low U concentrations and greater sorption at higher U concentrations. In all cases, sorption peaked between 5 and 50 minutes, and desorption was either completed by

the end of 8 hours for the lower concentrations or continued to proceed at a low rate for the higher concentrations; the experiments were ended after a week. The experiments indicate that the uranyl is sorbed on the carbonate surface, but then desorbs as the tetravalent, anionic, uranyl-tricarbonate complex, which keeps the U in solution. For natural systems, therefore, it is doubtful that U coprecipitation with carbonates would be an important sink for U.

3.0 Summary and recommendations

3.1 Expected behavior of U in the closed basins of interest

Figure III summarizes the expected behavior of U in a playa or terminal lake brine-evaporite system. In this specialized environment, U is postulated to be present in the fresh-water inflow stream. Minor amounts may also be contributed by wind-blown particulates. As the velocity of the inflow water slows, detrital deposition should remove sorbed U from solution. As evaporation and mixing with the brine begins to concentrate the inflowing solution, reversible U sorption on or minor coprecipitation with calcium and magnesium carbonates and calcium sulfates may occur. Finally, some U should be coprecipitated with evaporites precipitating in the halite-saturated zone. Diagenesis may resolubilize some sorbed and coprecipitated U. If sediments are or become reduced, the scavenging of U from solution by metal sulfides or organic surfaces should occur. As U(VI) enters reduced conditions, the reduction to U(IV) will result in the removal of U from solution by sorption on sulfides and organics, and by the precipitation of $UO_2(c)$.

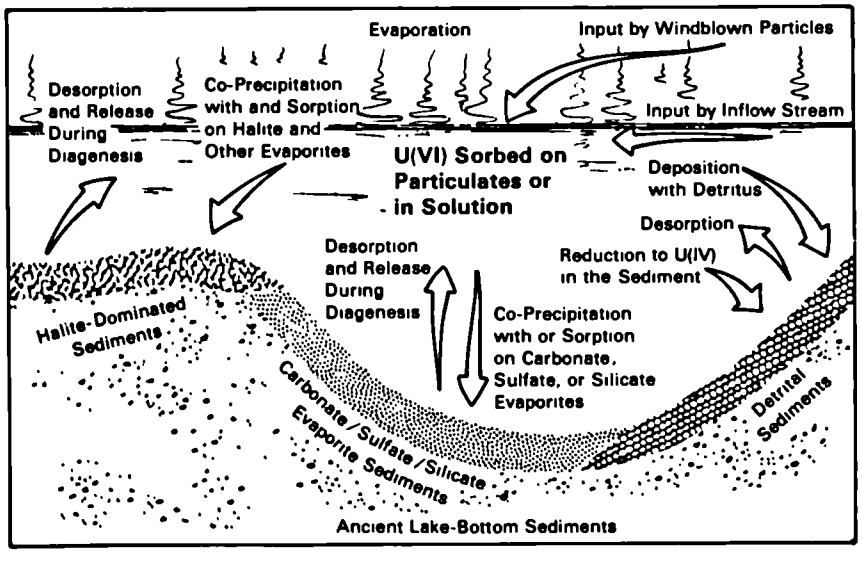

Figure III. Summary of Expected U Behavior in Playa or Terminal Lake Brine-Evaporite Systems.

Concentrations of U should, therefore, diminish in both the sediments and the brines as one moves from the inflow zone to the halite-saturated zone. Nevertheless, some U should be precipitated with the evaporites forming in the halite-saturated zone.

The dynamics of an evaporating brine (44) suggest that precipitation occurs at the surface, perhaps in a shallow zone of supersaturation; crystals that form then fall through the brine to the bottom. The crystals are, therefore, not at equilibrium with the brines below the surface unless these are also saturated with respect to the precipitating mineral. In well-mixed evaporation systems, managed to maintain depths of only 7.5 to 30.0 cm, the brine may eventually become supersaturated throughout, resulting in the growth of large crystals on the bottom (44). These conditions would probably not be encountered in natural systems, however, and evaporite mineral crystals would be expected to form at the brine surface and sink before substantial crystal growth could take place.

Crystals that reach the bottom will continue to be in dynamic equilibrium with overlying saturated brines, and the continual surface dissolution and reprecipitation that takes place bonds the individual crystals into a coherent but very rough layer of salt crystals covering the bottom of the lake. This layer has been observed by the author at the northern extremity of the Great Salt Lake, Utah. This dynamic system tends to allow coprecipitated metals, such as U, to be redissolved and scavenged by dissolved or particulate carbonate, phosphate, or organic materials in the brine. The rate of release from the salt crystals would probably be dependent on the location within the crystals.

3.2 Recommendations

The literature suggests that some trace-metal behavior in endorheic basins has been studied, but little information on U is yet available. An effort should be made to obtain and interpret natural analogue data for the U and Th decay series in selected closed basin brine-evaporite systems.

The quantitative study of the fate of U during evaporite-crystal formation at the brine surface, and diagenesis at the bottoms of saturated playa and terminal lakes, may lead to data on U coprecipitation, precipitation, sorption, and migration for a range of salt/brine environments. Endorheic basins with halite-saturated playa and terminal lake environments are scattered throughout the world (17), and the phenomena of interest are at or near the surface. Therefore, data should be readily obtainable from a number of locations representing a range of input and brine geochemistries, evaporite mineralogies and ages.

It is suggested that interested parties cooperatively identify a number of these environments and plan their characterization. The variety of environments that could be described may be sufficient to encompass the expected pH, Eh, U, co-solute, and evaporite mineralogy conditions pertinent to a nuclear waste repository in salt. Modelling of these competing processes, based on this characterization data, could provide experience and perhaps data that enhances the degree of confidence that may be associated with the modelling of spent nuclear fuel behavior in a hypothetical repository in salt.

Acknowledgment

This work was supported by the U.S. Department of Energy under contract DE-AC06-76RLO 1830.

References

1. COME, B. and CHAPMAN, N. (Eds.). (1986). Natural Analogue Working Group, first meeting, Brussels, November 5-7, 1985, final meeting report. Report EUR 10315 EN-FR, Commission of the European Communities, Brussels.
2. COME, B. and CHAPMAN, N. (Eds.). 1987. Natural Analogue Working Group, second meeting, Interlaken (CH), June 17-19, 1986, final meeting report. Report EUR 10671 EN-FR, Commission of the European Communities, Brussels.
3. GLASBERGEN, P. (1986). Special needs of modelers working in the field of geological disposal in rock-salt. Pages 86-89 in: Come, B. and Chapman, N. (Eds.). (1986). Natural Analogue Working Group, first meeting, Brussels, November 5-7, 1985, final meeting report. Report EUR 10315 EN-FR, Commission of the European Communities, Brussels.
4. U. S. DEPARTMENT OF ENERGY (1986). Nuclear Waste Policy Act (Section 112) Environmental assessment, Deaf Smith County site, Texas. DOE/RW-0069. Volume 1 Chapter 3: The site. Office of Civilian Radioactive Waste Management, Washington, D.C.
5. U. S. DEPARTMENT OF ENERGY (1986). Nuclear Waste Policy Act (Section 112) Environmental assessment, Deaf Smith County site, Texas. DOE/RW-0069. Volume 2, Chapter 6: Suitability of the Deaf Smith County site for site characterization and for development as a repository. Office of Civilian Radioactive Waste Management, Washington, D.C.
6. INTERA TECHNOLOGIES, INC. (1985). Preliminary analyses of scenarios for potential human interference for repositories in three salt formations. BMI/ONWI-553. Prepared for Office of Nuclear Waste Isolation, Battelle Memorial Institute, Columbus, Ohio.
7. WASTE ISOLATION SYSTEMS PANEL, THOMAS H. PIGFORD, Chairman (1983). A study of the isolation system for geologic disposal of radioactive wastes. National Research Council, National Academy of Sciences. Published by National Academy Press, Washington, D.C.
8. WOLLENBERG, H. A., BROOKINS, D. G., COHEN, L. H., FLEXSER, S., ABASHIAN, M., MURPHY, M. and WILLIAMS, A. E. (1984). Uranium, thorium and trace elements in geologic occurrences as analogues of nuclear waste repository conditions. Section 5.4, pages 464-491 in: Alexander, D. H. and Birchard, G. F. (Eds.). NRC nuclear waste geochemistry '83. NUREG/CP-0052. Proceedings of a conference held at Reston, Virginia, August 30-31, 1983. Published by the U.S. Nuclear Regulatory Commission, Washington, D.C.
9. SIMPSON, H. J., TRIER, R. M., LI, Y. H. and ANDERSON, R. F. (1984). Field experiment determinations of distribution coefficients of actinide elements in alkaline lake environments. Section 4.2, pages 326-342 in: Alexander, D. H. and Birchard, G. F. (Eds.). NRC nuclear waste geochemistry '83. NUREG/CP-0052. Proceedings of a conference held at Reston, Virginia, August 30-31, 1983. Published by the U.S. Nuclear Regulatory Commission, Washington, D.C.
10. BIRCHARD, G. F. and ALEXANDER, D. H. (1983). Natural analogues -- a way to increase confidence in prediction of long-term performance of radioactive waste disposal. In: Scientific basis for nuclear waste management VI, Mat. Res. Soc. Symp. Proceedings 15: 323-329.
11. SONNENFELD, P. (1984). Brines and evaporites. Published by Academic Press, Inc., Orlando, Florida.

12. LANGMUIR, D. (1978). Uranium solution-mineral equilibria at low temperatures with applications to sedimentary ore deposits. Geochimica et Cosmochimica Acta 42:547-569.
13. CHRISTENSEN, H. and BJERGBAKKE, E. (1982). Radiolysis of groundwater from HLW stored in copper canisters. KBS TR 82-02. Svensk Karnbransleforsorjning AB / Avdelning KBS, Stockholm.
14. NERETNIEKS, I. and ASLUND, B. (1983). The movement of radionuclides past a redox front. KBS TR 83-66. Svensk Karnbransleforsorjning AB / Avdelning KBS, Stockholm.
15. HOLSER, W. T. (1979). Mineralogy of evaporites. Chapter 8, pages 211-294 in: R. G. Burns (Ed.). Marine minerals. Mineralogical Society of America, Washington, D.C.
16. BRENNER-TOURTELOT, E. F., VINE, J. D. and BOHANNON, R. G. (1977). Lithium in the playa environment. Pages 169-182 in: Greer, D. C. (Ed.). Desertic terminal lakes. Proceedings from the International Conference, Weber State College, Ogden, Utah, May 2-5, 1977. Published by Utah Water Research Laboratory, Utah State University, Logan, Utah.
17. GREER, D. C. (1977). Desertic terminal lakes. Pages 1-24 in: Greer, D. C. (Ed.). Desertic terminal lakes. Proceedings from the International Conference, Weber State College, Ogden, Utah, May 2-5, 1977. Published by Utah Water Research Laboratory, Utah State University, Logan, Utah.
18. HOLSER, W. T. (1979). Trace elements and isotopes in evaporites. Chapter 9, pages 295-346 in: Burns, R. G. (Ed.). Marine minerals. Mineralogical Society of America, Washington, D.C.
19. TAYLER, P. L., HUTCHINSON, L. A. and MUIR, M. K. (1977). Heavy metals in the Great Salt Lake, Utah. Pages 109-124 in: Greer, D. C. (Ed.). Desertic terminal lakes. Proceedings from the International Conference, Weber State College, Ogden, Utah, May 2-5, 1977. Published by Utah Water Research Laboratory, Utah State University, Logan, Utah.
20. VAN LUIK, A. E. and JURINAK, J. J. (1978). A chemical model of heavy metals in the Great Salt Lake. Research report 34. Utah Agricultural Experiment Station, Utah State University, Logan, Utah.
21. THURBER, D. (1965). The concentrations of some natural radioelements in the waters of the Great Basin. Bull. Volcanol. 28, 195-201.
22. BELL, K. G. (1956). Uranium in precipitates and evaporites. U.S. Geological Survey Professional Paper 300:381-386.
23. MAYNARD, J. B. (1983). Geochemistry of sedimentary ore deposits. Published by Springer-Verlag, New York.
24. HAMBLETON-JONES, B. B. and TOENS, P.D. (1978). The geology and geochemistry of calcrete/gypcrete uranium deposits in duricrust: Namib Desert, South West Africa (Abstract). Economic Geology 37:1407-1408.
25. MANN, A. W. and DEUTSCHER, R. L. (1978). Genesis principles for the precipitation of carnotite in calcrete drainages in Western Australia. Economic Geology 73:1724-1737.
26. BRIOT, P. (1982). Formation of some uraniferous ores. Miner. Deposita 17:151-157. Title/abstract in English translation in Chem. Abstr. 96:202782z.
27. BRIOT, P. (1983). Hydrogeochemical environment of uraniferous calcrete from Yeelirrie (Western Australia). Miner. Deposita 18:191-206. Title/abstract in English translation in Chem. Abstr. 99:161675h.
28. RAWSON, R. A. (1980). Uranium in Todilto limestone (Jurassic) of New Mexico - example of a sabkha-like deposit. Pages 304-312 in: Rautman, C. A. (Ed.). Geology and mineral technology of the Grants

uranium region 1979. Memoir 38, New Mexico Bureau of Mines & Mineral Resources, Socorro, New Mexico.
29. LAUL, J. C., SMITH, M. R. and HUBBARD, N. (1985). Behavior of natural uranium, thorium, and radium isotopes in the Wolfcamp brine aquifers, Palo Duro Basin, Texas. In: Scientific basis for nuclear waste management VIII, Mat. Res. Soc. Symp. Proceedings 44: 475-482.
30. DUFFY, C. J. and OGARD, A. E. (1982). Uraninite immobilization and nuclear waste. LA-9199-MS. Los Alamos National Laboratory, Los Alamos, New Mexico.
31. OSMOND, J. K. (1980). Uranium disequilibrium in hydrogeologic studies. Chapter 7, pages 259-282 in: Fritz, P. and Fontes, J. Ch. (Eds.). Handbook of environmental isotope geochemistry, volume 1, the terrestrial environment, A. Published by Elsevier Scientific Publishing Co., Amsterdam.
32. Smith, M. J. et al. (1980). Engineered barrier development for a nuclear waste repository in basalt: an integration of current knowledge. RHO-BWI-ST-7, Rockwell Hanford Operations, Richland, Washington.
33. BOWIE, S. H. U. and PLANT, J. A. (1983). Natural radioactivity in the environment. Chapter 16, pages 481-494 in: Thornton, I. (Ed.). Applied environmental geochemistry. Academic Press Geology Series. Published by Academic Press, London.
34. MULLER, A. B. and DUDA, L. E. (1985). The uranium-water system: behavior of dominant aqueous and solid components. SAND83-0105, Sandia National Laboratories, Albuquerque, New Mexico.
35. COLLINS, G. A. (1975). Geochemistry of oilfield waters. (Developments in petroleum science, 1). Published by Elsevier Scientific Publishing Company, Amsterdam.
36. RICHARDS, F. A. (1965). Anoxic basins and fjords. Volume 1, Chapter 13 in: Riley, J. P. and Skirrow, G. (Eds.). Chemical oceanography. Published by Academic Press, London.
37. GOLDBERG, E. D. (1965). Minor elements in sea water. Volume 1, Chapter 5 in: Riley, J. P. and Skirrow, G. (Eds.). Chemical oceanography. Published by Academic Press, London.
38. ROBBINS, E. I. (1983). Accumulation of fossil fuels and metallic minerals in active and ancient rift lakes. Tectonophysics 94:633-658.
39. KELEPERTSIS, A. E. (1981). The geochemistry of uranium and thorium in some lower carboniferous sedimentary rocks (Great Britain). Chemical Geology 34:275-288.
40. BOROVEC, Z., KRIBEC, B. and TOLAR, V. (1979). Sorption of uranyl by humic acids. Chemical Geology 27:39-46.
41. BOROVEC, Z. (1981). The adsorption of uranyl species by fine clay. Chemical Geology 32:45-48.
42. CLARKE, F. W. (1924). The composition of the river and lake waters of the United States. United States Geological Survey, Professional Paper 135. U.S. Department of the Interior, Washington, D.C.
43. MORSE, J. W., SHANBAG, P. M., SAITO, A. and CHOPIN, G. R. (1984). Interaction of uranyl ions in carbonate media. Chemical Geology 42:85-99.
44. BUTTS, D. S. (1977). Solar evaporation chemistry of Great Salt Lake brines. Pages 125-129 in: Greer, D. C. (Ed.). Desertic terminal lakes. Proceedings from the International Conference, Weber State College, Ogden, Utah, May 2-5, 1977. Published by Utah Water Research Laboratory, Utah State University, Logan, Utah.

NATURAL ANALOGUES OF RADIONUCLIDE MIGRATION IN SEDIMENTS IN BRITAIN

P.J. HOOKER[1], N.A.CHAPMAN[1], A.B. MacKENZIE[2], R.D. SCOTT[2] & M.IVANOVICH[3]

1. British Geological Survey, Keyworth, Nottingham, NG12 5GG, UK
2. Scottish Universities Research & Reactor Centre, East Kilbride, Glasgow, G75 OQU, UK.
3. UKAEA, Building 7, Harwell Laboratory, Oxfordshire, OX11 ORA, UK.

Summary

Confidence in long-term predictions of radionuclide migration from a repository engineered within a shallow sedimentary sequence depends on the quality and accuracy of the relevant computer programs that are applied in the safety assessment. Far-field research models need to incorporate the correct mechanisms and geochemical processes of mobilisation, transport and retardation. A major theme, therefore, of this three year study is to examine a number of localities where pitchblende veins are associated with sediments and to establish geochemical relationships of speciation and distribution of the natural decay series elements. The principal processes of interest pertaining to these elements include mobilisation and diffusion into clays, retention onto organic material, and their isotopic interactions with colloids. Data are presented for two uraniferous localities under investigation, namely Needle's Eye on the Solway Firth coast near Dalbeattie, Scotland and a disused uranium mine at South Terras in Cornwall. The results illustrate the active processes of interest and provide a tentative basis for model testing.

1. Introduction

On the basis of earlier Survey work carried out under various uranium exploration programmes, the two analogue sites were chosen as being suitable localities to study uranium mobilisation and migration from discrete enriched sources into adjacent sediments. Each one (Figure 1) is in a shallow low temperature weathering environment, and each affords a relatively easy opportunity to derive geochemical data for the U/Th decay series radioisotopes. The results can be understood in terms of leaching, transport by advecting surface or groundwaters, perhaps involving suspended particulates, diffusion into clays, and retardation by organic material. The overall objective is to collect data for comparison with computer model calculations relating to long-term migration. This can be done in either a quantitative way, or in a qualitative manner, providing evidence for a particular process, or demonstrating the integrated effect of a variety of processes (1, 2).

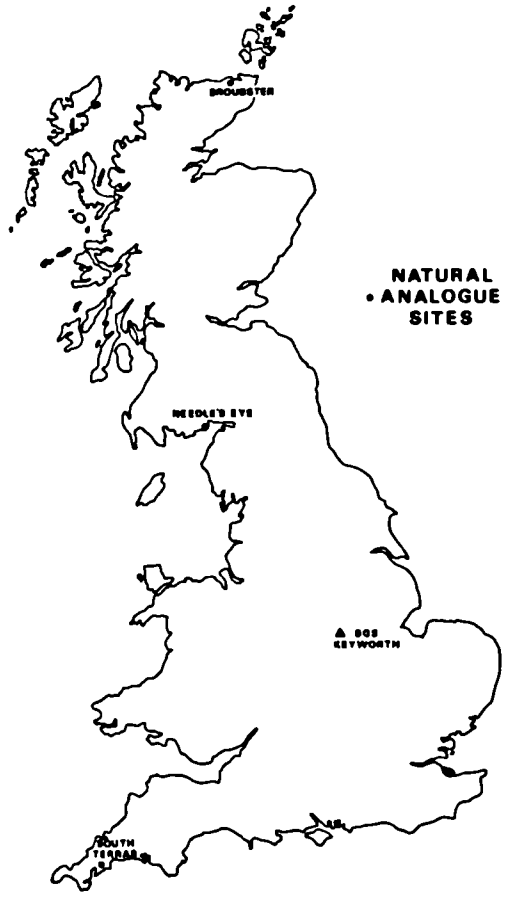

Figure 1: Natural analogue localities

2. Needle's Eye

2.1 Geological setting and objectives

The Southwick coast of the Solway Firth estuary in the Southern Uplands of Scotland is intersected by a suite of mainly northwest striking fissure veins which have been dated at about 185 + 20 Ma (3). At the Needle's Eye locality (Figures 2 and 3) the veins contain pitchblende and extend northwards for about 60m from the top of the cliff beneath periglacial deposits. They have been exposed in the cliff and traced radiometrically seawards for about 20m beneath mudflats forming a saltmarsh

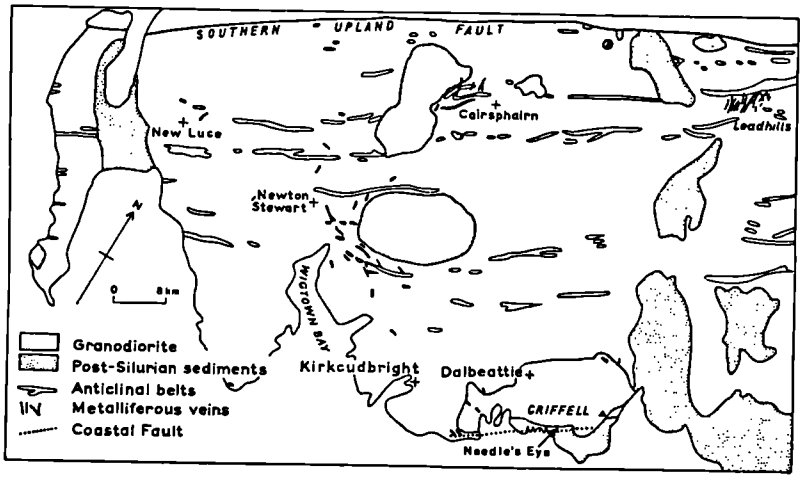

Figure 2: Sketch map, showing distribution of mineral veins and anticlinal belts within the western Southern Uplands (from ref. 3)

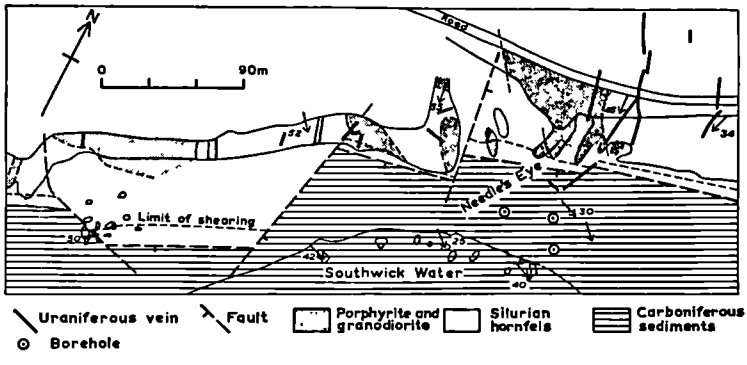

Figure 3: Geological map of Southwick cliffs and shore at the Needle's Eye site (after ref. 3).

known locally as the Merse. These post-glacial (ca. 10,000 years old) flood plain sediments mainly overlie a platform of Lower Carboniferous rocks, and represent a relatively stable accumulation of clay-rich estuarine alluvium. Apart from the vein anomalies, radiometric evidence is available for dispersion of leached uranium into the organic-rich top layers of the foreshore sediments, and for the deposition of anthropogenic radionuclides derived from weapons testing fallout and Sellafield effluent (4).

The prime objective at this natural analogue site is to obtain a concentration profile for the uranium decay series radionuclides in the clays of the sediments immediately overlying a pitchblende bearing vein situated about 20m from the base of the cliff. In order to establish whether or not uranium dispersed from the cliff veins could influence the required profiles at the proposed sampling site, a larger scale study of uranium migration in the area was necessary. This has involved analysing surface and groundwaters for uranium series elements, and the measurement of the radioelements in two sections excavated in the Merse deposits; the depth profiles of these can be regarded as 'controls'.

2.2 Results

The first of the two control sections (Pit 1) was dug in a peat bog area close to the base of the cliff in which the veins had been exposed by trenching. The second control point was chosen about 80m east of Pit 1 away from the vein outcrops in the cliff. This second control site (Pit 5) was one of a series lined across the Merse to the sea.

Pit 1 was found to be organic rich and anoxic from the surface to a depth of 110cm where bedrock was encountered. The control site was sampled in 10cm increments and some analytical results are shown in Table I.

Table I: Analytical data for the control sediment section of Pit 1, Needle's Eye.

Depth (cm)	Wet:Dry Ratio	% Loss on Ignition	% Organic Matter	% Pyrite	$^{137}Cs_{\bar{1}}$ cpmg	C-14 Age (yrs. BP)
0-10	5.10	86.3	72	0.31	0.056	NA
10-20	6.64	83.0	69	0.29	0.045	0
20-30	5.62	60.6	62	0.28	0.013	0
30-40	4.18	47.3	38	0.10	0.017	0
40-50	2.69	24.8	29	0.12	ND	0
50-60	3.07	30.8	26	0.11	ND	505
60-70	4.22	45.2	36	0.28	ND	520
70-80	3.40	34.4	37	0.29	ND	605
80-90	2.54	21.2	19	0.30	ND	670
90-100	2.90	25.4	25	0.18	ND	790
100-110	1.91	9.2	8	0.09	ND	NA

ND = not detected (below detection level); NA = not analysed

The organic content correlates with the % loss on ignition and shows a decrease from 72% at the surface to 8% at 100-110cm, with a sharp decrease at the 40-50 cm layer. This trend is matched by a decrease in the wet to dry ratio from 5.10 at the surface to 1.91 at 100-110cm with a minimum again being observed in the 40-50cm layer. The profile can thus be broadly split into two main sections: an organic rich layer of very high water content from the surface to about 45cm,underlain by a layer of lower water content and decreasing organic concentration with depth. Samples collected with a hand auger from the siltier less organic rich sediments at about 20m out from the cliff base likewise showed a saturated upper section with typically a particularly fluid layer at about half a metre's depth. This thin fluid layer represents a practical obstacle to coherent sampling beneath it.

The upper layer has been demonstrated to be'modern' by the presence of Cs-137 to a depth of 40cm. The absence of Cs-134 from these samples

suggests that the radiocaesium originates from bomb fallout rather than Sellafield waste. The presence of radiocaesium to 40cm depth is indicative of either mixing or rapid (relative to a 30 year half life) advection/diffusion of groundwater to this depth. These processes are responsible for the zero carbon-14 ages found for the layers down to 50cm (Table I and Figure 4).

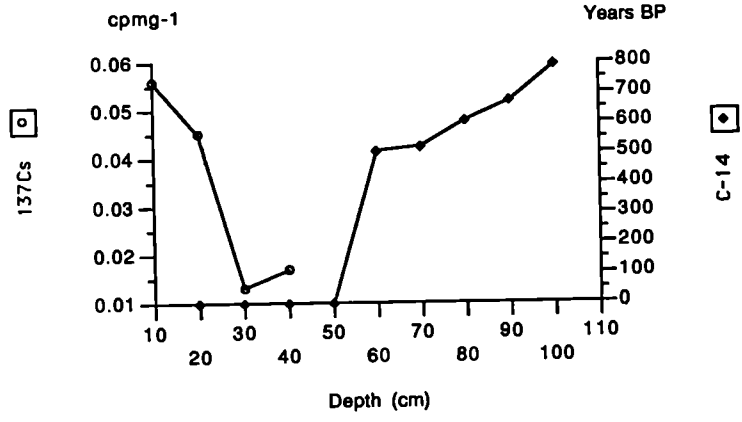

Figure 4: Depth profiles of Cs-137 and carbon-14 ages in control Pit 1, Needle's Eye

How far the apparent ages of the lower more clay-rich samples reflect an accurate time of deposition is open to question, and it would be useful to analyse deep samples of the deposits at the final proposed sampling locality to help constrain such times of perturbation.

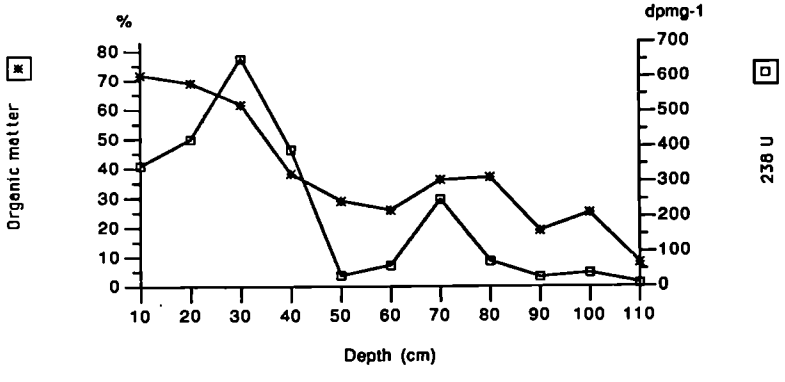

Figure 5. Uranium and organic matter profiles in control Pit 1, Needle's Eye

Table II shows the uranium and thorium results for the depth sections of Pit 1. The uranium concentrations furnish a profile broadly correlating with the organic matter determinations (Figure 5). The highest uranium values were measured in the layers above 40cm peaking at 659 dpm g^{-1} or 884ppm. The relative enrichment can be seen by comparison with the highest value of 9.2 dpm g^{-1} (153 m Bq g^{-1}) observed for the Loch Lomond sediment profile (5). With the exception of the 80-90 cm sample, all of the 234U/238U activity ratios were less than 1, suggesting a slight systematic depletion of 234U.

Table II. Uranium and thorium data for control sediments from Pit 1, Needle's Eye.

Depth (cm)	^{238}U	^{234}U	$^{234}U/^{238}U$	^{230}Th	$^{230}Th/^{234}U$	^{232}Th
0-10	390*	379*	0.97	5.4*	0.014	BDL
	348	342	0.98	-	-	-
10-20	422	400	0.97	-	-	-
	433	418	0.97	3.5	0.0084	0.30*
20-30	659	636	0.97	-	-	-
	591	581	0.98	7.6	0.013	0.59
30-40	394	377	0.96	9.3	0.025	0.67
40-50	30.4	29.6	0.97	2.51	0.085	1.00
	33.0	34.0	1.03	2.79	0.082	0.97
50-60	63.2	61.9	0.98	-	-	-
	58.9	58.2	0.99	2.76	0.047	0.94
60-70	250	245	0.98	5.13	0.021	1.26
	243	242	1.00	-	-	-
70-80	71.5	70.5	0.99	-	-	-
	70.5	68.6	0.97	2.43	0.035	0.98
80-90	27.8	28.2	1.01	2.83	0.10	1.09
	26.0	27.1	1.04	-	-	-
	28.4	29.1	1.02	-	-	-
90-100	40.0	39.6	0.99	-	-	-
	38.0	37.8	0.99	2.34	0.062	0.63
100-110	18.0	17.7	0.98	1.96	0.11	1.22
	17.7	18.0	1.02	1.95	0.108	1.08
Pitchblende from vein in cliff	$1.49_5 \times 10^5$	1.5×10^5	1.03	$2.82_5 \times 10^5$	1.83	BDL

*dpm g^{-1} dry weight. BDL = below detection level. Determined at SURRC by alpha spectrometry

It is interesting to see similar features present in the results for control Pit 5 (Table III) which revealed a thinner accumulation of sediments. Despite there being an order of magnitude less uranium in the Pit 5 deposits there is still seen a two layer distinction in distributions (Figure 6), with the top more organic rich horizon holding more uranium than the deeper section. Similar concentrations of Th-232 were measured for both controls, reflecting common deposition histories. At the same time, there are also very similar activities for Th-230, even though there is at least 10 times more parent U-234 in the sediments of Pit I. This indicates a tranport mechanism for Th-230 that is decoupled from U-234; control by particulates suspended in the incoming groundwaters is a possible explanation.

Table III: Available uranium and thorium data for control sediments from Pit 5, Needle's Eye.

Depth (cm)	^{238}U	^{234}U	$^{234}U/^{238}U$	^{230}Th	$^{230}Th/^{234}U$	^{232}Th
0-5	9.13*	9.16*	1.00	2.23*	0.24	0.37*
5-10	10.2	10.1	0.99	2.09	0.21	0.32
10-15	21.7	19.8	0.91	2.98	0.15	0.69
15-20	48.9	46.4	0.95	4.83	0.10	0.83
20-25	63.9	61.1	0.96	5.38	0.088	0.92
25-30	62.4	60.1	0.96	-	-	-
30-35	17.4	17.1	0.98	-	-	-
35-40	27.2	26.5	0.97	2.78	0.105	1.01
40-45	27.8	26.8	0.96	2.78	0.104	1.26
45-50	24.6	23.6	0.96	-	-	-
50-55	25.9	25.7	0.99	-	-	-
55-60	3.44	3.30	0.96	1.03	0.31	1.25

* dpm g^{-1} dry weight. Analysed by alpha spectrometry at SURRC.

These sediment uranium distributions require determinations of uranium in the associated surface and groundwaters in order to define an overall budget for mass transport. Some data are presented in Table IV. These results show how the U-poor surface waters percolating through the fractures of the Palaeozoic rocks of the cliff become enriched in uranium. After contact with the organic rich sediments near the base of the cliff, the emerging surface waters are again depleted.

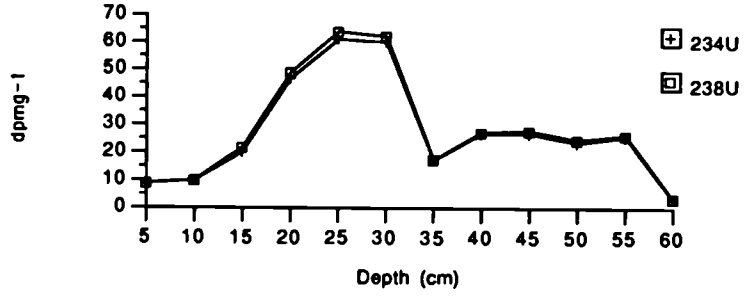

Figure 6. Uranium isotope profiles for control Pit 5, Needle's Eye

Table IV. Uranium series results for some water samples from Needle's Eye.

Sample	Date collected	^{238}U	^{234}U	$^{234}U/^{238}U$
Surface drain water at cliff top	Nov. 1985	0.73* ±0.05	0.84* ±0.05	1.15 ±0.10
Groundwater from cliff fissure	Oct 1985	18.2	16.6	0.91
	Nov 1985	28.8	27.8	0.96
Groundwater from upper 20cm of Pit 1	Oct 1985	46.9	44.8	0.96
Small stream near proposed sampling site, 20m from cliff	Oct 1985	2.05	1.95	0.95

* dpm l^{-1}; determined at SURRC

2.3 Discussion and conclusions.

The fissure sampled for groundwater is separated from a uranium mineralization vein by a distance of about 10m, suggesting that the bedrock of the cliff in general may also have to be regarded as a source of uranium. The high concentration of uranium in the anoxic soil at the base of the cliff in conjunction with the low values in the stream draining from the area suggest a highly efficient removal of uranium upon contact with the soil. A simple model involving leaching of uranium from the cliff as the soluble hexavalent ion followed by reduction to an insoluble tetravalent species on contact with the reducing soil at the base of the cliff can be suggested. The systematic depletion of 234U relative to 238U noted above for the soil profile is again observed for the water samples.

The following general conclusions can be drawn:

1. Uranium migration occurs in groundwater solution from the cliff area.
2. Efficient uranium fixation occurs in the upper organic rich layers of the soils at the foot of the cliff; the control sections showed decreasing levels of uranium with depth.
3. Uranium from the cliff area will contribute an insignificant amount of U at the proposed site for final depth profiling at 20m from the base of the cliff.

3. Studies at South Terras, Cornwall.

3.1 Introduction

The southern flank of the St Austell granite in Cornwall is characterised by a variety of mineral lodes (6,7). At South Terras a uranium lode was mined and until 1925 the tailings were re-worked for uranium and radium (6). Disused since 1929 the mine still has a number of spoil heaps which act as sources of leached natural decay series elements migrating into adjacent soils and streams. The North Shaft study area of the mine is bounded by the River Fal on its western margin. A tributary stream flows along the northern edge of the site. About 10m south of this stream lie two heaps. The streamwaters and intervening soils and groundwaters have been collected and analysed for U/Th series elements with the objective of finding evidence of colloidal transport.

3.2 Results

Two soil columns of alluvial silts were hand augered for analysis at points A and B, respectively 5 and 1.5m south of the stream. The data are presented in Table V. There are very high levels recorded for the top 15cm of the soils which are rich in organics and Fe_2O_3. Especially interesting are the disequilibria in the 230Th/234U ratios while the depletions in Th-228 with respect to Th-232 (Figure 7), imply recent mobilisation of parent Ra-228 (half-life of 5.75 years). Reinforcing this idea are the results in Table VI which refer to a groundwater collection made in pit ST1 dug 1m from the stream near hole B. The groundwater which was collected at 60cm below ground level in this pit had a pH of 6 and showed a 228Th/232Th ratio of 3.9.

Table V. South Terras radiometric data

Sample (depth cm)	Harwell Code	Isotopic content (dpmg-1) U-238	U-234	Th-230	Th-232	Th-228	Activity ratios U-234/U-238	Th-230/U-234	Th-230/U-238	Th-228/Th-232
B/1 (0-15)	3242	1631 5 ±24.4	1614 4 ±24 2	2339 4 ±32.1	3 10 ±0.37		0.99 ±0.01	1 45 ±0.03	1 43 ±0.03	
B/2 (15-30)	3243	32 89 ±1.22*	32 88 ±1 22	20 88 ±0.30	1 52 ±0.03	1 44 ±0.03	1 00 ±0.01	0 64 ±0.03	0 64 ±0.03	0 95 ±0 02
B/3 (30-46)	3244	53 11 ±2 57	53 79 ±2 60	68 04 ±1 02	1 20 ±0 03	1.19 ±0.03	1 01 ±0.01	1 27 ±0.07	1 28 ±0.07	0 99 ±0.02
B/4 (46-61)	3245	44 80 +1.41	45 36 ±1.42	82 99 ±1.27	1 06 ±0.02	0 92 ±0.02	1 01 ±0.00	1.83 ±0.07	1 85 ±0.07	0 87 ±0.02
B/5 (61 76)	3246	60 25 ±2 46	61 06 ±2 49	112 02 ±1.99	1.44 ±0.04	1 35 ±0 04	1 01 ±0.01	1.84 ±0.08	1.86 ±0.08	0 94 ±0.02
B/6 (76-91)	3247	24 96 ±0 78	25 14 ±0 78	23 64 ±0.38	1 29 ±0.03	1 26 ±0.03	1.01 ±0.01	0.94 ±0.04	0 95 ±0 04	0 98 ±0 02
A/1 (0-15)	3233	400 2 ±10 0	414 5 ±10 3	697 0 ±15.3	2.07 ±0.22	1 58 ±0 27	1.04 ±0.01	1 68 ±0 06	1.74 ±0 06	0.76 ±0.15
A/5 (60-75)	3237	54 94 ±1 63	54 47 ±1 62	14 75 ±0 70	0 33 ±0.01	0 09 ±0 03	0.99 ±0.03	0 27 ±0 02	0 27 ±0.02	0 29 ±0 03
A/9 (120-135)	3241	8 37 ±0 34	9 36 ±0 36	1.75 ±0.15	0 34 ±0.06		1.12 ±0.06	0 19 ±0.02	0 21 ±0.02	

*All quoted errors are 1σ uncertainties due to the nuclear counting statistics only

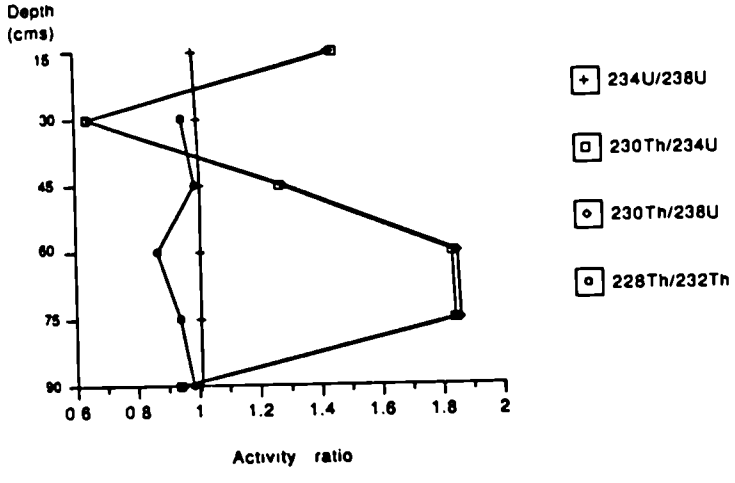

Figure 7. U/Th isotope profiles for augered section B, South Terras

Table VI: Comparison of U/Th series isotopes betwen pore water and soil particles in Pit ST1, South Terras

Sample	(U)	(Th)	$^{234}U/^{238}U$	$^{230}Th/^{234}U$	$^{228}Th/^{232}Th$
ST1 pit pore water (filtered)	50.2* ±2.1	0.67* ±0.21	1.03 ±0.03	0.14 ±0.01	3.9 ±1.5
ST1 soil particulates	519** ±38	14.5** ±0.8	0.81 ±0.01	0.51 ±0.04	1.17 ±0.97

* ppb ** ppm All errors 1σ. Harwell data.

Determinations on the stream water collections gave variable activity ratios but with 234U/238U generally ≥ 1, and with unusually high 230Th/-234U ratios ranging from 0.6 - 50. Uranium contents varied from 0.14 to 1.6 ppb (1.9 ppb for R. Fal); associated thorium concentrations were high ranging from 0.19 to 0.74 ppb (0.37 ppb for R. Fal).

3.3 Discussion

Active migration of U/Th isotopes in a direction away from the spoil heaps and surrounding shallow sediments into the stream and river has been demonstrated. The observed activity variations in the sediment profiles can be related to factors such as organic matter contents, the presence of secondary iron oxides, and the permeabilities of different layers. Some evidence has indicated that Th isotopic abundances in the silty pore waters bear some relationship with the suspended particulates. Likewise, the high Th-230 and Th-228 levels of the stream waters support the notion of pseudo-colloidal transport, but quantifying the speciation of this process will require refined sampling procedures.

4. Discussion

Radioactive disequilibria studies at both sites provide a potentially valuable insight into past and current migration processes for U/Th in near surface sediments. It is notable that for both situations the distributions of U favour the solid phase over the pore water phase by four orders of magnitude. This may represent a crude approximation to a Kd value of 10^4 ml/g for groundwater uranium interacting with organic rich and relatively reducing alluvial silts . Generally it is a difficult matter to derive an accurate in-situ Kd value for natural series isotopes (8).

Th-230 levels have been observed which exceed the grow-in expectations from parent U-234 for the Needle's Eye sediments. Similarly there is evidence of enhanced Th-230 additions to the stream waters at South Terras implying a tranport mechanism by particulates/pseudo-colloids. The ground and surface waters at South Terras also contain high 228Th/232Th ratios indicating preferential dissolution/surface-sorption of Ra-228.

Common to both sites are fixations of uranium in organics or iron oxyhydroxides and the mechanisms probably relate to reduction of hexavalent uranium. Whether these processes in such superficial and heterogeneous sediments can be sufficiently modelled depends not only on an understanding of the mechanisms but knowledge of the groundwater flows. Nevertheless, there is already much quantitative information emerging from

these studies and when the groundwater compositions have been determined and filtration tests carried out there will be a firmer basis for modelling.

ACKNOWLEDGEMENTS

Thanks are extended to BGS colleagu es who have contributed to this work, particularly Dr T K Ball, Dr I R Basham and Mr P D Roberts. Permission to work at Needle's Eye was given by the Scottish Wildlife Trust. This paper describes work carried out for the Department of the Environment as part of its research programme into radioactive waste management.

REFERENCES

1 CHAPMAN, N.A. and SMELLIE, J.A.T. (1986). Introduction and Summary of the Workshop on Natural Analogues to the Conditions around a Final Repository for High-level Radioactive Wastes. Chem. Geol. Spec. Iss. 55 (3/4), Proc. of Workshop on Natural Analogues, Lake Geneva, Wisconsin, USA, Oct. 1984.

2 COME, B and CHAPMAN, N.A. (editors)(1986). Natural Analogue Wo rking Group. First Meeting, Brussels, November 5-7, 1985. Commission of the European Comunities, Luxembourg, EUR 10315-EN, 223 pp.

3 MILLER, J.M and TAYLOR,K. (1966). Uranium mineralization near Dalbeattie, Kirkcudbrightshire. Bulletin Geol. Survey of Great Britain, 25, 1-18.

4 JONES, D.G., MILLER, J.M. and ROBERTS, P.D. (1984). The distribution of 137Cs in surface intertidal sediments from the Solway Firth. Marine Pollution Bulletin, 15, 187-194.

5. HOOKER, P.J., MacKENZIE, A.B., SCOTT, R.D., RIDGWAY, I.M., McKINLEY, I.G. and WEST J.M.(1985). A study of natural and long-term(10^3 - 10^4 yr) elemental migration in saturated clays and sediments. Part III. Rep. Fluid Proc. Res. Gp., Br. Geol. Surv. FLPU 85-9, British Geological Survey, Keyworth, UK, 76pp.

6 DINES, H.G. (1956). The metalliferous mining region of south-west England. Memoir of the Geol. Surv. of Great Britian. Vol.II, HMSO, London.

7 BALL, T.K., BASHAM, I.R. and MICHIE, U. McL (1982). Uraniferous vein occurrences of south-west England - paragenesis and genesis. In: Vein-type and similar uranium deposits in rocks younger than Proterozoic. IAEA, Vienna, TC-295/9, 113-158.

8 KRISHNASWAMI, S., GRAUSTEIN, W.C., TUREKIAN, K.K. and DOWD, J.F. (1982). Radium, thorium and radioactive lead isotopes in groundwaters: application to the in situ determination of adsorption-desorption rate constants and retardation factors. Water Resources Research, 18, 1633-1675.

Biogeochemical Studies of the Ra, U, Th and REE Deposit at Morro do Ferro: A Qualitative Application to Improve Confidence in Radionuclide Immobilization Processes

Paul Linsalata*, Eduardo Penna Franca# and Merril Eisenbud* *New York University Medical Center Institute of Environmental Medicine, Tuxedo, New York, U.S.A., #Universidade Federal do Rio de Janeiro, Rio de Janeiro, RJ, Brazil

A 60-80 million year old thorium and rare earth element (REE) deposit located within a small hill (Morro do Ferro or MF) in the state of Minas Gerais, Brazil, contains virtually none of the attributes deemed essential for the isolation of long-lived radionuclides emplaced in deep geological formations. High grade ore (0.5 to 3.0% Th and REE's) is found within 50m of the hill's surface on the southern flank with the richest portions within 10m of the surface. The underlying rock at MF (fine-grained nepheline syenite or tinguaite) is so highly altered (down to at least 400m) due to both weathering and hydrothermal activity such that apart from differences in radioactivity levels, one cannot distinguish the original host rock from the "ore" (Barretto and Fujimori, 1984). Perhaps the only "protection" afforded the ore body is a 1-3m surface cover composed of large aggregates of lateritic soil as radioactive as the "ore" beneath it, and several subsurface magnetite dikes (1-5m thick) which outcrop at various points along the southern face and have probably played a role in supporting the hill's structure. An extensive network of magnetite (and associated oxidation products) veinlets occurs randomly throughout the hill.

Precipitation at the site averages 170 cm y^{-1} and occurs mostly during a four month rainy season. The groundwater level is a subdued replica of the surface topography, with recharge from precipitation and discharge into a network of seepages at or near the hill's base forming a stream which flows year-round (base flow = 0.7 m^3 min^{-1}). Permeability measurements in and near the ore body give hydraulic conductivities between 10^{-4} and 10^{-5} cm s^{-1} and typical groundwater velocities of 7 to 34 cm day^{-1} (assuming an effective porosity of 2%).

Groundwater chemical data are very fragmentary and are based on samples taken during both dry and wet periods from an excavated adit and from relatively shallow bore holes within or near to the deposit (five holes with depths of 25-35m). Groundwaters were found to be acidic (pH 4.5-6.5), oxidising (Eh 300-500 mV) and apparently relatively dilute although quite variable with respect to complexing anion concentrations eg., HCO_3^- (5-10 as $CaCO_3$), F^- (0.02-0.8), $H_2PO_4^-$ (0.01-0.6) and SO_4^{-2} (0.02-0.6), (in ppm after Pivette, 1983 and others). Dissolved organic carbon concentrations (DOC < 0.45 uM) in groundwaters are considerably more consistant than are inorganic complexing anion concentrations and have been reported to range between 1-5 mg C l^{-1}. Although most of the DOC is associated with compounds having molecular weight equivalent diameters < 1,000 (50%), most of the Th (~75%) is associated with the humic fraction, particularly those compounds with equivalent diameters > 10,000 (Miekeley et al., 1985). A high positive correlation has been reported between "dissolved" Th and colloidal organic C (i.e., DOC > 1000 MWE) in groundwaters suggesting that Th is transported primarily in association with colloidal organic compounds.

Despite the physicochemical characteristics of the MF described above, the present day mobilization rates of elements with characteristic oxidation states of +4 (Th), +3 (La or Nd) and +2 (Ra) have been shown to be extremely low. Mean concentrations (in ug l^{-1}) in filtered (< 0.45 uM) stream water collected during baseflow regimes (i.e., seepage water) are 0.05 (Th), 0.3 (U), 0.3 (La), 0.8 (Ce), 1.7 pCi l^{-1} (Ra-228) and 0.2 pCi l^{-1} (Ra-226). Based on the ratios of the measured annual flux of these elements in solution to the respective ore body inventories, the fractional removal rates resulting from groundwater solubilization and seepage/stream transport are on the order of 10^{-9} y^{-1} for Th, Ce and La and 10^{-7} y^{-1} for Ra-228. Physical transport of the REE and Th by overland erosion during stormflow regimes results in mobilization rates which are several orders of magnitude greater. Based on the chemically analogous behavior of quadravalent Th and Pu (IV) (Th in surface environs may serve as a model for Pu in subsurface, reducing environs where Pu (IV) is expected to predominate), of trivalent

La and Am, Cm (III), and of Ra-228 and Ra-226, the low mobilization rates (long residence times) determined at MF for the natural analogues of the transuranic actinides under these quite unfavorable conditions, should insure the in-situ decay of the respective transuranic nuclides as well as of isotopes of Th and Ra-226 given the much more favorable conditions for isolation expected in a repository.

Based primarily on x-ray diffraction studies (Fujimori, 1983), a major reason for the retention of Th and REE's (as well as Ra) at MF appears to be related to the sorption of these elements on surfaces of kaolinitic clays dispersed throughout the weathered mantle. More specifically, preliminary findings using sequential leaching agents for removing these elements from exchangeable, carbonate, reductant-soluble (oxyhydroxides of Fe, Mn and Al) and organic phases of surface and subsurface bulk "ore" samples, have shown that between 15 to 50% of the total Th and REE content are associated with the reductant-soluble phase. Minor percentages occur in the remaining phases and in general, about 50% or more of the total concentrations are not released upon extraction with the various agents used.

It is probable that the same physicochemical processes which limit the mobilities of Th, REE's and Ra at MF may also limit the availability of these elements for incorporation into terrestrial food chains. Since 1983, work has progressed in establishing soil to plant and soil to animal transfer of these elements within the Pocos de Caldas plateau, which has the MF at its center. Concentration ratios (CR's = ug g^{-1} dry plant/ug g^{-1} dry soil) have been obtained in a field study involving the analysis of the edible portions of over 50 vegetable samples and 30 soil samples from 11 farms on the plateau. Plant/soil CR's were found to be lognormally distributed with median values listed in decending order as follows: Ra-228 (1.4×10^{-2}) ~ Ra-226 (8.6×10^{-3}) > La (5.5×10^{-4}) ~ Nd (3.4×10^{-4}) ~ Ce (2.6×10^{-4}) > Th (6.0×10^{-5}). Simplified, the order of plant uptake is: Ra(II) > REE(III) > Th(IV), where the stable oxidation state is indicated in parenthesis. Work is currently in progress on determining the relative availability of these elements in soil as well as the concentrations within animal tissues.

Finally, the ingestion of Th and REE's by members of two farm families living within the MF watershed was estimated by measuring the content of these elements in daily fecal samples. The rational here is that since these elements are poorly absorbed across the mammalian gut, the rate of output in the feces closely parallels the rate of intake. These studies revealed annual intakes of Th and La on the order of 4 and 12 mg y^{-1}. Since one family living only 1.5 km from the MF derived it's drinking and irrigation water from the same stream that receives drainage from the deposit, it was possible to estimate that only 5-9% of the annual intakes of Th and La was derived from consuming this water. The annual intake of Th-232 was determined to be less than 1% of the annual limit of intake recommended by the ICRP for members of the general public.

Although our studies at MF are far from complete, the data obtained to date from both geochemical and field biological programs suggest that although the actinide elements are hazardous when absorbed into the body, there exist geochemical barriers that would, under ordinary conditions, prevent these elements from leaving a waste repository and being incorporated into food and water.

The Poços de Caldas Project Feasibility Study: 1986-7.

John A. T. Smellie, Luiz Barroso Magno Jr[1], Neil A. Chapman[2], Ian G. McKinley[3], and Eduardo Penna Franca[4]

Swedish Geological AB, Uppsala, Sweden, [1]Nuclebras, Poços de Caldas, Brasil, [2]British Geological Survey, Keyworth, UK, [3]Eidg. Inst. fur Reaktorforschung, Wurenlingen, Switzerland, [4]Institute of Biophysics, Federal University of Rio de Janeiro, Brasil.

1. INTRODUCTION

Poços de Caldas is a small spa town lying in the 35 km diameter volcanic plateau of the same name, some 250km north of Sao Paulo in Brasil. The geology of the region comprises a complex of alkaline intrusives of Cretaceous age. These are associated with localised hot springs, deep hydrothermal weathering, and rich deposits of U, Th and rare earth elements (REE's). Eisenbud et al (1984) recognised the potential of the area for natural analogue studies in his work on the Th/REE deposit of Morro do Ferro, which assessed rates of mobilisation of Th as a Pu analogue. During the course of this work detailed reviews of the regional geology were prepared (summarised by Barretto and Fujimori, 1986). This work sparked off further interest in the potential of the area at a time when natural analogue studies were coming back into vogue, and a joint Swedish/Swiss/UK group visited both Morro do Ferro and the nearby C-09 Osamu Utsumi uranium mine in 1985 to consider a new programme of work. It was clear that given the technical interests of the groups concerned a number of attractive analogue possibilities were available and, with the interest and assistance of Nuclebras (the C-09 mine operators), the Brasilian Nuclear Energy Commission (CNEN), and several local Universities, a preliminary programme was defined. This programme took advantage of the very high U/Th series and REE concentrations in rocks which varied from highly altered clay-rich units, through to massive fractured formations, with apparently strong redox control of elemental mobility and distribution, to provide geochemical analogues of a number of processes of general interest and importance (as identified for example in the KBS-3 and Gewahr safety assessments of 1983 and 1985 respectively).

At this time very few analogue studies had attempted to link rock geochemistry to an appropriate hydrogeological system, and this was seen as one of the key areas where this study could contribute. Most 'transport' analogues have tried to to assess radionuclide mobility by using systems where the migration process has long-since ceased, and often took place at considerable depth under high temperatures. It is clear however, that most transport processes of significance to performance assessments take place in relatively shallow, low temperature groundwaters. At Morro do Ferro these have been responsible for the progressive erosion of the ore deposit, the concentration of residual Th and REEs in the near-surface zone, and the gradual mobilisation of Th as soluble and particulate fractions in surface run-off and shallow groundwaters. At the C-09 mine similar processes have concentrated pitchblende (UO_2) during the migration of a redox front which is localised around fracture zones in the rock. The programme was thus formulated to use both these environments as locations for two projects with somewhat overlapping aims. During the course of the 1985 visit simple conceptual models of the hydrogeochemistry of the two sites

were constructed from the sparse data available, and the following objectives identified.

1.1 Original objectives - C-09 mine.

- to determine concentrations and speciations of relevant elements in groundwaters from oxidising/reducing environments and to test existing mineral/solution equilibrium models.
- to study local mobilisation/deposition of uranium-series radionuclides (U, Th, Ra-isotopes) and the geochemical factors involved, paying special attention to processes around the redox front.
- to test models for the calculation of 'in situ' retardation factors of radionuclides in fractured crystalline rock.
- to investigate recent migration of radionuclides into or from the bulk crystalline rock at the contacts of water conducting fractures (extent of matrix diffusion)
- to quantify the role of groundwater colloids in the transport of U and other relevant elements
- to examine the influence of microbial activity on the mobility of radionuclides under natural conditions.

1.2 Original objectives - Morro do Ferro

- to assess the origin and nature of organic and inorganic colloids in this region
- to assess the degree of mobilisation and uptake of Th, other natural series radionuclides and REE as/on colloidal materials or as other (organic) complexes
- to assess colloid mobility through both the unsaturated and saturated zones as a function of distance from source along the flowpath.
- to assess the consequent contribution of colloids to radionuclide retardation/mobility, by integrating field data with laboratory studies of colloid partitioning and stability.
- to examine the influence of microbial activity on the formation and behaviour of colloids

It was recognised that as investigations got under way the original simple models would need to be modified, and that some of the objectives would prove unreachable, whilst further unforseen possibilities might emerge. Consequently the programme was planned to include both a pilot investigation (at the C-09 mine) and a one-year feasibility study aimed at obtaining an extensive spread of basic data in order to evaluate these original objectives. In this paper we report on the findings of this first year, the modifications to the programme that have proved necessary, and the revised targets that we are confident can be achieved in the final two years of the project.

We also use this programmed approach as an object lesson to non-geologists who are keen to use analogue data. Poços de Caldas is proving to be a fine example of the potentials, limitations and frustrations of natural analogues, and a reminder of the complexities of real natural systems.

2. THE FEASIBILITY STUDY

The feasibility study investigations were carried out at both the Osamu Utsumi uranium mine and Morro do Ferro. The main function of this phase of the work was to drill into those parts of the system considered potentially most useful, in order to confirm the simple

geochemical and hydrogeological concepts which had been developed. Suitable borehole locations were selected from large-scale reconnaissance studies of the geology and hydrogeology in these areas, together with borehole data related to earlier prospecting activities. The drilling programme at the two sites was initiated by a pilot hole in the Osamu Utsumi mine (Fig. 1); geological and hydrogeological information from this pilot phase was used to plan and execute the feasibility study phase, which is still in progress at the time of writing.

2.1 Osamu Utsumi Uranium Mine

The air-flush percussion pilot hole was drilled to 99m (Fig. 2), with systematic collection of rock chippings for chemical analysis every 4.5m. Three 10m holes were drilled nearby for hydrological purposes. The two subsequent feasibility study holes (9-1WC11 and 9-1VC24, hereafter referred to as boreholes F1 and F2 respectively; Fig. 2), were drilled using water-flush, rotary coring techniques, which resulted in a recovery rate better than 95%, to depths of 126m and 60m respectively. To avoid undue contamination and excess oxidation influencing the bedrock and the groundwater system, reducing artesian groundwater from an old flooded subterranean gallery system in the mine was used as a flushing medium during drilling. Microbiological sampling and geological logging of the core were carried out in parallel with the drilling, with subsequent sampling of the core for geochemistry/mineralogy. The three deep pilot and feasibility boreholes were geophysically logged, and hydraulically tested using inflatable packers. Significant inflow zones (major fractures) were identified and isolated using hydraulic packer systems, and sampling/monitoring of the groundwaters was carried out.

2.1.1 Geology: The recovered core showed the site to be dominated by tinguaite/phonolite, which is hydrothermally altered throughout the complete thickness drilled. Alteration due to low temperature weathering processes is variable in extent, having been facilitated by deeply plunging fracture zones and heterogeneities in rock properties. In the pilot hole the bedrock was found to be generally oxidised down to 25m, and reduced from 40m depth to the hole bottom, apart from a 1m zone at around 80m which coincided with a hydraulically conductive lamprophyre dyke. The section from 25-40m is characterised by an alternation of thin oxidised/reduced horizons corresponding to a series of penetrating fracture zones. The feasibility hole (F1) consists of phonolitic rock apart from a breccia zone at 105m and a dyke at 11m (Fig. 3). Oxidised bedrock dominates down to 69m. From 80m to the hole bottom at 126m the bedrock becomes increasingly competent and relatively 'fresh', with solution cavities due to leaching of pseudoleucite phenocrysts. The rock is less uniformly fractured than the upper 80m, with a trend to more discrete fractured or highly porous zones, often hydraulically conductive and lined with fresh pyrite, indicating a dominantly reducing groundwater environment. The shallower feasibility borehole (F2) reflects the main features described for the upper part of borehole F1.

The oxidised and reduced phonolites are characterised by the presence of limonite and pyrite, respectively. The oxidised phonolites are barren in sulphides; only hematite, hydrohematite and more diffuse, finely dispersed crystalline Fe-oxides/hydroxides, occur. In contrast, the reduced phonolites are characterised by pyrite with subsidiary sphalerite (sometimes as inclusion in pyrite); the pyrite has in many cases been partly oxidised to hematite/Fe-oxyhydroxides. The sulphides are typically fine-grained and dispersed throughout the rock matrix.

Gamma logging of the two feasibility boreholes (Fig. 3) indicated no major uranium mineralisation, although some fracture/cavity infillings observed from the core can be correlated with a marked peak at around 42m (borehole F1). Otherwise a small peak occurs at the redox boundary at 68m, and another at 104-105m, which correlates with a

washed-out clay horizon, absent from the drillcore, but detectable on the self potential and resistance logs. The point resistance log also shows a change in character between the predominantly oxidised and reduced sections, the main division of which occurs at around 70m depth.

The pilot hole chippings were analysed for U, Mo, Zr, S and K as part of the prospecting programme at the mine complex. Core samples were taken from strategic parts of the feasibility hole cores for specialised studies. These included representative samples from the oxidised and reduced zones, detailed profiles across the four redox fronts intersected, a profile across the water-conducting porous zone at 109.4-110.7m (borehole F1) which is also packered off and being sampled for hydrochemical studies, and samples from sealed and conducting fracture horizons. These samples have been distributed to several laboratories both within Brasil and abroad for a) mineralogical and microchemical investigations, b) whole-rock major and trace element geochemistry, c) whole-rock isotope geochemistry (uranium and thorium series; stable isotopes), and d) porosity, permeability and diffusivity measurements.

The pilot hole samples have uranium concentrations ranging from 100-3160 ppm with the higher contents (300-3160ppm) being associated with the more oxidised bedrock horizons. Sulphur is irregularly dispersed, although lower concentrations occur in the more oxidised horizons. The reduced bedrock is rich in pyrite, which is absent in the oxidised bedrock due to alteration. The K content is fairly uniform in the reduced bedrock, and a significant decrease is apparent in the oxidised bedrock due to weathering processes.

As yet few geochemical analyses are available for the feasibility boreholes. Preliminary investigations have confirmed that kaolinite is the most abundant clay mineral, ranging from 60-100 vol. %, with illite and illite-smectite mixed layers at 5-30 vol%, and subsidiary amounts of chlorite (2-15 vol%). Illite and chlorite show a tendency to decrease with depth. Smectite appears to occur only in the vicinity of the redox fronts, in one sample accounting for up to 70 vol% of the clay fraction. Studies are continuing to refine the clay mineralogy, and determine the relation between the U-content and the clay fractions.

Apart from some potassium depletion around the major conducting zone at about 110m, all the major elements show normal patterns typical of the Poços de Caldas plateau. Uranium is always enriched by a factor of 4 to 50 on the reduced side of the redox fronts, while thorium shows small enrichments on the oxidised sides, and also within the conductive zone at 110m. Rare-earth analyses show a normal pattern with a range of concentrations reflecting mineralogical variations.

The core samples were analysed by gamma spectroscopy in order to obtain approximate uranium concentrations, so that suitable sample sizes and analytical procedures could be selected for alpha spectroscopic analysis. Concentrations of individual nuclides were calculated assuming complete secular equilibrium in the ^{238}U decay chain in the reference material (DL-1A). The strongest uranium mineralisation observed, giving concentrations up to 2.8%, are associated with the redox front at 42m in borehole F1. Strong mineralisation is also apparent in the samples from drillcore 7-1WC11. The former mineralisation corresponds to nodular pitchblende. Otherwise the mineralised phonolites show pitchblende impregnations dispersed in the clay matrix associated with pyrite concentrations.

Disequilibrium within the ^{238}U chain is observed both in the sense of excess ^{238}U (based upon ^{234}Pa) and of excess daughters. For example, excess ^{238}U is observed in the mineralisation at 43m in borehole F1 while numerous samples exhibit an apparent excess of daughter radionuclides relative to ^{238}U. In a limited number of cases the decay chain is

at or near equilibrium. The samples therefore suggest differential movement and retardation of the uranium series radionuclides and this situation should be more quantitatively defined by future alpha spectroscopy.

2.1.2 Hydrogeology: Hydraulic testing of the pilot hole involved packer tests using 0.35m long inflatable packers separated by a 6.4m straddle. These tests, to determine the coarse distribution of pressure head and hydraulic conductivity, were made every 6.1m down the borehole. The distribution of hydraulic conductivity based on the length of the sections measured was found to be quite uniform (around $10^{-6}ms^{-1}$) which indicated that the bedrock is evenly fractured and can thus be considered as a porous medium. Pressure heads indicated the groundwater flow to have an upward vertical component.

Hydraulic testing of the two feasibility boreholes (Fig. 3) was carried out using an improved packer system, comprising 1m long inflatable packers separated by a 6.55m straddle. From 10-96m in the deeper hole (F1) and from 10m to the bottom of the shallower hole (F2) the hydraulic conductivity varied from 10^{-6} to 10^{-7} ms^{-1} and showed a tendency to decrease with depth in the former. From 4-10m, in common with the pilot hole, the value was very high ($1x10^{-4}ms^{-1}$) and coincided with those horizons of the boreholes in which flushing water was lost. From 96-124m in the deep hole the conductivity was also high ($2.5 \times 10^{-6}ms^{-1}$) and most of the water inflow was considered to originate at 110m, where the borehole intersects a major conducting pathway, indicated by the increased leaching textures in the bedrock, and by the marked response of the temperature log. This borehole was completed with a packer at 96.5m, so that groundwater sampling/monitoring would be possible from this major conducting zone. Borehole F2 was completed similarly at 45m, allowing groundwater sampling/monitoring from a 15m length of the borehole. In common with all the boreholes drilled at the mine, the groundwater heads indicate an upward vertical flow component. Groundwater enters the boreholes at all depths below 10m where the pressure of the water in the rock is higher than that in the borehole. Above 10m negative head values indicate that water is lost from the holes.

2.1.3 Groundwater Chemistry: The Osamu Utsumi mine groundwaters are being characterised in terms of chemical and isotopic composition, colloid concentrations and chemistry, and microbial activity. Although emphasis is being put on samples from the boreholes, other localities within and outside the mine are also being sampled to achieve a wider perspective for interpretation.

Two groundwater sampling point were isolated, as discussed above, based on the hydrogeological results from the two feasibility holes. These sampling points were supplemented by collecting water from two of the three shallow 10m holes near the mine drainage sump, from artesian water welling up from an old shaft, and from an artesian piezometric station located at a higher level on one of the peripheral benches of the mine. A representative surface water sample was collected from a stream outside the mine area to assess the recharge environment. Some of these sampling points are shown in Fig. 1.

For the hydrochemical studies, three programmes of analysis are being run in parallel. These are:

a) regular sampling at all locations and on site analysis of Fe(tot), Fe (II), U, F, $C0_3^{2-}$, HCO_3^-, SO_4^{2-}, S^{2-} and pH. These will be supplemented by dissolved oxygen and organic carbon.
b) monitoring the feasibility boreholes for pH, Eh (Pt and C electrodes), O_2, S^{2-}, temperature, and conductivity using a flow-through cell chemical unit. This monitoring will be carried out for sampling purposes until the groundwater is stable and representative.

c) sampling of (b) for the full hydrochemical analytical programme.

Programme (a) entails on site filtering (0.45μm) and stabilisation of the groundwaters which are then transported directly to the laboratory in the mine complex. Fe (tot) and Fe(II) contents are available within one hour of collection. For programme (c) the groundwater is collected in bulk and retained, filtered and/or stabilised within 3-4 hours of collection. These waters are then distributed for analysis. Samples for ^{222}Rn, ^{226}Ra and ^{228}Ra are prepared on site and counted using liquid scintillator or gamma spectrometry within 24 hours of collection.

The large volumes of water required for the colloid studies are taken from the feasibility boreholes in parallel with the samples for the main hydrochemical programme. Preliminary filtration of the groundwater (0.45μm) is carried out within 1-2 hours of collecting; ultrafiltration using filters with nominal cut-off limits of 100,000, 10,000 and 1000 MWU is normally carried out during the next 5-6 days. At the same time, groundwater samples are collected under sterile conditions for microbiological studies.

Only preliminary results are as yet available. Chemical monitoring of borehole F1 in particular, and of the other mine locations, has now been in progress for five months. This long-term monitoring was established to see whether the chemical stability of the deep groundwater was in any way influenced by fluctuations in rainfall, which are considerable in this region. Few significant chemical trends are apparent, although uranium content appears to show an increase in response to the build-up of the rainy season. As expected the shallow boreholes show a rapid response to the increase in rainfall coupled to erratic values for many of the measured parameters. This is not considered anomalous considering the near-surface, more oxidising environment of these groundwaters.

To date the preliminary monitoring and laboratory analytical data for the groundwaters from the feasibility boreholes, and the other sampling points in the mine, show a chacteristically reducing groundwater of low pH (5-6) and relatively low concentrations of dissolved ions. The reducing nature of the groundwaters, in addition to hydrogeological criteria which would support a deep, and therefore reducing source, is strongly supported by the dissolved iron contents (usually in the range of 1.4-2.0mg/l). In all cases the amount of Fe(II) present accounts for most of the iron content in the samples. This is further supported by the carbon probe Eh measurements which record values around -450mV. All indications are that reducing groundwaters now characterise the bedrock environment exposed at the present level of investigation at the mine, at least at depths greater than 10m. Thus, under present hydraulic conditions, reducing groundwater is flowing laterally and upwards through an oxidised upper bedrock horizon (approx 70m in thickness) which was characterised by an oxidising groundwater environment prior to mining operations. On reaching the surface these waters are oxidised, converting sulphide to sulphate, with a concurrent drop in pH, which can reach values as low as 1.5 in surface pools. Complex precipitation reactions and microbial activity are evident in this environment.

Few data are presently available from the colloid studies. Several samples have been ultrafiltered and are in the process of being analysed. Preliminary results indicate that a large proportion of the colloidal material is organic in nature.

2.1.4 Microbiology: Because micro-organisms are known to be important factors in many shallow hydrogeochemical processes (influencing pH, Eh, organic complexant concentration, for example), a limited microbiological study was included in the feasibility study. Both bedrock and groundwater samples were collected for examination. It is important that once the samples are collected, analysis should take place as soon as possible. Bedrock samples were collected from borehole F1 during drilling, as 10-20cms lengths

chosen as a function of depth and rock texture. Porous rock sections were preferred, as groundwater penetration (and therefore microbial access) would be more likely. To pick up any superficial microbial influence, sampling was carried out at smaller intervals near the bedrock surface. Upon removal, the core sample was immediately placed in clean plastic bags, the air expelled and the bag sealed. The samples were then stored in a cool box at about 5°C and transported to the laboratory.

Groundwater samples were taken from the same sampling points as described above for the hydrochemical programme. Samples were collected in 500ml autoclaved plastic bottles and considerable effort was made to maintain a reasonable asceptic technique. The bottles were filled to overflowing and the lid replaced without touching the lip of the bottle, stored at 5°C in a cool box and quickly transported to the laboratory.

Both core and water samples were tested for total aerobic/anaerobic heterotrophs, sulphate reducing bacteria, and sulphur oxidising bacteria. Samples were also processed for epifluoresence microscopy, but results are not yet available. No bacteria were isolated from core samples from hole F2, but some heterotrophs were obtained from F1. Bacteria were found in most of the groundwaters sampled (all groups). Thus the bacteria appear to be mobile/motile, and are not sorbed to rock material. This unexpected finding awaits confirmation from the microscopy studies.

2.2 Morro do Ferro

The feasibility programme for Morro do Ferro involved drilling three boreholes (Fig. 4). The two holes (MF10, MF11) near the gallery entrance have been completed; the third, to be drilled near the south stream, will be completed shortly.

Owing to rock instability drilling took much longer than anticipated. It was also essential to avoid mud and water-flushing techniques which would have resulted in contamination and leaching problems respectively. Good core recovery was given some priority as, in all earlier drilling at Morro do Ferro (dating back to the 1950's), core recovery from the mineralised upper 50m had never been adequate. Drilling thus utilised a simple dry-pushing method, using a short core barrel, which resulted in a core recovery of greater than 95% . This technique was successful in borehole MF10 to a depth of 60m (casing of the hole was necessary after 35m because of increasing instability) after which water-flush drilling with a double wall barrel was employed to a depth of 71m, with casing down to 62m. The dry-pushing technique was also used for borehole MF11 (some 6m away from MF10), to a depth of 45m, to provide a groundwater sampling point just below the groundwater table (normally at about 30m depth during the dry season)

The water used for flushing was near-surface in origin and transported from the C-09 mine complex, as the stream water available at Morro do Ferro was considered unsuitable, owing to the possible presence of nitrate and microbial contaminants.

2.2.1 Geology: Drilling was conducted within the magnetite breccia which exists between and around several major massive magnetite dykes. The thin magnetite vein infillings (normally 0.5 - 1.5cm but often up to 10cm in thickness) which comprise the breccias are still texturally distinct, though long since oxidised. Textural interpretation of the core was greatly facilitated by examining the gallery walls which have recently been enlarged for prospecting purposes. Besides magnetite, only limonite, hematite and pyrite can be observed microscopically. Scinitillometric logging of the complete core showed that only the upper 11m are significantly radioactive. With the exception of a zone between 15-19m, from 11-74m the activity does not exceed background levels.

In the first 11m there is a good correlation of high radioactivity with red-brown clay horizons (suspected to represent partially oxidised magnetite). White clay horizons (possibly clay-infilled old open fracture zones) do not appear to be mineralised. There is no obvious correlation between zones of high activity and the more massive, unaltered magnetite breccia infillings.

All of the rock penetrated by borehole MF10 is extensively altered. Although the dominant impression was of rock interacting with oxidising groundwaters, evidence of fresh pyrite at depth may infer some reduction, at least on a very localised scale. Owing to the casing in MF10 down to 62m, no geophysical logging of the hole was possible.

2.2.2 Hydrogeology: Previous hydrological investigations at Morro do Ferro (IPT Report, 1984) which involved the drilling of 9 piezometers to sample the upper part of the saturated zone, showed that the water table is a subdued reflection of the topography. At the top of the hill the water table is at least 80m below the surface, fluctuating by at least 20m between the wet and dry seasons. This represents the water which is stored and slowly released as base flow to the stream. In the valley bottoms the water table is at or near the surface, coinciding with seepages or discrete springs. The groundwater flow is downwards, maintained by a vertical component in the piezometric gradient.

Because of the necessity to case borehole MF10 down to 62m double packer testing techniques were not feasible. However, a slug test performed when the hole had penetrated the water table gave a bulk hydraulic conductivity of 1.6×10^{-6} ms^{-1}, and a second test performed using a single packer to isolate the lower section of the borehole from 64-74m gave a hydraulic conductivity of $1 \times 10^{-6} ms^{-1}$. Both of these relatively high values indicate an adequate groundwater supply for the considerable volumes of water required for the hydrochemical characterisation and colloid extraction programmes.

2.2.3 Groundwater Chemistry: Groundwater sampling and analysis have only just begun at Morro do Ferro; two preliminary samples have been collected using a dip-sampler. The first was a first-strike sample as borehole MF10 penetrated the groundwater table to a depth of 6m (ie 28.3-34.9m bgl), and the second from the same depth after borehole completion.

The samples were treated and distributed for hydrochemical characterisation using the same protocol to that described for the Osamu Utsumi mine. Both samples were also initially filtered (0.45µm) and ultrafiltered for colloid extraction. Supplementary samples for colloid extraction were collected from the unsaturated zone, represented by water percolating through the gallery roof. As with the C-09 mine, the colloidal material appears to be largely organic in nature, with evidence of strong complexation with Th.

2.2.4 Microbiological Investigations: A similiar sampling protocol to that described for the Osamu Utsumi mine was carried out. This involved a total of 10 samples taken from borehole MF10 to a depth of 61m. Analyses were identical to those performed at the C-09 mine, although only core material has been examined so far (from MF10). Heterotrophs were located throughout the borehole, with the very low numbers decreasing with depth. Again, the results await confirmation by epifluoresence microscopy.

3. DISCUSSION

The original plan of work at the C-09 Osamu Utsumi mine was structured around the distinctive fissure-flow system expected at this site. However, the feasibility study has shown that the hydrogeology is better described as a porous flow system - at least in the

upper 60m where the most distinctive redox and hydrolytic fronts are observed in the rock. Nevertheless, the possibility of deriving useful data on radionuclide retardation from the deepest fissure in borehole F1, which could be used to validate the extrapolation of laboratory sorption data, or of examining matrix diffusion in this zone, is not precluded. Although the flow system is thus not as discrete as was hoped, and distinctive geochemical gradients cannot be determined along localised flow paths, such retardation data as can be derived from the existing programme of measurements (physical properties and natural series radioisotopes) are relevant to any safety assessment for a fissured crystalline host-rock.

Assuming much higher priority than originally planned, however, is the geochemistry of the deep groundwaters. In particular, the relatively high colloid concentration - which appears to be predominantly organic in nature - represents an extreme scenario for repository safety analysis. Results to date indicate that such organic colloids influence the 'solution phase' (ie material passing a 0.45μ filter) concentration of particular elements (eg Lei, 1984). A major focus for further work is therefore the determination of parameters which influence the possible significance of such colloids to a far-field transport model: mechanisms of retardation (sorption, molecular filtration etc) and stability of the trace element/colloid association, with regard to the uptake/removal of the trace element or aggregation/disaggregation of the colloid itself.

A further key area of interest concerns the speciation and concentration levels of natural series elements in solution in the groundwaters in contact with the ore body. These data will have direct input to the equilibrium thermodynamic codes currently in use, and will also serve as a check on solubility limitation models of radionuclide mobilisation.

Two further, interlinked aspects of groundwater geochemistry which are of interest are the redox (and pH) conditions and the microbial activity. The experimental determination of redox potential, or of the extent of redox disequilibrium, is a major problem in many areas of nuclear waste management. In many national programmes, studies of the mechanisms of the geochemical processes controlling the redox conditions of natural groundwaters have been given a high priority. The redox profiles in both rock and groundwater observed in the boreholes at the mine can be considered as analogues of profiles occurring over much larger spatial scales at a repository site. Although the hydrological system probably precludes a study of redox boundary dynamics, more static, mechanistic studies are still possible. In particular, the relatively high U concentration in this region allows examination of the coupling of speciation of an important, variable oxidation-state element to major redox systems (eg Fe^{2+}/Fe^{3+}, SO_4^{2-}/S^{2-} etc). This can, at the least, be used as a qualitative test of the 'global Eh' concept generally applied in chemical thermodynamic models, but should also provide a more quantitative test of the models themselves and their associated databases.

Such redox reactions are, however, often very slow kinetically and, at low temperatures (<100°C) proceed only due to microbial catalysis. At the mine, such microbial oxidation of S^{2-} also gives rise to the production of protons ('acid') which also has marginal relevance for the operational phase of any repository in rocks with accessible sulphide (eg marls, clays). More generally microbial effects are now recognised to have considerable potential for influencing the performance of L/ILW repositories (particularly if near-surface) and this site offers the chance of examining both direct (eg uptake) and indirect (eg complexation with by-products - closely linked to the organic colloid study) effects of microbes on the speciation and mobility of a range of important elements (eg U, Th, Ra, Pb).

The main phase of work has now been planned to obtain detailed information on the topics discussed above, with a consequent increase in emphasis on hydrochemistry, and reduction

in effort on rock chemistry and physical properties studies. Two additional boreholes will be drilled to provide a deep groundwater sampling profile along the drainage direction of the mine, based on the current hydrology, and the original topography. Together with the feasibility hole, they will allow regular and routine water sampling in the influent zone above the ore-body, on the margin of the ore (feasibility hole), and in the most intensely mineralised zone near the old adit system. A semi-quantitative 2-D model of water movement will be constructed, and hydrochemical variations, specifically concerning speciation and concentration levels, will be related to rates of flow, recharge variations, residence times, the bulk rock chemistry of the orebody, and redox and microbial effects.

At **Morro do Ferro** the hydrogeological system is much as originally anticipated, but preferential conduction pathways (remnants of magnetite breccia) appear to play a more important role in water transport through the saturated zone then previously expected. The main original aim of this study was to examine the nature and transport of colloids derived from the Th ore body. The first part of the migration path is in unsaturated rock, so this part of the analogue is inherently qualitative as currently there is no prospect of being able to model colloid transport in such an environment. The main interest will remain with colloid behaviour in the saturated zone from hill slope to stream. In addition, from the point of view of repository safety assessment in argillaceous formations, a highly relevant, and potentially quantitative analogue is provided by the distinct flow paths through the very clay rich zones of the system. Solute diffusion from the main water conductors into the argillaceous matrix and the extent of retardation of colloids are key parameters which are of great significance (with highly non-linear consequences) to safety assessment transport models.

As for the C-09 mine, groundwater geochemistry and microbiology are also of interest at Morro do Ferro, but detailed analysis will only be possible in the saturated zone, where geochemical gradients appear to be less pronounced.

In general, the results of the feasibility study at both sites illustrate very clearly the problems associated with large analogue projects in complex geochemical environments. The project also shows that as soon as actual geological conditions can be determined, a mechanistic appproach with input from the modelling side aids timely identification of inappropriate studies, and allows serendipitous developments to be exploited readily. The results to date are very promising, and it appears highly likely that specific safety assessment models can be tested against data derived from this project. Work has now started on the main data gathering and interpretation phase, and the project is scheduled to be completed in late 1989.

4. ACKNOWLEDGEMENTS

This paper has been prepared by the project technical committee. However, many individuals and laboratories have contributed the data, expertise, and hard labour necessary to enable us to assemble this report. We would particularly like to thank the geological staff and colleagues in the chemical and microbiological laboratories at Nuclebras, Poços de Caldas, Dave Holmes and Julia West of BGS, Gus Mackenzie and colleagues of SURRC, Norbert Miekeley of PUC, Rio, and Tjerk Peters and his group at the University of Bern, who all participated actively in the feasibility study. Special thanks go to Nuclebras and CNEN for facilitating the work at all stages. The work was funded jointly by Nagra, SKB, and UK Department of the Environment.

5. REFERENCES

Barretto. P.C.M., and Fujimori, K. 1986. Natural Analogue Studies: Geology and Mineralogy of Morro Do Ferro, Brazil. *Chem. Geol.*, **55**, 297-312.

Eisenbud, M., Krauskopf, K., Penna Franca, E., Lei, W., Ballad, R., Linsalata, P., and Fujimori, K. 1984. Natural analogues for the transuranic actinide elements: an investigation in Minas Gerais, Brazil. *Environ. Geol. Water Sci.*, **6**, 1-9.

IPT, 1984. Geology, hydrology, geochemistry and radioactivity of Morro do Ferro: a critical review of the literature. Unpublished report of Instituto de Pesquisas Tecnologicas do Estado de Sao Paulo.

Lei, W. 1984. Thorium mobilisation in a terrestrial environment. Unpub. PhD thesis, New York University, New York, 414pps.

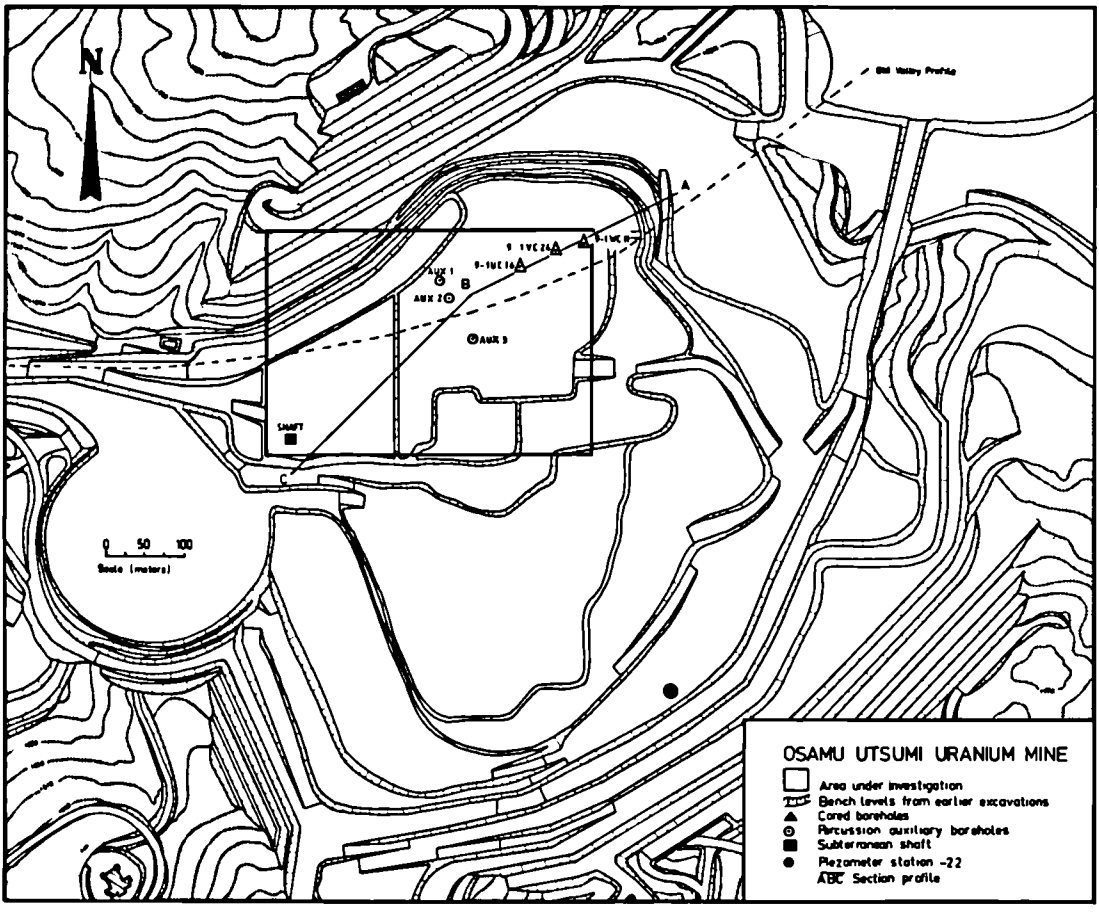

Figure 1: Position of the investigated area within the present extent of the mining operations. Indicated are the locations of the drilled boreholes, the piezometer station-22, the subterranean shaft, and the section profile (A-C) illustrated in Figure 2.

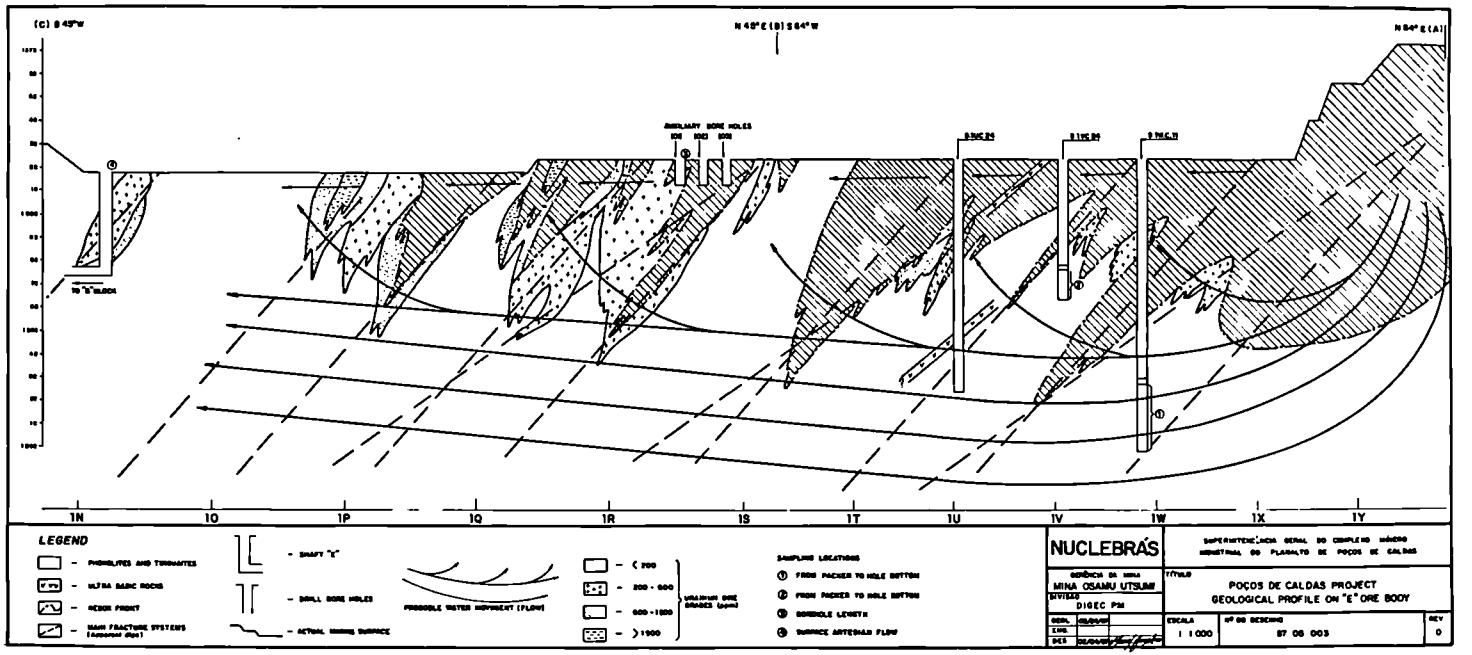

Figure 2: Section profile (A-C) from Figure 1 showing the relationships of the boreholes and groundwater sampling locations with the known geology, geochemistry and hydrology of the site.

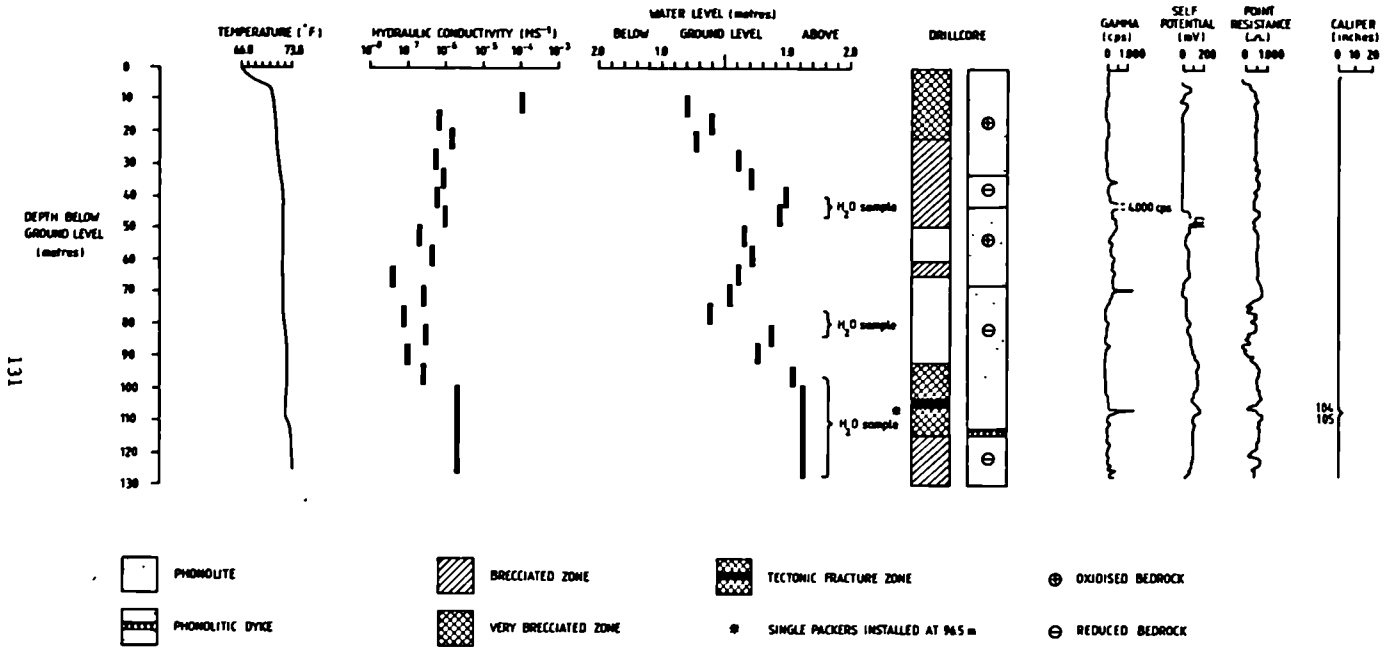

Figure 3: General features of Feasibility borehole 9-1WC11, Osamu Utsumi uranium mine, Pocos de Caldas.

MORRO DO FERRO

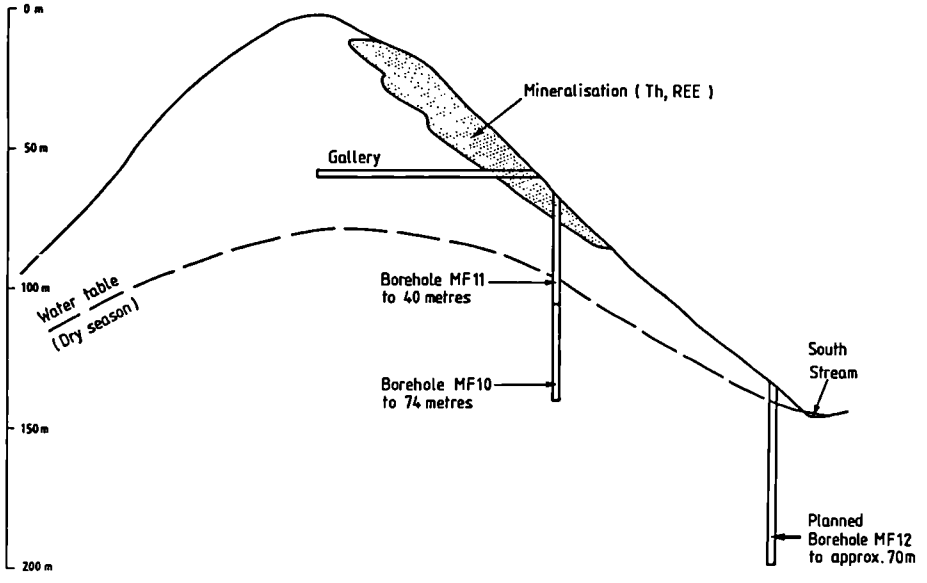

Figure 4: Location of the drilled feasibility boreholes MF10 and MF11 in relation to the mineralisation and the saturated and unsaturated bedrock zones.

SESSION 3 :

ANALOGUES FOR WASTE FORMS AND ENGINEERED BARRIERS

Chairman : F.P. SARGENT (AECL, CANADA)

Co-Chairman : P.L. AIREY (IAEA)

A 17th CENTURY BRONZE CANNON AS ANALOGUE FOR RADIOACTIVE WASTE DISPOSAL

R. O. Hallberg, P. Östlund and T. Wadsten.
Department of Geology
University of Stockholm

1.1 Introduction

Swedish Nuclear Fuel and Management Co. SKB, runs an intensive research in developing safe methods for the final deposit of used Swedish nuclear fuel. The present method is based on keeping the fuel in copper canisters embedded in clay at a depth of 500 meters in a crystalline rock.

By means of theoretical calculations, supported by experiments over short periods of time, it has been concluded that the corrosion effect on copper is very small. These conclusions would be further fortified if we had access to copper objects exposed to corrosive elements over a long period of time in an environment similar to that of the final storage.

One such analogue of corrosion processes is a bronze cannon, salvaged from the Swedish warship "Kronan" which sank in the Baltic Sea in June 1st 1676. The shipwreck is located about 3 nautical miles off the eastern coast of Öland at a depth of 26 m. The bottom sediment consists of sand of varying thickness down to a depth of maximally 0.5 m. The sand is underlain by glacial clay. The cannon was almost completely buried in a vertical position in the clay that consists of illite, montmorillonite and kaolinite.

1.2 Results

Microsond analyses of the bronze matrix show concentrations of Cu of about 96.3 %, Sn of about 3.3 %, Zn and Fe together < 0.5 %, and negligible amounts of Pb. All figures are given as percentages by weight of a total of 35 measuring points where the values obtained have been normalized to 100 %. The bronze matrix contains inclusions of slag products. They consist almost exclusively of a CuO phase (tenorite). In some cases an admixture of an FeO phase could be identified. The Cu-concentration in the bronze matrix shows a clear trend for values to be lower closest to the surface of the cannon in comparison with material deeper in the bronze matrix (Fig. 1). The scattering of the values in the data material is largely dependent on the spot analyses being made using given spacing along a straight line and that consequently a number of points have occurred in the vicinity of an inclusion which has influenced the analytical results. The spots which occurred in or adjacent to an inclusion of CuO gave such divergent results that they could easily be distinguished and rejected from the analytical material.

Two lines have been entered in Fig. 1 in order to determine the amount of copper leached out of the bronze matrix. These lines show the copper concentration of the cannon goods at deeper depths than 1 mm and the trends for decreasing copper concentrations in the surface layer. The former value is calculated to 96.3 % and the latter decreases from 96.3 % at a depth of 0.8 mm

to 95.2 at the surface. The density of the bronze matrix has been calculated to 8.82 g/cm^3. Using Figure 1 the leached amount of Cu can be determined to 4 mg per cm^2 cannon surface.

Cu was traced in the clay to a distance of about 4 cm from the cannon. Four consecutive layers of corrosion products were observed with the naked eye, the major components of copper being cuprite (Cu_2O) and malachite ($Cu_2CO_3(OH)_2$). Calculations of the amount of Cu in the corrosion products are difficult to make owing to the large variation in the material and therefore will give uncertain values but nonetheless can serve as a measure of the magnitudes concerned.

The copper concentration in malachite is 75 %. The thickness of the malachite layer varies but is around 0.05 mm. This would imply about 30 mg Cu on an area of 1 cm^2. Bearing in mind the variations we could then reach a value of 30 ± 30 mg Cu in the form of malachite per cm^2 cannon surface.

The copper concentration in cuprite is 89 %. The thickness of this layer varies more than for the malachite layer but a representative value is estimated to 0.2 mm. This means a copper concentration of about 160 mg per cm^2 cannon surface. We assess the variation to range from +100 to -150 mg Cu in the form of cuprite per cm^2 cannon surface. Thus, the total amount of released Cu per cm^2 cannon surface would for these two minerals vary between a few mg to about 350 mg with an average value of about 200 mg. In addition there are also other unidentified copper minerals.

The amount of Cu that leached from the cannon is made up of the sum of Cu in the clay and in the corrosion products malachite and cuprite. The dry weight of the clay per cm^3 clay volume was determined to 1.1 g. Using this value and the average concentration of Cu in the clay, the amount of diffused Cu per cm^2 cannon surface was calculated to 12.6 mg, 31.7 mg and 9.7 mg for three samples.

1.3 Discussion

The clay, partly consisting of montmorillonite, was packed tightly around the cannon and thus oxygen from the sea water could only penetrate the uppermost part of the clay and thereby influence the chemistry around the cannon. The uppermost 10 cm of the clay has a slightly brown tint while deeper layers are more grey in colour. The pore water in the clay contains Fe^{3+}. Consequently, the environment in the clay can be characterized as oxidizing. Measurements of pH in the clay show neutral values (7.0). Redox measurements give a mean value of +450 mV and suggest also an oxidizing environment. In a thermodynamic calculation the concentrations of Fe^{3+} and Fe^{2+} in the pore water give an Eh value of about +700 mV. The samples might have been oxidized to some extent before analysis but the thermodynamic calculations do not give absolute values for the Eh of the environment but can only be used as guidelines.

The identified minerals of the corrosion products on the cannon, Cu_2O, Fe_3O_4 and ZnS, indicate that most of them have been formed in an oxidizing environment.

A calculation of the general corrosion from pure copper material based only on the observed loss of 4 mg Cu per cm^2 during the period of 300 years in

which the corrosion had proceeded would result in a corrosion depth of 1.5 x 10^{-5} mm/year. In a situation with storage of expended nuclear fuel the copper capsules must withstand corrosion for 100 000 years. On the basis of the above-mentioned figure, this would imply a general corrosion of 1.5 mm. With a pitting factor of 5 (1) this would correspond to a maximum corrosion depth of 7.5 mm. However, a general corrosion of the cannon, which in turn will lead to a disapperence of the original outer bronze surface would result in larger corrosion figures than those above. An estimation of such a general corrosion is complicated by the fact that not only Cu of the bronze matrix but moreover Cu from the CuO inclusions has been leached.

The corrosion products have the same apperence all over the cannon. They do not show any tendency of diminishing in amount towards the muzzle, which was burried deepest in the clay. On these grounds oxygen is excluded as beeing of any significant importance as an oxidizing agent of the copper. it may have been of some importance in the uppermost 5 - 10 cm of the clay where time can allow for oxygen diffusion from the sea water but for the rest of the cannon the corrosion processes must be explained by means of other chemical reactions.

Highly probable reactions of the corrosion processes are suggested in Fig. 2. Among the proposed redox reactions there is one chemical reduction,

$$Cu^{2+} + e^- \rightarrow Cu \qquad (1)$$

which is in dynamic equilibrium with three oxidation processes,

$$Fe^{2+} + 2H_2O \rightarrow FeOOH + 3H^+ + e^- \qquad (2)$$

$$CH_2O + H_2O \rightarrow CO_2 + 4H^+ + 4e^- \qquad (3)$$

$$Cu \rightarrow Cu^+ + e^- \qquad (4)$$

The importance of each individual reaction for the release of copper, which on an average is 200 mg per cm^2 of cannon , can hardly be elucidated from existing data. 200 mg Cu corresponds to approximately 3 mM of Cu. The amount of malachite is equivivalent to ca. 0.5 mM of Cu, wich would infer 0.25 mM of CO_2 being produced by reaction (3). As this reaction involves four times more electrons per equivivalent of reaction (1), approximately 1/3 of the leached Cu can be explained by the oxidation of organic matter.

Iron constitutes a substantial part of the corrosion products (reaction (2)) but can probably not entirely account for the remaining 2/3 of the leached Cu. Whatever is left has to be split equal between reaction (1) and (4).

Would a contribution of a negliable amount of Cu by reaction (4) result in an unrealistic depth of the bronze matrix for a corrosive attack on CuO?

The area of the inclusions / cavities has been determined to be about 11 %. If we consider that the area of the inclusions is representative of their volume and that these, on average, lead to 200 mg Cu/cm^2, then the total depth of the corrosive effect on CuO can be calculated as illustrated below:

surface proportion of CuO in cm^2 x depth of corrosion in cm x density x Cu/CuO = 0.2g

0.11 x corrosion depth x 6.4 x 0.8 = 0.2

This gives a corrosion depth of about 3.5 mm. Presumably the corrosion has gone deeper since some of the inclusions have been isolated from corrosion attack and thus have not been able to contribute to the corrosion products. This can be observed as some of the inclusions at a depth of > 3 mm clearly show signs of leaching.

It is then clear that the completely dominating source of the Cu in the corrosion products must be the slag product CuO, which occurs in the form of inclusions in the bronze matrix. That the inclusions of CuO are the dominating source of leached Cu also explains why the corrosion in the cannon metal has reached as deep as 0.8 mm. Since the inclusions presumably to some extent are linked with each other, a system of cavities has been created which has allowed a leaching of the bronze to a greater depth than if it had been without slag products. Also no cuprite was observed in the cavities of the corroded inclusions, which would have been the case if there had been a direct reaction between the Cu of the bronze and the tenorite.

1.4 Conclusions

The cannon which was recovered in 1985 has been embedded for more than 300 years in a clay which largely has the same properties as the clay considered for use in the final storage of Swedish nuclear fuels.

The copper concentration in the bronze alloy is abnormally high, 96.3 % instead of a more normal 90 %, which makes it a suitable object in studies of copper corrosion.

The main corrosion products of copper are cuprite and malachite where the cuprite dominates.

The formation of cuprite involves a transformation of tenorite and can be explained by redox processes where Cu(s), Fe^{2+} and organic matter are the major electron donors.

References

1. HALLBERG, R.O., ENGVALL, A-G. and WADSTEN, T. (1984). Corrosion of copper lightning conductor plates. Br Corros. J., Vol. 19, No. 2

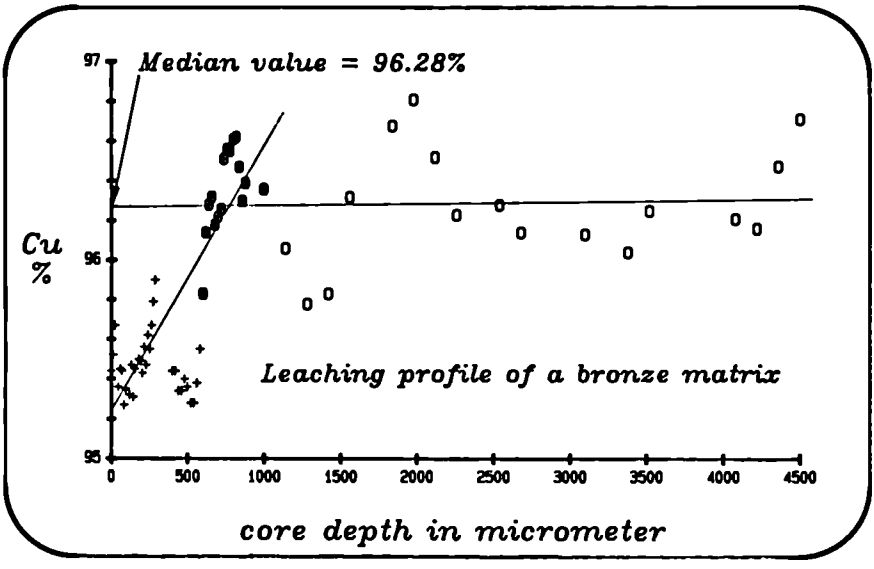

Fig. 1. Microprobe analysis of a core from the bronze cannon. Trend graphs of copper concentrations have been estimated by using data denoted by open circles for background values and data denoted by crosses for leached zone. Encircled crosses are common data for both estimates.

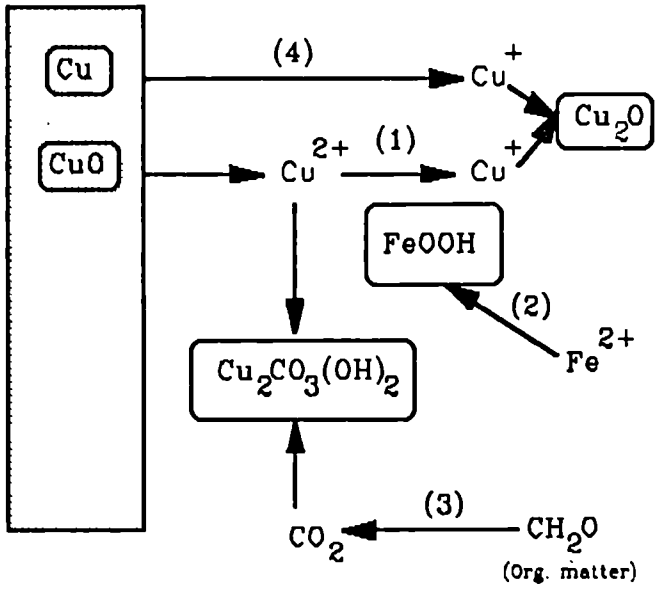

Fig. 2. Main chemical reactions of corrosion processes. For further explanations see text.

GEOCHEMICAL CONTROLS ON THE RETENTION OF FISSION PRODUCTS AT THE OKLO NATURAL FISSION REACTORS

DAVID CURTIS, TIMOTHY BENJAMIN, and ALEXANDER GANCARZ
Los Alamos National Laboratory, Los Alamos, NM, U.S.A.

ROBERT LOSS, KEVIN ROSMAN, and JOHN DeLAETER
Western Australian Institute of Technology,
Bentley, Western Australia, AUSTRALIA

JAMES DELMORE and WILLIAM MAECK
Idaho National Engineering Laboratory, Idaho Falls, ID, U.S.A.

A unique example of the utility of isotope geochemistry may be found in studies of the isotopic abundances of elements in samples from the Oklo uranium mine in the African Republic of Gabon. These studies demonstrate that two billion years ago, in a span of a few hundred thousand years, nuclear fission and associated processes profoundly changed the isotopic and chemical composition of discrete lenses of highly uraniferous rock within the mine (1,2). These changes can be quantified by characterizing operating parameters of the natural nuclear fission reactors and interpreting them in the context of the systematics of the nuclear reactions. Comparisons between the present, measured, composition of the natural reactor remnants and their calculated nuclear-reaction induced composition provides a quantitative characterization of compositional changes in the rocks during the last two billion years.

We have measured the abundances and isotopic compositions of uranium and eight fission product elements in samples from well-defined locations in an area containing the cross-section of a fossil reactor. The data have been used to examine the retention of fission products in the reactor zone and to explain this retention by analogy to properties of irradiated anthropogenic UO_2 reactor fuel. The analogy provides a consistent explanation for the distribution of fission products in the reactor zone samples. It suggests that the natural nuclear products formed a secondary mineral assemblage manifesting physical and chemical conditions localized on the scale of the uraninite grains. The partitioning of elements between these nuclear product bearing phases and those in the ambient environment was the primary control on the retention of nuclear products in the reactor zone. We suggest that ruthenium, palladium, and tellurium were quantitatively retained and molybdenum, and ^{99}Tc were partially retained in a metallic phase qualitatively similar to those observed in irradiated spent fuels (3,4,5). Fission products in solid solution with UO_2, such as neodymium and cadmium, interacted with the ambient environment of the reactor zone, despite the physical and chemical stability of the host phase. Small proportions of non-volatile neodymium were leached from uraninite, while virtually all of the volatile element cadmium was removed from the mineral.

A detailed discussion of the research has been submitted for publication elsewere.

Acknowledgements

This work was supported by the Office of Nuclear Waste Isolation, Battelle Project Management Division, Columbus, Ohio, the Australian Research Grants Scheme, and the U.S. Department of Energy, Office of Energy Research, Division of Engineering, Mathematics & Geosciences.

REFERENCES

1. International Atomic Energy Agency (1975). The Oklo Phenomenon. (Proc. Symp. Libreville, Gabon, 1975), STI/PUB/405, IAEA, Vienna.
2. International Atomic Energy Agency (1978). Natural Fission Reactors. (Proc. of tech. Comm., Paris, France, 1977), STI/PUB/475, IAEA, Vienna.
3. JEFFREY, B.M. (1967). Microanalyses of inclusions in irradiated UO_2. Journal of Nuclear Materials, 22, 33-40.
4. BRADBURY, B.T., DEMANT, J.T. MARTIN, P.M., and POOLE, D.M. Electron probe microanalysis of irradiated UO_2. Journal of Nuclear Materials, 17, 227-236.
5. KLEYKAMP, H. (1974). Formation of phases and distribution of fission products in an oxide fuel, in Behavior and Chemical State of Irradiated Fuels. (Proc. of Panel, Vienna, 1972), STI/PUB/303, IAEA, Vienna 157-166.

THE USE OF NATURAL ANALOGUES IN THE LONG-TERM EXTRAPOLATION OF GLASS CORROSION PROCESSES

W. Lutze and B. Grambow
Hahn-Meitner-Institut Berlin GmbH, FRG
R.C. Ewing and M.J. Jercinovic
University of New Mexico, Albuquerque, New Mexico, USA

Summary

One of the most critical aspects of nuclear waste management is the extrapolation of materials and systems behavior from short term experiments, typically on the order of one year, over comparatively very long periods of time. Safety and risk analyses have to rely on extrapolations and the respective findings have to be evaluated in the frame of licensing procedures. In this unique situation, any source of information that can lend support to the credibility of predicted behavior, should be exploited and investigated with great care. There are natural systems, e.g. the Oklo "reactor", which can provide evidence of radionuclide migration over very long periods of time and thus help to answer specific questions of interest. Natural glasses and minerals can serve as analogues for both glass and crystalline nuclear waste forms, and the alteration of the natural materials can be studied to infer information on the behavior of the man-made products in geologic environments. This paper reviews most of the work performed by the authors and their collegues in this field together with information available from literature and dicusses the extent to which natural glasses can be used to validate or verify predictions.

1. Introduction

One of the most critical aspects of the evaluation of radioactive waste forms is the extrapolation of their materials properties (as determined in short term experiments) over long periods of time. In this paper, we describe the application of natural analogues to questions concerning the corrosion of borosilicate nuclear waste glass as inferred from the study of natural glasses. This communication is based on a recent and more detailed paper by two of the authors, Ewing and Jercinovic (1).

The phrase "natural analogue" conveys the sense that in natural systems (usually of great age) there are situations or materials that are analogous to the conditions or materials of interest. It is important to define what is meant by such an analogy, as it leads immediately to the idea that there can be a "proof by analogy". In the broadest

sense, an analogy refers to a similarity between things otherwise unlike, that is a partial resemblance.

This view of "analogy" immediately limits what one may expect from this approach. Proof or "verification" of a hypothesis, e.g. the long-term durability of borosilicate glass can only be approached (never arrived at), and then only to the extent that details of one system correlate to the details of another system. The selection of the pertinent variables which are used to describe the phenomenon (e.g. temperature, pH, SA/V, flow rate) have a direct bearing on the validity of the conclusions.

When one considers the possiblity of using natural glasses as analogues for nuclear waste glasses, one must carefully frame the question, preferably in the form of a hypothesis that can be tested, either by confirmation in the laboratory of predictions developed from models or by confirmation in the field of "postdictions" derived from laboratory data and models, e.g.:

"Do natural glasses, as they exist in large scale geologic systems over long periods of time, provide confirmation of thermodynamic and kinetic models used to extrapolate the behavior of nuclear waste glasses to the long-term?"

In answering this question, we first have to establish a basis for suggesting that various silicate glasses behave analogously. Once we have established analogous behavior, we must place these similarities of behavior in the context of a general theory of glass corrosion. Once the general theory is confirmed, then we are justified in using it as a basis for extrapolation. Important questions that can then be answered are:

- -what is the corrosion mechanism?
- -what is the rate of corrosion?
- -does the corrosion mechanism change with time?
- -what effect do parameters such as temperature, pH, S/V, flow rate and solution composition have on the rate of corrosion?
- -what are the alteration products and what is their sequence of formation?
- -what factors do ultimately control the corrosion of nuclear waste glasses in the long-term?

There are a variety of glasses that form in the natural evironment: meteoritic glasses, impact glasses (tektites) and lunar glasses, rhyolitic glasses and basaltic glasses (2,3). These glasses range in age from most recent (volcanic glasses) to hundreds of millions of years old (some terrestrial, meteoritic and lunar glasses) and cover a wide compositional range (Table I). Natural glasses that have been considered as analogues for nuclear waste glasses are: a) tektites (13,14), b) rhyolitic glasses (4,15) and basaltic glasses (5-12). They can be grouped according to their silica content: a) tektites and rhyolitic glasses having silica contents of 70 to 75 wt % and b) basaltic glasses having silica contents in the range of 45 to 50 wt %. The former have been considered as analogues for high-silica, low-alkali formulations (e.g. the porous glass matrix encapsulated in a high-silica sleeve, (16)) and the latter as an analogue for the lower silica borosilicate glass formulations (6,7). It should be noted that the high silica contents for the HLW glasses in table I decrease by 10 to 30 % when the waste is added to the base glasses (frits). This decrease

Identification / Component	SRL 165	SON 68	SM 513	PNL 76-68	UK 209	GP 98/12	PO 422	tektite Philippine	rhyolite	basalt glass Hawaiite
	Composition in weight percent									
SiO_2	68.0	54.9	58.6	59.4	68.5	58.5	61.0	71.2	73.1	50.3
B_2O_3	10.0	16.9	14.7	14.3	15.0	11.0	19.9	-	-	-
Li_2O	7.0	2.4	4.7	-	5.4	-	4.3	-	-	-
Na_2O	13.0	11.9	6.5	11.3	11.2	17.5	1.4	1.5	3.5	4.9
K_2O	-	-	-	-	-	-	2.8	1.9	4.5	1.9
TiO_2	-	-	5.1	4.5	-	3.6	-	0.8	0.2	2.8
CaO	-	4.9	5.1	2.9	-	4.5	2.8	3.1	2.6	7.1
MgO	1.0	-	2.3	-	-	3.3	-	2.9	1.0	3.9
Al_2O_3	-	5.9	3.0	-	-	1.6	5.0	12.5	11.9	17.3
ZnO	-	3.0	-	7.6	-	-	2.8	-	-	-
ZrO_2	1.0	-	-	-	-	-	-	-	-	-
$MnO+Fe_2O_3$	-	-	-	-	-	-	-	5.3	2.6	11.0

Table I: Compositions of some HLW glass frits and of tektite, rhyolite and basalt glass samples. (Addition of waste oxides (10-30 weight percent, depending on the particular use of the various frits) brings the SiO_2 content of the waste glass down to about 50%).

applies, of course, to all other base glass constituents. Individual fission products are contained in the final glass at concentration levels hardly exceeding 2 wt%. The major differences between the waste glasses and the basaltic glasses can be seen in the significantly higher alkali contents, at least on a molar basis, and in boron oxide, which is not a constituent of natural glasses. To a certain extent, B_2O_3 could be considered as the counterpart to Al_2O_3 in the natural glasses. Both elements act as network formers at their respective concentration levels and help to stabilize the glass structure. It is still reasonable to assume that analogous behavior can only be expected as long as the nuclear waste glasses exhibit the properties of "typical" silicate glasses, i.e. the dominance of silica in the glass dissolution process and as a network former.

2. Tektites and Rhyolitic Glasses

Tektites occur as small rounded fragments ranging in size from fractions of a millimeter to tens of centimeters in diameter. They seldom occur as isolated objects rather are found as strewn-fields covering areas up to 10,000 km wide. They range in age from hundreds of thousands of years to 35 million years. It is rare that any alteration, hydration or devitrification effects are noted (2,3) Laboratory studies have been completed by Barkatt and coworkers (13,14) and leach rates (1.8×10^{-5} g m^{-2} d^{-1} or 2.6 μm/1000 yrs at 25°C) were measured. The extrapolated test results over the life time of tektites is in excellent agreement with the field observations of their extent of corrosion. The high durability is attributed to their high silica and alumina content and the low alkali content (<4 weight percent). $SiO_2 + Al_2O_3$ is usually at least 80 wt %. One can easily see the effect of variations from these compositional constraints in the reduced stability of rhyolitic glasses (which have higher alkali contents) and are often hydrated, altered and devitrified (4,15,17-20). As an example, figure 1 shows the chemically corroded surface of a rhyolitic glass with crystals in the pristine glass (6).

3. Basaltic Glasses

The specific use of basaltic glasses as analogues for nuclear waste borosilicate glasses was first made by Ewing (2,3) based on the similar silica contents of basaltic and borosilicate glasses and the fact that experimentally determined hydration rates on natural glasses had been confirmed by the measurement of hydration rind thicknesses on samples of great age (21-23); however, these early studies failed to recognize the important similarities between the altered layers of experimentally leached borosilicate glass and palagonite, the alteration product of basaltic glass corrosion. Allen (5) was the first to call specific attention to this similarity (25). Palagonites form in a wide range of geologic environments: a) in mid-ocean ridge environments when glass on pillow basalts reacts with sea water at approximately 4°C (9,26), b) in subglacial environments where the glass reacts with glacial melt water at 0°C (hyaloclastites) (9,26), c) when glass shards in layers of ash deposits associated with subaerial volcanic eruptions are altered by reaction with rainwater at ambient temperatures (or sea water when a crater is breached by the sea) (10), and d) when basaltic

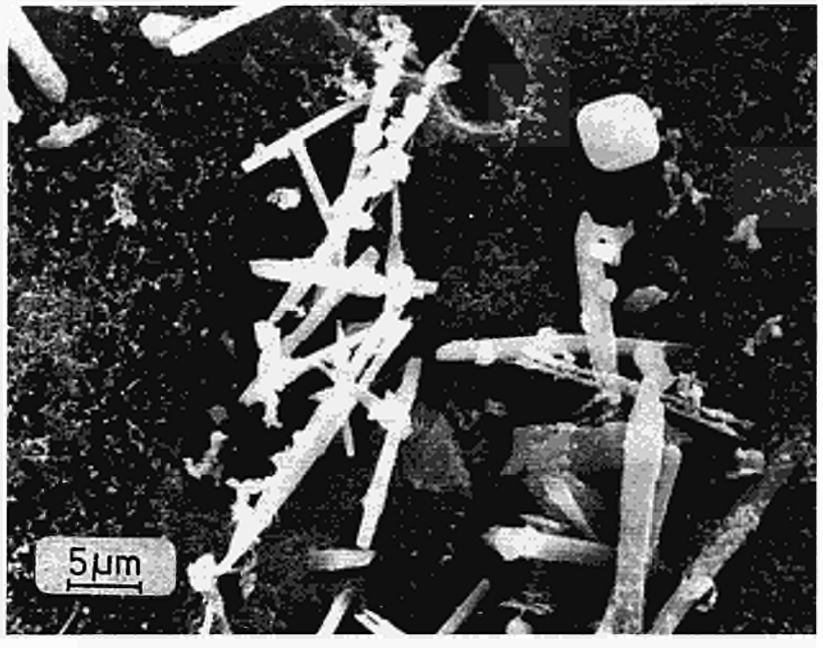

Fig. 1: SEM micrograph of a rhyolitic glass. The surface was corroded to make the devitrification products of the glass visible.

glass is altered in active geothermal environments either in the presence of water at > 75°C or water vapor (24,26). Thus, the geologic record provides a wide variety of environments with sufficient variation of temperature, flow rate, solution composition etc. under which basalt glass alteration can be studied.

Alteration experiments in the laboratory. In an effort to demonstrate analogous behavior in the presence of water, hydrothermal experiments were conducted on basalt and borosilicate glasses (200°C in a NaCl-solution, saturated at 55°C) for periods of time up to 30 days (6,7). In both cases, isometric analcime crystals were formed as surface precipitates, Si and Al being provided by the glass and the Na by the solution. At higher magnifications, repetitive sheet-like structures are apparent. Each sheet is covered by a mat of crystal rosettes (an unidentified clay). A similar multiple surface layer structure is common in naturally altered (3°C, sea water) basalt glasses. The similarity is further confirmed by analysis of the surface layers. All surface layers showed depletion in SiO_2 and CaO, relative to the parent glass; Al_2O_3 concentrations are approximately constant; and there were increases in the concentrations of TiO_2, FeO, MnO and Na_2O in the surface layers. Several glasses were investigated and surface layer formation could be related to glass composition. The higher the ratios of Mg, Al, Fe and Ti to Si in the glass, the higher the fraction of the surface layer formed relative to the total reacted glass.

In another context, workers in France (27-29), investigated sea water-basaltic glass interactions (50°C for runs between 1 and 595 days). The results of these experiments were important because they produced mats of surface crystals identified as hydrotalcite, $Mg_6Al_2CO_3(OH)_{16}4H_2O$, which had heretofore gone unidentified (but were certainly prominent) as alteration products on leached borosilicate glass. This is an important observation because hydrotalcite has not been reported in the alteration products of natural basalt glasses, suggesting that this is a transitory, metastable phase. One must remember that metastable phases can control solution compositions. The final composition of the surface layer evolves to that of saponite, a common phase in naturally altered basalt glasses.

Alteration in nature. Electron microprobe analyses of basaltic glass and corresponding palagonites have been obtained from a wide variety of geologic environments (12). In terms of absolute elemental concentrations, SiO_2, MgO and CaO are nearly always depleted in the palagonite relative to the glass. FeO and TiO_2 are retained, and Al_2O_3 concentrations are nearly constant, slightly depleted or even enriched (depending on pH). In general for fresh water alteration, the loss of elements from the glass (in order of greatest to least) is as follows: Na, K, Mg, Ca, Al, Si, Fe, Ti. In contrast to subaerially or fresh-water altered samples, those that have been altered by contact with sea water have retained Na and K (26).

A wide variety of crystalline phases (mainly clays and zeolites) form either by replacement of amorphous surface layers or by precipitation onto the surface layer. The nature of these phases reflect not only the composition of the original glass, but also the composition and time of contact with altering solutions. Phases may be formed from elements released during palagonitization or from material of external origin, and commonly as a mixture of both sources. Clays are the most common authigenic minerals, occurring as replacement of the palagonite and as a cement (11). Fe-rich smectites are abundant clays (Fe-Mg saponite being the most common). Zeolites are common in both fresh water and sea water altered basaltic glasses. Among Icelandic samples, however, zeolites are only abundant in: a) samples altered by sea water; b) fresh water samples older than 0.7 million years (rind thicknesses of at least 100 microns); c) samples exposed to alteration at elevated temperatures (26). All zeolite occurrences are associated with palagonite rinds which are somewhat depleted in aluminium relative to parent glass. The release of aluminum appears to be required before zeolites can form. Chabazite, $CaAl_2Si_4O_{12}{\cdot}6H_2O$, is the most abundant zeolite. Other important zeolites identified in natural samples which have appeared as reaction products in experimental studies include: a) analoime - $NaAlSi_2O_6{\cdot}H_2O$, b) phillipsite - $(K,Na,C)_{1-2}(Si,Al)_8O_{16}{\cdot}6H_2O$, c) thomsonite - $NaCa_2Al_5Si_5O_{20}{\cdot}6H_2O$. Tobermorite - $Ca_5Si_6O_{16}(OH)_2{\cdot}4H_2O$- and gyrolite - $Ca_2Si_3O_7(OH){\cdot}H_2O$ - which are not zeolites have also been identified in natural samples and experimental runs (12,24,30). As with the palagonites, the associated zeolites are more alkaline in sea water than those altered in fresh water. The formation of zeolites occurs only at low flow rates and when a substantial fraction of glass has been altered. Zeolites may thus be used to measure reaction progress (9).

There have been numerous attempts to establish the time dependence of corrosion of basaltic glasses by measuring rind thicknesses on samples

of known age (31-33). Rind thicknesses may vary from zero to greater than 1,000 microns (in general thickest for deep sea dredge samples) (9,26). The main difficulty is not only in establishing the age of the sample, but also in establishing duration of its contact with water. Even for deep sea dredge samples contact with water can be effectively stopped by the precipitation of authigenic cements. "Apparent" reaction rates (µm/1000 yrs) vary by as much as five orders of magnitude. Grambow et al. (9) have reconciled this wide range of "apparent" rates by describing the process with two rates: a) 3-20 µm/1000 yrs on the open sea floor where silica concentrations are in the range of 0.4 to 4 mg/l; b) 0.1 µm/1000 yrs in sediment covered sequences where the solution is at a Si-saturation. The results are shown in Fig. 2. Apparent rates of palagonite rind formation have been plotted to indicate their relationship to the forward rate and final rate of reaction in the glass dissolution process, as determined for borosilicate nuclear waste glasses. The slope of these curves was assumed to be one, indicating time independent reaction rates. The rate of reaction is high in solutions low in silica and about two orders of magnitude lower in silica saturated solutions. The glass then continues to react at a low rate which may or may not be constant in the long-term. A more extended data base for natural samples could help to understand the nature of the

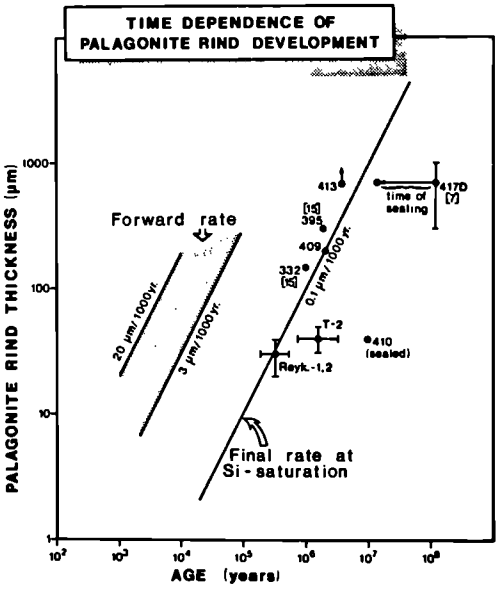

Fig. 2: Log-log-plot of palagonite rind thickness as a measure of reaction rates vs. age. The forward rate (higher rate) of reaction is assumed to determine the speed of corrosion when the basalt glass is in contact with fresh water (i.e. low in silica), whereas alteration proceeds with the final rate (lower rate) at Si-saturation. In this plot, the rate is the intercept of the curve with the y-coordinate.

long-term rate. In addition samples with even lower rates of reaction are considered (on the basis of geologic evidence) to have become sealed by authigenic cements; therefore, the time of contact with water is much less than the age of the sample.

One especially unique and useful study that deserves special mention is that by Jakobsson and Moore (24) in which they carefully studied the process of palagonitization in the basaltic tephra associated with the eruption of the volcanic island Surtsey in 1963-1967. Palagonitization was monitored via a drill hole which intersected a hydrothermal system (maximum temperature 150°C) due to intruding dikes beneath the cone. Detailed monitoring provided both time and temperature data for the system. Palagonitization was accompanied by the formation of a wide range of minerals of interest - calcite, chabazite, phillipite, analcime, tobermorite and smectite clays. The rate of palagonitization was strongly temperature dependent, doubling for every 12°C increase. At 100°C the measured rate was 3 μm/yr. The temperature dependence is similar to that of borosilicate glasses where doubling for every 10°C was found (39).

Modelling. There are only a limited number of examples in which models have been used to predict the long-term corrosion process in nuclear waste glasses and natural glasses. Jantzen and coworkers (34-37) have used a thermodynamic approach and have determined a logarithmic relationship between the glass corrosion rate (silica) and the extent of hydration and the calculated free energy of hydration. Based on these results, a "relative durability sequence" was established (from most to least durable): SiO_2, tektites, basalt glasses, and nuclear waste glasses. The results are shown in Fig. 3

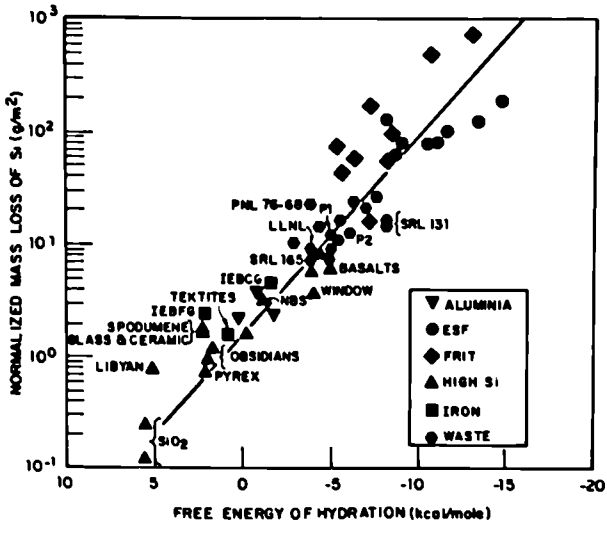

Fig. 3: Relation between the normalized mass loss of silicon and the free energy of hydration for various glasses.
(For a detailed explanation of the figure see ref. (36))

which has been reproduced from the work by Jantzen and Plodinec (36). Among the natural glasses, basalt glasses are the most comparable to nuclear waste glasses. The final conclusion, i.e. that nuclsar waste glasses such as SRP 165 are as durable as natural basalt glasses, however fails to take into account the wide variations in the observed durability of basalt glasses in natural environments.

In another approach, Grambow and others (9) have used the PREEQE "geochemical code" (38) to calculate the sequence of phase formation in basalt glass sea water reactions. The reaction path is calculated for an idealized closed system assuming congruent glass dissolution, precipitation of solid alteration products and the accumulation of soluble glass constituents in solution. The calculated sequence of phases: nontronite-saponite-phillipsite-chabazite is in agreement with the observed sequence:
palagonite-smectite(saponite)-phillipsite-gyrolite-chabazite-analcime.

Such an approach emphasizes ths importancs of metastable phases in controlling solution compositions. The sequence of clay mineral compositions which are precipitated (e.g. Fe-saponite vs. Mg-saponite) was found to depend on whether ferrihydrite or the less soluble lepidocrosite was used in the calculations. Additionally, examination of natural samples suggests that celadonite and chlorite are rare ("kinetically hindered") phases and can be excluded from the list of potential alteration products used in the computational simulation of solution concentrations. Similar calculations by Crovisier and others (29) confirm the results of these calculations and are consistent with static leaching tests using an artificial basaltic glass and sea water.

4. Conclusions

In the comparison of the corrosion behavior of natural glasses to nuclear waste form glasses, analogous behavior has been demonstrated between the results of laboratory experiments, empirical observations of natural occurrences and the results of calculations. The usefulness of the analogy in this case is substantiated by the wide variety of consistent results. The effects of temperature and solution compositions on the alteration products and corrosion rate have been determined and confirmed by the comparison of experimental, empirical and theoretical studies. Analogous behavior of borosilicate nuclear waste glasses and basalt glasses has been demonstrated by: a) the formation of similar reaction (alteration) products and surface morphologies with both types of glasses in the laboratory, b) similar reaction products on basalt glasses in the laboratory and in nature, c) the calculated (predicted) sequence of alteration products is in agreement with sequences observed in nature, d) comparable chemical durability was measured in the laboratory and predicted from thermodynamic calculations of energies of hydration.

Acknowledgement

Figures 1 and 3 were reproduced with permission of J. of Noncryst. Solids and Figure 2 of The Materials Research Society, Pittsburgh.

REFERENCES

1. EWING, R.C. and JERCINOVIC, M.J., in Scientific Basis for Nuclear Waste Management Vol X, 1987, eds. J.K. Bates and W.B. Seefeldt. (Materials Research Society, Pittsburgh 1987), in print.
2. EWING, R.C., in Scientific Basis for Nuclear Waste Management, Vol.1, edited by G.J. McCarthy (Plenum Press, New York, 1979), p.57.
3. EWING, R.C. and HAAKER, R.F., Natural Glasses: Analogues for Radioactive Waste Forms (Battelle PNL Report 2776/UC-70, 1979) 71 pp.
4. MALOW, G. and EWING R.C., in Scientific Basis for Nuclear Waste Management, Vol. 3, edited by J.G. Moore (Plenum Press, New York, 1981), p. 315.
5. ALLEN, C.C., in Scientific Basis for Nuclear Waste Management V, edited by W. Lutze (North-Holland, New York, 1982), p. 37.
6. MALOW, G., LUTZE, W. and EWING, R.C., J. Non-Crystalline Solids 67, 305 (1984).
7. LUTZE, W., MALOW, G., EWING, R.C., JERCINOVIC, M.J. and KEIL, K., Nature 314, 252 (1985).
8. BYERS, C.D., JERCINOVIC, M.J., EWING, R.C. and KEIL, K., in Scientific Basis for Nuclear Waste Management VIII, edited by C.M. Jantzen, J.A. Stone and R.C. Ewing (Materials Research Society, Pittsburgh, 1985) p. 583.
9. GRAMBOW, B., JERCINOVIC, M.J., EWING, R.C. and BYERS, C.D., in Scientific Basis for Nuclear Waste Management IX, edited by L.Werme (Materials Research Society, Pittsburgh, 1986) p. 263.
10. COWAN, R. and EWING, R.C., in Microanalysis-1986, edited by A.D.Romig Jr. and W.F. Chambers (San Francisco Press, Inc., San Francisco, 1986).
11. JERCINOVIC, M.J., EWING, R.C. and BYERS, C.D., in Advances in Ceramics, Nuclear Waste Management, edited by D.E.Clark, W.B.White and A.J.Machiels (American Ceramic Society, Columbus, Ohio) in press.
12. BYERS, C.D., EWING, R.C., JERCINOVIC, M.J., in Advances in Ceramics, Nuclear Waste Management, edited by D.E.Clark, W.B.White and A.J.Machiels (American Ceramic Society, Columbus, Ohio) in press.
13. BARKATT, Aa., BOULOS, M.S., BARKATT, Al., SOUSANPOUR, W., BOROOMAND, M.A., MACEDO, P.B., and O'KEEFE, J.A., Geochimica et Cosmochimica Acta 48, 361 (1984).
14. BARKATT, Aa., SAAD, E.E., ADIGA, R, SOUSANPOUR, W., BARKATT, Al., and ALTERESCU, S., Advances in Ceramics 20: Nuclear Waste Management II, edited by D.E.Clark, W.B.White and A.J.Machiels (American Ceramic Society, Columbus, Ohio) in press.
15. DICKIN, A.P., Nature 294, 342 (1981).
16. SIMMONS, J.H., MACEDO, P.B., BARKATT, Aa., and LITOVITZ, T.A., Nature 278, 729 (1979).
17. ZIELINSKI, R.A., Chemical Geology 27, 47 (1979).
18. ZIELINSKI, R.A., LIPMAN, P.W., MILLARD Jr., H.T., American Mineralogist 62, 426 (1977).
19. WHITE, A.F., Geochimica et Cosmochimica Acta 47, 805 (1983).
20. WHITE, A.F., Advances in Ceramics 20: Nuclear Waste Management II, edited by D.E.Clark, W.B.White and A.J.Machiels (American Ceramic Society, Columbus, Ohio) in press.

21. FRIEDMAN, I. and SMITH, R.L., American Antiquity 25, 476 (1960).
22. FRIEDMAN, I., SMITH, R.L. and LONG, W.D., Geological Society of America Bulletin 77, 323 (1966).
23. FRIEDMAN, I. and TREMBOUR, F.W., American Scientist 66, 44 (1978).
24. JACOBSSON, S.P. and MOORE, J.G., Geological Society of America Bulleting 97, 648 (1986).
25. EWING, R.C. and KRUMHANSL, J.L., American Nuclear Society Transactions 33, 280 (1979).
26. JERCINOVIC, M.J., EWING, R.C., KEIL, K., GRAMBOW, B., and LUTZE, W., Proceedings of the 5th International Symposium on Water-Rock Interaction, Reykjavik, Iceland, August 8-17, 1986 (in press).
27. CROVISIER, J.L., THOMASSIN, J.H., JUTEAU, T., EBERHART, J.P., TOURAY, J.C., and BAILLIF, P., Geochimica et Cosmochimica Acta 47, 377 (1983).
28. CROVISIER, J.L., EHRET, G., EBERHART, J.P., and JUTEAU, T., Sci. Geol. Bull. 36, 187 (1983).
29. CROVISIER, J.L., FRITZ, B., GRAMBOW, B., and EBERHART, J.P., Scientific Basis for Nuclear Waste Management IX, edited by L.Werme (Materials Research Society, Pittsburgh, Pennsylvania, 1986) p.273-280.
30. BATES, J.K., JARDINE, L.J., and STEINDLER, M.J., Science 218, 51 (1982).
31. MORGENSTEIN, M. and RILEY, T.J., Asian Perspectives XVII (2), 145 (1974).
32. HEKINIAN, R. and HOFFERT, M., Marine Geology 19, 91 (1975).
33. JUTEAU, T., NOAK, Y., WHITECHURCH, H., and COURTOIS, C., Initial Reports of the Deep Sea Drilling Project 51-53 (1979).
34. PLODINEC, M.J., JANTZEN, C.M., and WICKS, G.G., Advances in Ceramics, 8, edited by G.G.Wicks and W.A.Ross (American Ceramic Society, Columbus, Ohio, 1984) pp. 491-495.
35. PLODINEC, M.J., JANTZEN, C.M., and WICKS, G.G., Scientific Basis for Nuclear Waste Management VII, edited by G.L.McVay (North-Holland, New York, New York, 1984) pp. 755-762.
36. JANTZEN, C.M. and PLODINEC, M.J., Journal of Non-Crystalline 67, 207 (1984).
37. JANTZEN, C.M., Advances in Ceramics 20: Nuclear Waste Management II, edited by D.E.Clark, W.B.White and A.J.Machiels (American Ceramic Society, Columbus, Ohio) in press.
38. PARKHURST, D.L., THORSTENSEN, D.C., and PLUMMER, L.N., Water-Resources Investigations 80-96 (U.S. Geological Survey, Reston, Virginia, 1980).
39. CHICK, L.A. and TURCOTTE, R.P., Report PNL-4576 (1983).

GLASS STABILITY IN THE MARINE ENVIRONMENT

Z.H. ZHOU, W.S. FYFE and K. TAZAKI
Department of Geology
The University of Western Ontario
London, Ontario, Canada, N6A 5B7

Summary

Similarities in corrosion behavior have been found in static leaching experiments on natural (basaltic and rhyolitic) and waste form (PNL76-68, ABS-118) glasses in seawater and marine sediments. Grainy but cohesive magnesium-rich surface layers form on both natural and waste form glasses. Basaltic and ABS-118 glasses exhibit especially similar corrosion behavior and have comparable corrosion rates. As fresh basaltic and rhyolitic glasses are common in sediments as old as Miocene (~15 my) in two deep-sea drilling sites, it appears that fine natural glass can survive for a few million years. Metal encapsulated, massive glass pieces could therefore survive for millions of years if buried in appropriate marine sediments in the submarine environment.

1.1 Introduction

The chemical durability of nuclear waste forms is one of most important problems in disposal of such wastes. At this time most waste disposal systems involve a glass as the dilution matrix. The long-term stability of nuclear waste glasses must be predicted from extrapolations of short-term laboratory data and then verified, which is only possible by comparing the glasses with their closest natural analogues[1].

Glasses of different compositions are common natural materials, and the study of corrosion of natural glasses provide valuable information regarding the behavior of waste glasses, and may even suggest new glass compositions. Numerous workers[1-3] have shown that the corrosion behavior of basaltic glasses and waste glasses are similar in pure water and NaCl solutions. The experiments of this study document and compare corrosion behaviors of natural and radwaste glasses in seawater and in marine sediments, with experiments in distilled water for comparison. Naturally occurring volcanic glasses from two deep-sea drilling sites were examined to quantify the long-term stability of natural glasses in the submarine environment. This information is used to infer the long-term stability of radwaste glasses in such environments.

2. Experiments

2.1 Methods

Glasses chosen for study include PNL76-68, ABS-118, basaltic and rhyolitic. Both PNL76-68 and ABS-118 glasses were made from mixed oxide powders according to their formula[4]. HLW-oxides in ABS-118 were not

included. Basaltic glass (BG) was made from natural basalt (provided by Dr. W.R. Church) to which about one percent (by weight) of U_3O_8 was added. The powdered samples were fused at 1400°C in Pt crucibles; to ensure homogeneity, glass pellets from a first fusion were ground and fused for a second time. Each glass pellet was annealed at 550°C, cooled to room temperature, and cut into discs (~1.5 mm thick, 11.0 mm in diameter). The Rhyolitic glass (RG) is a natural sample from Mono Craters, California, which was directly cut into discs of the same size as the other glasses. All glass discs were polished with diamond powder and ultrasonically cleaned in an acetone bath. The composition of the glasses was analysed by electron microprobe and inductively coupled argon plasma (Table 1).

Table 1. Glass Composition

Glass			ABS-118		PNL 76-68	
Constituent	RG[a]	BG[a]	Intended	Analysed[b]	Intended	Analyzed[b]
SiO_2	77.35	48.79	50.99	54.54	40.00	40.25
Al_2O_3	12.48	15.39	5.53	5.59		
Fe_2O_3	0.63[c]	10.32[c]	3.27	3.30	11.10	11.02
MgO	0.02	8.19				
CaO	0.76	11.32	4.52	3.97	2.00	1.68
Na_2O	3.60	2.94	11.05	10.47	12.90	10.87
K_2O	4.60	0.40			0.10	0.09
TiO_2	0.08	1.12			3.00	3.14
MnO_2	0.05	0.19				
P_2O_5		0.12	0.34	0.44	0.50	0.58
UO_3		1.00	1.40	d		
B_2O_3			15.68	d	9.50	d
Li_2O			2.26	d		
Cs_2O					1.10	d
BaO					0.60	0.70
SrO					0.40	0.40
NiO			0.45	0.41	0.60	0.36
ZnO			2.82	2.90	5.00	5.05
Cr_2O_3			0.56	0.68	0.40	0.32
ZrO_2			1.12	1.14	1.90	1.88
MoO_3					2.40	d
CeO_2					3.0	d
La_2O_3					3.1	d
Eu_2O_3					1.0	d
Yb_2O_3					1.0	d
Total	99.58	99.09	99.99		99.96	

[a] Analyzed by electron microprobe; [b] Analyzed by inductively coupled argon plasma; [c] Total iron is given Fe_2O_3; [d] not analyzed.

The leachants used in experiments were distilled and deionized water (DIW), natural seawater (SW), and silica-saturated seawater (Si-SW). Natural seawater was collected from Massachusetts Bay, USA, by Dr. F.L. Sayles. Si-SW was prepared by adding silicic acid to natural seawater.

The corrosion tests were conducted following the MCC-1 procedures[5]. Specimen were placed on Teflon grids near the center of Teflon vials, and leachants were added to yield a surface area to volume ratio of 10 m^{-1}. Vials were placed in a conventional oven operating at 30°C or 90°C ±

0.5°C. In a simulated submarine environment at room temperature, oceanic muds were placed in a twenty liter plastic cylinder, and covered by a seawater reservoir. Nylon threads were attached to glass discs (of RG, BG, and ABS-118) buried in the muds.

After the allotted corrosion time (10, 30, 90, 180 days) solute concentrations of leachates were analysed using atomic absorption spectroscopy (for Zn, Fe), by colorimetric methods (for B and Si)[6], and by neutron activation (for U). The corroded glass surface was first investigated by optical microscopy, and the material on one face of each glass disc was scraped off, and analysed using X-ray diffraction (XRD), transmission electron microscopy (TEM), and scanning transmission electron microscopy (STEM). The other face of each glass disc was coated with gold, then observed by scanning electron microscopy (SEM) with energy dispersive X-ray analyzer (EDX), and secondary ion mass spectrometry (SIMS). The thickness of surface layers of corroded glasses was measured on the glass surface by a Dektak IIA Profilometer.

2.2 Results

The corrosion behavior of natural and waste form glasses in seawater at 90°C is strikingly similar. For both, a cohesive surface layer formed on the glass surface. At high magnification (Fig. 1), the surface layer appears as aggregates of rice-shaped grains. EDX data show that the surface layer has inherited the chemical composition of parent glass, but in all cases, significant amounts of Mg, with lesser amounts of Cl have been incorporated into the surface layers. SIMS analysis provided further evidence for such process and depletion of Na, Li and B.

The materials that make up surface layer are either amorphous or weakly crystalline as shown by XRD. TEM data confirmed XRD results. Most of surface layer material does not show an electron diffraction pattern, indicating its amorphous nature (Fig. 2-A). In runs of 30 days or longer, the surface layer consists dominantly of amorphous material, but also contains clay and sulphate minerals. Mg-rich clays such as lizardite and talc are most abundant (Fig. 2-B and 2-C). Less amount of kaoline minerals are also present. In both ABS-118 and Basaltic glasses, carbonate minerals were found as surface precipitates (Fig. 3). Carbonate crystals on basaltic glass surface were found after 30 days, and on ABS-118 after 90 days. Carbonates are not present on surfaces of PNL76-68 and Rhyolitic glasses.

Surface layers vary in thickness. PNL76-68 has the thickest surface layer, followed in order of decreasing thickness, by Rhyolitic, ABS-118 and Basaltic. ABS-118 and Basaltic glasses have reaction layers of comparable thickness. Note that surprisingly rhyolitic glass has a thicker reaction layer than basaltic glass.

The changes in leachate pHs resulting from corrosion in seawater at 90°C are shown in Fig. 5. It's quite obvious that pH change of leachate from PNL76-68, ABS-118, and basaltic glasses are similar, this is especially true for ABS-118 and basaltic glasses. Leachate pH resulting from rhyolitic glass is lower than those from other three glasses.

The weight losses of the glasses during corrosion in seawater at 90°C also show very similar trends (Fig. 6). After about 60 days, the weight losses of all glasses are less than zero, indicating the overall mass gain. The elemental mass loss of glasses during corrosion in seawater at 90°C varied with glass type and reaction time (Fig. 7-9). The Si loss from PNL76-68 and ABS-118 continue after 30 days, whereas that of basaltic glass decreases, indicating that back reaction was removing Si from solution (Fig. 7). Iron show similar behaviors to Si (Fig. 8). More U is lost from

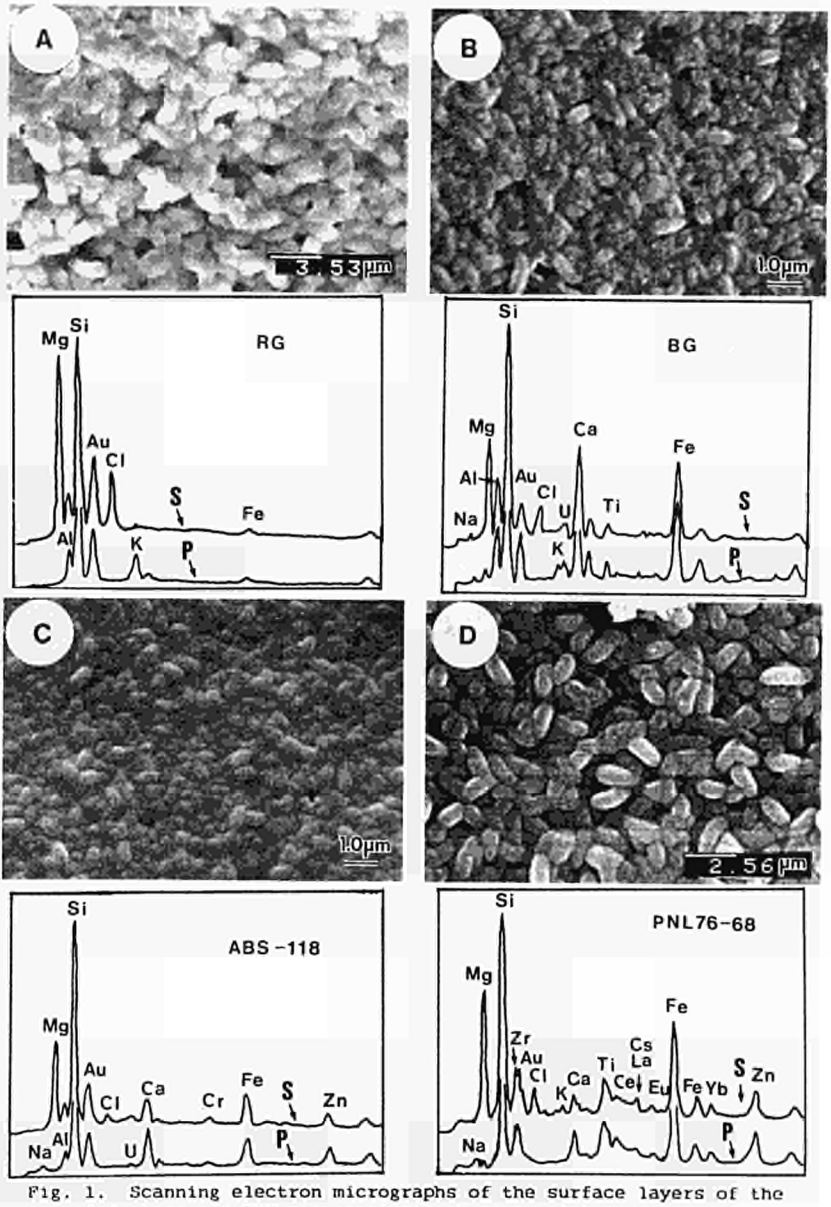

Fig. 1. Scanning electron micrographs of the surface layers of the corroded glass and EDX microanalysis of parent (p) and corroded (s) glasses (A. RG; B. BG; C. ABS-118; D. PNL76-68).

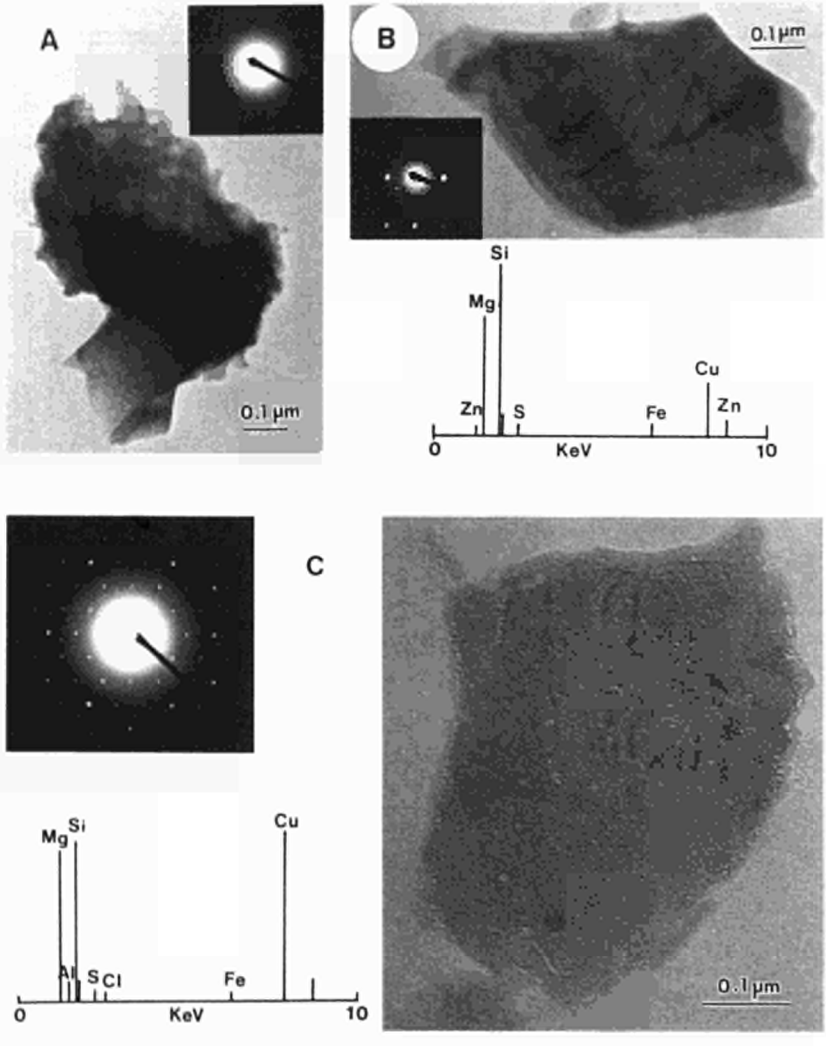

Fig. 2. Transmission electron micrographs of surface layer material and EDX microanalysis. A. Amorphous material present in surface layer of Basaltic glass after 90 days; B. Talc present in surface layer of PNL76-68 after 90 days. Copper peak in EDX is from sample grid; C. Lizardite present in surface layer of Basaltic glass after 180 days.

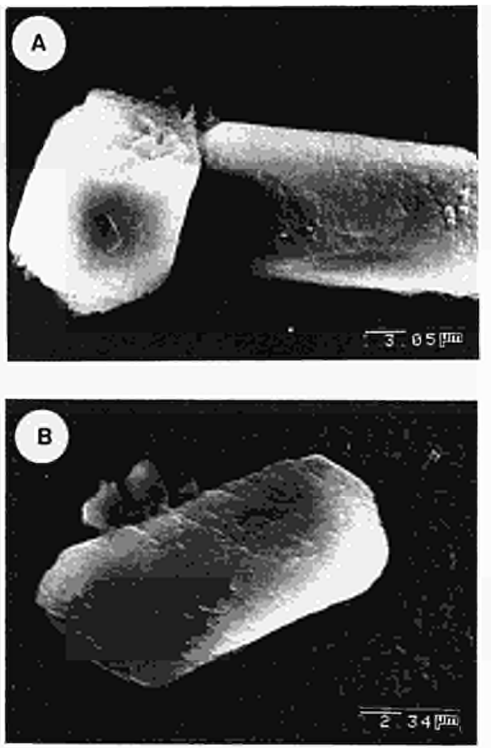

Fig.3 Carbonate precipitates on the surface of ABS-118(A) and Basaltic(B) glasses after 90 days corrosion in seawater at 90°C.

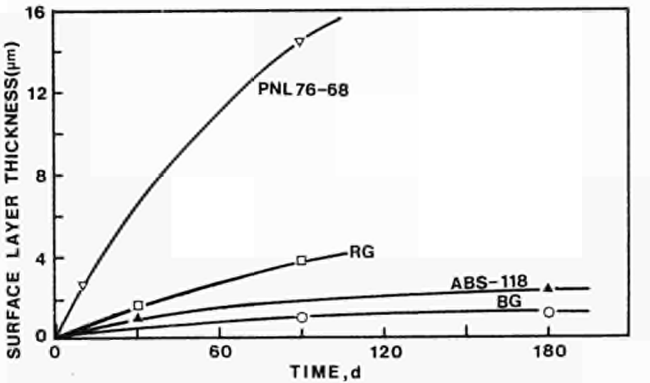

Fig.4 The thickness of surface layers developed during glass corrosion in seawater at 90°C.

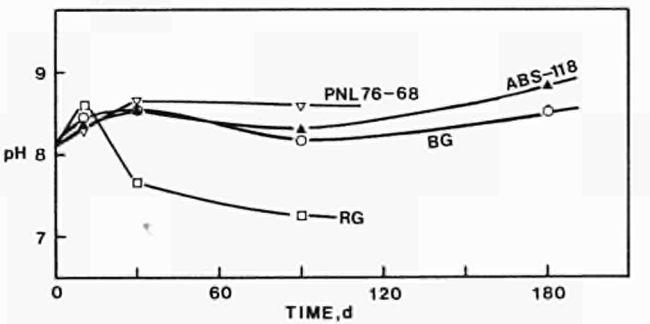

Fig.5 Leachate pH resulting from glass corrosion in seawater at 90°C.

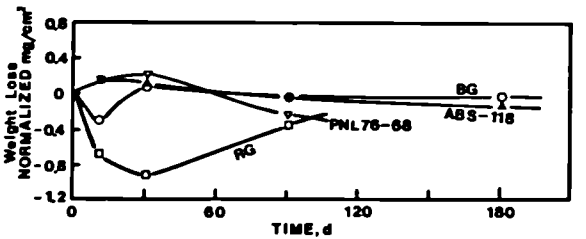

Fig 6 Normalized weight loss during glass corrosion in seawater at 90°C.

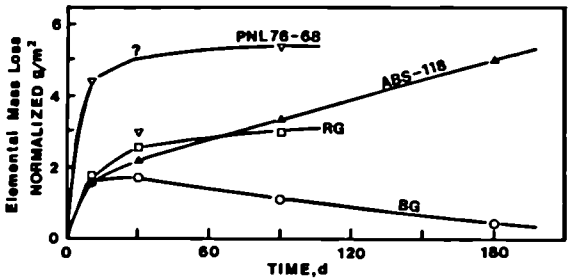

Fig.7 Normalized silicon loss during glass corrosion in seawater at 90°C.

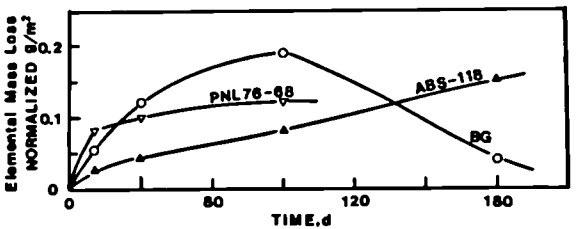

Fig.8 Normalized iron loss during glass corrosion in seawater at 90°C.

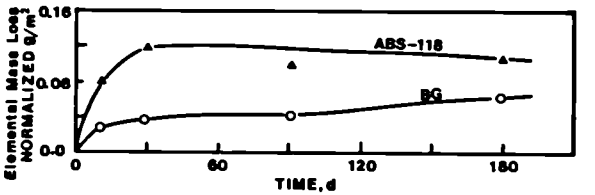

Fig.9 Normalized uranium loss during glass corrosion in seawater at 90°C.

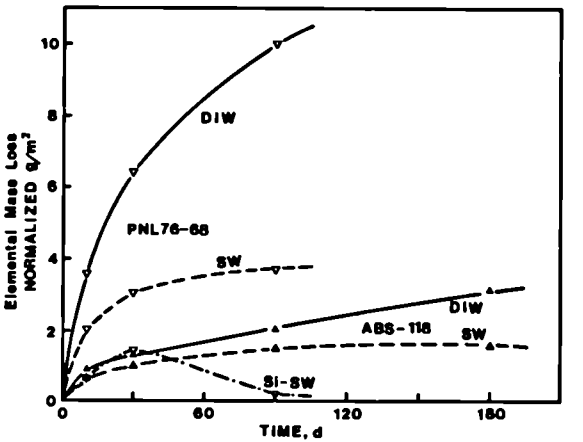

Fig.10 Normalized boron loss during glass corrosion in distilled water, seawater and Si saturated seawater at 90°C.

ABS-118 than from basaltic glass; however, after 30 days, nc more U is lost from ABS-118. It would be of interest to know the future uranium release of both glasses. Zinc in ABS-118 glass behaves in a similar manner to U.

Glass corrosion in DIW at 90°C is much faster than in SW at the same temperature. For example, boron release from both PNL76-68 and ABS-118 was higher in DIW than that in SW (Fig. 10). The release of boron from PNL76-68 is even lower in Si-SW than in SW. Details of leachant effect on glass corrosion will be discussed in a subsequent paper.

Glass corrosion in SW at 30°C proceeds more slowly than at 90°C. Few changes on ABS-118 and RG surface were detectable even after 180 days. In contrast, basaltic glass is more reactive: a very thin, grainy surface layer developed after 180 days at 30°C, and small carbonate crystals were also formed on the upper surface. However, in contrast with experiments at 90°C, Mg was not enriched in the surface layer. This difference may imply that the corrosion mechanism operative at the two temperatures is different.

Glasses emplaced in simulated marine sediments exhibit even fewer changes than those corroded in SW at 30°C. Very little amorphous material is present on glass surfaces even after 350 days, which suggests glass may be more stable in sediment pore water than that in seawater.

2.3 Discussion

The surface layers on corroded glass surfaces have long been considered as hydration layers, formed by counter-diffusion between hydrogen ions (such as H^+ and H_3O^+) in solution exchanging mobile ions (such as Na^+, Li^+ and K^+) in the glass network[7-9]. Accordingly, the surface layer is described as a gel. Recent studies[10,11,12], however, suggest that glass corrosion could be more complicated processes and surface layers of crystalline nature may be present[1,2,13]. In a Soxhlet-type leaching test, Murakami and Banba[14] found that the surface layers were made up of 10- to 100 nm crystalline and noncrystalline particles; the only crystalline phase they found was a sheet silicate. The data of this study show that the surface layer is composed dominantly of amorphous material, and that crystallinity of the layer increases with corrosion time. Mg-enrichment in the surface layer probably relate to the formation of Mg-silicates. This Mg-rich surface layer may act as a reaction barrier[12].

According to the surface layer thickness and normalized Si loss during corrosion, the relative reactivity in SW of the glasses may be arranged as follows:

Basaltic > ABS-118 and Rhylitic at 30°C

PNL76-68 > Rhyolitic > ABS-118 > Basaltic at 90°C

Both ABS-118 and Basaltic glasses have similar corrosion behavior and rates, this fact suggests that naturally occurring basaltic glasses may provide an effective analogue to nuclear waste form glass. It is surprising that rhyolitic glass is corroded faster than basaltic glass at 90°C because glass of high silica content is commonly believed[4] to be more stable than that of low silica content. However, a recent study[12] show that partial substitution by MgO or CaO for SiO_2 could increase the durability of a glass. This may explain the greater durability of basaltic vs. rhyolitic glass found in this study.

Numerous workers[15-17] have shown glass corrosion in most simulated ground water is no slower than that in distilled water. In contrast, the data of this study show that glass corrosion in seawater is much slower than that in distilled water, and in marine sediments, glass may even be more stable. This has important implications to be considered in discussions of continental and sub-seabed disposal of nuclear wastes.

3. Natural Glasses in Deep-Sea Sediments

Since, from the data presented above, it appears that the corrosion behavior and rates of waste form glass and its natural analogue are similar, the long-term stability of natural glasses could provide useful information on radwaste glass. Glassy materials are not only very common in oceanic sediments and submarine extrusive volcanics[18-19] but volcanic glasses of various ages in deep-sea sediments provide a unique opportunity to document the long-term stability of such glasses.

3.1 Methods

Glass bearing deep-sea sediments were collected from two DSDP cores, site 450 and site 436. Site 450 is located on the eastern side of the Parece Vela Basin, Philippine plate[20], site 436 on outer rise of the Japan Trench[21]. Samples were collected from youngest to oldest units (Fig. 11), ranging in age from <1 to 15 million years. Each sample was 3 cm^3 in size, and clays were separated from non-clays by washing; each fraction was collected for SEM and electron microprobe study. The age of glasses can be estimated from well-established fossil zones in the sediments[20,21] or can be dated by fission-track method[22].

3.2 Glass type and morphology

Colourless rhyolitic glass and brown basaltic glass are present in sediments of site 450, whereas most glass from site 436 is rhyolitic. Glass shards are 20-100 μm in size on average, and fresh glass shards are found at all depths in both cores. Fresh basaltic glass from site 450 (~10 my) is characterized by its integral acicular shape and smooth surface. Slightly older (~11 my) glass shards and pumice fragments from the same core are also quite fresh (Fig. 12-B). Fresh sideromelane from this core (Fig. 12-C) is about 12 million years old. The alteration of a basaltic glass shard (~14 my) from site 450 is indicated by ragged edges and the presence of alteration material on its surface (Fig. 12-D). Glass shards from site 436 are also very fresh, examples given in Fig. 12-E and 12-F.

These preliminary results suggest that both rhyolitic and basaltic glass particles of 20-100 μm in size do remain unaltered in deep-sea sediments for up to 15 million years. More detailed work is in progress to quantify the long-term stability of these glasses.

4. Conclusions

Results of these experimental studies of natural and waste form glasses in seawater and marine sediments, in conjunction with a study of natural glasses found in deep-sea sediments, lead to the following conclusions: A. Natural and waste form glasses, especially basaltic and ABS-118 glasses exhibit similarities in corrosion behavior in seawater and marine sediments. B. Both natural and waste form glasses are most stable in marine sediments, and are more stable in seawater than in distilled water. C. Fine natural glass particles could survive for up to 15 million years in deep-sea sediment. D. Metal encapsulated, massive glass pieces could probably survive for millions of years if buried in appropriate marine sediments in the submarine environment.

Acknowledgements:

The authors wish to thank Dr. F.L. Sayles for providing seawater and oceanic muds; Dr. W.R. Church for providing basalt sample and U.S. National Science Foundation for deep-sea drilling samples; John Forth and Ian Muir

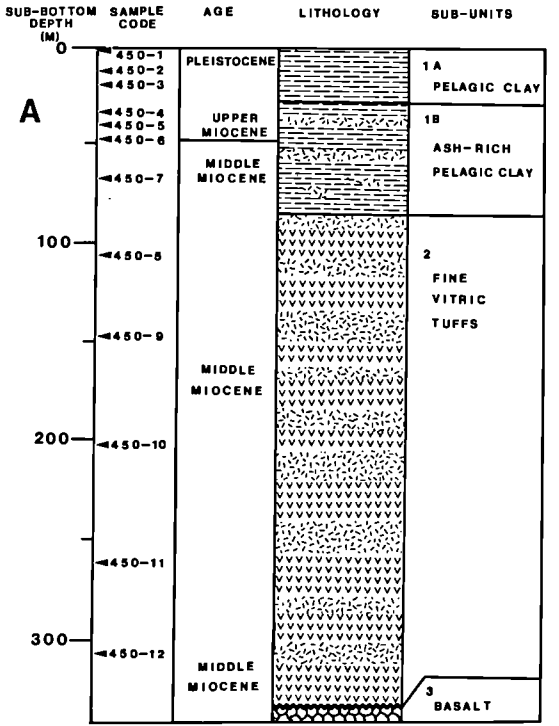

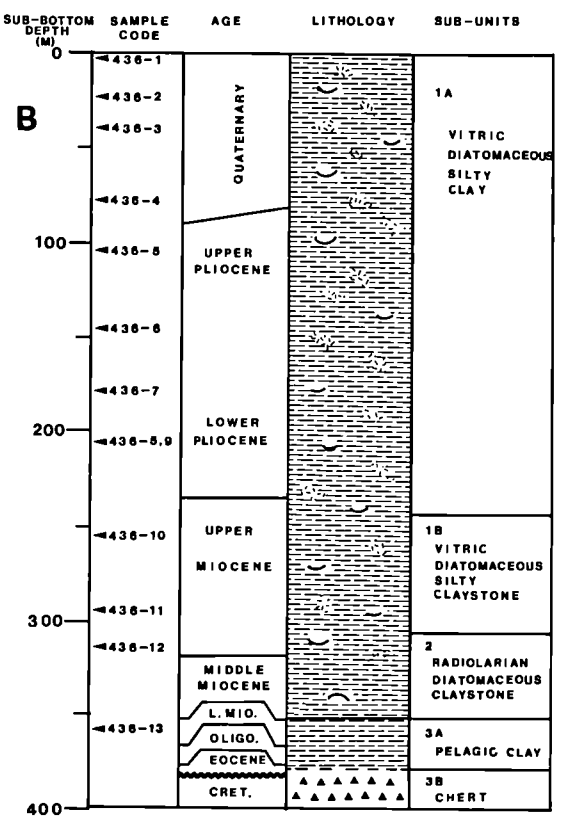

Fig.11 A. Lithology, age, and sampling position at site 450, modified from Kroenke et al.(1981).
B. Lithology, age, and sampling position at site 436, modified from Langseth et al.(1980).

for their help in glass making and preparation; Dr. J. Barbier for interpretation of TEM data. The financial support of this work is from Natural Sciences and Engineering Research Council of Canada.

References

1. LUTZE, W. et al. (1985). Alteration of basalt glasses: implications for modelling the long-term stability of nuclear waste glasses. Nature, 314, 252-255.
2. MALOW, G. et al. (1984). Alteration effects and leach rates of basaltic glasses: implications for the long-term stability of nuclear waste form borosilicate glasses. J. Non-Cryst. Solids, 67, 305-322.
3. BYERS, C.D. et al. (1985). Basalt Glass: an analogue for the evaluation of the long-term stability of nuclear waste form borosilicate glasses. Mat. Res. Soc. Symp. Proc. 44, 583-590.
4. GRAUER, R. (1985). Synthesis of recent investigations on corrosion behaviour of radioactive waste glasses. EIR-Bericht Nr. 538.
5. STRACHAN, D.M. et al (1981). MCC-1: a standard leach test for nuclear waste forms. Nucl. Tech., 56, 306-312.
6. GRASSHOFF, K. et al. (1983). Methods of seawater analysis. 2nd edition 419 pp., Verlag chemie, Weinheim.
7. DOUGLAS, R.W. and EL-SHAMY, T.M.M. (1967): Reaction of glasses with aqueous solutions. J. Am. Ceram. Soc., 50, 1-8.
8. DOUGLAS, R.H. (1979). Chemical Durability of Glass. in Doremus, R.H. and Tomozawa, M. ed. Treatise on materials Sci. and Tech., 17, 41-69.
9. MOORE, J.G. (1966). Rate of palagonitization of submarine basalt adjacent to Hawaii. USGS Prof. Paper, 550-D, D163-D171.
10. KUHN, W.L. et al (1983). Development of a leach model for a commercial nuclear waste glass. Nucl. Tech., 63, 82-89.
11. BARKATT, A. et al. (1985). Mechanisms of defense waste glass dissolution. Nucl. Tech., 73, 140-164.
12. ISARD, J.O. and MULLER, W. (1986). Influence of alkaline earth ions on the corrosion of glasses. Phys. Chem. Glasses, 27, 55-58.
13. BATES, J.K. (1985). The hydration alteration of a commercial nuclear waste glass. Chem. Geol., 51, 79-87.
14. MURAKAMI, T. and BANBA, T. (1984). The leaching behavior of a glass waste form - Part I: the characteristics of surface layers. Nucl. Tech., 67, 419-428.
15. LOKKEN, R.O. and STRACHAN, D.M. (1984). Long-term leaching of two simulated waste glasses, in Wicks, G.G. (ed.) Advances in ceramics, Vol. 8: Nucl. Waste Management. The Am. Ceram. Soc., Columbus, Ohio.
16. HERMANSSON, H.P. et al. (1983). Effects of solution chemistry and atmosphere on leaching of alkali borosilicate glass, in Brookins, D.G. (ed.) MRS Sci. Basis. Nucl. Wast. Manag. VI, North-Holland 143-150.
17. WESTSIK, J.H. Jr. et al. (1983). High-temperature leaching of an actinide-bearing, simulated high-level waste glass. PNL-3172 Pacific Northwest Laboratory, Richland, Washington.
18. SCHMINCKE, H.U. (1981). Ash from vitric muds in deep sea cores from the Mariana Trough and fore-arc region (South Philippine Sea) (Sites 453, 454, 455, 458, 459 and SP), Deep Sea Drilling Project Leg 60, in Init. Rep. DSDP Go. Hussong, D.M. et al. ed. 473-481.
19. BYERLY, G.R. and SINTON, J.M. (1979). Compositional trends in natural basaltic glasses from deep sea drilling project holes 417D and 418A, In Init. Rep. DSDP, 53. Donnelly, T. et al. ed. 957-971.
20. KROENKE, L. (1981). Site 450: East side of the Parace Vela Basin, in Init. Rep. DSDP 59. Orlofsky, S. ed. 355-403.

21. LANGSETH, M. (1980). Site 436: Japan outer rise, Leg 56, in Init. Rep. DSDP 56-57 Part 1. Lee, M. and Stout, L.N. ed. 399-446.
22. GANSEI, S.S. et al. (1980). Fission-Track age of volcanic glasses from ash layers at deep sea drilling project site 436, in Init. Rep. DSDP 56-57 Part 11. Lee, M. and Stout, L.N. ed. 1277-1279.

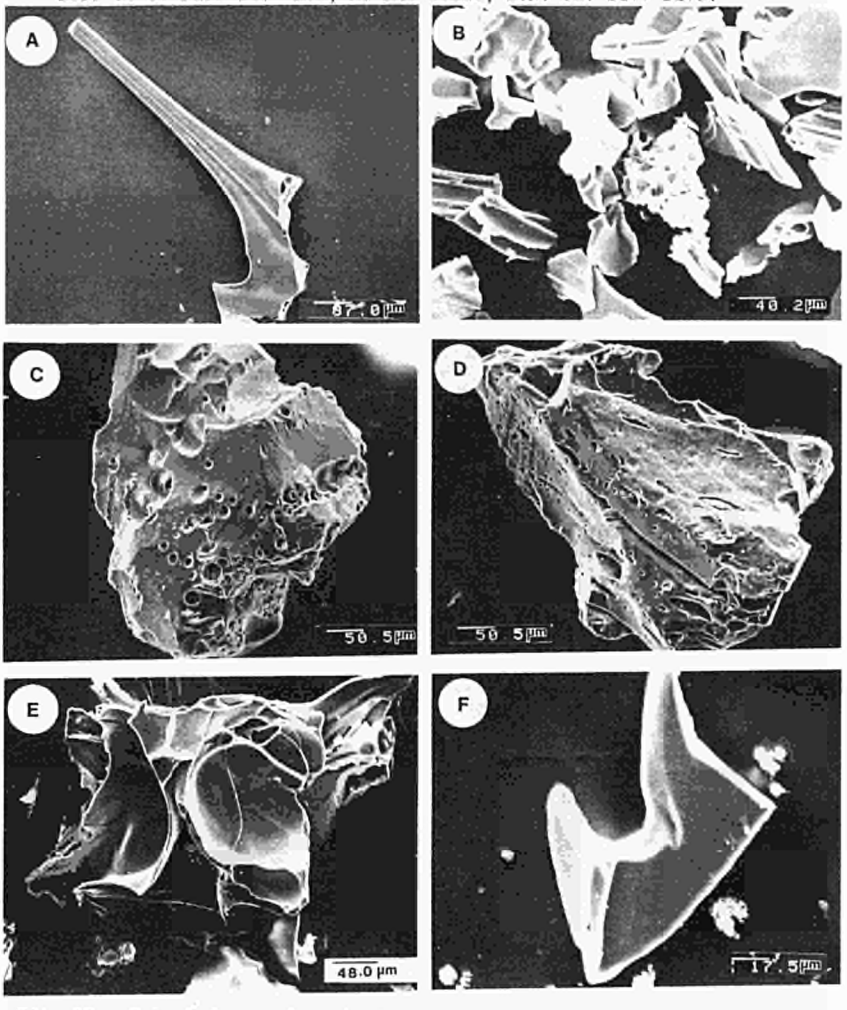

Fig. 12. Selected scanning electron micrographs of volcanic glasses from DSDP sites 436 and 450. A. A glass shard in 450-4; B. A general view of glassy material in 450-7; C. A fresh sideromelane in 450-10; D. A glass shard showing alteration in 450-11; E. A fresh glass shard in 436-1; F. A fresh glass shard in 436-12.

SESSION 4 :

ANALOGUES OF PROCESSES AFFECTING RADIONUCLIDE MIGRATION

PART 1

Chairman : I. NERETNIEKS (RIT, S)

Co-Chairman : B. SKYTTE-JENSEN (Risø NL, DK)

TESTING GEOCHEMICAL MODELS IN A HYPERALKALINE ENVIRONMENT

A.H. Bath 1), U. Berner 2), M. Cave 1), I.G. McKinley 2) and C. Neal 3)

1) British Geological Survey, Keyworth, Notts, NG12 5GG, U.K.
2) Eidg. Institut fuer Reaktorforschung, 5303 Wuerenlingen, CH
3) Institute of Hydrology, Wallingford, Oxon, OX108BB, U.K.

Summary

The near-field of a nuclear waste repository containing large volumes of cement and concrete will be highly alkaline and, probably, chemically reducing. A challenge in safety analysis is to determine the constraints on releases of particular radionuclides set by their low solubility in such an environment. Chemical thermodynamic models are usually used to calculate such solubilities but these are, inherently, oversimplifications of the real system and must be validated experimentally. These models can also be tested in natural analogue systems. A good analogue of aged concrete pore waters are the hyperalkaline springs found in the region of the Semail Ophiolite Nappe in Northern Oman. These have pH values of 10-12, are somewhat saline and are often extremely reducing, containing significant quantities of free hydrogen gas. In this study, thermodynamic model predictions of trace element solubility limits are compared with actual concentrations measured. Although somewhat crude, results indicate that predicted values are generally consistent with observations and give some indications of over-conservatisms associated with particular databases.

1.1 Introduction

Many nuclear waste repositories will contain large quantities of cement and concrete (e.g. components of waste, immobilisation matrix, backfill and engineering structures) and, in such cases, the chemistry of the near-field is usually dominated by this material. The pore waters of fresh cements and concretes are highly alkaline (pH generally around 13 or above) and consist primarily of a solution of Na and K hydroxides, the exact composition of which is dependent on cement/concrete type (1). With time, however, Na and K will be leached out and the water chemistry will be controlled by the less soluble $Ca(OH)_2$ and calcium silicates which comprise the bulk of the matrix (2,3). As deep groundwaters are generally reducing, the cement porewater would also become so after original trapped air is consumed by corrosion reactions. Anaerobic corrosion of contained metals or biodegradation of organic matrices might, in fact, lower the redox potential further and even result in significant formation of hydrogen (4).

Knowledge of the near-field chemical environment is important in repository safety assessment as it affects the solubility and speciation of radionuclides in the waste and hence their release rate and extent of retardation during transport. Equilibrium chemical thermodynamics provides the usual approach for evaluating elemental solubilities and speciation in aqueous solution. Application to nuclear waste problems is, however, somewhat limited by the availability of relevant data and hence many simplifying assumptions are generally involved in its use in this field. In particular, background data are very sparse for the rather extreme chemical conditions found in the pore waters of concrete or cement.

Data derived mainly under normal aqueous solution chemistry (neutral to acidic) must thus be extrapolated to the very alkaline environment expected. Relatively little laboratory data are available which would allow validation of model predictions - particularly under strictly reducing conditions - and this limits the weight which can be placed on model predictions.

1.2 Rationale for the study

At first sight, examination of groundwater from Oman in order to test thermodynamic geochemical models might seem a rather contrived use of analogues in a situation where a laboratory experimental approach is more relevant. Although certainly not a substitute for laboratory work, the analogue study is complementary as :

a) The chemical environment involved (high pH, very reducing conditions) is very difficult to simulate in the laboratory and is readily perturbed (e.g. by low-level CO_2 or O_2 contamination). Special approaches to ensure stable conditions e.g. pH or redox buffers, potentiostats etc. may introduce additional complications into the system (e.g. 5).

b) Experimental timescales may be insufficient for equilibrium to be reached, particularly for complex systems in which several solid phases are involved. Although natural groundwaters may not represent a complete equilibrium (6), they have reaction times much closer to those considered in a safety analysis context.

It must be noted that a major limitation to the analogue approach to testing solubility limits of trace species is uncertainty of the sources within the geological system and hence of whether concentrations observed reflect trace solubility limits or if release rates are insufficient to reach saturation concentrations. Thus, if predicted solubilities are above measured concentrations then the model is not necessarly conservative (in a safety analysis sense) but, if predictions are below measurements, the model is certainly in error (non-conservative). To be balanced against such a limitation is the fact that this type of study is relatively inexpensive!

1.3 Geological Setting

Hyperalkaline, calcium hydroxide rich springs are found in the region of the Semail Ophiolite Nappe in Northern Oman (Fig. 1). These have pH values of 10-12, are somewhat saline and are often extremely reducing, containing significant quantities of free hydrogen gas. At such springs, deposits of $Ca(OH)_2$ and $Mg(OH)_2$ and other anomalous minerals may be formed. It has been postulated that such waters are derived from low temperature serpentisation reactions at low water/rock ratios. The geochemistry of this rather peculiar environment has been discussed in detail by Neal and Stanger (7).

Fig. 1: The Semail Ophiolite Nappe. Sampling sites for this study are shown

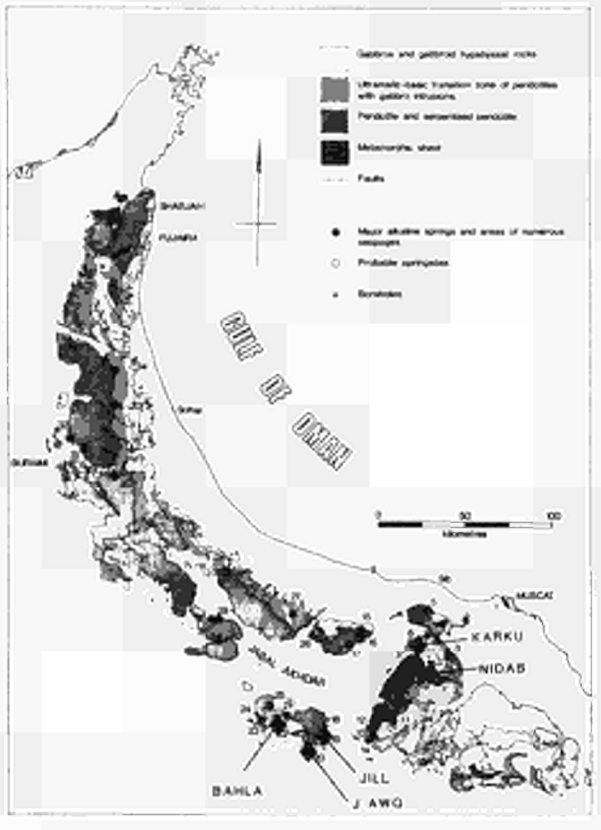

1.4 Chronological development of the project

The results of chemical thermodynamic calculations are very much dependent on the input data used which, for many of the elements involved in this study, involves fairly subjective selection from uncritically compiled databases. In order to avoid unconscious bias in this selection, a protocol was adopted which carefully separated the modelling and field measurement sides of the work. The chronological development of the project was thus:

1) Following the original suggestion of this analogue, the modelling group (at EIR) defined a "reference groundwater" based on reported major element chemistry of springs from this region. Existing safety analysis codes with associated databases were then used to calculate limiting solubility of relevant elements in this water. These values were published (8) and used as first estimates to help plan the field sampling trip (no previous measurements in this area of any of the elements involved are known).

2) After the sampling trip to Oman, in-situ measured parameters (temperature, pH, Eh, etc.) and major element concentrations measured on samples from 5 sites were sent to the modellers who then attempted to predict solubilities and speciation for these specific samples.

3) Finally, at a workshop, the model predictions were presented and only then were the measured values revealed for comparison.

2.1 Sampling and analysis

Five springs were sufficiently accessible to be sampled within the limitations of a short field visit; their locations are Nizwa Jill, Jebel Awq, Bahla, Karku and Nidab (Figure 1). All five are seepages with flowrates of ≤ 1 l s^{-1}.

Temperature pH, alkalinity and Eh were measured on each sample at the time of collection in the field. The pH electrode was calibrated with pH 7 and pH 13 buffer solutions (the latter being saturated $Ca(OH)_2$). Potentiometric alkalinity titrations were carried out in the field using a Hach digital titrator with a 1.6N H_2SO_4 acid cartridge; the hydroxide and carbonate end-points were detected as inflection points on a plot of pH against volume of acid titrated.

Samples for laboratory analyses of major and trace element chemistries were collected in ultraclean 500 ml FEP™ (a fluoro-polymer) bottles after filtration sequentially through 1µm, 0.45µm and 0.1µm membrane filters. The used filters were retained for residue analysis. At two sites only, 5 litre filtered (0.45µm) samples were collected for uranium and U/Th isotope analysis.

Total alkalinity and pH were again measured on samples after return to the laboratory at BGS Keyworth. These were carried out on a Radiometer TRS 822 recording titration system. The results compared extremely well with the field measurements. Anions (Cl, Br, SO_4, HPO_4 and NO_3) were determined on the unacidified sample by ion chromatrography (Dionex 2000i with AS4A anion separator and AG4A guard column).

Major, minor and some trace cations were analysed by inductively-coupled plasma optical emission spectrometry (ICP-OES) using an ARL 35000 instrument in the laboratory at BGS Wallingford. Solutions were acidified to 1% with HCL. Note that the ICP method analyses total S and P in solution, giving data which can be compared with the specific analyses for SO_4^{2-} and HPO_4^{2-} from ion chromotography, allowing an estimate of sulphur due to S^{2-}. The trace elements Ni, Zr, Co, Zn and La were found to be below detection limits for ICP-OES in all cases. Se was analysed by the generation of hydrogen selenide which was measured directly by atomic absorption.

A new ultra-sensitive analytical technique, inductively-coupled plasma source mass spectrometry (ICP-MS), was used in an attempt to quantify concentrations of some relevant analogue trace elements. The instrument used was a VG Isotopes PlasmaQuad™ in the Chemical Analysis Group at AERE Harwell (analyst: R.M. Brown). Samples were aspirated into the plasma

from solution acidified to pH <2 with HNO_3. Detection limits using single ion monitoring for many heavy elements by ICP-MS are between 0.1 and 0.01μg l^{-1} (ppb) and are therefore 2-3 orders of magnitude better than for ICP-OES. Although the technique is very sensitive for Ni, the original measurements of this element have to be considered suspect because the cone for transmitting ions into the mass spectrometer is made of nickel and therefore introduces a low but variable blank for this element. During the interpretation of raw analytical data from these samples, it was discovered that the Pd peak at m/e 105 suffers interference from $SrOH^+$, and as a result the low but detectable signal at this mass is not necessarily indicative of Pd abundance. Anlyses of Zr, Sn, Ce, Nd, Eu, Au, Th and U were attempted by ICP-MS; data are generally below limits of detection, even for this very sensitive technique.

2.2 Chemistry of the spring waters

The measured major ion chemistry of the five springs sampled is shown in Table I. The concentrations of species used in the model calculations are given in Table Ia, other species not used in the models but specified at the time of modelling are given in Ib while trace species not modelled but only reported after the modelling was complete are given in Ic. The measured concentration of the trace species modelled are reported separately in section 3.2.

These springs are all relatively warm (31-36 C) and, although in all cases pH falls into a narrow range (11.1-11.5), they differ quite significantly in redox conditions: Jebel is reasonably oxidising, Nizwa is intermediate and the other three are quite strongly reducing. The waters are all $NaCl/Ca(OH)_2$ type with Jebel having a significantly higher salinity than the others. Although, in general terms, the N and S redox systems follow the expected trends (high SO_4 and NO_3 in the oxidisng water, S^{2-} and NH_4^+ only in the most reducing systems), the redox couples involved are not in equilibrium with either each other or with the measured Eh. A significant amount of organic carbon is present in all cases and, in a parallel study, a range of microorganisms were detected in waters from both Nizwa and Karku (9).

2.3 Thermodynamic models and databases

The calculations reported here were performed using two well-known thermodynamic equilibrium codes, MINEQL and PHREEQE, which have been described in detail elsewhere ((10),(11) respectively). A version of MINEQL with an extansive actinide database (MINEQL/EIR-(12)) was used for modelling of U and Th. The speciation and solubility of these species were also evaluated using a database from the NEA (13). PHREEQE was used to model Se, Ni, Zr, Pd and Sn using a database compiled predominantly from the NEA (13), Benson and Teague (14) and Smith and Martell (15). Although this database has not been fully revieved, this work is currantly in progress. Components of this database have, however, been previously used in a waste management context (e.g. (16)). Due to uncertainties in thermodynamic data for sulphide minerals, and the lack of equilibrium of the S system, these species were not considered for the base calculations but are discussed qualitatively where relevant.

3.1 Model predictions

a) "Fission/activation products"

The elements Se, Pd, Sn, Zr and Ni were modelled and predicted solubility limit concentrations, dominant species in solution and solubility controlling solid phases are presented in Table II. Several

points should be noted:

1. The database used is rather small and there is a risk that important species are missing from the calculations. In general, neglecting an important solution phase species will result in under-estimation of solubility while missing an important solid phase will result in a "conservative" overestimate.

2. The quality of the data used is very variable. The importance of apparently small uncertainties in the source data (standard free energies or enthalpies of formation) cannot be overemphasised. Typically such errors would be in the range 1-10 kJ/mol for the species involved which translates to an uncertainty in the calculated solubility of a factor of about 10^3.

3. Se shows a marked difference in solubility between the oxidising and reducing waters due to the selenite/selenide transition. It should be noted, however, that the closely analogous sulphur system does not appear to be in equilibrium with the measured Eh while recent experimental work shows similar non-equilibrium for the selenate/selenite system (17). Hence, the overall applicability of an equilibrium approach to this element is difficult to justify.

4. The solubility of Pd is very low for the most oxidising case and totally negligible for all other waters. No real significance can be attributed to differences between concentrations at the 10^{-20}M level but it may be noted, in any case, that consideration of the PdS solid phase would further lower predicted Karku and Nidab solubilities by 9-10 orders of magnitude.

5. The solubility of Sn is calculated to be negligible in all cases but predicted values must be considered with caution as no data for stannates (e.g. $Sn(OH)_6^{2-}$) or organo-tin aqueous complexes were included in the database used.

6. The solubility of Zr is relatively high in all cases while that of Ni is relatively low. In the latter case, consideration of NiS as a solid phase would lower solubility further for Karku and Nidab by 5-6 order of magnitude (no data were found for an equivalent ZrS_2).

b) The actinides

The actinides Th and U were modelled using two different databases - one compiled at EIR for safety assessment modelling and one from the NEA. The results of these calculations will be discussed in more detail in a future paper but basically show:

1. The picture for Th is remarkably consistent for the two databases. In all cases $Th(OH)_4^o$ is calculated to be the major species in solution and ThO_2 to be the solubility limiting solid. While the NEA database results in a calculated saturation concentration of 10^{-10}M, the EIR database gives a value a factor of 5 higher. To some extent this can be explained by the relatively simple chemistry of this element - the constancy between springs is due to their almost identical pH. It is important that too much is not read into the consistency of the numerical values, however, as

this can equally reflect the fact that data for this element are relatively scarce and the same sources are used for both databases.

2. The U case is much more complicated. A general trend of decreasing solubility with more reducing conditions is observed but otherwise there are considerable differences between the two databases. (EIR: Jebel $4x10^{-4}$M, Nizva $2x10^{-7}$M; others $\sim10^{-6}$M; NEA: Jebel $5x10^{-3}$, Nizva $2x10^{-4}$, others $\sim10^{-9}$). The relative "conservatism" of the two databases thus varies between springs. A significant contribution to these differences arises from the somewhat "dubious" aqueous species $U(OH)_4^-$ (e.g. (18)) which is included at EIR but discarded by the NEA. The same limiting solid is predicted by both databases for Nizva (U_4O_9) and the most reducing springs (UO_2) but they disagreee for the most oxidising Jebel (EIR: $Ca(OH)_2(UO_2H_2SiO_4)_2$; NEA: U_3O_8).

3.2 Experimental measurements

The measured concentrations of the modelled trace elements are shown in Table III. It should be noted that in all cases concentrations are extremely low and below or very close to "state of the art" detection limits.

3.3 Discussion

For sake of comparison, the predicted saturation concentrations are also shown in Tabla III. Comparing the elements individually:

Se In all cases the model over-predicts concentrations. No obvious sink for Se is expected in the presence of relatively high S concentrations and hence it is expected that this simply reflects a source limitation.

Pd Measured values are significantly higher than predicted in most cases. Although tha measurements are suspect, Pd could be identified as an element in which experimental work would be needed to confirm the low model solubility.

Sn in all cases a very low concentration of Sn is observed which is, at least, consistent with the model but the difference of 10 orders of magnitude between predictions and the detection limit precludes further discussion.

Zr The predicted relatively high solubility of Zr is not reflected in the measured concentrations. This could be due to a source limitation, although Zr containing minerals occur widely over the earth's crust, or may indicate that an important solid phase is missing from the model database.

Ni Although the analytical data are suspect, they are consistent with the model predictions. This would not be so if NiS was considered as a solid phase and hence there is still a certain amount of uncertainty for this element.

Th Considering the errors involved, the Th experimental data are consistent with either database.

U In all cases, the U concentration is below that predicted by either database. In particular, the concentration for oxidising conditions is

especially low. Although this could be an artifact due to input of air into a previously reducing water, it might indicate that suggested species such as $Ca(OH)_2 \cdot UO_2(OH)_2$, which would lower solubility by ~ 10 orders of magnitude for oxidising conditions, actually exist in real life. If the latter is the case, both databases could be drastically overconservative for such conditions.

4.1 Conclusions

In general, it is found that measured concentrations of trace elements in hyperalkaline waters are consistent with the low solubility predicted by chemical thermodynamic models. Although the measurement data are poor, exceptions may be Pd and Ni (in the presence of sulphide) where the model under-predicts concentrations. On the other side, there is a strong indication that the model may considerably over-predict solubility of Zr and U (particularly under oxidising conditions).

4.2 Future work

The main limitation of this study is the very low concentration of the species of interest. Until more sensitive analytical techniques are available, it is unlikely that any continuation of such work in this area would be useful.

In the original plan of this study it was also intended to attempt to roughly classify the speciation of the elements by use of ion-exchangers (ie. specifying concentrations of anionic, cationic and, by differance, neutral species). In principle, this would provide a more rigorous test of the models (saturation would not need to be assumed) and, for example, could readily distinguish between the predictions of the two U databases for the most reducing solutions. Due to the very low concentrations involved, however, no hard data were obtained from this work. If, however, a technique of extractive concentration could be developed (e.g. passing large volumes of water through selective ion-exchangers), such a test of speciation predictions would be very valuable.

Finally, one area which may merit further study is the detailed geochemistry of the springs themselves. In the safety assessment field, models are being developed to predict the temporal evolution of cement/concrete pore water. The great similarity of mineral suites present in Oman with those expected in such a cement indicates that spacial profiles of alteration in the former may mimic temporal profiles of the latter and thus, at least qualitatively, provide some kind of model validation.

5. Acknovledgements

Special thanks are due to Dr. G. Stanger and Dr. J.C. Philp for their help during the field sampling. Thanks are also due to the many collegues in the U.K. and Switzerland who have contributed to this project and, in particular, to the Harwell analytical group. This work was jointly funded by U.K. Nirex Ltd. and NAGRA and we are grateful to Dr. R. Flowers and Dr. C. McCombie for their encouragement of this project.

References

1. Andersson, K., Allard, B., Bengtsson, M., Magnusson, B., (1983). Chemical composition of cement pore waters. Apendix X in K. Andersson. "Transport of radionuclides in water/mineral systems", Thesis Chalmers Institute of Technology, Gothenburg.
2. Glasser, F.P., Angus, M.J., McCulloch, C.E., Macphee, D., Rahman, A.A., (1985). The chemical Environment in Cements. Sci. Basis Nucl. Waste Manag., VIII, 849-858.
3. Berner, U., (1986). Radionuclide speciation in the porevater of hydrated cement. I The hydration model. EIR TM-45-86-28, Wuerenlingen.
4. Wiborgh, M., Hoeglund, L.O., Pers, K., (1985). Gas formation in a Type B repository and gas transport in the host rock. NAGRA NTB 85-17, Baden.
5. Meyer, R.E., Arnold, W.D., Case, F.I., (1984). Valence effects on the sorption of nuclides on rocks and minerals. NUREG/CR-3389 or ORNL-5978, Oak Ridge.
6. Lindberg, R.D., Runnells, D.D., (1984). Groundvater redox reactions: an analysis of equilibrium state applied to Eh measurements and geochemical modelling. Science, 225, 925-927.
7. Neal, C., Stanger, G., (1985). Past and present serpentinisation of ultramafic rocks; an example from the Semail Ophiolite Nappe of Northern Oman. J.I. Dever (ed), The Chemistry of Weathering, 249-275.
8. McKinley, I.G., Berner, U., Wanner, H., (1986). Predictions of radionuclide chemistry in a highly alkaline environment. Proc. Workshop "Chemie und Migrationsverhalten der Aktinoide und Spaltprodukte in natuerlichen aquatischen Systemen" Rep. PTB-SE-14, 77-89, Braunschveig.
9. Philp, J.C., Scringer, D.G., Voigt, N.J., Christofi, N., (1986). Microorganisms and microbial activity in hyperalkaline springwaters and sediments from Northern Oman. Napier College Report, Edinburgh.
10. Westall, J.C., Zachary, J.L., Morell, F.M.N., (1976). MINEQL - A computer programme for the calculation of chemical equilibrium composition of aqueous systems. MIT Technical Note 18.
11. Parkhust, D.L., Throstenson, D.C., Plummer, L.N., (1985). PHREEQE - A computer code for geochemical calculations (3nd revision). U.S. Geological Survey, Water-Resources Investigations 80-96.
12. Schweingruber, M., (1983). Actinide solubility in deep groundvater - estimates for upper limits based on chemical equilibrium calculations. NAGRA, NTB 83-24/EIR Bericht 507.
13. NEA, (1986). Extracts from the OECD/NEA chemical thermodynamic database, supplied by H. Wenner.
14. Benson, C.V., Teague, L.S., (1980). A tabulation of thermodynamic data for chemical reactions involving 58 elements common to radioactive vaste package systems. Lavrence Berkeley Lab. Rep. LBL-11448.
15. Smith, R.M., Martel, A.E., (1976). Critical Stability Constants, Plenum Press.
16. Early, T.O., Jacobs, G.K., Dreves, D.R., (1984). Geochemical controls on radionuclide releases from a nuclear vaste repository in basalt. Geochemical behaviour of disposed radioactive vaste, ACS Symp. Ser. 246, pp. 147-166.
17. Runnells, D.D., Lindberg, R.D., Kempton, J.H., (1987). Irreversibility of Se (VI)/Se(IV) redox couple in synthetic basaltic groundwater at 25°C and 75°C. Sci. Basis Nucl. Waste Manag., X, in press.
18. Bruno, J., Casas, I., Lagerman, B., Munoz, M., (1987). The determination of the solubility of amorphous $UO_{2(s)}$ and the mononuclear hydrolysis constants of uranium (IV) at 25°C. Sci. Basis Nucl. Waste Manag., X, in press.

Table I Chemistry of the Oman springs.
(all concentrations mg/l except * - µg/l)

	Nizwa Jill	Jebel Awq	Bahla	Karku	Nidab.
a) Species used in the model					
pH	11.24	11.39	11.41	11.44	11.16
Eh (mV)	-173	+33	-372	-363	-376
Temperature (C)	33	30.6	34.1	35.7	34.9
Na^+	218	603	189	258	130
K^+	9.2	27.8	8.4	11.2	3.6
Ca^{2+}	54.7	55.2	62.2	72.0	63.5
Sr^{2+}	0.27	0.62	0.14	0.28	0.27
Ba^{2+}	0.017	0.007	<0.002	0.003	<0.002
Li^+	0.017	0.024	0.021	0.021	<0.010
NH_4^+	<0.25	<0.25	0.58	0.31	1.54
Cl^-	291	858	275	351	193
SO_4^{2-}	0.91	34.1	0.19	2.39	5.6
S^{2-}	-	-	-	26.0	17.0
NO_3^-	0.38	31.2	0.18	0.43	0.20
Br^-	0.38	1.08	0.37	0.43	0.35
$[SiO_2]$	0.62	1.74	0.28	0.90	2.76
b) Species not modelled (known)					
CO_3^{2-}	0	0	0	0	0
Σ Al	<0.1	<0.1	<0.1	<0.1	<0.1
Σ Fe	<0.01	<0.01	<0.01	<0.01	<0.01
Σ Mn	<0.002	<0.002	<0.002	<0.002	<0.002
B	<0.02	<0.02	<0.02	<0.02	<0.02
Mg	<0.1	<0.1	<0.1	<0.1	<0.1
F	<0.05	<0.05	<0.05	<0.05	<0.05
c) Species not modelled (unknown)					
I	0.033	0.060	0.041	0.100	0.026
TOC	2.5	1.5	2.3	2.1	0.5
* Au	<0.09	<0.09	<0.09	<0.09	0.1
* Ce	<0.04	<0.04	<0.04	<0.04	<0.04
* Nd	<0.2	<0.2	<0.2	<0.2	<0.2
* Eu	<0.06	<0.06	<0.06	<0.06	<0.06

Table II Model predictions for Se, Pd, Sn, Zr and Ni

	Nizva	Jebel	Bahla	Karku	Nidab
pH	11.2	11.4	11.4	11.4	11.2
pe	-2.9	0.6	-6.1	-5.9	-6.2
Temp.	33	31	34	36	35
Se					
conc.	5e-3	5e-3	5e-7	5e-7	5e-7
soln.	SeO_3^{2-}	SeO_3^{2-}	Se^{2-}/HSe^-	Se^{2-}/HSe^-	Se^{2-}/HSe^-
solid	$CaSeO_3$	$CaSeO_3$	Se	Se	Se
Pd					
conc.	e-16	e-10	e-22	e-22	e-23
soln.	$Pd(OH)_2$	$Pd(OH)_2$	$Pd(OH)_2$	$Pd(OH)_2$	$Pd(OH)_2$
solid	Pd	Pd	Pd	Pd	Pd
Sn					
conc.	e-19	e-19	e-18	e-18	e-18
soln.	$SnOOH^+$	$SnOOH^+$	$Sn(OH)_3^-$	$Sn(OH)_3^-$	$Sn(OH)_3^-$
solid.	SnO_2	SnO_2	SnO_2	SnO_2	SnO_2
Zr					
conc.	5e-4	5e-4	5e-3	2e-3	1e-4
soln.	$Zr(OH)_5^-$	$Zr(OH)_5^-$	$Zr(OH)_5^-$	$Zr(OH)_5^-$	$Zr(OH)_5^-$
solid	$ZrSiO_4$	$ZrSiO_4$	ZrO_2	$ZrSiO_4$	$ZrSiO_4$
Ni					
conc.	3e-7	3e-7	3e-7	3e-7	3e-7
soln.	$Ni(OH)_3^-$	$Ni(OH)_3^-$	$Ni(OH)_3^-$	$Ni(OH)_3^-$	$Ni(OH)_3^-$
solid	NiO	NiO	NiO	NiO	NiO

conc. = saturation concentration (Molar): e-n = x 10^{-n}
soln. = dominant solution-phase species
solid = solubility limiting solid phase

Table III Predicted and observed concentrations of trace elements

	Nizwa	Jebel	Bahla	Karku	Nidab
Se					
Pre	5e-3	5e-3	5e-7	5e-7	5e-7
obs*	<3e-9	<3e-9	<3e-9	<3e9	<3e-9
Pd					
pre	e-16	e-10	e-22	e-22	e-23
obs	2.8e-9	6.6e-9	2.8e-9	2.8e-9	3.8e-9
Sn					
pre	e-19	e-19	e-18	e-18	e-18
obs*	<2e-9	<2e-9	<2e-9	<2e-9	<2e-9
Zr					
pre	5e-4	5e-4	5e-3	2e-3	1e-4
obs	<1e-9	<1e-9	1.1e-9	<1e-9	2.2e-9
Ni					
pre	3e-7	6e-7	3e-7	3e-7	3e-7
obs	<1e-8	<1e-8	2.7e-8	2.0e-8	3.4e-8
Th					
pre (EIR)	5e-10	5e-10	5e-10	5e-10	5e-10
pre (NEA)	1e-10	1e-10	1e-10	1e-10	1e-10
obs	<2e-10	<2e-10	<2e-10	<2e-10	<2e-10
U					
pre (EIR)	2e-7	8e-4	1e-7	1e-6	6e-7
pre (NEA)	2e-4	5e-3	3e-9	3e-9	2e-9
obs	<4e-11	4.2e-11	<4e-11	<4e-11	<4e-11

pre = predicted
obs = observed

concentration (molar)

* As noted in section 2.1, data are suspect and true concentrations are probably below detection limits.

SIMULATING THE MOVEMENT OF RADIUM AND LEAD AWAY FROM THE CIGAR LAKE URANIUM DEPOSIT

D.B. McCONNELL AND J.J. CRAMER
Whiteshell Nuclear Research Establishment
Atomic Energy of Canada Limited

Summary

The Cigar Lake uranium deposit in the Athabasca sandstone formation in northern Saskatchewan is under study as a natural analogue to various aspects of nuclear fuel waste disposal. The deposit consists of a high-grade ore body containing approximately the same amount of uranium as the expected inventory of a disposal vault. The deposit has a relatively simple geometry and groundvater flov system. Since 1984, data have been collected and compiled on the hydrogeochemistry and hydrogeological characteristics of the site, to study the distribution of uranium and associated elements in and around the deposit. As a part of this study, a simple model has been developed and tested for explaining the spatially varying part of the lead distribution in the sandstone above one region of the deposit. The observed distribution can be explained using reasonable values of the transport parameters. More detailed information about the site is required to test and refine the model further.

1. Introduction

In Canada and in several other countries, research programs are in progress to assess the concept of underground nuclear fuel vaste disposal in crystalline rock formations. To isolate the vaste, a combination of engineered barriers is to be set up within the natural barrier of the rock. (1,2) The vaste is immobilized within a durable container surrounded by a clay-based buffer material filling the rock cavity in vhich it is emplaced. Since transport of the radionuclides by groundvater is the only credible migration mechanism, the engineered barriers are designed to prevent groundvater penetration to the vaste on a short time-scale, and/or to retard the movement of radionuclides on a long time-scale. The long time-scale is dictated by the mobilities and half-lives of the vaste components, and may extend to hundreds of thousands of years for some high-level vastes.

Since 1982, Atomic Energy of Canada Limited (AECL) has conducted studies of naturally occurring processes that are analogous to those expected to occur in the disposal vault and its environment. A major component of this vork is the study of the sandstone-hosted uranium deposits in northern Saskatchevan. Through cooperation vith the exploration and mining companies, studies have been conducted on the deposits at Davn Lake, Key Lake and Cigar Lake. The vork reported here is based on the data gathered at the Cigar Lake site.

The uranium deposit at Cigar Lake is very large and rich, vith a relatively simple geometry. Because of its depth, more than 400 m, it has not been significantly affected by surface-controlled processes. The potential

of the deposit as a natural analogue to high-level waste disposal comes from its survival, relatively intact, for 1.3 billion years in a system open to groundwater, while at present having no obvious impacts at the surface.

As a part of the natural analogue program, this study has been initiated to explain the observed vertical distribution of lead in the sandstone above the deposit, using a simple model for the groundwater transport of the radioactive decay products of uranium toward the surface. As well as providing further insight into the processes at work in the natural system, the study has helped to identify extra data that must be obtained from such a site, for developing a useful analogue to radioactive waste migration.

The computer model has been implemented as a part of the SYVAC3 computer code, developed for simulating the performance of a disposal vault and its environment within the Canadian program for nuclear fuel waste disposal. (3) The agreement of the model results with a known analytical solution for a simple case helps lend credence to the SYVAC3 system and its ability to produce meaningful results from simulation models.

2. Physical and Chemical Characteristics Leading to the Model

The site has been described in detail elsewhere, (4-7) and only the relevant features will be described here. The mineralized zones of the deposit are situated along a ridge in the basement rock at a depth of just over 400 m. Figure 1 shows a plan view of the site, with the locations indicated for the borehole along which the distributions of elements were measured (Borehole 20), and those for which detailed geological and hydrological measurements were performed (Boreholes 75, 76, 137 and 139).

Boreholes 75, 76 and 137 were drilled into the main body of the deposit, where the bedrock and overlying layers are heavily fractured. The rock in the region of Borehole 20, however, is much less fractured and altered, and is better represented by the measurements from Borehole 139, even though the latter was not drilled into the ore deposit. Figure 2 shows a section through the region containing Borehole 139. The heavily mineralized zone (present in Borehole 20 at about 425 m depth) is absent, but would have been at the unconformity between the sandstone and bedrock, covered successively, as in the figure, with clay, sandy clay and finally an interval of over 400 m of relatively homogeneous sandstone extending to the overburden layer at the surface. The mineralized zone is thought to have formed approximately 1.3 billion years ago by the interaction of mineral-rich waters rising up through cracks in the basement rock and reacting with the minerals and waters present in the sandstone. Simultaneously, the rock just above the mineralized zone was depleted of silica and altered to form the sequence of progressively more sandy clay covering the deposit.

There is also evidence that from time to time, relatively brief episodes occurred during which the chemical conditions changed, resulting in the dissolution and transport of some of the deposited minerals into the upper layers. Such episodic events were likely responsible for the roughly uniform, elevated concentrations of these elements appearing in the sandstone above the deposit. (7) The measured distributions of elements associated with the ore, for example, cobalt, strontium and zinc, generally show high concentrations in the mineralized zone that decline to much lower, near-constant levels a short distance above the deposit, as illustrated in Figure 3. Lead, however, undergoes a more gradual decline over the first approximately 70 m above the ore zone, suggesting that its mode of deposition may differ, at least in part, from that of the other elements.

As part of the natural analogue studies, it is important to discover any contribution to the transport of uranium decay products from the deposit upvard to the surface. As a preliminary approach, it vas therefore decided to see vhether a simple transport model for the decay products of uranium could correctly describe the varying part of the lead distribution in the sandstone over the formation, assuming that the constant part vas produced by the same process that deposited the other elements. If the observed distribution could be explained vith this model using reasonable values of the transport parameters, it would indicate the possibility for the steady movement of significant amounts of decay products avay from the ore. There are, of course, other possible modes of lead transport that might produce the observed distribution during the episodic events that mobilized and transported lead; these may also have to be taken into account in a more complete model.

The key information for simulating the movement of uranium decay products avay from the ore layer is as follovs:

- the lead is entirely of radiogenic origin, and occurs at concentrations at least four times greater than that expected from the in situ decay of the uranium present in the sandstone (a fev parts per million) (7);
- the groundvater concentration of lead in the sandstone is very lov, and is consistent vith the relatively lov solubility of lead sulfide, vhich is prevalent in the sandstone;
- the uranium concentration in the groundvater is so lov as to rule out a significant transport of uranium avay from the deposit under present groundvater conditions (5);
- so little of the uranium and other minerals have migrated avay that it is probable a groundvater regime chemically like the present one has prevailed at the site for most of the life of the deposit.

We infer from the above information that the lead has precipitated out of the groundvater onto the sandstone host matrix, very near to its point of formation by decay of the parent nuclides. Further, the relative solubilities and half-lives of the members of the uranium decay series, shovn in Table 1, are such that only one nuclide, radium-226, combines the mobility and lifetime required to produce the observed spatial distribution in a flov regime similar to the present one. (The solubility characteristics quoted in the table vere derived from the groundvater data given in reference (5)).

We therefore suggest as a simple model for explaining the variation of the lead distribution, that dissolved radium-226 is transported out of the ore layer upvard toward the nearest discharge point at the bottom of Cigar Lake. In this model, the lead distribution vould reflect the concentration and rate of decay of the radium in the groundvater at the corresponding points in the sandstone, superposed on a constant background of lead deposited during episodes of different chemical conditions.

The radium transport process is taken to have continued during most of the time since the ore layer vas formed, except for episodes of relatively short duration in vhich the vater vas chemically different, and vas capable of dissolving some of the other elements in the ore zone. During these episodes, the vater vould have carried uranium, lead and several other elements up into the sandstone and distributed them more-or-less uniformly before the system returned to the normally prevailing conditions, causing these elements to precipitate out.

The physical extent of the mineralized zone is well known at the location of Borehole 20, and covers an area of several tens of square metres at relatively high concentrations of uranium ore. Since the borehole is located very nearly in the middle of Cigar Lake, it is assumed that the groundwater movement in the vicinity of the hole has been nearly vertical. Based on the relatively large area of the deposit, the inferred flow pattern and the relative homogeneity of the sandstone over this region of the deposit, we have simulated the ore layer by an infinite plane normal to the vertical groundwater velocity, at a depth of 425 m.

3. Model Description

At this initial stage, the system to be simulated is taken to be a 1-dimensional, homogeneous, porous medium through which radium-226 is being transported by a steady upward flow of groundwater. As the radium moves upward, it decays and deposits lead sulfide in the medium in amounts proportional to the local groundwater concentration of radium.

For a constant concentration entering at the bottom of the formation, the steady-state concentration distribution of radium from such a model satisfies the simple relation:

$$V[Ra]_x = -\lambda[Ra], \quad \ldots\ldots\ldots\ldots\ldots\ldots\ldots\ldots\ldots\ldots\ldots\ldots\ldots (1)$$

where [] signifies groundwater concentration, the subscript x denotes differentiation with respect to the height, x, above the deposit, V is the (retarded and dispersed) upward velocity of the dissolved radium, and λ is its decay constant.

In the absence of significant retardation and dispersion, the velocity V is the groundwater velocity. The lead distribution in the sandstone, {Pb}, at time t′, resulting from the solution of equation (1), is proportional to the integral of the local radium decay rate from t=0 to t′, and has the form:

$$\{Pb\} = A(t')\exp(-\lambda x/V), \quad \ldots\ldots\ldots\ldots\ldots\ldots\ldots\ldots\ldots\ldots\ldots (2)$$

where A(t′) increases linearly with time once the radium concentrations in the groundwater have reached steady state. This is a valid representation of the lead distribution as long as the time to steady state is short compared to the time, t′, at which the concentrations are measured.

Introducing retardation and longitudinal dispersion will, in general, alter the coefficient of x in the exponential of equation (2) (hereafter termed the slope of the logarithmic distribution). These two processes have opposite effects on its value. The equation then determining the distribution of radium concentration is:

$$R[Ra]_t + V[Ra]_x - D[Ra]_{xx} + R\lambda[Ra] = 0 \quad \ldots\ldots\ldots\ldots\ldots\ldots\ldots (3)$$

There is also a corresponding coupled equation for the distribution of lead concentration, {Pb}, deposited in the sandstone by radium decay. In these equations, there are separate sets of R, D and λ for radium and for lead, where R is the retardation constant, D is the dispersion coefficient, and λ is the decay constant. For the stable lead, λ is 0, and R is very large, because lead is effectively immobile. For a constant inflow of radium at constant concentration, the general solution of these equations retains an exponential spatial dependence, but with an x coefficient that depends in a complicated way on the values of R, D and V (see, for example, the steady-state solutions in reference 8 for the case in which there is no matrix

diffusion). As R, D and V are varied, the value of the slope of the logarithmic distribution can vary over a wide range.

The SYVAC3 computer code developed by AECL provides solutions to such coupled equations for decay chains of up to four members, and for a variety of initial conditions and boundary conditions. (9) One geosphere submodel, GEONET, that has been developed for simulating the crystalline rock environment of a vault with the SYVAC3 code (10), was modified to represent the model described here, treating the radium and lead as a two-member decay chain. Using GEONET, the concentration of lead in the sandstone could be estimated from a single SYVAC run, at a number of distances from the ore layer and for a chosen combination of R, V and D.

4. Results and Discussion

GEONET was used to obtain radium and lead distributions for the unretarded (R=1) and nearly dispersion-free (D=0.001) radium transport (equation 3), adjusting V to obtain an approximate fit to the observed lead distribution in Borehole 20. The lead distribution produced by the model from solving equation (3) and the corresponding coupled equation for lead has, as expected, the form of equation (2) for this simple case. The value of V obtained from the slope of the logarithmic lead distribution was about 0.03 $m \cdot a^{-1}$. The fit to the lead data is shown in Figure 4. A constant background value of 4.7 µg/g was subtracted before fitting the exponential.

The topographic relief of the area, supplemented by detailed measurements elsewhere in the region of the deposit, indicates that hydraulic gradients of about 0.01 can be expected along the vertical flow path below the discharge zone at the bottom of Cigar Lake. Combining this value with average values for the hydraulic conductivity and porosity of the sandstone formation, 5×10^{-7} $m \cdot s^{-1}$ and 0.16 respectively, gives a groundwater velocity of 1 $m \cdot a^{-1}$.

The difference between the estimate for V of 1 $m \cdot a^{-1}$ from the hydrological data and 0.03 $m \cdot a^{-1}$ from fitting the lead distribution data for the retardation and dispersion-free case suggests that retardation has a significant effect on the migration of radium in the medium, and must be taken into account. This implies that a value for R greater than 1 must be used in equation (3).

The retardation parameter, R, in equation (3) describes the retardation of the radium as it is carried through the sandstone by the groundwater. The mechanism most likely responsible for retardation is a combination of ion exchange and chemical sorption on the surface of minerals present in the sandstone, such as oxides of iron, as described for the analogous case of strontium transport in granitic sand. (12)

Dispersion effects can also be included through the relation $D = \alpha V + D_0$, where α is the dispersivity and D_0 is the molecular diffusion coefficient. The high porosity and low fluid velocity in the sandstone suggest that the mechanical dispersion is relatively small, and a value for the dispersivity of one tenth the path length (42.5 m) was used as being typical of such a system. (11)

The SYVAC3 code, incorporating equation (3) and the coupled equation for lead, was used to obtain lead distributions corresponding to various values of V, D and R. It was decided to allow R to vary in fitting the lead distribution, since of the three parameters, R, V and D, R could be estimated with the least confidence.

As a result of the fitting, the parameter set chosen to best represent the physical system was: $V = 1$ $m \cdot a^{-1}$; $D = 42.5$ m; and $R = 37$, where R was varied to fit the observed slope of the logarithmic distribution. The relation $R = 1 + \rho K_d / \varepsilon$, can be used in combination with the above R value,

and estimated values for the density, ρ, of 2.2×10^3 $kg \cdot m^{-3}$, and of the porosity, ε, of 0.16 (6), to give a value for the distribution coefficient, K_d, of 2.6×10^{-3} $m^3 \cdot kg^{-1}$. This value for K_d is about fourteen times lower than the values used to describe the analogous case of the transport of strontium in granitic sand. (12) However, it does correspond approximately to the ion exchange component of the retardation used in that model. Other transport measurements for Torpedo sandstone suggest that very lov values for K_d are appropriate for calcium. (13) A value for the radium sorption of 2.6×10^{-3} $m^3 \cdot kg^{-1}$ therefore seems to be reasonable for the Cigar Lake sandstone.

The sensitivity of the slope of the logarithmic distribution to variation of the parameters V, R, and D of equation (3) was also studied by varying them one at a time around the reference values given above. The resulting sensitivity curves are shown in Figure 5, with the parameters normalized to the reference values. As can be seen from the figure, the slope is very sensitive to changes in the velocity and retardation, and less sensitive to changes in the dispersivity.

It would be an easy task to use the full capability of the SYVAC3 system to incorporate distributions for V, D and R in the model to reflect both their variability and the accuracy with which they are known. However, the high sensitivity of the slope of the logarithmic distribution to these variables would result in a very wide range of slopes, using acceptable ranges of values of the variables, and no useful information would be obtained. To make further progress toward a more exact model, more detailed, integrated data sets for the site are needed, that would yield estimates for the local values of V, D and R, and of their variability on the scale used in the model.

6. Conclusions

A model has been developed to explain the variation of the distribution of deposited lead in the sandstone overlying a region of the Cigar Lake deposit. Reasonable values of the transport parameters used in the model can reproduce the distribution measured at the site. The model also reproduces the distribution calculated for the simple case of dispersionless, unretarded migration of radium via the groundwater.

Additional data are needed from the site in order to make further progress toward a detailed model for the lead distribution, and to compare its predictions with those derived from other possible deposition mechanisms. The most important data needed is a set of integrated hydrogeological and hydrogeochemical data from the same small region of the site, so that transport parameters can be estimated adequately. Measurements of the hydraulic gradient and conductivity, the porosity and tortuosity of the rock are needed for such a region, as well as the results of tracer tests to provide estimates of the dispersivity and retardation of elements of interest. Such data sets are also needed from more than one region to gain further insight into the range of the parameters to be encountered in large-scale simulations of radionuclide transport.

ACKNOWLEDGEMENTS

The authors would like to express their appreciation to B.W. Goodwin, T.W. Melnyk and D.M. LeNeveu for their helpful suggestions during the project and in reviewing this paper.

REFERENCES

1. KBS. (1983). Final storage of spent nuclear fuel. KBS-3, SKBF/KBS, Stockholm, 5 Volumes.
2. RUMMERY, T.E., and E.L.J. ROSINGER, E.L.J. (1983). The Canadian nuclear fuel waste management program. In International Conference on Radioactive Waste Management. Proceedings of a Conference held in Winnipeg, 1982 September 12-15. Canadian Nuclear Society, Ottava, Canada, pp 6-15.
3. ANDRES, T.H., FRECH K.J., KING, S.G., SHERMAN, G.R., and SKEET, A.M.M. (1987). The SYVAC3 Computer Program. Atomic Energy of Canada Limited Technical Record (in preparation).
4. CRAMER, J.J. (1986). Sandstone-hosted uranium deposits in northern Saskatchewan as natural analogs to nuclear fuel waste disposal vaults. Chem. Geology, vol. 55, pp 269-279.
5. CRAMER, J.J. (1986). A natural analog for a fuel waste disposal vault. CNS 2nd International Conference on Radioactive Waste Management, Winnipeg.
6. FOUQUES, J.P., FOWLER, M., KNIPPING, H.D. and SCHIMANN, K. (1986). The Cigar Lake uranium deposit - discovery and general characteristics. Can. Inst. Mining Bull., vol. 79, pp 70-82.
7. BRUNETON, P. (1986). Geology of the Cigar Lake uranium deposit. Saskatchewan Geological Society Conference on Economic Minerals of Saskatchewan, Regina.
8. SUDICKY, E.A., and FRIND, E.O. (1982). Contaminant transport in fractured porous media: analytical solutions for a system of parallel fractures. Water Resources Research, vol. 18, pp 1634-42.
9. WUSCHKE, D.M., GILLESPIE, P.A., MEHTA, K.K., HEINRICH, W.F., LENEVEU, D.M., GUVANASEN, V.M., SHERMAN, G.R., DONAHUE, D.C., GOODWIN, B.W., ANDRES, T.A., LYON, R.B. (1985). Second interim assessment of the Canadian concept for nuclear fuel waste disposal. Volume 4: Post-closure assessment. Atomic Energy of Canada Limited Report, AECL-8373-4.
10. GOODWIN, B.W., ANDRES, T.H., DAVIS, P.A., LENEVEU, D.M., MELNYK, T.W., SHERMAN, G.R., and WUSCHKE, D.M. (1986). Post-closure environmental assessment of a concept for the disposal of nuclear fuel waste. Submitted to Int. Journal of Waste Management and the Nuclear Fuel Cycle.
11. BEAR, J. (1975). Dynamics of fluids in porous media. American Elsevier Publishing Company.
12. MELNYK, T.W., WALTON, F.B., and JOHNSON, L.H. (1983). High-level waste glass field burial tests at CRNL: the effect of geochemical kinetics on the release and migration of fission products in a sandy aquifer. Atomic Energy of Canada Limited Report AECL-6836.
13. COATS, K.H., and SMITH, B.D. (1964). Dead-end pore volume and dispersion in porous media. Society of Petroleum Engineers Journal vol. 4, pp 73-84.

* Unrestricted, unpublished report, available from SDDO, Atomic Energy of Canada Limited Research Company, Chalk River, Ontario K0J 1J0.

TABLE I

URANIUM SERIES MEMBER	RELATIVE SOLUBILITY	HALF-LIFE [a]
U238	very low to low	4.468×10^{9}
Th234	very low	6.598×10^{-2}
Pa234	---	7.6×10^{-4}
U234	very low to low	2.44×10^{5}
Th230	very low	7.7×10^{4}
Ra226	moderate	1.620×10^{3}
Rn222	low	1.05×10^{-2}
Po218	---	5.8×10^{-6}
Pb214	very low	5.10×10^{-5}
At218	---	6×10^{-8}
Bi214	---	3.7×10^{-5}
Rn218	---	6.0×10^{-10}
Po214	---	5.20×10^{-12}
Tl210	---	2.51×10^{-6}
Pb210	very low	2.23×10^{1}
Bi210	---	1.37×10^{-2}
Po210	---	3.79×10^{-1}
Tl206	---	8.0×10^{-6}
Pb206	very low	stable

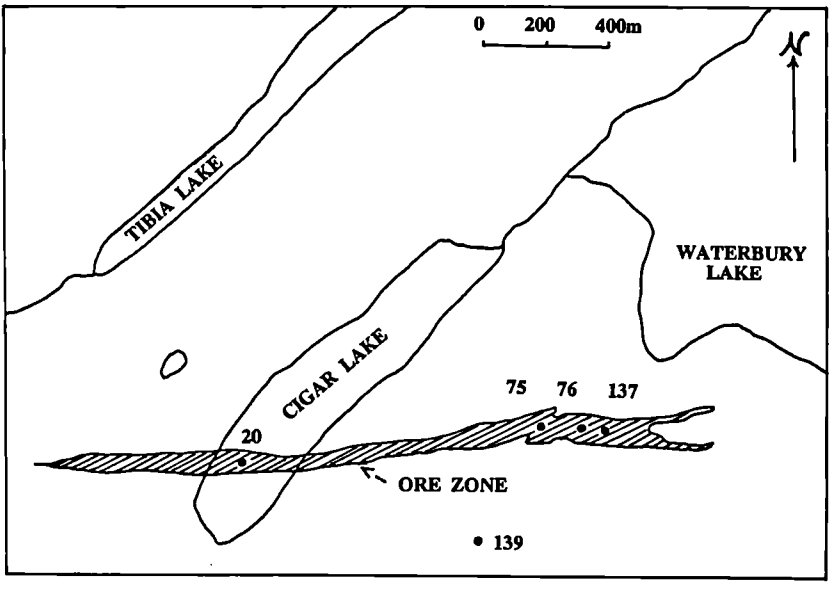

FIGURE 1: LOCATION OF DRILL HOLES AND OUTLINE OF CIGAR LAKE SITE

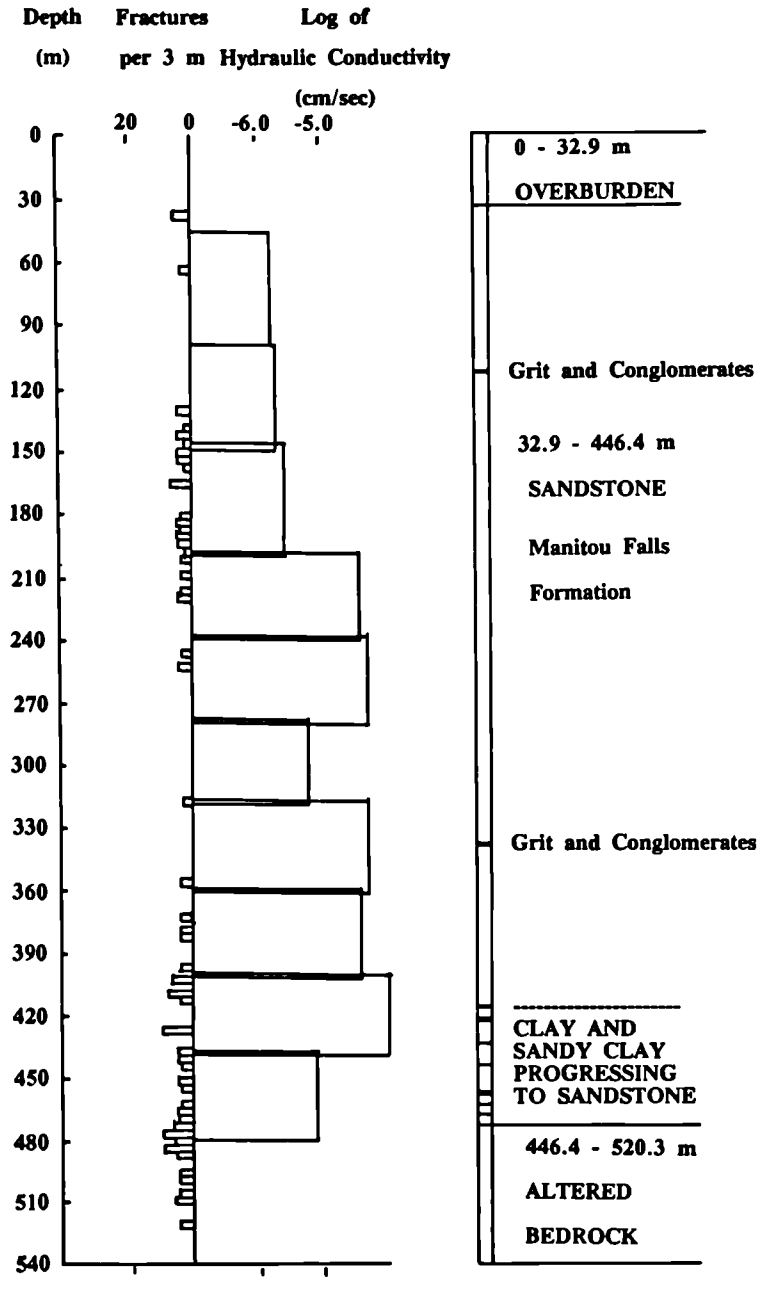

FIGURE 2: BOREHOLE 139 CHARACTERISTICS

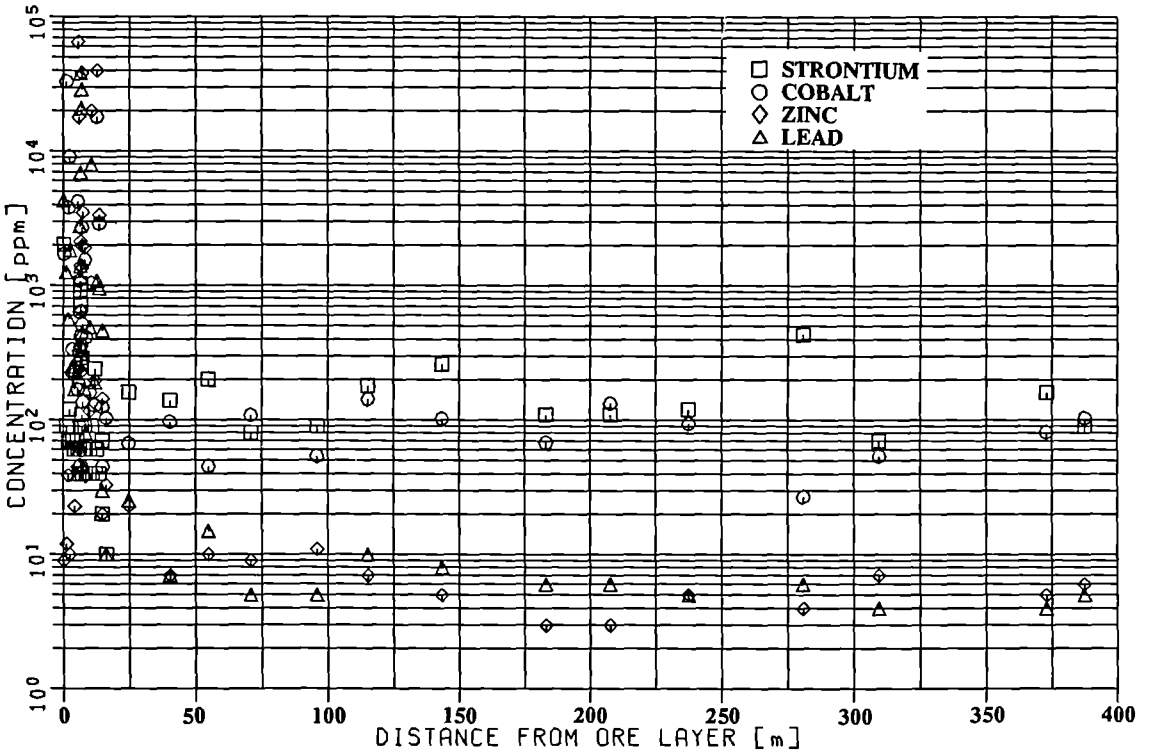

FIGURE 3: SAMPLE ELEMENT DISTRIBUTIONS FROM BOREHOLE 20

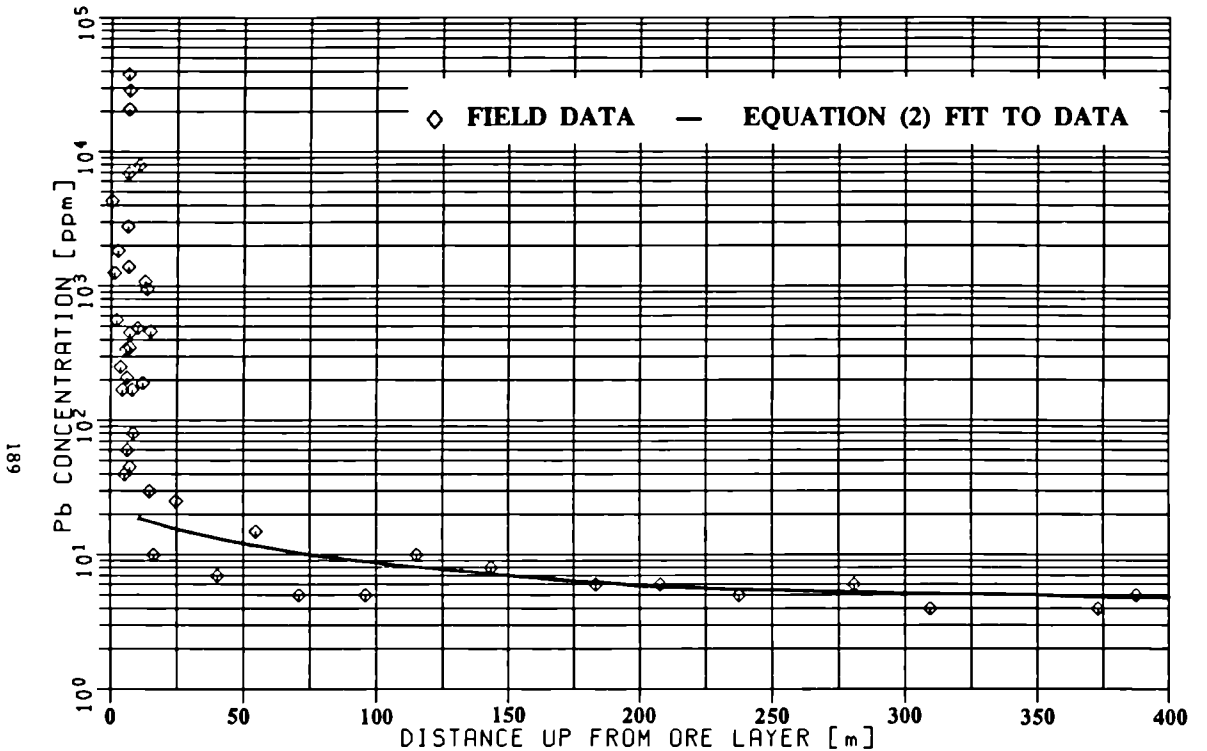

FIGURE 4: FIT OF EQUATION (2) TO BOREHOLE 20 Pb DATA

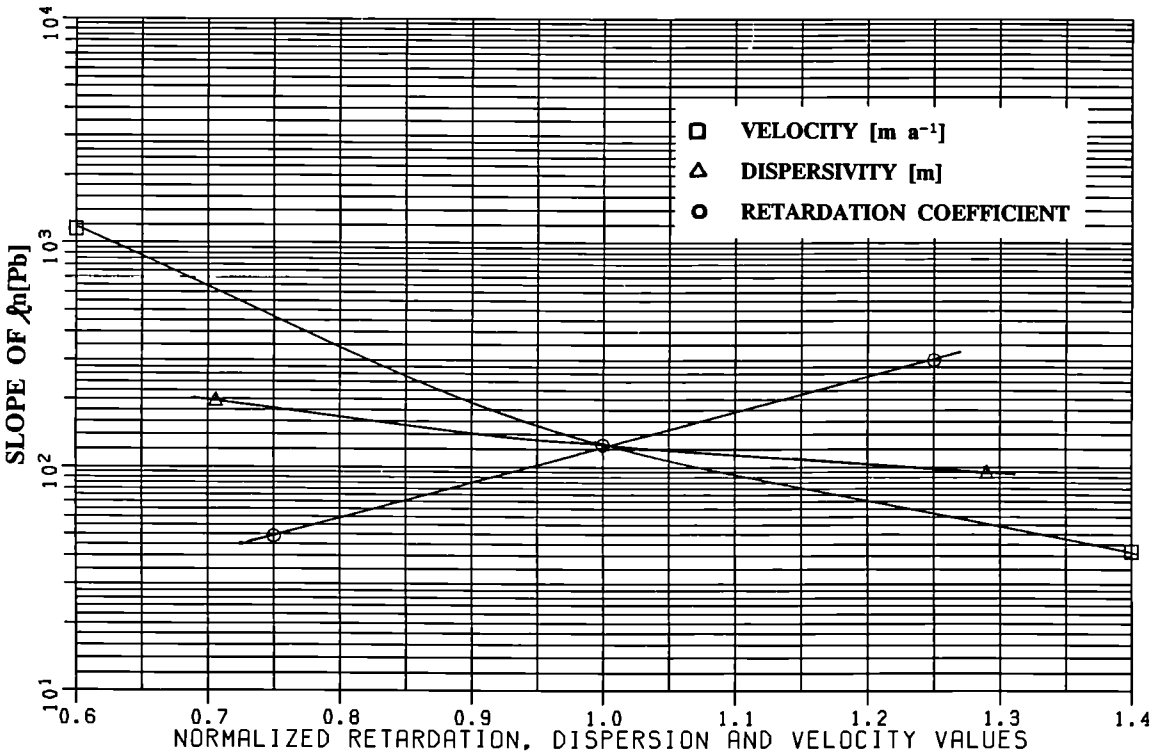

FIGURE 5: SENSITIVITY CURVES FOR VELOCITY, DISPERSION AND RETARDATION

HYDROTHERMAL ALTERATION SYSTEMS AS ANALOGUES OF NUCLEAR WASTE REPOSITORIES IN GRANITIC ROCKS
An example : The Langenberg hydrothermal system

L. GRIFFAULT*, M. JEBRAK**, B. LEMIERE**, P. PIANTONE**, J.F. SUREAU**
* Université de Poitiers.
** BRGM - BP 6009 - 45060 ORLEANS Cedex

Abstract

The results of this partial study on element distribution of a hydrothermally altered granite in the Langenberg site lead to conclude on :
- probable mobility for most part of major elements except SiO_2 and Al_2O_3 ;
- a pronounced mobility for light REE (La, Ce) ;
- a weak mobility for U ;
- no or weak mobility for heavy REE.

Comparison with chemical analogues for long-lived nuclides present in high-level radioactive waste are discussed.
Element mobilities are strongly controlled by intensive chemical parameters, e.g., pH or fCO_2, that destroy element-bearing minerals or allow crystallization of scavenger minerals.
According to the now admitted temperature for radwaste disposal of about 100°C for a far field, and data on stability of alteration paragenesis, it is possible to deduce that the alteration grade reached in granite, by induced hydrothermal system, will be clay facies.

1. Introduction

"The long-term safety of geological repositories will largely depend on our knowledge of geochemical mechanisms and on our capability to model the probable behaviour and migration of the radionuclide that might be released by the repository" (Joint OCDE-AEN, 1982). In order to draw up plausible prospective scenarios of migration or retention of elements, it is therefore necessary qualitatively and quantitatively to define interaction mechanisms between water and host rock to assess transfers according to the environmental physico-chemical parameters.

In laboratory, it is now possible to test low kinetic chemical reactions (about one year) or chemical balance evolution by stronger intensive parameters (compared with natural conditions) and thus to model them by means a thermodynamic calculation.

However it is still difficult to appraise the consequences of the evolution of a complex chemical system (precipitation, dissolution, absorption...) involving mineral phases whose crystallization, growth or dissolution are controlled by poorly-known kinetics over a period of time in the range of ten thousand to one million years, which is the probable average life-span of stored nuclear waste.

The historical analysis of geosystems selected for their analogy with repositories (geological environment) and that display traces of geochemical process to be tested, such as diffusion, hydrothermalism, natural fission, will provide real parameters for modelizing or comparison with existing models. These natural systems are reasonable constraints.

Such natural laboratories are found in the environment of mineral deposits and hydrothermal systems.

The analogical study will be more efficient if it deals with elements whose chemical behaviour can be considered as analogous to that of nuclide found in waste : Tc, Pa, Np, Pu, Am... (Chapman and Smellie, 1986).

The Langenberg site in the Vosges Mountains estearn France, which is the subject of the present work, is one of these natural laboratories.

The studied unweathered samples were provided by BRGM core holes drilled for fluorite exploration, completed by surface observations and rock sampling in the Langenberg area around a small well-defined hydrothermal system of the same generation.

2. Geological setting

The Ballons pluton massif lies within the eastern Vosges. It crops out over some thirty kilometers in length and five to six kilometers in width and is surrounded by Visean volcanosedimentary formations.

This massif is made up of heterogranular monzogranite characterized by orthose megaphenocrysts and is bound in the north and south by two zones of gabbroic, dioritic and monzonitic rocks.

To the east, the Ermensbach gabbro-diorite massif and the Sewen monzonite are distinguished from the main massif. Two little stocks of biotite leucogranite intrude the Ballons granite.

Forquin (1976) assumed a Middle Visean age for this complex based on the presence of :

- thermal-metamorphic halo in Visean volcano-sedimentary formations situated along the contact with Ballons related basic rocks ;
- monzonite fragments in the upper Visean pyroclastic layers.

This last observation led to suppose a shallow setting of the pluton. Nevertheless, due to structural observations, a younger age is given by André and Gagny (1981) for the monzogranite.

Some microgranites crosscutting this complex are described by Guerin (1967) in the southwest of the massif. Three types are distinguished :

- biotite and actinolite microgranite related to Crêtes magmatic group ;
- biotite and green hornblende microgranite linked with the Ballons magmatic group ;
- tourmaline microgranite which may be linked with the leucocratic Auxelles intrusions more to the south.

From a geochemical point of view, the Ballons monzogranite belongs to the shoshonitic association (Pagel and Leterrier, 1980) and has mainly a crustal origin.

The Ballons massif is intersected by a set of mineralized faults that can be classified into two main types :

- Mo, Cu, (U) stockwork and veins, located on the massif border, Chateau-Lambert district (Pagel and Ruhlmann, 1979) to the north and Goutte des Oeillets occurrences to the south ;
- F, Ba and Pb, Zn veins in N 20 to 45° E faults located in the south-western periphery of the massif (Langenberg), these veins are related to a Triassic paleosurface (Jébrak, 1984).

Alteration dispersion halos are associated with these mineralizations and were pointed out by the SNEAP regional and detailed multi-element prospection (Mouillac, 1974). Thus, one Cu-Mo anomaly, to the south of Ballon d'Alsace, parallel to the monzogranite margin, can be distinguished as well as a Pb, Zn, Ba anomaly around the Langenberg zone.

. Langenberg hydrothermal system, main outlines :

The emplacement of the Langenberg lode appears to be monophased and posterior to all hydrothermal events related to granite or pegmatite intrusions. It began with the formation of a silicified and chloritized granite breccia and continued with massive fluorite filling surrounding breccia fragments. Calcite, quartz and scattered cryatals of galena are associated with this mineralization.

The emplacement ends with layers of yellow fluorite, white barite and geodic quartz.

The presence of yellow fluorite is an indication on cooling duration of hydrothermal system : less than 100,000 years (Calas et al., 1972 ; Jébrak, 1986).

The depositional time of the mineralization can be inferred by structural data as demonstrated by the measurement of deformation directions which are conformable with north-south and northwest-southeast Permian overstretching events.

Temperature elevation induced by hydrothermal deposits is about 100 to 300°C as shown by hydrothermal paragenesis (see below).

The level of ore deposition deduced from the fracture position compared to the old pre-Triassic surface is weak. The summit of structures are very close to the surface level, 50 to 100 m, and the roots do not lie below 300 or 400 m.

The studies of $\delta^{32}S$, $\delta^{18}O$ and $^{87}Sr/^{86}Sr$ ratio on quartz and anhydrite of the Faymont hydrothermal system, Vosges (Arnold and Guillou, 1980 a et b, Michard et al, 1983) completed by REE studies on the Langenberg fluorite (europium anomaly and Yb/Gd ratio : Jébrak, 1986) led to assess the mixing of two origin fluids and to presume the participation of meteoric water.

Considering these general outlines, the analogy of nuclear waste repositories in granitic context and the Langenberg site is reasonable :

- size, 2 km x 300 m ;
- depth of emplacement = 0,5 km ;
- temperature elevation about 130 to 200°C ;
- duration of cooling 100,000 years ;
- meteoric water contribution during the hydrothermal events.

3. Samples and investigation methods

A variety of samples, showing various degrees and types of alteration was studied using the following techniques : (1) petrographic analysis, (2) electron microprobe analysis, (3) X-ray diffraction, (4) bulk chemical analysis, (5) X-ray fluorescence analysis.

Trace elements were analyzed by Inductively Coupled Plasma, REE by means of ion exchanges and Direct Current Plasma analysis with Tm as internal standard. The detection limits are about 0.1 to 0.5 according to the REE analyzed. The precision of the analysis is estimated at about 5 to 10 % below 5 ppm. U and Th are analyzed by X-ray fluorescence, the detection limit is about 2 ppm and analytical precision is estimated at about 10 %.

Alteration minerals are identified by X-ray diffraction on powders or oriented preparation. Dispersion is performed in distilled water by ultrasonic treatemed. Determination of clay minerals is carried out on natural, glycollated and heated samples (Brindley and Brown, 1980).

4. Mineralogical data

Three main types of hydrothermal alteration are distinguished in the samples from the Langenberg area :

- pervasive propylitization ;
- phyllite type alteration located near veins ;
- clay and carbonate alteration located near veins.

. Propylitization

. Petrological data :

Propylitization is a pervasive hydrothermal alteration affecting all the primary major minerals at the massif scale. This alteration shows no fracture control.

The main transformations are :

- chloritization epidotization of ferromagnesian minerals ;
- sericitization, epidotization, albitization and various stages of carbonatation of plagioclase.

Two main mineral assemblages are distinguished with carbonatation grade :

1) With chlorite-epidote-sphene with or without rutile-illite-calcite ;
2) With chlorite-calcite-illite-rutile.

Biotite shows various stages of alteration. Alteration begins along cleavage planes (001) where biotite looses its brownish color, and biotite layers are replaced by green chlorite. When propylitization is more advanced, biotite is entirely transformed into chlorite and has elongated shape of the primary mica.

Chloritization of biotite is accompanied by a development of epidote, sphene, with lenticular shape between (001) layers, and small scattered rutile crystals.

At the thin section scale, amphibole exhibits three main types of alteration : (1) only small lengthened chlorite crystals are identified along cleavage plane with incipient alteration ; amphibole crystals are invaded by (2) chlorite accompanied by patchy epidote or (3) calcite crystals with more advanced alteration.

Three alteration phases are identified in plagioclase crystals : illite, chlorite and epidote. Illitization is the main alteration phenomenon and when it develops in plagioclase it excludes other alteration phases.

Some samples contain chlorite veinlets.

. Chemical and cristallographic data :

Microanalyses and X-ray powder identifications were performed on the alteration phases of the two distinguished alteration paragenesis facies.

According to data :

- chlorites are brunsvigite (Foster, 1960) of IIb polytype ;
- epidotes with a Fe/Fe+Al ratio about 0.35 is of a pistacite type ;
- illites are 2 M 1 polytype, aluminous with octahedral Al^{VI} partly substituted by Fe and Mg, interlayer charges are balanced by K varying between 0.79-0.94 cation per formula*.

. Conclusions :

Minerslogical differences between the two main assemblages are controlled by CO_2 whose incressing fugacity allows calcite crystallization, probable Ca trapping and induces titanite transformation (Hunt and Kerrick, 1977) and epidote alteration.

* Calculated on the basis of 11 O.

At the crystal scale, with conservative volume hypothesis demonstrated by micrographic observation, biotite transformation into chlorite requires Fe^{2+} and Mg^{2+} supplies. According to previous observations, these elements must be considered as mobile elements brought in by fluids and trapped by neogenic chlorites.

The presence of epidote in these facies allows to determine a lower temperature limit at about 250 $\pm$ 50°C for a total pressure varying from 1 to 6 Kb (Liou, 1976). According to the mineral reactions involved in these hydrothermal processes (Helgeson, 1974 ; Rose and But, 1979) pH conditions are basic to neutral and CO_2 may be locally high enough to allow carbonatation.

. Phyllic-type alteration

. Petrological data :

Phyllic-type alteration characterized by extensive white mica crystallization is mainly developed along hydrothermal veins around on metre in thickness.

At a more advanced stage, granite structure is obliterated by newly formed phyllites.

Feldspar minerals are completely replaced by flakes of white mica which form clusters sheaves like of crystals (about 50 to 200 um in size). The shapes of amphibole crystals are not recognizable but former biotite is outlined by elongated white mica layers and residual rutile.

In these samples tourmaline is present but shows corroded zones containing quartz and white mica. The tourmaline probably corresponds to an earlier alteration (magmatic stage ?) entirely obliterated by the phyllic type facies. Scarce scattered calcite and pyrite are present.

. Chemical and crystallographic data :

The chemical composition of analyzed micas place them in the illite family with high interlayer charge (I.C.$\simeq$ 0.90 atom sum). They have high Mg content (about 0.15 atom per formula) and small Fe content (less than 0.6)*.

The compositions of the octaedral site is homogeneous and are not influenced by primary mineral chemistry. X-ray powder data classified these illites in 2 M 1 polytype.

. Conclusions :

Phyllic alteration is a strongly homogeneous alteration developed around hydrothermal veins.

Chemical data and X-ray powder data : high interlayer charge and 2 M 1 polytype infer that the facies were formed in temperature in the range of 300°C (Jacobs and Parry, 1979 ; Beaufort et al., 1983).

The mineralogical reactions involved in phyllic stage which display a strong H^+ fixation during destruction of primary silicates and systematic absence of chlorite result from the strong acidity of solution which has pH values below 3 (Montoya and Hemley, 1975 ; Lemière et al., 1986).

. Clay and carbonate alteration :

. Petrological data :

These alteration facies are also limited in veinlet walls with about ten centimeter development.

This late hydrothermal stage which affects rocks previously transformed by propylitization and phyllitization.

In all cases plagioclases are the most altered minerals and are entirely transformed into grey-yellow phyllites.

* Calculated on the basis of 11 O.

Previous propylitic chlorites are less affected and only in some samples are they transformed into clay minerals and ankerite.

In groundmass the typical minersls are clays and carbonates with dominant ankerite.

. Chemical and crystallographic data :

In theses facies 3 phases were identified on oriented samples by X-ray:

(1) Irregular illite-smectite mixed layer (Ro) with about 60 % of smectitic component (Velde, 1985), (2) illite and (3) kaolinite (Fig. 3).

Chemicsl composition of illite smectite Ro is mainly characterized by low K content (about 0.55 cation by formula*) and little Mg and Fe content ($\simeq$0.12 and $\simeq$0.10) respectively.

. Conclusions :

Clay carbonate alteration facies is a late alteration stage mainly controlled by carbonate-filled fractures.

Presence of Ro indicates a temperature of formation below than 100°C (Velde, 1985).

Fluids involved during clay-carbonate hydrothermal events are CO_2^- rich with neutral to basic pH because carbonates are precipitated.

5. Element distribution

. Major elements :

Estimation of gain and loss of major components during hydrothermal alteration based on norms system with assumed parent rock and studies on mean values of each group may be fruitful. It allows a correct semi-quantitative approach, whereas the density of samples must be known for a precise quantitative study.

Value gains and losses are summarized in Figure 4 for (a) propylitic, (b) phyllic and (c) clay-carbonate alterations.

The TiO_2 variations are not plotted because of their erratic behaviour due to heterogeneous distribution of the titaniferous mineral at the scale of analyzed samples.

SiO_2 and Al_2O_3 display no significant variation, less than 0.2. This allows a direct comparison of other element contents.

On the contrary salient changes are diplayed on L.O.I. for all the samples showing the most intense phyllic alteration.

Propylitization is distinguished from the other stages of alteration by a moderate gain in FeO, MgO and CaO.

Phyllic facies displays stronger negative variations in MgO, Na_2O and weak negative for K_2O anomaly.

Clay-carbonate alteration also exhibits negative variation in MgO and Na_2O, significant gain in CaO and a weak positive K_2O anomsly.

This study on major element behaviour during hydrothermal events led to the conclusion of a weak or no mobility for SiO_2 and Al_2O_3. The same observations were made on the Sibert porphyry-copper by Beaufort (1981).

Drastic variation on L.O.I. can be easily explained by crystsllization of more extensively hydrated or carbonated minerals such as phyllosilicates, epidote calcite etc...

The other elements display variation congruent with rock mineralogy :

- FeO, MgO, CaO gains in propylitic facies with crystallization of epidote, calcite and chlorite ;
- FeO, MgO losses during phyllite crystallization ;
- Na_2O losses and K_2O variations linked with feldspar and biotite destabilization and phyllite crystallizstion.

---

* Calculated on the basis of 11 O.

. Rare-earth elements :

According to literature data (Arhens, 1952 ; Shannon and Prewitt, 1970), two REE, Eu and Ce were chosen with a view to a comparison with Sr behaviour because of the following reasons :

- there is a possible similarity in radii ($\simeq$ 1.2 Å) and chemical crystallography behaviour ;
- Sr has served as an analog for Eu^{2+} (Phillpotts, 1970) ;
- feldspar is the main Sr bearing mineral in igneous rocks.

This comparison may be fruitful to model the primary Ca and Sr bearing mineral alteration but also secondary mineral crystallization.

Ce, Eu versus Sr behaviour are displayed in Figure 5 and Figure 6.

The different types of alteration facies are well distributed with Sr decrease, discrepancies on propylitic facies are not yet explained : they may correspond to incipient clay alteration. The more extended variation in REE content with increasing alteration is constituent with mineralogical observation. This diagram shows Ce, Eu and Sr depletion during hydrothermal alteration.

The comparison with trace element behaviour in clay and carbonate facies, phyllic facies and propylitic facies shows that carbonate plays the role of scavenger mineral precipitating the REE and restricting departure. The role of clay minerals cannot be defined, but according to Kamineni works (1986) they can display the same, but probably minor role.

Variation in Ce and Eu illustrated on Ce/Sr and Eu/Sr diagrams allows the utilization of mean values to describe REE content of each facies type.

The mean REE values show that there is a definite decrease of these elements in altered samples from propylitic facies to clay facies (data on unaltered facies are not yet available) except for heavy REE. This is shown in a Box-Whisker plot for La, Ce, Sm (Fig. 7).

The chondrite-normalized patterns of REE abundances in altered samples in Figure 8 display a clear cut depletion of light REE, La and Ce in clay and phyllic facies compared to propylitic facies. This phenomenon becomes weaker or undistinguishable with decrease of REE ionic radii.

However, the mobility and redistribution of these REE have been demonstrated convincingly for sea-floor alteration and low grade metamorphism (Frey et al., 1974 ; Floyd, 1977). REE mobility and depletion during rock alteration results either in sub-parallel dow-shifting of chondrite-normalized pattern or in significant negative fractionation for light REE due to a more pronounced mobilization of these elements owing to larger ionic radii which may influence their relative behaviour under certain conditions (Wood et al., 1976 and Lesher et al., 1976). Compared to propylitic facies, phyllic and carbonate facies display both behaviours :

- sub-parallel negative shifting with clay carbonate pattern ;
- negative fractionation for light REE with phyllic pattern.

. Uranium and thorium :

The U and Th contents of various types of altered samples versus Ce content are displayed in Figures 9 and 10.

Figure 9 shows that U concentrations decrease with alteration, three samples from altered facies show noteworthy high values above 30 ppm.

The weak depletion of U in phyllic and clay-carbonate facies compared with propylitic facies can be attributed to mobilization during hydrothermal events, the results are similar to those demonstrated by Kamineni (1985).

The three highly anomalous values may be due to scavenging by a favourable host mineral : two of these high U grades are related to with high CaO grade.

As U, Th display a weak depletion in concentration and alteration. No anomaly was detected.

6. Summary and discussion

The reaults and interpretation concerning the mineralized system of Langenberg brought out various aspects that are relevant to radwaate disposal :

- hydrothermal alteration of rocka ;
- element mobility during thermal water rock interaction.

. Hydrothermal alteration of rocka :

The hydrothermal faciea depicted cover a large range of temperature which overlaps the probable disposal temperature with :

- about 250 ± 50°C and higher, pervasive propylitic alteration ;
- about 300°C, phyllic alteration with common occurrence around the veina ;
- about 100°C, clay and carbonate alteration with common occurrence around the veins.

. Element mobility :

. Major elements :

At the aample scale most major elements were "mobile" during alteration proceases.

Propylitic alteration is characterized by CaO, MgO and FeO* gain.

Phyllic and clay alteration are characterized by Na_2O and MgO loas.

Carbonate mobility and sphene and epidote stability are strongly controlled by fCO_2 which leads to calcite crystallisation, possible massive carbonatation and CaO enrichment.

. Minor elementa :

Sr seems to be one of the more sensitive minor elements in the hydrothermal alteration. It displays the CaO rich mineral behaviour and therefore may be used with caution (mineralogical evidences) as an alteration index in granitic rocks.

The results and interpretation presented above in the section about REE, U and Th behaviour contain various aspects that are relevant and similar to the geochemical behaviour of far field waste disposal. The geochemical behaviour of U is quite similar to Pu and Np (Bagnal, 1972) ; under certain conditions, the geochemical behaviour of Th, ia similar to that of Pu (Krauskoft, 1984) ; and the geochemical behaviour of La and Nb is similar to Am snd Cm respectively.

According to the results of this study, REE, U and Th, mobilization during hydrothermsl processes can vary drastically with alteration facies.

The best example of departure is that of phyllic faciea in which a noteworthy depletion in light REE is emphasized by weak ratio La/Yb = 10.90 instead of 26 in propylitic facies ; a same but weak tendancy is noted for U.

These processes are strongly controlled by the mineralogy which destroys REE-bearing minerals : epidote, sphene... and does not allow cryatallization of minerals with favourable atructural aite to scavenge these released minor elements.

For clay and carbonate facies depletion in light REE, U and Th is less senaitive than in the previous phyllic facies, whereas epidote and sphene are destroyed because of high fCO_2. These resulta allow to suppose the presence of minerals favorable to the trapping of these elementa : calcite and perhaps clay minerals.

Strong U anomalies in three samples of phyllic and clay-carbonate facies display probable rich U minerals not yet determined. Precipitation or solution with complexation of U is extensively controlled by

oxydo-reduction conditions and carbonate concentration (Cramer, 1986). Precipitation in UO_2 with reducing local environment may be possible, but the presence of U in Fe oxyde is notorious (Kamineni, 1986).

. The approximation of pH with alteration parageneais shows that acidic solution favours light REE and generally U and Th depletion with strong destruction of the primary host minerals and do not allows cryatallization of mineral favourable to scavenging.

. Conclusions :

The results presented in this study suggest that mobilization of major and minor elements is possible, due to rock alteration either pervasive in whole rock, or limited along fractures.

The effects of these mobilizations are strongly controlled by the intensive parameters of hydrothermal fluid (pH or fCO_2, for example), that induce minerals which release or trap trace elements.

According to the data obtained, elements released, during alteration atage, can be redistributed and precipitated with variation of intensive parameters, in suitable aink in the inner part or outer part of hydrothermal syatems, for e.g. : carbonate filled fractures.

Within atability range of parageneses described above, and now admitted temperature for radwaste disposal about 100° for farfield, we can deduce that the alteration grade reached by induced hydrothermal system is clay facies.

REFERENCES

1. ANDRE, F. and GAGNY, C. (1981). Proposition d'un âge namurien pour le granite porphyroïde des Ballons, temoin vosgien d'un plutonisme à potentialité molybdénifère au Carbonifère supérieur. Congrés National des Sociétés Savantes, Perpignan, Avril 1981, III, p. 287-296.
2. ARHENS, L.H. (1952). The use of ionisation potentials. 1. Ionic radii of the elements. Geoch. Cosmochim. acta 2, p. 155-169.
3. ARNOLD, M. and GUILLOU, J.J. (1980). a) Dépôt d'anhydrite dans 17 filons métallifères hercyniens français : conséquences métallogéniques. C.R.A.S. Paris, Sér. D, t. 290, n° 3, p. 155-157.
   b) Les filons métallifères hercyniens. Origine de l'anhydrite et mécanisme de la pseudomorphose subsequente . Proposition d'un modèle. Sci. de la Terre, t. XXIV, n° 2, p. 173-194.
4. BAGNAL, K.W. (1972). The Actinide Elements. Elsevier, Amsterdam.
5. BEAUFORT, D. (1981). Etude pétrographique des altérations hydrothermales superposées dans le porphyre cuprifère de Sibert (Rhône). Thèse Université Poitiers.
6. BEAUFORT, D. and MEUNIER, A. (1983). A petrographic etudy of phyllic alteration surimposed on potassic alteration : the Sibert porphyry deposit (Rhône, France). Econ. Geol., vol. 78, p. 1514-1527.
7. CALAS, G., CURIEN, H., FARGE, Y. and MAURY, R. (1972). Cinétique de guérison des centres colorés de la fluorine jaune de Valzergues (Aveyron). Principe d'un thermomètre géologique. C.R.A.S. Paris, Sér. D, t. 274, p. 781-784.
8. CHAPMAN, N.A. and SMELLIE, J.A.T. (1986) - Introduction and summary of the Workshop. Chemical Geology, 55, p. 167-173.
9. CRAMER, J.J. (1986). Sandstone-hosted uranium deposits in northern Saskatchewan as natural analogs to nuclear fuel waste disposal vaults. Chem. Geol., 55, p. 269-279.
10. FLOYD, P.A. (1977). Rare earth element mobility and geochimical characterisation of spilitic rocks. Nature (London), 269, p. 134-137.
11. FOSTER, M.D. (1960). Interpretation of the composition of trioctaedral micas. U.S. Geol. Survey Paper, 354B, p. 11-49.

12. FOURQUIN, C. (1966). Données géologiques précisant l'âge des différentes phases de mise en place du granite du Ballon d'Alsace (Vosges méridionales). C.R.A.S t. 262, p. 1509-1512.
13. FREY, F.A., BRYAN, W.B. and THOMPSON, G. (1974). Atlantic Ocean floor : geochemistry and petrology of basalts from legs 2 and 3 of the Deep sea Drilling Project. J. Geophys. Res., 79, p. 5507-5527.
14. GUERIN, H. (1967). Les faciès de bordure du granite des Ballons. Bull. Serv. Carte Geol. Alsace Lorraine, 20, 1, p. 37-58.
15. HELGESON, H.C. (1979). Mass transfer among mineral and hydrothermal solutions. In geochemistry of hydrothermal ore deposits. Barnes John Wiley and Son ed. (2nd ed.). p. 568-606.
16. HUNT, J.A. and KERRICK, D.M. (1977). The stablity of sphene : experimentation redetermination and geologic implications. Geochim. et Cosmoch. Acta, 41, p. 279-288.
17. JACOBS, D.L. and PARRY, W.T. (1976). A comparison of the geochemistry of biotite from some Basin an Range Stocks. Econ. Geol., vol. 71, p. 1029-1035.
18. JEBRAK, M. (1984). Contribution à l'histoire naturelle des filons F-Ba du domaine varisque. Essai de caractérisation structurale et géochimique des filons en extension et en décrochement dans les massifs centraux français et marocain. Thèse d'Etat, Orléans.
19. JEBRAK, M. (1986). Devenir à long terme des stockages de déchets radioactifs en formation géologique : analogie avec l'altération des gisements minéraux. Rapport CCE, in press.
20. KAMINENI, D.C. (1986). Distribution of uranium, thorium and rare-earth element in the Eye-Dashwa Lake Pluton. A study of some analogue elements. Chemical geology, 55, p. 361-373.
21. KRAUSKOPF, K. (1984). Thorium as an analog for plutonium and rare-earth metals as analogs for heavier actinides. Abstr. Workshop or Radionuclide Migration, Natural Analog. to the Conditions around a Final Repository for HWL, organized by S.K.B.F. Chicago III.
22. LEMIERE, B., DELFOUR, J., MOINE, B., PIBOULE, M., PLOQUIN, M., ISNARD, P., and TEGYEY, M. (1986). Hydrothermal alteration and the formation of aluminous haloes around sulfide deposits. Mineral Deposits, 21, p. 147-155.
23. LESHER, C.M., GIBSON, H.L. and CAMPBELL, (1986). Composition-volume changes during hydrothermal alteration of andesite at Buttercup Hill, Noranda District, Quebec. Geochim and Cosmochim. Acta, Vol. 50, p. 2693-2705.
24. LIOU, J.G. (1973). Synthesis and stability relations of epidote $Ca_2 Al_2 Fe\ 3O12\ (OH)$. Jour of Petrol, 14, p. 381-413.
25. MICHARD, A., ARNOLD, M., GUILLOU, J.J., and SHEPPARD, S.M.F. (1983). Analyse S_{34}, $^{87}Sr/^{86}Sr$ de sulfates et O^{18} du quartz pseudomorphique de filons minéralisés à Ba-F. Coll. A.T.P. Geochimie Minérlogie CNRS. Bonnas, juin 1983, p. 272-277.
26. MONTOYA, J.W. and HEMLEY, J.J. (1975). Activity relations and stabilities in alkali feldspar and mica alteration reaction. Econ. Geol. 70, p. 577-583.
27. MOUILLAC, J. (1974). Géologie du granite des Ballons et de ses minéralisations à cuivre et molybdène associées (Vosges méridionales). Essai de contrôle métallogénique des résultats de la prospection. Thèse université Nancy.
28. OCDE-AEN Collectif (1982). Evacuation des déchets radioactifs dans les formations géologiques. Publication OCDE-AEN.
29. PAGEL, M. and LETERRIER, J. (1980). The subalkaline potassic magmatism of the Ballon massif (Southern Vosges, France). Shoshonitic affinity. Lithos 13, p. 1-10.

30. PHILLPOTTS, J.A. (1970). Redox estimation from a calculation fo Eu^{2+} and Eu^{3+} concentration in natural phases. Earth planet. Sci. Lett. 9, p. 257-268.
31. ROSE, A.W. and BURT D.M. (1979). Hydrothermal alteration. In geochemistry of hydrothermal ore deposits. Barnes - John Wiley and Son ed. (2nd ed). p. 175-235.
32. SHANNON, R.D. and PREWITT, C.T. (1970). Revised values of effective ioni radii. Acta Cryst. B, 26, p. 1046-1048.
33. SHANNON, R.D. (1976) - Revised effective ionic radii and systematic studies of interatomic distances in halides and chalcogenides. Acta Cryst. A, 32, p. 751-762.
34. WOOD, D.A., GIBSON, I.L. and THOMPSON, R.N. (1976). Elemental mobility during zeolite facies metamorphism of the Tertiary basalts of Eastern Iceland. Contrib. Mineral. Petrol., 55, p. 241-254.

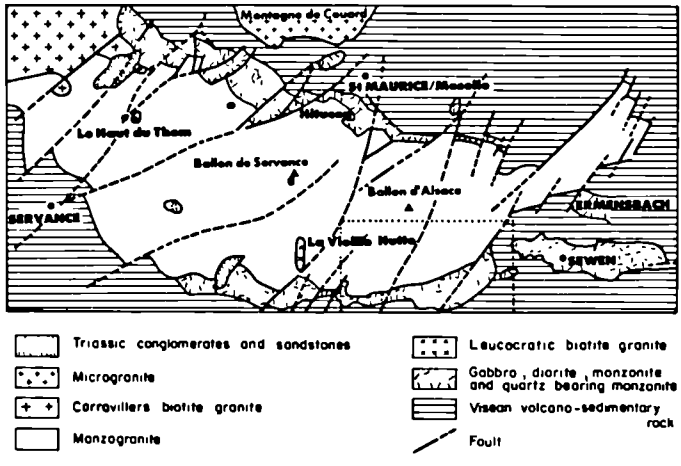

Fig. 1 - Geological map of Ballon d'Alsace complex (Mouillac, 1974).

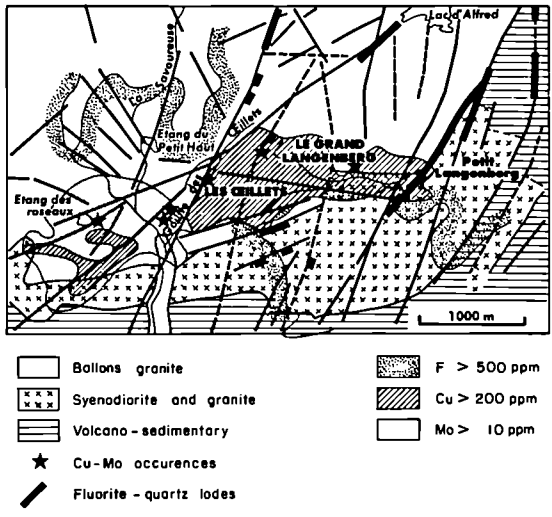

Fig. 2 - Detailled geological map of Oeillets and Langenberg areas showing geochimical anomalies.

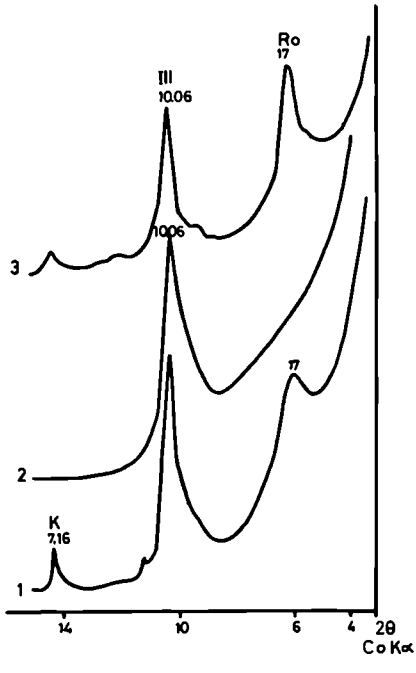

Fig. 3 - X.R.D. traces of irregular illite-smectite mixed layer (Ro), illite (Ill) and kaolinite (d_{hkl} are in A).
1 Glycollated,
2 Heated to 550°,
3 Li exchanged.

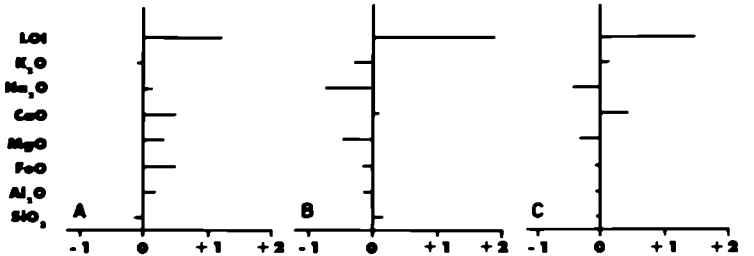

Fig. 4

- Gains and losses of major geochimical components during hydrothermal alteration expressed as percentage relative abundance to the assumed parent rock.
The value of each element mass balance index is calculated with the following equation :

$$BEL = \frac{PrEl}{PoEl} - 1$$

- PoEl, element average in weight % of samples with no or incipient atteration.

- PrEl, element average in weight % of samples with alteration type.
  A Propylitisation
  B Phyllic-type alteration
  C Clay and carbonate alteration.

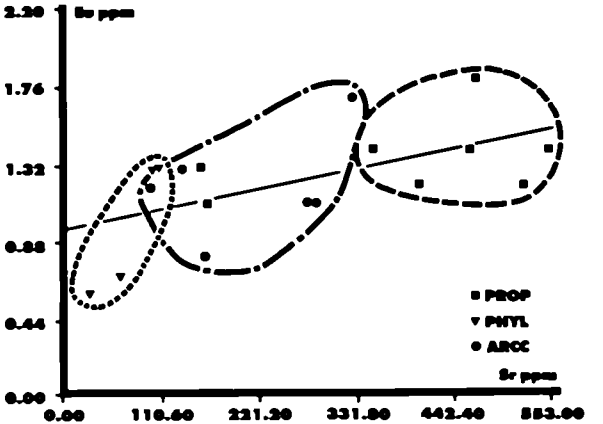

Fig. 5 - Sr versus Eu diagram.
Samples plotted are : prop. propylitic, phy. phyllic-type arcc. clay and carbonate alteration

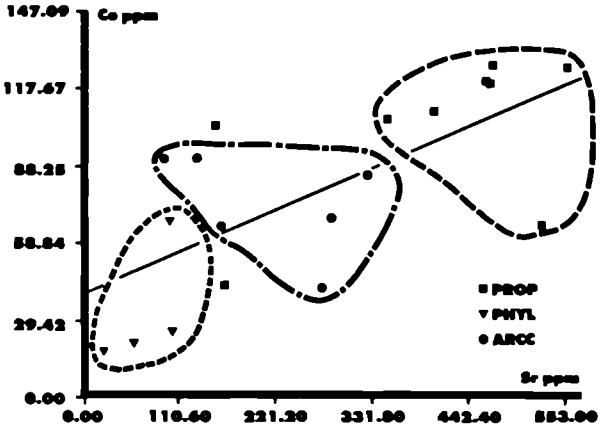

Fig. 6 - Sr versus Ce diagram.

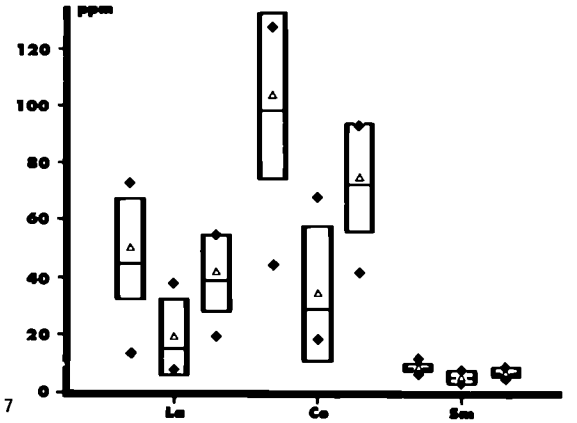

Fig. 7 - Box-Whisker plot for Lanthanum, Cerium and Samarium in samples of propylitic alteration (shaded), phyllic alteration (dotted) and carbonate alteration (white).
Symbols are : ◆ minimum-maximum - mean.
The size of box represent standard deviation.
The horizontal line within the box is the median.

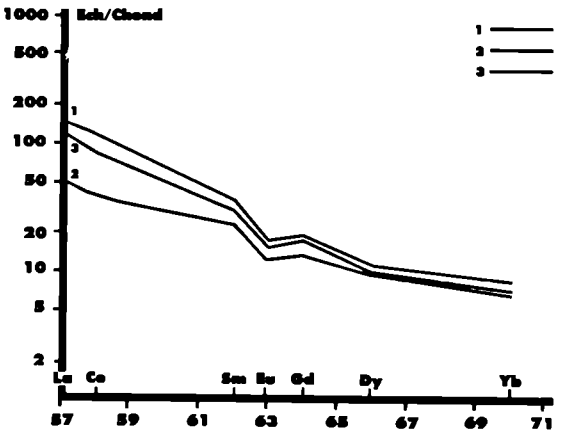

Fig. 8 - Chondrite patterns for REE in altered samples : (1) propylitic alteration, (2) phyllic-type alteration, (3) clay and carbonate alteration.

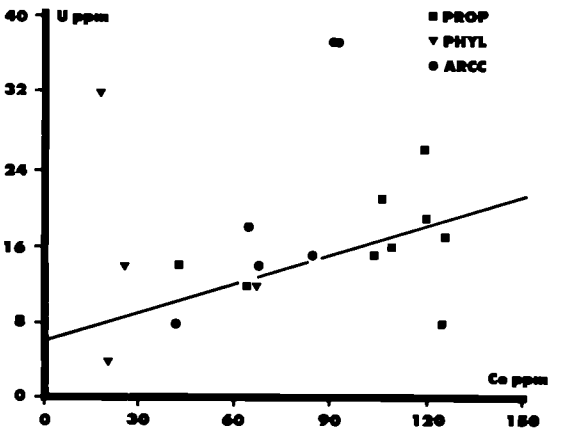

Fig. 9 - Ce versus U diagram.

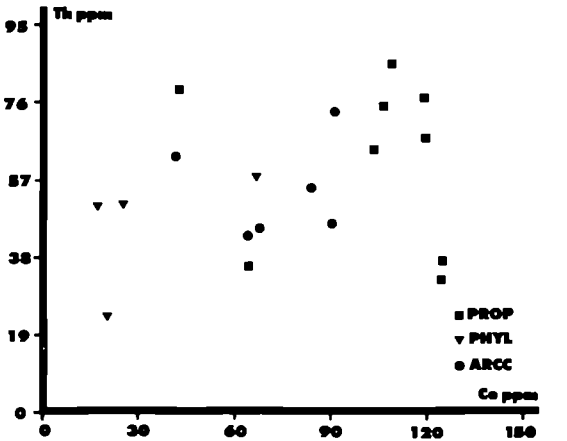

Fig. 10 - Ce versus Th diagram.

SOME GEOCHEMICAL AND MINERALOGICAL PECULARITIES OF DEPOSITS OF RADIOACTIVE MATERIALS AS EVIDENCE FOR RADIOLYSIS IN NATURE

I. F. VOVK
Divison of Nuclear Fuel Cycle
International Atomic Energy Agency

Summary

Geochemical and mineralogical features of deposits of radioactive materials have been reviewed in a search for the radiolytic effects established in laboratory experiments. The details of the review are presented. In particular, oxidation of organic matter, sulphides and other minerals and compounds containing elements of variable valence states, formation of specific minerals like wheweliite, hematitic halos and bleached zones around the uranium deposits, argillization and similar geochemical processes, to which oxidizing and reducing agents formed in groundwater radiolysis could contribute, are discussed. Special attention is given to the accumulation of hydrogen, oxygen, carbon dioxide and other specific gases, oxidized species in fluid inclusions in minerals and vaults in a number of uranium and potassium deposits, as well as to correlation between isotopic composition of some chemical elements (hydrogen, carbon, oxygen, sulphur) and uranium content, which can be best explained by radiolytic processes.

1. Introduction

Radiolysis of groundwater is an important factor in evaluating the chemistry of the "near-field" of HLW repositories. Natural radiolytic effects are also important in studies of uranium deposits as natural analogues of geochemical behaviour of some long-lived fission products (^{99}Tc and ^{129}I) and transuranic actinides (^{237}Np and ^{239}Pu).

The chemistry of both these groups of elements with all their differences displays one particular similarity: they can all exist in a number of valence states which are easily affected by reactions with products of water radiolysis. They may form various inorganic and organic compounds, including migration complexes which can be produced or destroyed in the process of groundwater radiolysis. These and other reasons discussed by Chapman et al. (4) place groundwater radiolysis among the important geochemical processes to be studied at natural analogues.

The uranium deposit at Oklo in Gabon is referred to nowadays as the most comprehensive analogue for final disposal of spent nuclear fuel, both in terms of the level of radiation and the amount of geological and geochemical information. Some of the observed geochemical processes (oxidation of uranium, reduction of iron, accumulation of free hydrogen in fluid inclusions) have already been interpreted in terms of radiolysis of groundwater and organic matter (5, 9).

However, the Oklo natural analogue alone cannot cover all geochemical aspects of water-rock system radiolysis. To obtain more or less a complete picture of radiolysis in nature, a variety of analogues must be studied. Thus, as it was rightly pointed out by Chapman et al. (4), both a further, more detailed examination of the Oklo analogue and identification of other locations for studying the resultant radiolysis profiles, would be extremely useful. Such locations may not be necessarily natural reactor sites. The extent of radiolytic alterations in a system depends on several factors such as integral absorbed dose, chemical composition, physical and physico-chemical properties of the system, etc. As far as the integral absorbed dose is concerned, values of 10^{10} - 10^{12} Gy, that is approximately as high as in Oklo uranium ore bodies, are characteristic for many other uranium deposits. Therefore, though the Oklo deposit is probably the most suitable choice for investigation of radiolytic effects in nature, it is not the only location where some of the effects in question can be traced.

The author's objective is to outline the major results of experimental laboratory studies of radiolysis with special emphasis on radiolysis of brines and heterogeneous water-rock systems and to discuss on this basis the geochemical and mineralogical zonation and some other characteristic features of deposits of radioactive materials which can be interpreted as evidence for groundwater radiolysis.

2. Radiolysis

Radiolysis of water and its solutions is one of the most advanced branches of radiation chemistry. Several extensive reviews on this subject have been published (7, 44) which typically contain the results of homogeneous radiolysis of simple aqueous solutions studied for academic purposes. This approach has led to understanding of the radiolytic processes under an idealized environment that may have limited application to both actual repository conditions and natural analogues. Laboratory and in-situ experimental studies of radiolysis of complex aqueous solutions and brines as well as heterogeneous water-rock systems simulating groundwater radiolysis in deep geological formations are now underway or being planned (18-21, 37, 44).

2.1 Water and aqueous solutions

The action of alpha, beta and gamma radiation on liquid water is to form reactive species, so-called primary radiolytic products, by electron excitation and ionization of water molecules. The most important are free radicals - hydrated electron, e^-_{aq}, hydroxyl and hydroperoxyl radicals, OH and HO_2, and hydrogen atom, H. The primary molecular products are hydrogen, H_2, and hydrogen peroxide, H_2O_2. Other important species are hydrogen and hydroxyl ions, H^+ and OH^-. The species e^-_{aq}, H and H_2 are reducing, while OH, HO_2 and H_2O_2 are oxidizing agents, e^-_{aq} and OH being most powerful.

The primary radiolytic products interact with themselves and with dissolved species to yield various secondary products the nature and quantity of which depend on a number of factors, in particular on the chemical composition of the irradiated solution. The efficiency of radiolysis, expressed by the G-value (number of radicals or molecules produced or destroyed per 100 eV of absorbed energy), and the total amount of an accumulated radiolytic product increases with increasing concentrations of so-called scavengers (reactive species) in solutions as they prevent the primary species from recombination into water molecules.

For example, G ($-H_2O$) for pure water varies with the kind of absorbed radiation (alpha, beta gamma) from 3.3 to 4.6 (7) while in some concentrated aqueous solutions it can reach 12-15 (41). Radiolysis of pure water produces only a very small equilibrium concentration of H_2. In solutions which contain high concentrations of OH scavengers (such as Cl^-, Br^-) and display synergistic interaction between the dissolved species, radiolysis may generate hydrogen and oxygen at a high equilibrium pressure. In experiments with brine, a total absorbed dose of gamma irradiation of 2.10^8Gy resulted in hydrogen and oxygen gas pressure of about 100 atm. Alpha radiation led to even higher equilibrium pressure (about 140 atm) at a lower total absorbed dose of 5.10^7Gy (18). The gas composition in both cases was 67% H_2 and 33% O_2 as would be expected for the stoichiometric value of $H_2/O_2 = 2$. In experiments on alpha radiolysis at lower total absorbed doses (9.10^3 - $3,6.10^4$Gy) H_2/O_2 ratios were 7 to 9 (28). The important point is that alpha radiolysis of brines in all cases creates extremely oxidizing conditions. Pederson et al. (28) reported that the effect of alpha radiolysis for the above cited doses was to raise the Eh values to about 1000 mV over unirradiated brines. This effect has been also observed by Gray and Simonson (18) and by Kim et al. (21) and can be linked to the presence of chlorine and other secondary oxidizing products Cl_2^-, ClO^-, etc.

There are examples of sharp increases of solubilities and dissolution rates of actinide compounds due to their oxidation apparently by the above species produced in the process of alpha radiolysis in concentrated chloride solutions (21). For other elements gamma radiolysis in this respect may be equally effective. Lieser et al. (25) found out that amount of released iodine increased from 8.10^{-5}% per Mrad of absorbed gamma irradiation for dry AgI to 4.10^{-4}% per Mrad, for wet AgI and to about 2.10^{-3}% per Mrad in saturated NaCl solution.

Organic matter and sulphur compounds when present in dissolved, suspended or colloidal forms may undergo radiolytic oxidation to form carbon dioxide and sulphates with a large variety of intermediate metastable species which, in case of sulphur, include thiosulphate, sulphite and others, and in case of some potential organic compounds (such as CH_4) can give rise to the formation of polymers. Radiolysis of carbon dioxide and nitrogen solutions may result in the formation of oxalic acid and nitric acid and NH_4^+, respectively. Other important radiolytic reactions in aqueous solutions include oxidation and reduction of metallic elements with variable valence state.

2.2 Water-rock systems

Radiolysis of heterogeneous and multicomponent water-rock system is still far from being completely understood. Very few of many possible mechanisms have been accurately recorded. It is apparent that they combine radiation effects both in liquid and solid phase, which however do not come to a simple arithmetic sum. Some processes, like mass and energy transfer under irradiation, changes in the rate and/or type of reaction initiated by irradiation in the presence of a phase boundary and changes in specific surface properties in irradiated heterogeneous systems, may appear to be the most important. It may be pointed out as an evidence for this that values of G (H_2) as high as 10 to 30 molecules per 100 eV have been reported for gamma radiolysis of water absorbed on the oxides, SiO_2, Al_2O_3, La_2O_3 (15).

The studies of the effects of irradiation on the stability of natural minerals in the presence of water confirm the predominantly destructive action of irradiation. Natural zircon displays increases in leach rates

of up to two orders of magnitude as a result of radiation induced amorphization (13). The results of experiments on the irradiation of the most widespread natural alumosilicates (quartz, feldspars, caolinite, chloride) show that both radiolysis of water and radiation damages in the subsurface layers of the mineral grains act in combination as a factor of mineral disintegration. A dose of 10^5-10^6Gy has been determined as the "threshold dose", marking the beginning of this effect (36). Disintegration of feldspars is the first stage of their alteration leading to argillization, which is potentially favoured by the radiolytic oxidation of organic matter and/or nitrogen contained in the water-rock system. A strong support for radiolytic argillization in nature comes from studies carried out by Simmons and Caruso (35). They discovered that uraniferous clay aggregates in granites include, as the host for uranium, non-clay minerals surrounded by smectite, nontronite or vermiculite.

The author's data (41) obtained in experiments of gamma irradiation of complex geological objects (bottom sediments of the Black Sea and the Mediterranean) demonstrate clearly that at least three major geochemical processes are caused by radiolysis of the water-rock system: salt enrichment of interstitial water (increase in TDS), production and accumulation of hydrogen and consumption of oxygen in oxidation of organic carbon, sulfur and perhaps other variable valence elements. They also show that salt enrichment is a complex function both of the radiolytic decomposition of water molecules, proved by the increase of Cl^- concentrations in interstitial water, and of accumulation of such TDS constituents as bicarbonates, sulphates and cations, particularly calcium, as a result of irradiation and interaction of water radiolysis products with the rock matrix. Storage of hydrogen (and carbon dioxide) in the gaseous phase, accumulation of bicarbonates and sulphates, iodine, iron, silica, nitrogen and other compounds in the liquid phase, was accompanied by corresponding decrease in content of organic carbon, sulphur and other elements in solid and gaseous phases. Typical post-irradiation values of pH were 6.8-7.5 in comparison with pre-irradiation values 7.0-8.9. Eh values dropped during irradiation from +550 mV to -200 - 340 mV. A very negative value of Eh (-500 mV) has been also reported by Jantzen and Bibler for irradiated granite and basalt groundwater (20).

Preliminary experiments on the effects of gamma irradiation of Boom Clay have indicated that, as in case of the irradiation of sea bottom sediments, the major radiolytic products were H_2 and CO_2 in the gas phase and SO_4^{2-} in the liquid phase. These phenomena are due to oxidation of pyrite and organic material both of which are present in Boom Clay (19).

Recent gamma radiolysis experiments have been conducted on aqueous systems representative of those that might be found in a repository in granite rocks by Tait et al. (37). Hydrogen was detected in all samples at concentrations ranging from 63 to 97 vol.%. Oxygen was detected in appreciable concentrations only in samples that did not contain granite with H_2/O_2 ratios close to 2. Oxygen was depleted from all capsules containing granite coupons or crushed granite. Samples which contained bentonite also showed a strong depletion of oxygen but in addition showed a significant proportion of CO_2, which is most likely resulted from the radiolytic oxidation of organic fraction in the natural bentonite clay (4.8 wt% organic by analysis). The pH values ranged from 6.5 to 10.6, the highest pH values correlate with those samples that had the highest leach rate (sodium borosilicate glass) and, thus, the highest release of Na^+.

The above short review of the experimental studies of the radiolysis of aqueous solution and water-rock systems shows that strong oxidants and

reductants are generated simultaneously. Molecular hydrogen is chemically inert toward low-temperature reactions and has much greater diffusional mobility than that of oxidizing species. So it can be selectively removed from locally irradiated water-rock system while the system itself becomes progressively oxidized and argillized with increased TDS in the liquid phase.

3. Deposits of radioactive materials

3.1 Absorbed doses

Durrani et al. (10) calculated that a uranium content of 0.5% in the region of low-grade ore of the Oklo deposit, situated adjacent to a quartz crystal, will impart to it a dose of 10^{10}Gy in 2.10^9 years from the alpha decay alone of the ^{238}U nuclei and that the uranium content in the core zone (up to 50%) would yield an alpha dose of 10^{12}Gy. The dose of alpha and beta irradiation from ^{235}U fission and ^{239}Pu decay for the period of the Oklo reactor operation was calculated to be 6.10^{25}MeV per ton of fuel (5) or 5.10^9J per kilogram of uranium ore (5.10^9Gy).

Proceeding from the dose rate values of 3050, 840 and 0.1 Gy/yr for the elements U, Th and K, respectively (41), it is easy to make rough estimations of the total absorbed dose for any deposit of radioactive material with known concentrations of the radioactive elements and the age of rocks of the deposit. For example, the total absorbed dose in the uranium ore of the Cigar Lake deposit, Canada (the average ore grade 14% U_3O_8 and the age of ore formation 1.10^9 years) is about 4.10^{11}Gy, in the potash ore of Verkhnekamsky deposit, USSR, represented by silvite (52,4%K, age 2.10^8 years) it is about 1.10^7Gy. For the nuclear core of the Oklo deposit similar calculations give total absorbed dose up to 3.10^{12}Gy.

3.2 Groundwaters and fluid inclusions

Calculations, based on the radiolytic yield of water decomposition 3 molecules per 100 eV, show that in a system in which hydrogen is evacuated and oxygen is either accumulated or consumed in oxidation reactions, doses of the order of 10^8Gy are sufficient to decompose all the initially contained water, resulting eventually in deposition of dissolved salts (43). Indeed, both fluid inclusions in minerals and groundwaters within the studied uranium ore bodies show salinites ranging from less than 1% to 26-30% (point of saturation of NaCl) and much higher (60-70%) in fluid inclusions containing salt crystals. Halides and other daughter minerals (sulphates, carbonates, oxidized iron, etc.) in such inclusions often do not dissolve even being kept under temperatures exceeding the homogenization temperatures which may indicate on the radiolytic concentration of the trapped solution and formation of the daughter minerals in the process of radiolytic oxidation of dissolved and host mineral substances (43). Due to this process the uranium content in fluid inclusions may reach values of $n.10^2$mg l^{-1} (27) and thus provide aqueous solutions with irradiation at the dose rate of up to several grays per year in addition to what they receive from the rocks.

Dubessy has measured in water-gas inclusions associated with uranium mineralization the following partial pressures of O_2 and H_2: Rabbit Lake deposit for P (O_2) from 7 to 60 bar, for P (H_2) from 0.02 to 2.4 bar; Cluff Lake deposit for P (O_2) from 4 to 30 bar, for P (H_2) from 0.5 to 2 bar; Oklo deposit for P (H_2) from 0.7 to 20 bar, for P (O_2) 0 bar. This latter result has been interpreted as joint radiolysis of water and organic matter, confirmed by the presence of CH_4 and CO_2 in several inclusions (9). CO_2, accompanied by CH_4 and C_2H_4, is the

major gas in fluid inclusions in samples from uranium deposits located in granites from Massif Central, France. Fluid inclusions show that there exists a clear relation between uranium grade and CO_2 concentration in the fluid (30). Kranz has determined in fluid inclusions in radioactive minerals, besides H_2 and CO_2 as major gases, He, CH_4, H_2S and a number of high-molecular organic compounds. This author points out that there exists a direct quantitative relationship between the content of some organic groups, in particular amino compounds, in inclusions and uranium and thorium content in minerals, which, in his opinion, suggests that these compounds originate through irradiation of mixtures of ammonia and methane (22). Enrichment in nitrogen compounds has been established for some uranium deposits of the USSR, where fluid inclusions within the ore bodies contain up to 1000 mg l^{-1} of bour nitrogen, in comparison with less than 100-300 mg l^{-1} in the adjacent host rocks (41).

3.3 Free gases

The release of gases containing hydrogen from the radioactive rocks has been known for a long time. At the Witwatersrand gold-uranium deposit, South Africa, brines associated with N_2-CH_4 gases with high content of He and H_2 also give rise to free gas jets. One of them, at the depth of 1426 m in the Crown Mine, had the following composition (vol.%): H_2-77.5; CH_4-11; CO_2-0.1; O_2-0.3; N_2+He+Ar-11.1 (14).

A halo of multicomponent gas (H_2, CO_2, CH_4) around a roll-type uranium deposit has been studied recently in the USSR (29). The data show that hydrogen is the most abundant gas (up 9 cm^3 per kilogram of rock), the content of carbon dioxide does not exceed 0.9 cm^3kg^{-1}. Maximum production of CO_2 is displaced down-dip from oxidation-reduction interface to the ore body, thus giving an evidence that in this particular deposit radiolytic oxidation of the scattered organic matter prevails over the oxidation by the dissolved atmospheric oxygen.

Radiolytic origin of free hydrogen gas accumulated in the salt vaults at potassium deposits has been discussed by the author elsewhere (41).

3.4 Organic matter

Detailed laboratory and field studies of the relationship of organic matter and uranium in geological formations gave convincing evidence that ionizing radiation from uranium and daughter products play an important role in physical and chemical changes known as maturation, polymerization, oxidation and/or degradation of organic matter (24, 34, 39, 42, 45). When multiple maturation populations are observed in organic materials derived from core samples, as a rule, the more mature organic constituents have been reworked from older sediments. Uranium deposits are exceptions to this rule. In core samples that pass through even comparatively young roll-front deposits, the extractable organic matter frequently exhibits various aspects of radiation damage (selective oxidation and/or thermal alteration) and a dual mode of thermal maturity is observed. Lower levels of maturation gradually give way to much higher alteration values as one approaches the zone where the uranium ore is most concentrated. This process reverses itself once the core hole passes through the roll-front into non-mineralized rocks (34). It is found at Oklo deposit that the organic material is oxidized and that the nearer to the reaction zone the greater the oxidation (39). Carbon-rich materials at a uranium deposit in Grants mineral belt have been severly degraded by radiation and organic matter now resembles amorphous carbon, having lost most of its hydrogen

and oxygen and its cellular structure (23). High concentrations of organic free radicals in the carbonaceous matter at the Vaal Reef gold-uranium deposit (Witwatersrand) suggest that radiation emitted from uranium played a unique role in the reconstitution and polymerization of the progenitor biochemicals (45).

3.5 Sulphur compounds

Combined effects of water radiolysis and radiation damage of mineral matrices are likely to significantly contribute to oxidation of sulphides in uranium deposits. Due to this, pyrite and other sulphide minerals decrease in abundance while sulphate concentrations, on the contrary, can increase with increasing maturity of uranium ore. This trend was first pointed out and explicitly explained on the basis of radiolysis for the Witwatersrand deposits by Myers: "Pyrite was depleted by the reaction that dispersed uraninite, buffering by pyrite moderated the oxidative dispersal of uranium. It follows that where pyrite was scanty or absent, uraninite was completely dissolved by the oxidizing effects of radiolysis" (26, p.AA-14). Pyrite depletion within ore bodies can be clearly seen in a number of roll-type uranium deposits. For example, at Benavides (South Texas) the percentage of the total iron disulphide content within the ore body is the lowest noted for reduced (sulphidized) zone. The highest values are determined in cores at some distance down the roll (16). Similar pattern of the distribution of FeS_2 in the reducing zone has also been observed in the Lamprecht and Felder deposits of Ray Point uranium district (17). It is consistent with the radiolytic model of sulphur oxidation. Thiosulphates formed in this process disproportionate into sulphides and sulphates and, thus, give rise to the formation of secondary sulphide and sulphate minerals down-dip hydraulic gradient.

Correlation between sulphate ion content in groundwater and radioactivity of water and rocks has been demonstrated earlier (41) and was explained on the basis of radiolytic model. In particular, it was shown that high content of sulphate ion (10.5-22.5 gl^{-1}) in fluid inclusions in minerals (pitchblende and calcite) of the nasturan stage at uranium deposit in volcanic rocks, most probably resulted from its radiolytic storage in contrast to the initial suggestion about the oxidation of pyrite by oxygenated groundwater. Detailed geochemical studies of the zone of sulphate-enriched waters closely associated with uranium deposits of the Ray Point district revealed that the oxidation of sulphide minerals and production of both aqueous sulphides and sulphates occur in the uranium ore bodies (17). However, the authors (17) were not able to indicate the source(s) of oxidants which would be adequate to produce the equivalent quantity of sulphate.

3.6 Host rock alteration

One of the most characteristic features of deposits of radioactive materials is their and/or host rock red coloration (gematitization). It is particularly pronounced in the potassium deposits as well as within and around the uranium ore bodies in crystalline rocks of the shields and granite massifs of the world. The geochemical cause of this phenomenon is still being discussed. It was shown that radiolysis is the most probable process leading to the oxidation of Fe^{2+} to Fe^{3+} and thus formation of the red colour of potassium deposits (41). It is also logical to assume that this process greatly contributes to the gematitization of rocks hosting uranium deposits in the absence of reducing agents other than iron (6, 42).

In uranium deposits associated with organic materials in redbeds

(such as anagenic deposits confined to petroleum accumulations, solid bitumen or organic trash pockets) an opposite process - bleaching (removal of red coloration) takes place. This phenomenon has been observed on the Colorado Plateau and other regions in the USA and USSR (1, 11, 42). The uranium-bearing organic matter with indigenous reducing capacity is bound to reflect this capacity by decoloration of adjacent usually coarser grained sediments (sandstones and conglomerates) from their normally red hues to a grey, green or white colour. The colour transition may be attributed to the reducing action of radiolytic hydrogen which has migrated into the porous red clastics causing reduction of Fe^{3+} to Fe^{2+}. The phenomenon has been used as a guide to ore because of strong correlation between thickness of ore and thickness of the alteration zone (1) and for the same reason it can be used as an evidence that the bleaching has been caused by radiolysis of groundwaters in the presence of acceptors of oxidative radiolytic species (organic matter).

Another well known process of uranium host rock alteration is argillization, i.e. replacement or alteration of the feldspars to form clay minerals. Besides the wall rocks adjacent to uranium veins, argillization is especially strongly marked in the zones of bleaching around the anagenic uranium deposits (11) where this process is apparently enhanced by radiolytic production of CO_2 and organic acids. The scale of argillization as in the coloration-decoloration cases is often proportional to the amount of uranium in the deposit thus reflecting its radiolytic potentiality.

Radiolysis of aqueous solutions of CO_2 or carbonates, as was mentioned above, produces oxalate ions giving rise to the formation of whewellite ($CaC_2O_4.2H_2O$). A significant amount of this rare mineral has been found in a number of hydrothermal uranium deposits and it was only natural to interpret such an association as a direct mineralogical indication of the radiolysis (3, 41).

The mineral assemblage in the alteration zone, defined by Brookins (2) as zone of retention surrounding the pitchblende, at Oklo, includes both sulphides and sulphates, carbonates, clay minerals, hematite and other oxides (2). However, in reaction zone clay minerals are predominant. Their possible origin has been described as precipitation from radiation-damaged "mud" into which original silicate minerals were transformed when they were exposed to the irradiation in the hot saline groundwaters (8).

3.7 Isotopes of light elements

Isotopic composition of some of the light elements (H, C, N, O, S) can be indicative for radiation-induced processes as far as kinetic and other effects of isotope fractionation are predictable on the basis of radiolytic model. Due to a higher rate of reactions among light isotopes it can be expected that in the reactions of recombination of radiolytically produced water constituents light water molecules form more preferrably. To keep the balance, free hydrogen gas and secondary products (hydrocarbons, clay minerals, oxides, sulphates, carbonates etc.) must be enriched in heavy isotopes of hydrogen and oxygen respectively. Radiolytic CO_2 formed in oxidation of organic matter must have relatively light values of $\delta^{13}C$. A large range of $\delta^{34}S$ can be provided by combination of intramolecular sulphur isotope exchange equilibrium and kinetic isotope effects during thiosulphate disproportionation.

A number of anomalies of isotopic composition of the light elements have been reported for the uranium deposits, though a few of them have

been interpreted as a result of irradiation. One such interpretation has been given by Leventhal and Threlkeld (24). They found that organic carbon associated with high-grade uranium ore, Grants, New Mexico, is heavy ($\delta^{13}C$ = -16.9 to -19.6 °/oo PDB) relative to the adjacent lower-grade samples (-22.7 to -26.4 °/oo). It is suggested that the heavy isotopic values for the organic residuum in the ore samples are related to alpha irradiation at a dose of 10^9Gy (24). Data on isotopic composition of carbonates which occur as inclusions and veinlets within high-grade ore of the Nabarlek uranium deposit, Australia, show marked ^{12}C ($\delta^{13}C$ = -13.1 to -19.7 °/oo PDB) and ^{18}O ($\delta^{18}O$ = 25.1 to 28.7 °/oo SMOW) enrichment compared to bedded carbonates ($\delta^{13}C$ ~ 0 °/oo, $\delta^{18}O$ ~ 13 to 19 °/oo) of similar age in the region (12). The extent of ^{12}C enrichment of the Nabarlek carbonates and the absence of the bedded carbonates in the area of the deposit led Ewers et al. (12) to the conclusion that they formed mainly from organically derived CO_2. Both, association with high-grade uranium ore and the extent of ^{18}O enrichment, allow one to conclude also that CO_2 resulted from radiolytic oxidation of organic matter. Formation of carbonates enriched in light carbon ($\delta^{13}C$ = -15.9 to -16.8 °/oo) at the Eldorado uranium deposits, Canada, correlates in time with the process of hematitization (33). Brine encountered in a sealed pocket at one of these deposits had $\delta^{18}O$ value of water molecules -16.2 °/oo (33), very low for brines, consistent however with the radiolytic model. δ D values of water hydrogen as low as -121 to -180 °/oo have been determined for fluid inclusions in ore albitite from a uranium occurrence, in comparison with values -45 to -79 °/oo for the inclusions in the host rocks (40).

The most negative values of $\delta^{34}S$ are usually confined to the ore bodies and their vicinities and correlate with the content of both secondary sulphides and uranium. This correlation may be considered as a proof of radiolytically induced redistribution of sulphur and its isotope fractionation through the formation and disproportionation of thiosulphate, especially when it is observed in the hypogeneous deposits where it is difficult to interprete in any other way than radiolytic. As an example one can mention the Echo Bay deposit in the crystalline rocks of the Canadian Shield where $\delta^{34}S$ values increase from -22 °/oo in sulphides deposited together or in the close vicinity of the uranium minerals to +27 °/oo in sulphides, spatially separated from the uranium ore. These values of $\delta^{34}S$ for vein sulphides are in sharp contrast to the monotonously constant values (2 to 5 °/oo) for sulphides of the bulk of rocks (32). Data on groundwater sulphur geochemistry obtained for the Ray Point uranium district help to understand the mechanism of such fractionation. The $\delta^{34}S$ values of H_2S and SO_4^{2-}, which are simultaneously present in groundwaters there and were most probably formed by radiation oxidation of sulphide minerals (with $\delta^{34}S$ -49.4 to 26.1 °/oo), vary from -61.2 to -36.6 °/oo and from -17.2 to 13.3 °/oo for H_2S and SO_4^{2-}, respectively. The corresponding values of fractionation factor Δ ($\delta^{34}S$) = $\delta^{34}S$ (SO_4^{2-}) - $\delta^{34}S$ (H_2S) are within the range from 30.2 to 52.3 °/oo with the mean for 10 samples 40.8 °/oo (17). They are consistent with the results of the experimental studies by Uyama et al. (38) of the intramolecular sulphur isoto e exchange in thiosulphate.

4. Conclusion

Water-rock interaction, which controls the migration of chemical elements in the geosphere, in its turn, may be affected by the process of radiolysis both in the high-level radioactive waste respositories and in

the deposits of radioactive materials. The major geochemcial effects of radiolysis include generation of free gases, predominantly hydrogen and carbon dioxide, potentially capable to change mineralogical and chemical properties of the host rocks (reduction and transfer of iron, transformation of feldspars and other relatively inert minerals into clays displaying high sorption qualities) as well as formation of chemical compounds, which, on one hand, may serve as migrating complexes (carbonates, thiosulphates, sulphates, organic acids and radicals, etc.) and, on the other hand, may, on the contrary, preclude the migration by co-precipitation (iron hydroxides, oxalates, sulphides, etc.). The final effect of radiolysis, therefore, is difficult to predict and, as the results will depend on the prevailing geochemical situation, it is necessary to have a number of natural analogues for the evaluation of this process.

Though effects of groundwater radiolysis in nature may be often partly or completely masked or eliminated by other processes like thermal and dynamic metamorphism, atmospheric weathering, hydrothermal alteration, etc., resulting in the same or similar mineralogical and geochemical changes, many of the known deposits of radioactive materials display nevertheless that or other geochemical feature relevant for recognition of radiolytic process. These features are bound to be more pronounced in the geochemical environment where natural radiolytic effects could be most effective, are best preserved and where other competing processes could be precluded by the geological situation. In other words, in addition to the Oklo deposit, some of the old high-grade uranium ore bodies in sedimentary rocks rich in organic matter, sulphides, feldspars and heavy minerals in zones of impeded water circulation may be probably selected for investigations as natural analogues of radiolysis.

REFERENCES

1. ADLER, H.H. (1974). Concepts of uranium ore formation in reducing environments in sandstones and other sediments. In Formation of Uranium Ore Deposits, IAEA, Vienna 141-168.
2. BROOKINS, D.G. (1978). Application of Eh-pH diagrams to problems of retention and/or migration of fissiogenic elements at Oklo. In Natural Fission Reactors, IAEA, Vienna 243-265.
3. BUGAENKO, L.T., DZHURINSKAYA, M.B., ZUBAKEV, V.E., KALYASIN, E.P., RUDNEV, A.V. and USPENSKY, V.A. (1983). Natural radioactivity and formation of whewellite in the uranium hydrothermal deposits. Dokladi Akademiyi Nauk SSSR, 271, N4, 962-963.
4. CHAPMAN, N.A., McKINLEY, I.G. and SMELLIE , J.A.T. (1984). The potential of natural analogues in assessing systems for deep disposal of high-level radioactive waste. NAGRA, NTB 84-41; KBS 84-16.
5. CURTIS, D.B. and GANCARZ, A.J. (1983). Radiolysis in nature: Evidence from the Oklo natural reactors. KBS TR 83-10.
6. DIMKOV, JU.M. and BRODIN, B.V. (1961). Concerning the red coloration of minerals in the uranium-bearing veins. Atomnaya Energiya, No.1, 35-41.
7. DRAGANIC, I.G. and DRAGANIC, Z.D. (1971). The radiation chemistry of water, Academic Press, New York.
8. DRAN, J.C., DURAUD, J.P., LANGEVIN, Y., MAURETTE, M. and PETIT J.C. (1978). Contribution of radiation damage studies to the understanding of the Oklo phenomenon. In Natural Fission Reactors, IAEA, Vienna 375-388.
9. DUBESSY, J. (1985). Contribution à l'étude des interactions entre paleo-fluides et mineraux á partir de l'étude des inclusions fluides

par microspectrometrie Raman. Consequences métallogeniques. These docteur es Science. L'institut national polytechnique de Lorraine.
10. DURRANI, S.A., KHAZAL, K.A.R., MALIK, S.R., PREMLIN, J.H. and HENDRY, G.L. (1975). Thermoluminescence and fission-track studies of the Oklo fossil reactor materials. The Oklo Phenomenon, IAEA, Vienna 207-222.
11. EVSEEVA, L.S., PERELMAN, A.I. and IVANOV, K.E. (1974). Geochemistry of uranium in the zone of hypergenesis. Atomizdat, Moscow.
12. EWERS, G.R., FERGUSON, J. and DONNELLY, T.H. (1983). The Nabarlek uranium deposit, Northern Territory, Australia: Some petrologic and geochemical constraints on genesis. Econ.Geol., 78, 823-837.
13. EWING, R.C., HAAKER, R.F. and LUTZE, W. (1982). Leachability of zircon as a function of alpha dose. In Scientific Basis for Nuclear Waste Management V, ed. W.Lutze, pp. 389-397, New York.
14. FRIDMAN, A.A. (1970). Natural gases of the ore deposits, Nedra, Moscow.
15. GARIBOV, A.A. (1983). Water radiolysis in the presence of oxides. In Proc. 5th Symposium on Radiation Chemistry, Budapest, 1982, Akademiai Kiado 377-384.
16. GOLDHABER, M.B., REYNOLDS, R.L. and RYE, R.O. (1978). Origin of a South Texas roll-type uranium deposit: II. Sulfide petrology and sulfur isotope studies, Econ.Geol. 73, 1690-1705.
17. GOLDHABER, M.B., REYNOLDS, R.L. and RYE, R.O. (1983). Role of fluid mixing and fault-related sulfide in the origin of the Ray Point uranium district, South Texas, Econ.Geol. 78, 1043-1063.
18. GRAY, W.J. and SIMONSON, S.A. (1984). Gamma and alpha radiolysis of salt brines. PNL-SA-12746.
19. IAEA (1985). Deep underground disposal of radioactive wastes: near-field effects. TR No.251.
20. JANTZEN, C.M. and BIBLER, N.E. (1985). The role of groundwater oxidation potential and radiolysis on waste glass performance in crystalline repository environments. DP-MS-85-28.
21. KIM, J.I., APOSTOLIDIS, Ch., BUCKAU, G., BUEPPELMANN, K., KANELLAKOPULOS, B., LIERSE, Ch., MAGIRIUS, S., STUMPE, R., HEDLER, I., RAHNER, Ch., STOWER, W. (1985). Chemisches Verhalten von Np, Pu und Am in verschiedenen konzentrierten Salzloesungen. RCM-01085.
22. KRANZ, R. (1967). Die geochemische Bedeutung organischer Verbindungen in den Einschluessen uran-haltiger Mineralien. Naturwissenschaften, 54, 469.
23. LEVENTHAL, J.S. (1980). Organic geochemistry and uranium in Grants Mineral Belt. New Mexico Bureau of Mines and Mineral Resources Memoir, 38, 75-85.
24. LEVENTHAL, J.S. and THRELKELD, C.N. (1978). Carbon -13/Carbon -12 isotope fractionation of organic matter associated with uranium ores induced by alpha irradiation. Science, 202, 430-431.
25. LIESER, K.H., COETZEE, P.P. and FOERSTER, M. (1985). Liberation of iodine from AgI during radiolysis. Radiochimica Acta, 38, 33-35.
26. MYERS, W.B. (1981). Genesis of uranium-gold pyritic conglomerates. In U.S. Geolog.Survey Prof.Pap. No.1161-A-BB, pp. AA1-AA26.
27. NAUMOV, G.B., MIRONOVA, O.F., SAVELYEVA, N.I. and DANILOVA, T.V. (1984). Content of uranium in hydrothermal solutions based on fluid inclusions studies. Dokladi Akademiyi Nauk, SSSR, 279, N6, 1486-1488.
28. PEDERSON, L.R., CLARK, D.E., HODGES, F.N., McVAY, G.L. and RAI, D. (1984). The expected environment for waste packages in a salt repository. In Scientific Basis for Nuclear Waste Management VII, ed. G.L.McVay, pp. 417-426, New York.

29. PEREVOZCHIKOV, V.G. and NATALCHENKO, B.I. (1985). A distal part of the bed oxidation zone of exogeneous epigenetic uranium deposits as a source of local gas formation. Izv. Vyssh. Ucnebn. Zaved., Geol.Razved, No, 67-70.
30. POTY, B.P., LEROI, J. and CUNEY, M. (1974). Fluid inclusions in uranium ores from intragranitic deposits in Limousin and Forez (Massif Central, France). In Formation of Uranium Ore Deposits, IAEA, Vienna 569-582.
31. REED, D.T. (1985). Effect of alpha and gamma radiation on the near-field chemistry and geochemistry of high-level waste packages. RHO-BW-SA-406 P.
32. ROBINSON, B.W. and OHMOTO, H. (1973). Mineralogy, fluid inclusions and stable isotopes of the Echo Bay U-Ni-Ag-Cu deposits, Northwest Territories, Canada, Econ.Geol. 68, 635-656.
33. SASSANO, G.P., FRITZ, P. and MORTON, R.D. (1972). Paragenesis and isotopic composition of some gangue minerals from the uranium deposits of Eldorado, Saskatchevan. Can. J. Earth Sci., 9, N2, 141-157.
34. SCHWAB, K.W. and PERRY, D. (1984). Effect of radiation on particulate organic matter associated with roll-front deposits. Am.Assoc.Pet.Geol.Bul. 68 (4), 526.
35. SIMMONS, G. and CARUSO, L. (1985). Uranium in clays of crystalline rocks. DOE/ER/04972-T2.
36. SPITSYN, V.I., BALUKOVA, V.D., KOSAREVA, I.M. and KABAKCHI, S.A. (1981). Experimental evaluation of changes in properties of natural minerals under irradiation. In Scientific Basis for Nuclear Waste Management III, ed. J.Moore, pp. 429-434, New York and London.
37. TAIT, J.C., WILKIN, D.L., HAMON, R.F. (1986). Gamma radiolysis effects on leaching of nuclear fuel waste forms: influence of groundwaters and granite on gaseous radiolysis products. AECL-8731.
38. UYAMA, F., CHIBA, H., KUSAKABE, M. and SAKAI, H. (1985). Sulfur isotope exchange reactions in aqueous system: thiosulfate - sulfide - sulfate at hydrothermal temperature, Techn.Report of ISEI, Ser.A, No.2, Okyama University.
39. VANDENBROUCKE, M., ROUZAUD, J.N. and OBERLIN, A. (1978). Geochemical study of the insoluble organic material (kerogen) in the Oklo uranium ore and the associated Francevillian schists. In Natural Fission Reactors, IAEA, Vienna 307-332.
40. VETSHTEIN, V.E. and SHCHERBAK, D.N. (1981). Pecularities of hydrogen isotope distribution in gas-liquid inclusions in sodium metasomatites. Dokladi Akademiyi Nauk UkSSR, ser.B, No.1, 3-5.
41. VOVK, I.F. (1979). Radiolysis of groundwater and its geochemical role, Nedra, Moscow.
42. VOVK, I.F. (1979). Some mineralogical and geochemical pecularities of uranium deposits in sedimentary rocks as a result of the groundwater radiolysis, Zap. Vses. Mineral. Obshch. No.4, 397-407.
43. VOVK, I.F. (1982). Brines of the crystalline basement of shields. Ukrainian Academy of Science, Kiev.
44. WALTERS, W.S. and WISBEY, S.J. (1986). A review of the literature realting to radiolytic oxidation. AERE R-11984.
45. ZUMBERGE, J.E., NAGY, B. and NAGY, L.A. (1981). Some aspects of the development of the Vaal Reef uranium gold carbon seams, Witwatersrand sequence: organic geochemical and microbiological considerations. In U.S. Geolog.Survey Prof. Pap. No.1161-A-BB, pp. 01-07.

EVIDENCE OF FOSSIL AND RECENT DIFFUSIVE ELEMENT MIGRATION IN REDUCTION HALOES FROM PERMIAN RED-BEDS OF NORTHERN SWITZERLAND

B. Hofmann*, J.P.L. Dearlove*++, M. Ivanovich+, D.A. Lever++, D.C. Green*+, P. Baertschi**, and Tj. Peters*.

*Department of Mineralogy and Petrology, Bern University, Baltzer-Strasse 1, CH-3012 Bern, Switzerland.

+Nuclear Physics Division B7, AERE Harwell, Oxfordshire. OX11 ORA UK.

++Theoretical Physics Division B424.4, AERE Harwell, Oxfordshire. OX11 ORA, UK.

*+Geology Department CCAT, East Road, Cambridge. CB1 1PT, UK.

*++Geology Department CCAT, East Road, Cambridge, UK and AERE Harwell, UK.

**NAGRA, Parkstrasse 23, CH-5401, Baden, Switzerland.

Summary

Spherical to oblate reduction haloes 1 to <100 mm diameter with mineralized cores are common in Permian red-beds of several NAGRA drillholes in Northern Switzerland. The cores of the haloes (0.1 to 10 mm diam.) show enrichments of many elements including analogue-relevant U, Th, Se, REE and Pd. The halo margins are marked by a sharp contrast between grey, hematite-free haloes and enclosing red, hematite-rich mudstone. The cores of the haloes are zoned with V concentrated at the margin and dominant U, Ni, As, Pb and Se in the centre of the core. The origin of the reduction haloes is due to a spherical redox-front that formed around isolated spots of a reducing agent in the red-bed during diagenesis. The spherical shape of the haloes indicates that their formation is due to diffusion-controlled migration of elements. K-Ar dating of vanadian mica (roscoelite) yielded Lower Cretaceous to Lower Jurassic ages. The fact that large haloes contain a much higher percentage of mineralized cores than small ones was taken as an indication that the mineralized halo cores may not be stable in the oxidizing red-bed environment and that element migration

is still taking place.
Uranium series disequilibrium profiles show that the cores contain concentrations of up to 35 wt% ^{238}U falling to an average 6ppm over 10 to 15 mm. Major accumulation and retention of ^{234}U appears to occur at the edge of the dark cores. It is possible that vanadium present in roscoelite mica may be responsible for the precipitation and retention of the ^{234}U. Uranium does not appear to accumulate preferentially at the halo margins. Bulk samples of surrounding red mudstone display complete uranium series isotopic equilibrium.
Mathematical modelling aimed at quantifying diffusion rates in low permeability rocks is in progress. Models constructed to describe these small scale processes may be useful in refining radioactive waste transport assessment codes.

1. Introduction

Reduction haloes are common in red-beds of Devonian, Permian and Triassic age from a wide range of localities: Germany (1,2), South Devon (3-5), Scotland (6), Oklahoma (7), East Greenland (8) and Northern Switzerland (9). Reductions haloes are spherical to oblate portions of rock which differ from the surrounding red-bed by the absence of hematite pigment and have a contrasting pale grey-green colour. The size of reduction haloes varies from less than 1 mm. to about 20 cm. Often, but not always, the haloes contain dark cores which are highly enriched in many elements, the most prominent being U, V, Ni, As and Se. Organic matter (carburan) is present in some cores. The spherical shape of the haloes, their occurrence in low permeability rocks, and the presence of steep concentration gradients suggest diffusive element migration towards and, possibly, away from the cores. A thorough investigation of this phenomenon can give valuable information about geochemical processes relevant to radioactive waste safety assessment codes. These processes include diffusive migration of many elements relevant to geochemical analogue studies such as U, Th, REE, Pa, Pd, and Se over geological time scales. In this context, reduction haloes provide several advantages in a detailed study:

(i) they are purely diffusive systems in low permeability rocks similar in mineralogy to hydrothermally altered, cataclastic crystalline rocks;

(ii) a wide range of elements is accumulated in halo cores;

(iii) reduction haloes are abundant in red-beds and can be studied under a variety of hydrogeological regimes;

(iv) their small size permits complete study in drill cores derived from great depths.

(v) the presence of a redox front can be used to study its effects on the mobility of several multivalent trace elements including uranium isotopes.

The results presented here were obtained in a pilot study of reduction haloes from NAGRA'S Kaisten borehole in Northern Switzerland. Mineralogical data from four other wells in Northern Switzerland have also been included (see Fig. 1). Five samples from the Kaisten core, each averaging 90 - 95 cm of homogeneous red mudstone, rich in reduction haloe ms were collected from 226.65 to 231.25 cm depth and used for chemical and bulk mineralogy analyses. One sample (Kai 230.00 m) containing two reduction haloes was used in a detailed uranium-series disequilibrium profile study.

For the sake of consistency, the following terms will be used in the text that follows: (i) cores = dark mineralised centres of reduction haloes; (ii) pale zone = spherical halo body devoid of hematite, showing no visible mineralisation; (iii) core margins = a sub-zone of the pale zone surrounding the halo core; (iv) hematite zone = host rock of the reduction haloes displaying red pigmentation due to the presence of hematite (see Fig. 2).

2. GEOLOGICAL AND GEOCHEMICAL BACKGROUND TO THE REDUCTION HALOES

Deep drilling and geophysical investigations carried out by NAGRA have confirmed recently the presence of a large tectonic graben in Northern Switzerland (10). The Permo-Carboniferous continental sedimentary infill of the graben with total thickness sometimes in excess of 2 km, is underlain and bordered by a crystalline basement similar to that outcropping in the nearby Schwarzwald massif (Southern Germany). Mesozoic and younger sediments cover most of the Paleozoic graben sediments (fig.1). The Kaisten drillhole is situated to the north of the graben, with Permian red-beds occurring between 125 and 297m depth.

2.1 Physical properties of reduction haloes and host rock (Kai 226.65-231.25 m).

Reduction haloes, comprising pale zone, core margins and core zone make up 6.2% by volume of the total rock and contain about 20% of the bulk rock uranium. Halo cores range from 0.002 to 0.09 % by volume of the total rock with a mean of 0.01 % by volume. Halo diameters vary from 1 to 50 mm. and display a bimodal frequency distribution with peaks at the 0-5 mm. and 25-30 mm. ranges. The reduction haloes are slightly oblate with a width to height ratio range from 1.10 to 1.85 (median 1.25, n=30). The lower ratios are attributed to halo compaction during diagenesis and the higher values may be due to higher diffusion rates along the bedding plane of the host rock.

The relationship between halo diameter and core diameter has been discussed by Hofmann (9) who concluded that a more stable reducing environment occurs in the centre of larger

haloes since diffusion distances for oxidising agents are shorter in the smaller haloes.

Bulk density/grain density measurements on thirteen samples yielded a mean total porosity of 11.6 vol % (s=1.04). Eleven mercury porosimetry measurements indicate pores with an equivalent radius of less than 63Å comprising 78 to 89% of total porosity. Pale zones have slightly larger equivalent pore sizes than hematite zones. Halo cores have a total porosity of 4.64 vol. % and an equivalent pore size of less than 63Å comprising 75 to 82% of the host rock. However, the halo cores also appear to have some secondary porosity in the 500 to 1500 Å pore-size range due to dissolution of specific core-cementing phases.

2.2 Mineralogy of reduction haloes and host rock (Kai 226.65-231.25m)

Bulk rock mineralogy was determined by diffractometry using LiF as an internal standard and total carbonate content was calculated from Coulometric CO_2 analyses. The core zone mineralogy was studied by reflected light microscopy, electron microprobe analyses and XRD (Guinier camera, diffractometer).

Alpha - autoradiographs were made by exposing polished sections to alpha - sensitive films (Kodak LR 115 II). Chemical analyses were performed by standard XRF procedures using Li-tetraborate glass tablets for major elements and pressed powder tablets for trace elements. U and Th were measured with a non-automatic XRF spectrometer following the procedure of James (11). FeO and B were measured by a spectrophotometric method, CO_2 and C_{org} by Coulometry.

The host rock mineralogy is dominated by clay minerals (60-65%) which support detrital grains of quartz, albite and potassium feldspar. The main clay mineral is illite (94%) associated with some chlorite (6%). Carbonate occurs as nodules of clear, iron-free crystals, and as microveinlets of iron-containing calcite and ankerite which post-date halo formation. Graphite, anatase, apatite, zircon, monazite, and hematite occur in trace quantities. The only mineralogical difference between the hematite and the pale zones is the absence of hematite in the latter. Forty mineral phases ubiquitous to halo cores were identified (Table 1). The most common minerals include roscoelite, uraninite, coffinite, rammelsbergite, niccolite and clausthalite. Mineral grain sizes range from less than 1 to 100µm. Pitchblende, the main uranium phase, occurs in the grain size range from less than 1 to 20µm.

Most ore minerals show textures indicative of replacement of clay minerals or detrital mineral grains. A few cores contain highly anisotropic, kerogen-type organic material. It is always associated with uraninite which causes radiation damage but does not contain uranium in amounts above the detection limit of the probe (100 ppm).

2.3 Geochemistry of reduction haloes and host rock (Kai 226.65-231.25m)

Microscopy, microprobe profiles and alpha - autoradiographs (see Fig. 4) nearly always show a concentric, cyclic distribution of elements (and their minerals). Analytical results for the bulk rock, hematite and pale zones and combined core material are listed in Table 2. For comparison, the average of three analyses of Permian bituminous mudstones from the Weiach borehole underlying the red-bed sequence is also given. Significant differences between the two are found in the iron oxidation state ratio (FeO/Fe_2O_3), the U/Th ratio, and the enrichment of As, B and Zn in the red-beds (see Table 2).

Three different trends of elemental behaviour can be distinguished in the reduction halo redox system relative to the bulk rock: (i) elements depleted in the hematite zone, enriched in the pale zone, and greatly enriched in the cores are U, REE, V, Cr, Ni, Co, Cu, Zn, As and Se; (ii) Pb is depleted in the pale zone and enriched in the cores; and (iii) Fe^{3+} and Th are depleted in the pale zone. The remaining elements display no significant mobility in the system. Most of the enriched elements form their own minerals. However, some are incorporated as minor constituents (eg. Cr in roscoelite, and REE and Th in uraninite). Combined mineralogical and geochemical analyses show that the following elements are enriched in halo cores:(C), (Mg),(P), S, K, (Ca), V, Cr, (Mn), Co, Ni, Cu, Zn, As, Se, Y, Mo, Pd, Ag, Sb, Te, REE, Au, Hg, Tl, Pb, Bi, (^{232}Th) and U (elements in brackets do not display systematic behaviour).

Fluid inclusions in calcite from Kaisten (227.10m) and dolomite from Riniken (910.78m), both in close contact with minerals from halo cores, show homogenization temperatures of 77 to 87 °C and salinities from 9 to 19 equivalent % NaCl. It is inferred that at the time of halo formation, pore waters may have been highly saline, oxidising and slightly alkaline. Present day groundwaters from the Permian red-beds at Riniken and Weiach are also reducing with quite high salinities although lower than the fluid inclusions (2). At Kaisten, however, groundwaters from the Permian-crystalline basement boundary (276.0-292.5m) are slightly oxidising and have lower salinities than both the fluid inclusions and the Riniken and Weiach boreholes. This may be due to infiltration and southward movement of fresh water into rocks of the Schwarzwald and the proximity to the surface of the Permian rocks at Kaisten.

The observed boundary between the pale/hematite zones is only an approximate indicator of the redox gradient at the time of halo formation. The absence of hematite formation within the pale zone indicates the stability of the redox conditions up to the present day.

2.4 Dating of reduction halo formation

The absolute dating methods K/Ar and U/Pb, complemented by estimates of overburden depth during halo formation, indicate the time when fossil element migration was terminated. The K/Ar dates on three nearly pure roscoelite separates from the Riniken borehole indicate closed system conditions from between 112 and 190Ma. These Lower Cretaceous to Lower Jurassic ages agree well with the 'compaction age' estimated as follows. The median of width to height ratio in Kaisten haloes is 1.25, corresponding to a compaction of 20% since halo formation. As present day porosity is 11.6%, porosity during halo formation is estimated to have been about 32% which corresponds to a burial depth range of approximately 500 to 800m. (13) or Middle to Upper Jurassic.

The U/Pb dating, notwithstanding analytical difficulties due to the fine grained nature of uraninite/lead minerals (clausthalite) separation, yield total lead 'ages' of between 82 and 120 Ma for Weiach and Riniken haloes. However, in Kaisten three separate samples (including one from a reduction zone in the crystalline basement) contain no detectable lead (less than 0.1%). Uraninite 'ages' from Kaisten samples therefore range from less than 10 Ma to 120 Ma.

These data indicate that most of fossil diffusion was terminated during the Mesozoic. In Kaisten, however uraninite deposition appears to have recommenced in response to a change in groundwater conditions during the Tertiary and possibly continued into the Quaternary.

2.5 Genesis of the reduction haloes

Reduction haloes are thought to form due to the presence of organic matter in the host rock. The cores serve as reduction sites causing the precipitation of mineral phases from pore fluids, the build-up of a concentration gradient and diffusive migration of elements towards the halo centres. Iron-rich pigment was dissolved due to changes in Eh, availability of different ligands, or both. The origin of the organic matter is unknown. However, it cannot be detrital because reduction haloes with identical mineral assemblages are also found in the crystalline basement. Furthermore, even in large cores no remnants of detrital organic matter are present. However, the concentric and cyclic distribution of elements in the cores makes it probable that the reductant was accumulating or being produced at the core margin at the same time as the trace elements were diffusing towards the core. In the absence of significant fluid movement (no hydrocarbon migration), it is possible that the organic matter was produced and/or immobilised by bacteria (14).

3. URANIUM SERIES DISEQUILIBRIUM PROFILES IN THE REDUCTION HALOES (KAI 226.65-231.25m)

A detailed uranium series disequilibrium study of two reduction haloes from Kaisten borehole was carried out in order to examine the diffusive migration of the isotopes of U, Th and Pa. Uranium series disequilibrium can be used to study the fractionation of radionuclides by comparing the activity of various parent/daughter pairs in a decay chain. If the rock mass remains geochemically undisturbed for periods commensurate with several times the longest daughter half-life then the daughter/parent activity ratios throughout the decay series will be unity. This state of secular radioactive equilibrium can be disturbed by a change in the chemical conditions in the rock resulting in daughter/parent fractionation due to differences in their respective chemistry. This state is reflected by the departure of their activity ratio from unity.

The mobility of U and Th at low temperature has been studied in considerable detail by Langmuir (15) and Langmuir and Herman (16) under a variety of chemical conditions. Under oxidising conditions ^{234}U enters solution more readily than ^{238}U due to its preference for a 6^+ valence state. Under reducing conditions uranium is relatively immobile. In contrast, all the thorium isotopes share a 4^+ valence state. Although thorium may form a variety of organic and inorganic complexes its mobility is limited by sorption processes since it hydrolyses rapidly onto a solid phase.

Pa is also insoluble and appears to hydrolyse more readily than thorium (17). Transport by adsorption onto suspended colloidal matter appears to be, as in the case of Th, the dominant mode of transport. In the diffusion system of reduction haloes some mobilization of Th and Pa cannot be ruled out.

3.1 Sampling for uranium series disequilibrium profile measurements

Uranium and thorium concentrations and activity ratios were determined by standard isotope dilution/alpha spectrometry techniques (18). Samples of halo material were extracted using a diamond tipped Burgess Vibrotool. Sampling was carried out from the halo margins towards the centre in order to reduce potential cross-contamination. Aliquots of uranium-rich cores were prepared in order to reduce the total uranium in each analysis. Sample sites are shown in Fig. 4. Two halo profiles (1 and 2) were selected along a continuous radial line joining two neighbouring cores (see Fig. 4A and 4B). Two additional profiles were selected perpendicular to profiles 1 and 2: profile 3 (L to N, Fig. 4C) and profile 4 (2H to 2N, Fig. 4B). The former profile is also perpendicular to the bedding plane of the host rock.

3.2 Results

The concentration profiles of ^{238}U and ^{232}Th are plotted as a function of distance from the centre of halo 1 (Sample E) in Fig. 5. The activity ratio profiles are plotted in Fig. 6. Isotopic concentrations for individual samples are given in (19). Although the $^{234}U/^{238}U$ and $^{230}Th/^{234}U$ activity ratios in profile 4 are significantly different from the other three profiles, these data have been included in the weighted averages presented in Table 3. The observed change in the details of profile 4 (see Fig.6) is thought to be caused by the coarser grained nature of the material in that profile and does not represent a fundamental departure from the general processes responsible for the profile shapes presented. For that reason and because of local inhomogeneities and difficulty in achieving reproducible data from small samples, it was thought appropriate for the purposes of the following discussion to combine the data from all four profiles into weighted averages for each zone (see Table 3).

The halo cores are characterised by the highest uranium and thorium contents, ranging from 0.3 to 35% by weight uranium and 28 to 3060 ppm Th. All uranium series radionuclide activity ratios are unity. The core margins display an excess of ^{234}U relative to ^{238}U and ^{230}Th, and a deficiency of ^{228}Th relative to ^{232}Th. The pale zone contains a deficiency of daughter radionuclides relative to their respective parent radionuclides. Weighted averages for individual samples from the hematite zone show a deficiency in ^{234}U and ^{230}Th relative to their respective parents. In contrast, homogenised hematite zone displays secular radioactive equilibrium for all activity ratios.

4. DISCUSSION

The high concentration gradients developed between the halo cores and the surrounding rock zones under relatively static pore water conditions indicate element mobility by liquid diffusion. The measured uranium series radionuclide parent/daughter activity ratios presented in Table 3 indicate that the diffusion timescales involved must therefore be commensurate with the half-lives of the longer-lived daughter radionuclides. Under these circumstances modelling the diffusion process is dependent on the unknown radionuclide concentrations in the pore waters.

Models considering inward and outward diffusion of uranium and daughter radionuclides are currently being developed and tested. Two geochemical scenarios are likely: (i) the porewater in the core zone is not in chemical equilibrium with the ore mineral phases, the latter are dissolved, and a porewater concentration profile similar to that in the solid develops leading to the outward diffusion of elements; and (ii) the porewater in the core zone is in chemical equilibrium with the ore phases and the porewater

concentration profile is an inverse of the solid phase profile leading to an inward diffusion of elements. The activity ratios presented in Table 3 indicate that recent inward diffusion of dissolved uranium and its deposition at the core margin is the most likely process. For this case, idealised solid and liquid phase diffusion profiles of uranium content and $^{234}U/^{238}U$ activity ratio in different zones of Kaisten reduction haloes are given in Fig. 7. An assumed $^{234}U/^{238}U$ activity ratio typically greater than unity in the porewater explains the observed excess of ^{234}U at the core margins. A corresponding small depletion of ^{234}U in the pale and hematite zones indicates the likely source for the accumulated uranium in the core margin.

Uranium profiles in NAGRA's deep borehole cores are basically fossil profiles (see section 2.4). At Kaisten, as already discussed, more oxidising conditions may be responsible for recent radionuclide transport. The measured uranium series disequilibria shown in Fig.5 and 6 are believed to represent a superposition of the fossil profile and a profile arising from recent processes responsible for the transport of uranium daughter products. Future work involves similar measurements on several haloes from other deep boreholes such as Riniken and Weiach, in which no recent transport is expected. This should allow a deconvolution of the curves obtained at Kaisten, in order to establish the relative importance of more recent processes such as those associated with alpha-decay and changes in solubility limits associated with the oxidising conditions. This work should help to obtain an understanding of the processes that are taking place and the basic uranium profiles across the haloes, along with the time-scale on which diffusion has been occurring, and assist in quantifying rates of migration under low-permeability conditions. Both should contribute useful information for safety assessment modelling.

5. CONCLUSIONS.

Reduction haloes are small, diffusion controlled redox systems involving the mobility of many elements. They are common occurrances in red-beds and may be regarded as sensitive indicators of recent water/rock interactions because of high concentration gradients observed in the solid phase. In haloes of the Kaisten borehole core, uranium has accumulated recently resulting in an observed ^{234}U excess with respect to ^{238}U at the halo margin. This is consistent with the well documented uranium behaviour in the sandstone roll-front deposits (20). The migration mechanisms involved and rates of accumulation or loss of elements relevant to the radioactive waste disposal studies may ultimately yield important parameters for safety assessment modelling. In order to develop the necessary transport models further, additional work on other haloes including protactinium and REE is necessary.

REFERENCES

1. EICHOFF, H.J and REINECK, H.E. (1952) Uran-Vanadiumkerne mit Verfarbungshofen in Gesteinen. - N. Jb, Miner, Mh. 1952, 294-314.
2. MEMPEL, G. (1960) Neue Funde von Uran-Vanadiumkernen mit Entfarbungshofen. - Geol. Rdsch. 49, 263-276
3. PERUTZ, M. (1939) Radioactive nodules from Devonshire, England, Mineralog. u. Ptrogr. Mitt. 51, 141-161.
4. HARRISON, R.K. (1975) Concretionary concentrations of the rarer elements in Permo-Triassic red-beds of Southwest England. - Geol. Surv. Great Brit. Bull. 52, 1-26.
5. DURRANCE, E.M., MEADS, R.E., BALLARD, R.R.B. and WALSH, J.N. (1978) Oxidation state of iron in the Littleham Mudstone formation of the New Sandstone Series (Permian -Triassic) of southwest Devon, England. - Geol. Soc. Am. Bull. 89 1231-1240.
6. PARNELL, J. (1985) Uranium/rare earth-enriched hydrocarbons in Devonian sandstones, Northern Scotland. - N. Jb. Miner. Mh. 1985, 132-144.
7. CURIALE, J.A., BLOCH, S., RAFALSKA-BLOK, J. and HARRISON, W.E. (1983) Petroleum-related origin for uraniferous organic-rich nodules of Southwestern Oklahoma. - Bull. Amer. Assoc. Petrol. Geol. 67, 588-608.
8. PERCH-NIELSEN, K., BIRKENMAJER, T., BIRKELUND and M. ALLEN (1975) Revision of Triassic stratigraphy of the Scoresby Land and Jameson Land Region, East Greenland, Gronlands Geol. Unders, Bull. 109, 51p, 1974.
9. HOFMANN, B. (1986) Small scale multi-element accumulations in Permian red-beds of Northern Switzerland. - N. Jb. Miner. Mh. Jg. 1986, H.8, 367-375.
10. MULLER, W.H., HUBER, M., ISLER, A. and KLEBOTH, JP. (1984) Erlauterungen zur "geologischen Karte der zentralen Nordschweiz 1:100 000". - Nagra Techn. Bericth 84-24, Baden.
11. JAMES, W. (1977) Parts-per-million determinations of uranium and thorium in geologic samples by x-ray spectrometry. - Analytical Chemistry 49, Wo7, G67-G69.
12. WITTWER, C. (1986) Probenahmen und Chemische Analysen von Grundwassern aus den Sondierbohrungen. - Nagra NTB 85-49, Baden.
13. FUCHTBAUER, H. and MULLER, G. (1977) Sediment - Petrologie, Teil II. Sedimente and Sedimentgesteine, - 3. Aufl., E. Schweizerbart'sche Verlysbuchhandlung, Stuttgart.
14. BUTTON, D.K. (1976) The influence of clay and bacteria on the concentration of dissolved hydrocarbon in saline solution. Geochim. Cosmochim. Acta 40, 435-440.
15. LANGMUIR, D. (1978) Uranium solution-mineral equilibria at low temperatures with applications to sedimentary ore deposits. Geochim. Cosmochim. Acta. 42, 547-570.

16. LANGMUIR, D. and HERMAN, J.S. (1980) The mobility of thorium in natural waters at low temperatures. Geochim. Cosmochim. Acta. 44, 1753-1766.
17. GASCOYNE, M. (1982) Geochemistry of the actinides and their daughters, in M. Ivanovich and R.S. Harmon (eds) Uranium series disequilibrium: Applications to environmental problems in Earth Sciences. Clarendon Press, Oxford, 33-35.
18. IVANOVICH, M. and HARMON, R.S. (1982) Uranium series disequilibrium: Applications to environmental problems in Earth Sciences, Clarendon Press, Oxford, pp571
19. IVANOVICH, M., DEARLOVE, J.P.L and LEVER, D.A. (1986) Uranium series disequilibrium profiles from reduction haloes in Permian red-beds of Northern Switzerland, AERE report G 4194.
20. OSMOND, J.K., COWART, J.B., and IVANOVICH, M. (1983) Uranium isotopic disequilibrium in groundwater as an indicator of anomalies, Int. J. Appl. Radiat. Isot. 34, 283-308.

TABLE 1: Mineral phases identified in reduction haloes of Northern Switzerland

Identification: (m) = microscopy, (e) = electron microprobe,
(x) = x-ray diffraction

Elements, intermetallic compounds

Silver Ag (m,e), gold Au (m,e), copper Cu (m,e), bismuth Bi (m,e), auricupride (Au, Cu) (m,e), electrum (Au, Ag) (m,e), Pd-Sb-phase, michenerite $PdBi_2$(m,e), whitneyite (Cu, As) (m,e), Cu-Ag-As-phase, Cu-Ni-As-phase.

Arsenides

maucherite Ni_3As_2(m,e), niccolite NiAs (m,x,e), rammelsbergite $NiAs_2$(m,x,e), safflorite $CoAs_2$(m,x,e), modderite CoAs (e).

Sulfides

chalcocite Cu_2S (m,x,e), anilite Cu_7S_4(m,e), digenite Cu_9S_5 (m,e), tennantite $Cu_{10}Zn_2As_4S_{13}$(m,e), galena Pb (m,e), covellite CuS (m,e), stromeyerite CuAgS (m,e).

Selenides

berzelianite Cu_2Se (m,e), klockmannite CuSe (m,e), crookesite $CuTlSe$ (m,e), clausthalite PbSe (m,e), bohdanowiczite $AgBiSe_2$ (m,e), guanajuatite Bi_2Se_3 (m,e).

Telluride: altaite PbTe (m,e)

Oxides

uraninite UO_2 (m,x,e), brannerite UTi_2O_6 (m,e), U-leucoxene $UO_2.nTiO_2$ (m,e), montroseite VOOH (m,e), cuprite Cu_2O (m,e).

Phosphate: apatite (m,x,e)

Silicates: roscoelite $KV_2(OH)_2AlSi_3O_{10}$ (m,x,e)
coffinite $USiO_4$ (m,e)

Chloride: Cu-Cl-(O?)-phase, possibly atacamite

TABLE 2: Major and trace-element geochemistry and bulk mineralogy of reduction haloes and host rocks (Oberrotliegendes, Kaisten) and bituminous peltic rocks (Autunian, Weiach)
(averages with standard deviation)

	Weiach Autunian		Kaisten bulk		Kaisten hematite zone		Kaisten pale zone		Kaisten cores
%	n = 3		n = 10		n = 5		n = 5		n = 1
SiO2	55.82	5.50	56.37	0.87	57.11	1.02	59.27	0.90	57.70
TiO2	1.04	0.09	0.85	0.02	0.87	0.02	0.89	0.03	0.82
Al2O3	20.54	2.25	17.65	0.56	17.56	0.95	17.71	1.00	16.92
Fe2O3	1.54	0.72	5.91	0.30	6.27	0.48	2.44	0.23	0.53
FeO	4.42	0.86	0.76	0.04	0.76	0.05	0.80	0.08	1.74
MnO	0.04	0.01	0.09	0.01	0.08	0.01	0.08	0.01	0.07
MgO	2.26	0.39	2.55	0.07	2.55	0.10	2.57	0.11	1.64
CaO	0.68	0.42	2.79	0.54	2.02	0.63	2.77	0.87	2.54
Na2O	1.58	0.67	0.47	0.09	0.51	0.06	0.59	0.19	0.52
K2O	3.88	0.35	6.02	0.20	6.12	0.38	5.98	0.40	6.00
P2O5	0.31	0.07	0.22	0.01	0.23	0.01	0.23	0.00	0.20
H2O+	4.43	1.26	3.74	0.23	3.39	0.15	3.74	0.17	3.13
CO2	0.50	0.29	2.10	0.46	2.08	0.47	2.11	0.66	1.76
Corg	1.24	1.23	0.00		0.00		0.00		0.00
Tr	0.21		0.22		0.21		0.24		2.96
ppm									
Ba	512	68	478	31	505	49	485	47	486
Rb	260	23	383	11	363	17	379	30	307
Sr	121	9	176	4	171	4	179	6	105
Pb	35	9	52	3	51	2	29	4	601

Th	29.8	3.3	17.5	0.6	18.0	1.0	15.2	1.0	10
U	9.8	4.0	7.9	0.6	6.5	0.6	12.9	4.2	1614
Nb	23	4	18	0	17	2	17	2	6
La	101	14	88	6	82	5	76	8	68
Ce	112	19	82	18	75	15	82	19	1279
Nd	48	12	23	9	19	0	20	13	99
Y	39	5	37	0.5	36	0.8	36	1.5	16
Zr	234	121	209	14	220	9	216	11	137
V	155	11	153	9.8	143	7.4	216	70	10420
Cr	107	18	93	3	90	3	88	4	156
Ni	53	7	57	3	50	1	71	16	2520
Co	24	7	22	0.8	21	1.1	17	3.5	379
Cu	33	16	9	1.3	9	1.6	15	2.7	142
Zn	84	9	109	3	105	4	108	6	146
Ga	32	5	24	1	24	0.8	25	2	21
Sc	26	5	24	1	23	0.9	24	2	18
As	5		102	16	74	4	292	182	10800
B	57	3	168	8	-		-		-
Se	1		1		1		1		85
%									
Quartz	20	7	21	2	25	2	24	2	22
Albite	3	1	4	2	3	1	2	1	5
K-spar	6	2	6	1	6	3	5	2	5
Calcite	0		4	1	4	2	4	2	4
Dolomite	0		1	0.5	1	0.5	1	0.5	0
Clay	71		61		59		65		64*
Illite	34	7			94	1	94	1	100**
Chlorite	12	2			6	1	6	1	
Kaolinite	54	9			0		0		

* includes ore minerals

** roscoelite

Table 3 : Weighted averages for uranium content and activity ratios in four zones

Zone (No of samples)	U Content	Th (ppm)	Activity ratios $^{234}U/^{238}U$	$^{230}Th/^{234}U$	$^{230}Th/^{238}U$	$^{228}Th/^{232}Th$
Core (5)	$^{+}(2\text{-}350)\times10^{3}$	$^{+}$28-3060	1.01 ±0.01*	1.01 ±0.02	1.02 ±0.02	-
Core margin (7)	$^{+}$7-1800	13.15 ±0.36	1.17 ±0.04	0.78 ±0.03	0.88 ±0.03	0.84** ±0.04
Pale zone (9)	6.28 ±0.07	17.59 ±0.25	0.91 ±0.02	0.97 ±0.02	0.93 ±0.03	0.81++ ±0.03
Hematite zone (6)	5.80 ±0.13	17.10 ±0.28	0.91 ±0.03	0.82 ±0.02	0.75 ±0.03	0.97 ±0.03
Bulk rock analysis (3)	7.08 ±0.17	16.11 ±0.24	0.95 ±0.03	0.99 ±0.03	0.95 ±0.03	0.97 ±0.02

* All uncertainties quoted are +1σ uncertainties due to nuclear counting only
\+ U and Th content ranges
** Four data points only
++ Eight data points only

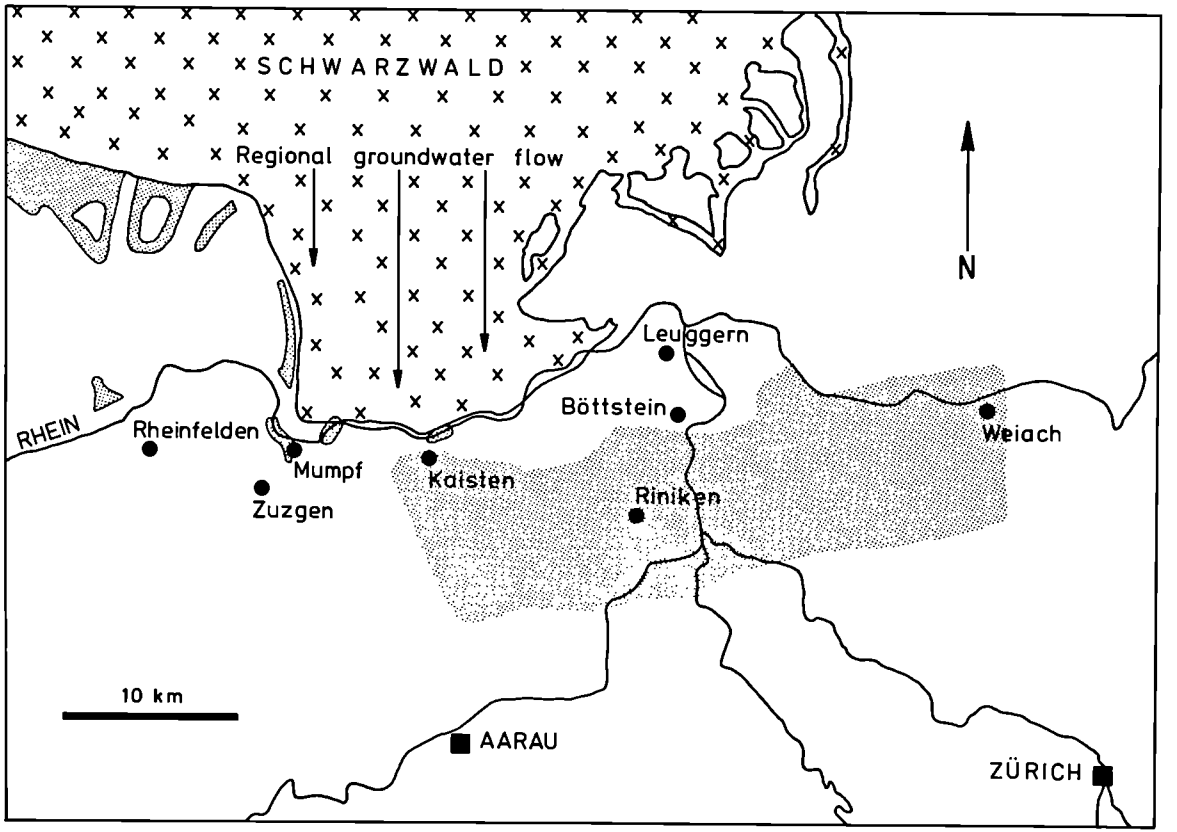

Fig.1 Map of sampling sites in Northern Switzerland. Area covered in crosses : crystalline rock outcrop; small dotted areas: surface exposures of Permian red-beds; large dotted area: proved subcrop of Permo-Carboniferous sediment; white area: Mesozoic and younger sediments.

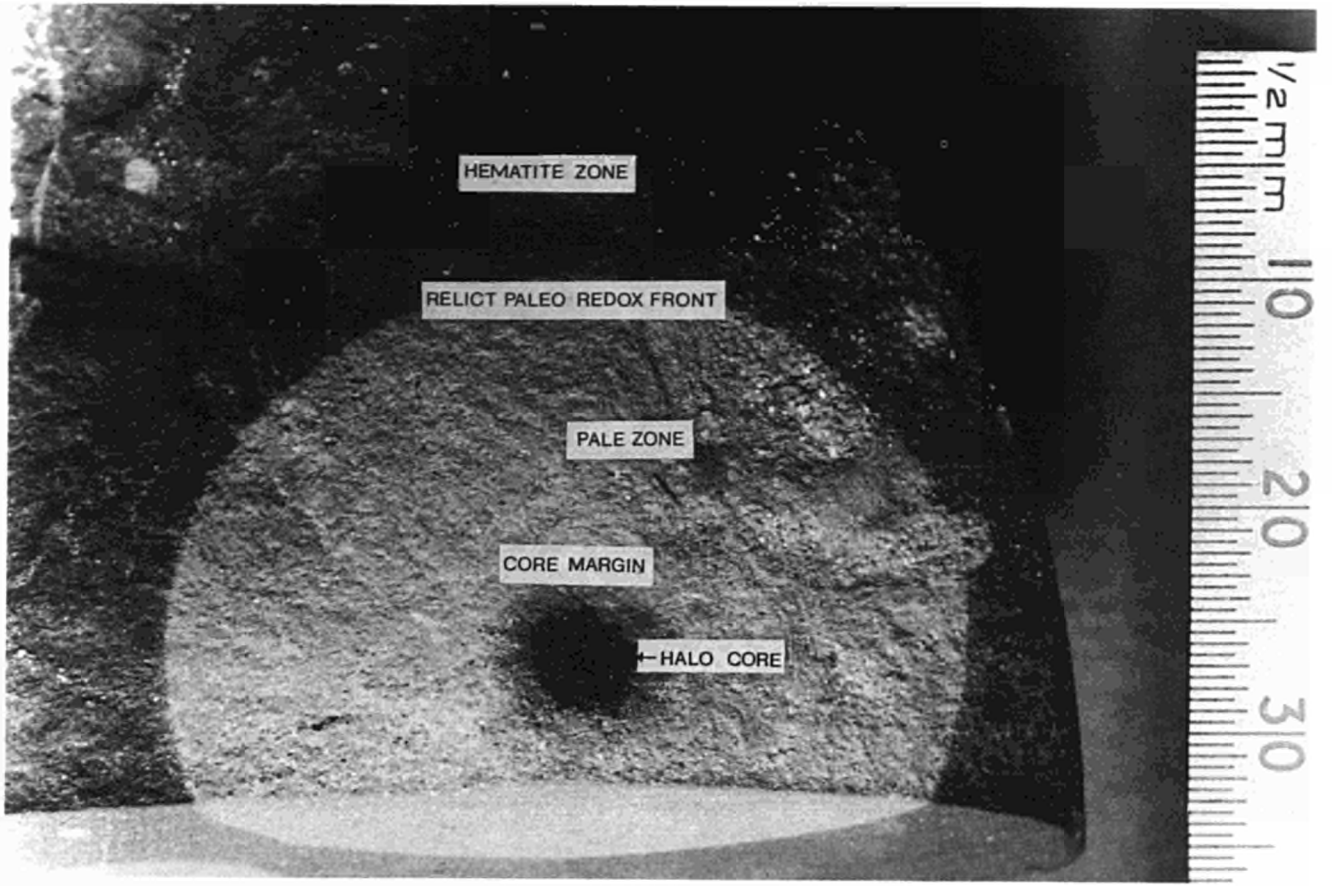

Fig.2 Reduction halo cross-section photograph showing the four zones: core, core margin, pale and hematite zones, and 'paleo' redox front.

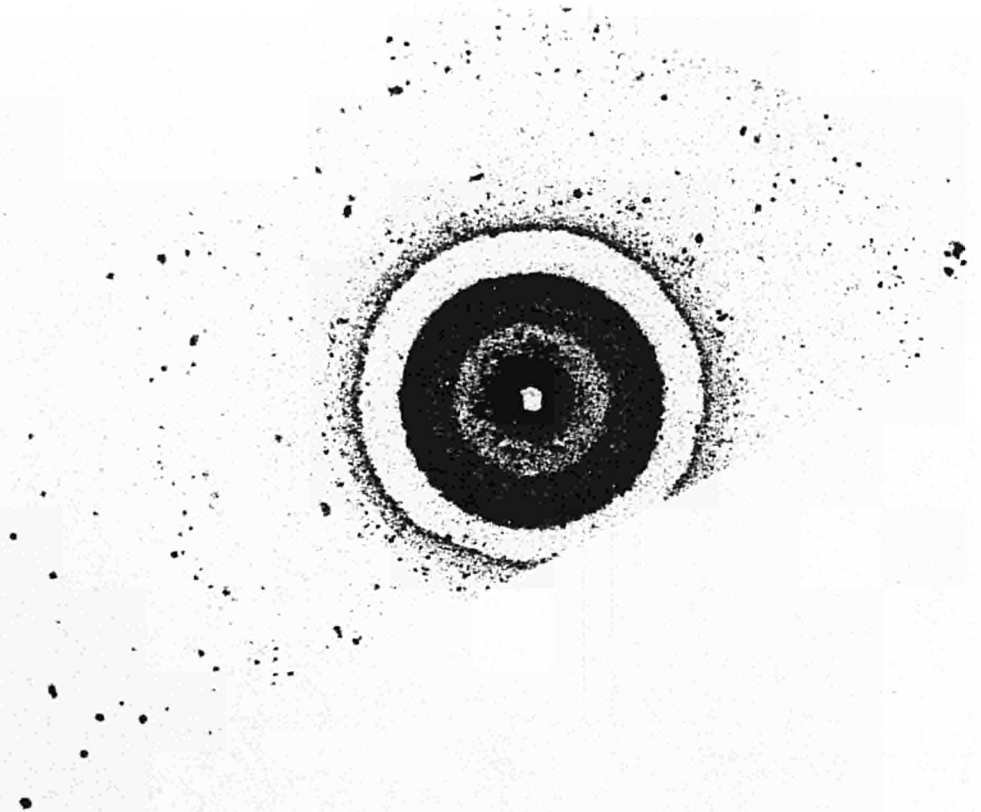

Fig.3 An alpha-autoradiograph of a reduction halo showing a concentric, cyclic distribution of uranium. Diameter of high-U core = 4mm. (Rheinfelden Weyerfeld 253.5m).

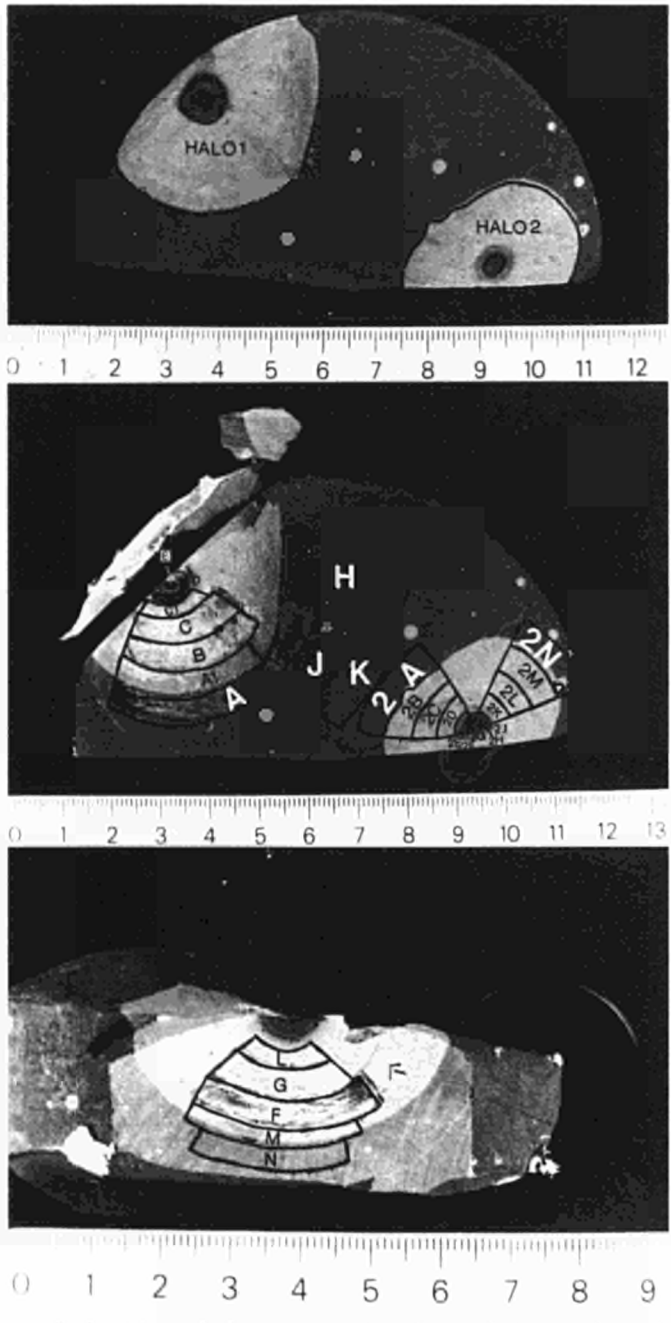

Fig.4 Reduction halo cross-section photographs showing the position of samples in Kai 230.0 used to construct the four uranium series disequilibrium profiles:

(a) two neighbouring halo cores, core margins, pale zones and common hematite-rich space between them (dark space);

(b) position of samples in profiles 1 (E to A), 2 (J to 2 G) and 4 (2H to 2N);

(c) position of samples in profile 3 (L to N).

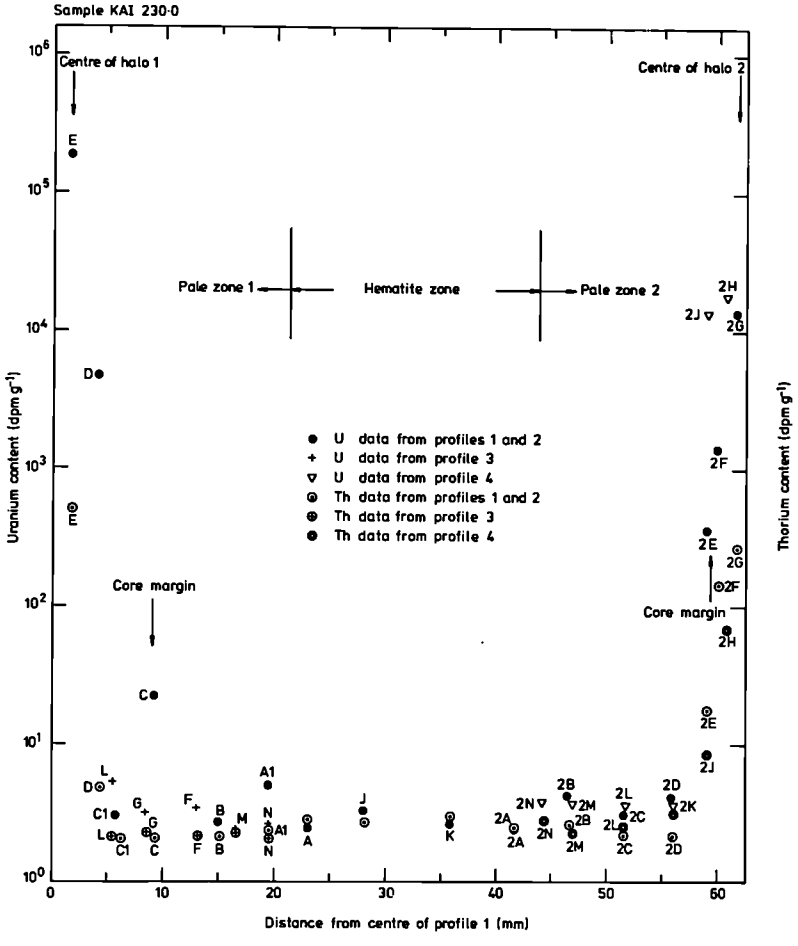

Fig.5 Plots of uranium and thorium contents against distance from centre of profile 1 for all four profiles.

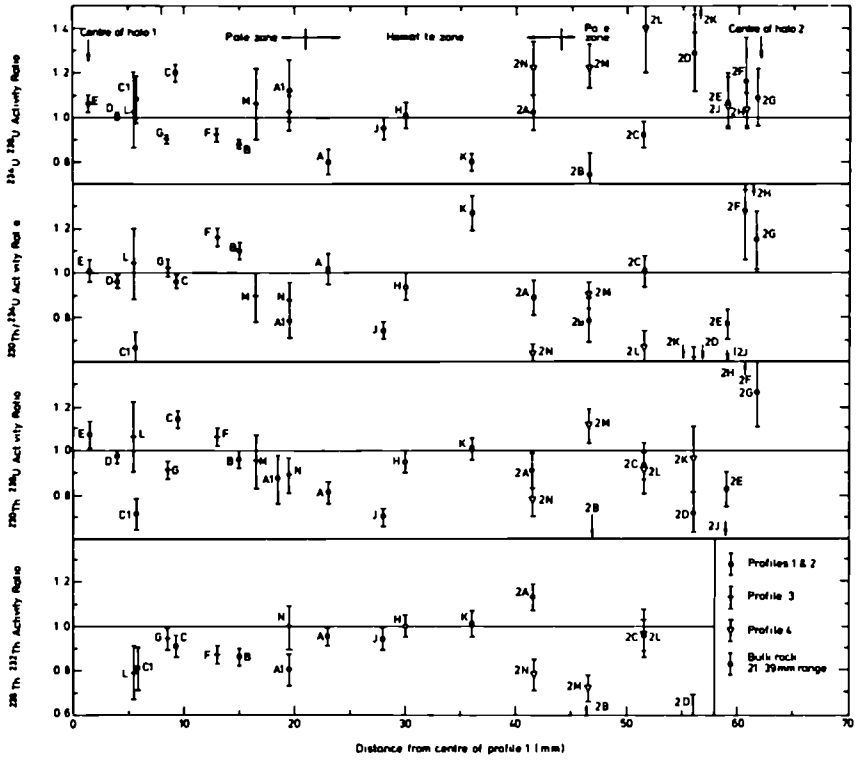

Fig.6 Plot of isotopic activity ratios against distance from centre of profile 1 for all four profiles

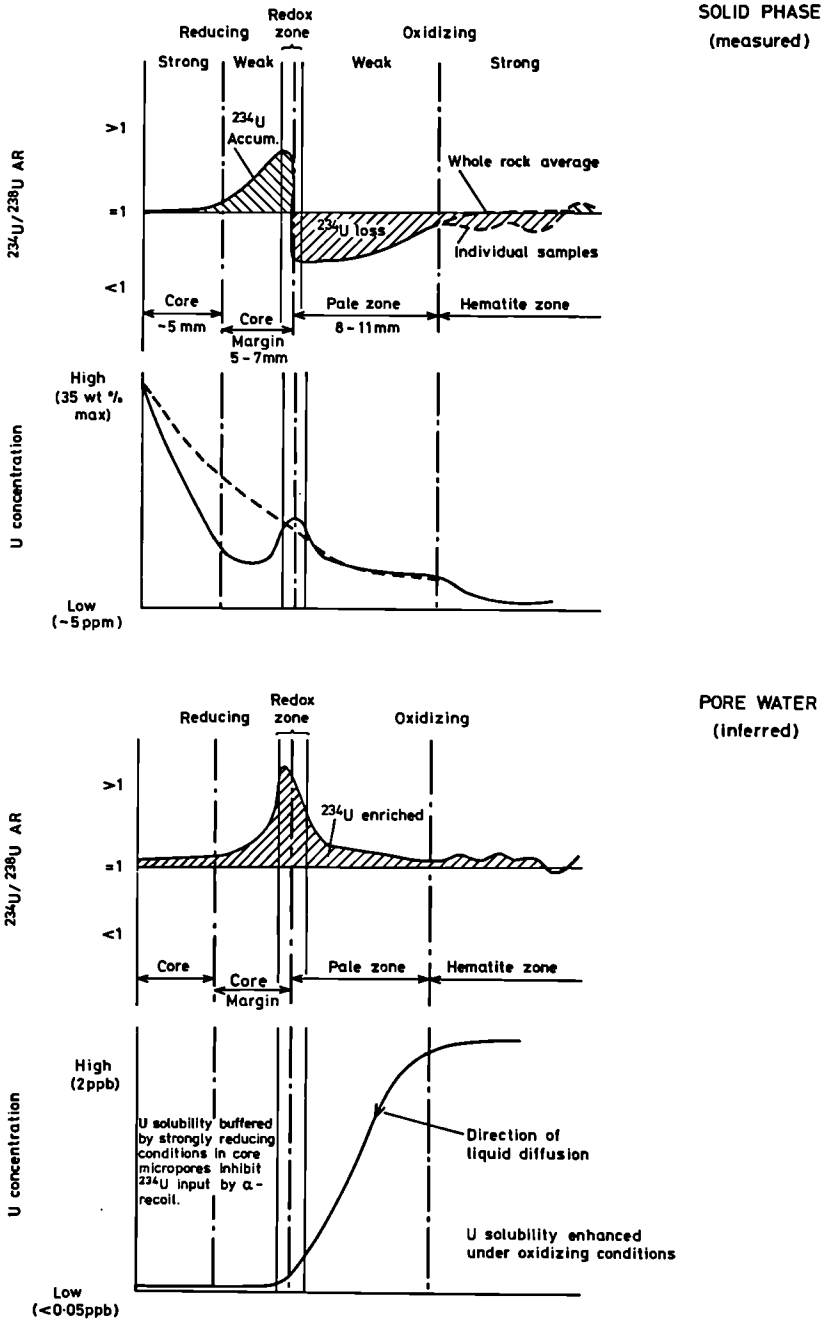

Fig.7 Idealised solid and liquid phase diffusion profiles of uranium content and $^{234}U/^{238}U$ activity ratio in different zones of the Kaisten reduction haloes.

MODELLING ISOTOPE DISTRIBUTIONS IN BORECORES

P. Herzog

Federal Institute for Reactor Research, EIR, Wuerenlingen

Summary

The distribution and possible mobilisation of natural radionuclides in the neighbourhood of a water-bearing fracture in rocks may provide valuable information for the understanding of transport mechansims thought to determine the long term behaviour of a radioactive waste repository.

A one-dimensional diffusion transport model of a three member decay chain including sorption (linear adsorption isotherm) is presented. The rock adjacent to a water-bearing fissure has been modelled as a porous, homogeneous, isotropic and infinite medium. A further assumption is that the bulk rock phase does not act as a radionuclide source and, hence, does not contain any minerals or/and impurities of the radionuclides of interest. From the isotopic concentrations in the water of the fracture, assumed to be in a steady state, boundary conditions are extracted. Initial conditions are specified, e.g. at the time when the fissure opened. We present analytical expressions and discuss diffusion from rock to fissure for the ^{238}U - series members. We show results for two representative environments with respect to sorption (reducing, oxidising).

1 Introduction

The long term behaviour of a nuclear waste repository located in the geosphere is of major concern in safety analysis. As this is mainly determined by the mechanisms of radionuclide geosphere transport over very long timescales it seems appropriate to look at those natural systems where radionuclides have been mobile for long periods of time. The distribution of natural radionuclides within the rock may provide valuable informations about the mechanisms involved in transport [1].

In this paper we shall consider the transport of three members of the ^{238}U decay chain in a system where water was circulating in a fissure penetrating a relatively impermeable rock. Concentration profiles transverse to the fracture (e.g. in borecores taken across the fracture) may illustrate the history of radionuclide migration into the rock or into the water-bearing fissure.

In the next section we shall present a simple transport model for such rock-fracture systems, present analytical solutions and discuss its implications and limitations. In a further section we shall draw conclusions from this study.

2 A transport model for radionuclide migration in a rock/fracture system

2.1 Mathematical formulation

Consider a rock/water interface together with its adjacent rock matrix. We shall assume that the rock behaves as a homogeneous, isotropic porous medium. (Thus we are not going to consider rocks with internal fracture networks and/or rocks with U-series minerals as constituents). Provided that the penetration depth of radionuclides or the width of the depleted zone (depending on the sign of the concentration gradient from the water bearing fissure to the rock matrix) is much smaller (even for long periods of time) than a typical spatial scale of the problem at hand allows to model the rock as an infinite medium along the normal to the fracture plane (z-axis). The simplest model for the fracture is an infinite plane-parallel slit (containing the x- and y-axis) of a certain width containing water in a physico-chemical steady state. As a consequence of these assumptions the concentration profiles along the z-axis will be invariant under translations in x- and y-direction (ie. we neglect transversal diffusion); thus, the transport into or out of the fissure (along the $\pm$z-axis) can be modelled as one-dimensional. From these considerations it is obvious that any property of the rock/water interface (z=0) is irrelevant; it is only the location where we shall state one of our boundary conditions for the transport equation.

As radionuclides can be adsorbed at the porespace-surfaces the basis of our model is a system of coupled differential equations describing diffusive transport of a three member decay chain; provided that the parameters do not vary in space and time we get:

$$(\partial/\partial t)\,(\varepsilon C_1+(1-\varepsilon)\rho S_1) = D_1\ \partial^2/\partial z^2\ (\varepsilon C_1) - \lambda_1(\varepsilon C_1+(1-\varepsilon)\rho S_1) \qquad (1.1)$$

$$(\partial/\partial t)\,(\varepsilon C_2+(1-\varepsilon)\rho S_2) = D_2\ \partial^2/\partial z^2\ (\varepsilon C_2) - \lambda_2(\varepsilon C_2+(1-\varepsilon)\rho S_2) + \lambda_1(\varepsilon C_1+(1-\varepsilon)\rho S_1) \qquad (1.2)$$

$$(\partial/\partial t)\,(\varepsilon C_3+(1-\varepsilon)\rho S_3) = D_3\ \partial^2/\partial z^2\ (\varepsilon C_3) - \lambda_3(\varepsilon C_3+(1-\varepsilon)\rho S_3) + \lambda_2(\varepsilon C_2+(1-\varepsilon)\rho S_2) \qquad (1.3)$$

$$\text{Kinetic equations : } (i=1,2,3)\ S_i(z,t)=f(z,t,C_i(z,t)) \qquad (2.i)$$

For notation see Appendix.
The appropriate initial and boundary conditions that have to be specified in order to solve these equations will be specified below.

By making the assumption that S_i depends linearly on C_i (i.e. sorption is an instantaneous and reversible process) we can state eqs. (2.i) in an explicit form.

$$S_i(z,t) = K_d^{(i)}\ C_i(z,t) \qquad (2.i)'$$

Using the relation (A.1) the eqs. (1.i) can be rewritten as:

$$\partial C_1/\partial t = D_1/R_1\ \partial^2 C_1/\partial z^2 - \lambda_1 C_1 \qquad (1.1)'$$

$$\partial C_2/\partial t = D_2/R_2\ \partial^2 C_2/\partial z^2 - \lambda_2 C_2 + (R_1/R_2)\,\lambda_1 C_1 \qquad (1.2)'$$

$$\partial C_3/\partial t = D_3/R_3\ \partial^2 C_3/\partial z^2 - \lambda_3 C_3 + (R_2/R_3)\,\lambda_2 C_2 \qquad (1.3)'$$

As initial conditions we choose spatially constant but different concentrations for each nuclide.

$$C_i(z, t=0) = \alpha_i \qquad (3.i)$$

The idea behind this choice is the assumption that the considered nuclides were distributed uniformly over the whole available porespace before the fracture opened. As boundary conditions we choose general Dirichlet-type conditions.

$$C_i(z=0, t) = \beta_i \qquad (4.i)$$

$$C_i(z=\infty, t) = \gamma_i(t) \qquad (5.i)$$

In the infinite medium approach the functions $\gamma_i(t)$ of eqs. (5.i) cannot be chosen freely since in the limit $z \to \infty$ the eqs. (1.i)' become Bateman-like ordinary differential equations in time: $\gamma_i(t)$ have to be solutions of these equations, eqs. (3.i) being the initial conditions.

The solutions to the eqs. (1.i)', taking into account the initial and boundary conditions, eqs. (4.i) and (5.i), are given by

$$C_1(z,t) = \alpha_1 E_1(z,t) + \beta_1 F_1(z,t) \qquad (6.1)$$

$$\begin{aligned} C_2(z,t) = {} & \frac{\kappa_{21}}{\delta_{21}}\alpha_1\lambda_1 E_1(z,t) + \left(\alpha_2 - \frac{\kappa_{21}}{\delta_{21}}\alpha_1\lambda_1\right)E_2(z,t) \\ & + \mu_2^2\frac{\kappa_{21}}{\varrho_{21}}\beta_1\lambda_1 F_1(z,t) + \left(\beta_2 - \mu_2^2\frac{\kappa_{21}}{\varrho_{21}}\beta_1\lambda_1\right)F_2(z,t) \\ & - \kappa_{21}\lambda_1\left(\frac{\alpha_1}{\delta_{21}} - \mu_2^2\frac{\beta_1}{\varrho_{21}}\right)R_{21}(z,t)\,(1-\delta(0|\sigma_{21})) \end{aligned} \qquad (6.2)$$

$$\begin{aligned} C_3(z,t) = {} & \frac{\kappa_{31}}{\delta_{31}}\alpha_1\frac{\lambda_1\lambda_2}{\delta_{21}}E_1(z,t) + \frac{\kappa_{32}}{\delta_{32}}\lambda_2\left(\alpha_2 - \frac{\kappa_{21}}{\delta_{21}}\alpha_1\lambda_1\right)E_2(z,t) \\ & + \left(\alpha_3 - \frac{\kappa_{32}}{\delta_{32}}\lambda_2\left(\alpha_2 - \frac{\kappa_{21}}{\delta_{21}}\alpha_1\lambda_1\right)\right)E_3(z,t) + \mu_2^2\mu_3^2\frac{\kappa_{31}}{\varrho_{31}}\beta_1\frac{\lambda_1\lambda_2}{\varrho_{21}}F_1(z,t) \\ & + \mu_3^2\frac{\kappa_{32}}{\varrho_{32}}\lambda_2\left(\beta_2 - \mu_2^2\frac{\kappa_{21}}{\varrho_{21}}\beta_1\lambda_1\right)F_2(z,t) + \left(\beta_3 - \mu_3^2\frac{\kappa_{32}}{\varrho_{32}}\lambda_2\left(\beta_2 - \mu_2^2\frac{\kappa_{21}}{\varrho_{21}}\beta_1\lambda_1\right)\right)F_3(z,t) \\ & - \kappa_{31}\lambda_1\frac{\sigma_{21}\lambda_2}{\varrho_{32}\sigma_{21} - \sigma_{32}\varrho_{21}}\left(\mu_3^2\frac{\alpha_1}{\delta_{21}} - \mu_2^2\mu_3^2\frac{\beta_1}{\varrho_{21}}\right)R_{21}(z,t)\,(1-\delta(0|\sigma_{21})) \\ & - \kappa_{31}\lambda_1\frac{\sigma_{32}\lambda_2}{\varrho_{32}\sigma_{21} - \sigma_{32}\varrho_{21}}\left(-\mu_2^2\frac{\alpha_1}{\delta_{21}} + \mu_2^2\mu_3^2\frac{\beta_1}{\varrho_{21}}\right)R_{31}(z,t)\,(1-\delta(0|\sigma_{31})) \\ & - \left(\kappa_{32}\lambda_2\left(\frac{\alpha_2}{\delta_{32}} - \mu_3^2\frac{\beta_2}{\varrho_{32}}\right) + \kappa_{31}\lambda_1\frac{\sigma_{32}\lambda_2}{\varrho_{32}\sigma_{21} - \sigma_{32}\varrho_{21}}\left(\mu_2^2\frac{\alpha_1}{\delta_{32}} - \mu_2^2\mu_3^2\frac{\beta_1}{\varrho_{32}}\right)\right)R_{32}(z,t)\,(1-\delta(0|\sigma_{32})) \end{aligned} \qquad (6.3)$$

The functions $E_i(z,t)$, $F_i(z,t)$ and $A_{ij}(z,t)$ as well as $\delta(x|y)$ are defined in the Appendix, too.

2.2 Model application

In the following application of our model we shall concentrate on the (^{238}U-^{234}U-^{230}Th) system. The half-lifes $\tau_{1/2}$ (decay constants, respectively) of these nuclides are given by.

$\tau_{1/2}$ (^{238}U) = 4.468×10^{9}yr : λ_1 = 1.551×10^{-10}yr^{-1}
$\tau_{1/2}$ (^{234}U) = 2.440×10^{5}yr : λ_2 = 2.841×10^{-6}yr^{-1}
$\tau_{1/2}$ (^{230}Th) = 7.700×10^{4}yr : λ_3 = 9.002×10^{-6}yr^{-1}

The quantities

$D_1 = D_2 = D_3 = 1\times10^{-10}$m^2/s = 3.154×10^{-3}m^2/yr
$\rho = 2.5\times10^{3}$kg/m^3
$\varepsilon = 0.03$

will not be varied.

As some groundwaters show activity ratios that are in the neighbourhood of $(\lambda_2C_2/\lambda_1C_1)=3$; $(\lambda_3C_3/\lambda_2C_2)=1/20$, we also fix the boundary conditions at the fracture/rock interface with the idea that the porewater adjacent to the fissure has the same composition as the water in the fracture [3,4]. A typical ^{238}U concentration value in waters is 1×10^{-9} mol/l [3]. Thus we completely specified the boundary condition at z=0:

$C_1(z=0,t) = \beta_1 = 1\times10^{-9}$mol/l
$\lambda_2\beta_2/\lambda_1\beta_1 = 3$: $\beta_2 = 3(\lambda_1/\lambda_2)\beta_1 = 1.64\times10^{-13}$ mol/l
$\lambda_3\beta_3/\lambda_2\beta_2 = 1/20$: $\beta_3 = (3/20)(\lambda_1/\lambda_3)\beta_1 = 2.58\times10^{-15}$ mol/l

What the initial concentrations α_i are concerned two situations may occur: either $\alpha_i>\beta_i$ or $\alpha_i<\beta_i$; in the former case we will have diffusion from the rock towards the fissure and in the latter diffusion will take place from the fissure towards the rock. As space is limited we shall discuss only the case $\alpha_i>\beta_i$. For further discussion see Ref. [5].

As the bulk part of uranium is ^{238}U we fix α_1 (= porewater concentration of ^{238}U at t=0) to be close to the U solubility limit concentration; we choose $\alpha_1 = 5\times10^{-9}$ mol/l for definiteness. In addition we assume that before fracture opening the ^{238}U-chain has attained radioactive equilibrium with respect to total activities in the whole rock body. Therefore the inital conditions are:

$\alpha_1 = 5\times10^{-9}$ mol/l

$(\lambda_2R_2C_2(z,t=0)/\lambda_1R_1C_1(z,t=0)) \simeq \lambda_2/(\lambda_2-\lambda_1) \simeq 1.00$:
$\alpha_2 = \alpha_1(\lambda_1R_1)/(\lambda_2R_2) = 5.459\times10^{-5}\ K_{21}\alpha_1$

$(\lambda_3R_3C_3(z,t=0)/\lambda_2R_2C_2(z,t=0)) \simeq \lambda_3/(\lambda_3-\lambda_1) \simeq 1.00$:
$\alpha_3 = \alpha_1(\lambda_1R_1)/(\lambda_3R_3) = 1.723\times10^{-5}\ K_{31}\alpha_1$

In the subsequent parameter variations for the $K_d^{(i)}$-values (see eqs. (2.i)') we shall consider a case where the nuclides are in an environment of reducing eH-conditions and a case where the eH-conditions are oxic.

Case A1) Reducing eH-conditions [6]

$K_d^{(1)} = K_d^{(2)} = K_d^{(3)} = 1 m^3/kg$

$R_1 = R_2 = R_3 = 8.083 \times 10^4$

$\alpha_2 = 2.73 \times 10^{-13}$ mol/l, $\alpha_3 = 8.61 \times 10^{-14}$ mol/l

Case A2) Oxic eH-conditions [6]

$K_d^{(1)} = K_d^{(2)} = K_d^{(3)} / 100 = 0.01 m^3/kg$

$R_1 = R_2 = 8.093 \times 10^2$, $R_3 = 8.083 \times 10^4$

$\alpha_2 = 2.73 \times 10^{-13}$ mol/l, $\alpha_3 = 8.63 \times 10^{-16}$ mol/l

The porewater concentration profiles are shown in Fig. 1 for case A1) and in Fig. 2 for case A2). The nuclides are characterised by —·— for ^{238}U, by —··— for ^{234}U and by —···— for ^{230}Th. The range shown is two meters (fissure at z=0m). We plotted results for three different times $t_1=10^4$yr, $t_2=10^6$yr and $t_3=10^8$yr after fissure opening. In trying to interpret these results the following observations emerge:

1) By increasing (lowering) the retardation factor of the mother nuclide, ^{238}U, with respect to a reference case it is clear that the porewater - concentration of this nuclide drops (increases).
2) The location of the front where diffusion starts to mobilise the nuclides in the porewater can be readily understood for times that are smaller than the half-lives of the considered nuclides: Under this condition we may drop the decay terms in eqs. (1.i)': All the equations decouple and we only have to solve the ordinary diffusion equation with the diffusion coefficient D_i being replaced by (D_i/R_i); its solutions for the approximate concentrations $\bar{C}_i$ (z,t) are given by:

$$\bar{C}_i(z,t) = \alpha_i + (\beta_i - \alpha_i)\,\mathrm{erfc}\left(\frac{k_i z}{2\sqrt{\lambda_i t}}\right) \qquad (7.i)$$

$$\bar{C}_i(z,t=0) = \bar{C}_i(z=\infty,t) = \alpha_i \;;\; \bar{C}_i(z=0,t) = \bar{C}_i(z,t=\infty) = \beta_i$$

By defining the depletion front $\bar{z}_i$ as the location where the concentration has dropped to 90% of the initial concentration (equivalent to the concentration at $z=\infty$) we have $\bar{C}_i(\bar{z}_i,t) = {}^9/_{10}\,\bar{C}_i(z=\infty,t) = {}^9/_{10}\alpha_i$ and thus get an implicit equation for $\bar{z}_i$:

$$\mathrm{erfc}\left(\frac{k_i \bar{z}_i}{2\sqrt{\lambda_i t}}\right) = \frac{1}{10}\,\frac{\alpha_i}{\alpha_i - \beta_i} \qquad (8.i)$$

This relation implies $\bar{z}_i = 2u_i(\alpha_i,\beta_i)\sqrt{(D_i/R_i)t}$ where $u_i(\alpha_i,\beta_i) = \mathrm{erfc}^{-1}[\alpha_i/(10(\alpha_i-\beta_i))]$ is a proportionality constant, ie. the depletion front depends linearly on $\sqrt{t}$ and $1/\sqrt{R_i}$. (The characteristic $\sqrt{t}$-law for diffusion processes). The proportionality constants $u_i(\alpha_i,\beta_i)$ and the quantitiy $\bar{z}_i/\sqrt{t}$ are given in the following table:

Case	$u_1(\alpha_1,\beta_1)$	$\bar{z}_1/\sqrt{t}$ [m·yr$^{-\frac{1}{2}}$]	$u_2(\alpha_2,\beta_2)$	$\bar{z}_2/\sqrt{t}$ [m·yr$^{-\frac{1}{2}}$]	$u_3(\alpha_3,\beta_2)$	$\bar{z}_3/\sqrt{t}$ [m·yr$^{-\frac{1}{2}}$]
A1)	1.085	4.287×10^{-4}	0.813	3.212×10^{-4}	1.152	4.551×10^{-4}
A2)	1.085	4.284×10^{-3}	0.813	3.212×10^{-3}	-----	----------

Since $\alpha_2/(\alpha_3-\beta_3)|_{A2} < 0$, it is clear that we cannot define a depletion front for ^{230}Th in case A2); its concentration gradient points toward the rock. [In the framework of the exact calculations this also happens for ^{234}U at times that are longer than $\tau_{1/2}(^{234}U) = 2.440\times10^5$yr (case A1) and case A2) at $t=t_3 = 10^6$yr; see the corresponding figures]. For $t=t_1 = 10^4$yr, a timescale where our assumptions to derive eqs. (7.i) are certainly valid, we get in case A1) $\bar{z}_1(t=t_1) = 4.3\times10^{-2}$m, $\bar{z}_2(t=t_1) = 3.2\times10^{-2}$m and $\bar{z}_3(t=t_1) = 4.6\times10^{-2}$m, whereas in case A2) we get $\bar{z}_1(t=t_1) = 4.3\times10^{-1}$m and $\bar{z}_2(t=t_1) = 3.2\times10^{-1}$m; this is in fair agreement with the result of the exact calculation where the depletion front is defined as $C_i(\bar{z}_1,t) = {}^9/_{10}\gamma_i$ (t).

As the half-life of ^{238}U is very long, $\tau_{1/2}(^{238}U) = 4.468\times10^9$yr $\gg t_3=10^6$yr, eq. (8.1) for the depletion front $\bar{z}_1$ is valid for all times considered : For $t=t_3 = 10^6$yr after fissure opening we expect the ^{238}U depletion front at 4.3m (43m) for case A1) (case A2)). As this is far outside the range considered, the ^{238}U porewater concentration at z=2m, $t=t_3 = 10^6$yr will be strongly reduced: Exactly this reduction can be seen in the figures; of course, it is stronger in case A2) than in case A1). This depletion of ^{238}U at $t=10^6$yr within the range considered is also responsible for the depletion of the daughter ^{234}U and of ^{230}Th.

3) In Table 1 we listed the total activity ratios $R_i\lambda_iC_i/R_k\lambda_kC_k$, i=2,3 and k=1,2. In case A1) we see that for a large z-range ($0.35m \sim z \lesssim 2m$) and for all times t_2,t_3 the ratios show the radioactive equilibrium value ($\simeq$ secular equilibrium value) of unity : Taking into account the experimental errors, usually of the order of 10%, we would conclude from total activity ratios alone, that even after 10^8 years (after fracture opening) nuclide mobilisation occured only in a zone ~0.35m thick adjacent to the waterbearing fissure. In the previous sections we have given reasons why such a conclusion would be wrong: The depletion front of ^{238}U extends as far as 4.3m (43m) in case A1) (case A2)) from the fissure. Activity ratio measurements have to be accompanied by concentration measurements if mobilisation of nuclides has to be shown: Nuclides having the same transport influencing characteristics (D_i,R_i in this model, but also solubility limits etc.) can move along being in radioactive equilibrium. In case A2), where the retardation factor of ^{230}Th is ~100 times larger than the retardation factor of U, the ^{230}Th/^{234}U ratio reaches radioactive equilibrium within the first ~0.25m, whereas ^{234}U/^{238}U shows disequilibrium extending beyond the range considered. This far reaching disequilibrium of ^{234}U/^{238}U is the result of the lower retardation factor of U in this case compared to case A1): A lowering of $R_{i,2}$ by 100 results in the same "2/1"-value at a distance z as the "2/1"-value with the original $R_{i,2}$ at z/10. This is clearly exemplified:

$$R_2\lambda_2C_2/R_1\lambda_1C_1(z=0.1m)\big|_{A1} - R_2\lambda_2C_2/R_1\lambda_1C_1(z=1m)\big|_{A2} = \begin{cases} 1.40 & , t=t_2 \\ 1.76 & , t=t_3 \end{cases}$$

$$R_2\lambda_2C_2/R_1\lambda_1C_1(z=0.1m)\big|_{A1} - R_2\lambda_2C_2/R_1\lambda_1C_1(z=2m)\big|_{A2} = \begin{cases} 1.11 & , t=t_2 \\ 1.19 & , t=t_3 \end{cases}$$

The pattern of disequilibrium for $^{230}Th/^{234}U$ in case A2) shows an experimentally non-detectable minimum at $t=10^6$yr, this results because at this time the transport term $(D_2/R_2)(\partial^2 C_2/\partial z^2)$ for ^{234}U is still important whereas for ^{230}Th $(D_3/R_3)(\partial^2 C_3/\partial z^2)$ is negligible compared to the decay term $-\lambda_3 C_3$.

It is readily understood why "3/2" is always larger than unity: As ^{234}U has been mobilized within a larger range than ^{230}Th, leading to a depletion of ^{234}U within that range, we expect the activity ratio $R_3\lambda_3 C_3/R_2\lambda_2 C_2$ to be larger than unity.

3 Discussion

This note has to be understood as a first step in modelling radionuclide migration in the region of a water-bearing fissure. Unfortunately, the results obtained in the previous sections cannot be compared with experimental data collected so far, for several reasons:

α) Theoretical reasons:
Many of the rock/water systems subjected to experimental investigations involve rocks that contain ^{238}U-series mineral grains and/or ^{238}U-series impurities in other minerals. (All the crystalline borecores with a fissure are such systems). Thus one of our main assumptions, namely no ^{238}U-series minerals/impurities, excludes interpretation of data from such systems. - It is evident that such grains will strongly influence the porewater/adsorbed phase concentrations of all ^{238}U series nuclides; hereby elemental solubility limits, themselves dependent on chemical conditions and responsible for precipitation/dissolution, play an important role that cannot be neglected.

β) Experimental reasons
Most of the experiments performed on such rock/water systems have given incomplete information for modelling purposes [7]. From the discussion in the previous sections, however, a list of measurements, that should be carried out on such rock/water systems, emerged.

1) A detailed analysis of the water in the fissure (--> boundary conditions); it also might give indications of the age of the fissure.
2) Measurement of rock parameters:
   - Density ρ
   - Porosities ε (flow porosity, connected porosity)
   - Diffusivities D_i for nuclide i
   - Detailed mineralogy
3) Sorption experiments with the elements of interest under reducing or (and) oxic conditions in order to determine sorption isotherms. For these experiments a (natural or artificial) water, which is in chemical equilibrium with the rock, should be used (--> speciation).
4) A special effort should be made to extract the different phases (eg. the porewater and the adsorbed phase); together with a detailed mineralogical analysis (see 2)) this allows a deeper insight into possible transport mechanisms to be modelled. These different phases should be examined for the different isotopes separately in order to understand their share in the elemental solubility limit if attained.

A final remark: In this note we only considered the transport of three members of the ^{238}U-decay chain. In some instances it might be useful to also know the concentration profile of ^{226}Ra: As the halflife of

^{226}Ra is only $\tau_{1/2}$ (^{226}Ra) = 1.600×10^{3}yr and this is much smaller than $\tau_{1/2}$ (^{238}U) = 4.468×10^{9}yr we may also use eqs. (12.i) for the system ^{234}U–^{230}Th– ^{226}Ra for times $t \ll \tau_{1/2}$ (^{238}U). It is clear that appropriate initial and boundary conditions should be chosen.

Appendix Notation

C_i [mol/m^3] : Concentration of nuclide of i-th generation (i=1: parent; i=2: child; i=3: grandchild) in porewater.
S_i [mol/kg] : Concentration of nuclide of i-th generation adsorbed on the rock matrix.
D_i [m^2/s] : Diffusion coefficient for nuclide of the i-th generation. Space and time independent.
λ_i [s^{-1}] : Decay constant of nuclide of the i-th generation.
ε [-] : Connected rock porosity (Space and time independent).
ρ [kg/m^3] : Rock density.

$$R_i = 1 + (1-\varepsilon)(\rho/\varepsilon)K_d^{(i)} \tag{A.1}$$

$$\kappa_{ij} = R_j/R_i \tag{A.2}$$

$$\delta_{ij} = \lambda_i - \lambda_j \tag{A.3}$$

$$\mu_i^2 = R_i/D_i \tag{A.4}$$

$$k_i = +\sqrt{\mu_i^2\lambda_i} = \sqrt{(R_i/D_i)\lambda_i} \tag{A.5}$$

$$\rho_{ij} = k_i^2 - k_j^2 = (R_i/D_i)\lambda_i - (R_j/D_j)\lambda_j \tag{A.6}$$

$$\sigma_{ij} = \mu_i^2 - \mu_j^2 = (R_i/D_i) - (R_j/D_j) \tag{A.7}$$

$$E_i(z,t) = \operatorname{erf}\left(\frac{k_i z}{2\sqrt{\lambda_i t}}\right) e^{-\lambda_i t} \tag{A.8}$$

$$F_i(z,t) = \frac{1}{2\sqrt{\pi}} e^{-\lambda_i t - (k_i z)^2/(4\lambda_i t)} \left\{ G\left(\frac{-2\lambda_i t + k_i z}{2\sqrt{\lambda_i t}}\right) + G\left(\frac{2\lambda_i t + k_i z}{2\sqrt{\lambda_i t}}\right) \right\} \tag{A.9}$$

$$A_{ij}(z,t) = \frac{1}{2\sqrt{\pi}} \left[e^{-\lambda_i t - (k_i z)^2/(4\lambda_i t)} \left\{ G\left(-\sqrt{\frac{\mu_i^2\delta_{ij}}{\sigma_{ij}}}t + \frac{k_i z}{2\sqrt{\lambda_i t}}\right) + G\left(\sqrt{\frac{\mu_i^2\delta_{ij}}{\sigma_{ij}}}t + \frac{k_i z}{2\sqrt{\lambda_i t}}\right) \right\} - (i \leftrightarrow j) \right] \tag{A.10}$$

$G(z=x+iy)$ is a function related to the complementary error function [2]

$$G(z) = \sqrt{\pi}\exp(z^2)\operatorname{erfc}(z) = \sqrt{\pi}\exp(x^2-y^2+2ixy)\operatorname{erfc}(x+iy) \tag{A.11}$$

$$\delta(x|y) = \begin{cases} 1 & x = y \\ 0 & x \neq y \end{cases} \tag{A.12}$$

References

[1] The literature on natural analogues is plentiful. See e.g. "Natural analogue working group; Second Meeting, Interlaken (CH), June 17-19, 1986" ed. B. Côme and N. Chapman.
To be published as CEC Report No. EUR 10671.

[2] "Handbook of Mathematical Functions" ed. M. Abramovitz and I.A. Stegun, Dover Publication, New York, 1970.

[3] NAGRA "Hydrogeologisches Untersuchungsprogramm Nordschweiz, Wasseruntersuchungen". For $^{234}U/^{238}U$ activity ratios in water.

[4] NAGRA NTB 85-06 Sondierbohrung Boettstein / Ergebnisse der Isotopenuntersuchungen; W. Balderer, H. Loosli, Physikalisches Institut der Universitaet Bern; Januar 1985. For $^{230}Th/^{234}U$ activity ratios in water.

[5] F. Herzog; "Modelling isotope distributions in bore cores", EIR internal report, TM-45-86-30, Wuerenlingen, 1986.

[6] I.G. McKinley, J. Hadermann; "Radionuclide Sorption Database for Swiss Safety Assessment" EIR-Bericht Nr. 550, 1984.

[7] A.B. Mackenzie, R.D. Scott; " Analysis of Granites for natural analogue studies. Final report to NAGRA/KBS, 1986. P.J. Hocker, A.B. Mackenzie, R.D. Scott, I.M. Ridgway, I.G. McKinley, J.M. West; "A study of natural and long-term (103-104yr) elemental migration in saturated clays and sediments". Part III, BGS Report FLPU 85-9. 1985.

Table 1 Total activity ratio profiles for times t=t = 10^6yr and t=t = 10^8yr after fracture opening. The notation "2/1" for $R_2\lambda_2C_2/R_1\lambda_1C_1$ and "3/2" $R_3\lambda_3C_3/R_2\lambda_2C_2$ is used.

A	case A1)				case A2)			
	t=10^6yr		t=10^8yr		t=10^6yr		t=10^8yr	
z[m]	"2/1"	"3/2"	"2/1"	"3/2"	"2/1"	"3/2"	"2/1"	"3/2"
0.0	3.00	0.05	3.00	0.05	3.00	5.00	3.00	5.00
0.1	1.40	0.86	1.76	0.78	2.65	1.89	2.81	1.92
0.2	1.11	1.00	1.29	0.99	2.37	1.21	2.65	1.22
0.3	1.04	1.00	1.11	1.02	2.15	1.06	2.50	1.05
0.4	1.01	1.00	1.04	1.02	1.97	1.02	2.36	1.02
0.5	1.00	1.00	1.02	1.01	1.83	1.02	2.23	1.01
0.6	1.00	1.00	1.00	1.01	1.71	1.02	2.12	1.00
0.7	1.00	1.00	1.00	1.00	1.61	1.02	2.02	1.00
0.8	1.00	1.00	1.00	1.00	1.53	1.02	1.92	1.00
0.9	1.00	1.00	1.00	1.00	1.46	1.02	1.84	1.00
1.0	1.00	1.00	1.00	1.00	1.40	1.03	1.76	1.00
1.1	1.00	1.00	1.00	1.00	1.35	1.03	1.69	1.00
1.2	1.00	1.00	1.00	1.00	1.30	1.03	1.63	1.00
1.3	1.00	1.00	1.00	1.00	1.27	1.03	1.57	1.00
1.4	1.00	1.00	1.00	1.00	1.23	1.03	1.52	1.00
1.5	1.00	1.00	1.00	1.00	1.21	1.03	1.47	1.00
1.6	1.00	1.00	1.00	1.00	1.18	1.03	1.43	1.00
1.7	1.00	1.00	1.00	1.00	1.16	1.03	1.39	1.00
1.8	1.00	1.00	1.00	1.00	1.14	1.03	1.36	1.00
1.9	1.00	1.00	1.00	1.00	1.31	1.03	1.32	1.00
2.0	1.00	1.00	1.00	1.00	1.11	1.03	1.29	1.00

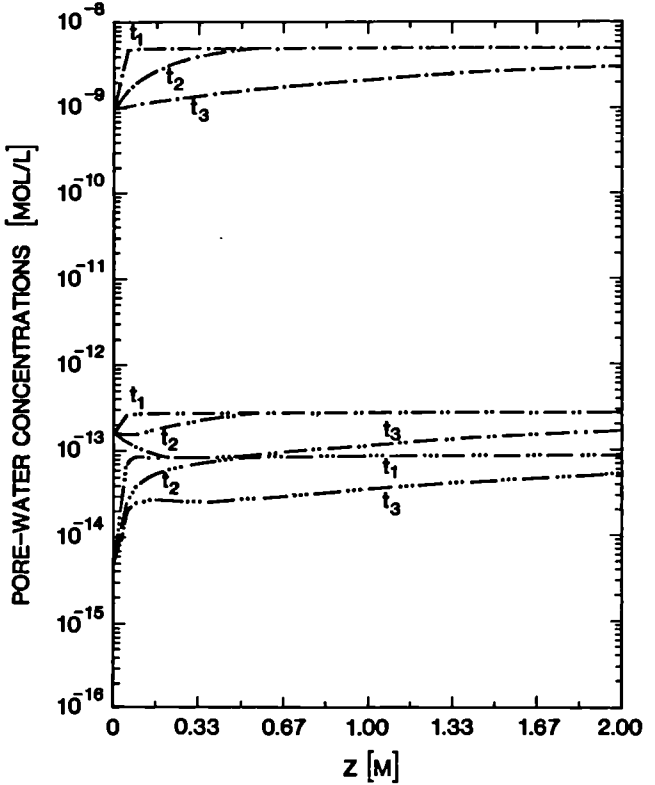

Figure 1:

Pore-water concentration profiles for ^{238}U (——·——), ^{234}U (——··——) and ^{230}Th (——···——) in case A1). Concentrations of each nuclide are plotted for three different times, $t_1 = 10^4$yr, $t_2 = 10^6$yr and $t_3 = 10^8$yr after fissure opening.

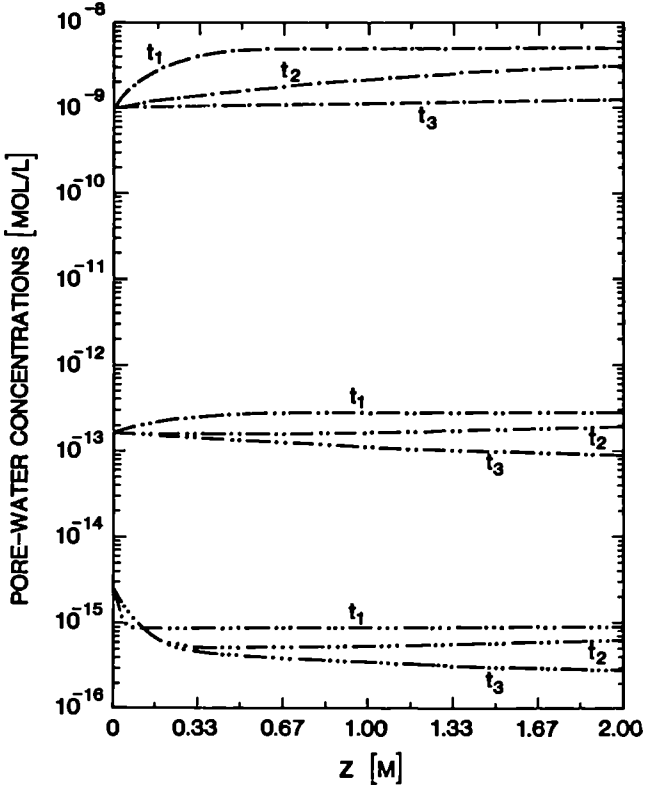

Figure 2:

Same as Fig. 1 but for case A2).

Long-term solute diffusion in a granite block immersed in sea water

N.L. Jefferies.
Chemistry Division,
Harwell Laboratory,
Oxfordshire, UK.

June 1987

Abstract

Solute diffusion profiles for Cl^-, Br^-, F^- and SO_4^{--} have been measured in a granite block which was immersed in the sea at Falmouth, Cornwall, for 30 years. The apparent diffusion coefficient and the solute accessible porosity have been estimated from the Cl^- and Br^- profiles, and these values have been compared with previously obtained laboratory data. SO_4^{--} and F^- are partially sorbed in the granite block, and their sorptivity is estimated from an analysis of their pore water concentration profiles.

1. Introduction

The matrix properties which control solute transport in granitic rocks have previously been examined (1). Laboratory experiments were performed to determine both the intrinsic diffusion coefficient (Di) and the rock capacity factor (α) using through-diffusion techniques in which steady-state diffusion of a solute under a constant concentration gradient is established across a membrane of rock. Di and α are defined as:

$$F = D_i \frac{dc}{dx} \quad \ldots\ldots 1$$

- where F is the steady-state flux per unit cross-sectional area of rock, and $\frac{dc}{dx}$ is the concentration gradient across the sample.

$$\alpha = \phi + \rho R_d \quad \ldots\ldots 2$$

- where ϕ is the solute-accessible porosity of the porous medium, ρ the density and R_d the distribution ratio.

However, because of the low diffusivity of granite it has not been possible to obtain laboratory data for Di and α on granite samples thicker than 5 cm (1). The object of this work, therefore, was to identify larger specimens of granite which have been undergoing natural diffusion processes for longer, known, periods of time, in order to study diffusion over greater distances.

2. Experimental Considerations

The principle of the experiment was to examine trace element profiles developed in a block of granite as a result of its immersion in sea water. Solutes in the sea water will diffuse into the block and, conversely, solutes present at higher concentrations within the block will diffuse outwards. Anion profiles have been examined in this study, since these elements will be weakly-sorbed or non-sorbed and therefore will be most mobile.

Because of the low matrix porosity and permeability of the granite it is not possible to directly extract the pore water from within the rock. Similarly, because of the high Cl^- and F^- concentrations of the granite studied (average contents of $\sim$ 500 and 1400 ppm respectively (3)), it is not possible to simply dissolve the rock to measure the total halide concentrations, because only a small proportion will be partitioned into the pore water.

It is therefore necessary to allow solutes within the granite to diffuse out into a reservoir of water and, after sufficient time has elapsed to allow out-diffusion to proceed to equilibrium, to measure the concentration of solutes in that reservoir. The concentration of leachable anions in the granite (expressed as μg of anion per g of rock) can be calculated from a knowledge of the rock mass and reservoir volume.

In order to reduce the time required for out-diffusion of the anions, the granite was crushed to a finer particle size. However, the partitioning of the halides in the granite must be appreciated before deciding upon the optimum particle size. The halides, in addition to substituting in trace amounts into hydrous minerals are also concentrated in fluid inclusions within the granite. These isolated pockets of fluid, with dimensions up to 20 μm, represent 'fossil' hydrothermal waters trapped in quartz during its recrystallisation. Analysis of fluid inclusions from unmineralised granites in SW England reveals salinities of up to 40 wt% NaCl (4). Clearly, if these inclusions are fractured during crushing of the granite, additional halides will be released to solution, and will obscure the pore water composition trends. Therefore, the granite in this study has been crushed to a particle size of 1 cm; large enough to minimise fluid inclusion fracturing, but small enough to allow out-diffusion equilibrium to be attained in 1-2 weeks.

3. Experimental Details

In 1956, a number of freshly blasted granite blocks were transported from a Cornish granite quarry and placed in front of the East Pier, Falmouth Docks, in order to act as wavebreaks. The blocks were entirely immersed in sea water, except at Spring low tides when their upper surfaces were exposed.

In February, 1987 two blocks of dimensions approximately 1.5 x 1.0 x 0.6 metres, were recovered. Petrological examination of the blocks confirmed that they had been obtained from the Carnmenellis pluton, and were of the coarse-grained megacrystic biotite granite variety. Samples of fresh, unweathered granite of this variety were obtained in order to determine the levels of trace elements which can be leached from granite which has not been immersed in sea water.

A 40 mm diameter core was obtained from one block by rotary drilling, using a demineralised water flush so as not to introduce contaminants. The core was drilled parallel to the short axis of the granite block. The experimental details are shown diagrammatically in Figure 1. This core was then sectioned at 3 cm intervals along its length, producing samples weighing approximately 100 g, and crushed to a particle size of 1 cm. 40 ml of AnalaR water was added to each sample, which was stored in a watertight container. Three granite samples, taken from quarries on the Carnmenellis pluton, were crushed to the same particle size and treated in the same manner.

In order to investigate the effect of particle size on the 'leachable' trace element concentrations, granite samples from the Carnmenellis pluton were also crushed to a grain size of less than 2 μm and placed in AnalaR water as before. At this particle size, all anions partitioned into fluid inclusions would be released and leached from the granite.

After 50 days the granite samples were removed from the solutions which were then analysed for Cl^-, Br^-, F^-, SO_4^{--} and NO_3^- using ion chromatography.

4. Results

(i) Granite 'backgrounds'. These samples of fresh biotite granite were collected from the Carnmenellis pluton and had not been immersed in sea water. As Table 1 demonstrates, the leachable concentrations of Cl^- and F^- are strongly dependent upon the particle size of the crushed granite. SO_4^{--} concentrations increase only slightly with the finer particle size, whilst Br^- is consistently below the limit of analytical detection (<0.002 μg/g).

Table 1

Particle Size	Cl^-	F^-	SO_4^{--}	Br^-
1 cm	1.2 - 2.6	1.1 - 1.9	1.6 - 2.2	<0.002
2 μm	33.3 - 95.0	24.2 - 46.6	4.5 - 9.3	<0.002

Anion concentrations leached from fresh biotite granites, Carnmenellis. Values expressed as μg anions leached per g granite (μg/g).

(ii) Anion profiles in the granite block. Cl^-, Br^-, F^- and SO_4^{--} profiles are plotted in Figures 2 and 3. NO_3^- was consistently below the analytical detection limit and is not considered further. The Cl^- and Br^- profiles are flat at concentrations of approximately 28 μg/g and 0.08 μg/g respectively (Figure 2). These concentrations are factors of 15 and >40 times higher than those leached from the granite 'backgrounds'.

In contrast the F^- and SO_4^{--} profiles display maxima at depths of between 5-14 cm into the block (Figure 3). Concentrations of leachable F^- and SO_4^{--} in the central parts of the block are similar to those in the 'background' granites.

5. Discussion of Results

The diffusion coefficient obtained from an analysis of the profiles is the apparent diffusion coefficient, Da. This is the appropriate coefficient to use when the distance that a species has diffused is being considered (2). It is related to the intrinsic diffusion coefficient, D_i, by:

$$Da = \frac{D_i}{\alpha} \qquad \ldots\ldots 3$$

where $\alpha = \phi + \rho Rd$.

The distribution ratio, Rd, is defined as the concentration of the nuclide partitioned onto the solid phase divided by the equilibrium concentration remaining in solution.

A limited amount of laboratory data has previously been obtained for the biotite granites of the Carnmenellis pluton (1). The intrinsic diffusion coefficient, Di, has been measured at $3 \times 10^{-14} m^2 s^{-1}$ and α (using 0.1M KI as the solute) at approximately 10^{-3}. Sorption of I^- at high concentrations is considered to be weak and therefore the porosity (ϕ) of the Carnmenellis biotite granites is estimated at 10^{-3}.

The principal assumption in the following analysis is that the block was in a saturated state (ie all pores were filled with water) prior to its immersion in the sea. If this was not the case, sea water will be drawn into the block and this would require a modification of the analysis used to interpret the pore water profiles.

The pore network in the granite is dominated by micro-fractures developed in quartz. Measurement of the apertures of these fractures, using SEM, indicates apertures of the order of 1 μm or less. These preliminary observations are in agreement with previous investigations of pore structure in granitic rocks (5) and indicate that free drainage of the pores will not occur. Therefore, evaporation of pore water in the block is the only means by which the block can dry out. The rate at which the block dries out can be calculated by balancing the diffusive flux of water vapour out of the rock against the rate at which the menisci recede ie

$$Do_w \psi \frac{\Delta Cg}{\ell} = \frac{d\ell}{dt} \phi C_w \qquad \ldots\ldots 4$$

- where ΔCg is the difference in concentration of the water vapour between the surface of the block and the surface of the meniscus ($g\ m^{-3}$)
- ℓ is the distance over which the water vapour must diffuse out of the block (m)
- C_w is the density of water ($kg\ m^{-3}$)
- t is time(s)
- Do_w is the free water diffusion coefficient for water vapour in air ($m^2 s^{-1}$)
- ψ is the diffusibility of granite (the intrinsic diffusion coefficient divided by the free water diffusion coefficient for any solute diffusing through a porous medium).

Integrating 4 gives:

$$\ell = \left(\frac{2\ Do\ \psi\ \Delta Cg\ t}{\phi\ C_w}\right)^{1/2} \qquad \ldots\ldots 5$$

- and by inserting a typical laboratory-derived value for ψ (2×10^{-8}) and assuming a 60% relative humidity gives:

$$\ell = 2.3 \times 10^{-6}\ t^{1/2} \qquad \ldots\ldots 6$$

This indicates that the pore water in the granite block will evaporate to a depth of 1 cm in 0.6 years, and to a depth of 10 cm in 60 years. The long times required for significant evaporation to occur imply that the block will not have appreciably dried out before being immersed in the sea.

Therefore, on the assumption that the pore water trace element profiles have developed in response to diffusional fluxes into or out of the granite block while it was immersed in the sea, Da for various solutes can be estimated. The appropriate relationship which links Da and ℓ, the distance over which diffusion has taken place in time, t, is $\ell = \sqrt{Da\ t}$.

The results of the investigation into the effect of particle size on leachable anion concentrations in fresh samples of biotite granite, collected from quarries, are as expected. When the rock was crushed to a particle size comparable with the size of fluid inclusions in the rock, the concentrations of leachable F^- and Cl^- increase markedly (Table 1), indicating that a significant proportion of these elements are present in the liquid phase. In contrast, the SO_4^{--} concentration, derived in the rock by oxidation of pyrite, is only slightly affected by the degree of crushing.

(i) Cl^-, Br^- profiles (Figure 2).

The concentrations of leachable Cl^- and Br^- within the block are consistent with the model that the pore water has $[Cl^-]$ and $[Br^-]$ identical to that of sea water ($\sim$19000 µg/g and 67 µg/g respectively) and that $\alpha = 1.3 \times 10^{-3}$. This value of α is similar to the estimated value of ϕ and suggests that Cl^- and Br^- are essentially non-sorbed in the granite. A minimum Di can be calculated from these profiles and yields $Da \geq 9 \times 10^{-11} m^2 s^{-1}$. The calculated Di is, therefore, $\geq 10^{-13} m^2 s^{-1}$, at least a factor of 3 higher than that measured in the laboratory.

(ii) F^- and SO_4^{--} profiles (Figure 3).

The shape of the F^- and SO_4^{--} profiles suggests that their development has not been the result of a one-stage process. The SO_4^{--} concentrations at the faces of the block are consistent with the pore water having $[SO_4^{--}]$ identical to that of sea water ($\sim$2700 µg/g) and $\alpha = 1.5 \times 10^{-3}$. It should be noted that this value of α is in good agreement with both laboratory-derived data (1) and those obtained from analysis of Cl^- and Br^- profiles.

The leachable concentration of sulphate, however, increases to a maximum at depths of between 11 and 14 cm into the block. This profile is clearly not to be expected if the pore water concentrations have developed as a result of high $[SO_4^{--}]$ sea water diffusing into initially low $[SO_4^{--}]$ pore water.

The fluoride profile is even more pronounced. In this profile, the leachable F^- concentrations at the faces of the block suggest that $[F^-]$ in the pore water is 1000 times that of the sea water, indicating that F^- is in the process of diffusing out of the block into the sea.

A possible explanation for the initially high F^- and SO_4^{--} concentrations at the edges of the granite block are that these elements have been released to solution while the block was undergoing in-situ weathering in the quarry. The faces of the granite block are natural fracture surfaces and therefore weathering has progressed into the block through these surfaces as a result of water circulation in the pluton.

Sulphate is produced by oxidation of pyrite as the redox front advances into the block, whilst fluoride is released during the weathering of micaceous minerals, particularly biotite. The F^- and SO_4^{--} released by the weathering process will be partially resorbed, due to their substitution for OH^- groups in newly formed hydrous minerals. This partial sorption of F^- and SO_4^{--} explains their much lower mobility, compared to Cl^- and Br^-, in the granite block after its immersion in the sea. The high pore water concentrations at the edge of the block are maintained due to slow desorption of SO_4^{--} and F^-, but during the diffusion process the maximum concentration both decreases and migrates in position towards the interior of the block, resulting in the conversion from the initial 'U' shaped concentration profile to the 'M' shaped profile now observed.

The distribution ratios for SO_4^{--} and F^- can be estimated by an analysis of the distance, ℓ, over which diffusion has taken place.

(i) SO_4^{--}

ℓ is approximately 0.12 m
$t = 9.8 \times 10^8$s

Therefore, $Da = 1.5 \times 10^{-11} m^2 s^{-1}$. If D_i is $10^{-13} m^2 s^{-1}$, as estimated above, then $\alpha = 7 \times 10^{-3}$. ϕ, estimated from the Cl^- and Br^- profiles is 1×10^{-3} which gives $\rho Rd = 6 \times 10^{-3}$.

(ii) F^-

ℓ is approximately 0.05 m
$t = 9.8 \times 10^8$s

Therefore, $Da = 2.5 \times 10^{-12} m^2 s^{-1}$. Using the same assumptions as above, $\alpha = 0.04$ and therefore ρRd is approximately 0.04.

The values of Di obtained from an analysis of pore water profiles in the granite block are equal to, or greater than, $10^{-13} m^2 s^{-1}$. This is a factor of at least 3 times greater than the 3 laboratory-generated Di values previously reported for fresh Carnmenellis biotite granite (1). However, diffusion through fracture surfaces of Carnmenellis granite has also been investigated in the laboratory, and has demonstrated that Di is enhanced in the rock adjacent to the fracture by up to 200 times (6). It is possible, therefore, that the diffusivity of the granite block is higher than the original estimate of $3 \times 10^{-14} m^2 s^{-1}$. This can be examined further by laboratory through-diffusion experiments on samples taken at various distances from the faces of the granite block.

6. Conclusions

This preliminary experiment has demonstrated the potential for the measurement of solute migration in granite, as a result of the rock being immersed in sea water for a known period of time. Diffusion of Cl^- and Br^- from the sea water into the block has gone to equilibrium, indicating a higher diffusivity for the granite than previously expected. In addition to solute diffusion from the sea water into the granite, there has also been out-diffusion of some solutes into the sea. It is believed that high concentrations of such solutes, eg F^- and SO_4^{--}, were generated at the margins of the block due to weathering processes.

Therefore, there is a potential for measuring out-diffusion of other partially sorbed nuclides which have been released from original mineral phases during weathering of the granite. However, this depends upon an understanding of the pore water profiles developed across a granite block which is undergoing progressive in-situ weathering in a quarry.

7. Acknowledgements

I wish to thank Falmouth Docks and Engineering Co. for granting permission to remove the granite blocks and Mr. V.M.B. Watkins of Elcon Western (Electrical) Ltd. for supervising their removal and for obtaining core samples. Ion chromatography analyses were performed by Environmental and Medical Sciences Division, Harwell. Finally, thanks are due to Dr. D. Lever and Mr. P.J. Bourke for their help during this work, and for their comments on, and improvements to, the original manuscript.

This work has been commissioned by the Department of the Environment as part of its radioactive waste management research programme. The results will be used in the formulation of Government policy, but at this stage they do not necessarily represent Government policy. I acknowledge partial funding of this research by the Commission of the European Communities under contract number FI.1W.0074UK(H).

References

(1) D.A. Lever and M.H, Bradbury (1985). Rock-matrix diffusion and its implications for radionuclide migration. Mineralogical Magazine, 49 pp 245-254.

(2) D.A. Lever (1986). Some notes on experiments measuring diffusion of sorbed nuclides through porous media. Harwell Report AERE R 12321.

(3) R. Fuge and G.M. Power (1969). Chlorine and fluorine in granitic rocks from SW England. Geochimica et Cosmochimica Acta, 33 pp 888-893.

(4) A.H. Rankin and D.H.M. Alderton (1985). Fluids in granites from south west England. In: High Heat Production Granites, hydrothermal circulation and ore genesis. Institution of Mining and Metallurgy, London pp 287-300.

(5) M.M. Wadden and T.J. Katsube (1982). Radionuclide diffusion rates in igneous crystalline rocks. Chemical Geology, 36, pp 191-214.

(6) M.H. Bradbury (1985). Measurement of important parameters determining aqueous phase diffusion rates through crystalline rock matrices. Journal of Hydrology, 82 pp 39-55.

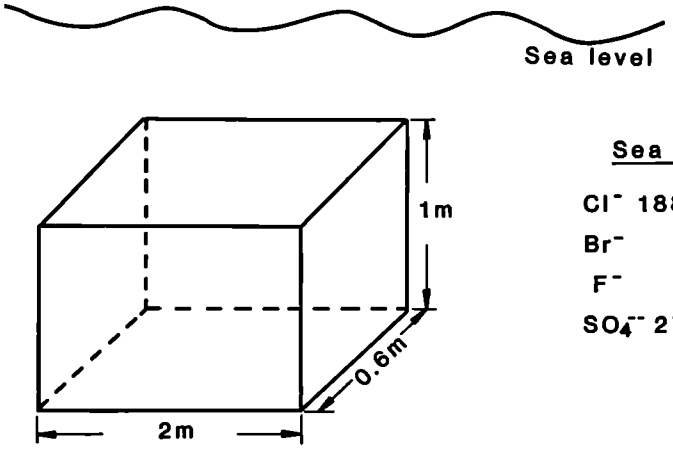

Granite block. Immersed in sea water for 30 years. 0.6 metre long core taken from block after it had been raised from the sea.

Sea water

Cl^-	18800 µg/g
Br^-	67 µg/g
F^-	2 µg/g
SO_4^{--}	2700 µg/g

Fig. 1. Sketch of the experiment

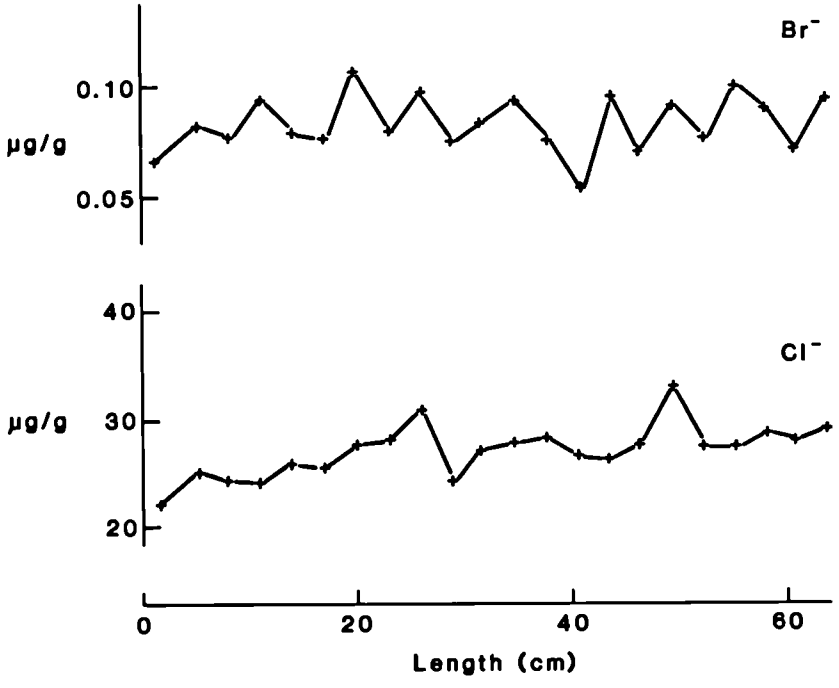

Fig. 2. Leachable Br^- and Cl^- profiles for granite block (concentrations presented as ug (anions leached) per g (granite)).

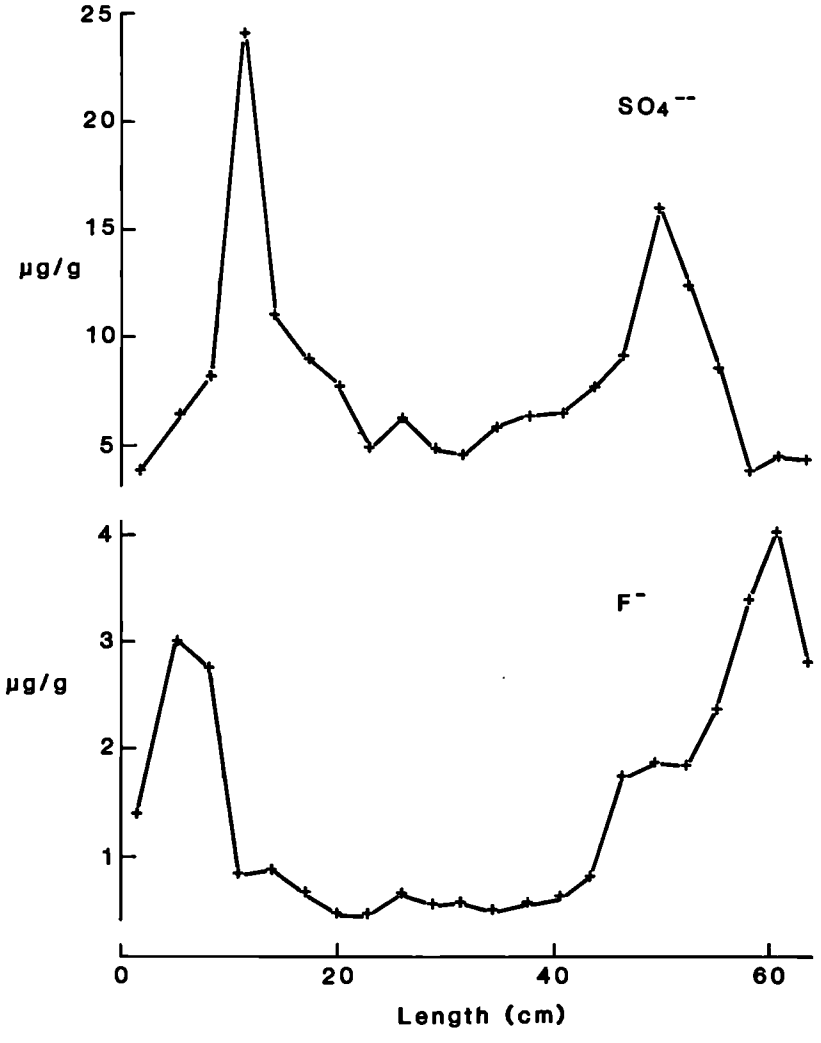

Fig. 3. Leachable SO_4^{--} and F^- profiles from granite block (concentrations presented as µg (anions leached) per g (granite)).

ELEMENT DISTRIBUTION ACCROSS VEINS IN THE EAST BULL LAKE GABBRO ANORTHOSITE LAYERED INTRUSION, ALGOMA DISTRICT, ONTARIO - AN EVALUATION OF MATRIX DIFFUSION.

P.PINTO COELHO
Departmento of Geology
The University of Western Ontario
London, Ontario, Canada, N6A 5B7

Summary

The East Bull lake pluton is cut by macrofractures filled with alteration minerals (veins) predominantly represented by prehnite, calcite, quartz and feldsprs. The chemical composition of such veins is compared to the wall rock chemistry in order to evaluate the behaviour of natural elements during alteration as a guide to radionuclide migration throughout the complex in the case of nuclear waste disposal in the area. The element distribuition accross veins to the wall rock gives an idea of matrix diffusion from veins. Matrix diffusion is one of the processes responsible for retardation mechanisms in the intrusion. Matrix diffusion designates the radionuclide penetration in the rock matrix, thus effectively removing them from the main fluid flow field (1). This process is particularly important in the control of dispersion of non-sorbing radionuclides such as iodine and tritium. Therefore, how far into the wall rock alteration in element distribuition occurs, indicates how far matrix diffusion may happen. These data can be obtained from the observation of element concentration with distance to veins diagrams. As observed in diagrams from East Bull lake, "matrix diffusion" occurs in the intrusion at distances varying between 3.2 and 6.5 cm from the vein (fluid source). The wall rock composition is affected closer to the vein, mainly for Ba (3.2 cm), while U and Zr seem to go as far as 6.5 cm into the wall rock. All the major elements (except Fe2O3) concentration varies up to 5.0 cm far from veins. The same happens for Sr except for the deepest anorthosite samples. Dispersion of iron, titanium, volatiles and rubidium occur as far as 4.0 cm from the fluid source. Th is between the "matrix diffusion" of Ba and most major elements while P2O5 follows most of the major elements.

1.1 Introduction:

The behaviour of radionuclides inside a rock in the

case of release from the waste vault, depends on the concentration of the radionuclides in the dispersion fluid, the rock permeability, sorption and flow regime. To approach this problem one can perform an experiment of fluid percolating through a rock sample with constant or different concentrations of radionuclides in the fluid and under different physico-chemical conditions. At best, this procedure is an attempt to reproduce the conditions of percolation in the natural media. Also, concentration of radionuclides in solution is an estimate, based on various Eh, pH and T. Another approach is to consider the natural behaviour of elements similar to radionuclides that will eventually scape from the waste. Such distributions, due to alteration in the rock, are a consequence of physico-chemical characteristics of fluids, that have been percolating the media for the geologic history and best reflect the nature of percolating fluids, eliminating the problem of temperature and pressure assumptions as well as fluid composition of the laboratory experiment. In addition, the resulting element concentrations in alteration and wall rock phases are a consequence of fluid percolating through a very much larger sample size, being more representative of the geologic environment where the waste will be hosted. Notice also that by analyzing elemental distribuition at different depths and in different rock types one is able to estimate which elements are fixed, which are added and which are mobile. Element distribution curves accross fluid pathways will allow one to establish a trend for the intrusion through regression analysis. The resulting trend will represent an average elemental distribution curve during alteration. Based on this trend, if initial element (or equivalent radionuclide) concentration in the waste vault is assumed, by applying the equivalent regression equation one can estimate the amount of radionuclides that will leave the system in the case of leakage.

One of the most important parameters of waste disposal geologic media is its capacity to retain radionuclides in case of release from the waste container. This capacity is generally known as "sorption". "Sorption involves all the physical and chemical processes which transfer dissolved species, either reversibly or irreversibly, from the aqueous to the rock phase "(2). Sorption results from the direct interaction of the solute, in the percolating fluid with the solid phase or percolating media. Molecular filtration, ion exclusion, ion-exchange, physical absorption, mineralization, precipitation and diffusion into "dead-end" pores (2) are the main sorption mechanisms (fig.1). Therefore, sorption will depend on several physico-chemical conditions of the solution (fluid) and of the solid phase. Sorption and retention factors are also a function of element concentration and distribution throughout alteration.

Matrix diffusion is one of the processes responsible for retardation of elements contained in fluids, percolating the intrusion. The penetration of radionuclides in the rock

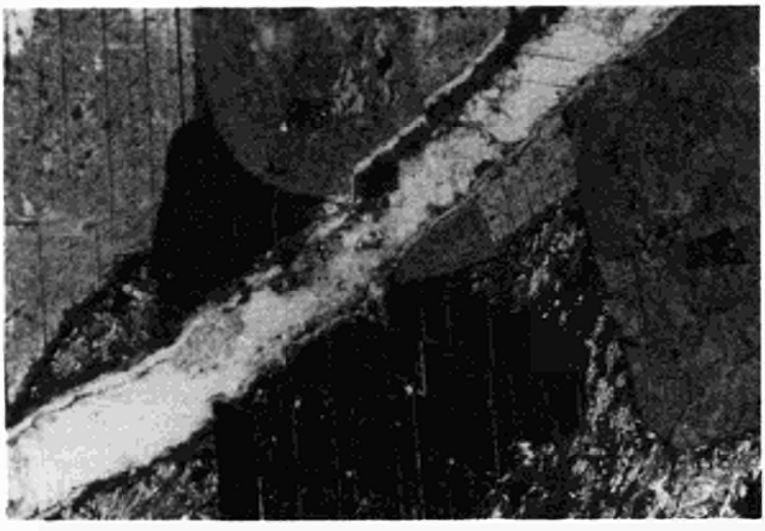

Plate 1 - Sharp contact wall rock / vein and lateral showing tensile displacement. Chlorite and calcite are the main minerals in the vein. Sample EBL2DH/26.00 - 26.16 m. (30.5 X).

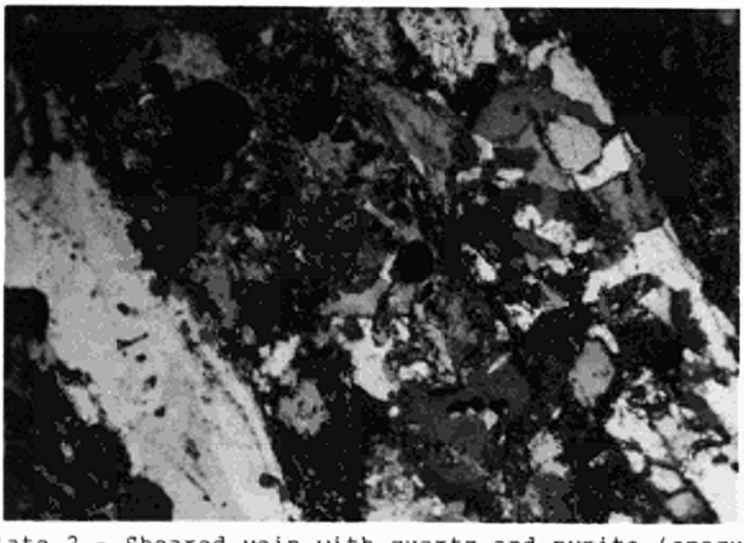

Plate 2 - Sheared vein with quartz and pyrite (opaque) from EBL1DH/261.20 m. (30.5 X).

matrix, removing them from the fluid flow, is particularly important in the control of dispersion of non-sorbing radionuclides such as iodine and tritium. Vein alteration in rocks show the pathways of fluids migrating through this media. The boundaries of alteration in the wall rock show how far the fluid was able to leach and precipitate into the rock, thus providing an indication on how far matrix diffusion may occur. Certainly, the "matrix diffusion" of each particular element will also depend on the phisico-chemical characteristics of each element. Other factors such as rock and fluid characteristics are already fingerprinted in the characteristics of natural veins.

To know matrix diffusion in a particular media, the distribution of natural elements accross veins must be obtained. To evaluate how the radionuclides, contained in the high level waste, will be affected by this proccess, one may look at the behaviour of their natural analogues.

The distribution of the analogues should reflect the distribution of radionuclides, considering the fluid and rock conditions will repeat in a future fracturing and vein filling event. With this approach, one may consider the distribution of U, Th, La, Nd, Br, Sr and Ba as being representative of the radionuclides of Pu, Np, Cm, Am, I and Ra. Ra occurs in aqueous solution as Ra+2 with very similar chemistry to Sr and Ba. Also existent Sr sorption data are in agreement with in situ geochemistry of Ra (2). The analogy between Th and Pu is mentioned in (3), (4) and (5). Airey and Ivanovich (3) although recognizing the several oxidation states for Pu, indicate that in a moderate Eh and pH range, characteristic of most natural environments including those potential disposal sites, a similar behaviour is expected for Pu and Th. These same authors, addressing other works, indicate the "striking" similarity in equilibrium constants for the two elements. Further, they refer to the similar behaviour of Np+4 and U+4. In addition, Krauskopf (5) points out that the stable solid form for both elements under most conditions, is the dioxide and that the principal dissolved species in equilibrium with it is the undissociated hydroxide. In the same paper he indicates a partial analogy between Th and Np. These elements present similar concentrations in a great part of the Eh and pH ranges expected in a repository. Nd is similar to Am and Cm since they are present in the natural environment in the +3 oxidation state and the ionic radii of such ions are approximately identical (Nd+3 = 1.05 A, Cm+3 = 1.06 A and Am+3 = 1.05 A). Also since La chemical properties are similar to Nd, both elements are used as analogues of Cm and Am (3). Eisenbud et al. (4) and Krauskopf (5) also refer to La and Nd as analogues for Cm and Am. Br and I are geochemically similar. They are both biophilic elements and are enriched in organic rich soils and sediments (6). The use of Br as an analogue for I is also suggested by Cramer (7). This means that depending on the concentration of radioelements that enter the rock system, their distribution can be approached by the analysis

of the distribution of their analogous elements. This paper presents the results of natural element (or respective oxide) distruibution accross veins in the East Bull lake gabbro-anorthosite intrusion as a guide for the interpretation of matrix diffusion of radionuclides.

1.2 Sampling and sample description:

Eight samples from depths varying between 25.90 m to 736.50 m in drill cores EBL 1 and EBL 2 were selected for major and trace elemente analysis. Figure 2 provides the location of drill holes that are correlated in figure 3. The samples included portions of drill core represented by anorthosites, gabbros and troctolites. X-ray fluorescence was used to determine whole rock geochemistry. Detection limits for this method are around 0.01 % for major elements and 10 ppm for trace elements (8). Thorium was determined by instrumental neutron activation with 0.1 ppm detection limit. Uranium levels were determined by neutron activation using the delayed neutron counting technique. Samples were crushed in an agate mill to 200 mesh for analysis. The agate mill adds 0.1 - 0.3 % silica to the actual rock content (8). Analysis were performed by X-ray Assay Laboratories.

Gabbro and anorthosite samples show partial metamorphism to greenschist facies. The original mineralogy is mainly represented by clinopyroxene (augite and pigeonite), high temperature plagioclase (andesine-labradorite), opaques (magnetite?) and traces of intergranular quartz. Plagioclase is altered to clinozoisite, zoisite, and subordinately, sericite. The metamorphic minerals do not replace the plagioclases entirely, usually occupying twinning planes or porphyroblastic inclusions. In general, no more than 30 % by volume of feldspars are replaced by metamorphic minerals. Mafic minerals are altered to tremolite-actinolite and hornblende. Chloritization is also a major feature with chlorite filling microfractures. This alteration due to metamorphism affects almost 70% (by volume) of the original mafic minerals.

Troctolite samples are represented by olivines, augite, minor orthopyroxene, labradorite-bytownite and biotite. Alteration minerals include iron oxides, serpentine, chlorite and talc (?).

Studied veins fill macrofractures of drill cores. These contain mainly prehnite, calcite, quartz, chlorite and epidote as filling material. Quartz veins are generally sheared. Veins show well defined boundaries in sharp contact with the wall rock constituting a straight plane. Lateral continuity of veins is apparently large as indicated in some outcrops in the area. The thickness of vein filling macrofractures varies approximately between 2 and 8 mm. Core samples show that veins may be accompanied by up to 7 cm of alteration (dispersion ?). Displacement along vein is predominantly perpendicular to the walls, indicating tensional stress (Plate 1). Alternatively quartz-filled

fractures are usually accompanied by some shearing (Plate 2). Veins are generally multilayered suggesting a paragenetic sequence of chlorite, followed by calcite, prehnite, feldspars, quartz, chlorite again and calcite. A lack of oriented core samples for the present study precluded delineation of macrofracturing trends. Some data obtained for EBL 1 cor samples, how ever, shows fracture planes dipping from 10o to 65o .

Samples were obtained from each vein and respective wall rock at variable distance from the vein. The results were plot in a binary diagram of percentage with distance to the vein.

1.3Results:

The results show that vein chemistry is very simple in agreement with a simple mineralogy as observed in thin sections and X-ray diffraction analysis. The predominant elements in veins are Si, Al, Ca, Fe and volatiles (H2O, CO2). Locally (one sample) K is high. Among the trace elements, Ba and Cr are the most important. In relation to the intrusion, veins are low in TiO2, MnO, MgO, Na2O, Fe2O3 (total), Sr, Th and Cr. They are enriched in CaO, H2O + CO2 + other volatiles (LOI) and Rb. They are practically invariable, when compared to wall rock, in terms of mean SiO2, Al2O3, Nb and P2O5 content.
Ba and K are generally low and similar to wall rock values.

How far into the wall rock vein alteration occurs, indicate how far matrix diffusion may happen. These data can be obtained from the observation of element concentration with distance to veins diagrams. These are diagrams are constituted by individual lines that roughly represent distinct levels inside the East Bull lake intrusion and its different rock types. When shallow and deep samples present opposite behaviour, in relation to their chemical content across veins, it suggests that besides local fluid mobility, vertical mobility throughout the pluton is redistributing elements along veins. As a consequence, the resulting regression analysis for all samples should be very poor for this element or be represented by a regression line close to the horizontal, near the veins. A similar distribuition of elements, across veins, with depth, represented by individual distribution lines of similar trend, means that the element remained mostly in the wall rock (immobile element) or was carried out of the system during vein alteration. These two cases are possible when general depletion towards vein is observed. On the other hand, if a general increase towards vein is observed for a particular element and it is not accompanied by a relative depletion of the element in the wall rock, when compared to similar rock types, this may represent an addition to the system.

The establishment of a regression line for each element or oxide in relation to vein distance is done with the intent of defining how an element concentration varies

with distance to vein due to alteration.

The applied regression models followed equations I, II, III and IV. Nonlinear regression analysis was done by the Gauss method.

$Y = B_1+(B_2 X)^{B_3}$ equation I

$Y = B_1+B_2X^{B_3}$ equation II

$Y = B_1+B_2B_3^{X}$ equation III

$Y = B_1+B_2e^{(XB_3)}$ equation IV

where:

Y = element concentration (% or ppm)

X = distance to veins (cm)

B_1 = initial concentration (constant)

B_2 and B_3 = regression factors

Besides regression parameters, important data to be considered during evaluaton of the regression results is the sum of squares of the residues (S) (Table 1). The larger the (S), the poorer the regression fit. However, this does not mean very much if one does not take into account the graphical representation. It is suggested here that poor regression is a reflection of variation in the concentration of the element in the percolating fluid, and consequently its final concentration across the rock. It is also evident, from element concentration data and observation of graphics, that S equal or very close to zero only means a smaller sample with concentrations close or at the detection limit of a particular element, or yet that element concentration is given by small numbers (low order of magnitude). This last case occurs because the sum of the squares of residuals does consider the absolute difference between observed and predicted values. It is this author's opinion that a better evaluation of the regression quality would be given by the mean value and standard deviation to zero the better the regression. However it is out of the scope of this work to discuss mathematical aspects. What is important is the similarity of the resulting regression line to the individual distribution lines. The variable depth and/or rock composition could be introduced as an attempt to obtain better regression lines. However, if these variables affect the regression results, a correction of the constant value (B_1) may provide the necessary adjustment of the regression function to the respective element distribution. Therefore, if the individual distribution lines are similar to the regression curve, the regression can be adjusted as function of rock type (composition) or depth as desired. This adjustment, by varying constant value, should also be used to estimate radionuclide distribution as mentioned before.

Data for La, Nd, Cs, Zr and Y are not suitable or analytically representative or at least do not show a defined trend in the present study. However, for radioelements belonging to the Th, U and Sr family (Figures 4,5 and 6) and their analogues it is possible to estimate their distribution, in case of release into the rock, by the respective regression analysis for these elements. Iodine and Br were not detected in this study.

As observed in the diagrams distance to veins with element concentration, "matrix diffusion" occurs in distances varying between 3.2 and 6.5 cm from the vein (fluid source). The wall rock composition is affected closer to vein, mainly for Ba (3.2 cm)(Figure 7), while U and Sr seem to go as far as 6.5 cm into the wall rock. All the major elements (except Fe2O3) concentration varies up to 5.0 cm far from veins. The same happens for Sr with exception of the deepest anorthosite samples. Dispersion of iron (Figure 8), titanium (Figure 9), volatiles (Figure 10) and rubidium (Figure 11) occur as far as 4.0 cm from the fluid source. Th is between the "matrix diffusion" of Ba and most major elements while P2O5(Figure 12) follows most of the major elements. This means that elements like U and Zr (Figure 13) or their radionuclide analogues, will show the highest diffusion from a fluid percolating a major fracture. They will be followed by all the major elements, except Fe and Sr. Among the least dispersive elements are Ba and Th. Comparatively, Fe, Ti and Rb will show intermediate dispersion. Notice that this behaviour is exclusively related to the physico-chemical conditions of the percolating fluid and solid media at East Bull lake and cannot be extrapolated for different conditions. It is interesting to note, however, that this behaviour is particularly in accordance with the relative mobility of U, Th, Ba and Rb in geologic media. On the other hand the pronounced diffusion of Zirconium, a relatively immobile element, may be justified by its association with Uranium in some minerals.

REFERENCES:

1. MILNES, A.G. (1985). Geology and radwaste. Academic press inc. (London) Ltd. 328 pp. London.
2. McKINLEY, I. G. and HADERMAN, J. (1984). Radionuclide sorption database for Swiss safety assessment. EIR-Berich Nr. 550/NAGRA NTB 84-40 report. 108 pp. Wurenlingen.
3. AIREY, P.L. and IVANOVICH, M. (1984). Geochemical analogues of high level radioactive waste repositories. In Smellie, A.T. (ed.), SKB technical report 84-18 - Natural analogues to the condition around a final repository for high-level radioactive waste - Proceedings of the natural analogue workshop held at Lake Geneva, Wisconsin, U.S.A. (October 1-3, 1984), pp. A3:1 - A3:18.
4. EISENBUD, M., KRAUSKOPF, K., PENNA FRANCA, E., LEI,W., BALLARD, R., LINSALATA, P. and FUJIMORI, K. (1984). Natural analogues for the transuranic actinide elements: an investigation in Minas Gerais, Brazil. In Smellie, A.T. (ed.), SKB technical report 84 -18 - Natural analogues to the condition around a final repository for high-level radioactive-waste. Proceedings of the natural analogye workshop held at Lake Geneva, Wisconsin, U.S.A. (October 1 - 3,

1984),pp.C1:1.
5. KRAUSKOPF, K. (1984). Thorium as an analogue for plutonium and rare earth metals as analogues for heavier actinides. In Smellie, A.T. (ed.), SKB technical report 84 - 18 - Natural analogues to the condition around a final repository for high-level radioactive-waste. Proceedings of the natural analogue workshop held at Lake Geneva, Wisconsink, U.S.A. (October 1 - 3, 1984), pp. C2:1 - C2:19.
6. FUGE, R. (1974). Bromine - 35 O. II. Relation to the other halogens. In Wedepohl, K.H. (exec. ed.), Handbook of Geochemistry, Vol. II-3, pp. 35-O-1.
7. CRAMER, J.J. (1984). Natural analogues to nuclear fuel waste disposal in crystalline rocks: an overview. In Smellie, A.T. (ed.), SKB technical report 84 - 18 - Natural analogues to the condition around a final repository for high-level radioactive-waste. Proceedings of the natural analogue workshop held at Lake Geneva, Wisconsin, U.S.A. (October 1 - 3, 1984),pp. A4:1 - A4:17.
8. X-RAY ASSAY LABORATORIES LIMITED (XRALL)(APRIL 1984). Schedule of fees and services. 9pp. Don Mills, Ont., Canada.

TABLE 1: Non linear regression parameters. All Y results in % except for (*) = ppm.

Y	B1	B2	B3	S	Equation
SiO_2	53.733847	-0.63944548	-0.78955302	1064.365	2
Al_2O_3	-63.337	0.998	83.192	538.925	1
CaO	12.942061	1.0001023	-6133.6692	1181.6178	3
MgO	3.0257435	0.94892401	0.79246115	365.237	2
Na_2O	-34.229	1.002	36.649	56.551	1
K_2O	0.162	0.904	1.075	25.707	1
Fe_2O_3	4.514988	1.0223161	0.73538204	321.877	2
MnO	-4.329	1.002	4.386	0.049	1
TiO_2	0.10934276	0.034433112	0.66293853	0.265	2
P_2O_5	0.029858475	0.008422027	0.19602594	0.015	2
LOI	148.68881	-144.54875	-0.0012426153	67.550	4
Th*	-0.73620203	1.0000917	68.443155	0.875	3
U*	-0.77437247	1.0001000	-11.166497	0.251	3
Cr*	-22328.672	1.002	22412.688	3.871×10^6	1
Rb*	3683.8513	-3632.5150	0.00091212852	3.206×10^4	4
Nb*	-32.319	1.002	50.892	2172.122	1
Y*	8.999	1.000	1.000	zero	1
Zr*	17.946	0.717	11.155	2174.971	1
Sr*	-282.664	-0.999	523.625	4.555×10^5	1
Ba*	42237.314	-41802.778	0.00082436699	1.601×10^6	4

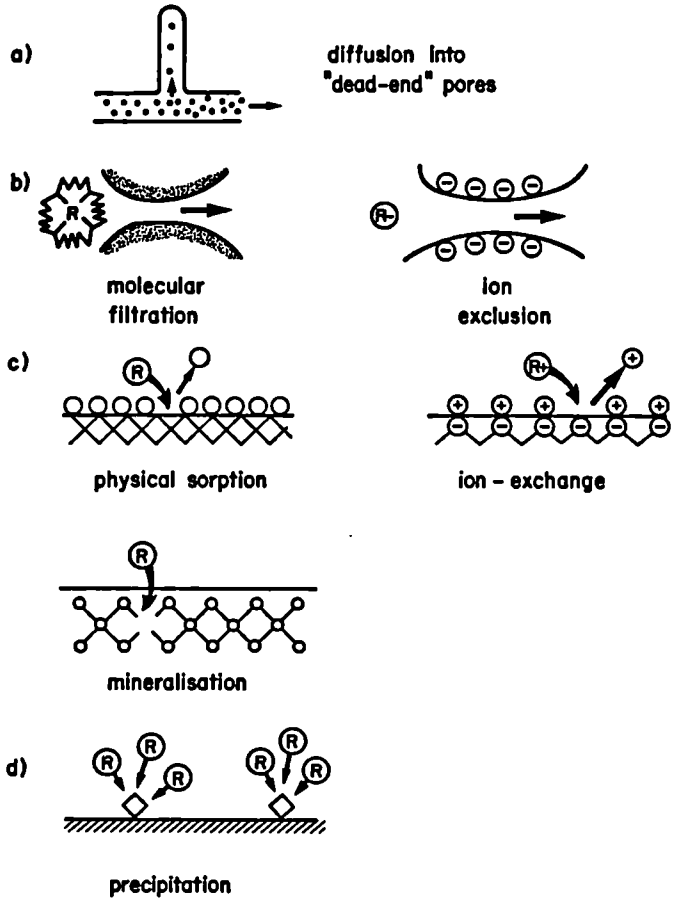

FIG. 1 . Sorption mechanisms (after McKinley and Hadermann, 1984).

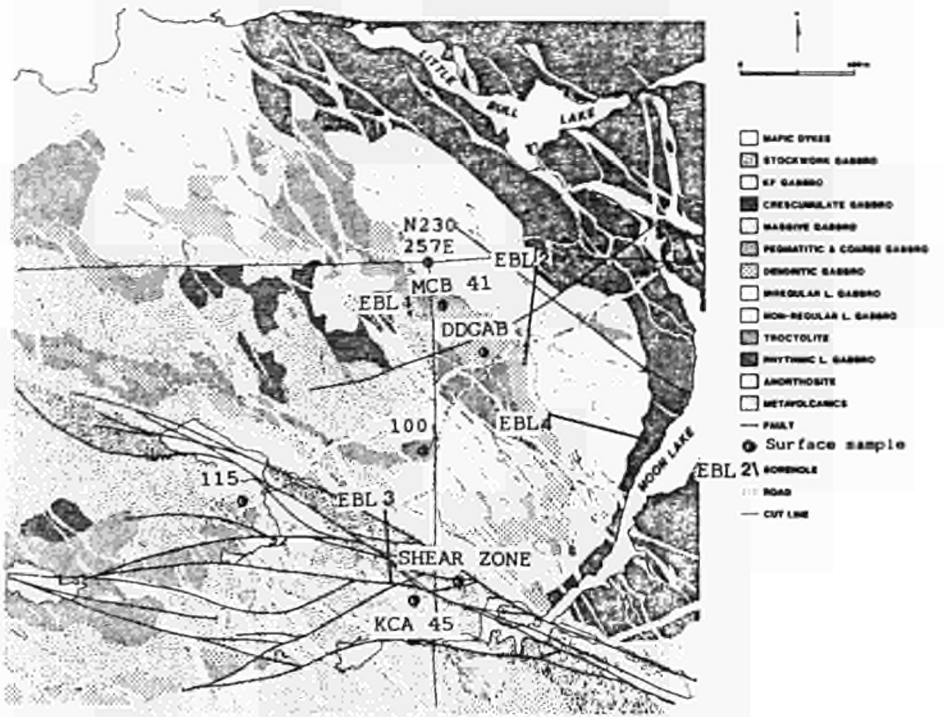

FIG. 2 . Surface sample and drillhole location. (Geology after Ejeckam et al., 1985).

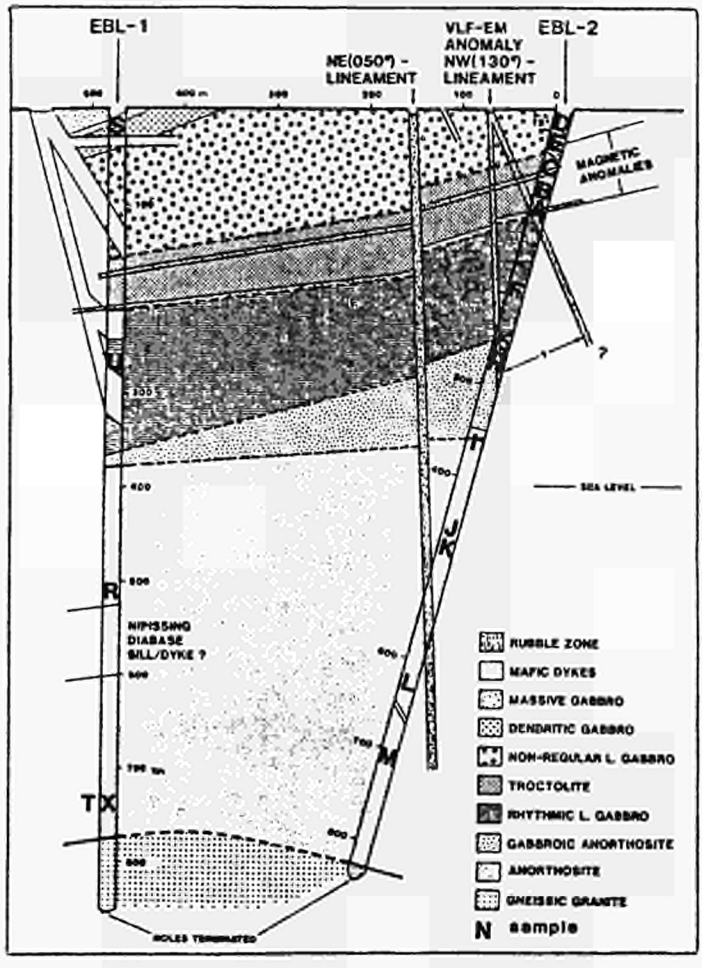

FIG. 3 . Geologic cross section through EBL-1 and EBL-2 drill holes (after Ejeckam et al., 1985).

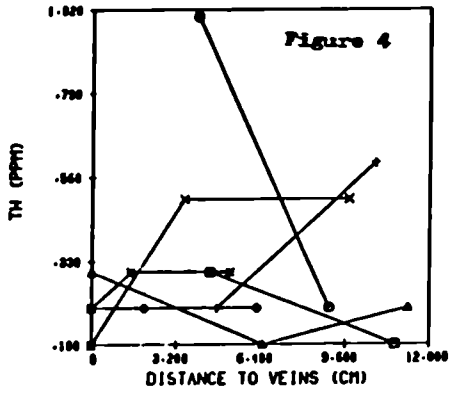
Figure 4
TH (PPM)
DISTANCE TO VEINS (CM)

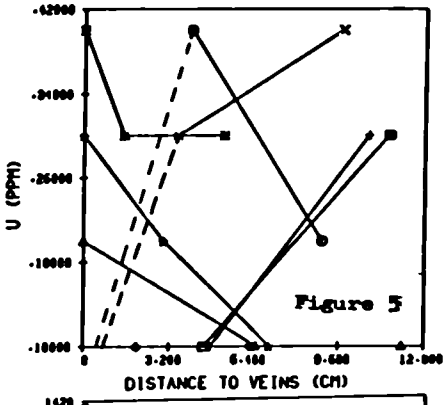
Figure 5
U (PPM)
DISTANCE TO VEINS (CM)

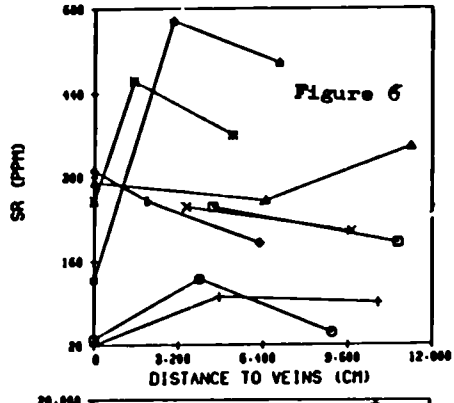
Figure 6
SR (PPM)
DISTANCE TO VEINS (CM)

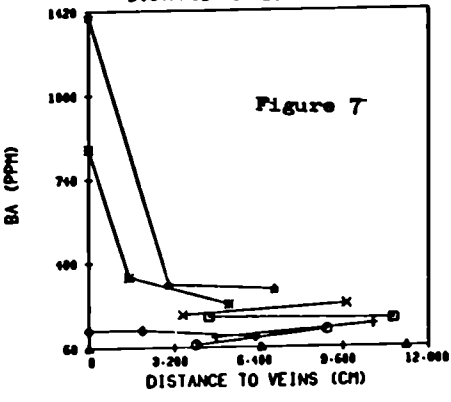
Figure 7
BA (PPM)
DISTANCE TO VEINS (CM)

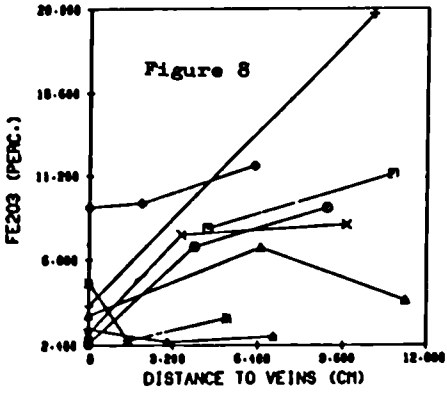
Figure 8
FE203 (PERC.)
DISTANCE TO VEINS (CM)

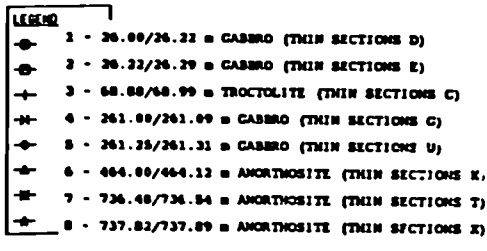
LEGEND
1 - 26.00/26.22 m GABBRO (THIN SECTIONS D)
2 - 26.22/26.29 m GABBRO (THIN SECTIONS E)
3 - 60.80/60.99 m TROCTOLITE (THIN SECTIONS C)
4 - 261.00/261.09 m GABBRO (THIN SECTIONS G)
5 - 261.25/261.31 m GABBRO (THIN SECTIONS U)
6 - 464.00/464.12 m ANORTHOSITE (THIN SECTIONS K)
7 - 736.48/736.84 m ANORTHOSITE (THIN SECTIONS T)
8 - 737.82/737.89 m ANORTHOSITE (THIN SECTIONS X)

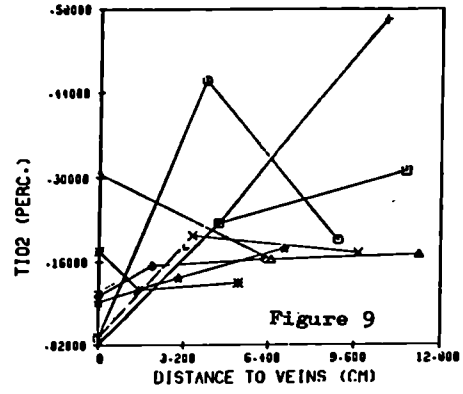
TIO2 (PERC.)
.58000
.44000
.30000
.16000
.02000
Figure 9
0
3.200
6.400
9.600
12.000
DISTANCE TO VEINS (CM)

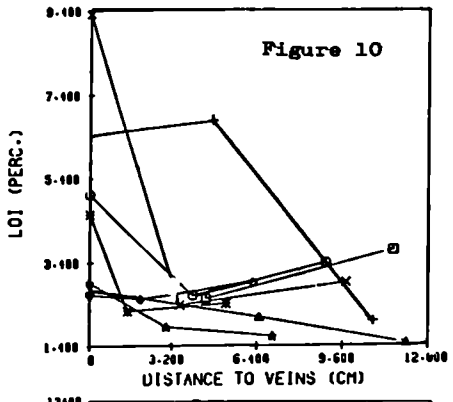
LOI (PERC.)
9.400
7.400
5.400
3.400
1.400
Figure 10
0
3.200
6.400
9.600
12.000
DISTANCE TO VEINS (CM)

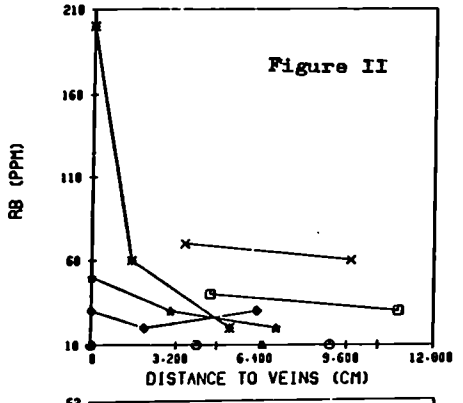
RB (PPM)
210
160
110
60
10
Figure II
0
3.200
6.400
9.600
12.000
DISTANCE TO VEINS (CM)

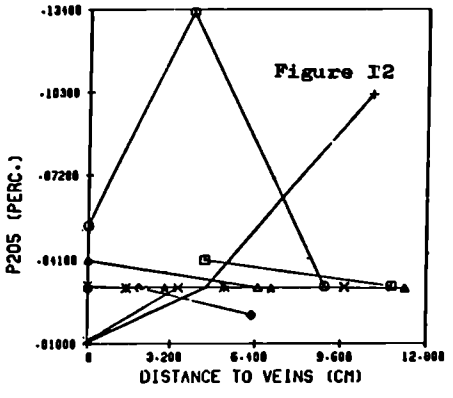
P205 (PERC.)
.13400
.10300
.07200
.04100
.01000
Figure I2
0
3.200
6.400
9.600
12.000
DISTANCE TO VEINS (CM)

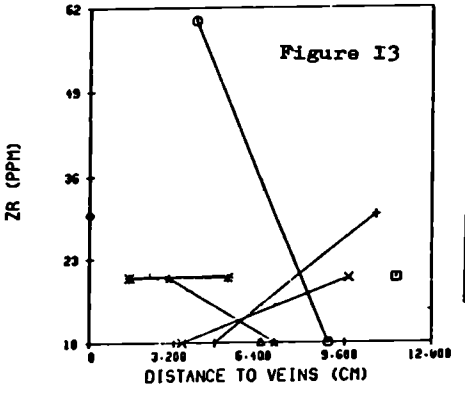
ZR (PPM)
62
49
36
23
10
Figure I3
0
3.200
6.400
9.600
12.000
DISTANCE TO VEINS (CM)

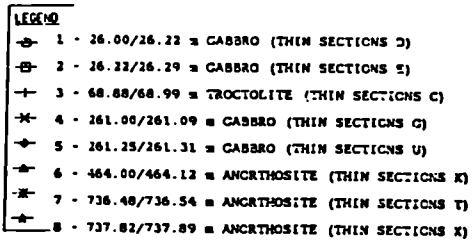
LEGEND
1 - 26.00/26.22 = GABBRO (THIN SECTIONS D)
2 - 26.22/26.29 = GABBRO (THIN SECTIONS E)
3 - 68.88/68.99 = TROCTOLITE (THIN SECTIONS C)
4 - 261.00/261.09 = GABBRO (THIN SECTIONS G)
5 - 261.25/261.31 = GABBRO (THIN SECTIONS U)
6 - 464.00/464.12 = ANORTHOSITE (THIN SECTIONS K)
7 - 736.48/736.54 = ANORTHOSITE (THIN SECTIONS T)
8 - 737.82/737.89 = ANORTHOSITE (THIN SECTIONS X)

MARYSVALE NATURAL ANALOG STUDY: FEASIBILITY PHASE ANALYTICAL RESULTS

Michael Shea
Office of Waste Technology Development
Battelle Memorial Institute
7000 S. Adams St.
Willowbrook, IL 60521 USA

SUMMARY

The Marysvale Natural Analog Study is being conducted by the Office of Waste Technology Development for the U.S. Department of Energy. The major focus of this study is the elucidation of the mass transport of nuclides in a hydrothermal system associated with some uranium (uraninite-pyrite-fluorite) veins within quartz monzonite and granite. The objectives of the study include: (1) determining the nature of the mineralizing hydrothermal system in terms of thermal, spatial, temporal, and chemical parameters; (2) determining the extent of the element/fluid migration; and (3) identifying the geochemical and geohydrologic processes controlling this movement. Feasibility phase analytical results include: (1) the importance of identifying fractures within the host rock; (2) the detection of the mobility and immobility of some very important and extremely important radionuclides of concern; (3) the modelling of Ar transport will help define non-sorptive, conservative mobility parameters within the fractured granitic rock.

1.0 INTRODUCTION

The purpose of the Marysvale Natural Analog Study study is to measure and model mass transport associated with some hydrothermal uranium-molybdenum veins that have been deposited within epizonal granitic rocks (quartz monzonite and granite) near Marysvale, Utah. This natural analog study will help elucidate processes of mass transport which may be applicable to radioactive waste isolation. The study is investigating the spatial distribution of selected elements and their nuclides upon whole rock, mineral, and water samples from the study area.

Previous geological studies in the region include work by [1, 2, 3, 4, 10]. these studies were concerned with the general geology of the Marysvale region, and with the mineralogy and formation of the ores. The Marysvale area has also been studied as a natural analog for radwaste isolation [5, 6, 8]. Some of the results reported here have been presented earlier [8, 9].

2.0 RESULTS TO DATE

2.1 Oxygen and Hydrogen Stable Isotopes

Preliminary results based on oxygen isotope data have been reported [7, 8]. The principle conclusion drawn from whole-rock oxygen and hydrogen isotopic data is the high degree of control by fractures on the movement of the hydrothermal fluids. The a priori conceptual model (working hypothesis) anticipated that the main controls of the hydrologic regime would be large scale discontinuities, e.g. fault planes. The host rock between these major hydrologic features was assumed, as a first approximation, to behave isotropically in relation to the hydrothermal effects. However, the hydrothermal fluids did not behave as pervasively as anticipated, but were controlled by smaller scale discontinuities, e.g. fractures [8].

The $\delta^{18}O$ values for plutonic rocks (quartz monzonite and granite) of the Marysvale study area range from +6.7 to +0.1 per mil. The initial $\delta^{18}O$ values for quartz monzonite and local meteoric water are estimated to be approximately +7 and -14 per mil, respectively (Figure 1). Meteoric water similar to that found today is believed to have been the source for the hydrothermal fluids. Model calculations for apparent water/rock ratios at 200 C range from <0.1 to ~1 [10].

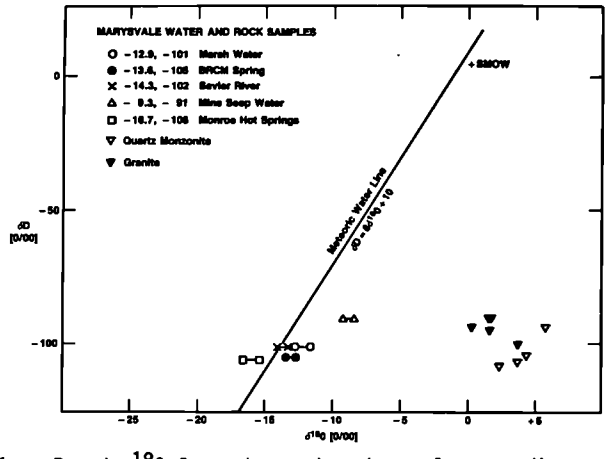

Figure 1. δD and $\delta^{18}O$ for water and rock samples near Marysvale, Utah. Rock samples show oxygen isotope shift due to equilibration with water similar to modern meteoric values around Marysvale.

A sample containing a quartz monzonite-granite interface exhibits a notable depletion in ^{18}O in subsamples nearest to the boundary, relative to distal subsamples [8]. This suggests that there was enhanced water/rock interaction at the interface, either by increased fluid flow or residence time, and that the hydrothermal event post-dates the emplacement of the quartz monzonite and granite.

Preliminary oxygen and hydrogen isotopic analyses have also been performed on mineral separate samples. These analyses suggest substantial ^{18}O isotopic heterogeneities among minerals presumably from hydrothermal alteration. Equilibrium temperatures calculated from some mineral pairs appear to fall within the range of plutonic cooling.

2.2 Elemental Analysis

Whole rock and mineral samples have been analyzed for major, minor, and trace elements by various methods, including ICP, XRF, and INAA. These analyses are used to note elemental distribution within the mineralized hydrothermal system, and support other techniques, suck as isotopic analyses. Covarience analysis is being used to determine if there is any coupling between elements within the system.

Of particular interest is the distribution of the Rare Earth Elements (REE). This group includes some elements that either themselves have been identified as radwaste nuclides of concern, or can proxy for such nuclides. The REE pattern for the quartz monzonite is typical of normal plutonic rocks, and explainable by usual petrologic processes. The conventional REE/chondrite patterns for the Marysvale quartz monzonite show no apparent distinction between those hydrothermally altered and unaltered (Figure 2). With regard to the quartz monzonite-granite contact sample mentioned above, each subsample pair is indistinquishable from its mate, although the ^{18}O data show a marked change (Figure 3). Thus, it appears again that the hydrothermal event had no appreciable affect upon the REE pattern of typical quartz monzonite or granite, although some small amount of change (<10%) would not be discernible.

A parallel statement regarding hydrothermally altered and unaltered granite cannot be made since there are no corresponding "fresh" granite samples. However, REE/chondrite patterns for two subsamples from a granite sample containing a cross-cutting ore vein are distinctly dif-

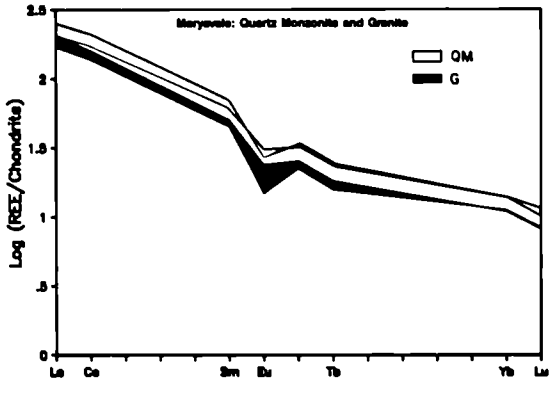

Figure 2. REE/Chondrite normalized data for Marysvale whole-rock samples. Patterns are typical of normal plutonic processes. There is no apparent effect from hydrothermal alteration

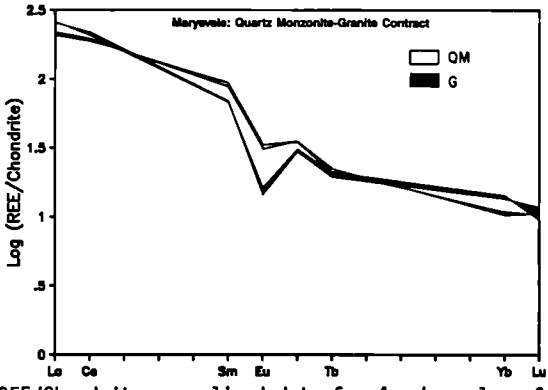

Figure 3. REE/Chondrite normalized data for 4 subsamples of an intrusive contact sample from Marysvale, Utah. Even though $\delta^{18}O$ values for each subsample pair are markedly different, REE patterns are analytically indistinguishable.

ferent from other granite samples (Figure 4). It is interesting to note that the subsample nearest (~1 cm) the vein (MVF-53A) shows Ree depletion relative to the subsample (MVF-53B) furthest (~5 cm) from the vein, possibly indicating leaching of REE in the granite by the hydrothermal fluids after an initial REE enhancement. Further, these REE/chondrite patterns are quite similar to those for ore vein samples (Figure 5), indicating the influence of the mineralizing hydrothermal fluids on the granite near the cross-cutting vein. Ore sample MVF-11 may represent ore deposited by fluid which had partially equilibrated with the enclosing plutonic rock.

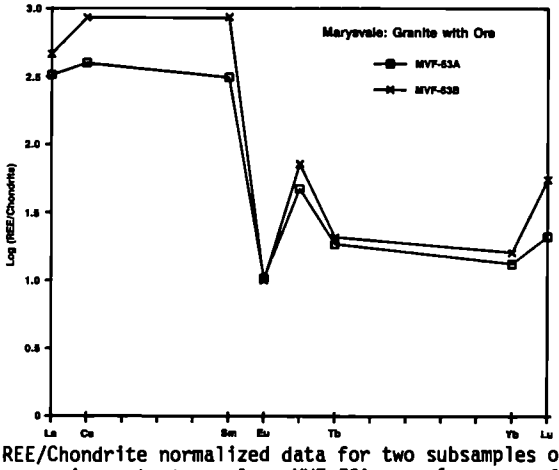

Figure 4. REE/Chondrite normalized data for two subsamples of granite/ore vein contact sample. MVF-53A was ~1 cm away from vein. MVF-53B was ~5 cm away. Patterns indicate that hydrothermal fluids did not act as simple REE enrichment. Patterns are also markedly different from other granite samples.

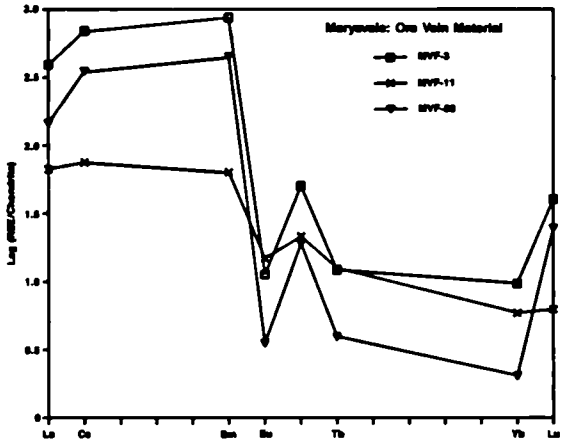

Figure 5. REE/Chondrite normalized data for three ore samples from Marysvale, Utah. Patterns show marked difference between ore and plutonic rocks. MVF-11 may represent ore fluid more equilibrated with plutonic rock.

2.3 Ar-Ar

The $^{40}Ar/^{39}Ar$ method of age dating has been used on some selected hydrothermal biotite and chlorite separates from both plutonic host rock bodies. The results give flat and reproducible plateau ages, and suggest that excess argon 40 is present within the biotite phases of the quartz monzonite (Figure 6). The apparent excess Ar 40 may have been extracted from the surrounding country rocks, or due to recoil loss of 39 Ar during irradiation.

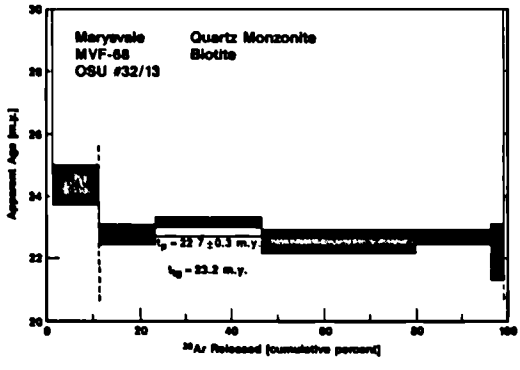

Figure 6. ^{39}Ar release spectra for biotite from a relatively undisturbed ($\delta^{18}O$ = +6.7) quartz monzonite sample near Marysvale, Utah. Spectra may show evidence of excess Ar.

The $^{40}Ar/^{39}Ar$ biotite ages of the granite is analytically indistinguishable from quartz monzonite biotite ages (Figure 7). Chlorite sepctra from the granite are disturbed, and show evidence for excess ^{40}Ar (Figure 8). Plateau minimums for granite chlorites have no apparent age significance.

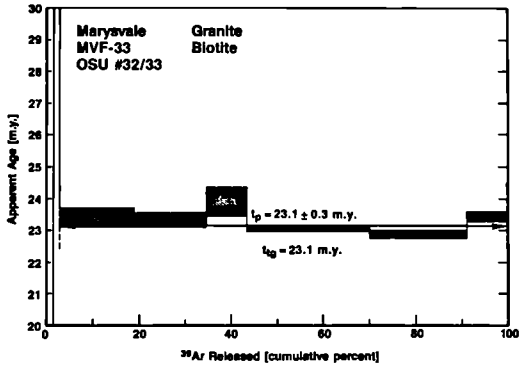

Figure 7. ^{39}Ar release spectra for biotite from a typical ($\delta^{18}O$ = +1.3) granite sample near Marysvale, Utah. Even though there is no apparent evidence for excess Ar, plateau age is greater than quartz monzonite which is intruded by granite.

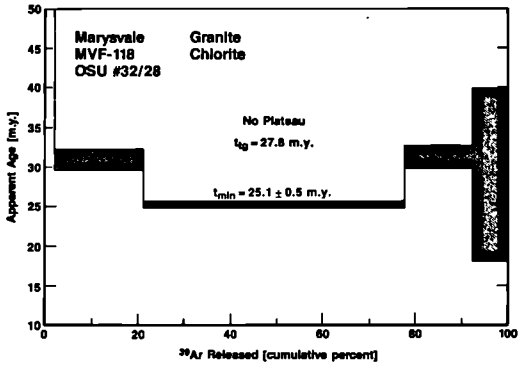

Figure 8. ^{39}Ar release spectra for chlorite from a typical ($\delta^{18}O$ + 1.2) granite sample near Marysvale, Utah. Sample shows evidence of excess Ar. Plateau minimum has no apparent age significance.

The Ar/Ar age of biotite from a quartz monzonite sample (MVF-1) within a foot of a major ore vein is apparently unaffected, although there is some evidence of excess ^{40}Ar (Figure 9). The non-resetting of the biotite indicates that the hydrothermal system was less than ~300 C, the closure temperature for biotite. The Ar release spectra from chlorite of the same sample shows strong evidence of excess ^{40}Ar. The plateau minimum age is similar to the reported age of mineralization (18-19 m.y.).

Previous age dating by others, using various standard methods, has shown a large spread in ages for both intrusive bodies. The new Ar/Ar data will result in revisions to the previously proposed chronology of igneous activity at Marysvale. Biotite from a relatively undisturbed ($\delta^{18}O$ = +6.2) quartz monzonite sample (MVF-66) has been used as an internal monitor, with a determined age of 22.8 +/- 0.3 m.y. A new Ar/Ar application which is able to more precisely determine age differences will be attempted in order to distinguish the quartz monzonite and granite ages.

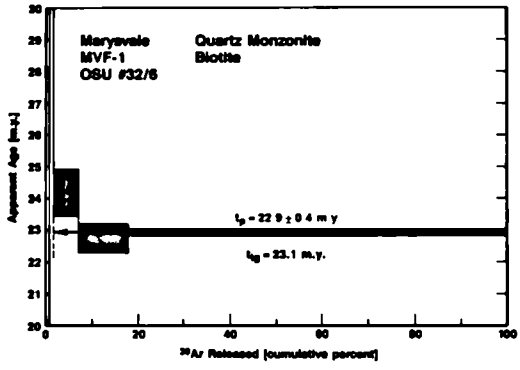

Figure 9. ^{39}Ar release spectra for biotite from a quartz monzonite sample ($\delta^{18}O$ = + 2.3) approximately 1 foot from a major mineralized vein. The age is slightly greater than that for fresh quartz monzonite. Spectra may show evidence for excess Ar.

2.4 Uranium and Thorium Disequilibrium

Preliminary, low precision alpha spectroscopy has been used on selected rock samples to determine the activities of thorium 228, 230, 232, and uranium 234, 235, 238. Based upon these data, it appears that the quartz monzonite host rock has experienced a preferential leaching of uranium over thorium within the recent past (<1 million years) relative to the reported mineralization age of ~18 million years (Cunningham et al., 1982). The apparent disequilibrium is markedly high (Figure 10). Further work, using more a precise technique, is planned.

2.5 Rb-Sr

Rb and Sr isotopic compositions have been determined for selected quartz monzonite and granite whole-rock samples. Both data sets have been plotted on Sr-evolution diagrams (Figures 11 and 12).

The Rb-Sr data for the quartz monzonite shows that the rock has been variably disturbed in terms of Rb-Sr systematics. The "isochron age" obtained (28.2 +/- 5.6 m.y.)has a linear regression correlation coefficient (0.8943) insufficient to allow age significance to be applied to a best fit line. This may be due to the relatively small range in $^{87}Sr/^{86}Sr$ ratios (~0.7-1.4). It is anticipated that planned mineral separate Rb-Sr

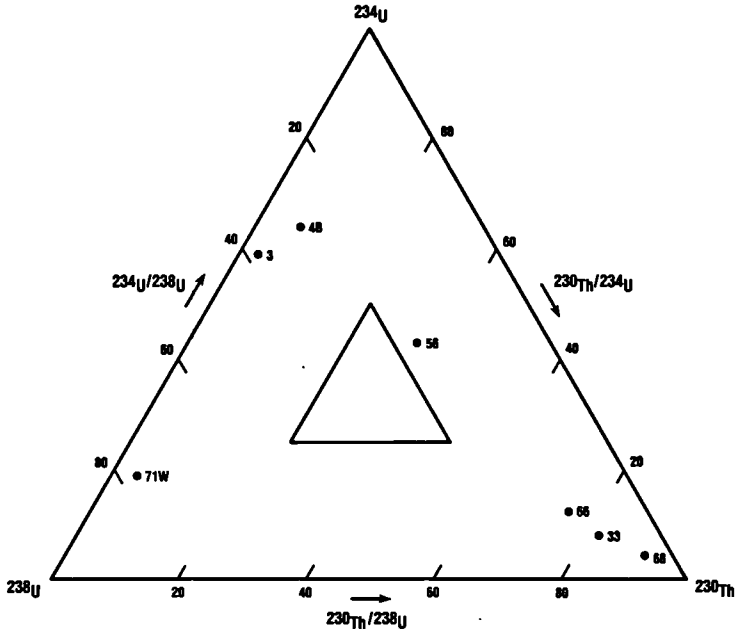

Figure 10. Ternary activity diagram for activity ratios from Table 2b for Marysvale samples. These preliminary values show evidence for marked U-Th disequilibrium in the recent past (<1 million yrs). Typical values plot within central triangle.

analysis of biotite, K-feldspar, and plagioclase will allow meaningful age dating by this technique. The preliminary Rb-Sr "age" obtained is significantly higher than the Ar/Ar age. If Rb-Sr whole-rock and mineral separate systematics continue to give an age older than the Ar/Ar age, this would imply that (1) there is a significant difference between the "cooling" ages of RB/Sr and Ar/Ar for the Marysvale quartz monzonite, or (2) the quartz monzonite has either lost Rb or gained radiogenic from the quartz monzonite "isochron" (0.705393 +/- 0.000089) may indicate some degree of crustal contamination.

The granite whole-rock Rb-Sr data gives an apparently significant (r=0.9969) "age" of 35.3 +/- 1.2 m.y. and an initial $^{87}Sr/^{86}Sr$ value of 0.705274 +/- 0.000104. The apparent "age" of the granite is markedly higher than that of the quartz monzonite, and is therefore not geologically significant, since the granite is known to cross-cut and intrude into the quartz monzonite. The granite is ubiquitously altered, and therefore likely to have had its Rb-Sr isotopic composition disturbed. This disturbance is possibly responsible for the apparent isochron.

The initial isotopic Sr values of the quartz monzonite and granite are analytically indistinquishable, and support the hypothesis that the two intrusives are consanguineous.

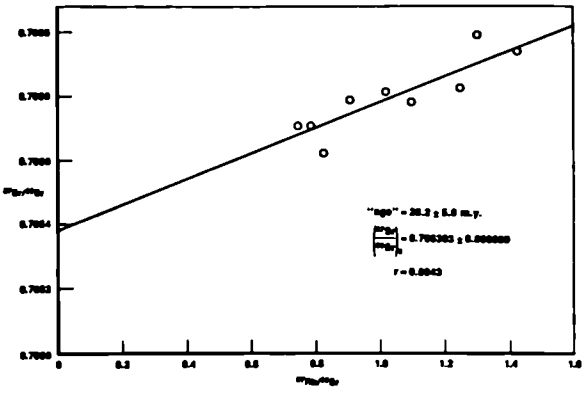

Figure 11. Whole-rock Rb-Sr "isochron" of the quartz monzonite central intrusive near Marysvale, Utah. The samples have been variably disturbed giving a correlation coefficient too low to allow age significance to be applied to the slope of the line.

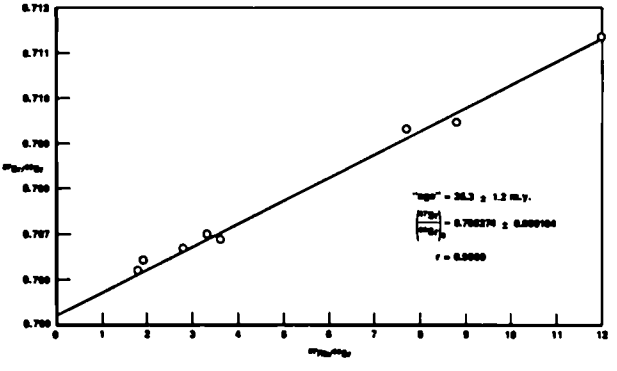

Figure 12. Whole-rock Rb-Sr "isochron" of fine grained granite near Marysvale, Utah. Even though the correlation coefficient might allow time significance to be placed on the slope of the line, the age derived is too old based on Ar/Ar and field relationships.

Further study of these initial isotopic Sr values may help elucidate the nature of possible mass transport processes.

Whole-rock granite $^{87}Sr/^{86}Sr$ and $1/Sr$ data appear to lend themselves to a double-mixing model (Figure 13). The data suggest that a water/rock interaction of relatively radiogenic ^{87}Sr rich hydrothermal water with granite is superimposed on an earlier, non-hydrothermal "petrologic" mixing trend. The petrologic mixing may be due to deuteric, second boiling processes, or subliquidus assimulation and mixing of xenolithic material.

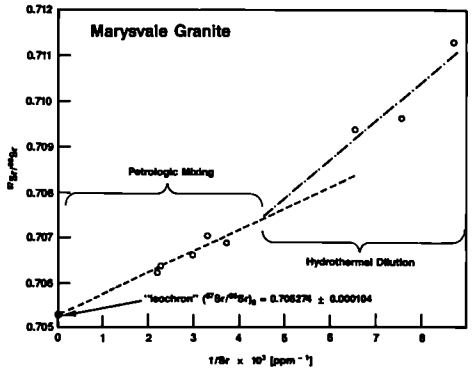

Figure 13. Whole-rock $^{87}Sr/^{86}Sr$ and 1/Sr mixing lines for fine grained granite near Marysvale, Utah. Fitting of two mixing lines through data suggest that there may be a mixing of relatively radiogenic Sr rich water with granite (hydrothermal dilution), superimposed on a previous, non-hydrothermal mixing trend (petrologic mixing).

3.0 CONCLUSIONS

3.1 Major Findings

- hydrothermal fluids highly controlled by fractures (not just large scale faults).

- ^{18}O distribution is heterogenious down to the meter scale.

- ^{18}O distribution is heterogenious among various minerals due to hydrothermal alteration.

- REE were apparently immobile during hydrothermal event except in proximity (~1 cm) to veins.

- REE patterns for ore samples are distinct from granitic rocks.

- ore fluid REE pattern apparently superimposed on rock REE pattern close to veins.

- excess Ar present in measured phases may be an effective tracer of fluids through quartz monzonite.

- new Ar ages will result in revisions to the previously proposed chronology of igneous activity at Marysvale.

- Ar spectra plateaus apparently unaffected even in proximity to veins (<0.3 m).

- non-resetting of biotite Ar ages indicates fluids <300 C.

- preliminary U and Th activity measurements indicate marked disequilibrium.

- there has been apparent leaching of U within the recent past (<1 million years).

- Rb-Sr systematics disturbed by hydrothermal event.

- Rb-Sr ages are significantly higher than Ar/Ar ages.

- $(^{87}Sr/^{86}Sr)_o$ values for the quartz monzonite and granite indicate that they are consanguineous.

- relatively high $(^{87}Sr/^{86}Sr)_o$ values may further indicate crustal contamination.

- a double-mixing model may explain isotopic and chemical Sr data, where hydrothermal water/rock interaction trend is superimposed on a non-hydrothermal mixing trend.

3.2 Applicability to Radioactive Waste Isolation

- isotopic and chemical data point out the importance of identifying fracturing within the repository host rock.

- REE data indicates that, depending on the waste form used, some very important radionuclides of concern (Sm, Eu, Cm[Nd], and Am[Nd]) may be relatively immobile.

- modeling of Ar transport will help define non-sorptive, conservative mobility parameters within fractured granitic rock.

- U and Th disequilibrium data indicate the remobilization of U in oxidizing environments.

- Rb-Sr data show that some extremely important radionuclides of concern (Sr, Ra[Sr], and Cs[Rb]) will be affected by hydrothermal processes, and allow for the possibility to model this disturbance.

4.0 ACKNOWLEDGEMENTS

The author thanks Prof. K. A. Foland, Larry Gaber, Jeff Linder, and Fritz Hubacher of The Ohio State University with whom working together is both productive and pleasant. Also thanks to Dr. Bob Laughon of OWTD for assistance rendered. This work is supported through DOE contract DE-AC02-83CH10139.

REFERENCES

1. Cunningham, C. G., and T. Steven (1979), "Uranium in the Central Mining Area, Marysvale District, West Central Utah," U.S. Geol. Surv. Map I-1177.

2. Cunningham, C. G., et al. (1982), "Geochronology of Hydrothermal Uranium Deposits and Associated Igneous Rocks in the Eastern Source Area of the Mount Belknap Volcanics, Marysvale, Utah," Economic Geology, 77:453-463.

3. El-Mahdy, O. (1966), Origin of the Ore and Alteration in the Freedom No. 2 and Adjacent Mines at Marysvale, Utah, Ph.D. Thesis, Univ. of Utah.

4. Kerr, P., G. Brophy, H. Dahl, J. Green, and L. Woolard (1957), Marysvale, Utah, Uranium Area - Geology, Volcanic Relations, and Hydrothermal Alteration, Geol. Sc. Amer., Spec. Paper 64.

5. Shea, M. (1982), Uranium Migration Associated With Some Hydrothermal Veins at Marysvale, Utah: A Natural Analog for Radioactive Waste Isolation, M.S. Thesis, University of California at Riverside.

6. Shea, M. (1984), "Uranium Migration At Some Hydrothermal Veins Near Marysvale, Utah: A Natural Analog for Radwaste Isolation", Materials Research Society Symposium Proceedings, 26:227-238.

7. Shea, M., and K. A. Foland (1984), "Marysvale Natural Analog Study: Preliminary Oxygen Isotope Relations," in Proceedings of the Natural Analogue Workshop, Lake Geneva, SKB Report 84-18, D5:1-22.

8. Shea, M., and K. A. Foland (1986b), "Marysvale Natural Analog Study: Preliminary Oxygen Isotope Relations," Chemical Geology, 55:281-295.

9. Shea, M. and K. A. Foland (1986b), "Marysvale Natural Analog Study: Results of Phase I", American Chemical Society National Meeting, Anaheim [abstract].

10. Steven, T., C. Cunningham, C. Naeser, and H. Mehnart (1979), Revised Stratigraphy and Radiometric Ages of Volcanic Rocks and Mineral Deposits in the Marysvale Area, West Central Utah, U.S. Geol. Surv., Bulletin 1469.

SESSION 4 :

ANALOGUES OF PROCESSES AFFECTING RADIONUCLIDE MIGRATION

PART 2

Chairman : D. BROOKINS (Univ. New Mexico, USA)

Co-Chairman : G. de MARSILY (EMP, F)

NATURAL COLLOIDS AND GENERATION OF ACTINIDE PSEUDOCOLLOIDS IN GROUNDWATER

J.I. Kim, G. Buckau and R. Klenze
Institut für Radiochemie, TU München, 8046 Garching, FRG

Summary

Natural colloids in the Gorleben aquifer systems have been investigated as for their chemical composition, quantification and size distribution. Humic substances appear to be the major organic materials in these groundwaters, generating humic colloids which are analysed to be humic acid (and fulvic acid) loaded with a large number of trace heavy metal ions. These metal ions are natural homologues of actinides and some fission products in trivalent, tetravalent and hexavalent state. Concentrations of trivalent and tetravalent heavy metal ions are linearly correlated with the DOC concentration in different groundwaters. The DOC is found to be present as humic colloids. The Am^{3+} ions introduced in such a groundwater readily undergo the generation of its pseudocolloids through sorption or ion exchange reactions with humic colloids. The chemical behaviour of Am(III), being similar to the trivalent metal ions, e.g. Fe^{3+}, REE etc. found in natural colloids, has been investigated by laser induced photoacoustic spectroscopy.

1. Introduction

Natural colloids are ubiquitous in groundwaters and by introducing actinide ions they readily generate actinide pseudocolloids through sorption or ion exchange reactions. The chemical composition and size distribution of natural colloids are different from one groundwater to another, depending on the geochemical properties of each given aquifer system (1). They may be composed of inorganic oxide or hydroxide aggregates if the groundwater is poor in organic substances, or of organometallic polymer coagulates if the aquifer system contains humic substances which are the most common organics in groundwater (2,3). All natural colloids, however, contain a large number of trace heavy metals, rare earth elements (REE), Zr, Hf, Th, U etc., which are chemically natural analogues of actinides and some fission products in trivalent, tetravalent or hexavalent state (4). A careful investigation of natural colloids in a given aquifer sy-

stem may, therefore, give an insight into the possible migration phenomena of fission products and actinides through colloid transportation.

The present paper deals with quantification, size distribution and chemical characterization of natural colloids in the Gorleben aquifer systems. The generation of actinide pseudocolloids is investigated by tracing a groundwater with the Am^{3+} ion. Thus produced Am pseudocolloids are speciated by various methods for chemical and physical characterization.

2 Experimental

Groundwater is sampled under nitrogen atmosphere into a 50 L aluminium container, of which the inner wall is electropolished or teflonated prior to its use, and transported to the laboratory under air tight conditions. The water is kept in contact with the original sediment during transportation. The water is divided in a special inert gas box (Ar plus 1 % CO_2) into glass bottles (3 L volume) with air tight covers and stored in a refrigerator at 10 °C under light shield. 1 % CO_2 gives rise to the maintenance of the HCO_3^- concentration about 10^{-2} mol L^{-1} in groundwaters of pH = 7.5 ~ 8.2. This condition corresponds closely with deep aquifer systems of the Gorleben area in Germany.

Analyses of major groundwater components are carried out, after filtration at 450 nm, by inductively coupled plasma atomic emission spectroscopy (ICP-AES) and high performance ion chromatography (HPIC). The trace inorganic constituents are determined by a special method of monostandard neutron activation analysis (MS-NAA) (5,6). Size fractionation of colloids is made either by ultrafiltration or by ultracentrifugation. The DOC concentration in groundwater is analysed by a DOC analyser (UV-DOC-UNOR:MAIHAK Co.) and the separation of humic acid and fulvic acid is carried out by the commonly used acid-base process (7). Following the precipitation of humic acid in 0.1 M HCl, the supernatant is passed through a XAD-8 (Rohm and Haas Co.) column to fix fulvic acid, which is then eluted with 0.1 M NaOH.

The generation of pseudocolloids is investigated in groundwaters traced with ^{241}Am either by dissolving Am hydroxide precipitate or by spiking the Am^{3+} ion in the groundwater in question. The traced groundwater is then stored under light shield and Ar (1 % CO_2) atmosphere for 5 months before carrying out the speciation. The speciation is undertaken spectroscopically using laser induced photoacoustic spectroscopy (LPAS) (8-10), which provides a sensitivity of spectral work 2 ~ 3 orders of magnitude higher than attainable by conventional spectrophotometry.

3 Results and discussion

3.1 Chemical composition of natural colloids

A large number of groundwaters from the Gorleben aquifer systems are analysed to quantify major and trace inorganic constituents which are present either as colloids or as dissolved ionic species. The inorganic cations and anions with concentrations greater than 10^{-6} mol/L are con-

sidered as major constituents, whereas those less than 10^{-6} mol/L are defined as trace constituents. The Fe concentration varies considerably from one groundwater to another , i.e. from $< 10^{-7}$ mol/L to 5 x 10^{-5} mol/L. Therefore, this element belongs to both categories. As dissolved organic carbon (DOC), humic or fulvic acid is found in nearly all Gorleben groundwaters with a wide variety of concentrations, ranging from <0.1 mg C/L to 100 mg C/L.

From a close examination of the analytical results it is observed that in groundwaters with a DOC concentration less than 1 mg C/L, Fe and other trace heavy elements are present in very low concentrations, often beyond the detection limit, while in groundwaters abundant with DOC (>1 mg C/L) the concentrations of trivalent and tetravalent elements are increasing linearly with the DOC concentration. No correlation has been found for the major constituents like Na^+, Ca^{2+}, Mg^{2+}, SiO_3^{2-} etc. Similarly the hexavalent UO_2^{2+} ion does not show a concentration correlation with DOC.

In figs. 1-6, concentrations of major and trace inorganic elements are illustrated in relation with the DOC concentration in different Gorleben groundwaters. As being apparent from fig. 1 and 2, there is no particular relation between concentrations of major elements of divalent or anionic state and DOC. The concentration of Ca and Mg varies randomly from one water to another in three orders of magnitude (fig. 1), while the variation of Si concentration is rather narrow (fig. 2). In general, Si concentrations in groundwaters in contact with original geomatrices are distinctively higher than in model waters conditioned for one year with geomatrices. The reason may be the slow dissolution kinetics of Si compounds, resulting in an unequilibrated condition even after one year contact time.

As shown in figs. 3-5, the concentrations of trivalent and tetravalent elements demonstrate a linear correlation with the DOC concentration, giving rise to an average slope of one for all elements, irrespective of differences in the concentration range of each element. This fact implies that a certain form of complexation process with DOC prevails in the dissolution of trivalent and tetravalent metal ions in groundwaters under investigation. The DOC found in Gorleben groundwaters is composed mainly of humic or fulvic acid. Their strong complexation with metal ions of higher oxidation state ($Z > 2+$) is so fully the characteristics of a type to generate colloids as a natural stabilization. Humic or fulvic acid present in Gorleben groundwaters loaded with heavy metal ions of groundwater constituent, therefore, appears to be colloidal species whose chemical behaviour become different from monomeric complexes. Such species are called "humic colloids" in this paper in order to distinguish them from metal humate complexes. The spectroscopic speciation of the two different species are discussed in the later section.

As shown in fig. 6, concentrations of the hexavalent uranylion does not show any particular relation with the DOC concentration. A preliminary examination of its relation with the carbonate concentration shows a certain dependency, because a carbonate complexation probably better stabilizes the uranylion in groundwater. However, further investigations are necessary for its concrete verification.

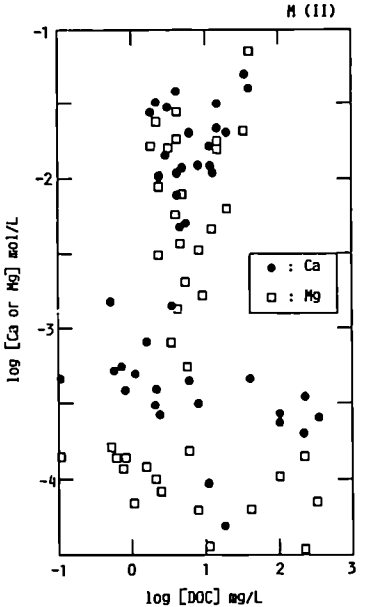

Fig. 1: Concentrations of Ca and Mg (mol/L) found in different Gorleben groundwaters plotted in relation with the DOC concentration (mg C/L)

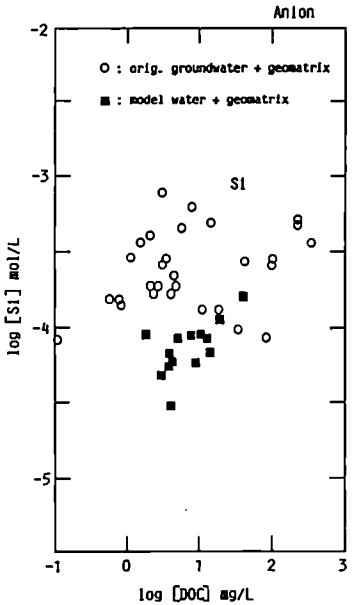

Fig. 2: Concentrations of Si (mol/L) found in different Gorleben groundwaters plotted in relation with the DOC concentration (mg C/L). The original groundwaters have been always, while the modelwaters have been only for one year, in contact with corresponding geomatrices prior to analysis

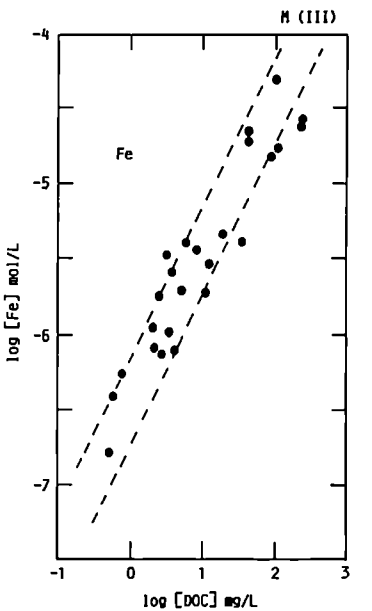

Fig. 3: Concentrations of Fe(III) (mol/L) as afunction of the DOC concentration (mg C/L) in different Gorleben grundwaters

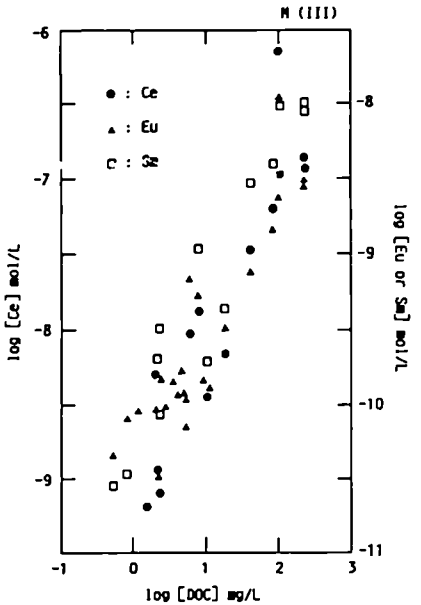

Fig. 4: Concentrations of trivalent trace rare earth elements (mol/L) as a function of the DOC concentration (mg C/L) in different Groleben groundwaters

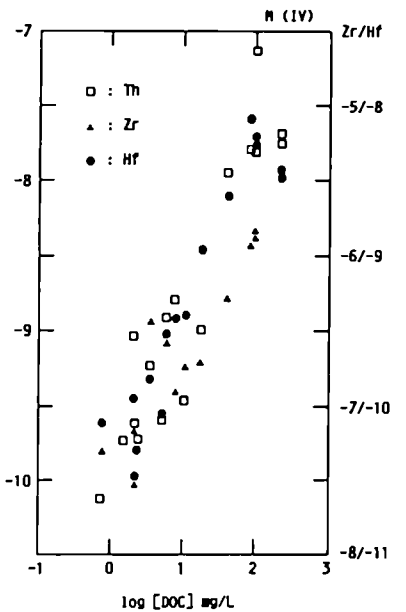

Fig. 5: Concentrations of tetravalent trace heavy metal elemtnts (mol/L) as a function of the DOC concentration (mg C/L) in different Gorleben groundwaters

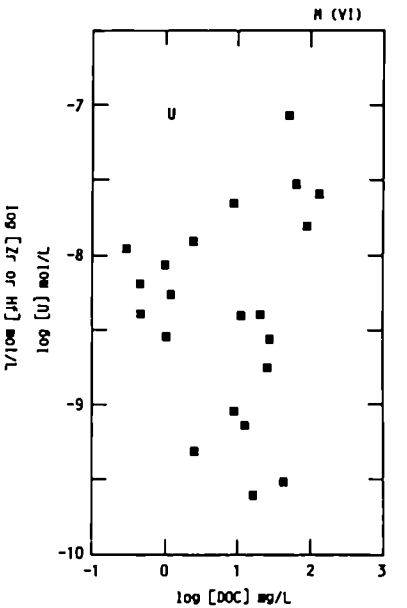

Fig. 6: Concentration of U(VI) found in different Gorleben groundwaters plotted in relation with the DOC concentration (mg C/L)

3.2 Humic colloids

In the Gorleben aquifer system, groundwater colloids are found mostly as humic colloids. The average size of these aggregates is considerably larger than the average molecular size of humic acid separated from the same groundwater. The size evaluation of a typical humic acid from the Gorleben aquifer systems, using a Sephadex column of molecular sieving type, has shown an average value of 11.000 Mwt. unit. Since humic acid is present as a humic colloid in groundwaters by loading heavy metal ions (cf. figs. 3-5), the size fractionation of the colloids can be evaluated by analysing the concentration of a particular metal ion, e.g. Fe^{3+}, which appears quantitatively bound to the humic colloid.

A typical example is shown in fig. 7 for the size evaluation of humic colloids by ultrafiltration with different pore sizes. The groundwater (Gohy-1012) under investigation contains DOC with 7.8 mg C/L, which is analysed to be 80 % humic acid and 20 % fulvic acid by the so called acid base process (7). The successive ultrafiltration of the original groundwater with decreasing filter pore size leads to a concentration decrease of Fe^{3+} in the filtrates. After acidifying the groundwater to pH = 3, the Fe concentration in the filtrates becomes somewhat increased, suggesting the release of Fe from humic colloids. When the groundwater is conditioned with 10^{-3} mol/L EDTA for three months, the major amount of Fe remains in the filtrates. The phenomenon can be explained by the EDTA complexation of Fe^{3+}, extracting Fe^{3+} ions from humic colloids and stabilizing them as monomeric Fe-EDTA complexes in solution.

A similar effect of EDTA complexation has also been observed for other trivalent and tetravalent metal ions in the same groundwater (cf. elements shown in figs. 4 and 5) (3). These natural homologues of fission products and actinides are readily released from humic colloids and changed into more stable EDTA complexes. By the ultrafiltration study, it is confirmed that the major part of trace heavy metal ions in the groundwaters is quantitatively associated with humic colloids and therefore the concentration of these ions increases, as shown in figs. 3-5, with an augmentation of the humic colloid concentration, which is directly related with the amount of DOC.

In a groundwater poor in humic substances, the colloid generation is in general caused by the aggregation of metal hydroxides. Such colloids of inorganic nature also contain metal ions of trivalent and higher oxidation state, which are sensitive to hydrolysis. They are natural analogues of fission products and actinides (3-4). Under the variation of geochemical conditions, inorganic colloids are much less stable than humic colloids (3).

3.3 Generation of Am pseudocolloids

In a groundwater rich in humic colloids, the Am^{3+}ion is readily sorbed on them and thus undergoes the generation of its pseudocolloids. Such a process is demonstrated in fig. 8. In the Gohy-1012 groundwater containing 7.8 mg C/L DOC, which is present mainly as humic colloids, the

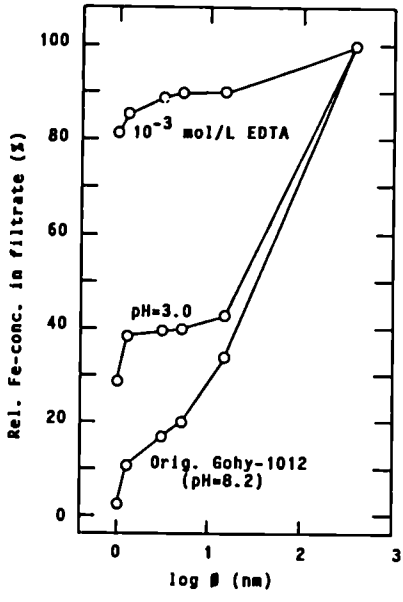

Fig. 7: Concentrations of Fe(III) in groundwater filtrates from the successive ultrafiltration at different pore sizes. The filtration is carried out for the original Gohy-1012 groundwater (pH = 8.2), after acidifying it to pH = 3.0 and after conditioning with EDTA (final conc. 10^{-3} mol/L EDTA)

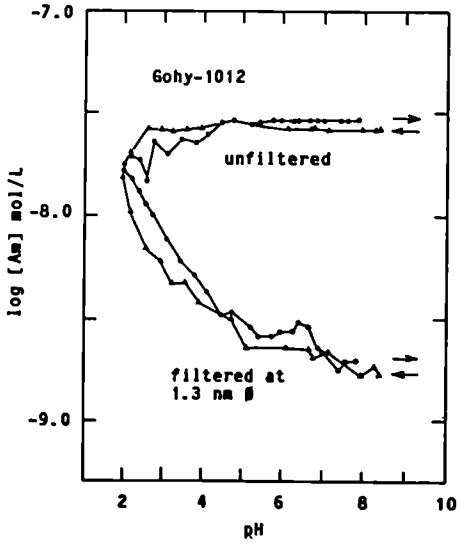

Fig. 8: Generation of Am(III) pseudo-colloids (humic colloids) in the Gohy-1012 groundwater by dissolving Am hydroxide precipitate and diluting it with fresh groundwater. The pH titration is made from pH = 8.4 to 2.5 and back titrated. The Am concentration is determined in unfiltered solutions and filtrates at 1.3 nm pore size

Am^{3+} ion is introduced by dissolving its hydroxide precipitate and diluting it with the fresh groundwater. The groundwater traced with Am^{3+}, having pH = 8.4 and 2.63 x 10^{-8} mol/L Am, is titrated with 0.1 M HCl down to pH = 2 and back titrated with 0.1 M NaOH up to pH = 7.8. The Am concentration is measured in unfiltered solutions and filtrates from the pore size of ca. 1.3 nm (5000 Dalton cut-off). In the unfiltered solution the Am concentration remains nearly constant until pH = 2.5 and decreases to 1.78 x 10^{-8} mol/L at pH = 2, whereas in the filtrates at 1.3 nm the Am concentration increases continuously with decreasing pH. The back titration from pH = 2 to pH = 8 shows a reversible phenomenon as for the change in Am concentrations both in unfiltered solutions and filtrates at 1.3 nm.

The results shown in fig. 8 can be interpreted as follows: the Am^{3+}ion introduced is sorbed on the humic colloids present in the groundwater, thus producing its pseudocolloids which can be then filtered nearly quantitatively by ultrafiltration at 1.3 nm pore size. While decreasing pH, the Am^{3+}ion is released from the humic colloids and found in the filtrates in a growing amount with decreasing pH. At pH = 2, slightly over 60 % Am is recovered in the solution. Under this condition humic colloids may be transformed into humic acid which, through over protonation, starts to produce suspended particulates of metastable state and hence to precipitate slowly. The particulates may contain the rest Am ions (40 %) which disappear from the solution through sedimentation. The back titration to alkalic solutions regenerates Am^{3+}ions quantitatively into the solution as pseudocolloids which are again filterable from the solution by ultrafiltration.

3.4 Speciation of Am pseudocolloids

In the Gohy-1012 groundwater, which is relatively rich in humic substances and hence in humic colloids, upon introducing Am(III) the generation of Am(III) pseudocolloids dominates over carbonate complexation. The process is partly explained in fig. 8. The chemical state of the Am^{3+}ion in this process has been investigated spectroscopically in order to demonstrate the generation of Am(III) pseudocolloids and the exchange reaction of Am(III) on humic colloids in this groundwater. Since the solubility constraint of Am(III) in groundwater does not allow a direct speciation of its soluble species by conventional spectrophotometry, the laser-induced photoacoustic spectroscopy (LPAS) is used for the purpose. This new method enables the speciation of Am(III) for concentrations down to 10^{-8} mol/L (8-10).

The Gohy-1012 groundwater traced with Am(III), as described in section 3.3, is used for the speciation without dilution in order to have a sufficient amount of Am(III) in the solution. Fig. 9 shows the spectroscopic features of the Am(III) traced groundwater in the region of Am(III) absorption bands, e.g. 503 nm for the Am^{3+}ion and 506.5 nm for the Am-humate complex ion. The groundwater with an initial Am concentration of 2 x 10^{-6} mol/L (spectrum (a)) does not show either of the Am species which are expected to be observed in the case of their presence. Instead, a re-

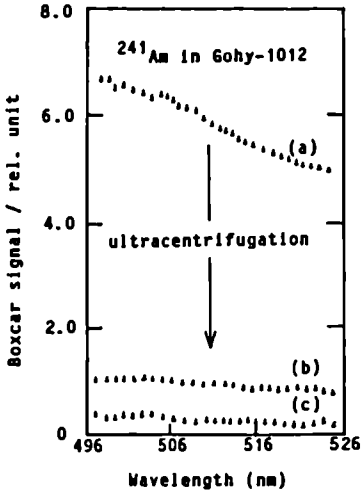

Fig. 9: Photoacoustic spectra of Am pseudocolloids (humic colloids) in the Gohy-1012 groundwater before (spectrum (a)) and after centrifugation at 4×10^4 g for 5 h (spectrum (b)) and at 6×10^5 g for 24 h (spectrum (c)). Spectra are taken absorption region of Am(III) (cf. ref. 4).

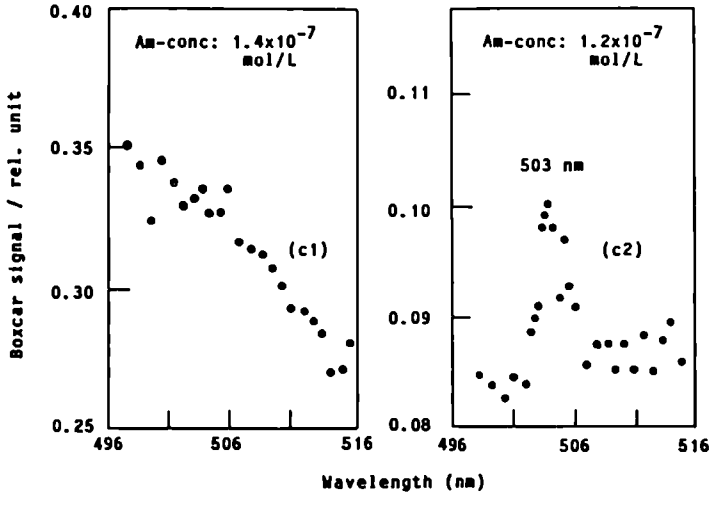

Fig. 10: Photoacoustic spectra of Am pseudocolloids (humic colloids) in the Gohy-1012 groundwater (cf. spectrum (c)) in fig. 9) before (spectrum (c1)) and after acidification for 5 month (spectrum (c2)). In spectrum C2 the absorption peak of the Am(III) ion is distinguished at 503 nm.

latively high base line is observed with increasing absorptions to the UV direction, which is attributable to humic colloids present in the solution. By ultracentrifugation at different centrifugal forces, a decrease in the humic colloid concentration is observed as shown by the spectra (b) and (c) which are taken for the solutions centrifuged at 4 x 10^4 g for 5 h and 6 x 10^5 g for 24 h, respectively. Ultrafiltration leads to the same result that suggests the absence of the detectable amount of Am(III) ionic species.

The centrifuged solutions are then acidified to 1.2 M HCl and left for many months. The humic colloids are precipitated but no Am^{3+} ion is detectable in solutions immediate after acidification. Starting from one month after acidification, the Am^{3+} ion can be monitored in all solutions and its concentration growth is observed along with the elapsing time. After 5 months the absorption band of Am^{3+} becomes well distinguished in all three solutions (cf. fig. 9), indicating the desorption of Am^{3+} from its pseudocolloids. The spectroscopic results for the solution (spectrum (c) in fig. 9) before and after acidification are illustrated in fig. 10 for comparison.

The spectrum c1 in fig. 10 shows the presence of humic colloids, which is identical to the spectrum (c) in fig. 9 and magnified for its ordinate scale, whereas the spectrum in fig. 10 illustrates the absorption band of the Am^{3+}ion at 503 nm. Although the base line of spectrum (c1) is substantially decreased by precipitation of humic colloids upon acidification, the floculating particulates in the solution cause scatterings observed in the spectrum (c2). However, the absorption peak of Am^{3+} at 503 nm is well distinguished. Upon neutralizing the solution to pH = 8, the same spectrum (c1) of humic colloids is reproduced and the reversible phenomenon of fig. 8 has been thus verified spectroscopically.

In natural aquifer systems, humic substances are ubiquitous in a wide variety of concentrations. Whenever humic substances are present, it is most likely that they are generating humic colloids as groundwater colloids through loading of heavy metal ions. In groundwater it is difficult to distinguish metal humate complexes from humic colloids only by ultracentrifugation or ultrafiltration, because both are large in size and water soluble. The distinction can only be made spectroscopically. For example, the Am(III) humate ion has a distinctive absorption band at 506.5 nm with the molar extinctions coefficient of 300 $cm^{-1}mol^{-1}L$ (4), while the humic colloid containing Am(III) does not show any absorption peak as demonstrated already in fig. 9.

Groundwater colloids, as composed of humic colloids or of other inorganic colloids, contain always natural analogues of fission products and actinides. A careful investigation of such natural colloids, as for their chemical composition, size distribution and stability, will certainly lead to a better understanding of the geochemical behaviour of actinides as well as some fission products of higher oxidation state in a given groundwater and hence the plausible interpretation of their migration phenomena.

References

1. Yariv, S. and Cross, H. (1979). Geochemistry of Colloid Systems, Springer-Verlag, Berlin.
2. Kim, J.I. (1986). Chemical Behaviour of Transuranic Elements in Natural Aquatic Systems, in: Handbook of the Physic and Chemistry of the Actinides, Eds. Freedman, A.J. and Keller, C., Elsevier Science Publishers B.V., Amsterdam.
3. Buckau, G., Stumpe, R. and Kim, J.I. (1986). J. Less-Common Metals, 122, 555.
4. Kim, J.I., Buckau, G. and Zhuang, W. (1986). Humic Colloid Generation of Transuranic Elements in Groundwater and their Migration Behaviour, 1986 MRS-Meeting, Symp. L., Paper No. L11.2 (proceedings in print).
5. Kim, J.I., Stärk, H. and Fiedler, I. (1980). Nucl. Meth. Instr. 977, 577.
6. Kim, J.I. (1981). J. Radioanal. Chem. 63, 121.
7. Stevenson, F.J. (1982). Humic Chemistry, John Wiley + Sons, New York.
8. Stumpe, R., Kim, J.I., Schrepp, W. and Walther, H. (1984). Appl Phys. B34, 203.
9. Schrepp, W., Stumpe, R., Kim, J.I. and Walther, H. (1983). Appl. Phys. B32, 207.
10. Stumpe, R. and Kim, J.I. (1986). Laser-Induced Photoacoustic Spectroscopy for the Speciation of Actinides in Natural Aquatic Systems, RCM-02386, pp 176.

NATURAL ANALOGUE STUDY OF THE DISTRIBUTION OF URANIUM SERIES RADIONUCLIDES BETWEEN THE COLLOID AND SOLUTE PHASES IN THE HYDROGEOLOGICAL SYSTEM OF THE KOONGARRA URANIUM DEPOSIT N.T., AUSTRALIA

* M. IVANOVICH, **P. DUERDEN, **T. PAYNE, **T. NIGHTINGALE
*G. LONGWORTH, *M.A. WILKINS, +R.B. EDGHILL, ++D.J. COCKAYNE and +B.G. DAVEY

*Nuclear Physics Division, AERE Harwell, OX11 ORA, U.K.

**AAEC, Lucas Heights, NSW 2232, Australia.

+Dept. of Soil Science, University of Sydney.

++Electronmicroscopy Unit, University of Sydney.

Summary

There is an urgent need to establish a body of empirical data on the 'real world' behaviour of natural colloids in order to model realistically the subsurface transport of radionuclides. The colloid sampling technique used in the present project is based on an ultrafiltration system capable of concentrating particles whose size is greater than 10,000 MW and has an option for fractionating the concentrated colloids into particle size groups. The sampled colloids are not exposed to the atmosphere prior to or during concentration thus ensuring the same redox conditions as in the aquifer at sampling depth. Five boreholes at the Koongarra uranium deposit were sampled jointly by AAEC, Lucas Heights and AERE Harwell personnel during August 1986. Samples of groundwaters, pure aqueous phase, particulate (greater than 1 μm diam. particle size) and colloid (less than 1 μm diam. particle size) fractions were collected. All samples were taken in duplicate and have been characterised by the laboratories in UK and Australia in terms of their physical, chemical and actinide isotopic composition. Radiometric data are interpreted in terms of the fraction of the radionuclides associated with the colloid concentrates and the isotopic equilibrium between the pure aqueous and colloid phases.

1. Introduction

Studies of radionuclide migration in the terrestrial environment have become of major importance with the need for disposal of radioactive waste from the nuclear power industry. Extensive modelling of the radionuclide migration following a breach in a waste repository has been carried out. One approach to the problem of predicting future transport of activity has been to study natural or

geochemical analogues where the effects of past transport over geological times may be evaluated (1). One such analogue is the system comprising the uranium deposits in the Alligator Rivers region of the Northern Territory of Australia. No particular natural analogue can be used to model all facets of radionuclide migration, and the aim of the present study is to assess the importance of colloids in sub-surface transport (2). The migration of radionuclides from a repository is largely determined by the movement of groundwater and its interactions with the host rock. However significant amounts of the relatively insoluble radionuclides such as ^{232}Th, ^{230}Th and ^{231}Pa may be associated with groundwater colloids, which could result in their increased mobility. If colloidal transport is found to be significant then linear distribution coefficients (K_d) between solid and liquid phases should not be used to describe the solute/host rock interaction.

The use of uranium series disequilibrium (USD) measurements can yield the actinide isotopic inventory of the colloids. Here naturally occurring isotopes of U, Th and Ra are used as natural analogues for the important elements Np, Pu, Am and Cm.

Several radionuclides, particularly those of thorium, occur only in barely detectable levels in aqueous systems. It is necessary therefore to concentrate colloidal particles from very large volumes of water (of the order of 10^3-10^4 L). Clearly the colloids must not be significantly altered during collection. Previous experience has shown that if the water is not sealed against atmospheric oxidation or loss of CO_2 during collection, further colloids may be created. These problems may be avoided by use of an ultrafiltration rig used in the recirculation mode with a sealed atmosphere. In this mode groundwater is pumped around a circuit comprising an anisotropic hollow fibre cartridge and a collection tank (typically 20L). This provides both a continuous supply of ultrafiltrate and a colloidal concentrate in which the colloids are retained in an aqueous medium of the same ionic strength and redox potential found at the sampling depth. Whereas such an ultrafiltration procedure may be used in the field the alternative of ultracentrifugation cannot.

There will be inevitable delays between collection and analysis of samples and therefore it is necessary to investigate both the stability of the samples and the choice of suitable containers for transport.

It is essential that the colloids be fully characterised, in terms of their physical, chemical and mineralogical properties.

The aim of this collaborative programme is to assess the role of groundwater colloids in the sub-surface transport of radionuclides. To this end, the following questions are being addressed:

1. What are the fractions of radionuclides associated

with the natural colloids and the solute phase?
2. How do USD measurements carried out in separate laboratories compare?
3. How stable are the sampled natural colloids during collection and transport to the analytical laboratory?
4. What are the controlling conditions for the establishment of isotopic equilibrium between colloid and solute phases?
5. Is it possible to establish the relative ages of the colloid and solute phases?
6. How is the mineralogical composition of the colloids related to that of the hard rock?

2.1 Equipment and sample collection

Five drill holes were sampled at the Koongarra uranium deposit in the Alligator Rivers region in August 1986. Four of these, PH49, PH56, PH55 and PH14 intersect the uranium mineralisation of the No 1 ore body which is contained in Mg-rich chloritized schists. The remaining hole KD2 should reflect the down-flow hydrogeochemical dispersion from the No. 1 ore body.

Groundwater was pumped from the drill holes by a submersible pump placed below the water table. The holes were pumped for several hours before sampling to ensure that the groundwater was representative of the aquifers. Table 1 provides a summary of the sample collection for the experiment with PH14* being a repeat measurement in borehole PH14.

The water was pumped through a nominal 5μm filter (Microclean II G78B2) then a 1μm Nuclepore QR-type filter cartridge. This cartridge was chosen because of its well defined particle size cut-off and the high flow rates achievable due to its large surface area (1.7 m^2).

A 200 L holding tank was located between the Nuclepore filter and the ultrafiltration system. This was allowed to continuously overflow so that excess water produced by the pump could be dispersed and air be prevented from entering the system.

The colloid concentration was carried out using an Amicon DC10LA ultrafiltration system equipped with dual hollow fibre cartridges having a nominal cut-off of 10,000 MW. The total surface area of the cartridges was 17,600 cm^2 which allowed the colloids from approximately 1200 L of groundwater to be concentrated into a volume of less than 20 L within 8 hours.

The equipment was operated in a recirculation mode in which a high velocity of groundwater within the hollow fibres reduced fouling and maintained an adequate flowrate throughout the colloid concentration.

The flow in all the lines was measured by flowmeters. Every holding tank in the collection system was equipped with a gas supply of a mixed N_2/CO_2 atmosphere at a pressure slightly above 1 Atm to maintain carbonate equilibrium in the groundwater. The gas filled the void space above the

water level and prevented atmospheric oxygen entering the apparatus. Redox potential, pH, dissolved oxygen, bicarbonate and conductivity in the inlet groundwater and the ultrafiltrate were monitored thoughout the colloid concentration operation to determine whether the chemistry of the groundwater was being altered by passage through the ultrafiltration system.

Samples of groundwater and ultrafiltrate were taken at intervals throughout the operation for radiochemical and elemental analysis and a final ultrafiltrate sample was collected immediately prior to stopping ultrafiltration. These samples were acidified to pH <1 with HNO_3 and stored in polyethylene bottles. Large volume samples (20 L) were taken when thorium analyses were required. Special sampling procedures were required for collection of samples for physical analysis, as the colloid should be maintained in its natural form. At the end of the colloid concentration, colloid concentrate and ultrafiltrate samples were transferred to airtight borosilicate glass and PVC bottles, without contact with atmospheric oxygen. Both plastic and glass bottles were used because it has not been established which are preferable for sampling.

The Amicon hollow fibre cartridges were backflushed with 0.1 M HCl after each operation and the washings collected for elemental and radionuclide analysis. The 5μm and 1μm prefilters were taken to the laboratory for analysis. New prefilters were used at each drill hole and the hollow fibre cartridge was prepared by running a volume of groundwater through prior to the colloid concentration operation.

2.2 Uranium series measurements and sample characterisation

The isotopic activities of uranium and thorium radionuclides in the appropriate decay chains were measured using isotope dilution/alpha spectrometry. These measurements were made on 0.2-0.7L samples in each laboratory, with the exception of ultrafiltrate measurements at AAEC where 25L samples were used.

The short-lived ^{227}Th (half-life ~19 days) was measured in the analyses of PH14 and PH49, and time was allowed for it to equilibrate with the longer-lived parent, ^{227}Ac. Following ^{227}Th separation from ^{227}Ac during the analytical procedure, allowance was made for the ^{227}Th decay and the appearance of daughter activities in the spectrum. Thus the analysis of ^{227}Th yielded the activity of ^{227}Ac in the sample.

The elemental analyses of the colloid concentrate and ultrafiltrate for each drill hole were carried out using Inductively Coupled Plasma-Emission Spectroscopy (ICP-ES) and total organic carbon contents were measured in a TOCSIN analyser. Photon correlation spectroscopy was used to study the colloid concentrate, in order to get an idea of mean colloidal particle size and concentration.

The collected <1 μm size samples were examined under Transmission Electron Microscopy (TEM) and the 1-5 μm size particle fractions from the prefilters were examined with Scanning Electron Microscopy (SEM). Each instrument was fitted with energy dispersive analysis facilities.

3. Results

Throughout the following text differentiation between Harwell and AAEC data is made only when essential to the discussion.

3.1 Uranium series measurements

The alpha spectra for samples in glass containers were analysed for uranium, yielding ^{238}U activities which varied from 0.1 dpm kg^{-1}(KD2) to 176 dpm kg^{-1}(PH49) while the $^{234}U/^{238}U$ activity ratios in colloid concentrate and ultrafiltrate, were equal and had the value unity except for PH14(0.75), PH14*(0.79) and PH56(0.8). Agreement was obtained between uranium measurements in the two laboratories to within about 5%.

Thorium activities found by AAEC were of the order of 2 x 10^{-3} dpm kg^{-1} (ultrafiltrate) and 8 x 10^{-2} dpm kg^{-1} (colloid concentrate) for ^{230}Th and were below the detection limits of 10^{-3} dpm kg^{-1} (ultrafiltrate) and 15 x 10^{-3} dpm kg^{-1} (colloid concentrate) for ^{232}Th. For about half the samples somewhat higher values were obtained by Harwell. The reasons for this are still being investigated and in the meantime AAEC values of thorium concentrations are adopted.

The percentage activities of ^{238}U and ^{230}Th associated with the colloid phase were obtained by subtracting the activity for the concentrate volume of ultrafiltrate from that for the colloid concentrate and dividing by the concentration factor. These are shown in table 2. The colloid phase activity ratios $^{234}U/^{238}U$ and $^{230}Th/^{234}U$ were found to be close to unity and 10^{-2} - 10^{-3} respectively.

The results of a detailed analysis of various fractions collected from boreholes PH14 and PH49 are given in tables 3 and 4. The amount of each isotope associated with the size fractions is given as a percentage of the total amount carried in unfiltered groundwater. The radionuclides on the prefilters were determined by an acid leach whereas the retention on the Amicon filters was determined by analysing the solution which had been used to backflush the filter.

3.2 Chemical characterisation

There was little variation between the elemental concentrations in the colloid concentrate and ultrafiltrate samples for each borehole. Agreement between Harwell and AAEC laboratories was good apart from iron levels, typically

0.4 ppm (AAEC) and 0.01 ppm (Harwell). In the case of PH14 additional measurements were obtained for the material retained on the Amicon filter.

3.3 Physical characterisation

Evidence for colloidal particles in the colloidal concentrates and in the ultrafiltrates was found using transmission electron microscopy and associated energy dispersion spectrometry for microanalysis. Very little material was obtained for any of the <1µm samples examined, with centrifuged samples giving only a scattering of particles on the grids. The pump holes closest to the fault line gave the greatest variety of colloids. These included crystalline and non-crystalline magnesium silicates, titanium-rich particles and gold. However, all samples were dominated by iron-rich particles, possibly secondary, i.e. having formed since collection. The colloids mostly appeared in small clusters of particles with the same chemical composition. At no time were alumino-silicate clay-like particles observed in the <1µm samples.

The samples changed with time in respect of the observed particles. Those samples examined after months of storage displayed only Fe-rich particles with various other elements incorporated. In addition, the colloid concentrate samples showed up to 10 times the number of these particles than in the corresponding ultrafiltrate. Although the particles were mostly 1µm or less, a few larger particles were seen. In PH56 in particular, one 15µm and one 5µm size particle were seen, but particles of this size were not seen in any of the other samples.

Photon correlation spectroscopy measurement also indicated the presence of colloidal material for PH14 and PH49, but none was seen for KD2, PH55 or PH56. Values were obtained for the translational diffusion coefficient of 2.0 x 10^{-10} cm ^{2} s^{-1} (PH14) and 3.6 x 10^{-10} cm ^{2} s^{-1} (PH49), leading to values of particle hydrodynamic radius of 13.80 µm (PH14) and 7.72µm (PH49). These are clearly greater than the size range determined by the Amicon filter (1µm - 1nm) and are either due to aggregation or an artefact of the measurement carried out on a sample with a multi-modal particle size distribution.

On the 1 µm Nuclepore prefilter, only clay-like particles were seen. These had chemical compositions corresponding to chlorite, micas and kaolinite. Some appeared to have iron-rich coatings. For all particle sizes uranium was only associated with species rich in iron. No clogging of the filter pores was seen.

4. Discussion

4.1 Chemical characterisation

A comparison of the elemental analyses of the ultrafiltrate and colloidal material (including the material retained by the Amicon filter) for PH14 suggests that within

the accuracy of the measurements, K, Na, Mg, Si, Ca and Mn are not associated with colloidal material below 1 μm particle size. The only elements for which elemental analysis provides evidence of colloidal transport are thorium, actinium, iron, uranium, and possibly aluminium (Al levels are close to detection limits).

The lower levels of iron found by Harwell can be ascribed to the fact that unlike the AAEC samples, they were not acidified before analysis, which could lead to oxidation and precipitation of iron.

4.2 Physical characterisation

The electron microscopy results for the colloid concentrate phase clearly show that the colloids changed with time, with the fraction of iron-rich particles increasing, presumably produced from iron in solution. It is not known what changes if any occurred during concentration. To answer this question it will be necessary to study the colloidal phase in the unfiltered and prefiltered water as well as the colloid concentrate, directly after collection.

The presence of large (~10μm) particles in the stored colloid concentrates found in the PCS measurements, suggests that the colloidal material has undergone flocculation. Particle of this size must contain between 10^3-10^9 colloidal particles. Since the light scattering intensity is relatively weak, it can be severely distorted by the presence of a few aggregates. In addition interpretation of PCS data is difficult when there is a wide range of particle sizes.

4.3 Uranium series measurements

The results of the radiometric measurements on all phases including filter residues, for PH14 and PH49 (tables 3,4) show that the bulk of uranium resides in the ultrafiltrate, and the bulk of the thorium resides in the 1-5 μm size fraction as might be expected from their relative solubilities and the tendency for thorium to adsorb under natural redox conditions. It is unlikely that all the activity held by the 1 μm and 5 μm prefilters is removed by an acid leach. In fact, when the 1 μm filter used in the collection of sample PH49 was acid leached, a large quantity of insoluble material was also removed. Comparison of the isotopic signatures in the acid-soluble and insoluble fractions suggested that the particles consisted of typical uranium bearing ore coated with a layer of 'mobile' material.

Substantial activities of the radionuclides were retained by the Amicon filter. If it is assumed that these filter-retained activities originate in colloidal particles rather than species adsorbed from solution then, the colloid fraction of the sub-1 μm fraction for uranium is increased from 0.05% to 1.4% for PH14 and from 0.4% to 1.3% for PH49. Colloid fractions of the sub-1μm fraction for ^{230}Th

are increased from 4.5% to 11% for PH14 and from 35% to 82% for PH49. At PH49 approximately equal amounts of ^{227}Ac are associated with the colloid concentrate and the Amicon filter, and the total colloidal ^{227}Ac in the sub 1 μm fraction is at least 85%.

The concentration of ^{230}Th and ^{227}Ac in groundwater are close to detection limits. However, readily measurable levels of both these isotopes were retained by the Amicon filter at PH14 and PH49. The $^{227}Ac/^{230}Th$ ratio was 2.8 $\pm$ 0.3 at PH49 and 3.1 $\pm$ 0.2 at PH14. The presence of ^{227}Ac on the colloid filter with an activity greater than ^{230}Th is in marked contrast to the solid phase where ^{230}Th is always in excess. This indicates that ^{227}Ac is more mobile in groundwater than ^{230}Th.

To a certain extent the observed difference in partition of uranium and thorium isotopes between the colloid and solute fractions is not surprising. The uranium is in the oxidized uranyl form, which forms soluble complexes with a wide range of ligands. The close similarity of the $^{234}U/^{238}U$ activity ratios for ultrafiltrate, colloid concentrate and the material retained by the Amicon filter suggests chemical equilibrium between the solute and colloid phases. Thus the uranium associated with the colloid (particulate) fraction has probably been adsorbed from solution. On the other hand, thorium occurs almost entirely in the +4 oxidation state and has little tendency to form soluble complexes in geochemical systems. Thorium-232 is primordial and occurs mainly in weather-resistant primary minerals. It was identified only in the >1μm particulates which consisted of coarse particles of geological material.

Although the uranium and thorium activities associated with the colloid phase are found to be very small for the Koongarra uranium deposit, in a radioactive waste repository it is likely that the activity phase distributions will be different. These will depend for example upon the physical and chemical form of the radioactive waste and on the chemical conditions in the near-field which control its speciation.

5. Conclusions

(1) Most elements which are present in measurable levels in unfiltered groundwater are either contained within or adsorbed on particles above one micron in size, or are dissolved. The majority of uranium is dissolved, whereas almost all the thorium and actinium are associated with particulates above 1μm in size. For these radionuclides colloidal particles comprise only a small fraction of the total radionuclide content in unfiltered groundwater.

(2) About 1-2% of the uranium activity and 10-70% of the thorium activity in the sub-1μm fraction are associated with the colloid phase.
(3) Results obtained in the Harwell and AAEC laboratories for isotopic activities are in good agreement for uranium and the discrepancies found for the thorium activities may be attributed partly to the small sample sizes and partly to the difficulty of measuring very low thorium levels in groundwater samples using alpha spectrometry.
(4) There is evidence for changes in the colloidal material after storage for several months, with the colloids being dominated by iron-rich particles. Although colloidal material is collected in the ultrafiltration rig, which has a measurable load of uranium and thorium activities, it is not clear whether the physical characteristics of the colloid material are changed on concentration. To check this, electron microscopy and photon correlation spectroscopy should be carried out on unfiltered and prefiltered water and colloid concentrate as soon as possible after collection.
(5) Since the $^{234}U/^{238}U$ activity ratios of colloid and solute phases are approximately equal, the two phases are in chemical equilibrium in respect of the uranium isotopic contents.
(6) Measurable levels of uranium, thorium and iron are retained by the Amicon filter and may be colloidal. The presence of actinium in the fraction retained by the Amicon filter may indicate an association with colloidal particles and is evidence for actinium mobility in groundwater. The level of ^{230}Th in the <1μm-filtered groundwater and colloidal particles is very low and indicates that it is the least mobile of the radionuclides studied.
(7) More information about the physical characteristics of the colloids is needed before a calculation of their long term stabilities and ages can be attempted. Electron microscopy measurements are currently in progress to determine the mineralogical content of the colloids in an effort to relate it to the mineralogy of the hard rock. An effort will be made to obtain more meaningful information about colloid particle size, concentration etc. from photon correlation spectroscopy measurements. Analysis of the radiometric data for the fractionated colloid samples is also in progress.

The results presented here are part of an on-going project in which both techniques and analytical methods are being constantly evaluated and improved. At this stage it is already clear that the use of measurements of actinide isotopic activities and activity ratios coupled with techniques of colloid collection and characterisation can provide useful information with respect to modelling of radionuclide transport in hydrogeological systems.

ACKNOWLEDGEMENTS

This work received financial support from UKDOE (Contract No.UKDOE PECD 7/9/373) and USNRC (Contract No. NRC-04-81-172). The authors gratefully acknowledge the assistance of David Garton at the AAEC who designed and assembled the colloid sampling equipment, and the analytical assistance of Miss Sandra Hasler at AERE,Harwell. Thanks are due to Mr Roger Brown at AERE, Harwell and Mrs Debra Alewood at CSIRO, Lucas Heights Research Laboratories for elemental and TOC analyses.

REFERENCES

1. AIREY, P.L and IVANOVICH, M, (1986), Geochemical Analogues of High-Level Radioactive Waste Repositories, Chem. Geol. 55, 203-213
2. IVANOVICH, M and HARDY, C.J., (1986), Identification and Measurement of Colloids in Groundwater, Proceedings of second meeting of natural analogue working group, Interlaken, 17-19 June, 1986.

TABLE 1: SAMPLE COLLECTION DETAILS : KOONGARRA PROJECT

Sample	Date	SWL (m)	Pump Set at (m)	Ultra-filtrate Volume	Concent-ration Factor	Flow Rate L/min	Comment
KD 2	21/8/86	5.27	20	2060	147	4.9	Concentration with 10,000 MW
PH 55	22/8/86	4.35	15	1313	66	3.5	Concentration, then fractionation with 0.1 µm only
PH 14	23/8/86	5.14	20	1182	131	2.6	Concentration only
PH 14*	25/8/86			1115	56	2.5	Concentration, then fractionation with 0.1 µm and 100,000 MW filters
PH 49	26/8/86	6.89	15	891	45	2.3	Concentration, then fractionation 0.1 µm and 100,000 MW with Harwell rig
PH 56	27/8/86	5.03	15	510	85	2.1	Concentration with 10,000 MW
	27/8/86	5.03	15	944	157	7.9	Concentration with 100,000 MW

SWL = STANDING WATER LEVEL

TABLE 2: PERCENTAGE ACTIVITIES OF ^{238}U AND ^{230}Th ASSOCIATED WITH COLLOIDS FOR PARTICLE FRACTIONS <1μm.

SAMPLE	^{238}U (%)	^{230}Th (%)
KD2	0.20	N/A
PH55	0.30	18
PH14	0.05	4.5
PH14*	0.15	6.5
PH49	0.40	35
PH56	0.25	21

TABLE 3: SIZE PARTITIONS (%) FOR ISOTOPES IN PH14 PUMPED GROUNDWATER

FRACTION	^{238}U (%)	^{234}U (%)	^{232}Th (%)	^{230}Th (%)	^{227}Ac (%)
>5 μm	3.7	3.9	-	5.0	33
1 - 5 μm	5.5	5.4	>80	93.0	57
Amicon filter	1.2	1.3	<1.3	0.16	1.4
Colloid	0.1	0.1	<0.4	0.08	<0.4
Ultrafiltrate	89.5	89.3	<20	1.77	<15

TABLE 4: SIZE PARTITIONS (%) FOR ISOTOPES IN PH49 PUMPED GROUNDWATER

FRACTION	^{238}U	^{234}U	^{230}Th	^{227}Ac
>5µm	14.6	13.3	34.9	~45*
1 - 5µm	13.5	12.4	65.0	~55*
Amicon filter	0.7	0.7	0.05	1.5
Colloid	0.3	0.3	0.006	1.3
Ultrafiltrate	70.8	73.3	0.012	2.5

* Full ingrowth of ^{227}Th has not yet occurred.

COLLOID BENCHMARK EXERCISE: AN INTERLABORATORY STUDY OF SAMPLING AND CHARACTERISATION TECHNIQUES FOR NATURAL COLLOIDS IN OXIC GROUNDWATER.

C.A.M. ROSS, C. DEGUELDRE*, M. IVANOVICH** and G. LONGWORTH**
Fluid Processes Research group, British Geological Survey, Keyworth, UK.
*Eidgenössisches Institut für Reaktorforschung,Würenlingen, Switzerland. **Uranium Series Disequilibrium Section, Nuclear Physics Division, Harwell Laboratory, UK.

Summary

Natural colloids have been identified as potentially important in the transport of radionuclides in groundwater. This paper presents the results of a comparative study of two methods of colloid sampling; pulsed, cross-flow ultrafiltration and tangential diafiltration. In this study a comparison was made of colloid populations, composition and size distributions in colloid concentrate samples taken in the field, of a poorly mineralised groundwater abstracted from fractured Permo-Triassic sandstone in the English East Midlands. The actinide isotopic activities associated with the colloids were also determined, using isotope dilution/alpha spectrometry, at Harwell. In order to study the effects of storage on natural colloids, additional groundwater samples were stored for approximately two months before fractionation using the cross-flow filtration and diafiltration methods previously applied to field samples. Preliminary results from this intercomparison exercise indicate that; (i) no artefacts are produced by either colloid concentration method, although some aggregation of colloidal particles may occur on storage of aqueous colloid concentrates, (ii) good agreement on colloid populations and size distributions is obtained by different laboratories applying scanning electron microscopic analysis to cross-flow ultrafilters and (iii) limited fractionation of solutes is caused by diafiltration of low salinity water, in particular uptake of sodium.

1.0 Introduction

Natural colloids may be important in the transport of radionuclides in groundwater, and could significantly affect any analysis of repository safety. A range of techniques including ultrafiltration, ultracentrifugation and dialysis have been used as a means of isolating or concentrating colloids in groundwater but, to date, no comparison has been made of these methods to identify possible sampling artefacts. During the Second Natural Analogue Workshop in Interlaken, it was proposed that the CEC should co-ordinate a comparative study of sampling methods for natural groundwater colloids. This exercise was felt to be complementary to existing work on comparison of techniques for colloid characterisation being undertaken within the framework of the MIRAGE II programme and offered a means of comparing both sampling and analytical techniques.

2.0 Selection of a reference groundwater

The reference groundwater for this exercise was selected after preliminary screening of groundwater samples from three different aquifer systems; glacial clays, Ispra (Varese, Italy), consolidated sandstone, Markham Clinton (UK) and fractured granite, Felslabor Grimsel (Switzerland). Groundwater samples were characterised by laser induced photoacoustic spectroscopy (LIPAS), at the Institut für Radiochemie der Technischen Universität München (TUM). Colloid populations were estimated by comparison with LIPAS spectra for a standard solution of 220 nm diameter latex beads of known concentration. These preliminary analyses (1) showed that the groundwaters all contained similar colloid populations of the order 10^9-10^{10} particles per litre. The Markham Clinton site, which is a public water supply

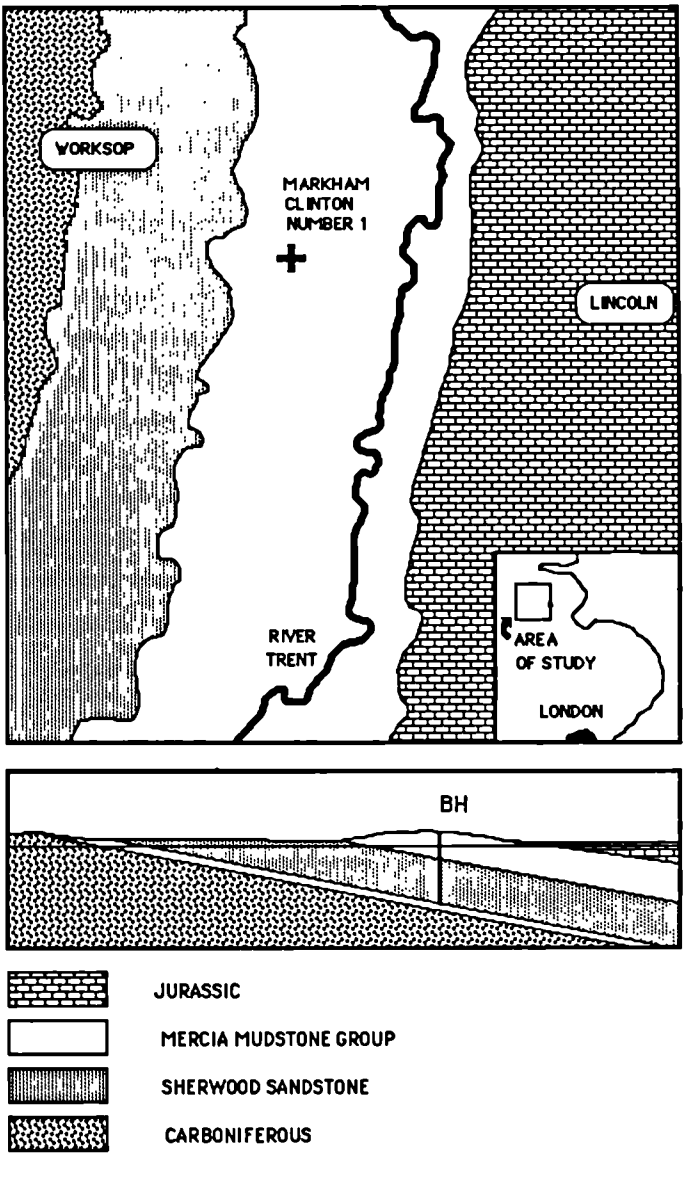

Figure 1. Sketch map and schematic cross-section showing the location of the Markham Clinton Borehole.

borehole, was chosen for the intercomparison exercise on the basis of (a) good access to the site, (b) essentially unlimited water supply and (c) stable and well-characterised groundwater chemistry. The use of an established abstraction borehole also ensured that any colloids introduced or created during drilling and construction of the borehole had been flushed from the system. In addition the Markham Clinton groundwater has a high uranium content (ca.5 µg/l) offering potential for 'age-dating' colloids using uranium-series disequilibrium data (see e.g. (2)).

2.1 Markham Clinton - Location of site and previous research.

The Markham Clinton pumping station is situated in the English East Midlands (National Grid Reference SK 711727) approximately 20km west of Lincoln and 150km north of London (figure I). A complex of three boreholes abstracts groundwater from the Sherwood sandstone aquifer at a rate of approximately 10^6 litres/hour, contributing to the public water supply for Nottingham. This geochemical evolution of this aquifer has been studied extensively in the past (3,4); the Markham Clinton site was also included in an intercomparison study of groundwater dating methods by the International Atomic Energy Agency (5).

The Sherwood Sandstone aquifer comprises a complex of Triassic continental red beds deposited in a major fluvial system in the East Midlands Basin. The sandstone is overlain unconformably by Triassic marine mudstones, and was uplifted and eroded in the mid-Tertiary before Pleistocene glaciation, which left Drift deposits over approximately half of the sandstone outcrop. The sandstone is predominantly poorly cemented quartz, with significant amounts of detrital and authigenic orthoclase and microcline feldspars, together with detrital muscovite, biotite and illite. Sand grains are coated with haematite and amorphous iron oxides which give the sandstone its distinctive red colouration. Calcite and dolomite may form up to four percent of the rock weight, occurring as isolated mineral grains and clots, and preserved as orginal cement. The groundwater abstracted at Markham Clinton is calculated to be at near-equilibrium with calcite and dolomite, and slightly oversaturated with amorphous ferric hydroxide (4). The general direction of groundwater flow in the basin is downdip to the east and regional groundwater velocities of 0.7-4 ma^{-1} have been calculated for this aquifer. Carbon-14 dating suggests that the 'age' of the Markham Clinton groundwater is of the order 3500-7000 years (5).

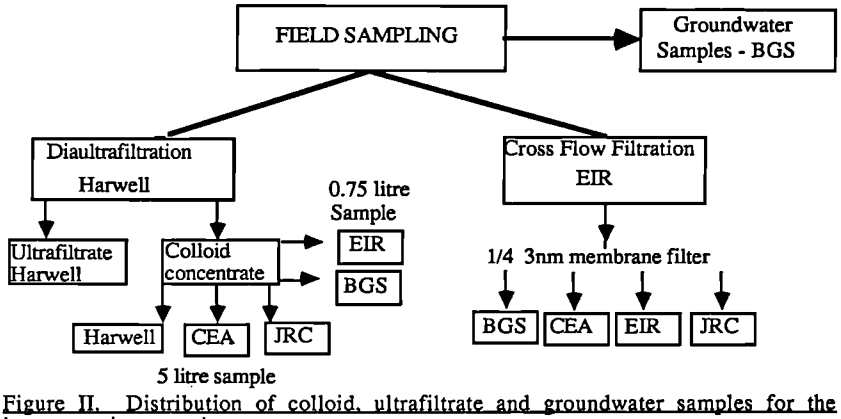

Figure II. Distribution of colloid, ultrafiltrate and groundwater samples for the intercomparison exercise.

2.2 Colloid Sampling.

Two main types of sample were collected for the intercomparison exercise; membrane filters from cross-flow filtration and aqueous colloid concentrates from the tangential

diafiltration. The distribution of samples for this study is summarised in figure II.

2.2.1 Cross-flow ultrafiltration - equipment and methodology.

The ultrafiltration rig used for cross-flow isolation of colloids was developed at EIR (6). The main components of the system are:

(1) Amicon mini-reservoir (RC800, No. 6024) containing water to be analysed.

(2) pretreatment system for water saturation and filtration of gas used to pressurise ultrafiltration cell.

(3) Amicon pulsed-flow mini ultrafiltration cell (model 3, No. 5106).

(4) electromagnetic valve system to control the transfer of fluid from the mini-reservoir to the ultrafiltration cell (Galtek No. 203-1214 and No. 203-3414).

(5) electromagnetic valve system to control the gas pressure in the ultrafiltration cell and reservoirs.

(6) automatic water-level control system for the mini-cell, comprising two pairs of infra-red sources and detectors (IFM Electronique, Opto effector OE 0002/3), producing signals which are amplified (Verstarker OV110-typOV5012) and linked back to the valve control system (this system can also be manually controlled).

(7) flushing circuit to allow rinsing of filter membrane to remove e.g. excess salts when filtering saline groundwater (not used in this exercise).

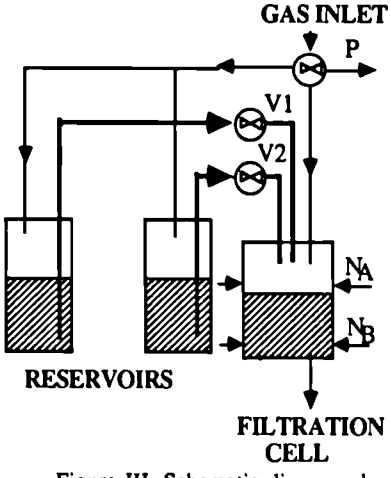

Cycle	NA	NB	V1, V2, P
(1)	0	0	1
(2)	0	1	1
(3)	1	1	0
(4)	0	1	0
(1)	0	0	1

Figure III. Schematic diagram showing the water-level control system, and valve operating sequence for the EIR cross-flow ultrafiltration equipment.

The commercially-available Amicon mini-cell was modified by replacing the safety valve with an electronically controlled injection system (Figure III). The injection system consisted of two modified Amicon mini-reservoirs, which feed into the mini-cell via Teflon tubing. The sample flow is controlled by electromagnetic valves; a third valve controls the inflow of gas to the reservoirs and filtration cell. Previous experiments had shown an optimum gas pressure of 1-2 bars giving a filtration rate of 0.05-1.0 ml/minute, depending upon the type of membrane used (6). Although the gas can be matched in composition to that in equilibrium with the groundwater, high purity nitrogen was used in this exercise. The water level in the filtration cell was monitored by the automatic level system, and both the gas and water flows regulated automatically. The control system, which can also be operated manually, is described in detail by Degueldre and Thomi (6). The complete apparatus was enclosed in a flexible plastic housing, which excluded atmospheric particulates, and which can also be flushed with an appropriate gas mixture for anaerobic operation and sample

manipulation. Using this system three colloid isolates were prepared, each with approximately 150 ml water, on 25 mm diameter (active surface area 75 mm^2) Amicon XM50 membranes (nominal pore size 3nm); groundwater was bled into the filtration system via a continuous flow loop from the borehole. The three filters were subsequently quartered and colloid populations estimated independently by the four laboratories (JRC, Italy; CEA, France; EIR, Switzerland and BGS, UK).

2.2.2 Diafiltration - equipment and methodology

The Harwell geocolloid sampling rig comprises four main components:

(1) Prefilter - Gelman 1µm pleated membrane filter cartridge (No. 12632).

(2) Amicon DC 10LA ultrafiltration system (No. 5472)

(3) Amicon hollow fibre industrial size ultrafiltration cartridge,10,000 Daltons MW (1-2nm) particle size cut-off.

(4) 20litre high density polyethylene sample container, fitted with regulator valve, gas-pressure relief valve (for nitrogen input) and inlet and outlet connectors with automatic shut-off connectors for sample dispensing.

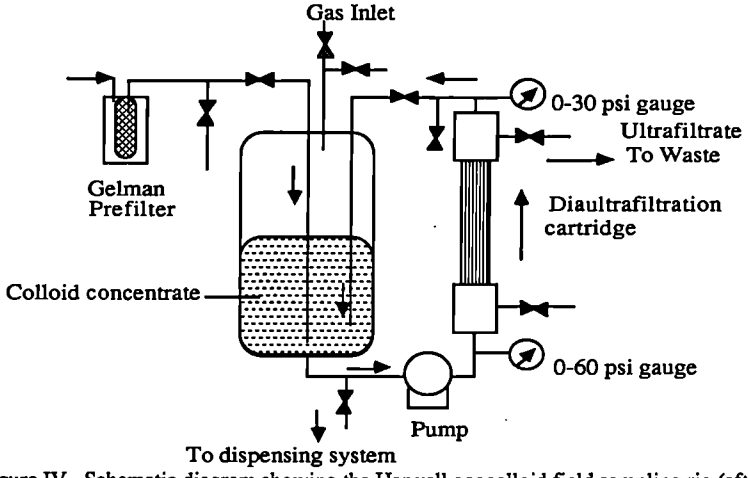

Figure IV. Schematic diagram showing the Harwell geocolloid field sampling rig (after Ivanovich et al.(7))

The arrangement of this apparatus is shown schematically in figure IV. An aqueous colloid concentrate was prepared at the borehole, simultaneously with the preparation of the membrane filters, using the standard industrial-size Amicon ultrafiltration rig fitted with a 10,000 Daltons MW cut-off, Hollow Fibre industrial-sized cartridge. The sampling rig is used in the recirculation mode in which the groundwater is pumped around a circuit consisting of a 20l reservoir and the Hollow Fibre Cartridge Filter. The cartridge consists of a bundle of hollow fibres stacked so that the water enters along their axes. Water passing through the fibre walls (cut-off 10,000 MW), i.e. the ultrafiltrate, is drained to waste (Figure IV). Water flow through the rig was balanced by manually operating inflow and back-pressure valves. In this way the reservoir sample becomes progressively enriched in colloids; the colloid concentrate.

After priming the diafiltration rig with prefiltered groundwater, 1474 litres of water were passed through it over a period of approximately five hours. Twenty litres of colloid concentrate (representing a concentration factor of 73.7) were collected in the reservoir and dispensed to the high density polythene container using a slight overpressure of nitrogen gas; subsamples of this concentrate were dispensed into amber glass bottles, via a manifold

incorporating automatic shut-off connectors, and shipped for analysis to the participating laboratories. On completion of the sampling exercise both the Amicon cartridge and the Gelman prefilter were backflushed with 0.1M hydrochloric acid, in the laboratory, to remove collected particulates and sorbed species for uranium series analysis.

2.2.3 Groundwater samples.

Throughout the sampling exercise groundwater samples were collected, and preserved for major and trace element analysis, at regular intervals; labile parameters (temperature, pH, Eh, dissolved oxygen and conductivity) were measured at the borehole. A 20l sample of ultrafiltrate was also taken at the beginning and end of the diafiltration run, as well as 20l of prefiltered (1μm) groundwater.

In order to study the effects of sample storage on the natural colloid populations, additional groundwater samples were collected in an Amicon stainless steel, pressurised sample bottle and in pressurised, platinised aluminium containers, supplied by TUM. These samples were stored for approximately two months before fractionation using the two different methods previously applied in the field.

3.0 Results

3.1 Characterisation of cross-flow ultrafiltration membranes

3.1.1 Scanning and transmission electron microscopy

The quartered membrane filters were examined by scanning electron microscopy (SEM). Very similar electron micrographs were obtained by the four participating laboratories (8,9) typically showing flaky amorphous silica/quartz particles, clays (illite/smectite?), iron oxide, calcite and clots and fibres of organic material. A representative micrographs is shown in figure Va. The first filter to be collected (filter I) also showed single rods and colonies of bacteria which were much rarer on the second and third filters; it seems likely that these bacteria are contaminants which have been introduced during the connection of the ultrafiltration cell to the borehole supply. These seem to have been washed out of the system during the first filtration run over a period of about 12 hours. The deposition of bacteria on the filter surface appears to have distorted the flow across the membrane and filter I showed a much more heterogeneous particle distribution across the membrane surface than the two collected subsequently.

EIR also attempted to analyse filter III using TEM, preparing the sample by washing the colloids off the membrane filter onto a bronze grid. However because of the relatively small number of particles it was difficult to differentiate the groundwater colloids from artefacts of the sample preparation; bidistilled water used to wash the membrane filter contains a comparable number of particles to this groundwater (12).

3.1.2 Estimation of colloid populations

Particle numbers and sizes were quantified by three of the laboratories. EIR analysed electron micrograph negatives using an automatic Quantimet system for image analysis. The individual particle areas were measured and converted to a circle diameter of equivalent area; a size distribution was then obtained by summing numbers of particles of equivalent diameter, over a total area of 1600 μm^2. Artefacts, such as the bacteria and membrane defects, were manually eliminated from the particle count. BGS obtained an estimate of the particle population by manual counting of electron micrographs, covering ten areas of between 570 and 2000 μm^2 for each filter, again eliminating obvious artefacts. CEA-FAR estimates of particle numbers, using a similar methodology, were lower, although both the cross-flow membrane and the aqueous colloid concentrate gave consistent populations (cf. section 3.2.3). The results from the three laboratories are given in table I.

These data show a large uncertainty in the population obtained for filter I, reflecting the uneven distribution of particles on the membrane caused by the deposition of bacteria. The population found on filter III shows a much smaller standard deviation, reflecting the more

Table I. Markham Clinton Groundwater - Colloid Population estimated by Direct Counting of Membrane Filters.

Filter Number	BGS Population (particles/litre) Mean ± Standard deviation	EIR/CEA Population (particles/litre) Mean ± Standard deviation
I	[1]$6.18 \pm 3.41 \times 10^7$ (56%)	[3]$2.0 \pm 0.5 \times 10^8$ (25%)
II		[4]1×10^6
III	[2]$1.14 \pm 0.15 \times 10^8$ (13%)	[4]1×10^6

[1]particles of ≥ 0.1μm resolved, mean of 10 counts over separate areas of 2000 μm^2
[2]particles of ≥ 0.05μm resolved, mean of 10 counts over separate areas of 570 μm^2
[3]EIR Quantimet estimate, integrated over area of 1600 μm^2
[4]CEA analysis particles of ≥ 0.1μm resolved, counted over several areas of ca. 500 μm^2

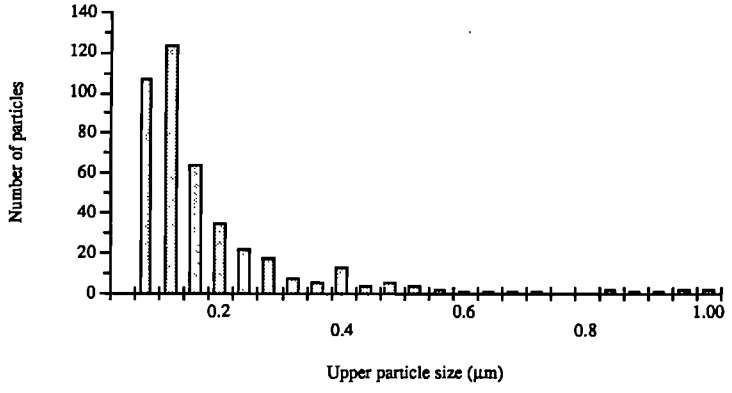

Figure VI. Typical particle size distribution obtained by Quantimet analysis of filter I (EIR data)

homogeneous distribution of particles, in the absence of bacterial contaminants. These populations compare quite favourably with the original LIPAS estimate of ca. 10^9 particles/litre (1). It is quite possible, particularly for filter I, that small sub-micron particles, which predominate, have been masked by larger aggregates and particles. The difference between the CEA analyses and those from BGS and EIR reflects the particle-size resolution obtained by the laboratories; CEA and the first BGS analyses only include particles greater than 0.1μm in diameter, excluding a large number of the smaller particles found at higher resolution (cf. section 3.1.3). Generally it is likely that the SEM counts underestimate the colloid population; the original LIPAS estimate may be the most realistic.

Figure V. Typical electron micrographs of membrane filters (a) prepared directly and (b) from colloid concentrate.

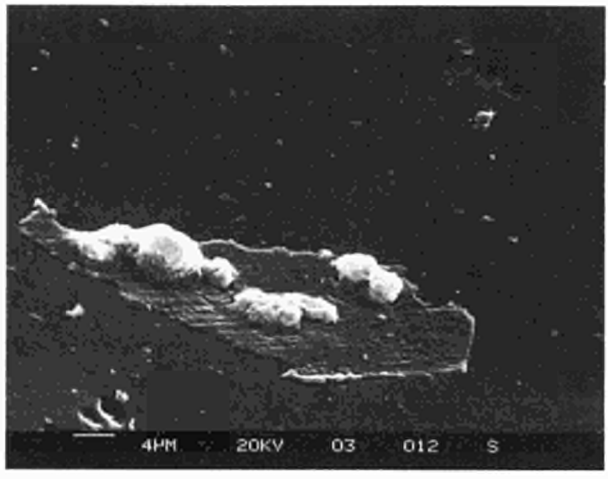

Fig. Va Cross-flow ultrafilter III (BGS): Organic flake with dolomite overgrowth on surface; numerous submicron particles in background.

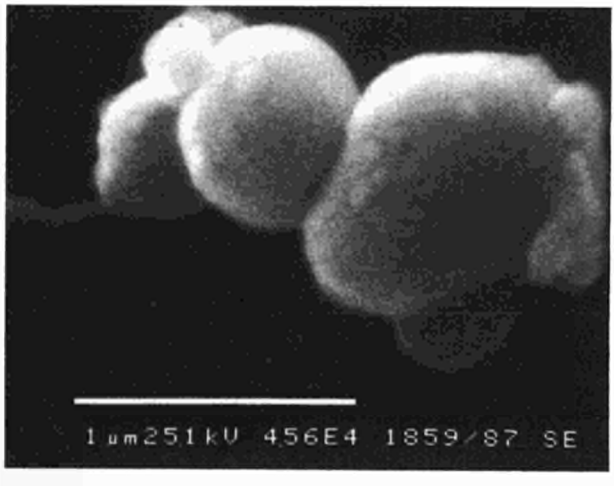

Figure Vb.Cross-flow ultrafilter prepared from aqueous colloid concentrate (EIR): Typical field of view showing colloid aggregate.

3.1.3 Particle Size distribution

A summary of the typical particle size distribution obtained from filter I, by Quantimet analysis, is given in figure VI. This shows the predominance of particles of the order 0.1 μm, at the lower limit of SEM resolution; it is difficult to resolve particles of less than 0.04μm diameter although their presence cannot be discounted.

3.1.4 Colloid Analysis - SEM/EDX

SEM examination of the filters suggests that the isolated micron-sized particles are similar in morphology and composition to the smaller particles which are more typical of this groundwater. Since it is difficult to obtain an EDX spectrum for particles of less than one micron, three of the laboratories (BGS, CEA-FAR and JRC) measured representative spectra for these larger particles. The spectra typically showed significant X-ray signals for Ca, Si, Al, Mg, K, Na, Mn, Fe and Zn; a large Cl peak from the membrane was always present, and there is some evidence that Zn is also present in the membrane.

3.2 Analysis of aqueous colloid concentrate

3.2.1 Elemental analysis of groundwater,ultrafiltrate and colloid concentrate

Groundwater, ultrafiltrate and colloid concentrate samples were analysed for major and trace cations by ICP/AES, by Harwell, JRC and BGS, and for anions using standard wet chemical methods by JRC and BGS. The results of these chemical analyses are summarised in table II. There is generally good agreement between the laboratories; the 1975 groundwater analysis by BGS demonstrates the stability in composition of the Markham Clinton groundwater, with time. To date only calcium, magnesium, sodium, potassium, TOC, manganese, barium, strontium and silicon have been analysed in the groundwater, ultrafiltrate and colloid concentrate. Figure VII compares the concentrations of calcium, magnesium, sodium, potassium and silicon in these three fractions; results are shown for the colloid concentrate for the three laboratories. It seems clear that sodium is depleted in the ultrafiltrate and colloid concentrate. Although there appears to be a similar depletion of potassium, the values measured in groundwater on 20/1/87 were also quite variable, although generally by less than $\pm 0.1 mgl^{-1}$. It is similarly difficult to be certain of the apparent increase of alkaline earth metals in the ultrafiltrate and colloid concentrate (figure VII), given the slight variation in groundwater quality during the extended sampling period.

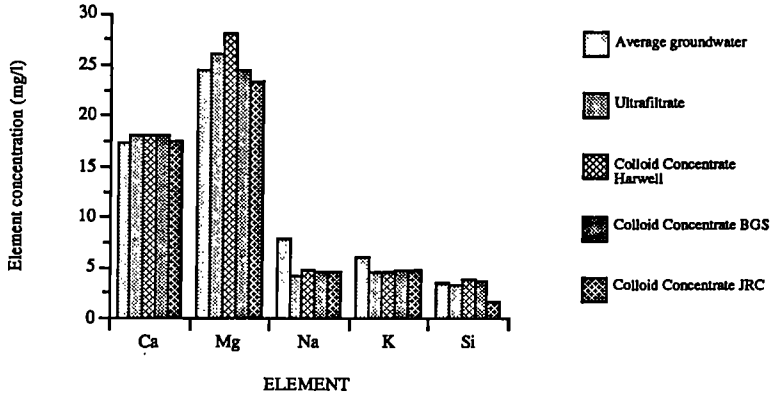

Figure VII. Concentration of major elements in groundwater, ultrafiltrate and colloid concentrates. (Maximum analytical error ±5%)

Silicon concentrations are very similar in all of the samples with the exception of the JRC colloid concentrate, which also shows depletion of magnesium. This difference may reflect the effects of sample storage, since the other laboratories completed analysis very soon after sample collection. It is not possible to compare the manganese data since these all approach detection limits; the TOC data appear unreliable and show considerable analytical variance between samples.

Sample† Species	GW1	GW2	GW3	UF	CCH	CCB	CCJ
			Concentration mg/l				
pH	8.05	7.82	7.6	-	-	8.3	7.9
Conductance	-	250	252	-	-	-	371
Ca	18	17.2	16.9	18	18	18	17.5
Mg	25	24.5	24.2	26	28	24.5	23.4
Na	4.1	7.75	8.9	4.15	4.7	4.6	4.6
K	4.7	6.37	3.93	4.5	4.6	4.81	4.7
Cl	7.1	7.47	8.39	-	-	8.62	11.9
SO_4	15	9.07	8.53	-	-	9.43	9.6
HCO_3	173	192	193	-	-	180.3	164.7
NO_3	2.5	2.08	2.06	-	-	2.52	1.5
NO_2	<2	<2	<2	-	-	<2	-
F	0.054	<0.1	<0.1	-	-	<0.1	0.08
Br	0.054	<0.05	<0.05	-	-	<0.05	-
HPO_4	0.01	<0.5	<0.5	-	-	<0.5	0.02
TOC	<0.1	5.1	-	1.3	1.0	-	0.2*
Fe	0.006	<0.02	<0.02	-	-	<0.02	0.1
Mn	.002	<0.004	<0.004	0.01	0.01	<0.004	-
Si	-	3.56	3.48	3.3	3.9	3.58	1.8
Al	-	<0.065	<0.065	-	-	<0.065	0.2
Ni	0.005	<0.085	<0.085	-	-	<0.085	-
Co	0.001	<0.035	<0.035	-	-	<0.035	-
Sr	0.15	0.12	0.12	0.12	0.13	0.11	-
Ba	-	0.44	0.43	0.47	0.50	0.43	-

Table II. Groundwater, colloid concentrate and ultrafiltrate compositions.

†Sample Code
GW1 - BGS analysis groundwater sample, 1/3/75
GW2 - BGS analysis averaged groundwater sample, 20/1/87
GW3 - BGS analysis groundwater sample, 12/2/87
UF - Harwell analysis ultrafiltrate average, 20/1/87
CCH - Harwell analysis colloid concentrate, 20/1/87
CCB - BGS analysis colloid concentrate, 20/1/87
CCJ - JRC analysis colloid concentrate, 20/1/87

* value reported as mg/l O_2 ($KMnO_4$ method), - indicates not measured.

All major cation analyses ±5% (or less)

It has been suggested that salt exclusion and sample contamination may occur as a result of ultrafiltration (10) and there may also be uptake of trace elements by HF filter membranes (11). The concentration of colloids in the sample is too low to affect the composition of the ultrafiltrate or colloid concentrate. A possible explanation for the similar changes in composition of the ultrafiltrate and colloid concentrate is that some sodium is taken up on the Amicon filter cartridge and/or on the reservoir walls and connecting tubes of the diafiltration rig; ion exchange with alkaline earth metals may also occur. Further laboratory work is required to check this. Similar data should also be collected for the cross-flow ultrafiltration system. However the depletion of both magnesium and silicon in the JRC colloid concentrate sample may indicate a real change in composition with storage, possibly reflecting aggregation

and settling of colloids.

3.2.2 Fractionation of uranium series elements

Groundwater samples were prepared for isotopic diluton/alpha spectrometry by acidifying and boiling down the samples, spiking them with the appropriate U and Th isotopes, and separating the uranium and thorium fractions to produce electroplated alpha sources. These were then counted in the Harwell alpha spectrometer. The uranium isotopic concentration in the colloid concentrate, ultrafiltrate and prefiltered groundwater were found to be of the order of 3 dpm kg^{-1} for ^{238}U and 7 dpm kg^{-1} for ^{234}U. Corresponding values for the thorium isotopes were appreciably lower; about 10^{-3} dpm kg^{-1} for ^{232}Th, about $2x10^{-2}$dpm kg^{-1} for ^{228}Th and about $4x10^{-3}$ for ^{230}Th. The isotopic results are summarised in table III.

Fraction	ISOTOPE (dpm/1474l)				
	^{238}U	^{234}U	^{228}Th	^{230}Th	232Th
Unfiltered Water	4913±78	10953±162	56.±5.9	14.7±1.4	5.9±1.5
Total <1μm	4655±121	10454±268	25.1±1.5	16.2±1.5	1.5±0.5
>1 μm (Filter)	0.65±0.04	1.14±0.04	0.05±0.02	0.21±0.01	0.044±0.007
Colloid Concentrate	61±1.7	138±4	0.2±0.1	0.32±0.06	0±0.01
Amicon filter	4.3±0.1	9.47±0.14	0.06±0.03	0.041±0.006	0.04±0.43
Ultrafiltrate Start of fractionation	4712±110	10578+243	28±3	5.8±1.5	0.87±0.43
Ultrafiltrate End of fractionation	4731±109	10585±240	26±3	5.8±1.5	1.45±0.72

Table III. Activities of uranium and thorium isotopes associated with different size fractions.

Comparison of the actinide isotopic activities in the various phases (table III) indicates that not all the activities held by the 1μm prefilter and the Amicon filter (10,000 MW) are removed by leaching. For this reason the activities on the >1μm particulates were determined from the difference in activities of the unfiltered and prefiltered groundwater. Similarly the colloid fraction together with the activity held on the Amicon filter were found from the difference in activities in the prefiltered groundwater and the ultrafiltrate (table IV).

Most of the uranium is contained in the ultrafiltrate (table IV). The bulk of the ^{228}Th and ^{232}Th activities are associated with the > 1μm particulate phase, while most of the ^{230}Th activity (64%) is contained in the colloid phase (including that held by the Amicon filter). Upper limits for the colloid fraction were obtained of 3%, 10% and 18% for uranium, ^{228}Th and ^{232}Th.

	ISOTOPE				
Fraction	^{238}U	^{234}U	^{228}Th	^{230}Th	^{232}Th
>1μm particles	5±3	5±3	50±12	0±13	75±38
Ultrafiltrate	95±4	95±4	44±7	36±10	30±16
Colloid concentrate and Amicon Filter	0±3	0±3	6±10	64±17	5±18

Table IV. Percentage distribution of U-238, U-234, Th-228, Th-230 and Th-232 between particulate, ultrafiltrate and colloid phase (including Amicon filter residue)

3.2.3 Physical characterisation of aqueous colloid concentrate

The particle population is more difficult to characterise directly in the aqueous colloid concentrate. Harwell and JRC both attempted to determine the particle size distribution directly in the colloid concentrate using photon correlation (dynamic light scattering) spectroscopy. In both cases the particle population proved too low for reliable interpretation of the spectra, although the Harwell data suggested that aggregation had occurred, indicating an equivalent hydrodynamic radius of 9.7μm. It may be that only a relatively small number of particles have aggregated, masking the spectral contribution from smaller particles. This may also be an artefact of the measurement carried out on a sample with a multi-modal particle-size distribution. However aggregation is compatible with the chemical analyses obtained by JRC, suggesting loss of magnesium and silicon on storage of the colloid concentrate.

JRC have also carried out preliminary ultracentrifugation experiments, doping the colloid concentrate with ^{241}Am(III) to act as a marker for the particulates, which should sorb Am(III) quite strongly. These experiments clearly show uptake of the added Am, but are difficult to interpret because of the range of particle sizes present in the sample (9).

CEA-FAR obtained a particle population for the colloid concentrate by cross-flow ultrafiltration of 50-70ml of colloid concentrate onto an Amicon XM 50 membrane filter; SEM micrographs of the carbon coated membrane were prepared and counted. A population equivalent to 2×10^6 particles/litre was obtained, which agrees closely with the CEA estimate from direct membrane filtration. The slight increase in population observed with the colloid concentrate sample may also reflect aggregation, bringing more particles within the limit of resolution of SEM. Figure Vb shows a representative micrograph (EIR) of a membrane filter prepared from the colloid concentrate, and clearly demonstrates particle aggregation. Bacteria were also observed in the EIR sample prepared from the colloid concentrate and, generally more aggregates were found, although the agreement between the two methods is encouraging.

Further work is planned on the separation of colloids from the aqueous concentrate by cross flow ultrafiltration, by the other participating laboratories.

4.0 Effects of water sample storage

Samples of groundwater were collected for colloid fractionation, by cross-flow ultrafiltration and diaultrafiltration, after approximately 2 months storage. These have yet to be analysed.

5.0 Conclusions

This intercomparison exercise has demonstrated that it is possible to isolate and enumerate natural groundwater colloids, with good reproducibility using cross-flow ultrafiltration. The results from the diaultrafiltration colloid concentration system are more ambiguous. Although the study is not fully complete, the following conclusions and recommendations for further work can be made:

(1) Cross-flow membrane ultrafiltration provides reproducible colloid samples which are relatively easy (if time-consuming) to enumerate by analysis of SEM micrographs. However the present resolution of 0.05-0.1μm obtainable with SEM places a restriction on the size of colloid particles which can be distinguished.

(2) Samples produced by diafiltration in the form of an aqueous colloid concentrate are more difficult to characterise. A reliable technique is needed to determine the colloid particle size and population directly. However present work on determining the colloid population by ultrafiltration of the concentrate agrees quite closely with the values obtained by analysis of membranes prepared directly. There is also some evidence that the composition of the colloid concentrate changes with time.

(3) The HF diaultrafiltration system appears to take up alkali metals and, possibly, release alkaline earth metals (ion exchange?). This needs to be checked in the laboratory and similar data collected for fluids contacting the cross-flow ultrafiltration membrane.

(4) Isotope dilution/alpha spectrometry has been used to put limits on the percentage activities of natural-series isotopes associated with the colloid and particulate phases. Upper limits for the colloid fraction were obtained of 3%, 10%,18% and 64% for uranium, ^{228}Th, ^{232}Th and ^{230}Th.

(5) Neither colloid isolation method is without disadvantages. If the aim of the investigator is to simply to enumerate the particle size distribution and population, then the cross-flow filtration method is simpler to perform and analyse and gives reliable data, once the sampling system is flushed of contaminants. However if large colloid samples are required for use in, for example, sorption experiments or uranium series analyses the diaultrafiltration system is easier to operate for large sample batches; the alteration of the physical state of the colloids should be investigated further.

6.0 Acknowlegements

This study could not have been undertaken without the co-operation of Severn Trent Water Authority, in particular Peter Wade, who allowed us to use the Markham Clinton borehole and provided considerable practical assistance. Steve Hitchman, Dave Holmes, and Mike Wilkins are thanked for their help in taking the samples. Mark Cave performed many of the groundwater analyses and Tony Milodowski spent several days enumerating and analysing membrane filters. The efforts of the members of the other participating laboratories, particularly Drs. Bidoglio, Moulin, Billon, Kim and Buckau are also gratefully acknowledged. This study was funded jointly by the UK Department of the Environment and the CEC, with contributions from EIR and NAGRA.

This paper is published by permission of the Director of the British Geological Survey (Natural Environment Research Council).

7.0 References

1. KLENZE, R. and KIM, J. I. (1986). Characterisation of groundwater colloids by laser induced photoacoustic spectroscopy. Institut für Radiochemie der Technischen Universität München, Report No. RCM 03286.

2. IVANOVICH, M. and HARDY, C.J. (1986). Identification and measurement of colloids in groundwater. Natural Analogue Working Group, Interlaken, Switzerland, 17-19 June 1986.

3. BATH, A.H., EDMUNDS, W.M. and ANDREWS, J.N. (1979). Palaeoclimatic trends deduced from the hydrochemistry of a Triassic sandstone aquifer, United Kingdom. In: "Isotope Hydrology" (Proc. Symp. Vienna, 1978). Vol II, pp. 545-568, I.A.E.A., Vienna, 1984.

4. EDMUNDS, W. M., BATH, A.H. and MILES, D.L. (1982). Hydrochemical

evolution of the East Midlands Triassic sandstone aquifer, England. Geochim. Cosmochim. Act., 46, 2069-2081.
5. ANDREWS, J.N., BALDERER, W., BATH, A.H., CLAUSEN, H.B., EVANS, G.V., FLORKOWSKI, T., GOLDBRUNNER, J.E., IVANOVICH, M., LOOSLI, H. and ZOJER, H. (1984). Environmental isotope studies in two aquifer systems: A comparison of groundwater dating methods. In: "Isotope Hydrology 1983", pp. 535-576, I.A.E.A., Vienna, 1984.
6. DEGUELDRE, C.A. and THOMI, H. (1986)
Réalisation d'une cellule de diaultrafiltration à injection pulsée. EIR Internal Report Number: TM-42-86-37 (8/12/1986).
7. IVANOVICH, M., LONGWORTH, G. and WILKINS, M.A. (1987). Preliminary report on the collection and characterisation of colloids from Markham Clinton, January 1987. Unpublished Harwell Report.
8. MOULIN, V. (1987). Preliminary experimental results for the interlaboratory exercise on colloid sampling and characterisation. Unpublished report CEA-FAR, pers. comm.
9. BIDOGLIO, G. (1987). Preliminary experimental results for the interlaboratory exercise on colloid sampling and characterisation. Unpublished report JRC ISPRA, pers. comm.
10. JOLLEY, R.L. (1981). Concentrating organics in water for biological testing. Environ. Sci. Technol., 15 (8), 874-880.
11. SALBU,B., BJÖRNSTAD, H.E., LIDSTRÖM, N.S., LYDERSEN,E., BREVIK, E.M., RAMBAK, J.P. and PAUS, P.E. (1985). Talanta, 32, 907 et seq.
12. DEGUELDRE, C., GIOVANOLI, R., GRIMMER, H., NAEF, E. and PORTMANN, A. (1987). Sampling and Characterisation of Markham Colloids. EIR Internal Report: TR-42-87-11.

APPLICATION OF OPEN SYSTEM MODELLING TO STUDIES OF SECONDARY MINERALIZATION (KOONGARRA) AND ROCK MATRIX DIFFUSION (KRÄKEMÄLA)

C Golian and P Duerden
Australian Atomic Energy Commission

Summary

The open system modelling technique was developed to interpret the results of the natural analogue study being conducted in the Alligator Rivers region of the Northern Territory of Australia. The model was prepared in a general form, and then compared with other open system models. A modified version of the model was used to study the movement of uranium in the secondary mineralization deposit at Koongarra. The results were consistent with a general understanding of a roll front effect. The average overall uranium mobility rate had leaching characteristics near the original ore deposits which systematically changed to a deposition mechanism farther from the primary body. The derived timescale for the event was in agreement with the results of other modelling attempts. A second modified version of the open system model allowed uranium mobility in the region of a water conducting fracture in crystalline rock to be modelled. Experimental data by Smellie, MacKenzie and Scott from a Kräkemäla granite sample containing a fracture were used to test the model. The calculated uranium mobility rate supported the assumption that the radionuclides can disperse into the rock matrix through a diffusion mechanism.

1.1 Introduction

Mathematical modelling studies of natural analogues can be divided into two separate groups. The framework of the first utilizes an extensive number of hydrodynamic dispersivity, molecular diffusion or variably defined sorption mechanisms, and the second uses radiochemical data for an evaluation of open or closed systems.

A number of hydrodynamic models are available. However, owing to the complexity of the geohydrological medium, they can be used with varying degrees of accuracy. Accuracy depends on the availability of geohydrological data, a comprehensive physical description of the modelled system and an adequate mathematical treatment of the hydraulics and geochemistry. Hydrodynamic models (1-5) are based on idealised fundamental physical phenomena which, of necessity, deal only with global variations of physical and chemical parameters. Inadequacy of the hydrogeological characterization of the sites studied is a common problem of mathematical modelling.

The importance of an accurate determination of, for example, the aperture of the water-conducting fractures in crystalline rock or their spacing is commonly stressed (4). This can be overcome in a laboratory environment, by measuring the parameters required for the modelling, e.g. the diffusion coefficient, and applying the acquired data to field

conditions (5). For practical reasons, the modelling is often simplified by omitting from the mathematical description some of the transport processes, because they are negligible or because they lack sufficient manageable input data. However, once the parameters have been incorporated in the model, they introduce an element of uncertainty which is especially uncontrollable when the effect of a particular process is difficult to estimate. A typical example of this effect is the reduction of the model from three dimensions to one dimension in which the results of transport are analysed in one arbitrarily chosen orientation. In this case, radionuclide movement in the selected dimension is taken to be representative of the whole system.

The open system mathematical approach represents the other extreme of radionuclide transport modelling. By definition, it is a reduced modelling approach, based on essentially comprehensive experimental data which consists of activity ratios (ARs) of radionuclides in rock samples taken from chosen localities. Additional information on radionuclide distribution and ARs in local groundwater is usually also available.

In the open system model, the physical movement of the radionuclides in geological strata is not investigated because of its uncertainty; rather, the model looks at the final results of the leaching and deposition processes, i.e. the alteration of the activity ratios.

Although the problems incurred in the hydrodynamic models have much less effect in this approach, the open system method has inherent limitations and inadequacies, but they are mainly conceptual and less dependent on the availability of experimental data.

A number of open system uranium models have been developed (6-10). Most are designed to deal with a particular dating assignment, e.g. shell, bone, coral or soil profile dating.

2.1 Lucas Heights Open System Model

Open system mathematical modelling was undertaken at Lucas Heights in support of an extensive experimental program based on studies of radionuclide migration around uranium deposits in the Alligator Rivers region of the Northern Territory of Australia (11-13). The mathematical framework of the model was based on the measured results of authogenic and allogenic changes in the ratios of uranium isotopes and some of their daughter products, e.g. thorium.

It was initially assumed that thorium is immobile in soluble form. However, recent experimental data have suggested the possibility of colloid transport. The uranium leaching or deposition processes were assumed to be first order processes, i.e. deposition/leaching rates were proportional to the concentration of accessible uranium in the ore deposit. A similar approach was used in the Hille model (6), although it is difficult to support in the case of a deposition process in which there is an undefined correlation between the level of uranium in the rock and that in the groundwater.

This model also assumes that at time t = 0, following a known or undefined sequence of events, water commenced to move through the given geological system, thus mobilizing the accessible uranium. Time t = 0 is not necessarily a point value, but may represent a very extended initial period; however, on the relevant timescale it is of neglible duration.

From the model description presented in an earlier publication(13), the generating equations for uranium-238, uranium-234 and thorium-230 are formulated as follows:

$$-\frac{dU_8}{dt} = \lambda_8 U_8 + \xi U_8 \quad , \tag{1}$$

$$-\frac{dU_4}{dt} = \lambda_4 U_4 + R\xi U_4 - \lambda_8 U_8 \quad , \tag{2}$$

$$-\frac{dTh}{dt} = \lambda_0 + Th - \lambda_4 U_4 \quad , \tag{3}$$

where U_8, U_4, Th are uranium-238, uranium-234 and thorium-230, respectively and λ_8, λ_4, λ_0 are the corresponding decay constants, ξ is the leaching/deposition rate, and R is the ratio of ^{234}U to ^{238}U leaching/deposition rates, and is usually the AR found in groundwater adjacent to the deposit.

In the mathematical formalism, the leaching/deposition rate is presented in the form of decay constants with a minus sign for deposition and a plus sign for a leaching process.

The solution of equations (1), (2) and (3) can be expressed as U_4/U_8, Th/U_4 activity ratios indicated as Su and St respectively:

$$Su = Su(t_0)e^{(b-a)t} + \frac{\lambda_4}{b-a}\left(e^{(b-a)t} - 1\right) \tag{4}$$

$$St \times D = St(t_0)e^{(a-\lambda_0)t} + \frac{\lambda_0}{a-\lambda_0}\left(e^{(a-\lambda_0)t} - 1\right) +$$

$$+ \frac{\lambda_0\lambda_4}{(b-a)(a-\lambda_0)(b-\lambda_0)Su(t_0)}\left[(b-a)e^{(a-\lambda_i)t} + \right.$$

$$\left. + (a+\lambda_0)e^{-(b-a)t} + \lambda_0 - b\right] \tag{5}$$

where $D = 1 + \frac{\lambda_4}{(b-a)Su(t_0)}\left(1 - e^{-(b-a)t}\right)$,

$a = \lambda_4 + R\xi$, and

$b = \lambda_8 + \xi$.

The model was used in a four-zone model to interpret the Ranger, Jabiluka and Nabarlek uranium deposits. In particular, the uranium residence time in each zone and the relevant leaching/deposition rates were calculated. The model was extended to describe the distribution of radionuclides in specific minerals so that the isotopic fractionation between amorphous iron, crystalline iron and clay/quartz phases could be rationalised. In addition, the model was compared against other open system models. These included the model developed by Rosholt et al. (9) and used to interpret a large data set on the deposition of alluvial, aeolian and other materials. An attempt was made to interpret the parameters λ_0 and the Rosholt model calibration curve. The model also proved to be satisfactory when it was compared with Hille's model (6) and used to interpret data for mollusc samples obtained by Szabo and Rosholt (8). The calculation of time-leaching rate domains, shown in Figure 1 demonstrates the good agreement between the models. The basic set of equations in the model was suitably flexible for application to specific open system requirements.

Two further examples which demonstrate the adaptability of the model are given below. In the first, a modified version is used to describe the

formation of the secondary mineralization deposit at Koongarra. The second uses an alternate approach to interpret uranium mobility in the region of a water conducting fracture.

3.1 Modelling the Koongarra Secondary Mineralization Deposit

3.2 Koongarra Deposit

The Koongarra deposit consists of an area of the original ore body and a region of extended secondary mineralization. The primary zone contains uraninite veins within steeply dipping quartz-chlorite schists of the lower member of the Cahill Formation (14). The secondary mineralization area is in the shape of a tongue-like fan which is oriented along the general direction of strong groundwater flow (Figure 2) and is formed in weathered schists which extend from almost the surface to the bottom of the weathered zone at 25-30 m.

Samples were taken from the centre layer of the secondary mineralization fan, starting from a position close to the primary ore body and extending away from it in a southerly direction. The layer 15-20 m below the surface is the more uranium rich part of the fan. The area is also characterised by a dominant horizontal water flow pattern. However, close to the fault there is strong recharge, possibly from the lower levels, where there is seepage of surface water along the whole length of the fan during the wet season.

3.3 Modelling

The basic model was modified to include a more realistic representation of the leaching/deposition processes so that the leaching/deposition rate is related to the actual uranium concentration in rock and water, and to the system adsorption ability represented by the adsorption coefficient K_d. The adsorption coefficient is defined as the ratio of the weight of uranium adsorbed per unit weight of adsorbate to the weight of dissolved uranium per unit volume of solution after adsorption equilibrium has been attained.

The change in uranium concentration in the rock due to radionuclide mobilization is given by a double expression. The first part describes the actual leaching/deposition rate and is called 'uranium in/out flow' whilst the second indicates the direction of the flow, which determines the overall leaching or deposition character of the process. The latter part of the expression is a function of the uranium concentration in both the adsorbate and the groundwater and is proportional to the K_d of the system.

The change in urania concentration in rock due to mobilization of these radioisotopes in groundwater, (A) can be expressed as follows:

$$A = F.(q \frac{C}{C^W} - 1)$$

where C^W is the uranium concentration in water, C is the uranium concentration in rock, V is the volume of rock, Π is the porosity, S^W is the U4/U8 activity ratio in groundwater, q is the leaching/deposition factor ($\sim \frac{1}{K_d}$), F is the uranium in/out flow $F = C^W.V.\Pi.\phi$, and ϕ is the transport rate (>0).

The expression in brackets signifies the result of the radioisotope transport, where $(q \frac{C}{C^W} > 1)$ indicates a leaching process and $(q \frac{C}{C^W} < 1)$ the deposition of mobilized radioisotopes.

The generating equations (1), (2) and (3) were modified to include this representation of the deposition/leaching process:

Uranium-238

$$-\frac{dU_8}{dt} = \lambda_8 U_8 + A_8 \quad , \tag{6}$$

$$= (\lambda_8 + q\Pi\phi)U_8 - \phi U_8^W \quad . \tag{7}$$

Uranium-234

$$-\frac{dU_8}{dt} = \lambda_4 U_4 - \lambda_8 U_8 + A_4 \quad , \tag{8}$$

$$= (\lambda_4 + Rq\Pi\phi)U_4 - \lambda_8 U_8 - R\phi U_4^W \quad . \tag{9}$$

Thorium-230

$$-\frac{dTh}{dt} = \lambda_0 Th - \lambda_4 U_4 \quad . \tag{10}$$

The solution of these equations can, as before, be presented in a convenient form for activity ratio calculations.

First, the 'normalized' decay rates are introduced:

$$Q_8 = \frac{\lambda_8 U_8}{\lambda_8 U_8(0)} \ , \ Q_4 = \frac{\lambda_4 U_4}{\lambda_8 U_8(0)} \text{ and } Q_0 \frac{\lambda_0 Th}{\lambda_4 U_4(0)} \quad .$$

Thus

$$Q_8 = e^{-bt} + \frac{\phi}{b} S(1 - e^{-bt}) \tag{11}$$

$$Q_4 = Suu(0)e^{-at} + \frac{\phi}{a} S(\frac{\lambda_4}{b} + RS^W)(1 - e^{-at}) + \\ + \frac{\lambda_4(b-\phi S)}{b(b-a)} (e^{-at} - e^{-bt}) \tag{12}$$

$$Q_0 = Stu(0)e^{-bt} + \frac{\lambda_0\lambda_4(b-\phi S)}{b(b-a)(b-\lambda_0)Suu(0)} (e^{-bt} - e^{-\lambda_0 t}) + \\ + \frac{\lambda_0}{a(a-\lambda_0)Suu(0)} (a\ Suu(0) - R\phi SS^W + \\ + \frac{\lambda_4(a-\phi S)}{b-a}) (e^{-\lambda_0 t} - e^{-at}) + \\ + \frac{\phi S}{a\ Suu(0)} (\frac{\lambda_4}{b} + RS^W)(1 - e^{-\lambda_0 t}) \quad , \tag{13}$$

where $a = \lambda_4 + q\Pi R\phi$,

$b = \lambda_8 + q\Pi\phi$,

$S = \frac{\lambda_8 U_8^W}{\lambda_8 U_8(0)}$,

$S^W = \frac{\lambda_4 U_4^W}{\lambda_8 U_8^W}$,

$Suu(o) = \frac{\lambda_4 U_4(0)}{\lambda_8 U_8(0)}$,

$Stu(o) \quad \frac{\lambda_0 Th(0)}{\lambda_4 U_4(0)}$.

These 'normalized' rates are then used to present the expression for relevant activity ratios:

$$Suu = \frac{\lambda_4 U_4}{\lambda_8 U_8} = \frac{Q_4}{Q_8} , \qquad (14)$$

$$Stu = \frac{\lambda_0 Th}{\lambda_4 U_4} = \frac{Q_0}{Q_4} . Suu(0) . \qquad (15)$$

3.4 Initial and Boundary Conditions

The major difficulty of this procedure is that there is a greater number of variables than available equations. The usual approach is to select the largest possible ranges for the variables, and calculate for any systematically chosen combination of values. The calculated ARs are then compared with experimental data and rejected or accepted on the basis of given matching criteria. These criteria are determined by reference to the precision of the experimental results. Apart from the preselected ranges of the variables, it is also necessary to predetermine the initial conditions and, if required, other boundary conditions.

In many cases, initial ARs in rock or groundwater can be set up by accepting the general assumption of the model, e.g. that at time = 0, the primary deposit is in an unperturbed state and probably is equilibrated; thus $^{234}U/^{238}U = 1.00$ and $^{230}Th/^{234}U = 1.00$. In the region of the secondary mineralization, the value of $^{234}U/^{238}U(0)$ is set to be equal to the ratio in which the water deposited the uranium. The reason for this assumption is that the uranium carried by groundwater and deposited in a particular region overwhelmed, in mass terms, any uranium initially present in the region during the 'time zero period'. Furthermore, bearing in mind the assumption that thorium does not travel, the initial value $Si(0) = {}^{230}Th/^{234}U(0)$ is set to be zero.

It was also assumed that the total time of formation of the secondary mineralization fan is related linearly to the total length of the fan because of the constant advancement of the roll front. The age of a particular region of the fan is thus inversely proportional to the normalized distance between the region and the centre of the primary ore body.

Other parameters such as R, the ratio of the urania leaching rates, and ξ, the leaching/deposition rate, were allowed to vary freely in the ranges R = 0.40–2.00 and -40×10^{-6} to 40×10^{-6} y^{-1}, respectively.

Figure 3 represents graphically the results of the modelling and shows the relationship between averaged rate of leaching/deposition and the position of the sample and corroborates the predicted behaviour in the secondary mineralization region. The region closer to the primary ore body was dominated by the leaching process throughout its formation, but further from the original ore body the process shows overall deposition characteristics. This is in agreement with the hypothetical mechanism for the moving roll front.

The timescale of the process has not been determined unequivocally owing to the intrinsic nature of this mdelling approach. It can be said, however, that the age of the process is at least 700 ky and extends into the region of several My, but it is self-evident that the sensitivity of any method based on the half-life of uranium-234 diminishes rapidly beyond about 1 My.

An additional and significant result of the modelling was the determination of the value of R. Although a large range of R was allowed for during computation, the constraints of the modelling provided solutions with values restricted to the narrow range of 0.80–0.85, a value which is in pleasing agreement with the data for modern groundwater from bore holes in the system (12).

The advantage of imposing an age-distance relationship is clearly demonstrated when we consider the results obtained from a series of samples which represent the vertical distribution of the uranium in the secondary mineralization fan in a section close to the original ore body. The sample depths ranged from 0-50 m of the DDH 52 drill core. In the modelling, all samples were treated as individual cases, no restrictive conditions interlinking the development of this vertical profile being used in the computation routine.

The rate-time curves for each sample are shown in Figure 4. It can be seen that they exhibit the typical outcome of the general open system approach. The solutions, being in the form of sometimes large leaching/deposition rate-time domains, are the result of an incomplete site description and a lack of sufficient constraints. However, even with these imprecise results it is possible to point to the general trend of the uranium deposit displacement. The leaching process can be seen to be strongest near the surface, probably due to percolating surface water during the wet season, with the rate then decreasing markedly for the samples near the bottom of the weathered zone.

4.1 Rock-matrix Diffusion

4.2 Sample description

Radionuclide diffusion into the rock matrix is thought to be an important retardation mechanism for the migration of contaminants from radioactive waste repositories. The crystalline rock body can contain rich, hydraulically connected fracture systems which allow free circulation of underground waters and could facilitate the movement of radionuclides through the rock. It is then possible that the material is adsorbed on the fracture surface and may diffuse into the crystalline matrix thus decreasing the rate of advancement of the pollutants. We have used the open system model to evaluate this process using data reported by Smellie et al. (15) in a detailed study of natural radionuclide migration in crystalline rock. Rock drill core samples from three locations in Sweden and Switzerland were selected from water-conducting fractures. The sample from Kräkemäla (Sweden) drill core is typical of the Gotemar coarse-grained granite and is macroscopically homogeneous. However, the mineralogical composition shows considerable variety, being mainly quartz, plagioclase and potash feldspar with many accessory minerals.

The contained fracture was in fact a series of parallel micro-fissures up to about 10 mm in width with the fissure surfaces being coated by an FeOOh-oxide layer. Smellie also reported that the effect of the fracture zone, in the form of FeOOH-oxide dustings, is visible up to 20 mm into the host rock.

4.3 Formulation of uranium migration model

In order to model the uranium and thorium distribution in the water conducting fracture, it was assumed that uranium can be leached from the rock and dissolve in the groundwater, and uranium from the water can be adsorbed on the fracture filling minerals. In addition direct groundwater to rock transfer can occur along grain boundaries.

In contrast to the previous example where we considered the movement of groundwater through weathered rock, here water has flowed mainly through the fracture and dispersed into small fissures and intergrain space. In this version of the model it was necessary to evaluate the leaching and deposition processes separately. Recoil was also included as a separate process as it was suspected of having special improtance in determining the mobility of uranium in the fracture region. The efficiency of the recoil transfer was related to the surface between the liquid and solid phases.

It was assumed that uranium concentration in the intergrain water was constant over geological time and the modern thorium distribution pattern closely resembles the original thorium signature.

Additional information on the distribution of iron pattern, variation of its oxidation ratio, the distribution of rare-earth elements and the general mineralogy of the sample is also very valuable in determining the initial conditions for solving the model equations. It is well known, for example, that uranium and thorium affiliate with iron phases (12), and rare-earth elements and thorium have similar distribution patterns.

4.4 Mathematical formulations

The change of uranium-238 concentration in a given region of crystalline rock in the vicinity of a water conducting fracture can be written as

$$-\frac{dU_8}{dt} = \lambda_8 U_8 + \xi U_8 - \delta U_8^{W} \tag{16}$$

whilst equations (17) and (18) model the authigenic and allogenic changes in ^{234}U and ^{230}Th in the same region.

$$-\frac{dU_4}{dt} = \lambda_4 U_4 - \lambda_8 U_8 + R\xi U_4 - R^{W}\delta U_4^{W} - \phi_u \lambda_8 U_8^{W} \tag{17}$$

$$-\frac{dTh}{dt} = \lambda_0 Th - \lambda_4 U_4 - \phi_{Th}\lambda_4 U_4^{W} \tag{18}$$

where δ is the deposition rate (water to rock), R^{W} is the $U_4/_8U$ activity ratio of uranium deposit, ϕ_u, ϕ_{Th} are the recoil coefficients for U_4 and Th (water to rock), and U_4^{W}, U_8^{W} is the uranium(^{234}U or ^{238}U) in water.

The above set of equations is then solved analytically with the solutions being presented as before in the form of normalized decay rates:

$$P_8 = \frac{\lambda_8 U_8}{\lambda_8 U_8(0)}\ ,\ P_4 = \frac{\lambda_4 U_4}{\lambda_4 U_4(0)} \text{ and } P_0 = \frac{\lambda_0 Th}{\lambda_4 U_4(0)}$$

viz

$$P_8 = W_1 e^{-bt} + \frac{\delta}{b} S \tag{19}$$

$$P_4 = (Su(0) - W_2)e^{-at} + \frac{\lambda_4 W_1}{b-a}(e^{-at} - e^{-bt}) + W_2 \tag{20}$$

$$P_0 = \frac{1}{Su(0)}(Su(0)Stu(0) - W_3)e^{-\lambda_0 t} + \frac{\lambda_0\lambda_4 W_1}{(\lambda_0 - b)(b-a)\ Su(0)}(e^{-\lambda_0 t} - e^{-bt}) + \frac{\lambda_0}{(\lambda_0 - a)Su(0)}(Su(0) + \frac{\lambda_4}{b-a}W_1 - W_2)(e^{-at} - e^{-\lambda_0 t}) + \frac{W_3}{Su(0)} \tag{21}$$

where $a = \lambda_4 + R\xi$,

$b = \lambda_8 + \xi$,

$S = \frac{\lambda_8 U_8^{W}}{\lambda_8 U_8(0)}$,

$Su^{W} = \frac{\lambda_4 U_4^{W}}{\lambda_8 U_8^{W}}$,

and $W_1 = 1 - \frac{\delta}{b} S$,

$W_2 = \frac{\lambda_4}{a} (\frac{\delta}{b} + R\frac{\delta}{\lambda_4} Su^W + \phi_u)S$,

$W_3 = W_2 - \phi Th Su^W S$,

$Su(0) = \frac{\lambda_4 U_4(0)}{\lambda_8 U_8(0)}$,

$Stu(0) = \frac{\lambda_0 Th(0)}{\lambda_4 U_4(0)}$.

With the uranium concentration and the ARs also expressed as functions of the normalized decay rates such that

$$U = U(0) \times P_8 \tag{22}$$

$$Suu = \frac{\lambda_4 U_4}{\lambda_8 U_8} = \frac{P_4}{P_8} \tag{23}$$

$$Stu = \frac{\lambda_0 Th}{\lambda_4 U_4} = \frac{P_0}{P_4} \times Suu(0) \tag{24}$$

Initial values for the $^{234}U/^{238}U$, ^{230}Th, ^{234}U ARs of the samples were set at 1.0, which is equivalent to an equilibrium condition before start of flow of water, the range of ARs being restricted to 0-1.00 with 0.1 progression increments. The R values were set in the 0.0-2.7 range and R^W values in the range 1.00-2.7 with 0.15 increments. The groundwater is considered to have an excess of ^{234}U and urania ARs as high as 3.00.

The leaching rate was allowed to vary from 8×10^{-5} y^{-1} to zero, and the deposition rate δ from 0 to 8×10^{-5} y^{-1} in 0.5×10^{-6} y^{-1} increments. The value of Su^W was related to modern R and R^W values and a number of values for ϕ_u, ϕ_{Th} (the recoil coefficients) in the 0-0.2 range were used.

4.4 Results and Discussion

The experimental data show that the uranium concentration decreases sharply from the region of the fracture surface and then has little variation. This is in marked contrast to the thorium concentration which fluctuates over the entire rock section. At about 10-12 cm from the fracture there is a local increase in the concentration of both radioisotopes. The $^{234}U/^{238}U$ activity ratio shows excess of ^{238}U near the surface but falls below 1.00 for the region between 3-12 cm, and the $^{230}Th/^{234}U$ activity ratio is less than 1.00 near the surface. This suggests that the high $^{234}U/^{238}U$ disequilibria and $^{230}Th/^{234}U$ deficit near the fracture surface may be due to competing deposition and leaching processes with possible groundwater to rock recoil of ^{234}U.

The modelling results presented in Figure 5 support this general observation. The uranium migration rate, obtained by calculation of the net result of the local leaching and deposition processes and the possible effect of the recoil mechanism, is shown as a function of distance from the fracture surface.

The migration rate curve shows local fluctuations which probably reflect among other tendencies, the mineralogical variability of the rock matrix. The general trend of migration rate with distance was obtained by 'smoothing' the migration rate curve. This indicates however, that the net rate goes through a maximum near the fracture surface and then decreases systematically with distance. The area near the fracture surface

is in the region of strongest depositional activity and penetration of deposited uranium into the matrix. This is balanced however, by general leaching and diffusion mechanisms which remove uranium from the uranium-bearing minerals in the matrix.

The other promising result of these studies is the similarity of the uranium gradient pattern to the migration pattern, which as can be seen from Fick's diffusion law in its simplest form,

$$\frac{dU}{dt} = D \frac{dU}{dx} ,$$

where D - diffusion coefficient,
is the basic requirement for a diffusion process. However, the pattern similarities cannot be extended to a direct proportionality of the migration rate and the uranium gradient because the mineralogical composition of the sample varies considerably from the fracture face, so the diffusion coefficient D could not be constant for the entire sample.

A timescale for the leaching and deposition processes along the sample was established, with the starting event occurring at least 700±200 ky ago.

5.1 Conclusions

The modelling of uranium migration on the basis of uranium series disequilibria can effectively determine at least the qualitative features of the leaching/deposition processes. Moreover it can be used to establish a basis for understanding the mechanism of uranium movement.

An essential pre-requisite for open system modelling is the acquisition of additional information about the geological system, a common property which allows the individual computing routines to be 'interlinked', and thus reduce the uncertainty of 'fitted' parameters.

In general however, the method of computation is relatively uncomplicated and the data base necessary for modelling the site is reduced to a range of radiochemical characteristics. The basic modelling approach is not site-specific and its results can be applied to the prediction of rates of transport and the timeframe at a radioactive waste repository.

The minimum age of 700±200 ky for the Koongarra region of secondary mineralization which was derived with the present open system modelling scheme is comparable with results obtained by Lever (13) when using a range of hydrodynamic transport models and available geo- and hydrological data.

The qualitative open system model solutions of the horizontal migration and the vertical distribution conform with a general understanding of roll front effects.

The agreement of the derived $^{234}U/^{238}U$ ratio in groundwater (parameter R) with data for local modern groundwater, supports the general basis for both the horizontal and vertical modelling approaches.

The modelling of uranium and thorium distribution in crystalline rock near the water-conducting fractures established the similarity of the migration rate and the uranium gradient patterns, and indicates the presence of a diffusion mechanism. The migration rate has deposition process characteristics in an area close to the fracture face, but further away the leaching mechanism is dominant. This is affected however by local mineralogy and Fe distribution patterns.

In the region near the fracture face there is a retention of strongly implanted uranium, such as ^{234}U from recoil resulting from the net effect of competing leaching and deposition activities. The overall decrease in the uranium concentration in this part of the rock was accompanied by

markedly high $^{234}U/^{238}U$ ARs, whereas the ^{230}Th remained unequilibrated with its ^{234}U parent. This zone required particular attention during modelling owing to an increase in the significance of recoil. At the present time, the recoil parameters are only 'fitted' in the computing routine, and a more reliable method of estimation is required.

6.1 References

1. TANG, E.H., FRIND, E.O. and SUDINCKY, E.A. Contaminant Transport in Fractured Porous Media: Analytical Solution for a Single Fracture, Water Resour. Res. 17 (1981), 555.
2. LEVER, D.A. Modelling Radionuclide Transport at the Koongarra Uranium Deposit, Natural Analogue Working Group (Second Meeting), Interlaken, 17-19 June 1986. To be published as EUR 10671.
3. GRISAK, G.E. and PICKENS, J.F. Solute Transport through Fractured Media, Water Resour. Res., 16, No 4 (August 1980), pp. 719-30.
4. LEVER, A.A. and BRADBURY, H.H. Mineral. Mag., 49 (1985), 295.
5. BRADBURY, M.H., LEVER, D.A. and KINSEY, D.V. In Scientific Basis for Radioact. Waste Management V (Elsevier, 1982), pp. 569.
6. HILLE, P. An Open System Model for Uranium Series Dating, Earth Planet. Sci. Lett., 42 (1979), 138-143.
7. ROSHOLT, J.N. Open System Model for Uranium Series Dating of Pleistocene Samples. In Proceedings of Symposium on Radioactive Dating Methods and Low-level Counting, Monaco, 1967 (IAEA, Vienna), pp. 299-311.
8. SZABO, B. and ROSHOLT, J.N. Uranium Series Dating of Pleistocene Molluscan Shells from Southern California - An Open System Model. J. Geophys. Res., 74 (1969) 3253-60.
9. ROSHOLT, J.N. Uranium Trend Dating of Quaternary Sediments, US Geological Survey Open File Report 80-1087, 1980.
10. ROSHOLT, J.N. Uranium Trend Systematics for Dating Quaternary Sediments, US Dept of the Interior, Geological Survey, Open File Report 85-298, 1985.
11. AIREY, P.L., ROMAN, D., GOLIAN, C., SHORT, S., NIGHTINGALE, T., LOWSON, R.T. and CALF, G.E. Radionuclide Migration around Uranium Ore Bodies - Analogues of Radioactive Waste Repositories, USNRC Contract NRC-04-81-172, Annual Report 1982-83, AAEC Report C40 (1984) (NUREG/CR-391, Vol. 1).
12. AIREY, P.L., ROMAN, D., GOLIAN, C., SHORT, S., NIGHTINGALE, T., PAYNE, T., LOWSON, R.T. and DUERDEN, P. Radionuclide Migration around Uranium Ore Bodies - Analogues of Radioactive Waste Repositories, USNRC Contract NRC-04-81-172, Annual Report 1983-84, AAEC Report C45 (1985).
13. AIREY, P.L., GOLIAN, C. and LEVER, D.A. An Approach to the Mathematical Modelling of the Uranium Series Redistribution within Ore Bodies, Topical Report, AAEC/C49, June 1986.
14. SNELLING, A.A. Urananite and its Alteration Products, Koongarra Uranium Deposit. In Proceedings of IAEA International Symposium Uranium in the Pine Creek Geosyncline, Sydney, 4-8 June 1979, Ed. J Ferguson and A.B. Goleby (IAEA, Vienna, 1980), p. 487.
15. SMELLIE, J.A.T., MacKENZIE, A.B. and SCOTT, R.D. An Analogue Validation Study of Natural Radionuclide Migration in Crystalline Rocks using Uranium-Series Disequilibrium Studies. Paper presented to First Meeting of Natural Analogue Working Group, Brussels, 5-7 November 1985. EUR 10315 EN-FR

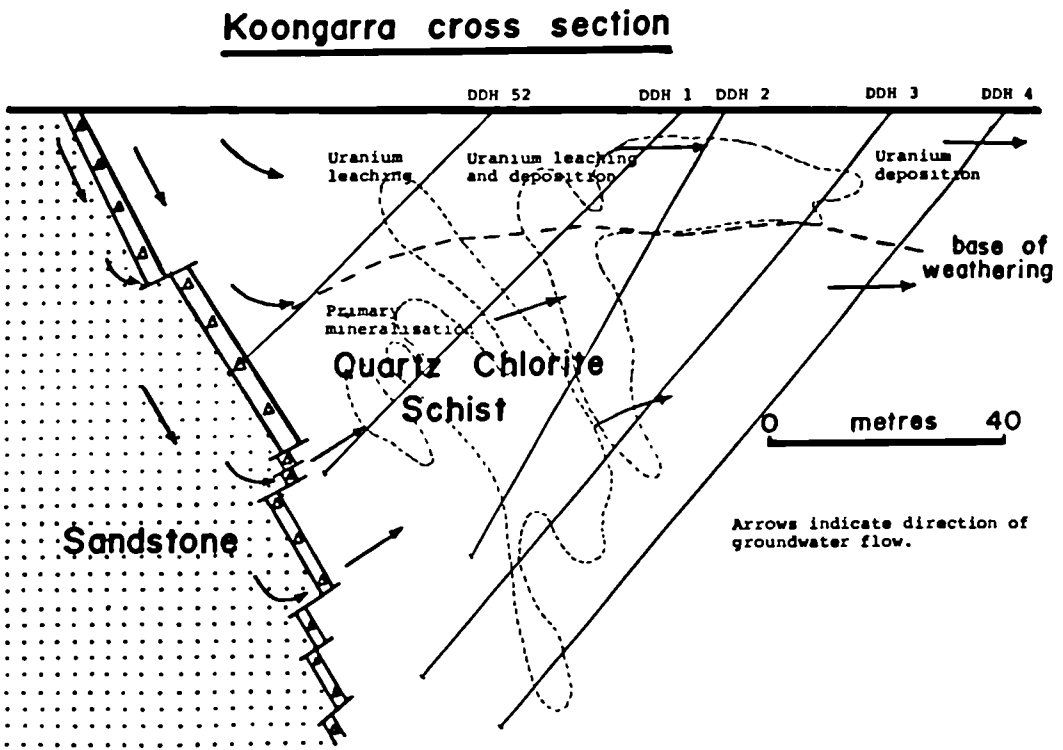

Figure 1 Section through the Koongarra ore body.

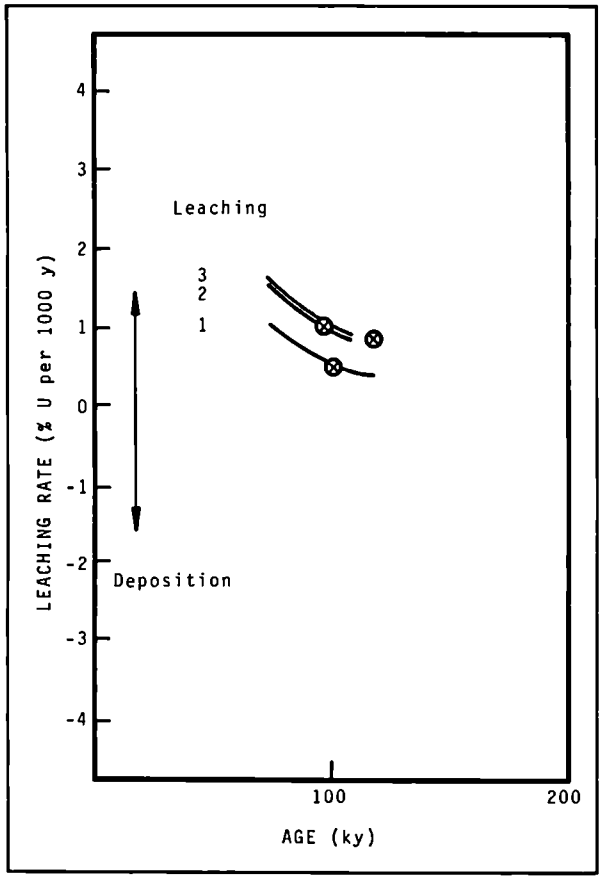

Figure 2 Dating of shells (data of Rosholt and Szabo (8)). Comparison of Hille's (6) model results and time-leaching domains obtained using the current model.

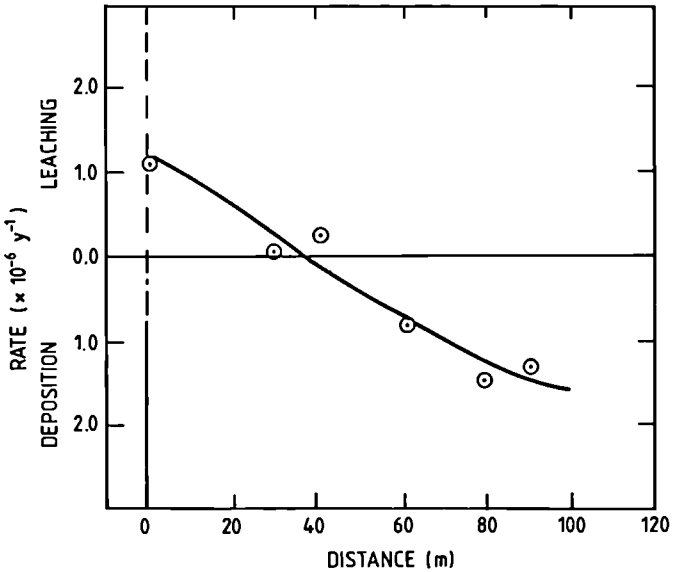

Figure 3 Modelling of Koongarra 'dispersion' formation. Average uranium transport rates versus distance of the original deposit.

Figure 5 Average uranium migration rate and uranium gradient for Kräkemäla sample.

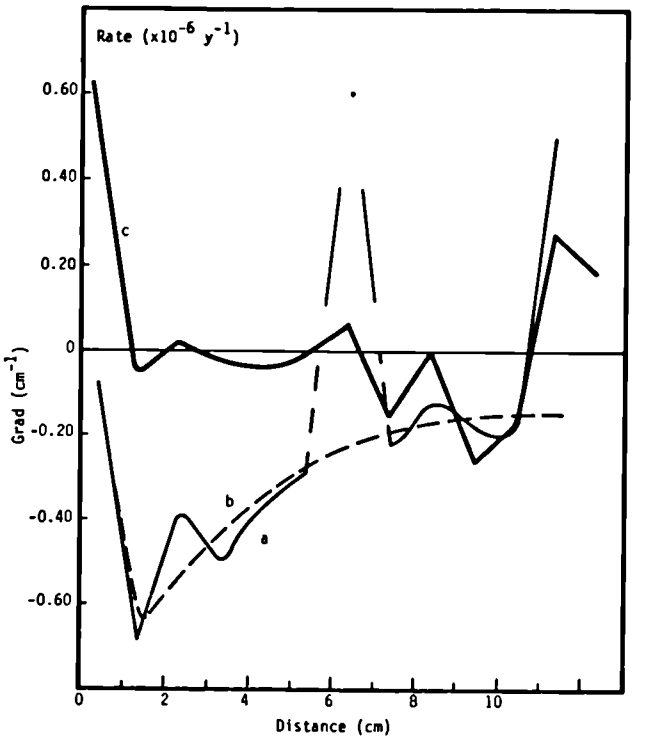

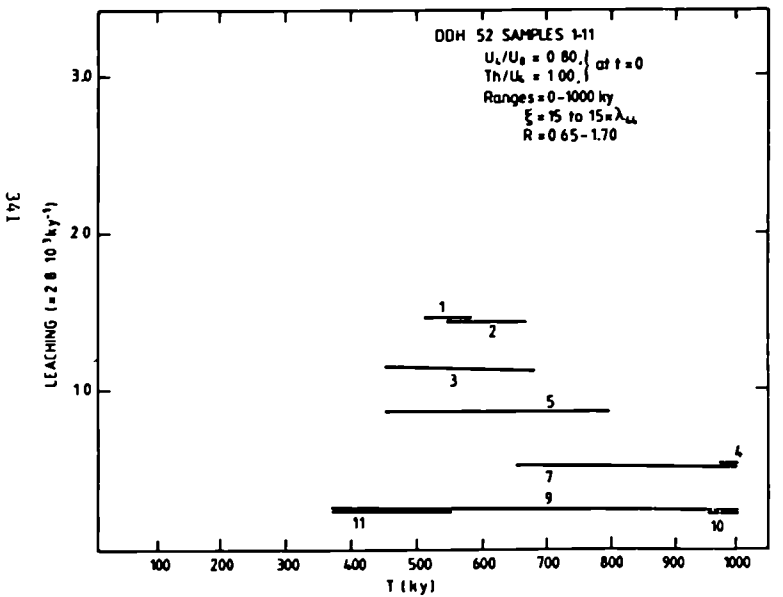

Figure 4 Leaching rate-time domains for a vertical drill core in the Koongarra ore body.

A NATURAL ANALOGUE FOR NEAR-FIELD BEHAVIOUR IN A HIGH LEVEL RADIOACTIVE WASTE REPOSITORY IN SALT: THE SALTON SEA GEOTHERMAL FIELD, CALIFORNIA, USA

W. A. ELDERS
Institute of Geophysics and Planetary Physics
University of California
Riverside, California, 92521, USA

Summary

In the Salton Sea Geothermal Field (SSGF), in the sediments of the delta of the Colorado River, we are developing a three-dimensional picture of active water/rock reactions at temperatures of $\leq 300°C$ and salinities of 7 to 25 weight percent to produce quantitative data on mineral stabilities and mobilities of naturally-occurring radionuclides. The aim is to produce data to validate geochemical computer codes being developed to assess the performance of a Commercial High-Level Waste (CHLW) repository in salt. Among the findings to date are: (1) greenschist facies metamorphism is occurring; (2) brine compositions are fairly similar to those expected in candidate salt repository sites; (3) U and Th concentrations in the rocks are typical for sedimentary rocks; (4) the brines are enriched in Na, Mn, Zn, Sr, Ra, Po and strongly depleted in U and Th relative to the rocks; (5) significant radioactive disequilibria exist in brines and solid phrases of the SSGF. The disequilibria in the actinide series allow estimation of the rates of brine-rock interaction and understanding of hydrologic processes and radionuclide behaviour. Work is continuing emphasizing the reactions of authigenic clay minerals, epidotes, feldspars, chlorites and sulphates. So far, adapting geochemical codes to the necessary combination of high salinity and high temperature has lagged behind the natural analogue study of the SSGF so that validation is still in progress. In the future our data can be also used in validating performance assessment codes which couple geochemistry and transport processes, and in design of waste packages and back fill compositions.

1.0 Introduction

For some thirty years, when discussions first began in the U.S.A. on the concept of mined geological repositories for CHLW, salt has been one of the leading candidates for a host rock (1). However prediction of the performance of a repository in salt, or in any other rock type, requires

ability to model the long-term performance of the specific site and the engineered barrier system. Such performance assessment can only be partially satisfied by laboratory measurements and field tests, which must then be extrapolated to the larger scales, longer times, and higher degrees of complexity likely in a high-level nuclear waste repository. Acceptance of the predictions of the hydrological, transport and geochemical behaviour made by such mathematical modeling requires validating the necessary computational codes against quantitative results derived from real data and known processes, which have operated over long time spans under conditions similar to those anticipated in a salt repository, i.e. to study natural analogues. The methodology for model verification and validation for near-field performance assessment for a salt waste repository is described elsewhere (2).

The geological record provides numerous examples of long-lived natural laboratories where processes relevant to possible behaviour in CHLW repositories have occurred, some of which are the subject of presentations at this conference (3). However most natural analogues studied involve processes which are long since ended, so that it is necessary to make numerous assumptions in modeling the conditions responsible for their occurrence. On the other hand, active geothermal systems offer substantial advantages over "fossil" hydrothermal systems as natural analogues, in that we can study, not only the effects of water/rock interactions at elevated temperatures, but the processes themselves. In an active geothermal system, being drilled to produce steam for electric power, we can make direct observations of the temperature, depth and fluid pressure at which hydrothermal alteration occurs, and sample the fluid and rock chemistry directly. Similarly, we can make direct observations of the parameters such as porosity and permeability which control mass and energy transfer. Furthermore, we are much better able to estimate the age and duration of heating and water/rock reactions (4). Such direct field observations and measuremsnts of natural hydrothermal processes can result in critical input to the development and validation of computer models. However it is clear that data used to develop a computer model must be kept distinct from data used to validate it. In 1982 my colleagues and I began the search for a suitable geothermal field in which to acquire data for geochemical model validation of a salt repository as part of a programme funded by the Office of Nuclear Waste Isolation.

2.0 Choice of the SSGF

Unfortunately we know of no instances of salt domes or salt beds with temperatures at economically drillable depth comparable to peak temperatures estimated to be likely in a high-level waste repository (5). Development of high temperature hydrothermal systems is inimical to the survival of salt. However, the Salton Sea Geothermal Field (SSGF), on the delta of the Colorado River, in the Imperial Valley of Southern California, offers an attractive target for study for a number of reasons. It is the largest and hottest known hot brine hydrothermal system in North America. The SSGF is only one of a number of geothermal fields currently undergoing commercial development as sources of electric power in the Salton Trough of Southern California and Northern Mexico (Figure 1). The Salton Trough is a structural depression at the head of the Gulf of California, which has been partially filled with the Late Miocene to recent detritus of the Colorado River (6). The depression is an active

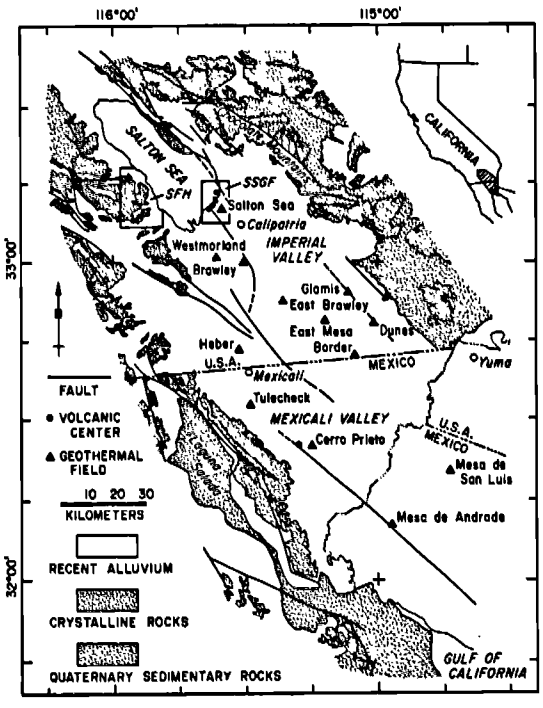

Figure 1.

Map of the geothermal fields and volcanic centers in the Salton Trough of southern California and northern Mexico (SSGF = Salton Sea Geothermal Field; SFH = San Felipe Hills where rocks stratigraphically equivalent to those of the SSGF at crop out).

rift zone at the transition between the divergent tectonics of the East Pacific Rise, to the south, and the transform fault tectonics of the San Andreas Fault system to the north. The tectonics of the Trough is dominated by "leaky" transform faults, producing tensional zones in which intrusion of basaltic and rhyolitic magmas occurs periodically. These intrusions are the heat sources of the high temperature geothermal systems. The progressive growth of the delta of the Colorado River has effectively isolated the Salton Trough from the Gulf of California to the south. Water entering this closed basin can only escape by evaporation. The depression has consequently undergone cycles of flooding and dessication as the Colorado River changed its course, alternately flowing south to the Gulf or north into the closed basin (7, 8).

Although bedded salt or salt domes have not yet been penetrated by drilling, the SSGF was chosen as a natural analogue of a salt repository for the following reasons: (a) It is a well-known hydrothermal system under commercial development with wells, subsurface data and samples available for study. (b) Temperatures within it exceed 300°C and thus span the range expected in a salt repository. (c) It is the most saline system in the Salton Trough with groundwater salinities (70,000 to 250,000 mg/kg TDS) spanning the range of brine compositions expected in and around a salt repository. (d) The sedimentary section is similar to that surrounding potential salt host rock horizons. (e) The geothermal system has been active for more than 25,000 years, a time scale of interest for a CHLW repository (9).

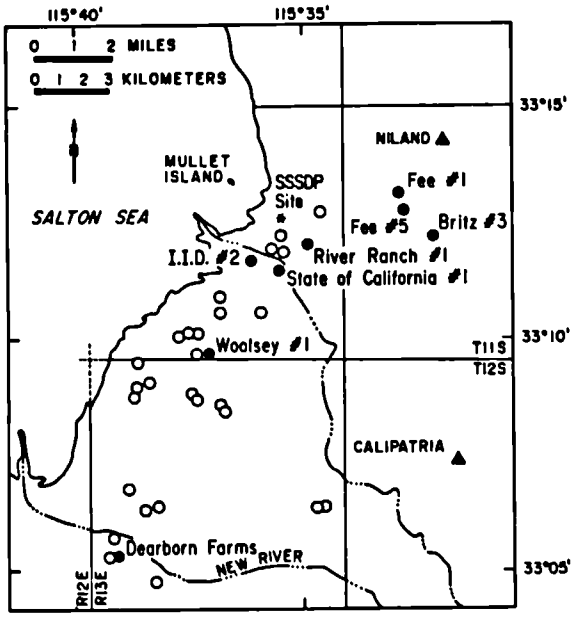

Figure 2. Location of deep geothermal wells and the Salton Sea Scientific Drilling Project research well in the SSGF: filled circles = wells studied for this report; open circles = other wells; asterisk = SSSDP well.

During this analogue study we have acquired samples and data from about two-thirds of the almost 50 geothermal boreholes, ranging from 1.5 to 3.3 km deep, which were drilled in the SSGF. Some of these wells currently supply steam to two operating electrical power plants and more plants are planned for construction in the next two years. Between October 1985 and April 1986 a research borehole, the Salton Sea Scientific Drilling Project, was drilled on the east side of the field to a depth of 3.2 km where a temperature of 355°C was measured. This well released to the public domain a wealth of data and samples from the SSGF including brine samples from two different depths, and 225 m of rock cores demonstrating a transition from unconsolidated lake and deltaic sediments into hornfels with greenschist facies mineralogy (10).

3.0 Geology and Geochemistry of the SSGF

The strata containing the geothermal brines consist of deltaic mudstones with interbedded quartzo-feldspathic siltstones and sandstones with clay or carbonate cements. Detrital phyllosilicates are chiefly smectite, illite, and kaolinite, with lesser amounts of biotite, chlorite and muscovite (11). In response to the temperatures exceeding 300°C at depths of 3 km, or less, over an area considerably more than 100 km^2 (Figure 2) active greenschist facies metamorphism is occurring (12). The

gross stratigraphy in the drilled part of the field consists of an upper clay-silt-evaporite lacustrine sequence, up to 400 m thick in the centre of the field, and a lower interbedded mudstone-sandstone deltaic sequence (9).

The SSGF brines are concentrated Na, Ca, K chloride solutions containing low amounts of SO_4^{-2}, H_2S and HCO_3^-. They range between 7 and 28% by weight of total dissolved solids, depending on depth and location, with concentrations highly stratified with depth. Typical values of dissolved components in the more saline boreholes near the centre of the field (in mg/kg) are:

Cl	83,000	- 155,000	Na	40,000	-	59,000	
Ca	13,000	- 59,000	K	7,000	-	15,000	
Fe	200	- 1,200	Mn	500	-	1,100	
Zn	300	- 800	Li	90	-	290	
SiO_2	180	- 400	Pb	40	-	100	
Cu	0.5	- 8	Ag	0.8	-	1.4	(9)

The very high concentrations of dissolved components are now believed to be derived from dissolution of non-marine Plio-Pleistocene evaporites associated with lacustrine sediments containing bedded anhydrites (after gypsum). Fluid inclusions in these anhydrites contain halite crystals (13). Active base-metal ore deposition is going on in this system (14).

Figure 3 compares the brine chemistry from the IID No. 2 well, which lies near the centre of the field and attained a temperature of about 315°C at approximately the 1,700 m sample depth, with brine chemistry from Fee No. 5 well from near the eastern margin of the field where a temperature of 290°C was reached at about 3,000 m (4). In spite of the marked difference in temperature gradients, the brine analyses are essentially identical. For comparison, the compositions of fluid inclusions in salts and a range compositions of fluids which might intrude a nuclear waste repository in salt in the Permian Basin of Texas are shown (15). The SSGF brines are rather similar to the brines likely to be encountered in CHLW repositories in salt in the USA especially for the elements, Cl, Na, Ca, and K. However, the SSGF brines differ from them in having a lower Mg content as they are not derived from marine evaporites and because above 225°C they precipitate Mg-rich chlorite. Furthermore, the SSGF brines are enriched in Fe, Mn, Zn, Sr, B, Ba, Li, Si, and Pb relative to the brines from the proposed CHLW repository aite in Texas, because these elements are leached from the sediments at elevated temperatures. Eh and pH conditions for the SSGF brines are difficult to determine directly due to differences in sampling conditions and reservoir conditions. However, measured Eh values ranging from 0.17-0.25 volts and pH estimates of 4-6 are consistent with the observed mineral assemblages (16).

4.0 Analog Studies of the SSGF

We are using a combination of mineralogical and geochemical methods to develop a three-dimensional picture of temperature, salinity, lithology, mineralogy, and the chemistry of interactions between reservoir rocks and the hot brines. The techniques employed include optical microscopy and quantitative x-ray diffraction for mineralogical modal analysis, x-ray fluorescence and induced neutron activation for rock analysis, electron microbeam analysis for mineral analysis, fission track

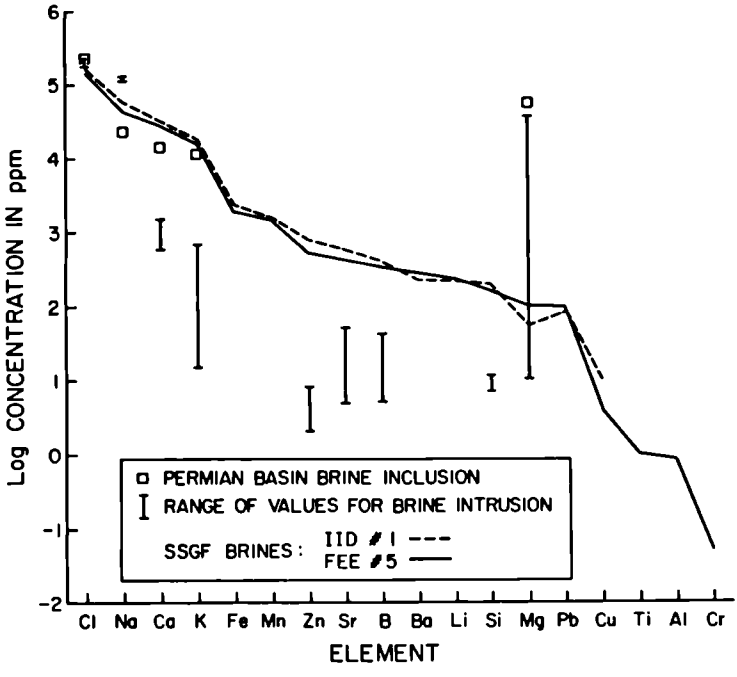

Figure 3. Analyses of brines from a central well (IID No. 2) and a marginal well (Fee No. 5) in the SSGF. For comparison, an analysis of brines in inclusions in Permian salts from a possible salt repository site in Texas, and the range of values which has been suggested for brines which could intrude these salt deposits is included [Permian salt brine data are from (15)].

radiography for ^{235}U analyses, mass spectrometry for hydrogen, oxygen, carbon and sulphur isotopic ratios, fluid inclusion analyses using heating and freezing microscope stages, analysis of U and Th decay chains using α and γ spectrometry and β counting, and fluid analysis by atomic absorption and inductively coupled plasma techniques.

4.1 Mineral Reactions

With increasing temperature and depth four progressive zones of hydrothermal alteration may be distinguished (11, 17). These are (1) at < 190°C a dolomite/ankerite zone with mixed layer smectite/illites; (2) 190-325°C, a calcite/chlorite zone with illite/phengite; (3) 325-360°C a biotite zone with actinolite, albita and epidote; and (4) above 360°C a garnet zone with biotite and actinolite. These mineralogical changes are accompanied by progressive recrystallizations leading to porosity reductions and formation of hornfelsic textures.

4.2 Geochemical Computer Code Validation

An important aspect of this study is validation of computer codes for geochemical interactions in aqueous systems which are being developed for application to the Civilian Radioactive Waste Management Program of the U.S. Department of Energy. In this study the codes being tested consist of the EQ3/6 software package, a thermodynamic equilibrium code with kinetic capability (18, 19). It models water-mineral interactions as a function of temperature and pressure. The EQ3NR speciation-solubility code calculates aqueous speciation and mineral saturation indices from water analyses. EQ6 is a reaction path code which can be used to simulate mineral/water interactions at temperatures up to 300°C and over long times. There is an option to use Pitzer's equations to calculate activity coefficients in aqueous solutions and EQ6 has been upgraded to model open flow-through systems.

We have analyzed brines and assemblages of authigenic minerals apparently in equilibrium with them for about 12 wells in the field. Figures 4A and 4B show some typical results of using EQ3 to calculate the activity ratios of brines, and then plotting the data for a wide range of compositions on activity diagrams, calculated by the methods of reference (20). The two wells from Cerro Prieto (see Figure 1) produce fluids with approximately 20,000 mg/kg of total dissolved solids, the intermediate brines from the SSGF contain 70,000-100,000 mg/km of total dissolved solids, whereas the hypersaline brines contain 23 to 25 weight per cent of dissolved solids. At quartz saturation, at 300°C and 86 bars of fluid pressure, these brines, ranging over an order of magnitude in concentration, plot as a coherent group. This is consistent with the similarity in hydrothermal minerals observed at Cerro Prieto and in the Salton Sea Geothermal Field over a wide range of salinity.

Although for these components the code predicts mineral assemblages similar to those which are observed to occur, this is in general not true for other dissolved species. Thus so far, further development of the code to work at high temperatures and high salinity simultaneously is proving difficult, consequently validation of the computer codes is an on-going activity.

4.3 Fission Track Radiography

Among the studies of the migration and retardation of elements of interest in CHLW, perhaps the easiest to analyze is U because its distribution can be deduced from fission tracks induced by spontaneous decay of ^{235}U in its host minerals. We used a combination of INAA to determine total concentration of U and fission tracks to determine its location in the rock. We then compared U concentrations in subsurface mudstones and sandstones, over a range of temperature of 325°C with those seen in stratigraphically equivalent, but unaltered, rocks at outcrop in the San Felipe Hills (Fig. 1).

A relatively uniform concentration of U is observed throughout the field, independent of depth, temperature, or salinity (Fig. 5), particularly in mudstones and siltstones. Sandstones are slightly more variable showing their highest U concentration in detrital zircon, epidote or sphene. The U distribution in the San Felipe Hills is similar. In both the Salton Sea Geothermal Field and the San Felipe Hills the sediments contain between 0.2 to 7 mg/kg of U.

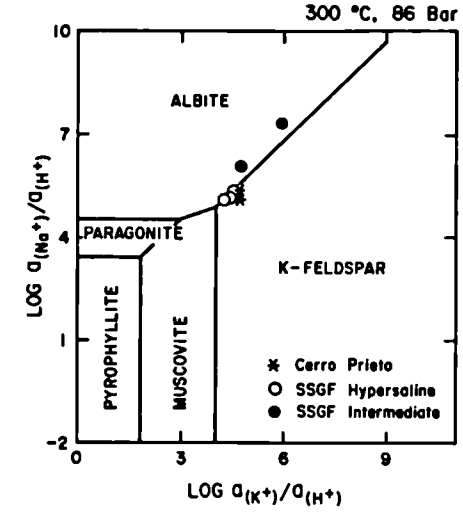

A

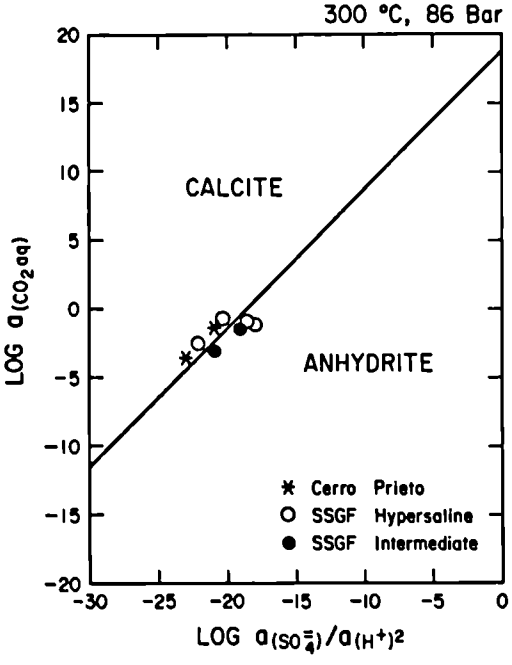

B

Figure 4. Examples of activity ratio mineral phase diagrams for geothermal fluids in the Salton Trough. The activity ratios are calculated for three types of brines ranging from 7-25% wt of total dissolved solids using EQ3 (19). When plotted on the activity diagrams they predict mineral assembles similar to those observed (20).

Upper diagram: Sodium and potassium activities and stability fields of alkali feldspars.

Lower diagram: Carbonate and sulphate activities and stability fields of calcite and anhydrite.

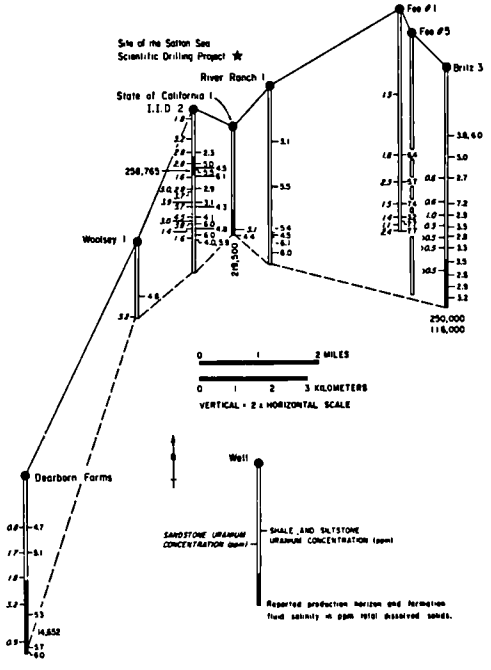

Figure 5. A "fence" diagram showing concentrations of Uranium in shales and sandstones from the SSGF. Well locations are as shown in Figure 2. Brines in Britz No. 3 well come from two separate horizons. Salinity data are from (4).

Table 1 shows that these rocks and a sample of a Holocene lake bed have very similar U and Th concentrations. These similarities suggest that the distribution of these elements is due to detrital processes rather than diagenetic or hydrothermal reactions. A minor exception to this suggested immobility of these elements is seen in the deepest and hottest part of the SSGF where certain samples are slightly enriched in U. Fission track analysis shows that the enriched amount of U is concentrated in locally developed authigenic epidote. This retention of U in epidote above 300°C suggests that U can be mobilized on a microscopic scale, but it is retarded if epidote is forming.

4.4 U-Th Decay Chains

Determination of Rc, the rock/brine concentration ratios, [where $R_c = (dpm/g)_{rock}/(dpm/g)_{brine}$] for the naturally-occurring U and Th series radionuclides in the SSGF vary from 1 for isotopes of Ra, Pb, and Rn, to

TABLE I. RANGE AND AVERAGE U AND Th AMOUNTS IN SANDSTONES, SHALES, AND MUDSTONES FROM THE SALTON SEA GEOTHERMAL FIELD (SSGF) AND SAN FELIPE HILLS AREA (SFH), IN PPM.

	SSGF SANDSTONES	SSGF SHALES	SFH SANDSTONES	SFH MUDSTONES	HOLOCENE LAKE CAHUILLA MUDSTONE
No. of analyses	30	42	5	5	1
U:Range ppm.	<0.5 to 5.7 ± 0.3	2.5 ± 0.6 to 7.2 ± 0.5	0.5 ± 0.3 to 3.7 ± 0.3	2.3 ± 0.4 to 4.2 ± 0.3	—
Average U	2.2	4.6	2.4	3.3	2.3 ± 0.4
No. of analyses	6	11	5	5	1
Th:Range ppm.	2.4 ± 0.07 to 13.2 ± 0.2	8.3 ± 0.2 to 20.0 ± 0.3	2.9 ± 0.2 to 7.4 ± 0.3	10.7 ± 0.4 to 13.4 ± 0.4	—
Average Th	6.6	14.0	4.2	11.7	11.8 ± 0.4

$5x10^4$ for ^{238}U and ^{234}U, and $5x10^5$ for ^{232}Th (21, 22). The high sorptivity of ^{238}U and ^{234}U suggests uranium is retained in the +4 oxidation state in these reducing conditions. On the other hand the relatively high solubility of lead and radium appears to be due to chloride complexing (22).

Comparison of $^{238}Ra/^{236}Ra$ ratios in the brine with those of their parents $^{232}Th/^{230}Th$ in the rocks indicates that radium equilibration is achieved within the mean life of ^{228}Ra (8.3 yrs), in brine samples from some wells but not in others. This suggests different rates of water/rock reaction in different wells. These differences are supported by different ^{226}Ra, ^{210}Pb and ^{222}Rn concentrations and also by material balance calculations for $^{228}Ac/^{228}Ra$. A material balance calculation for ^{18}O and ^{226}Ra, assuming steady state, yields fluid residence time in the SSGF of 10^2–10^3 years, and suggests water/rock mass ratios of 0.7. This suggests the system formed 2–$4x10^4$ years ago (22).

5.0 Current and Future Work

Work is continuing to obtain data to validate the equilibrium geochemical computer code and to study radionuclide partitioning between minerals and brine over a range of temperature, salinity and lithology. Special emphasis is being given to clay mineral reactions, the influence of solid solution on the stability of authigenic epidote, feldspars, chlorites, sulphates and smectites, determination of reaction paths from mineral paragenesis and mineral vein sequences, and radionuclide retardation and diffusion. As the geochemical code develops we will continue attempts at validation. We believe that the next step will be to couple these geochemical codes with mass and heat transfer codes. The data from the SSGF natural analogue are equally applicable to such transport models.

6.0 Acknowledgments

This is paper UCR/IGPP-87/19 of the Institute of Geophysics and Planetary Physics, supported by Battelle's Office of Nuclear Waste Isolation Contract E512-08300. The results reported here are the work of the Geothermal Resources Group at University of California, Riverside, and our colleagues at the University of Southern California working under that contract. Special thanks are due to A. E. Williams for help in preparing Figure 4.

REFERENCES

1. NATIONAL ACADEMY OF SCIENCES (1957). The disposal of radioactive waste on land. Report of the Committee on Waste Disposal, H. H. Hess, Chairman. National Academy of Sciences, Washington D. C., U.S.A., Publication No. 519, 142 pp.
2. OFFICE OF NUCLEAR WASTE ISOLATION (1984). Performance assessment, plans and methods for the salt repository project. Battelle Memorial Institute, Columbus, Ohio, U.S.A., Publication No. BMI/ONWI-513, 146 pp.
3. BROOKINS, D. G. (1984). Chemical aspects of radioactive waste disposal. Springer Verlag, New York, U.S.A., 347 pp.
4. ELDERS, W. A. and MOODY, J. B. (1985). The Salton Sea geothermal field as a natural analog for the near-field in a salt high-level nuclear waste repository. Materials Research Society Symposia Proceedings. Volume 44, Pittsburg, Pennsylvania, U.S.A., pp. 565-572.
5. CLAIBORNE, H. C., RICKERTSEN, L. D. AND GRAHAM, R. F. (1980). Expected environments in high-level nuclear waste and spent fuel repositories in salt. Oak Ridge National Laboratory, Oak Ridge, Tennessee, U.S.A., Publication No. ORNL/TM-7201.
6. ELDERS, W. A., REX, R. W., MEIDAV, T., ROBINSON, P. T. and BIEHLER, S. (1972). Crustal spreading in Southern California. The Imperial Valley and the Gulf of California formed by rifting apart of a continental plate: Science, Vol. 178, No. 4056, pp. 15-24.
7. ELDERS, W. A. (1979). The geological background of the geothermal fields of the Salton Trough in Geology and Geothermics of the Salton Trough, W. A. Elders (editor) University of California, Riverside, Campus Museum Contrib. Vol. 5, pp. 1-19.
8. LACHENBRUCH, A. H., SASS, J. H., and GALANIS, Jr., S. P. (1986). Heat flow in southernmost California and the origin of the Salton Trough. Jour. Geophys. Res., Vol. 90, No. B7, pp. 6709-6736.
9. ELDERS, W. A. and COHEN, L. H. (1983). The Salton Sea geothermal field, California as a near-field natural analog of a radioactive waste repository in salt. Battelle Memorial Institute, Columbus, Ohio, U.S.A. Publication No. BMI/ONWI-513, 146 pp.
10. SASS, J. and ELDERS, W. A. (1986). The Salton Sea Scientific Drilling Project. Geothermal Resources Council Transactions, Vol. 10, pp. 473-478.
11. MC DOWELL, S. D. and ELDERS, W. A. (1983). Allogenic layer silicate minerals in borehole Elmore 1, Salton Sea geothermal field, California. Amer. Min., Vol. 68, No. 11, pp. 1146-1159.
12. MUFFLER, L. J. P. and WHITE, D. E. (1969). Active metamorphism of upper Cenozoic sediments in the Salton Sea geothermal field and the Salton Trough, Southeastern California. Geol. Soc. Amer. Bull., Vol. 80, pp. 157-182.

13. MC KIBBEN, M. A., ELDERS, W. A. and WILLIAMS, A. E. (1986). Saline brines and ore-forming processes in the geothermal systems of the Salton Trough in Guptil, P. D., Gath, E. M. and Ruff, R. W. (eds.) Geology of the Imperial Valley, California. South Coast Geological Society, Guidebook No. 14, pp. 144-151.
14. MC KIBBEN, M. A. and ELDERS, W. A. (1985). Fe-Zn-Cu-Pb mineralization in the Salton Sea geothermal system, Imperial Valley, California. Econ. Geol., Vol. 80, pp. 539-559.
15. CLARK, D. E. and BRADLEY, D. J. (1984). Definition of the Waste Package Environment for a repository located in salt. Proceedings of the 1983 Civilian Radioactive Waste Management Information Meeting. U. S. Dept. of Energy, Washington, D. C. Conf. — 831217, pp. 284-289.
16. MAIMORI, A. (1982). Mineral recovery from Salton Sea geothermal brines. Geothermics, Vol. 11, pp. 239-258.
17. MC DOWELL, S. D. and ELDERS, W. A. (1980). Authigenic layer silicate minerals in borehole Elmore 1, Salton Sea geothermal field, California, U.S.A. Contributions to Mineralogy and Petrology, Vol. 74, pp. 293-310.
18. WOLERY, T. J. (1979). Calculation of chemical equilibrium between aqueous solution and minerals: the EQ3/6 software package. Lawrence Livermore National Laboratory, report UCRL-52658, 39 pp.
19. WOLERY, T. J. (1983). EQ3NR A computer program for geochemical aqueous speciation — solubility calculations: User's Guide and documentation. Lawrence Livermore National Laboratory, report UCRL-53414, pp. 1-191.
20. BOWERS, T. S., JACKSON, K. J. and HELGESON, H. C. (1984). Equilibrium activity diagrams for coexisting minerals and aqueous solutions at pressures and temperatures to 5kb and 600°C. Springer-Verlag, Berlin, 397 pp.
21. ZUKIN, J. G. (1986). Uranium and Thorium series isotopes in the Salton Sea geothermal field, southeastern California: Their applications in determining the rates of brine-rock interaction and radionuclide transport. Unpublished M. S. Thesis, University of Southern California, 156 pp.
22. ZUKIN, J. G., HAMMOND, D. E. and KU, T. L. (1986). Uranium-Thorium series isotopes in brines and reservoir rocks from two deep geothermal well holes in the Salton Sea geothermal field, southeastern California. Geochemica et Cosmochimica Acta (In press).

THE GEOCHEMISTRY OF NATURAL TECHNETIUM AND PLUTONIUM

David B. Curtis, John H. Cappis, Richard E. Perrin, and Donald J. Rokop
Isotope Geochemistry Group
Los Alamos National Laboratory, Los Alamos, NM 87501 U.S.A.

June Fabryka-Martin
Dept. of Hydrology and Water Resources
University of Arizona, Tuscon, AZ 85721 U.S.A.

ABSTRACT

It is generally assumed that element 43—technetium—and element 94—plutonium—are exclusively anthropogenic, found in nature only as contaminants. However, these nuclides also occur naturally as transient products of nuclear processes. In nature, ^{99}Tc is produced by ^{238}U spontaneous fission and ^{235}U neutron induced fission and subsequently destroyed, with a half-life of 2.13 x 10^5 y, by radioactive decay. Plutonium-239 is produced naturally by ^{238}U neutron capture and decays with a half-life of 2.41 x 10^4 y. Rates of production of these nuclear products depend on the neutron fluence in the geologic environment, and the abundance of their mutual parent, uranium. Therefore, once the production and decay rates are equal (a condition we will refer to as nuclear equilibrium) samples of those environments should contain correlated abundances of the two elements. If the nuclear parent and daughters are undisturbed, such a state of equilibrium will be achieved in about 10^6 y. Chemical changes with respect to these three elements in this time frame can be identified and quantified by comparing measured abundances with those predicted by the systematics of nuclear equilibrium. Thus, determination of the abundances of ^{99}Tc, ^{239}Pu, and U should provide a useful tool for studying aspects of the chemistry of geologic environments during the last million years.

We have found very few reported determinations of natural ^{239}Pu and ^{99}Tc abundances. These results were obtained by measuring radioactive decay rates of the nuclides after their separation from kg of host material. Reported concentrations of each nuclide are on the order of 10^{-12} g/g U. These procedures are extremely tedious and have not been used extensively in geochemical studies. We have developed analytical procedures using isotope dilution mass spectrometry to measure as little as 10^{-15} g of these elements in as much as 10 g of geologic material.

This capability provides a practical means of utilizing these nuclear products in geochemical studies. Such research is particularly relevant to issues associated with the design and evaluation of geologic repositories for nuclear wastes.

The first experiment constitutes a test of principle of the systematics of nuclear equilibrium and is designed to examine the chemical stability of Tc and Pu in uranium minerals from a variety of geologic settings. Our first results are consistent with those predicted by nuclear systematics, suggesting that these minerals have effectively retained the nuclear products on a million year time scale.

A complementary experiment is designed to examine the retention and transport of Tc, Pu, and U at Koongarra, a uranium deposit located in the Northern Territory of Australia. This deposit has been altered in recent geologic history by rapidly flowing aquifers fed by high seasonal rainfall. An oxidizing region, called the weathered zone, extends from the surface to a depth of about 30 m. It is distinguished by the alteration of primary uranium minerals and the dispersion of uranium along the hydrologic gradient. At greater depths the geochemical environment is reducing. Primary uranium minerals have been altered in this region, but there is no evidence of the massive uranium migration seen in the shallower zone. Rock samples were obtained from cores taken during the resource assessment of the mine. These samples represent materials along the hydrologic gradient in both the oxidizing weathered zone and the reducing deeper region. In addition, water was sampled from wells penetrating the ore along the hydrologic gradient. Abundances of ^{99}Tc, ^{239}Pu, and U are being measured in these samples to study the formation and reaction of Tc and Pu solutes and examine the effects of the redox conditions on the migration and retention of these multivalent elements. Our first measurements show Tc enrichment relative to U in water collected from the most uraniferous portion of the deposit.

This work is sponsored by the U.S. Department of Energy, Office of Energy Research, Division of Engineering, Mathematics & Geosciences, and the Australian Atomic Energy Commission.

THE USE OF URANIUM-SERIES DISEQUILIBRIUM FOR SITE CHARACTERIZATION AND AS AN ANALOGUE FOR ACTINIDE MIGRATION

M. GASCOYNE
Applied Geoscience Branch
Atomic Energy of Canada Limited

Summary

Uranium-series isotopic disequilibrium in any rock or mineral phase is a powerful indicator for determining 1) how recently alteration has occurred, 2) the type of rock-water interaction that has occurred and, hence, the chemical conditions prevailing at that location, and 3) how actinides migrate under natural subsurface conditions. Since all geological formations contain trace amounts of U and Th, the disequilibrium technique is, therefore, an important tool in any site selection and characterization studies of prospective sites for geological disposal of nuclear wastes.

To illustrate this application, measurements of uranium-series disequilibrium in three plutons in the Canadian Shield have been obtained together with supporting data from groundwater analyses. Disequilibrium between 238U, 234U, 230Th and 226Ra is generally not observed in visibly unaltered rock nor in fracture-filling minerals and adjacent rock where the minerals are of a high-temperature origin. Disequilibrium is observed, however, in rock immediately adjacent to, or rubble within, water-bearing fractures, and in some fractures containing low-temperature secondary minerals.

Uranium-series data for a buried hydrothermal granite in Montana, USA, indicate negligible actinide mobility over the last 10^6 years. This result suggests that radionuclide migration from a vault in a hydrothermal regime will be minimal.

A procedure is described for applying decay-series methods to the characterization studies involved in site selection for nuclear waste disposal.

1. Introduction

The safe disposal of nuclear fuel wastes requires their isolation from the biosphere for a long period of time. Canada, together with several other countries, is investigating the potential of burial within an engineered vault deep in plutonic rock formations as a method of isolation. Because laboratory validation of this disposal concept is impossible for the time period required, any evidence for the stability of naturally occurring analogues to the components of the disposal system is valuable and, at least, qualitatively useful for validation. Unfortunately, most natural analogues are site-specific and may be relevant to only a small part of the overall disposal system concept. Of more universal application is the study of uranium- and thorium-decay series isotopes in the rock at a proposed disposal location. This is a type of analogue that provides data on the recent history of natural radionuclide migration, the

mechanisms causing it and the prevailing geochemical conditions in the rock and associated groundwaters. This application was first described in detail by SCHWARCZ et al. (1).

The presence of secular radioactive equilibrium between parent-daughter pairs in natural decay series for a mineral or whole rock sample is evidence for immobility of the radionuclides and the absence of low-temperature alteration (weathering) processes. Characteristic patterns in some of the daughter/parent radioactivity ratios can be seen in rocks that have been altered in the last 10^6 years: $^{234}U/^{238}U < 1.0$, $^{230}Th/^{234}U > 1.0$, $^{226}Ra/^{230}Th \neq 1.0$, $^{228}Th/^{232}Th < 1.0$, etc. ROSHOLT (2) has summarised the processes which lead to these characteristic patterns and these are shown in Table I.

A subsidiary application of disequilibrium studies involves analysis of specific mineral phases to determine their suitability as hosts for actinides and fission products in the event of disposal of used UO_2 fuel or reprocessed wastes. Such minerals include monazite, sphene, uraninite, zircon, perovskite, etc. Most of these minerals are found in plutonic rocks as accessory phases or vein infillings, and sometimes they contain significant concentrations of U, Th, Ra, and the rare earth elements (the stable analogues of some fission-product radionuclides). Observation of secular equilibrium in the Th- and U-decay-series isotopes in these minerals is an indication of their resistance to alteration or leaching and, hence, their suitability as host phases.

If disequilibrium can be measured for any radionuclide activity ratio in a whole rock or mineral sample, this indicates that:

1. one or the other of the nuclide pair has been mobilized,
2. this mobilization has occurred recently and within the last 10^6 years (the exact time scale depends on the ratio affected),
3. the geochemical conditions causing this nuclide to migrate can be defined.

TABLE I

SUMMARY OF ALTERATION PROCESSES AND THEIR AFFECTS ON U-SERIES RATIOS (AFTER ROSHOLT, 1983)

Process Number	Process Description	Isotope Effect	Typical Activity Ratio Values $\frac{^{234}U}{^{238}U}$	$\frac{^{230}Th}{^{234}U}$	$\frac{^{226}Ra}{^{230}Th}$	Typical Occurrence
1	U leaching (chemical)	no fractionation of ^{234}U from ^{238}U, excess ^{230}Th generated	~1.0	>>1.0	≤1.0	near-surface bulk leaching of an already weathered rock; oxidising environment
2	U leaching (chemical + recoil)	some fractionation of U isotopes, preferential loss of ^{234}U from recoil disrupted sites, excess ^{230}Th generated	≤1.0	>1.0	≤1.0	near-surface leaching of relatively fresh rock; mildly oxidising environment
3	U leaching (recoil)	some fractionation of U isotopes	<1.0	≥1.0	<1.0	intermediate to deep location little U leaching; Ra leaching in high salinities; reducing environment
4	U addition (recoil + sorption)	$\frac{^{234}U}{^{238}U}$ ratio of groundwater attained	>1.0	<1.0	~1.0	moderate depth location; no leaching; at a redox front
5	U, Th addition (recoil + sorption)	disequilibrium induced in surface of adjacent rock	>1.0	>>1.0	≤1.0	shallow to moderate depths; most noticeable in well fractured rock with high U in groundwater

This paper briefly reviews some of the results of disequilibrium studies on plutonic rocks with particular application to the Canadian Nuclear Fuel Waste Management Program (CNFWMP). Interpretations of the processes and time scales involved are presented. A scenario for application of disequilibrium studies in site selection and characterization procedures is presented.

2. Decay-Series Disequilibrium

The decay series for the three primordial isotopes: ^{238}U, ^{235}U and ^{232}Th is shown in Figure 1 in terms of the half-lives of the daughter radionuclides. Under closed-system conditions, the radioactivity level attained by each daughter isotope in any decay series is equal to that of the parent. Radioactivity ratios of isotopes in that series are, therefore, in equilibrium and equal to unity (1.00). Longer-lived nuclides have more geological significance because, during their lifetime, they may become separated from their parent by physical or chemical processes (e.g., gaseous diffusion, dissolution). If the separation distance is large, secular radioactive equilibrium for the sample analysed may no longer hold. Such "disequilibrium" is usually expressed by values > 1.00 or < 1.00 for the daughter/parent radioactivity ratio and can be detected by modern analytical techniques if there is greater than about 4% deviation from equilibrium. Because of the tendency of the system to return to radioactive equilibrium after the fractionating process, the extent of disequilibrium between any members of a series depends on the amount of fractionation that occurred and the time elapsed since that process or event.

It is therefore possible to determine if a rock body is open or closed to radionuclide migration by whether or not radioactive equilibrium presently exists in all minerals in the rock. Furthermore, the presence of disequilibrium in any of the decay series gives insight into the geochemical conditions that gave rise to this condition, and, from the half-lives of the radionuclides involved, indicates the time scale over which the migration has occurred. The useful time ranges for various parent-daughter pairs in the three natural decay series are limited by the precision with which isotopic ratios may be measured and are generally equivalent to about five half-lives of the daughter nuclide.

Determination of the ratios $^{234}U/^{238}U$, $^{230}Th/^{234}U$, and $^{226}Ra/^{230}Th$ for a given rock or mineral sample will indicate whether these radionuclides have migrated over periods extending from the present to about 1.5 Ma, 350 ka and 8 ka ago, respectively. A detailed discussion of the concepts and applications of uranium-series disequilibrium studies, and their use in nuclear fuel waste management has been given by SCHWARCZ et al. (1).

In the study of natural radionuclide migration in plutonic rock, it is essential to obtain information on the concentrations of decay-series nuclides in the associated groundwater. Knowledge of the water chemistry, its age and flow regimes in the rock is also required to interpret the significance of rock mineral disequilibria data. Examples of the application of decay-series methods in the Canadian Program, which incorporate some or all of the above studies are given below.

3. Methods

Uranium- and Th-series isotopes in whole rock or mineral separates are generally analysed by either acid digestion or fusion techniques, followed by ion exchange and thin source plating. The prepared sources are then counted by alpha spectrometry and individual isotope activities determined by reference to an added tracer. Groundwater samples are also analyzed by the above processes except that radon isotope activities are

usually determined by a scintillation counting method. Details of these methods can be found in references 2, 3, 4 and 5.

4. Applications of Decay-Series Studies in the CNFWM Program

4.1 Mineral Stability

Perovskite, zirconlite, monazite, sphene and uraninite have been proposed by international scientists as potential host mineral phases for fission product vastes (6, 7). The rationale for this is largely the stability of the natural occurring minerals to radionclide migration over long periods of geological time. However, other data are necessary to support these findings, e.g., stability in the temperature range 0 to 200°C, stability in fresh and/or saline groundwaters, sensitivity to radiation damage, capacity for incorporating percent quantities of radionuclides in the crystal structure, etc. Studies of natural analogue minerals generally offer relatively little of this information.

Similarly, fev studies have described the use of Th- and U-series disequilibria for determining the integrity of the mineral phases vith respect to alteration. More frequently, disequilibria data are obtained from analysis of contacting solutions during the leaching of a mineral to demonstrate the effects of radiation damage caused by alpha recoil decay (8).

The mineral sphene (titanite) has been proposed as a host for re-processed nuclear fuel vaste in the Canadian Nuclear Fuel Waste Management Program (9). Considerable data have been obtained on both natural and synthetic sphene that describe its stability in groundvater (10, 11) and vith respect to leaching of radionuclides (10, 12) and susceptibility to radiation damage (13, 14).

To assess the stability of sphene over geological time periods, U series disequilibrium methods have been used to analyze 21 natural sphene samples (11). The samples were mostly vein infillings and mineral separates from felsic igneous and metamorphism rocks, mainly from Ontario, Canada. The samples were analysed for $^{234}U/^{238}U$, $^{230}Th/^{234}U$ and $^{226}Ra/^{230}Th$ radioactivity ratios. Uranium and Th concentrations ranged from 40 to 1900 mg/kg and 40 to 1100 mg/kg, respectively. Secular radio-active equilibrium vas observed in all but six samples, four shoved ^{234}U deficiency, one had 26% ^{226}Ra deficiency and one had 100% ^{226}Ra excess (Figure 2). Of these, two exhibiting disequilibrium were found to contain the alteration products anatase and calcite. Although about 30% of the samples analysed had suffered radiation damage, there was no clear correlation vith the presence or absence of U-series disequilibrium. GASCOYNE (11) also compared U-Th-Pb ages for sphenes reported in the literature vith 68 U-Th-Pb zircon ages or other age measurements for the same rock formation. Age agreement vas very good and in many cases the sphene ages gave more consistent and reliable results than any other method.

The results of these studies demonstrated the stability of sphene to metamorphism and alteration processes over geological time (10^7 to 10^9 a) and to lov-temperature (veathering) processes over the last 10^6 a. Sphene vas found to retain radionuclides and daughter products in its structure better than zircon and other U-rich accessory minerals. Up to 30% meta-mictization of the sphene mineral did not appear to induce radionuclide loss. These results, although based entirely on natural sphene minerals, support the contention that a sphene-based glass-ceramic is a suitable and durable host for Canadian nuclear fuel vaste.

A different perspective on mineral stability to lov-temperature alteration processes has recently been described by LATHAM and SCHWARCZ (15, 16). Weathered surface samples of granite from the Eye-Dashva Lakes pluton near Atikokan, northwestern Ontario, were subjected to standard

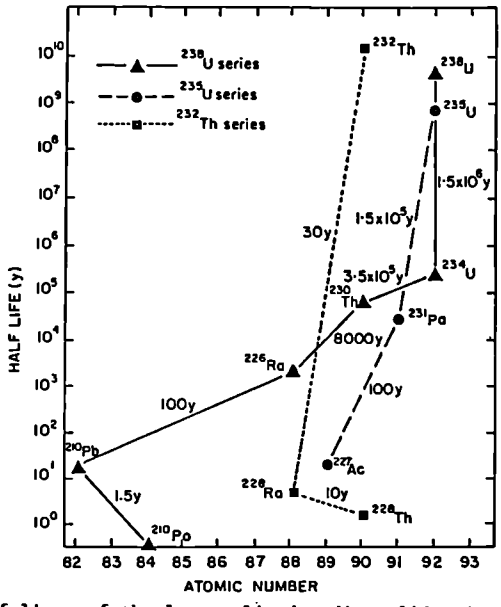

Figure 1: Half-lives of the longer-lived radionuclides in the natural decay series of U and Th. Useful time periods of each decay transition are shown.

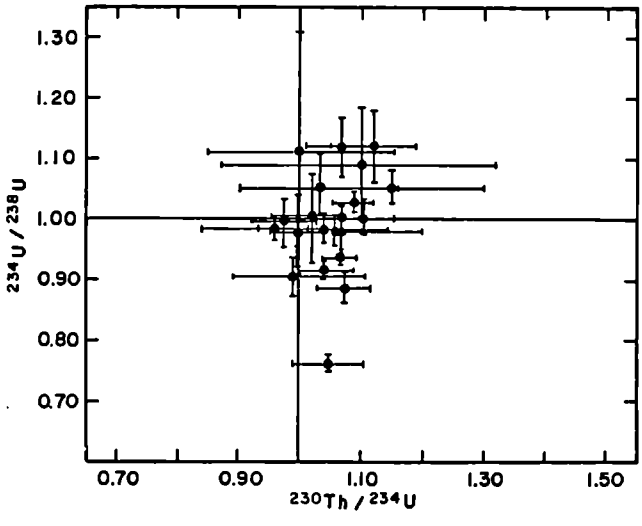

Figure 2: Variation of U-series activity ratios for 21 natural sphene samples (11). Error bars are ± 1σ.

mineral separation techniques, and each fraction analysed for $^{234}U/^{238}U$ and $^{230}Th/^{234}U$ activity ratios. For most samples, all three fractions (mafics, quartz + feldspar, zircon + sphene) showed depletion of ^{234}U relative to ^{238}U and enrichment of ^{230}Th relative to ^{234}U. This was most distinct in the quartz + feldspar fraction. The zircon + sphene fraction, which contained between 20% and 60% of total U, was generally closest to secular equilibrium with significant disequilibrium only observed in one case (the $^{230}Th/^{234}U$ ratio was 1.25 ± 0.05).

These results further indicate the resistance of sphene to weathering and migration of radionuclides. In contrast, the ferromagnesian and felsic minerals are readily susceptible to this migration, in part due to their ease of alteration and to the tendency for actinides to be loosely bound in their structure or present on grain boundaries (1).

4.2 Low-Temperature Rock Alteration

Most decay-series studies have examined disequilibria in whole rock samples of igneous and metamorphic bodies. In the CNFWMP, rocks from each of three plutons (Figure 3) have been analysed for evidence of U-series disequilibrium as part of a more general study of geochemistry and hydrogeology of the areas. SCHWARCZ and LATHAM (17) attempted to determine $^{234}U/^{238}U$ and $^{230}Th/^{234}U$ in altered and unaltered core samples of the East Bull Lake gabbro/anorthosite, near Massey, Ontario. They experienced analytical problems due to the low levels of U and Th in the rock (concentrations were less than 0.4 mg/kg U and 1.5 mg/kg Th) and high Fe concentrations (Fe interferes in the chemical extractions). Of the more reliable results obtained, altered (serpentinised) cores were found to have $^{234}U/^{238}U$ ratios as low as 0.86 (± 0.17) and $^{230}Th/^{234}U$ ratios up to 1.4 (± 0.3). Unfortunately, the poor counting statistics for many samples does not allow clear conclusions to be drawn except that the same patterns were observed in the East Bull Lake gabbro as have been noted in disequilibrium studies of other plutonic rocks.

In a similar study of surface samples of the Eye-Dashva Lakes granite, near Atikokan, Ontario, LATHAM and SCHWARCZ (15) observed frequent depletion of ^{234}U and excess of ^{230}Th giving $^{234}U/^{238}U$ ratios between 0.82 and 1.01 and $^{230}Th/^{234}U$ ratios between 1.12 and 1.78. Disequilibrium was also noted between ^{232}Th and ^{228}Th indicating loss of the intermediate nuclide ^{228}Ra. GASCOYNE and SCHWARCZ (18) analysed borehole cores from the same area and observed similar trends in near-surface cores and heavily altered cores that penetrated fracture zones. Mobility of ^{228}Ra was not seen except that over 100% ^{226}Ra excess was found in a highly fractured core at a depth of 94 m and a 20% ^{226}Ra deficiency occurred in an altered, gypsum-containing, fractured sample at a depth of 1050 m. The results of these two studies are shown in Figure 4. The more heavily altered cores lie some distance from secular equilibrium, whereas the less altered pink and grey granite samples, and those containing high-temperature, fracture-filling minerals, such as epidote, are within 2σ of equilibrium.

From their study, GASCOYNE and SCHWARCZ (18) concluded: 1) most bulk-rock and mineral-infilled samples had not experienced measurable radionuclide migration in recent geological time (up to 10^6 a), 2) disequilibrium was only found in altered rocks and usually those that were associated with fractures and low-temperature infilling minerals, 3) ^{234}U was more mobile than ^{238}U probably due to alpha-recoil and damaged-site leaching processes and 4) ^{226}Ra mobility may have been enhanced in saline- and retarded in fresh-water environments.

In a more detailed application of Th- and U-series disequilibria to plutonic rocks, GASCOYNE and CRAMER (19) analysed surface samples and borehole cores from various depths in the Lac du Bonnet granite batholith, Manitoba. The cores and one surface sample were all adjacent to frac-

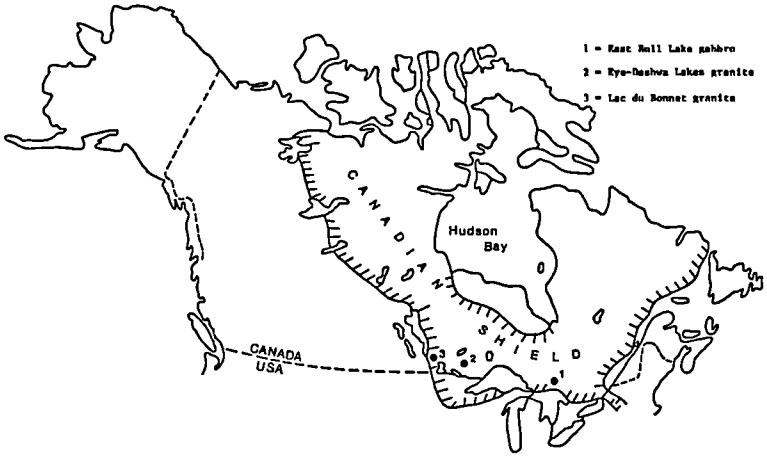

Figure 3: Location of the research area plutons on the Canadian Shield which have been sampled for decay-series studies.

tures, and had a visible alteration profile consisting of 1) unaltered pink granite, 2) hematite-rich red granite, 3) clay-rich beige granite and calcite- or clay-rich fracture surface.

Major, minor and rare earth element (REE) analyses of cores from a depth of about 150 m showed loss of Ca and Na, gain then loss of Fe, and gain of K, U and REE towards the fracture surface (Figure 5). These characteristics correlated with the progressive alteration of plagioclase feldspars, hematisation followed by bleaching of the granite, and increasing illite content towards the alteration surface. Uranium was associated with both the hematite and illite but only showed significant isotopic disequilibrium close to the fracture surface, in the bleached, illite-rich portion. This suggested that the hematisation was relatively ancient (i.e., $> 10^6$ a ago) and that both Fe-removal and illite formation were the main processes occurring at present time that might affect Th- and U-series isotopes.

Samples from this depth gave the lowest values of $^{234}U/^{238}U$ ratio for altered rock so far observed in the Canadian Program (0.66 ± 0.02), whereas $^{230}Th/^{234}U$ ratios were close to equilibrium (Figure 5). These results indicate the intensity of ^{234}U preferential leaching processes, which probably occur by significant recoil loss of ^{234}U to the groundwater (process 3 in Table I). This interpretation is supported by the equilibrium values for $^{230}Th/^{234}U$ ratios and indicates intense ^{234}U mobility within possible 10^3 to 10^6 a. All REE were enriched in the more altered part of the core, but the total REE content was lower than in unaltered parts of cores from the surface and greater depths. The coincidence of REE enrichment in the most altered rock and significant U-series disequilibrium suggested that REE mobilization may have been a recent phenomenon.

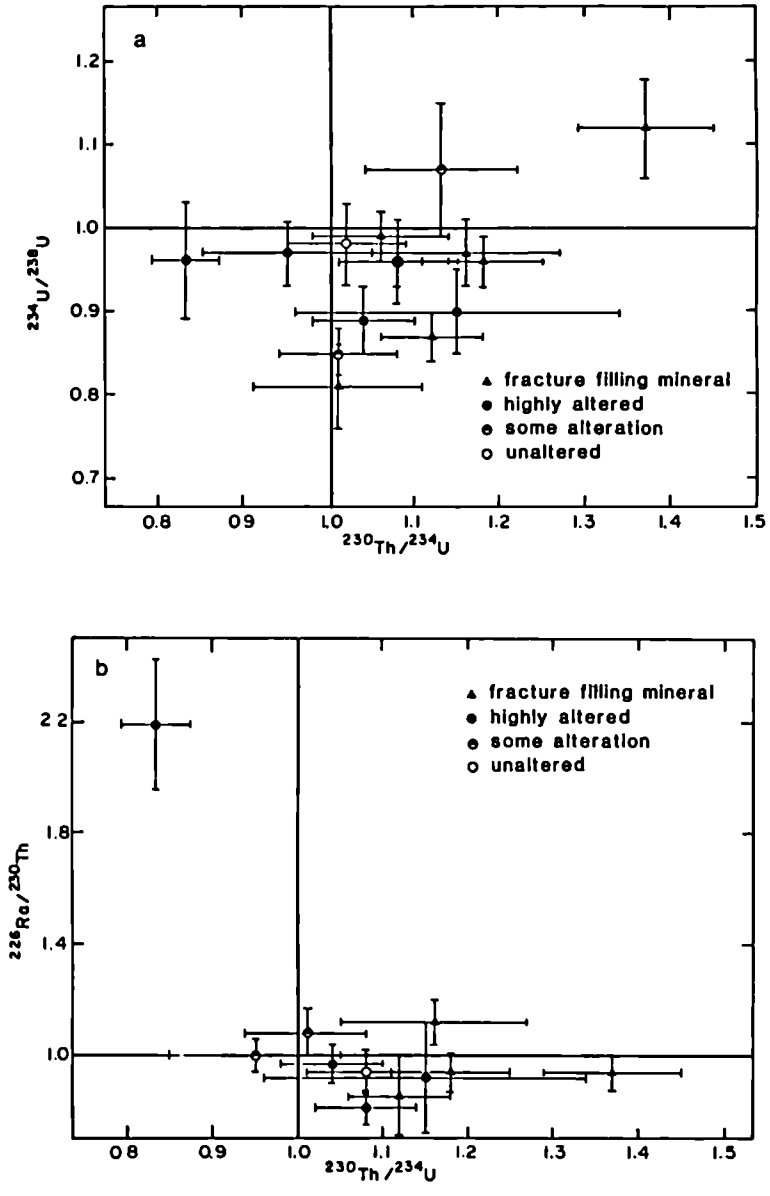

Figure 4: Variation of (a) $^{234}U/^{238}U$ and (b) $^{226}Ra/^{230}Th$ with $^{230}Th/^{234}U$ activity ratios for Eye-Dashva Lakes granite core samples (after 18).

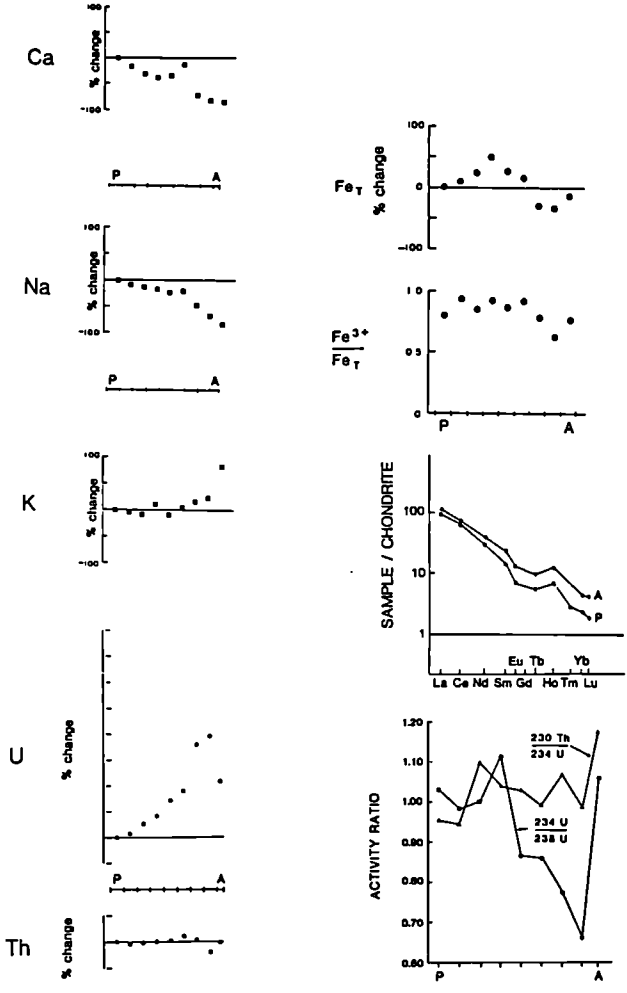

Figure 5: Variation of major, minor and rare earth element content, and of U-series activity ratios, with distance (~ 1 cm intervals) between relatively unaltered rock (P) altered rock at the fracture surface (A) for a core at ~ 150 m depth in a fracture zone in the Lac du Bonnet granite (after 19).

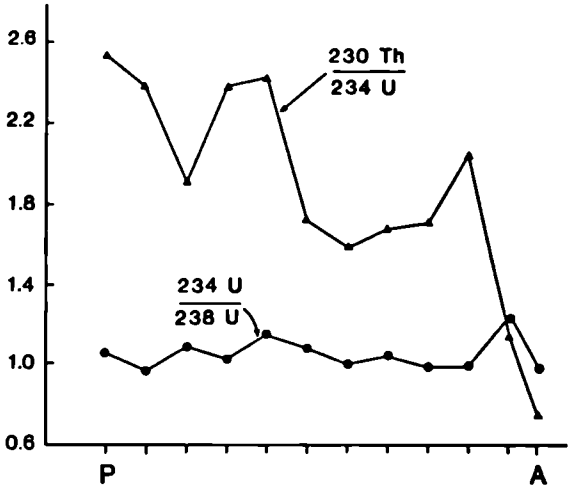

Figure 6: Variation of U-series activity ratios for a fracture-containing surface rock sample from the Lac du Bonnet granite (19). Horizontal scale is as Figure 5.

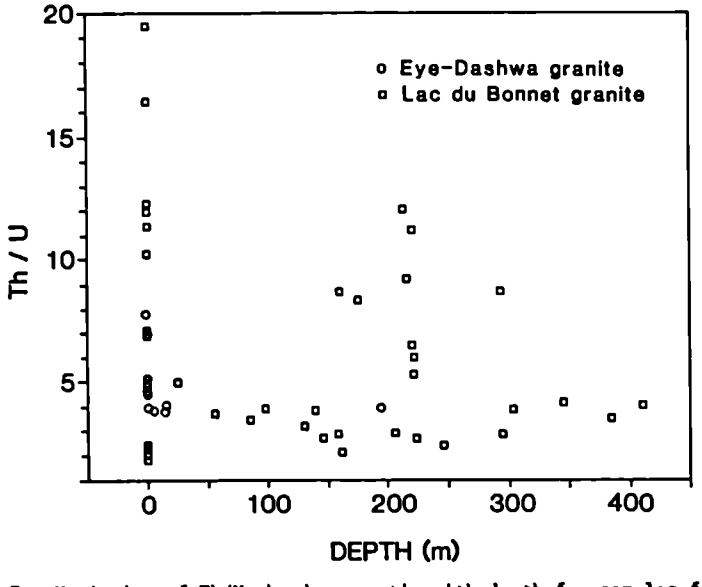

Figure 7: Variation of Th/U abundance ratio with depth for samples from the Lac du Bonnet and Eye-Dashwa Lakes granites (after 19).

The surface sample showed relatively little of the above trends, possibly because the fracture had a lesser role in alteration of the rock compared with the pervasive surface weathering conditions that had been imposed on the sample. Nevertheless, the U-series data (Figure 6) showed high $^{230}Th/^{234}U$ ratios (up to 2.5) and surprisingly stable, equilibrium values for $^{234}U/^{238}U$ ratios. These results are typical of process 1 in Table I indicating intense U leaching without isotopic fractionation. The high $^{230}Th/^{234}U$ ratios suggest that this leaching occurred within a time $<< 3.5 \times 10^5$ a.

A core from about 730-m deep in the granite was relatively intact and showed only slight Ca, Na and K variations towards the fracture surface. Increases in Fe and U were associated with chlorite in the fracture; the lack of U-series disequilibrium indicated that this was a relatively ancient mineralization (i.e., older than 10^6 a).

Indication of more pervasive leaching of U than shown in the fracture profiles was also noted (19) from the high Th/U abundance ratios in supposedly 'unaltered' rock away from the fracture face of the surface and shallow-depth cores. High ratios were also observed in many surface samples of granite (Figure 7) suggesting that loss of U may be one of the earliest processes in low-temperature alteration of granite, occurring even before alteration of plagioclase, ferromagnesian minerals, etc. These ratios indicated that up to 80% of the initial inventory of U had been leached from the rock, implying that U was present in the Lac du Bonnet granite in a more labile form than in the Eye-Dashwa Lakes granite. This is borne out by the lower Th/U ratios for comparable samples from the Eye Dashwa Lakes studies described above (see Figure 7).

The U-series isotope data from these two studies showed that U was being leached from granite at the surface and in permeable fracture zones down to at least 100 m, but, below this depth, most U mobility occurred via the α-recoil mechanism and selective leaching of the more mobile decay-product daughters. Weathering processes at the surface gave rise to U removal without isotopic fractionation, thereby accumulating excess ^{230}Th. At greater depth, redox conditions limited the solubility of U, caused the greatest degree of ^{234}U loss and, because loss occurred on or soon after formation, near-equilibrium $^{230}Th/^{234}U$ ratios were maintained.

4.3 The Role of Groundwater

An important part of the study of the Lac du Bonnet granite batholith (19) involved analysis of groundwaters from depths approximately corresponding to the rock data. High U concentrations (up to ~ 1 mg/L) and relatively low $^{234}U/^{238}U$ ratios (1.6 to 3.0) were observed in shallow Ca- or Na-HCO_3 type groundwaters (20), in agreement with the Th/U data and isotopic evidence for rapid U-loss from surficial rocks. At depths of 100 to 300 m, however, U concentrations were much lower (< 100 µg/L), $^{234}U/^{238}U$ ratios higher (3 to 7), and the rock data indicated less active U leaching but greater isotopic fractionation. The complexity of processes occurring at these depths was noted from the variety of isotopic patterns seen in a subsidiary study of fracture zone rubble samples. This suggested that uranium deposition and re-solution processes, perhaps controlled by a moving redox front, were occurring here on a recent geological time scale (probably within the last 10^4 a).

The studies of the East Bull Lake gabbro/anorthosite and Eye-Dashwa Lakes granite in the Canadian Program did not describe the U concentration and isotopic characteristics of groundwater from the sampling horizons. A limited amount of data is now available to support this work (21, 22), but direct correlations are difficult because the rock- and water-sampling programs were conducted independently of each other.

Groundwater at East Bull Lake contains less than 5 µg/L U at all

depths and, where measurable, the $^{234}U/^{238}U$ ratios are low (between 1.0 and 1.4). These results suggest that U is not enriched in fracture coatings and, therefore, a source of α-recoil ^{234}U is absent. This conclusion is supported by rock and mineral analyses (D.C. KAMINENI, Personal Communication).

In the Eye-Dashva Lakes pluton, surface and shallow groundwaters contain some U (up to 10 µg/L (22)) but far less than observed in the Lac du Bonnet area. Recently, however, concentrations as high as 250 µg/L have been observed for groundwater from a depth of about 150 m in a major fault zone. In spite of the low concentrations in shallow groundwaters, high levels of Rn in shallow groundwaters near faults and prominent surface lineaments were observed (22), indicative of groundwater discharge areas.

4.4 Hydrothermal Alteration

Disposal of nuclear fuel waste in a vault in plutonic rock imposes a thermal gradient on the surrounding rock. Within a short period of time after closure, temperatures as high as 100°C will be attained in the adjacent rock formation. The study of Th- and U-series disequilibria in low-temperature alteration and weathering processes in plutonic rocks (as described above) may, therefore, not be fully relevant as an analogue for potential actinide migration in the vicinity of a vault. Natural analogues for this type of higher temperature system have been described (23) but many are fossil contacts between high temperature intrusives and the surrounding, cooler, country rock. Few are currently active hydrothermal systems. Of the latter, fewer still have been examined for the mobility of actinides using Th- and U-series disequilibria.

In a study partly sponsored by the Atomic Energy Control Board of Canada, core was examined from a 2.1-km deep, percussion and core-drilled borehole in the Empire Creek Stock, Marysville, Montana, USA (24). This granite body is about 40-Ma old and contains an active hydrogeothermal circulation system that maintains a temperature of about 90°C below ~ 500 m. Much of the core is altered and veined; secondary minerals include sericite, kaolinite (from feldspar), chlorite (from biotite) and quartz (in the veining). Uranium-series analyses of selected samples from the borehole are shown in Table II. The samples of core show greater enrichment in U and Th than cuttings obtained during percussion drilling. This may be due to sorting of cuttings during transit up the borehole (the heavy, actinide-rich fraction will tend to sink and be lost). Uranium is enriched over Th in all samples relative to normal terrestrial abundances (Th/U ratios range from 2.2 to 4.7 compared to 4.6, the crustal abundance ratio).

All $^{234}U/^{238}U$ ratios lie within $\pm 2\sigma$ of secular equilibrium (1.00), indicating that neither ^{234}U nor ^{238}U have been selectively leached from, or deposited onto, the samples over the last 10^6 a. All $^{230}Th/^{234}U$ ratios lie within 3σ of equilibrium, indicating no isotopic mobility in the last ~ 3×10^5 a. These results suggest that much of the observed mineralogical alteration is fossil or is occurring very slowly, so that U-series equilibria are maintained. Unfortunately, $^{226}Ra/^{230}Th$ ratios were not determined in this study. These may have shown some response to the hydrothermal system because radium is often mobile under these conditions and, because of the short ^{226}Ra half-life, the ratio is more sensitive to migration than the actinide isotopic ratios. In addition, no data exist regarding the concentration and isotopic nature of actinides and their daughters in groundwaters in the rock body.

These results confirm some of the textural and mineralogic evidence obtained from the Empire Creek Stock borehole which suggest that much of the alteration occurred during an earlier period, following intrusion. However, the presence of a vigorous convective circulation of groundwater

TABLE II

URANIUM AND TH CONCENTRATIONS AND ISOTOPE ACTIVITY RATIO DATA FOR ALTERED CORE AND CUTTING SAMPLES FROM THE EMPIRE CREEK STOCK BOREHOLE, MARYSVILLE, MONTANA

Sample No.	Type*	Depth (m)	U mg/kg	Th mg/kg	$\frac{^{234}U}{^{238}U}$	$\frac{^{230}Th}{^{234}U}$	Description
5-6	co	305	21.3	49.9	0.98±0.03	1.00±0.04	Strong alteration to sericite, biotite and quartz
8-28-16	co	-710	8.3	39.0	1.01±0.06	1.01±0.09	Less altered rock
10-30-4A	ms(1.2)	-1000	239	606	1.09±0.03	0.98±0.05	Separate from less altered rock
10-30-4B	ms(0.65)	-1000	57	-	1.05±0.07	-	Separate from less altered rock
12-30	co	1298	30.5	108	1.01±0.02	1.11±0.05	Kaolinised feldspars, fracured zone
14-34	co	1636	17.7	46.6	0.95±0.03	0.98±0.05	Less altered rock
1525/30	cu	465	14.8	32.5	1.01±0.04	0.97±0.06	From water-bearing fracture zone
1910/15	cu	582	10.0	39.1	0.98±0.04	1.10±0.06	From major water-bearing zone
2920/25	cu	890	12.0	-	0.99±0.05	-	Fracture zone
3385/90	cu	1032	10.9	32.1	0.97±0.04	0.98±0.06	From major water-bearing fracture zone
4015/20	cu	1224	17.7	44.1	0.99±0.03	0.92±0.05	Fracture zone
6735/40	cu	2053	10.7	-	1.02±0.04	-	From major water-bearing zone

* co = core, cu = cuttings, ms( ) = magnetic separate at ( ) amperage

in the body, coupled with extensive fracturing and high rock porosity at great depth (24) suggest that rock alteration is occurring rapidly at present. Under these conditions, considerable actinide mobility might be expected; however, this does not occur, as shown by the U-series data. These results suggest that the onset of convective circulation in granite due to the presence of a nuclear fuel waste vault, is unlikely to increase the mobility of actinides leaking from the vault.

5. Modelling of Decay-Series Results

Attempts at modelling actinide mobility from Th- and U-series data tend to fall into three main types: 1) descriptive models of U accumulation and dissolution (18, 19, 25, 26, 27); 2) semi-empirical mathematical models, such as open system and uranium-trend models (28, 29, 30); and 3) process models, such as the etch model (31, 32) and the leach model (15).

The descriptive models use graphs of isotope ratios (e.g., $^{230}Th/^{234}U$ versus $^{234}U/^{238}U$) to visually describe the relation of the sample to secular radioactive equilibrium (e.g., see Figure 6 this report), and to infer the migration process from the quadrant the data occupy. The semi-empirical models have been mainly applied to highly altered and weathered deposits, such as paleosols and sediments, and are not further considered here. The models of LATHAM and SCHWARCZ (15) are applicable to the types of actinide migration seen occurring naturally in

plutonic rocks of the Canadian Shield. They found that their results from the Eye Dashva Lake granite best fitted a model of U leaching (i.e., U removal from the rock matrix) rather than U etching (i.e., U removal at the rate of mineral surface dissolution). In the leach model, the rate of removal depends on the U concentration available to the groundwater, and so, as might be expected, leaching of U decreases as the rock becomes more weathered. The etch model was rejected for surface and near-surface weathering because the high $^{230}Th/^{234}U$ ratios predicted by this model were not observed and the high porosities expected by congruent dissolution of U and matrix were not encountered.

The lack of U depletion in the weathered rocks, and the generally low $^{230}Th/^{234}U$ ratios in the Eye-Dashva Lake surface samples led LATHAM and SCHWARCZ (15) to propose that U leaching was a slow process, occurring at a rate that was less than the decay rate of ^{230}Th and controlled mainly by the low permeability of the rock. However, this interpretation was compromised by the fact that the observed disequilibrium values in the weathering rinds of samples had almost certainly been attained since the last glaciation, thus implying ^{234}U loss in the last 10^4 a. LATHAM and SCHWARCZ (15) concluded that the ratios observed were largely due to rapid leaching of labile U present in the rock in low concentrations on grain boundaries. Once this had been removed, leaching slowed and isotopic ratios tended closer to unity.

The results for the Lac du Bonnet granite, (19), further support the leach model described above. Although higher $^{230}Th/^{234}U$ ratios were observed in surface samples (up to 2.5) than seen by LATHAM and SCHWARCZ (up to 1.78), the greater depletion of U relative to Th in the surface samples of this granite body (maximum Th/U = 24) suggests that a steady-state value of $^{230}Th/^{234}U$ had been reached, and the rate of removal of ^{234}U was equal to the rate of decay of excess ^{230}Th. This interpretation implies that alteration of the surface granite samples began prior to their exposure following deglaciation 15 000 a ago. This is not unreasonable because alteration is observed in samples up to 250-m deep at present. Alternatively, the high $^{230}Th/^{234}U$ ratios coupled with high Th/U ratios in surface samples of the Lac du Bonnet granite, may indicate that most of the U is present in a labile form, i.e., sorbed on grain boundaries or contained in phases that are rapidly altered.

The complexity induced by the presence of labile and non-labile U, varying surficial exposure histories, and the various migration processes involved (i.e., etch, leach, α-recoil, etc.) make it difficult to determine quantitatively any reliable age data or U-removal rate information. For this reason, Th- and U-series disequilibria are best used qualitatively to detect actinide mobility in a plutonic rock and to estimate a time scale based simply on presence or absence of secular equilibrium between isotope pairs.

6. The Application of Decay-Series Methods to Site Selection

Selection procedures for a site for disposal of nuclear fuel waste require minimal disturbance and incursion of the rock. Drill holes will therefore likely be few and well-spaced, and their locations will also be based on extensive use of surface and airborne geological and geophysical surveys. A summary of methods based on decay-series equilibrium techniques, which could be applied to the site selection process is given in Table III. One of these non-incursive methods, is the detection of faults, other structural discontinuities and groundwater discharge zones by measurement of radon gas concentrations in soil, air or surface waters. The usefulness of this method and of accompanying helium measurements has recently been demonstrated for the Carnmenellis granite, Cornwall, U.K., (33). The technique has been applied within the Canadian Program for part

of the Eye-Dashva Lakes pluton (21).

During the drilling of boreholes for site characterization, the chemistry and radioisotopic composition of groundwaters (Table III) should be determined as soon after drilling as possible to limit contamination and inflow of other waters. Whole rock samples of the core should be taken

TABLE III

PROPOSED METHODOLOGY FOR THE APPLICATION OF THORIUM- AND URANIUM-SERIES DISEQUILIBRIUM TECHNIQUES TO SITE SELECTION PROCEDURES IN NUCLEAR FUEL WASTE DISPOSAL

Item	Sampling Procedure	Isotopic	To Determine	Evidence
1.	Soil gas & surface water	Rn, He	Lineaments; discharge zones	High Rn, He
2.	Surface outcrops	U, Th, Ra	Extent of alteration	Th/U and U-series ratios
3.	Surface sediments	Leachable U, Th, Ra	Extent of contribution to groundwater radio-chemistry	High U, Ra in leachables
4.	Surface waters	U, Ra, Rn	Discharge zones for shallow groundwaters; local mineralisations	High U, Ra and $^{234}U/^{238}U$
5.	Groundwater	U, Ra, Rn	Local deposition/dissolution areas; redox conditions	High or low U, Ra, Rn, $^{234}U/^{238}U$
6.	Core - Unaltered	U, Th, Ra	State of equilibrium	Th- and U-series ratios
	- Altered profile	U, Th, Ra	Patterns of disequilibrium	Th- and U-series ratios
	- Rubble, gouge material	U, Th, Ra	Patterns of disequilibrium; redox conditions in zone	Th- and U-series ratios
	- Fracture-filling calcite or gypsum	$^{230}Th/^{234}U$	Radiometric age	$^{230}Th/^{234}U < 1$ if mineral is < 350,000 a
	- Other fracture-filling minerals	U, Th, Ra	Relative age; patterns of disequilibrium	Th- and U-series ratios
	- Thin sections	Fission track	Distribution of U in minerals, grain boundaries, etc.	Higher track densities

where there is no obvious alteration and analysed to check that secular equilibrium holds. Core showing alteration profiles should be analysed for U-series disequilibria for all depths to determine the patterns and controls of naturally-occurring radionuclide movement. These data may also give insight to the alteration history of the rock body and distances of migration of radionuclides into the rock matrix. Where sufficient core is available (or if actinide concentrations are high), analysis of mineral separates by U-series methods should be attempted to identify phases exhibiting disequilibrium and/or locations of labile U. Analysis of samples of fracture gouge will probably indicate the most current migration processes occurring in the rock; an effort should be made to correlate these data with the water radioisotopic composition and hydrogeological flow patterns.

Finally, attempts should be made to date any fracture-filling minerals (e.g., calcite, gypsum) by the $^{230}Th/^{234}U$ age-dating technique to indicate depositional processes occurring within the last ~ 3×10^5 a (34). In addition, fission track analysis should be used on altered and unaltered core thin sections to determine the distribution of U.

Conclusions

Thorium- and, particularly, uranium-series disequilibrium methods have proved useful in identifying the mobility of actinides in plutonic rock bodies and associated groundwaters in the Canadian Shield. The presence of radioactive disequilibrium between naturally occurring decay-series isotope pairs in whole rock or mineral separates has indicated

mobility of some actinide isotopes within the last 10^6 a. Disequilibrium is most often found in surface and near-surface altered samples and actinide leaching rates have been modelled from disequilibria data. The lack of mobility of actinides in a convective circulation system surrounding a nuclear fuel waste vault suggests that these radionuclides may be retarded by the geosphere when leaking from a vault emplaced deep in plutonic rock. This type of study is invaluable in characterizing locations selected as potential disposal sites.

REFERENCES

1. SCHWARCZ, H.P., GASCOYNE, M. and FORD, D.C. (1982). Uranium series disequilibrium studies of granitic rocks. Chem. Geol. 36, 87-102.
2. ROSHOLT, J.N. (1983). Isotopic composition of uranium and thorium in crystalline rocks. J. Geophys. Res. 88, (89), 7315-7330.
3. GASCOYNE, M. (1982). The determination of U-Th-Ra isotopic ratios in granitic rocks. Techn. Memo. 82-1, Dept. of Geology, McMaster University, Hamilton, Ontario.
4. LALLY, A.E. (1982). Chemical Procedures. In: Uranium Series Disequilibrium: Applications to Environmental Problems (eds. M. Ivanovich and R.S. Harmon), Clarendon Press, Oxford.
5. GASCOYNE, M. and LAROCQUE, J.P.A. (1984). A rapid method of extraction of uranium and thorium from granite for alpha spectrometry. Nucl. Instrum. Methods Phys. Res. 223, 250-252.
6. HAAKER, R.F. and EWING, R.C. (1981). Natural analogues for crystalline radioactive waste forms. Part II. Non-actinide phases. In: Scientific Basis for Nuclear Waste Management (ed. J.G. Moore), 3, 299-306, Plenum Press.
7. FLORAR, R.J., ABRAHAM, M.M., BOATNER, L.A. and RAPPAZ, N. (1981). Geologic stability of monazite and its bearing on the immobilization of actinide wastes. In: Scientific Basis for Nuclear Waste Management (ed. J.G. Moore) 3, 507-514, Plenum Press.
8. EYAL, Y. and FLEISCHER, R.L. (1985). Preferential leaching and the age of radiation damage from alpha decay in minerals. Geochim. Cosmochim. Acta, 49, 1155-1164.
9. HAYWARD, P.J. and CECCHETTO, E.V. (1982). Development of sphene based glass ceramics tailored for Canadian waste disposal conditions. In: Scientific Basis for Nuclear Waste Management, (ed. S.V. Topp), 4, 91-98, Elsevier, N.Y.
10. HAYWARD, P.J., HOCKING, W.H., MITCHELL, S.L. and STANCHELL, M.A.T. (1984). Leaching studies of natural and synthetic titanite, a potential host for Canadian nuclear fuel processing wastes. Can. Mineral. 21, 611-623.
11. GASCOYNE, M. (1986). Evidence for the stability of the potential nuclear waste host, sphene, over geological time, from uranium-lead ages and uranium-series measurements. Appl. Geochem. 1, 199-210.
12. BANCROFT, G.M., METSON, J.B., KANETKAR, S.M. and BROWN, J.D. (1982). Surface studies on a leached sphene glass. Nature, 299, 708-710.
13. VANCE, E.R. and METSON, J.B. (1985). Radiation damage in natural titanites. Phys. Chem. Minerals, 12, 255-260.
14. VANCE, E.R., KARIORIS, F.G., CARTZ, L. and WONG, M.S. (1984). Radiation effects on sphene and sphene-based glass-ceramics. In: Advances in Ceramics (eds. G.G. WICKS and W.A. ROSS), 8, 62-70, Am. Ceramic Soc..
15. LATHAM, A.G. and SCHWARCZ, H.P. (1987a). On the possibility of determining rates of removal of uranium from crystalline igneous rocks using U-series disequilibria. 1. A U-leach model, and its applicability to whole rock data. Appl. Geochem. 2 in press.

16. LATHAM, A.G. and SCHWARCZ, H.P. (1987b). On the possibility of determining rates of removal of uranium from crystalline igneous rocks using U-series disequilibria: 2. Applicability of a U-leach model to mineral separates. Appl. Geochem. 2 in press.
17. SCHWARCZ, H.P., and LATHAM, A.G. (1985). Uranium-series disequilibrium analyses of core and surface samples from East Bull Lake. Unpub. Interim Report to Atomic Energy of Canada Limited, Pinawa, Manitoba.
18. GASCOYNE, M. and SCHWARCZ, H.P. (1986). Radionuclide migration over recent geologic time in a granitic pluton. Isot. Geosci. 59, 75-85.
19. GASCOYNE, M. and CRAMER, J.J. (1987). History of actinide and minor element mobility in an Archean granitic batholith in Manitoba, Canada. Appl. Geochem., 2 in press.
20. GASCOYNE, M. (1987). High levels of uranium and radium in groundwaters at Canada's Underground Research Laboratory, Lac du Bonnet, Manitoba, in preparation.
21. BOTTOMLEY, D.J., GASCOYNE, M., ROSS, J.D. and RUTTAN, J.T. (1986). Hydrogeochemistry of the East Bull Lake pluton, Massey, Ontario. Atomic Energy of Canada Limited Technical Record, TR-382*.
22. LAROCQUE, J.P.A. and GASCOYNE, M. (1986). A survey of the radioactivity of surface water and groundwater in the Atikokan area, northwestern Ontario. Atomic Energy of Canada Limited Technical Record, TR-379*.
23. CHAPMAN, N.A., MCKINLEY, I.G. and SMELLIE, J.A.T. (1984). The potential of natural analogues in assessing systems for deep disposal of high-level radioactive waste. Nagra Technical Report NTB 84-41.
24. TAMMEMAGI, H.Y., HAVERSLEW, B. and STURCHIO, N.C. (1986). Investigations of the Empire Creek Stock, Montana, as an analogue to a nuclear waste repository. Chem. Geol., 55, 375-386.
25. THIEL, K., VORWERK, R., SAAGER, R. and STUPP, H.D. (1983). ^{238}U fission tracks and ^{238}U-series disequilibria as a means to study recent mobilisation of uranium in Archean pyritic conglomerates. Earth Plan. Sci. Lett., 65, 249-262.
26. SMELLIE, J.A.T. and ROSHOLT, J.N. (1984). Radioactive disequilibria in mineralised fracture samples from two uranium occurrences in northern Sweden. Lithos, 17, 215-225.
27. SMELLIE, J.A.T., MACKENZIE, A.B. and SCOTT, R.D. (1986). An analogue validation study of natural radionuclide migration in crystalline rocks using uranium-series disequilibrium studies. Chem. Geol. 55, 233-254.
28. ROSHOLT, J.N. (1985). Uranium-trend systematics for dating Quaternary sediments. U.S. Geol. Surv. Oper. File Rep. 85-298, 34 p.
29. SZABO, B.Z. and ROSHOLT, J.N. (1969). Uranium series dating of Pleistocene Molluscan shells from Southern California - an open system model. J. Geophys. Res., 74, 3253-3260.
30. AIREY, P.L. and ROMAN, D. (1981). Uranium series disequilibria in the sedimentary uranium deposit at Yeelirrie, Western Australia. J. Geol. Soc. Australia, 28, 357-363.
31. ANDREWS, J.N., GILES, I.S., KAY, R.L.F., LEE, D.J., OSMOND, J.K., COWART, J.B., FRITZ, P., BARKER, J.F. and GALE J. (1982). Radioelements, radiogenic helium and age relationships for groundwaters from the granites of Stripa, Sweden. Geochim. Cosmochim. Acta, 46, 1533-1543.
32. LATHAM, A.G. and SCHWARCZ, H.P. (1986). Models of uranium etching and leaching: Their applicability to estimating rates of natural uranium removal from crystalline igneous rocks using U-series disequilibrium data from the Eye-Dashwa Lakes pluton. Atomic Energy of Canada Limited, Technical Record TR-353*.
33. GREGORY, R.G. and DURRANCE, E.M. (1987). Helium, radon and hydrother

mal circulation associated with the Carnmenellis radiothermal granite of southwest England. J. Geophys. Res. in press.
34. MILTON, G. (1987). Paleohydrological inferences from fracture calcite analyses. Appl. Geochem. 2 in press.

* Unrestricted, unpublished report available from SDDO, Atomic Energy of Canada Limited Research Company, CVhalk River, Ontario KOJ 1JO.

REDISTRIBUTION OF NATURAL ^{129}I AMONG MINERAL PHASES AND GROUND WATER IN THE KOONGARRA URANIUM ORE DEPOSIT, N.T., AUSTRALIA

J.T. FABRYKA-MARTIN
Department of Hydrology and Water Resources, University of Arizona

D. ROMAN
Australian Atomic Energy Commission

P.L. AIREY
International Atomic Energy Agency

D. ELMORE
Environmental Research Division, Argonne National Laboratory

P.W. KUBIK
Nuclear Structure Research Laboratory, University of Rochester

Summary

Redistribution of fission-product ^{129}I between ore and ground water is being evaluated in field studies at four uranium ore deposits. Most attention has been given to the Koongarra deposit. Weathered primary ore samples have atomic $^{129}I/U$ ratios ranging from 5 to 22% of values predicted for equilibrium, indicating preferential loss of ^{129}I relative to U during weathering. Samples from zones of relatively recent U deposition under slightly oxidizing conditions show considerable enrichment in ^{129}I relative to U, which is attributed to sorption of ^{129}I onto Fe oxide or clay surfaces.

Water samples from the four deposits also indicate strong partitioning of ^{129}I into ground water during weathering of the ore. Maximum ^{129}I concentrations and $^{129}I/I$ ratios occur in boreholes nearest the primary ore bodies; these values are generally 1 to 2 orders of magnitude higher than those for boreholes up-gradient of the deposits. ^{129}I contents in the water drop sharply with distance down-gradient of the Koongarra deposit, which is consistent with the significant sorption indicated by drill-core analyses.

1.0 Introduction

Fission product ^{129}I ($T_{1/2}$, 1.6×10^7 yr) is produced along with ^{131}I and stable ^{127}I in reactor fuel elements. Over 99% of the iodine remains trapped until the fuel is reprocessed, when it is volatilized and can be captured by a variety of recovery methods. Final waste forms that are commonly proposed involve incorporation of insoluble solid forms of iodine in a matrix of cement, low-melting glass, bitumen or epoxy resin.

The most likely scenario by which ^{129}I would be transported back to the biosphere is as a consequence of the invasion of the waste by ground water. Because of its long half-life, radioactive decay is insignificant as a process for diminishing the ^{129}I concentration of the waste. Hence,

other processes for reducing the specific activity of iodine reaching the surface are important to consider. These include leach resistance of the waste, dilution by stable ^{127}I, and retardation by geologic media along the flowpath to the surface.

Numerous laboratory studies have been conducted over the past decade for the purpose of characterizing the behavior of iodine ions with minerals which could be encountered by ^{129}I along the flowpath to the surface in order to model the rate of nuclide migration relative to water. Sorption of iodine by most minerals is quite small. The tendency for sorption is commonly expressed by a distribution coefficient, K_D (mol/g solid per mol/ml solution). In fresh ground water at near-neutral pH, K_D values for I^- sorption on most silicate minerals lie within the range 1 to 10 ml g^{-1} (4). K_D values of 0.8 to 53 ml g^{-1} measured for sorption of I^- on soils were tentatively attributed to amorphous Fe and Al oxide coatings on silt-sized particles (25). Studies have also focussed on the identification of minerals which would be stable within the repository environment and which could be incorporated into backfill in order to retain ^{129}I in the repository. Significant sorption of I^- (up to K_D of 10^3 ml g^{-1}) is reported for minerals containing Hg, Pb, Ag, and Cu (4,5). Sulfide minerals containing Cu, Pb and Fe are particularly efficient sorbents (23).

Although such studies provide useful and necessary information for modelling studies and for elucidating possible retardation mechanisms, extension of laboratory results to the natural environment is of doubtful validity for several reasons (2). Sorption behavior depends upon pH, Eh, ground-water chemistry and accessible mineral surfaces, which cannot be readily reproduced in the laboratory and which are likely to vary along the flowpath in the real world. Sorptiveness of a given mineral may vary with time due to slow alteration of the surface. Laboratory timescales may not be sufficiently long for the system to achieve equilibrium distributions. Consequently, determination of ^{129}I distributions in appropriate natural analogs provides a useful extension of laboratory results and test of predictions based on those results.

An uranium ore deposit is a good candidate as a natural analog of retardation processes in the far field of a waste repository, provided that the deposit and its geochemical history are well-characterized (2,3). Iodine-129 concentration profiles in ground water down-gradient of deposits permit evaluation of the migration rate of ^{129}I relative to water. Comparison of concentrations in solution to that sorbed onto reactive mineral surfaces provides an estimate of the distribution coefficient, K_D. In addition, uraninite and pitchblende may behave as natural analogs of unreprocessed spent fuel elements (17). Mechanisms and rates of loss of ^{129}I from these minerals in nature provide a comparison for rates of transfer from waste to ground water in a repository.

Since 1981, the Australian Atomic Energy Commission (AAEC) has been evaluating the distribution of numerous radioactive products of U decay and fission in mineral phases and ground water around four U ore deposits in the Alligator Rivers Uranium Province, Northern Territory, Australia. Well-defined mineralogical relationships, variety of geochemical environments within each deposit, and accessibility of ore and ground water for sampling make these sites useful for testing hypotheses about the relative mobilities of radionuclides on a geologic timescale. The current status of the research program and description of the deposits (Koongarra, Nabarlek,

Ranger, and Jabiluka) are presented in Ref. (1,3). With respect to ^{129}I, research has focussed on modeling the production of this fission product within the ore, mobilization of ^{129}I induced by weathering of the ore, and migration in ground water. Chlorine-36 has also been measured in the ore in order to assess the variability of in-situ neutron fluxes and to estimate residence times of U in younger parts of the deposits. Its concentration in ground-water is used in this study as a check for the presence of bomb-pulse ^{129}I.

2.0 Description of the study area

2.1 Study region

The uranium deposits are hosted by quartz-muscovite-chlorite schists, with common accessory minerals including biotite, pyrite, hematite, tourmaline, apatite, sphene, zircon, epidote-group minerals, and gypsum (18). Although carbonate minerals do not occur within the ore zones, the ore deposits are always located near massive beds of dolomite and/or magnesite. The host schist is extensively weathered to an average depth of about 20 meters, ranging up to 35 meters at Ranger (18,22). Above the water table, common weathering products are Fe and Al oxides and hydroxides, kaolinite, and montmorillonite (3).

In the unweathered zone, uraninite and pitchblende comprise the primary mineralization and are associated with intense chloritization. In the weathered zone, the most common secondary uranium minerals are saleeite (Mg uranyl phosphate) and sklodowskite (Mg uranyl silicate). A rich variety of other uranyl oxides, silicates, phosphates, and vanadates has also been recognized at all of the deposits (18,22).

The area has a summer monsoonal climate, with nearly all of the annual rainfall of 1.3-1.4 m occurring between December and March. Annual evaporation is 2.2 m. Water tables fluctuate several meters during the year, sometimes reaching the surface during the wet season and receding to depths of 7 m at Koongarra and 15 m at Ranger and Nabarlek during the dry season (18).

2.2 The Koongarra deposit

In the past two years, our work has concentrated on the Koongarra deposit. Here, the primary ore consists of uraninite and various alteration products and extends to a depth of about 100 m (Figure I). Immediately above this zone, from the surface to a depth of about 30 m, the original ore has been greatly altered by weathering under oxidizing conditions (22). Ground water flowing through the deposit has produced a dispersion fan of secondary U minerals and U sorbed onto Fe oxides and clays, extending about 100 m down-gradient of the main ore body.

Recharge to the unweathered schist occurs by downflow along both sides of the reverse fault separating Kombolgie sandstone from the host schist and by crossflow from sandstone into schist at depth through a brecciated zone (22) (Figure 1). Water entering from the sandstone is slightly oxidizing, as indicated by hematite staining of the sandstone. Elsewhere, the weathered schist is believed to act as a relatively impermeable capping that limits downward percolation of surface waters flooding the area during the wet season.

3.0 Model for in-situ production of ^{129}I

Comparison of measured ^{129}I concentrations to those predicted for equilibrium conditions is the basis for interpretation of the results in terms of degree of retention by ore minerals, rates of transfer from ore to water, and retardation by sorptive surfaces down-gradient of the deposit. ^{129}I is produced in uranium ore by spontaneous fission of ^{238}U and thermal-neutron induced fission of ^{235}U. The ^{129}I content of the ore as a function of residence time of U, t_u, is given by

$$N_{129}(t_u) = [N_{238}\,\lambda_{sf}\,Y_{sf} + \Phi_n\,N_{235}\,\sigma_{235f}\,Y_{if}]\left[\frac{1 - \exp[-(\lambda_{129} + \lambda_L)\,t_u]}{\lambda_{129} + \lambda_L}\right]$$

atoms g^{-1} yr^{-1} (Eqn. 1)

where N_{238} and N_{235} = atomic concentrations of ^{238}U and ^{235}U (atoms g^{-1}), λ_{sf} = spontaneous fission decay constant for ^{238}U (8.5×10^{-17} yr^{-1}), Y_{sf} = spontaneous fission yield at mass 129 (3×10^{-4}), Y_{if} = yield at mass 129 for thermal-neutron induced fission of ^{235}U (0.0074), σ_{235f} = thermal-neutron capture cross-section of ^{235}U for a fission event (583×10^{-24} cm^2), Φ_n = thermal-neutron flux (neutrons cm^{-2} yr^{-1}), λ_{129} = decay constant for ^{129}I (4.3×10^{-8} yr^{-1}), and λ_L = leach fraction for irreversible transfer of ^{129}I from mineral to water.

The thermal-neutron flux is determined by ore geochemistry and can be approximated for the Alligator Rivers deposits as a function of U content (14). With this simplification, the ^{129}I content of ore is estimated for a closed system at equilibrium

$$(N_{129})_{eq} = 1470\,[U] + 0.477\,[U]^2 \quad \text{atoms } g^{-1} \quad \text{(Eqn. 2)}$$

where [U] is uranium concentration in ppm. The first term on the right-hand side accounts for contribution of ^{129}I from spontaneous fission, and the second term accounts for induced-fission production. For U concentrations less than 300 ppm, only the first term is significant, and the equilibrium atomic ratio $^{129}I/U$ is 6×10^{-13}. Above this threshold concentration, induced fission becomes increasingly important, causing an exponential increase in the equilibrium atomic ratio. For ore containing 1000, 10,000 and 100,000 ppm U, for example, predicted equilibrium atomic ratios are 7.7×10^{-13}, 2.5×10^{-12}, and 2.0×10^{-11}, respectively.

Loss of ^{129}I from U minerals into ground water occurs by direct recoil into the water; release by dissolution or recrystallization of the host mineral; implantation by recoil into an adjacent grain, followed by etching of the fission damage track; and diffusion through the mineral lattice. In the present study, these mechanisms are lumped into a single parameter, the leach fraction λ_L, which is defined as the ratio of the amount of ^{129}I leached in a year to the total amount of ^{129}I present in the solid phase at the beginning of the year.

4.0 Analytical methods

In 1983 and 1985, iodine was extracted from ground water in the vicinity of four uranium deposits in the Alligator Rivers region: Ranger, Koongarra, Nabarlek and Jabiluka. Borehole locations relative to the deposits are shown in figures in Ref. (1,3). The method of collection is by pumping 1000 or more liters of filtered ground water through a resin bed containing 600 to 1000 cm^3 of anion-exchange resin (100-200 mesh Dowex 1-X8). In the laboratory, iodine is stripped from the resin and purified by the method described in Ref. (13).

Chloride was extracted from the same boreholes as were sampled for ^{129}I analysis. Two methods were used. In 1983, nearly all Cl^- samples were collected by passing about 40 liters of ground water through a column of anion-exchange resin (20-50 mesh Dowex 1-X8, NO_3^- form). In the laboratory, Cl^- is eluted with 2M $NaNO_3$ and precipitated as AgCl by adding a slight excess of 1M $AgNO_3$. For other samples, AgCl was precipitated directly by adding 1M $AgNO_3$ to ground-water acidified with HNO_3. In all cases, AgCl precipitates were subsequently purified by dissolution in NH_4OH, addition of $Ba(NO_3)_2$ and filtering to remove sulfate (as $BaSO_4$), and reprecipitation of AgCl following evaporation of NH_3 or neutralization with HNO_3.

Several drill-core samples were selected from the Koongarra and Ranger No. 3 uranium prospects to be processed for ^{129}I and ^{36}Cl analysis. The procedure is carried out in a closed system under vacuum and involves leaching the ground samples with HF, oxidizing I^- to I_2 with H_2O_2, and distilling the volatile halogen species into a liquid N_2 trap (19). Iodine is reduced with H_2SO_3 and the two halides are precipitated as Ag salts. Koongarra sample locations are shown on Figure I. Additional sample information and preliminary interpretation of results are described in Ref. (14).

Final sample forms are AgCl and AgI, which are ready for isotopic analysis by tandem accelerator mass spectroscopy (TAMS) at the University of Rochester. Instrumentation is described in Ref. (9,10).

5.0 Measurements and interpretation of ^{129}I contents of uranium ore

5.1 Results for weathered primary ore

Ore samples from the weathered top of the Koongarra primary ore body have atomic ratios $^{129}I/U$ ranging from 5 to 22% of predicted equilibrium values (Samples 5-7, Table I and Figure I). The residence time of U in the primary ore (900 My) is sufficiently long for equilibrium to have been established with respect to ^{129}I concentrations before the weathering front advanced to this depth. Weathering initiated one to three million years ago (3), and elevated $^{36}Cl/Cl$ ratios in weathered ore indicate that the rate of loss of U during weathering is rapid relative to the half-life of ^{36}Cl (3.01×10^5 yr) (14). Activity ratios for isotopes in the U-decay series suggest that the remaining U recrystallized in place to form secondary U minerals, as opposed to being transported and reprecipitated (3). Hence, we interpret the depleted $^{129}I/U$ ratios of these samples as indicating preferential loss of ^{129}I relative to U during weathering. The rate of U leaching is on the order of 10^{-7} to 10^{-6} yr^{-1} in this part of the Koongarra deposit and up to 10^{-5} yr^{-1} in the other deposits (1,3); λ_L for ^{129}I thus must be $>> 10^{-7}$ yr^{-1}.

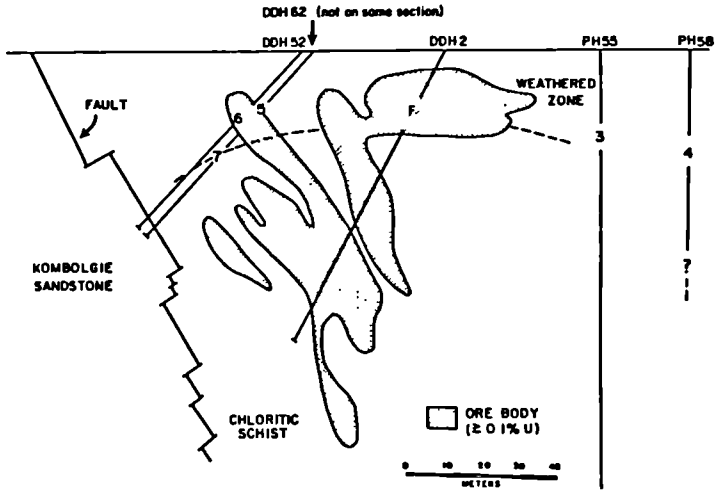

Figure I. Schematic cross-section of Koongarra uranium deposit, showing locations of drill-core samples listed in Table I

Table I. Measured iodine-129 contents of uranium ores (Ref. 13)

Sample	Zone of U leaching (L) or deposition (D) (a)	$^{129}I/I$ ratio 10^{-15} (± 1 σ)	^{129}I content 10^5 atoms/g (± 1 σ)	Atomic ratio $^{129}I/U \times 10^{-13}$ Meas.	Predicted (b)
Ranger 3 drill-core samples					
2	D - oxidized ore	59 ± 33	3.9 ± 2.2	130	5.8
8	L - unsaturated zone	62 ± 76	4.0 ± 4.9	6.5	6.3
9	D - oxidized ore	88 ± 30	5.7 ± 2.0	130	5.8
Koongarra drill-core samples					
3	D - dispersion fan	73 ± 32	1.9 ± 0.8	3.0	6.3
4	D - dispersion fan	22 ± 45	0.6 ± 1.2	27	5.8
5	L - weathered ore	912 ± 65	58.5 ± 4.2	2.1	27
6	L - weathered ore	107 ± 29	2.8 ± 0.8	1.6	7.1
7	L - weathered ore	782 ± 312	51.2 ± 20.4	1.7	29

(a) Based on location of sample relative to U transport models described for these deposits in Ref. 1 and 3.
(b) Equilibrium atomic ratio calculated using equation (2) in text.

Two other studies have touched on the question of retention of ^{129}I by uranium minerals. In the Oklo uranium deposit of Gabon, less than 1% of fission-product Xe was retained by the ore, and both Xe and I are believed to have migrated out of the deposit during the time that the reaction zones were active (15). In contrast, significant retention of ^{129}I for some uranium minerals is suggested by the high ^{129}I contents measured for 19 ore samples from various localities (7). Atomic ratios $^{129}I/U$ are reported for six of these minerals and range from 1.3×10^{-12} to 5.9×10^{-11}, far above the value for spontaneous-fission production alone. Unfortunately, degree of ^{129}I retention cannot be calculated from these data because mineral ages and geochemical environments, which are necessary for estimating equilibrium quantities of ^{129}I, are not known.

5.2 Results for samples from dispersion fans

Down-gradient of Koongarra and in oxic zones of dispersed U at Ranger, preliminary results suggest enrichment of ^{129}I relative to U (Table I). The residence time of U in these zones is too short for ^{129}I production to be significant (14). Such relative enrichment is thus attributed to sorption of ^{129}I onto reactive mineral surfaces at a rate that is comparable to that for U sorption or deposition.

Surface FeOH groups are the most likely sites for I^- sorption. Hematite, goethite, and ferrihydrite (amorphous Fe oxide) are major constituents of clay-sized fractions in the upper 30 or more meters (3). The efficiency with which these minerals scavenge I^- from solution depends upon particle size, degree of crystallization and ground-water pH and is greatest for finely-divided, freshly-precipitated Fe oxides at low pH (8,16,24, 25). Kaolinite and montmorillonite, which are also present, sorb only minimal quantities of I^- in fresh water with pH > 5 (4,5,8). Local groundwater pH is in the range 6-8 (3).

6.0 Measurements and interpretation of ^{129}I contents of ground water

6.1 Results

Results of ^{129}I analyses for ground waters are reported in Table II, in which boreholes are arranged approximately in the direction of the hydraulic gradients for Koongarra and Nabarlek. Although all ground-water samples collected for this study have $^{129}I/I$ ratios considerably higher than that estimated for atmospheric background (1×10^{-12}, Ref.11), a systematic pattern is still apparent. Among the 1983 sample suite, ground waters collected upgradient of ore deposits have the lowest ratios, ranging from $2\text{-}7 \times 10^{-12}$. Ratios for samples collected from boreholes intersecting primary ore zones have the highest ratios, ranging from $19\text{-}645 \times 10^{-12}$. Those collected down-gradient of deposits are variably lower but still well above background and range from $13\text{-}45 \times 10^{-12}$. The three Koongarra wells resampled for ^{129}I in 1985 have higher ratios than the 1983 suite of samples. However, in both years, $^{129}I/I$ ratios and ^{129}I concentrations are highest in ground water extracted from the primary ore zone and decrease down-gradient.

Results of ^{36}Cl analyses for ground waters are also reported in Table II. Ratios range from $<85 \times 10^{-15}$ to a high of $11{,}340 \times 10^{-15}$ at PH 94 (Koongarra). Unlike the case of ^{129}I, no trend is apparent between Cl isotope ratios and sample location relative to U deposits.

Table II. Iodine-129 and chlorine-36 concentrations in ground water, 1983-1985

Borehole ID and location (a)		Year	$^{129}I/I$ (10^{-12}) (b)	^{129}I 10^5 atoms/liter Concentration (c)	$^{36}Cl/Cl$ (10^{-15})	^{3}H (T.U.) (d)	^{14}C (pmC) (d)
Koongarra							
KD-1	up	1983	6.4 ± 1.4	0.24 ± 0.05	148 ± 20	1.0	64
		1985	84 ± 8	3.2 ± 0.3	(e) 267 ± 16		
					(f) 76 ± 9		
PH 49	in	1983	645 ± 106	92 ± 15	152 ± 22	0.9	51
		1985	911 ± 134	130 ± 19	(e) 169 ± 13		
					(f) 184 ± 29		
PH 55	down	1983	45 ± 5	4.3 ± 0.5	153 ± 17	0.9	92
		1985	106 ± 9	10 ± 0.9	(f) 196 ± 18		
PH 139	down	1985	68 ± 8	6.5 ± 0.8	(f) 392 ± 36	---	---
PH 94	down	1983	---	---	1723 ± 187	4.7	101
		1984	---	---	11340 ± 910		
Nabarlek							
RN20472	up	1983	7.1 ± 1.5	15 ± 3	---	---	---
OB 20	up	1983	5.2 ± 0.6	5.4 ± 0.6	82 ± 12	2.7	96
RN21038	up	1984	---	---	155 ± 15	---	---
OB 25	down	1983	23 ± 4	78 ± 13	495 ± 51	0.8	85
RN20473	down	1983	13 ± 4	24 ± 7	67 ± 15	1.2	138
RN20476	down	1983	---	---	185 ± 18	---	---
TB 36	down	1983	---	---	104 ± 18	1.8	87
Ranger							
RN20099	up	1983	1.6 ± 0.5	0.3 ± 0.1	140 ± 15	0.8	---
9722	up	1983	---	---	125 ± 16	0.6	56
79/6A	in	1983	83 ± 22	20 ± 5	228 ± 23	1.0	---
Jabiluka-2							
148	in	1983	19 ± 2	6.3 ± 0.7	61 ± 29	---	---

(a) in = well intersecting primary ore deposit
up = well upgradient of deposit or otherwise outside its influence
down = downgradient of deposit and possibly influenced by it

(b) Results reported ± one standard deviation. 1983 measurements have been revised from those reported in Ref. 11 on the basis of a review of the raw data and remeasurement of some of the samples.

(c) Iodine concentrations for 1985 samples assumed to be the same as those measured in 1983.

(d) Source of tritium and ^{14}C data: Ref. (3). Samples were collected in 1983 and earlier.

(e) Cl sample collected at beginning of pumping for ^{129}I sample

(f) Cl sample collected at end of pumping for ^{129}I sample

6.2 Origin of ^{129}I in ground water

Ratios above the background $^{129}I/I$ ratio of 1×10^{-12} could arise from three sources: technological ^{129}I carried in with rain water, leaching of ^{129}I from geologic formations, and leaching from U ore deposits.

Even far removed from the influence of U deposits, subsurface production could be a significant source for ^{129}I in local ground water. Background U concentrations in the rocks are generally above average. Kombolgie sandstone, the formation immediately up-gradient of the Koongarra deposit, contains about 7 ppm U. This corresponds to an equilibrium ^{129}I content of 8300 atoms/g with an isotope ratio $^{129}I/I$ of 20×10^{-12} (assuming 0.2 ppm I as an average value for sandstone). Thus, leaching from the local aquifers probably is responsible for ^{129}I concentrations above background in ground water up-gradient of the deposits. However, it is not sufficient to account for the high ^{129}I levels in ground water from the deposits or down-gradient of them.

Atmospheric $^{129}I/I$ ratios in the post-1950 era are on the order of 10^{-12} to 10^{-9} due to testing of thermonuclear devices and operation of fuel-reprocessing plants. The possibility that elevated ^{129}I concentrations and $^{129}I/I$ ratios in ground water are due to technological ^{129}I must be considered. One way to distinguish between these two sources is to look for the presence of other man-made nuclides, especially mobile species such as tritium, ^{14}C, and ^{36}Cl. Concentrations of these species that are considerably above atmospheric background are more likely due to man's activities than to natural mechanisms.

However, this criterion must be applied with caution. A strong correlation among anthropogenic concentrations of these nuclides in the atmosphere or in ground water is not expected because isotope production, release, and degree of dilution by stable counterparts vary with source and location. In addition, relative radionuclide concentrations in ground water will vary from those in the atmosphere according to rates of wash-out from the atmosphere and retention in the ground. Finally, one must consider that all of these radioisotopes are also produced in the lithosphere to some extent (6). This proviso is particularly relevant in the case of ^{36}Cl in the vicinity of U ore deposits, in which high neutron fluxes lead to $^{36}Cl/Cl$ ratios of the order 10^{-12} to 10^{-10} (14). Obviously, very little Cl would need to be leached from ore by ground water in order to obtain a considerable increase in isotope ratio above background, which is $<1 \times 10^{-13}$ for this area.

With these thoughts in mind, we examined ^{36}Cl, ^{14}C, and tritium contents of the local ground waters (Table II). Bomb-pulse ^{36}Cl is clearly present in Koongarra borehole PH 94, which also contains elevated levels of tritium and ^{14}C, and is probably present in PH 139 as well. Of the other wells at Koongarra, the variability of $^{36}Cl/Cl$ ratios in KD-1 is suggestive of a small component of bomb-pulse water although to a much less extent than PH 94. Consequently, ^{129}I levels for KD-1 and PH 139 in 1985 should be viewed with suspicion; they may not be due entirely to natural sources. However, ^{129}I in PH 49 and PH 55 must be derived from the U deposit.

At the other ore deposits, a small component of bomb-pulse water may be present in Ranger 79/6A and in OB-20, TB-36, and RN 20473 at Nabarlek. However, the amount is probably insufficient to explain the high $^{129}I/I$

ratios and ^{129}I concentrations, which we therefore attribute to natural sources.

6.3 Evidence for transfer of ^{129}I to and from ground water

Results for water samples indicate strong partitioning of ^{129}I into ground water during weathering of primary ore, which is consistent with the depleted $^{129}I/U$ ratios of ore samples from this zone. Atomic ratios $^{129}I/U$ in Koongarra ground waters range from 2×10^{-11} to 9×10^{-10} and are thus enriched by 1-3 orders of magnitude relative to the average equilibrium ratio for the source minerals, 1.3×10^{-12}, assuming an average U content of 4000 ppm (20).

Down-gradient of the primary ore deposits, ^{129}I concentrations decrease due to dilution and to removal from solution by sorption. At Koongarra, average ^{129}I concentrations decrease from 1×10^{7} atoms l^{-1} in PH 49 to 7×10^{5} atoms l^{-1} in PH 55 about 80 m down-gradient. Based on conductivity and $^{36}Cl/Cl$ measurements for the water, the effect of dilution is negligible; essentially all of the decrease can be attributed to ^{129}I sorption. This trend is consistent with significant ^{129}I sorption onto mineral surfaces indicated by ^{129}I analyses for drill-core samples from zones of U deposition at Koongarra and Ranger (Section 5.2).

An apparent sorption ratio of 300 ml g^{-1} can be estimated based on the average ^{129}I concentration for PH 55 (7×10^{2} atoms ml^{-1}) and ore sample 3 (2×10^{5} atoms g^{-1}). This ratio corresponds to a retardation factor of 1/1500 to 1/4000 for the velocity of ^{129}I relative to water (assuming bulk density of 2.5 g cm^{-3} and porosity between 0.2 and 0.5 (3)). The sorption ratio is considerably higher than ratios reported for ferric hydroxide and limonite at pH 6-8 in laboratory studies (10-20 ml g^{-1} (4,5)). Thus, at the field site, irreversible coprecipitation or occlusion of I^{-} in the mineral lattice (5,23) may also be occurring. The latter mechanism would be enhanced by the Koongarra ground-water chemistry which is supersaturated with respect to Fe oxides.

At Koongarra, ^{129}I buildup in water in the weathered orebody and subsequent decrease down-gradient is quite striking. The trend at the other deposits is not nearly so dramatic. One would expect ^{129}I concentrations in water from the Nabarlek orebody to be even higher than that at Koongarra because a large part of this deposit was also within the zone of weathering, leading to the formation of a dispersion fan (21). In addition, the ore at Nabarlek has a considerably richer U content than Koongarra ore (average 2.5% U, compared to 0.4% at Koongarra, Ref. 20). However, the Nabarlek deposit has been completely mined out, and the closest borehole (OB 25) to the original ore-body is 300 m down-gradient. Any ^{129}I leached from the ore-body would probably be considerably diluted or removed from solution by sorption by this point. The Jabiluka 2 and Ranger 3 ore deposits are mostly below the zone of weathering and may have retained most of their ^{129}I contents.

Acknowledgements. We are indebted to A. Snelling, P. Duerden, and T. Nightingale for assistance in collecting field samples and for helpful discussions. Advice and encouragement from S.N. Davis have been particularly appreciated. R. Teng, T. Hemmick, and N. Conard assisted with isotopic measurements. This research is being funded by the U.S. Nuclear Regulatory Commission and the Australian Atomic Energy Commission.

REFERENCES

1. AIREY, P.L. (1986). Radionuclide migration around uranium ore bodies in the Alligator Rivers region of the Northern Territory of Australia - analogue of radioactive waste repositories - a review. Chem. Geol., 55:255-268.
2. AIREY, P.L. and IVANOVICH, M. (1986). Geochemical analogues of high-level radioactive waste repositories. Chem. Geol., 55: 203-213.
3. AIREY, P.L. et al. (1982-1986, yearly reports). Radionuclide migration around uranium ore bodies - analogue of radioactive waste repositories. (U.S. Nuclear Regulatory Commission Contract NRC-04-81-172), Annual Reports 1981-82, 1982-83, 1983-84, 1984-85.
4. ALLARD, B. et al. (1980). Possible retention of iodine in the ground. Proc., Intl. Symp. on the Sci. Basis for Nucl. Waste Mgmt., 2:673-680.
5. ANDERSSON, K., TORSTENFELT, B. and ALLARD, B. (1983). Sorption of radionuclides in geologic systems. Report 1983, SKBF-KBS TR 83-63.
6. ANDREWS, J.N. et al. (1987). The in-situ production of radioisotopes in rock matrices with particular reference to the Stripa granite. Submitted to Geochim. Cosmochim. Acta.
7. BRAUER, F.P. and STREBIN, R.S., Jr. (1982). Environmental concentration and migration of ^{129}I. Environmental Migration of Long-Lived Radionuclides. IAEA, Vienna, pp. 465-475. IAEA-SM-257/43.
8. COUTURE, R.A. and SEITZ, M.G. (1984). Sorption of anions of iodine by iron oxides and kaolinite. Nucl. and Chem. Waste Management, 4:301-306.
9. ELMORE, D. et al. (1979). Analysis of ^{36}Cl in environmental water samples using an electrostatic accelerator. Nature, 277:22, Errata 246.
10. ELMORE, D. et al. (1980). Determination of ^{129}I using tandem accelerator mass spectrometry. Nature, 286:138-139.
11. FABRYKA-MARTIN, J., DAVIS, S.N. and ELMORE, D. (1987). Applications of ^{129}I and ^{36}Cl in hydrology. Submitted to Nucl. Instr. Meth. Phys. Res. B.
12. FABRYKA-MARTIN, J. et al. (1985). Detection of natural fission products in ground water. ANS Trans., 92:190-191.
13. FABRYKA-MARTIN, J. et al. (1985). Natural iodine-129 as an environmental tracer. Geochim. Cosmochim. Acta, 49:337-347.
14. FABRYKA-MARTIN, J. et al. (1987). Iodine-129 and chlorine-36 in uranium ores, 2. Discussion of AMS measurements. Submitted to Isot. Geos.
15. FREJACQUES, C. and HAGEMANN, R. (1976). Conclusions from studies of the Oklo Natural Reactors. Proc., Intl. Symp. on the Mgmt. of Wastes from the LWR Fuel Cycle, Denver CO, 11-16 July 1976. CONF-760701, pp 678-685.
16. FUGE, R. (1974). Iodine, Ch. 53 in: Handbook of Geochemistry, Vol. II, Pt. 4 (K.H. Wedephol, ed.), Springer-Verlag, New York.
17. HAAKER, R.F. and EWING, R.C. (1980). Uranium and thorium minerals: natural analogues for radioactive waste forms. Proc., Intl. Symp. on the Sci. Basis for Nucl. Waste Mgmt., 2:281-288.
18. KNIGHT, C.L. (ed.) (1975). Economic Geology of Australia and Papua New Guinea 1. Metals. Australasian Institute of Mining and Metallurgy, Monograph Series No. 5, Victoria, Australia.
19. ROMAN, D. and FABRYKA-MARTIN, J. (1987). Iodine-129 and chlorine-36 in uranium ores, 1. Preparation of samples for analysis by AMS. Submitted to Isot. Geos..
20. RYAN, G.R. (1977). Uranium in Australia, pp. 24-42 in: M.J. Jones (ed.), Geology, Mining and Extractive Processing of Uranium. Inst. of Mining and Metallurgy, London.
21. SHIRVINGTON, P.J. (1980). $^{234}U/^{238}U$ ratios in clay as a function of

distance from primary ore. Proc. Intl. Uranium Symp. on the Pine Creek Geosyncline 1980. IAEA, Vienna, pp. 509-520.
22. SNELLING, A.A. (1980). Uraninite and its alteration products, Koongarra uranium deposit. Proc. Intl. Uranium Symp. on the Pine Creek Geosyncline 1980. IAEA, Vienna, pp. 487-498.
23. STRICKERT, R., FRIEDMAN, A.M. and FRIED, S. (1980). The sorption of technetium and iodine radioisotopes by various minerals. Nucl. Tech., 49:253-266.
24. WHITEHEAD, D.C. (1974). The sorption of iodide by soil components. J. Sci. Fd. Agric., 25:73-79.
25. WILDUNG, R.E. et al. (1974). Pertechnetate, iodide and methyl iodide retention by surface soils. BNWL-1950 Pt. 2, 37-40.

MECHANISMS AND QUANTITATIVE EVALUATIONS OF RADIONUCLIDE FIXATION IN GEOSPHERE

S. NAKASHIMA and H. NAKAMURA
Department of Environmental Safety Research
Japan Atomic Energy Research Institute
Tokai, Ibaraki, 319-11 Japan

Summary

Among many mechanisms involved in radionuclide migration-fixation in geosphere, several mechanisms concerning fixation of dissolved metal ions in aqueous media into rocks and sediments have been elucidated. Fixation of groundwater elements in crystalline phases has been studied on the red altered granitic rocks along fractures. Electron microscopic techniques are useful in characterizing the microphases which are possible sites for radionuclide fixation. Infrared microspectroscopy can be a good tool for analyzing spatial distributions of water in altered rocks which should be related to the alteration front. Fixation of radionuclides by reducing agents in geomedia has been studied experimentally in order to determine kinetic and thermodynamic parameters of these reactions. The determination of reaction rates is very important for the long-term quantitative evaluation of these processes, especially for slow reactions. All these studies have pointed out some geochemical approaches useful to evaluate long-term radionuclide fixation in geomedia.

1. Introduction

Application of natural phenomena to the safety evaluation of radioactive waste disposal has many approaches covering various disciplines. Among many aspects of this "natural analogue" study, a) elucidation of mechanisms of trace element migration-fixation processes in geosphere which might also work for waste radionuclides, and b) evaluation of their quantitative aspects in a geological time scale, are of primary importance.

Study of microphases in minerals and rocks, which are supposed to play an important role in radionuclide migration-fixation, is now in progress. The characterization of microphases in minerals such as microinclusions, crystal defects, crystal boundaries and metamict minerals by means of microanalytical devices will provide useful informations on possible sites for radionuclide fixation and on the long-term stability of fixed radionuclides in these sites. An example of this approach is presented below.

Fixation of trace elements by natural organic matter such as

coaly substances, porphyrins and some bacteria are also important processes in evaluating the radionuclide immobilization in geosphere. This type of study will be first concentrated on the characterization of natural organic matter which are effective to reduce polyvalent ionic species of actinides and technetium and then on the long-term quantitative evaluation of this phenomena by means of kinetic parameters of responsible reactions. An example of an active micro-reducing-environment in sediments causing a rapid fixation of technetium is also presented here.

2. Fixation of groundwater elements in crystalline phases

2.1 Red coloration of feldspars along fracture

Occurence of red feldspars are common in alteration zones of feldspar-bearing rocks, especially granitic rocks. This phenomenon can be considered to be a clear evidence of groundwater-rock interaction. The origin of red color of these altered feldspars has been considered to be the presence of iron, but its chemical form in feldspars has not yet been well established. Iron can be present in the crystal structure, as iron-bearing microcrystals such as hematite (1) or as iron staining on the grain boundaries and cleavage planes (2).

2.2 Microphase characterization in minerals

Scanning electron microscopy equipped with energy dispersive X-ray analyzer (SEM-EDX) was applied to characterize the microphases in a red feldspar from altered granitic rock from Northwest Kyushu, Japan. Red feldspars are observed only in alteration zones along fractures (Fig.1). Among feldspars of this altered zones, white feldspars are also recognized together with red feldspars.

SEM-EDX analyses of these altered feldspars having both whitish and reddish parts indicate that potassium rich parts correspond to the whitish parts. The reddish parts appear to correspond to the Na-Ca rich parts (Plagioclase molecule: $NaAlSi_3O_8$-$CaAl_2Si_2O_8$). Iron is found to be present in a part of these Na-Ca rich parts in the order of 20 μm, while no iron was detected by this SEM-EDX technique in plagioclase feldspars from less altered zone. Quantitative analyses of these Fe rich phases in red altered feldspars reveal that they are epidote group minerals [$Ca_2(Al,Fe^{3+})_3Si_3O_{12}(OH)$], which contains generally Fe^{3+} replacing Al^{3+} of the crystal structure. But these minerals have greenish , yellowish or greyish colors and do not show pink or red colors except for the presence of Mn^{2+} in Ca site, which is not the case here. We should then look for submicron iron containing microphases in order to elucidate the origin of the red color of these altered feldspars.

Transmission electron microscopy equipped with energy dispersive X-ray analyzer (TEM-EDX) was used to search for submicron phases in red altered feldspars. This technique reveals the presence of iron minerals in the order of 0.5 μm. We are now trying to characterize these microcrystals by means of electron diffraction technique in order to know if they are iron oxides such as hematite (Fe_2O_3) or iron hydroxides such as goetite ($FeO{\cdot}OH$).

A tentative explanation of the red color in the altered feldspars studied here is the presence of iron containing submicron microphases such as hematite in plagioclase feldspars. These irons, which can be

supplied by groundwaters during alteration of iron bearing minerals (for instance, hornblende in this study), might be precipitated as iron oxides or hydroxides into favorable sites in minerals. Similar phenomena can be supposed for some dissolved radionuclides in groundwater.

Trace element fixation in the form of microinclusions in minerals can be the main mechanism of water-rock interaction in the present case. On the other hand, it should be noted also that calcium sites in rocks can be one of the possible sites for the fixation of dissolved metal cations, having higher valence states and larger ionic radii. In fact, rare-earths, U and Th are commonly found to be present in Ca-containing natural minerals such as allanite. The close exchange relationship between Ca and U in the course of water-rock interaction has been already noticed (3). The calcium sites in minerals, together with microinclusions, grain boundaries and crystal defects, are then considered to play an important role in the radionuclide immobilization.

These results suggest applications of microphase characterization techniques to the study of trace element migration and fixation in rocks, as a natural analogue to the radioactive waste disposal.

2.3 Water in altered minerals

A first trial of the application of infrared microspectroscopy to the characterization of minerals is in progress (4). The infrared spectra of 20x20 μm area of the above mentioned feldspars were measured. Red altered feldspars appear to have higher content of molecular water (peak around 3630 cm^{-1}) than less altered white feldspars. This result shows an evidence of hydrolysis of feldspars along groundwater paths. Analyses of spatial distribution of water (OH and H_2O) by means of infrared microspectroscopy can be then useful in evaluating spatial distribution of influence of groundwater which is related to alteration front.

2.4 Alteration front in rocks

The studied red coloration of feldspars in granitic rocks are limited to only a few centimeters width from the fracture (Fig.1). This width of red colored zone can be considered to be an example of spatial limit of groundwater-rock interaction : alteration front.

A numerical model for the evaluation of this alteration front was applied recently by FUJIMOTO (1987) to explain spatial distributions of natural alteration zones of rocks (5). The author employed the term $\rho V/Ak$ as an indicator of the alteration width, based on the following one dimentional mass balance equation in the case where the diffusion of an element in water is negligible compared with the water velocity:

$$\frac{\partial C_i}{\partial t} = - V \frac{\partial C_i}{\partial x} + \frac{Ak}{\rho} (C_{ieq} - C_i) \qquad (1)$$

C_i, C_{ieq}: concentration of species i in water and that in equilibrium state.
ρ, V : density of water and water penetration velocity
A : contact area of rock and water
k : rate constant of a first-order reaction such as dissolution and precipitation
t : time
x : distance from the starting point of rock column.

This approach can be used in evaluating quantitatively the spatial limit of water-rock interaction, by taking the mass flux direction perpendicular to the fracture in our case of the red altered granitic rock.

3. Fixation of U by natural organic matter

Mechanisms and quantitative aspects of uranium fixation by natural organic matter were studied experimentally by using two lignite samples having different degrees of diagenetic evolution (6,7,8). Lignite is known to be associated with important uranium deposits (9).

3.1 Fixation mechanisms

When the aqueous uranyl solution is heated with lignite samples at 20°- 200°C, the first phenomenon observed is fixation of uranyl ions on the organic matter (Fig.2). The high rank lignite (Gardanne) fixed uranyl ions in the form of stable organo-uranyl compounds, while the low rank lignite (Arjuzanx) fixed them by a simple ion exchange to form uranyl-carboxyl compounds. The quantity of fixed uranyl is around 0.5 mmol/g lignite.

3.2 Reduction mechanisms

At higher temperatures (120°- 200°C) of the experiment, reduction of uranyl ions into uraninite (UO_2) was observed for both lignite samples. The dehydrogenation of lignite was responsible for the reduction of uranyl ions:

$$RH_2 + UO_2^{2+} \longrightarrow R + UO_2 + 2\ H^+ \qquad (2)$$

RH_2 represents an organic geopolymer containing oxygenated functional groups and hydrocarbonaceous moieties, and R its dehydrogenated form. In the case of the high rank lignite, the detailed study of the reaction by means of infrared spectroscopy indicates that the organic functional groups responsible for the uranyl reduction are hydroxyl groups and aliphatic hydrocarbons. This study shows the way of elucidating types of active natural organic geopolymers for redox sensitive radionuclides.

3.3 Reduction kinetics

The further experiments were conducted in order to determine kinetic parameters of the reduction reaction (2)(Fig.3). The partial orders of the reaction were determined to be 1 for uranyl ion and 1 for organic matter:

$$d[UO_2^{2+}]/dt = - k\ [UO_2^{2+}][RH_2] \qquad (3)$$

$[RH_2]$ denotes the weight of organic matter in a unit volume of water (g/l for instance). The activation energy of the reaction (E) can be expressed by using the apparent rate constant $k_{app} = k[RH_2]$ and the apparent Arrhenius factor $A_{app} = A[RH_2]$, for the case of constant $[RH_2]$, as follows (R: gas constant, T: absolute temperature):

$$k_{app} = A[RH_2]\exp(-E/RT) = A_{app}\exp(-E/RT) \qquad (4)$$

The equations (3) and (4) give the following equation (5) :

$$\ln [UO_2^{2+}] = \ln[UO_2^{2+}]_o - A_{app}\ t \exp(-E/RT) \qquad (5)$$

Uranyl content of a groundwater having an initial uranyl content of $[UO_2^{2+}]_o$ after a time t of contact with lignite at a temperature T can be then calculated by this equation.

3.4 Long-term evaluation

The rate constants and activation energies of the uranyl reduction process were determined at 180°- 200°C (Fig.4: E = 28 ± 2 kcal/mol and $A_{app} = 5.3 \times 10^8\ s^{-1}$ for the system lignite 200 mg - 0.1 M UO_2Cl_2 10 ml; $[RH_2]$ = 20 g/l). The reaction is fast at these diagenetic or hydrothermal conditions.

Supposing that the same rate limiting process of the reaction (precipitation of uraninite) is expected for lower temperatures and the kinetic parameters determined above can be used for lower temperatures, we can calculate the time necessary to precipitate uranium from groundwater at lower temperatures. An example of the calculation for 40°C, which can represent the temperature condition of radwaste disposal, is presented here.

Let us consider the groudwater containing 10 ppb of uranyl ions which is in contact with the organic material with the weight ratio of 1:10 ($[RH_2]= 10^4$g/l). By using $A_{app}= 500 \times 5.3 \times 10^8\ s^{-1}$, the time necessary to precipitate 90 % of dissolved uranyl can be calculated as 0.36, 9 and 220 years respectively for activation energy (E) values of 26, 28 and 30 kcal/mol. These time scales are of great importance for the estimation of reaction kinetics in the safety assessment of high-level waste disposal. It should be noted that the accuracy of the values of the activation energy is essential for evaluating the long-term behaviour of this process. The same accuracy is needed for the temperature condition of the reaction. Theoretically speaking, doubling the amount of organic matter should divide by two the time necessary to obtain the same reduction yield. The water-organic matter ratio is also important in this consideration.

3.5 Model with water flow

The evaluation above discussed is based on the static condition of water-organic matter contact. In this case, the amount of uraninite precipitation is limited by the uranyl content of the groundwater. By this static process, it is not possible to form uranium deposits having high uranium contents (only 1 ppb U in the present case). We should then consider the water renewal in order to precipitate more uranium.

If the groundwater is renewed ideally after 90 % of precipitation yield, we need 10^6 times longer time than the static condition to form uranium deposits having 0.1 % U (ex., 9 million years for E=28 kcal/mol).

Now, supposing that the groundwater is flowing with a rate of 10^{-3} cm/s through 1 m^3 of organic matter mass, groundwater should be renewed every 28 hours. This renewal time is too fast to precipitate further uraninite comparing with the reaction time calculated above (ex.,9 years for E=28 kcal/mol). Consequently, the uranium deposit formation should need no shorter period than the ideal renewal case. The groundwater flow is effective for the faster accumulation of

uraninite, only if the water renewal time is shorter than, but remaining about the same order of, the reaction time (relatively high flow rate at higher temperature conditions, in the present case).

These calculations indicate that the formation of uranium deposits at low temperatures needs considerable time even in geological time scale (ex., 9 million years at 40°C) and so that higher temperature conditions are favorable for the uranium deposits associated with organic matter. In fact, the temperature conditions of some of these types of important uranium deposits were estimated to be around 100°- 200°C (9,10,11).

3.6 Equilibrium consideration

The equilibrium points of the uranyl aqueous solution - lignite system were observed at 180°- 200°C (Fig.3). The equilibrium constants $k_{eq} = [H^+]^2/[UO_2^{2+}]$ were determined experimentally and we can use the following equation to estimate equilibrium uranyl contents of groundwater in contact with lignite at various pH values:

$$\log[UO_2^{2+}] = - \log k_{eq} - 2\ pH \qquad (6)$$

Based on this equation, we can expect the precipitation of uraninite to reach equilibrium at these temperatures in natural aqueous media containing uranyl ions in the order of 10 ppb, for the pH values greater than 4.

This equilibrium consideration is useful for the fast reaction in a geological time scale. On the other hand, very slow reactions such as uraninite precipitation at low temperatures should be studied in detail to determine accurate kinetic parameters which permits long-term evaluations.

4. Fixation of Tc in sediments

An example of a real micro-reducing-environment in geomedia was revealed by a redox-sensitive tracer diffusion experiment. Quantitative aspects of technetium fixation are also discussed below.

4.1 Diffusion of Tc in sediments (12)

Several series of measurements, at room temperature, of diffusion coefficients of pertechnetate anion were made on selected samples of deep-sea sediments from North-east Atlantic ocean and on Na-bentonite samples, in order to evaluate diffusivity of "non-sorbing" ions in sediments.

Linear correlations on a logarithmic scale between the apparent diffusion coefficeints and the porosities of the sediments were observed on both of the two materials. The diffusion coefficients of "non-sorbing" ions can be thus estimated by the porosities of sediments.

4.2 Fixation of Tc in sediments (13)

A very small value of the apparent diffusion coefficient was obtained on a deep-sea sediment sample containing black parts rich in pyrite (Fig.5). Technetium appeared to be fixed by these black parts which are local accumulations of pyrite replacing diatoms in a diatom-pigment rich part of calcareous sediments. These black materials are considered to be indicators of a "micro-reducing-environment" in deep-sea sediments, which might be in close relation with bacterial

activities. This microenvironment can be supposed to have a reducing capacity, which is still active even under oxic condition of the experiments, and cause the fixation of technetium possibly in the form of oxides or hydroxides of lower oxidation states. This study proves the real efficiency of radionuclide fixation-retardation processes in sediments, which are fast enough to occur during the diffusion process.

4.3 Tc fixation experiments

The fixation rates of technetium by various reducing agents, such as ferrous iron containing minerals and some natural carbonaceous materials, have been determined experimentally. An example of the results on the fixation of technetium by magnetite is presented here. By means of the change, as a function of time, of pertechnetate content of aqueous solution in contact with magnetite, the first order rate constant was determined to be 3.8×10^{-6} s^{-1} at room temperature. This reaction reaches an equilibrium in about 30 hours. This technetium fixation process is thus fast enough to occur in the course of diffusion process in sediments.

The equilibrium point of the system gives the equilibrium constant $k_{eq} = 1/[TcO_4^-]^2[H^+]^2 = 5.5 \times 10^{31}$ and the standard free energy of the reaction $\Delta G_r^\circ = -43 \pm 2$ kcal, assuming the following reaction:

$$2\ TcO_4^- + 6\ Fe_3O_4 + 2\ H^+ = 2\ TcO_2 + 9\ Fe_2O_3 + H_2O \qquad (7)$$

These equilibrium parameters provide direct quantitative bases for the fixation of radionuclides in geomedia, if the reaction kinetics can be neglected in the quantitative evaluations.

REFERENCES

1. DEER W.A., HOWIE R.A. and ZUSSMAN J.(1966). An introduction to the rock forming minerals. Longman, London.
2. ISSHIKI N.(1958). Notes on rock-forming minerals(3) Red coloration of anorthite from Hachijo-jima. J.Geol.Soc.Japan, 64, 644-647.
3. NAKASHIMA S.(1987). Infrared microspectroscopy of minerals: a new microphase characterization technique in earth sciences. JEOL News, 27,1. (in Japanese)(in press)
4. NAKASHIMA S. and IIYAMA J.T.(1983). Behavior of uranium during the formation of granitic magma by anatexis (II). Influence of major element cations on the mobility of uranium. C.R.Acad.Sci.Paris, t.296, serie II, p.1425-28. (in French)
5. FUJIMOTO K. (1987). Factors to controll the width of a partially altered zone. Mining Geology, 37. (in Japanese)(in press)
6. NAKASHIMA S., DISNAR J-R., PERRUCHOT A. and TRICHET J. (1984). Experimental study of mechanisms of fixation and reduction of uranium by sedimentary organic matter under diagenetic or hydrothermal conditions. Geochim.Cosmochim.Acta, 48, 2321-29.
7. NAKASHIMA S., DISNAR J-R., PERRUCHOT A. and TRICHET J. (1987). Fixation et réduction de l'uranium par les matières organiques naturelles: mécanismes et aspects cinétiques. Bull.Mineral.Spec.Issue (in press)

8. NAKASHIMA S., DISNAR J-R., PERRUCHOT A. (1987). Kinetic study of uranium reduction by sedimentary organic matter underdiagenetic or hydrothermal conditions. submitted to Geochim.Cosmochim.Acta
9. BREGER I.A.(1974). The role of organic matter in the accumulation of uranium. The organic geochemistry of the coal-uranium association. Formation of Uranium Deposits. Proc.Sym.IAEA,Athens, 6-10 May 1974, IAEA-SM-183/29, p.99-124.
10. PAGEL M.(1975).Détermination des conditions physicochimiques de la silicification diagénétique des grès Athabasca (Canada) au moyen des inclusions fluides. C.R.Acad.Sci.Paris,t.280,Serie D,2301-04.
11. BROOKINS D.G.(1980). Syngenetic model for early proterozoic uranium deposits: evidence from Oklo. Uranium in the Pine Creek Geosyncline, Proc.Sym.IAEA,Vienna,1980,p.709-719.
12. NAKASHIMA S., KITA H., SHIMOOKA K. and NAKAMURA H. (1987). Diffusion of technetium in deep-sea sediments and bentonite. ESOPE Final Report, JRC Report Series, CEC (to be published).
13. NAKASHIMA S., KITA H. and MITAMURA H. (1987). Technetium fixation in deep-sea sediments - a possible micro-reducing-environment -. ESOPE Final Report, JRC Report Series, CEC (to be published).

Fig.1 Schematic drawing of a red altered granitic rock sample from Northwest Kyushu, Japan.
F : fracture filled with prehnite: $Ca_2(Al,Fe^{3+})_2Si_3O_{10}(OH)_2$
: feldspars with dots representing schematically the density of reddish color
: quartz
: black to greenish black minerals such as hornblende and chlorite.

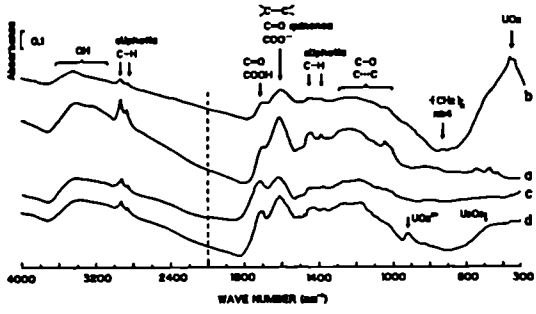

Fig.2 Infrared spectra of two purified lignite samples and their reaction products with uranyl solutions:
a) Gardanne lignite (G): a high rank lignite.
b) Reaction product of the system G 100 mg - 0.1 M UO_2Cl_2 10 ml after 262 hours of heating at 180°C.
c) Arjuzanx lignite (A): a low rank lignite.
d) Reaction product of the system A 100 mg - 0.1 M UO_2Cl_2 10 ml after 4 hours of heating at 180°C.

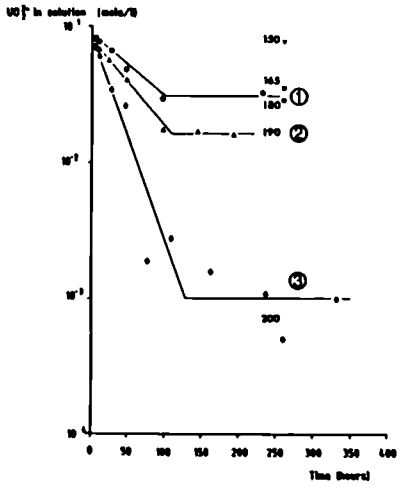

Fig.3 Variation of uranyl contents in aqueous phase as a function of run duration.
●1,▲2,◆3: experiments with 100 mg of Gardanne lignite and 10 ml of 0.1 M UO_2Cl_2 at 180°C(1), 190°C(2) and 200°C(3).
▽,□,○,◇ : Results of the same type of experiments conducted during 262 hours at 150°C(▽), 165°C(□), 180°C(○) and 200°C(◇).

Fig.4 Variation, as a function of temperature, of apparent rate constants k_{app} of reduction and dehydrogenation processes in the system lignite - 0.1 M UO_2Cl_2 (L):
1G: uranyl reduction by Gardanne lignite (G); 200 mg G - 10 ml L.
2G: uranyl reduction by G : 100 mg G - 10 ml L.
3A: uranyl reduction by Arjuzanx lignite (A); 100 mg A - 10 ml L.
4G: dehydrogenation of G in the same system as 2G.
5A: dehydrogenation of A in the same system as 3A.

Fig.4

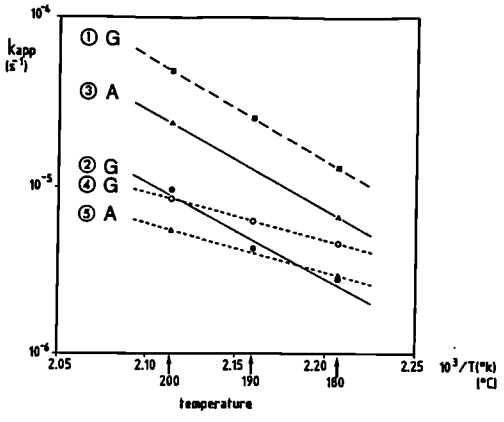

Fig.5

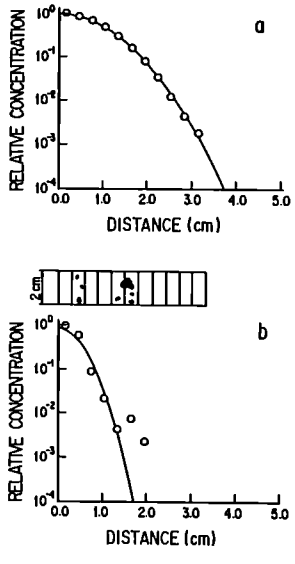

Fig.5 Diffusion profiles of pertechnetate anion in deep-sea sediments.
(a): Calcareous deep-sea sediment sample; Apparent diffusion coefficient $D_{app} = 5.9 \times 10^{-10}$ m^2/s.
(b): Calcareous deep-sea sediment sample with a schematic drawing of the sample containing black spots rich in pyritized diatoms. Retardation of pertechnetate diffusion is observed on this sample; $D_{app} = 1.2 \times 10^{-10}$ m^2/s.

SESSION 5

PANEL :

"HOW FAR ARE WE WITH NATURAL ANALOGUES?"

Chairman	:	F. Girardi	(JRC, Ispra)
Co-Chairman	:	T. Papp	(SKB, Sweden)
Members	:	N.A. Chapman	(BGS, UK)
		I.G. McKinley	(EIR, Switzerland)
		F.P. Sargent	(AECL, Canada)
		I. Neretnieks	(RIT, Sweden)
		D.G. Brookins	(Univ. of New Mexico, USA)

1. Chairman's Opening Statement (F. Girardi)

The theme of this last session is to be "How far are we with natural analogues ?". Obviously, the debates must also cover "What remains to be done in this field, and what are the priorities".

I would like first to give my own point of view about the importance of work on natural analogues. I think it can easily be summarized by drawing a "utility plane of analogues", in which the two axes would represent the increasing "value" of analogues, respectively for engineered barriers and for "far field" (i.e. disposal scenario) analogues. Needless to say, the ideal replica of a whole real repository would lie at the upper right corner of the plane.

My opinion would be that analogues of engineered barriers build up confidence in models, whereas analogues of "disposal scenarios" build up confidence in modellers.

Considering the presentation we had during the Symposium, it would seem to me that the area of "analogues for disposal scenarios" is rather well covered by the on-going programmes, whereas more work should be done on analogues of barriers. In this respect, the example of the bronze cannon corrosion seems to be a very valuable one.

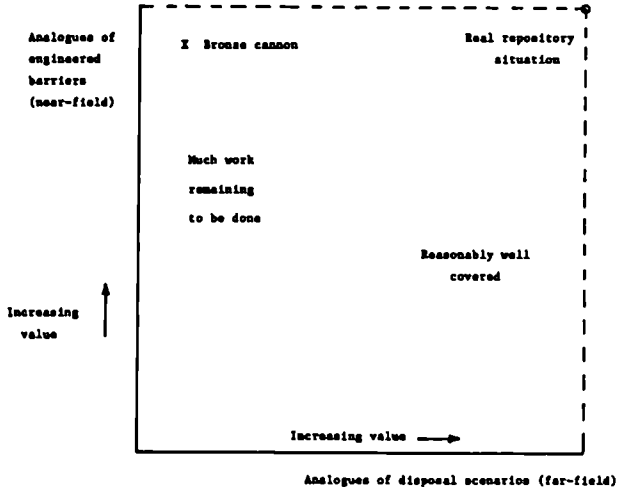

Diagram of the "Utility Plane of Analogues"

2. Panel Members Statements

N.A. Chapman

The basic issue I would like to address here is the quantitative versus the qualitative roles of natural analogues. During these three days, we have seen lots of examples of data on interesting analogue occurrences related to specific processes; but we have had very few examples of fully quantitative data, and even fewer cases where such data have been taken up by safety assessment modellers and used to justify their arguments. This may simply reflect the present paucity of real safety assessment (only two or three exist); we may actually be too early to see natural analogues achieving their full or real potential.

There are some examples where we can use natural analogue data to add to our numerical geochemical databases, but generally even the most quantitative results (e.g. diffusion rates, corrosion rates, solubility limits, etc) are really only making us ask more questions about our understanding of the process involved, or our interpretation of which mechanisms are important.

Now, this is in itself not a bad thing. Indeed, it is a very good thing, because it continually increases our understanding, and thus our confidence in the models we construct, and which go to build up any performance assessment. However, it is largely a qualitative application.

Now in the past, being hard-nosed scientists, we have tended to denigrate qualitative uses. But perhaps this is where the real value of natural analogues lies; as illustrative tools: they allow us, as scientists, to build up understanding and confidence. On the same basis they have a qualitative role in the presentation of the results of performance assessments to the public and regulators. Our models and their numerical predictions are largely inscrutable to most people. Comparison of the processes we predict will occur, to ones which we know to occur, is a digestible and comprehensible means of demonstrating to the public that our own ideas have a sound basis in the real natural world.

Thus, we will continue to receive quantitative "wish-lists" from the performance assessment modellers, and the field people will continue to respond by seeking good analogue data. But don't expect clean, hard, unimpeachable numbers all the time. Analogues, by nature, are "dirty" and often difficult to interpret unambiguously.

So an "alternative" view is that analogues are principally qualitative tools, but we should not worry too much that they are, as this use alone will be invaluable in presenting our safety cases.

I. McKinley

I would tend to go one step beyond this position and argue that natural analogues are probably also, right now, quantitative tools.

As regards the major site studies, the "big three" (Cigar Lake, Alligator Rivers and Poços de Caldas) all seem to be developing well without evidence of superfluous replications. In all cases, the input from the modelling side, which has been much discussed at previous meetings of the CEC Natural Analogue Working Group, seems to be now well established. One remaining problem, however, which also seems evident in the other studies covered (Sandstone uranium deposits, endorheic basins and UK sediment sites) is the lack of input from these with experience in (or responsibility for) safety assessment.

Most of the studies are (or include) "transport" analogues. Even though "Kd" values may be derived, it seems that the calculations always involve assumptions of dubious validity. From the safety assessment viewpoint, a more qualitative appraisal of the rôle of perturbing mechanisms (e.g. colloïds, organics) may be more relevant.

All of the studies include some appraisal of "geochemistry" which often seems to be the easiest direct analogue, allowing immediate checking of conceptual models or even the conservatism of chemical equilibrium codes and their associated databases. Such work would be even more powerful if technology for appraisal of aqueous phase speciation, at even its crudest level, could be developed.

To sum up, it seems to me that we are now, via natural analogues, in a position to investigate the phenomena in details, and to make reliable comparison with detailed models.

F.P. Sargent

Let us leave for a while the debate about "qualitative" and "quantitative" uses of analogues; our first task should be to determine how good "good enough" needs to be for the validation of performance assessment.

In this respect, we must bear in mind the inevitable limitations of all analogues. The geological records are often incomplete, and errors in age determination may be large. Critical parameters are sometimes not well known. Finally, the configuration are seldom identical or directly analogous to those of a real repository.

However, despite this, natural analogues provide the only means by which extrapolation of long-term behaviour, by models, can be confirmed.

Secondly, we must be also aware of the negative use of analogues. There are many examples of "negative analogues" which might undermine confidence (of the public and/or regulators) in predictions of performance assessment and in disposal concepts.

The first example would be the one of bentonite seams which, exposed to surface conditions, show fractures which do not heal, contrary to our commonly adopted views about this material. Another example is the case of very large-scale (some km^3) kaolinization of granite bodies due to hydrothermal phenomena. Finally, one can argue that the Cigar

Lake uranium ore body was formed and concentrated because large quantities of uranium were transported by groundwaters over very long distances and timespans, therefore indicating a strong large-scale mobility of uranium at this time. We must consider these natural phenomena, and be able to refute or mitigate them; of course we must first understand them after careful studies.

These "negative analogues" may therefore show positive consequences, by leading us to set design criteria, or modify our disposal concepts; finally, they can be converted to positive arguments, of the form "such phenomenon would not be possible in a disposal configuration because of...".

To conclude, I would like to support the suggestion, made during the Symposium, to "re-visit" the OKLO fossil reactors, with our improved awareness of what natural analogues can bring to waste disposal studies.

I. Neretnieks

I will not try and summarize all papers in my session, but instead I will pick a few items from my personal fields of interest.

As regards the needs for natural analogues in safety assessment, I think that they can show whether some ideas or concepts advocated by safety assessment people are correct or not. In this respect, we have come a long way since the last conference in Lake Geneva (1984); now we can try to quantify many observations.

Let us turn now to more specific topics. The studies of hyperalkaline waters are of direct relevance for the disposal scenarios involving concrete materials; some data are still missing but the work brings useful indications for experimentalists about what is still needed.

As regards radiolysis, the numerous observations collected are suggestive and have direct bearing on the mechanisms of redox conditions close to disposed spent fuel canisters. The studies of reduction haloes show that precipitation at the redox front is an essential process for radionuclide release from the "near-field". Investigations of uranium distribution in borecores, of chloride ion penetration in granite blocks, and of data from hydrothermal veins in granite all address essential questions.

Now I would like to give some personal comments. Although we have come a long way (as previously stated), we no doubt still have a long way to go. We presently have very few, if any, conclusive results from natural analogues, which can be used for validating transport models. On the positive side, I think that a forum like this is one of the essential part of a "validation" or "understanding" process. The debates inspired me (and, I think, many others) to further investigations and exchanges of thoughts and information within our "natural analogue community".

D.G. Brookins

It was pointed out in this Symposium, and in Stockholm at the GEOVAL conference earlier this month, that natural analogues can be extremely useful to both the technical community and to the public. Let me comment on both areas.

We have seen this week that there is indeed a widespread interest in natural analogues, and considerable progress made in many key areas, and disappointingly little attention given to other key areas.

On the positive side, I would like to emphasize that much of the work is tied to carefully conceived and carried out investigations. Further, the modellers are cognizant of the importance of natural analogues, as are many experimentalists; but there still exists communication gaps which must be closed. Conferences such as this one are a great help in this respect.

On the negative side, I think that analogues for widely differing water-to-rock ratios at different pressure and temperature conditions are of great importance, but few actual studies involving radionuclides have been carried out. Further, stable isotopic studies (S, C, H and especially O) are important to problems of water-to-rock ratios, water movement, paleohydrology, mineral paragenesis and many other areas; yet studies in the radwaste natural analogue field are few. Finally, relatively few uranium deposits, or other high actinide sources, have been studied. We have here summarized the studies in some of these, and it is apparent that we have barely scratched the surface.

Now I would like to identify some specific needs. Concerning the OKLO site, they would be as follows: stable isotopic analyses (with a view to radiolysis); more detailed geochronology; more detailed chemical, probe, SEM, STEM, etc, studies, coupled with speciation studies of fission products and actinides; hydrology and paleohydrology; more studies of organics. As regards natural analogues for bedded salt, we are now aware of the paucity of such analogues; must there not be more ? Interest should be given to dykes, playas, etc. Finally, attention should be paid to the behaviour of actinides in hydrothermal and geothermal systems, especially when pressure, temperature, and water chemistry are known; included here are uranium deposits at elevated temperatures.

Turning now to the "public perception" point of view, I would like to recall that the anti-nuclear message starts in early elementary school in the USA. On the other hand, high-school and college students can understand natural analogue messages more easily than health arguments based on probabilities. Therefore we, in the natural analogue field, need to communicate our findings and our "trans-science" obervations to the public, and especially the news media. Furthermore, we need to integrate natural analogue reasoning into total elementary and sophisticated risk assessment studies.

. Status of the work on natural analogues as seen from the viewpoint of a safety assessor (T.Papp)

A substantial broadening of the interest in natural analogues is seen, especially for validation of models in geochemistry, nuclide transport and glass leaching.

Obviously, there is no lack of potential analogues. There seems, however, to be a need for a mechanism evaluating the priorities, e.g. what is the safety importance of each phenomena that is modelled ? What are the parameter spans of interest for various concepts ? What degree of validation is required for a model in a safety assessment ?

Many of these priorities are site and concept- specific and must be dealt with independently by the research organizations. There might, however, also be a need for some internationally coordinated action which could supplement already ongoing efforts trying to establish an international consensus in performance assessment practice and methodology.

With regard to ongoing activities two specific items might have an impact on the studies of natural analogues.

The first is the project on scenarios that was recently launched by the Performance Assessment Advisory Group (PAAG) referring to the Radioactive Waste Management Committee of the OECD-NEA. The intention is to compile a background on scenarios that have been investigated. How have the various groups evaluated them and how have they established the probabilities for them ? This will be a basis for an international discussion with the intention to see whether a consensus can be reached on the practice and methodology, including rules on what scenarios must be covered and when a scenario can be discarded. Especially for natural scenarios this might also result in a priority list for the need of natural evidence to enhance the confidence in the relevance of the scenario models.

The other items is the present work on sensitivity and uncertainty (a workshop was recently arranged in Seattle by NEA on this subject). A major trend in safety assessment today is to try to complement the deterministic assessment models by models that can handle uncertainties. A number of those codes have now been developed using distributions as input parameter and propagating them through the assessment sequence to result in a probability consequence distribution as an output.

Due to limitations in computer time and capacity these submodels representing the various components or subsystems of the repository must be very simplified compared to the normal research models you are working with. Here again I see a need for a future action by groups such as this on natural analogues. The validation of such simplified models will not be easy and has not yet been discussed in detail. It might be that the acceptance of the assessment results will depend on our ability to find a suitable balance between models simple enough to be handled probabilistically and models realistic enough to be validated by natural analogues.

4. Summary of the discussion

The subsequent discussion involved many members of the audience in debate with the panel. Four main issues emerged:

(i) "qualitative vs quantitative" uses of analogues;

(ii) disenchanted opinions

(iii) suggestions for further investigations

(iv) opinion from regulators, or concerning public perception

"Qualitative vs quantitative" uses of analogues

Natural analogue studies must be carried out with the objective to increase confidence in the performance assessment of radioactive waste disposal, and also make public perception easier.

Advocates of the "qualitative" uses of natural analogues emphasized the fact that the identification of processes operating in Nature was indeed possible, whereas unambiguous quantification of these latter was often beyond the scope of present capabilities, due to the complexity of natural situations. An example of this is the Uranium-series disequilibrium method, a commonly applied tool, which generally only gives indications whether particular phenomena take place or not. In this respect, natural analogues play an irreplaceable role, simply by illustrating which phenomena need to be accounted for in a correct description of transport and other processes.

It was pointed out, however, that even apparently qualitative analogues, e.g. the Cigar Lake ore body, could bring quantitative elements, such as the fact that groundwater from this site meets the requirements for drinking water as regards uranium concentration.

Additionally, it was stressed on various occasions that the quantitative use of analogues for disposal studies should be given priority as often as possible. This is already possible for instance when studying the degradation products of volcanic natural glasses; these results allow the testing of extrapolations for waste glass products from laboratory data via the use of mathematical models. Further, quantitative data are the objective when it comes to studying the transport of uranium, colloïds, iodine, etc, in the environment. Mainly for colloïds, it is necessary to understand phenomena (a qualitative role) and to quantify them. In this respect, initiatives such as the "CEC colloïd benchmark" are of great value and should be expanded.

Finally, it must be borne in mind that performance assessment studies must include both the geosphere and the biosphere. For the l tter, the only possible quantitative validation of models lies in the use of carefully conducted field measurements, such as those carried out at the Morro do Ferro site. There is a need for more biosphere analogues, which were barely addressed at this conference.

Disenchanted opinions

The large number of ongoing natural analogue studies should not lead to the impression of an anarchic proliferation of diverging, unconnected research programmes. Caution and judgment must be the necessary first step before embarking into new research on natural analogues. It was recalled that the initial enthusiasm about OKLO dropped when the site became a simple "playground for radiochemists" bringing no more useful results for performance modelling; fears were expressed that today's major programmes could run into the same problems. Furthermore, some pessimism appeared at the recent GEOVAL symposium concerning the useability of analogues for performance assessment studies (although this mainly concerned the quantitative aspect of analogues). Finally, it was pointed out that none of the presently studied analogues showed the "five desirable attributes" identified by Chapman et al. in 1984. However, even "imperfect" natural analogues are presently the only acceptable method by which long-term safety predictions can be substantiated.

Suggestions for additional research

The above remarks largely went to show that the specialists are well aware of the limitations of the "natural analogue tool", and suggestions were also given for possible improvement of the present situation.

It would appear that most analogue research is now concerned with hard, fractured rocks. Therefore, more studies on other rock types should be encouraged. In the same line, careful attention should be paid to identify analogues of those radionuclides which are shown (by safety studies) to be the major contributors to dose-to-man, i.e. not only transuranium elements and iodine, but also Technetium, etc.

Chemical processes are probably the area in which most efforts are being directed; very few examples of natural analogues of physical processes are presently studied. Therefore, "coupled analogues" should be paid more attention.

Finally, it was indicated that the OKLO site might become the subject of renewed attention from the International Atomic Energy Agency (IAEA) in the next years.

Regulators' viewpoint - Public perception

With a view to public perception, the consensus of regulators would seem to be that natural analogue studies should be simple and presented as simply as possible, so that they are understandable by the lay public. As regards the scientific community, the maximum benefit will be obtained from natural analogues (either qualitative or quantitative) if and when links are increased between performance assessment modellers and natural analogue modellers. The means of using analogue data in direct support of performance assessments, both in justification and presentation of their results, is to be the topic of the next CEC Natural Analogue Working Group (NAWG) meeting in 1988.

POSTER PRESENTATIONS

IN LABORATORY, ON SITE, IN SITU SAMPLING AND CHARACTERIZATION OF GRIMSEL COLLOIDS - PHASE I.

C. A. DEGUELDRE
Hot Laboratory,
Eidgenoessisches Institut fuer Reaktorforschung,
CH-5303 WURENLINGEN

Summary

The characterisation of Grimsel colloids has been carried out after sampling the natural colloids by pulsed diaultrafiltration in situ/on site i.e. in the NAGRA Felslabor Grimsel or in laboratory i.e. EIR Wurenlingen after transfer of water samples. In the first phase, colloid speciation, size distribution and concentration are reported from SEM/EDX investigations on dry flat ultrafiltration membranes, in addition colloid species are estimated by running a thermodynamic code. The parameters from the water analytical survey have been very constant (e.g. T=285K, pH=9.7) for more than one year. Calculation of saturation indices indicates that from the most concentrated elements i.e. Ca, Si, C, F, S; quartz, calcite and fluorite should precipitate in "in situ" conditions (i.e. log PCO2 =-5.5), while in laboratory (atmospheric conditions pH=8) calcite is dissolved. In laboratory and on site/in situ sampling by pulsed diaultrafiltration yields the production of microsamples of colloids investigated by SEM/EDX. The colloid concentration is 2-5 10E10 particles per litre, the size distribution reported from 40 to 1000 nm is a continuous decay starting from small size e.g. 40-80 nm (120 items per 200 umE2) and decreasing for the larger e.g. 720-760 nm (1 item per 200 umE2). EDX analysis indicates that Si is present as colloidal material, however, its small concentration yields the conclusion that composite colloids including silica have been generated e.g. with part of the 360ppb DOC.

1 INTRODUCTION

Since colloids have been indentified as potential key species for the transport of radionuclides, a colloid survey including determination of species concentrations and size distribution has been scheduled before and during the migration experiment in the Felslabor Grimsel (FLG). As far as water transport has been suspected to alter colloid population, colloid sampling by pulsed diaultrafiltration (PDUF) has been done in laboratory (EIR Wurenlingen) as well as on site/in situ (FLG) in the migration zone (Figure I).

Table I summarizes our analytical approach. It includes for the first phase the sampling work by PDUF in the in situ conditions the colloids by PDUF or the transfer of the water matrix in stainless steel container prior to separation by PDUF in laboratory under similar thermodynamic conditions (P,T,V,P1...Pi). From the analytical survey of the water, saturation indices are calculated from the average elementary concentrations. As result, inorganic species suspected to precipitate are at first researched as colloid in the experimental approach. The SEM/EDX work concerns in laboratory or in situ prepared ultrafiltration membrane. Concentration, size distribution and elementary speciation result from these investigations.

Phase II and III deal with advanced microscopic and microbeam techniques. As an example TEM investigations have been used very succesfully for colloids characterization <1,2>. In addition the application of classical analytical methods (e.g.AAS) will allow us to define colloidal elementary compositions. Accuracy of these data will be checked by changing the matrix volume.

2 SITE AND WATER DESCRIPITION

The FLG and particularly the migration zone are described in NAGRA reports <3>. Water data resulting from the analysis carried out by EIR or for NAGRA are reported on Table II. The composition of this rather basic and slightly mineralised water is very stable with time and does not present any seasonal change.

3 THERMODYNAMIC PREDICTIONS OF COLLOID SPECIES

The in situ pH of 9.7, the temperature of 285 K and the total pressure of 1 Atm correspond a partial pressure of carbon dioxide of 10E-5.5 Atm. In these circumstances the major components that are supposed to precipitate are quartz, calcite and fluorite. These species should be present as major inorganic colloid. Other species such as hydroxoapatite, fluoroapatite, kaolinite, hematite, goethite and alpha iron hydroxyde present positive log IAP/KT (saturation index), however, they should appear as minor colloidal constituants because P, Al and Fe are only present at the ppb level. They are just mentioned in the phase I for sake of completeness.

Any contact with air increases the carbon content and the pH of the water in equilibrium with air drops to 8. Figure II shows the

effect of the carbon dioxide partial pressure on the FLG water pH. Among the major colloidal constituants, calcite is dissolved before pH 8 while quartz and fluorite are yet precipitated for PCO2 = 1 Atm. The only way to dissolve quartz would be either to increase the pH over 10 or heat the system over 310 K.

4 COLLOID SAMPLING BY PDUF

Pulsed diaultrafiltration has been carried out with Grimsel water under nitrogen or argon containing vpm of CO2 or O2. For the PDUF carried out in the laboratory (EIR) the water after being sampled in stainless steel bottles under anaerobic conditions is injected in the ultrafiltration rig. The water is kept under the local overpression (1 Atm) and transfered in the laboratory (Wurenlingen) were the separation work can be performed.

PDUF has been used in situ/on site since last year using for pressurisation similar gas as in laboratory. However, in situ, the sampling is carried out in flow conditions. During PDUF, the pressure in cell is 1 Atm, while the injections require a 0.1 atm overpressure for the water spikes. The sample after PDUF are dryed under inert gas and the membranes are transfered in small container to the laboratory.

5 SEM/EDX INVESTIGATIONS

Membranes are sticked on sample carrier with carbon paste and coated with 20 nm gold, silver, carbon or gold paladium mixture. The later preparation allowing better morphological investigations because the lateral resolution is improved. In all the cases after a PDUF of some tens of ml, the membrane is homogeneously covered with colloids. Figure III shows a typical micrograph with rather spherical colloids whose diameters range from 40 to 1000 nm. Smaller are not clearly detected. They can be counted and from the average number of colloids calculated for the active surface of the membrane (0.8 cmE2) and for a given volume of water diaultrafiltrated, the colloid concentration can be deduced. We calculated 2+1 10E10 and 4+2 10E10 pt.1E-1 as first results respectively for the in laboratory and for the in situ PDUF. This result is to be compared with KIM's LPAS <4> which measured 0.6 10E10 pt.1E-1. It is premature from this preliminary result to give a definitive experimental answer to the question of relevance of sampling in laboratory or in situ.

Size distributions as reported on Figure IV are obtained by quantimetric investigations of the micrograph negatives. The quantimeter discriminates the elementary composite colloids from their aggregates. Similar results were obtained making manually discrimination and counting. Actually, in the controlled conditions artefacts (bacteries, dust ...) do not affect the results because their concentrations are <0.01.

The elementary analysis by EDX gives as background a Cl spectrum due to chloride sorption in the membrane during the PDUF. Even the largest spherical colloids (2 um) did not exhibit any typical peak ascribable to plain inorganic items . However, by differential EDX

between membrane and colloid some small peaks of Si where found. For this study, the membrane was coated with silver and Figure V presents an exemple of differential spectrum.

6 CONCLUSION

With a concentration of some 10E10 pt.1E-1 the slightly mineralized anaerobic granitic water flowing in FLG could be representative for sampling/characterization exercise because its concentration is located between Markham 10E8 and Gorleben 10E12. In addition, the geology and hydrogeology of the Grimsel site are of direct relevance to many waste disposal programs. The natural granitic colloids are composed of silica associated with dissolved organic carbon. The colloid concentration (for a density of 1-2) should range from 200 to 500 ppb.

7 ACKNOWLEDGEMENTS

Acknowledgements are due to E. Naef and R. Giovanoli for their SEM/EDX work, H. Grimmer for adapting the quantimet program and B. Bayens for running the code PHREEQ using the analytical data of the water provided by EIR and NAGRA.

REFERENCES

<1> DEGUELDRE C. A., GIOVANOLI A., KEIL R., MOHOS M., WERNLI B., (1985) Caracterisation des colloides naturels dans une eau granitique de reference. EIR TM-42-85-54.

<2> WARBICK A., EGE G.M., HENKELMAN R.M., et al (1979) An evaluation of radiocolloid sizing techniques. J. Nucl. Med. 18; 827-834.

<3> NAGRA, BGR, GSF, (1985) Grimsel Test Site, Overview and Test Programs NAGRA NTB 85-46.

<4> KLENZE R. KIM J. I. (1986). Characterization of groundwater colloids by laser induced photoacoustic spectroscopy. TUM, Report No. RCM03286.

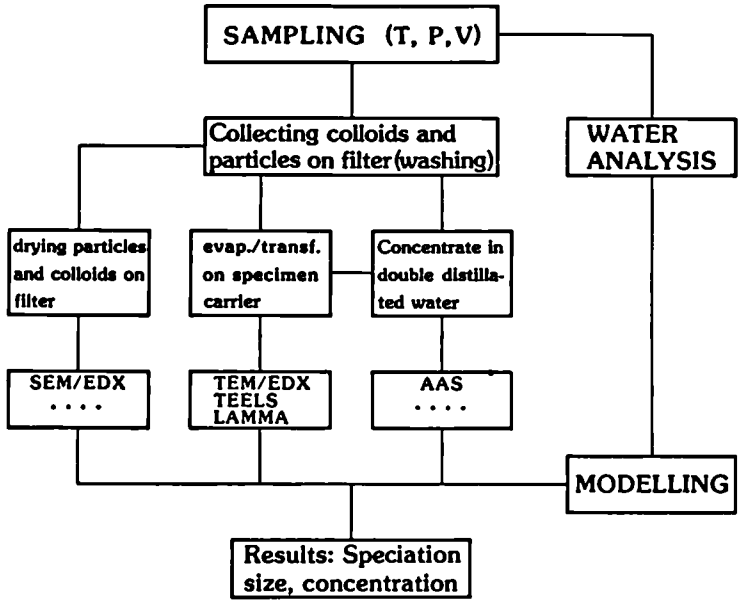

Table I: Analytical program : phase I

TOTAL MOLALITIES OF ELEMENTS

ELEMENT	MOLALITY	LOG MOLALITY
CA	1.370096D-04	-3.8632
MG	8.000561D-07	-6.0969
NA	6.850480D-04	-3.1643
K	4.000281D-06	-5.3979
FE	9.000631D-07	-6.0457
MN	2.700189D-07	-6.5686
AL	2.500175D-06	-5.6020
BA	2.200154D-07	-6.6575
SR	1.830128D-06	-5.7375
SI	2.000140D-04	-3.6989
CL	1.550109D-04	-3.8096
TOT ALK	4.200295D-04	-3.3767
S	6.200435D-05	-4.2076
B	6.200435D-06	-5.2076
P	2.100147D-07	-6.6778
F	3.300231D-04	-3.4815
LI	1.150081D-05	-4.9393

----DESCRIPTION OF SOLUTION----

PH =	9.7000
PE =	-0.1000
ACTIVITY H2O =	1.0000
IONIC STRENGTH =	0.0012
TEMPERATURE =	12.0000
ELECTRICAL BALANCE =	-4.5073D-05
THOR =	1.5398D-03
TOTAL ALKALINITY =	4.2003D-04
ITERATIONS =	10
TOTAL CARBON =	2.9112D-04

---- LOOK MIN IAP ----

PHASE	LOG IAP	LOG KT	LOG IAP/KT
CALCITE	-8.3575	-8.4179	0.0605
ARAGONIT	-8.3575	-8.2644	-0.0931
DOLOMITE	-18.9451	-16.7747	-2.1704
SIDERITE	-14.2096	-10.3648	-3.8448
RHODOCHR	-11.0587	-10.3405	-0.7182
STRONTIT	-10.2195	-9.2819	-0.9376
GYPSUM	-8.2375	-4.6149	-3.6226
ANHYDRIT	-8.2374	-4.2403	-3.9971
CELESTIT	-10.0995	-6.5856	-3.5139
BARITE	-11.0067	-10.1832	-0.8235
HYDROXAP	-1.6792	-2.2128	0.5336
FLUORITE	-10.9519	-11.1174	0.1655
CHALCEDY	-3.8135	-3.6772	-0.1363
QUARTZ	-3.8135	-4.2139	0.4003
GIBBSITE	9.1296	9.5319	-0.4024
KAOLINIT	-38.3127	-38.5635	0.2508
SEPIOLIT	-42.7861	-40.9656	-1.8205
HEMATITE	11.6540	-2.9772	14.6313
GOETHITE	5.8270	0.9699	4.8571
FEOH3A	5.8270	4.8910	0.9360
PYRITE	-102.1855	-18.8576	-83.3279
FES PPT	-55.8961	-3.9150	-51.9811
VIVIANIT	-48.7523	-36.0000	-12.7523
PCO2	-6.8950	-1.2986	-5.5963
O2 GAS	-52.1844	-2.8984	-49.2861
H2 GAS	-22.2912	-3.0912	-19.2000

Table II: Grimsel water analytical data and IAT/KT (saturation index) results.

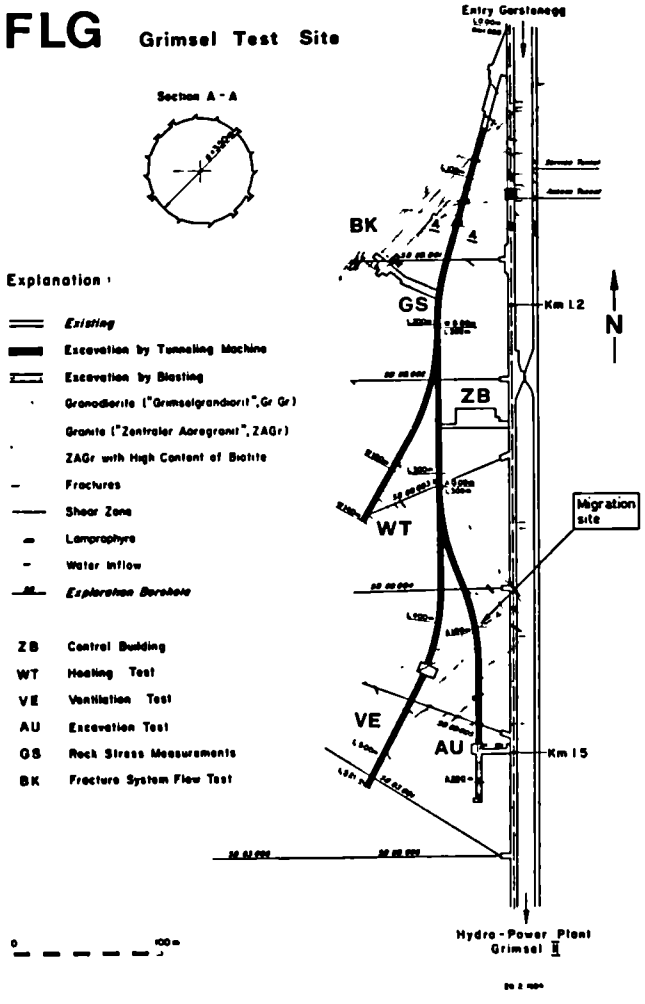

Figure I: Felslabor Grimsel plan with migration zone.

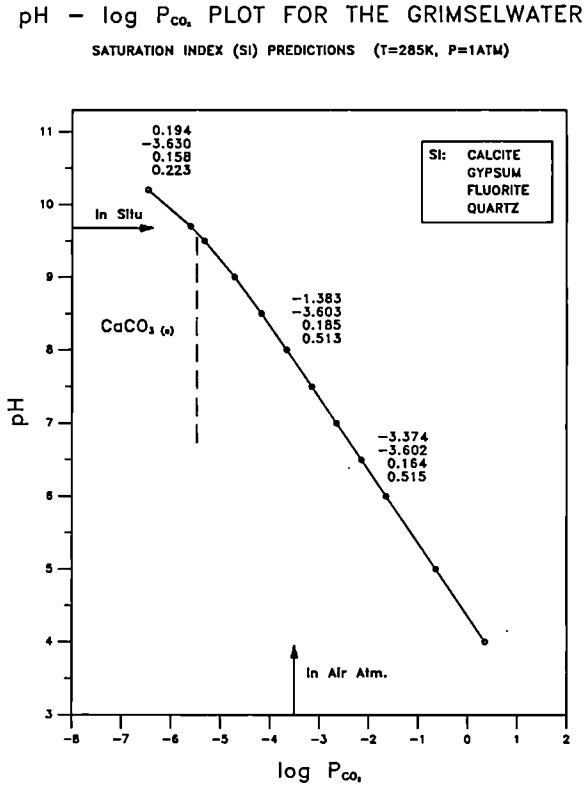

Figure II: pH - logPCO2 predictions.

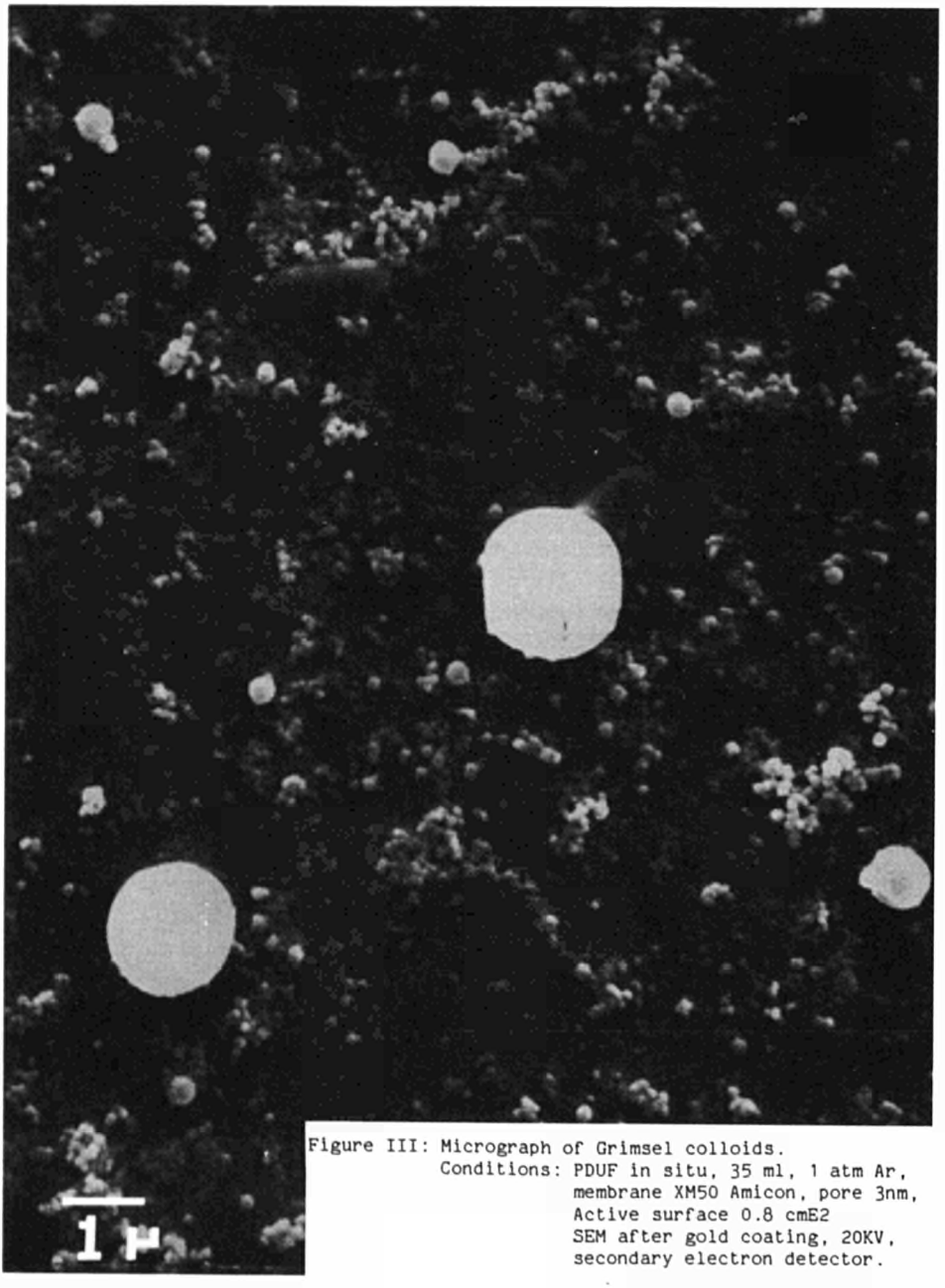

Figure III: Micrograph of Grimsel colloids.
Conditions: PDUF in situ, 35 ml, 1 atm Ar,
membrane XM50 Amicon, pore 3nm,
Active surface 0.8 cmE2
SEM after gold coating, 20KV,
secondary electron detector.

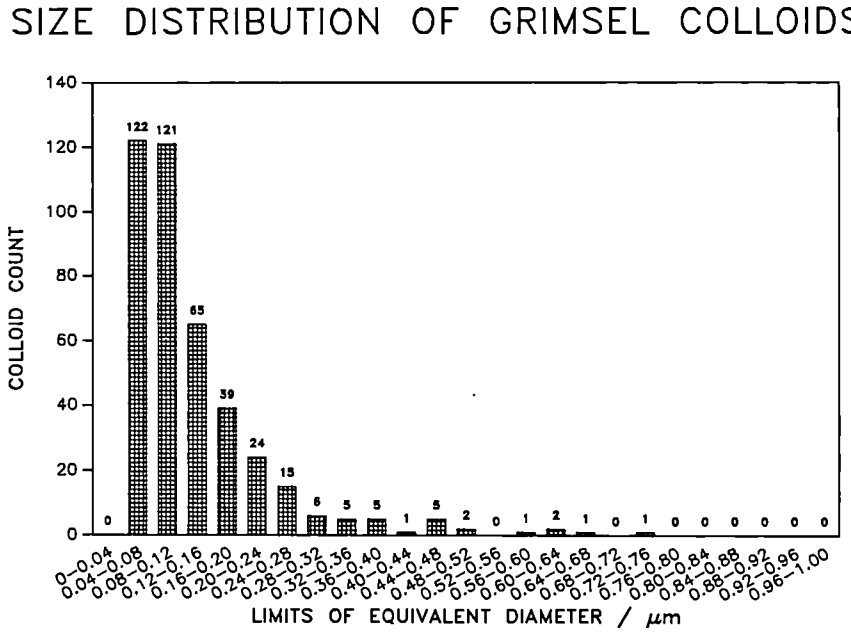

Figure IV: Size distribution of Grimsel colloids.

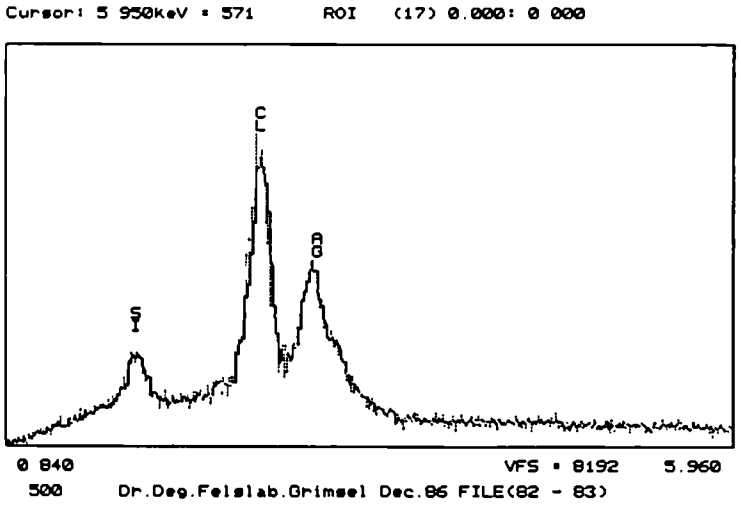

Figure V: Colloid EDX spectrum, filter coated with silver
Cl peak due to the membrane.

HYDROLOGICAL MODEL STUDIES AND NATURAL ISOTOPE DATA AS INDICATION FOR GROUNDWATER FLOW IN DEEP SEDIMENTARY BASINS

P. GLASBERGEN
RIVM
P.O. Box 1
3720 BA Bilthoven
The Netherlands

Summary

The study of the flow system in deep aquifers is relevant to the safety assessment studies of geological disposal of radioactive waste. Because, deep aquifers are the first porous medium in which migration of radionuclides can occur, it is essential to establish whether the direction of this flow permits migration toward shallow fresh-water aquifers and finally to the biosphere.

Although natural isotopes provide indications about the age and origin of groundwater, interpretation of the findings is difficult. A hypothesis about the flow system can be reached on the basis of an interpretation of natural isotopes taking into account the paleogeographic situation. To reduce the uncertainty associated with the interpretation of natural isotopes, we made an inventory of all available oxygen-18 and carbon-14 data concerning The Netherlands, which we divided into two sets, i.e., data originating from areas outside the area of Zechstein salt deposition and data from salt- influenced aquifers. The first series of ^{18}O data was combined with ^{14}C data which yielded a curve of ^{14}C-age vs. ^{18}O. The ^{18}O data of the second series was corrected with help of this graph which enabled the calculation of the contribution of dissolved rock-salt.

Another approach to obtain support for such a hypothesis is the construction of a model. Groundwater flow lines can be calculated and travel times, starting from surface infiltration, estimated. These models can show the likelihood of the flow system assumed for the hypothesis. It is concluded that the best results can be obtained by combining both approaches -isotope hydrology and groundwater modelling- to reduce the uncertainty about the deep groundwater system.

1. Introduction

For estimation of the migration of radionuclides released from deep disposal facilities in geological formations it is essential to quantify the components of the geohydrological system in the overlying sediments. For example, the groundwater flow in the hydrological basin must be known. In The Netherlands, rock-salt formations of Zechstein age are being studied as potential disposal medium. The formations overlying the Zechstein Group form a continuous cover occasionally perforated by salt domes. Because it is so large and is partly covered by the sea, a complete geohydrological characterization of the NW European Basin (fig. 1) is not possible in the present state of our knowledge. The Basin is surrounded by the Fenno-Scandian High in the north, the Rhenish Massif and several Central European blocks in the south, and the Western British Highs in the West. The thickness of the sediments overlying the Zechstein increases to over 8 km in the central parts of the basin (1).

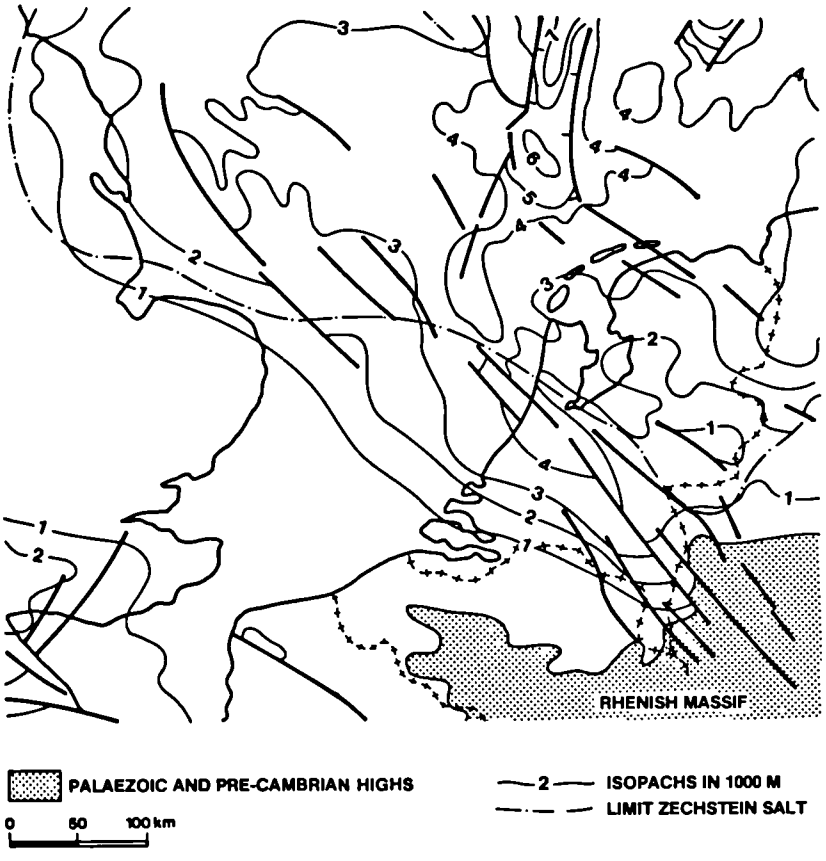

fig. 1 Isopachs for Late Permian to Quaternary sediments (after Ziegler, 1982).

A very slow flow of groundwater might occur in deep strata above the impermeable Zechstein salt formation. If this is the case, the direction of flow might be determined by the topographic difference in height between the coastal area and the infiltration area, which is situated in Germany and Belgium. Infiltration toward the boundaries of the Basin takes place in the outcrop zones, but quantification of the system is not yet feasible. Large parts of the NW European Basin are covered by seas, but it is not known whether the groundwater flow in deep aquifers extends into those areas. For the more or less W-E running southern limit of the Basin in general, the horizontal groundwater flow could be from south to north/northwest.

To obtain more information about the flow in the deep parts of the NW European Basin, we collected data on natural isotopes and applied these to a hypothetical geohydrological model of infiltration and flow. Most of these data concerned the groundwater in Upper-Tertiary/Quaternary aquifers. Little is known about groundwater in deeper aquifers.

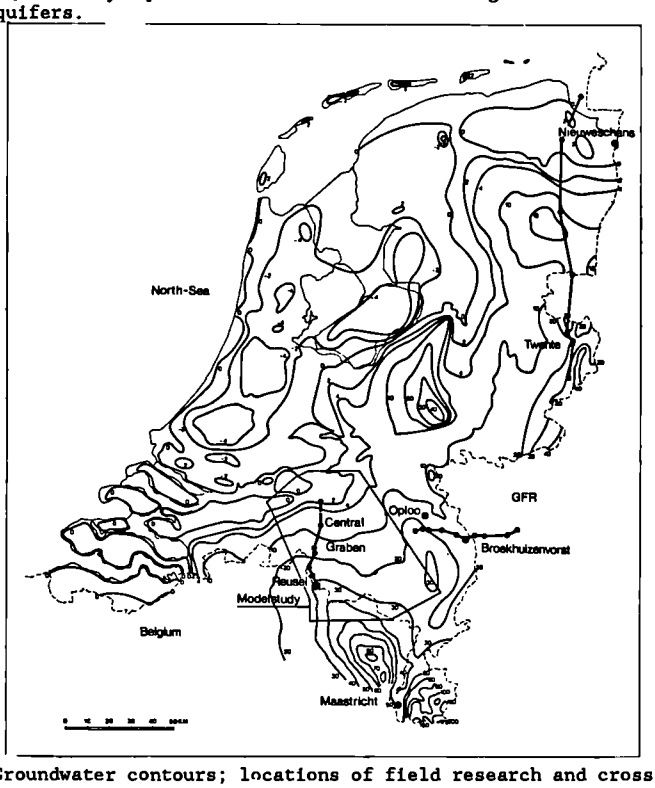

fig. 2 Groundwater contours; locations of field research and cross-sections.

2. Available boreholes and preliminary interpretation of results

Some geohydrological information about the boreholes used for this study will be briefly summarized here. The locations of these holes are shown in fig. 2.

The oldest formation, which was reached by a borehole, is situated in Maastricht. Two screems have been placed in this borehole, at a 480 m in the Upper Devonian and the other at 240 m in the Dinantian. Fig. 3 shows a simplified cross-section with indication of the lithology. The possible infiltration area is situated about 10 km south of Maastricht. The piezometric heads, which are several metres above ground level, and the existing groundwater contour maps of the area, do not permit any firm conclusion concerning the origing of the groundwater. Some groundwater quality parameters are summarized in

Table I Some parameters of groundwater quality in the investigated boreholes.

Location :		Maastricht	Oploo	Reusel	Broekenhuisenvorst	
Nieuweschans						
Depth :		480 m	513 m			
Formation :		Devonian	Lower Paleocene/ Cretaceous	Lower Oligocene	Lower Oligocene	Eocene
Parameter	Unit					
Cl^-	mg/l	5300	12300	720	12839	74419
SO_4^{2-}	mg/l	390		7	230	1276
HCO^{3-}	mg/l	852	510	1310	514	157
Na^+	mg/l	3800	7070	823	7200	43019
Ca^{2+}	mg/l	170	550	17	610	1718
Mg^{2+}	mg/l	82	270	5.6	290	966
Br	mg/l	8.7	45.5	2.7	20.2	111
^{18}O	o/oo SMOW	-8.20	-5.91	-7.26	-6.52	-3.47
D	o/oo SMOW	-56.2	-37.5	-48.7	-44.5	-26.7
^{14}C	o/o	3.0	0.85	2.4	3.4	1.97

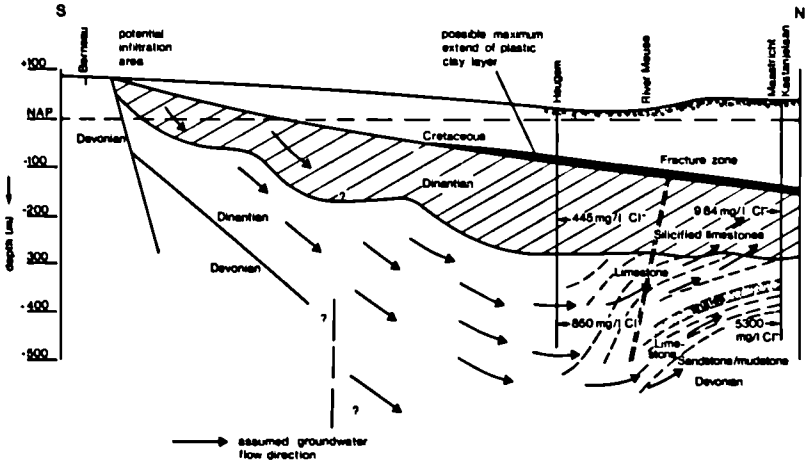

fig. 3 Simplified cross-section Berneau. Maastricht, showing the assumed flow system.

table I. The ^{14}C age can be roughly estimated at 25,000 years. This means that the water could have infiltrated during the very cold period in the Middle Weichselian. The ^{18}O value confirms infiltration in a cold climate, because at present the ^{18}O value in the assumed infiltration area is -8.1 °/oo. A well test gave an average hydraulic conductivity of 1.55 x 10^{-7} m/s over the screen lenght of 20 m (2). This value is probably determined predominantly by the effects of cracks. Core tests yielded an average porosity of 0.6 % (3). Taken together, these data support the hypothesis that the origin of this groundwater lies in a southern infiltration area (see fig. 3).

In the Oploo borehole a screen has been placed at 513 m on the boundary between the Tertiary and the Cretaceous in a limestone aquifer. Due to the relatively great hydraulic conductivity of the aquifer, an origin of this groundwater in the south-eastern direction, where the Tertiary wedges out, can be assumed.

In the same region, isotope data have been obtained from a number of wells. These wells situated more or less on a flow line. Differences in ^{14}C allowed calculation of flow velocities and hydraulic conductivity. A numerical model was made for this area. Only transmissivities determined from pumping tests and hydrological boundary values were used to calculate the head of the groundwater. Calibration improved the transmissivity pattern (fig. 4). The final

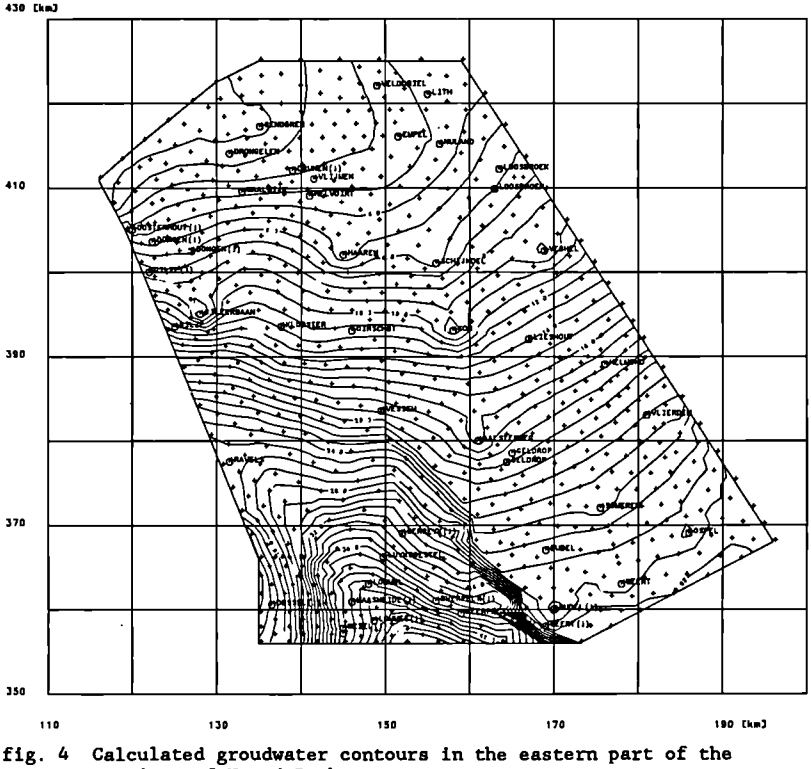

fig. 4 Calculated groudwater contours in the eastern part of the province of Noord-Brabant.

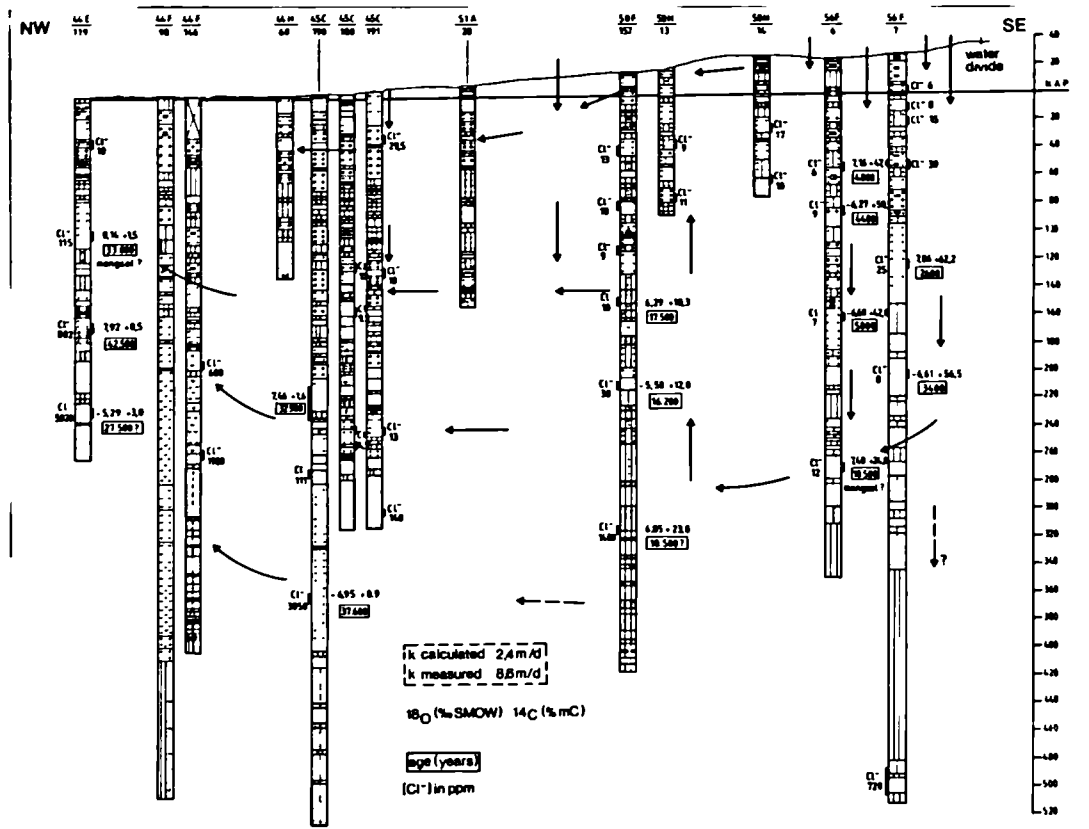

fig. 5 Geohydrological cross-section through Noord-Brabant, showing the assumed flow system.

outcome of the numerical model was a conductivity of 8.6 m/d (4), whereas use of the travel times calculated with ^{14}C data for the main aquifer (see fig. 5) gave a conductivity of 2.4 m/d (5). Although this difference is very hardly surprising in view of the uncertainties associated with the ^{14}C interpretation, it is easier to explain if we consider the paleohydrological situation in this area. During colder periods more than 10,000 years ago, the gradient could have been less sharp due to higher natural groundwater levels in the lower river valleys and less infiltration in the southern higher sandy soils. At present the lower soils are artificially dewatered.

The Reusel borehole (56F7) at the right in the profile in fig. 5 has a screen at 490 m which is below the extremely impermeable Oligocene Boom clay. The Berg sand aquifer is only 20 m thick, but it extends very far (fig. 6). The outcrop area is located along an E-W running line north of Brussels. A water divide in the shallow aquifer lies close to Reusel. The transmissivity of the aquifer was shown by a slug-test to be 0.2 m^2/d, which means that, taking the small gradient to the south into account, the ^{14}C age of about 30,000 years cannot be explained by horizontal flow originating from the outcrop area. Analysis from clay samples taken from the overlying clay confirmed a vertical infiltration of fresh water. The most probable explanation of the Berg sand water quality would seem to be infiltration of water from overlying aquifers, which slowly replaces the original marine pore water. The still high chloride content of this aquifer can be explained by assuming that the aquifer is also or was formerly fed by water with a higher salinity flowing upward from deeper aquifers.

At Broekhuizenvorst in a borehole in the same geological formation a screen was placed at 539 m. The hydraulic head is about 12 m above the surface of the ground, which implies that the origin of

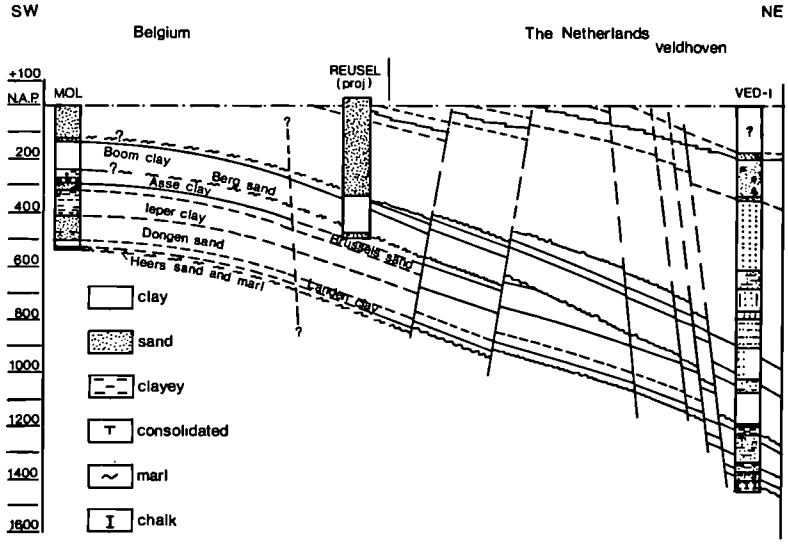

fig. 6 Cross-section through the Reusel borehole.

this Berg sand water must lie in a topographically higher area. The ^{14}C analysis provided evidence supporting a considerable age of the Berg sand water, i.e., in the range of 35,000 - 40,000 years. The transmissivity determined by a well test is 0.18 m^2/d, which is in close agreement with the results for the Reusel borehole (6). The area under study lies in a tectonic unit situated between the faults bordering the Central Graben and the Krefeld High (fig. 7). In general, the groundwater flow is in this area from Germany toward The Netherlands. The water quality points to deep circulation. Carboniferous groundwater in this area often shows high sodium-chloride concentrations (7). Although infiltration along nearby faults might offer an explanation the expected very low effective porosity of the Carboniferous (1%) points to an area of origin lying some tens of kilometres to the SE.

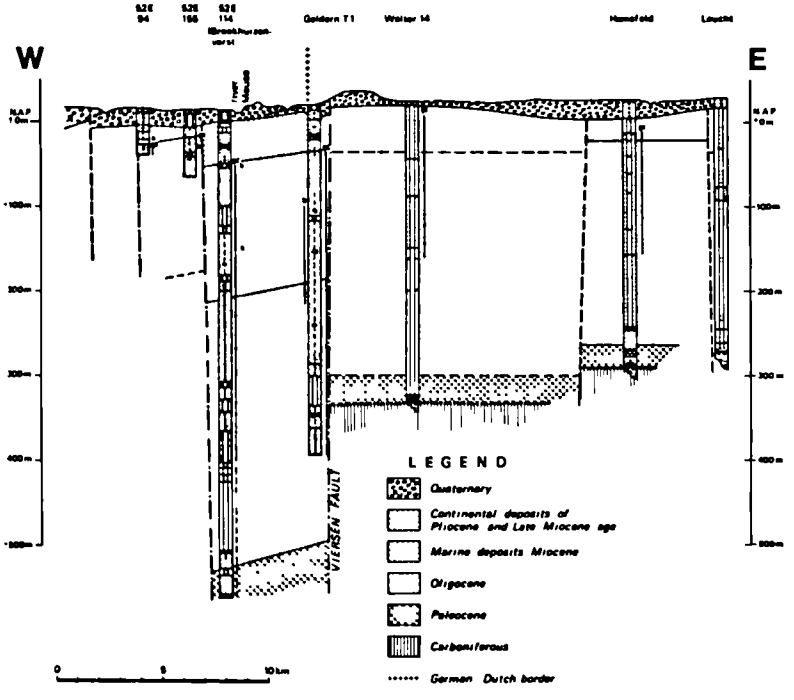

fig. 7 Cross-section through the Broekhuizenvorst borehole.

One of the boreholes studied is situated within the area of Zechstein salt deposition. The Nieuweschans borehole was provided with a 45-m screen extending to a depth of 582 m in an Eocene aquifer. According to the distance from the Eocene outcrop, the water in this aquifer is remarkably young (about 30,000 - 35,000 years). At various times after the Weichselian ice age the region was covered by a

shallow sea. Alterations in the topographic conditions make it impossible to define a specific hydraulic gradient as to either direction or magnitude. In samples from the overlying clay salt-concentration increases with depth. The quality of the groundwater found in the Eocene aquifer is determined primarily by the dissolution of halite, which has also led to high concentrations of a number of other ions such as Ca, Mg, Sr, and Br (8). The young age of this groundwater can in all likelihood be explained by percolation along permeable rocks lying against the flank of a nearby salt dome. About 5 km to the east there is indeed a salt dome which has penetrated the Eocene and also the overlying Oligocene clay.

3. Results of local research

Among the results of the local studies the large differences in salinity are the most remarkable. The explanation of salt concentrations in deep groundwater might lead to conclusions about possible contacts between groundwater flowing in deep aquifers and rock-salt and might also permit estimation of the rate of dissolution of the rock-salt. This latter process is of importance for the determination of the long-term isolating capacity of the rock-salt.

Under conditions prevailing in The Netherlands there are several sources of sodium-chloride: 1. rain-water, in very small concentrations, 2. sea-water intrusion, 3. dissolution of solid rock-salt, 4. diffusion from adjacient layers and 5. combinations of these sources.

For identification of the origin of the salt present in solution, the ratios between various ions can be helpful. Furthermore, ratios between natural isotopes and between other ions can be used for this purpose. We shall start with the relationship between chloride and bromide. In samples representing mixtures of fresh-water and sea-water, Br/Cl ratios lie in the range of 25-50 x 10^{-4}. Water containing dissolved sodium-chloride shows lower ratios. Measurements made during the experimental flooding of a potash mine in Germany gave ranges from 12-20 x 10^{-4} (9).

The graph of Cl vs. Br (fig. 8a) shows clearly that Reusel fits on the drawn dilution line starting from the sea-water point. Both the Nieuweschans and the Broekhuizenvorst wells are influenced by dissolved minerals with a lower Br content. It is remarkable that the Maastricht groundwater shows almost the same Br/Cl ratio, although the evaporites with which it could have been in contact, are not of Zechstein but of Carboniferous or Devonian age. When the available Dutch data are plotted as Br vs. TDS and the results are compared with those in the literature it becomes evident that the data points of the Maastricht II, Broekhuizenvorst, and Nieuweschans wells fall to the left of the seawater evaporation curve (fig. 8b); on the other side of the curve, where Br is enriched, the line A-D represents the findings of Frape and Fritz (10) for groundwater in the Canadian Shield. Except for Oploo the Dutch data show depletion of Br and are comparable to the data on dissolved salt in the flooded German salt mine Hope (9). The shift of the data points for the Dutch wells can therefore be explained by the uptake of dissolved rock-salt, as already suggested in connection with the local studies.

Plotting of Cl^- vs. ^{18}O (fig. 9) gives a set of curves for several ^{18}O values. The curves start from the sea-water point (^{18}O=o). All types of groundwater orginating from rainwater or sea-water intrusion should fit between this set of curves. This holds for the a-e and Reusel wells. The other investigated wells fall outside the

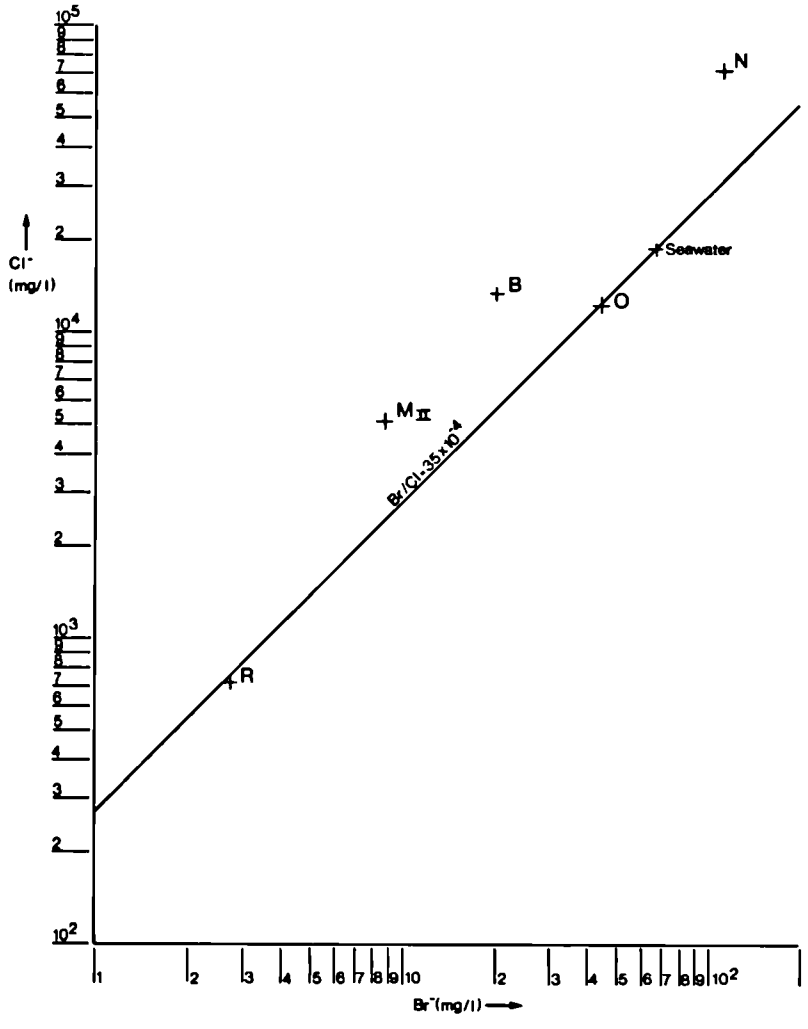

fig. 8a Plot of Cl vs. Br.

drawn curves. When an ^{18}O value for these waters is estimated, the share of the chloride orginating from dissolution or from the original groundwater can be determined by finding the intersection of a line running parallel to the vertical axis and the choosen ^{18}O curve. Before that, however it must be known whether the initial groundwater is influenced by evaporation. The points should lie on the theoretical line for the deuterium - ^{18}O relation. Broekhuizenvorst and Reusel

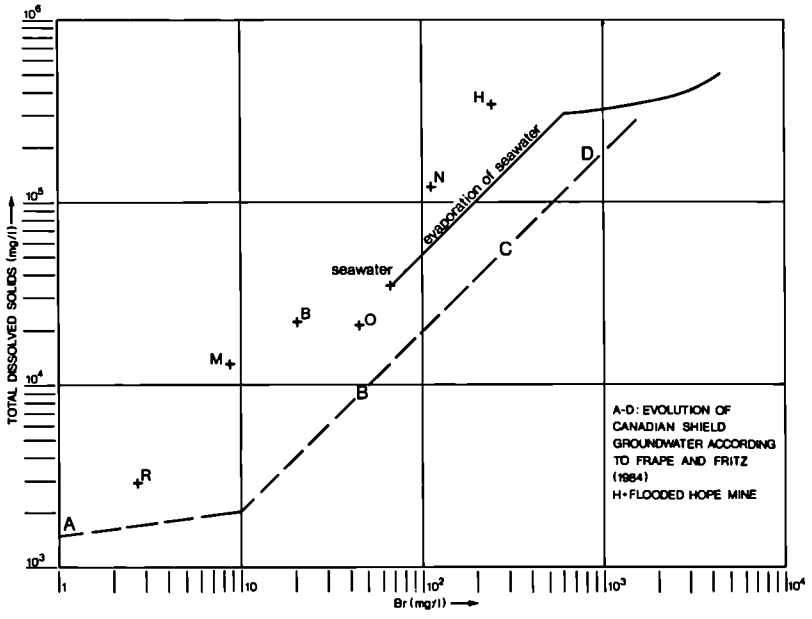

fig. 8b Plot TDS vs. Br.

satisfy this relation. The relation for Cl^- vs. $\delta^{18}O$ cannot be used to establish the ^{18}O content for Nieuweschans because of the influence of evaporation. This problem can be solved if a curve for ^{18}O vs. ^{14}C can be constructed, which can only be done on the base of ^{18}O values that are not influenced by evaporation. All of the available data were used to obtain the graph in fig. 10. This graph is an extension of the one published by Glasbergen and Mook, which covered approximately 15,000 years (10). From the position of the Broekhuizenvorst well in this graph an ^{18}O value of about -8 $^0/_{oo}$ seems acceptable. In terms of fig. 9, the chloride content of the original groundwater at Broekhuizenvorst would be about 4000 mg/l. Around the Nieuweschans data point the position of the graph is not sharply defined. But an ^{18}O value of -8.5 to -9 $^0/_{oo}$ seems reasonable. Without evaporation the ^{18}O value could have been about -5 $^0/_{oo}$. Corrected for mixing, the content could lie within the range of 5000 to 10,000 mg/l (see fig.9).

4. A prognosis of flow in the deep parts of the Basin

The geochemical information supplied by the above mentioned analyses proves that for all the locations studied the age of the groundwater supports the existence of a hydrological cycle in the Dutch part of the NW European Basin extending into deep aquifers. The outer Basin boundary crosses Belgium south of Brussels and north of Maastricht, curves south into Germany over Bonn and then runs north to Dusseldorf and Enschede before turning eastward into Germany. The topographic height along the boundary should lead in general to

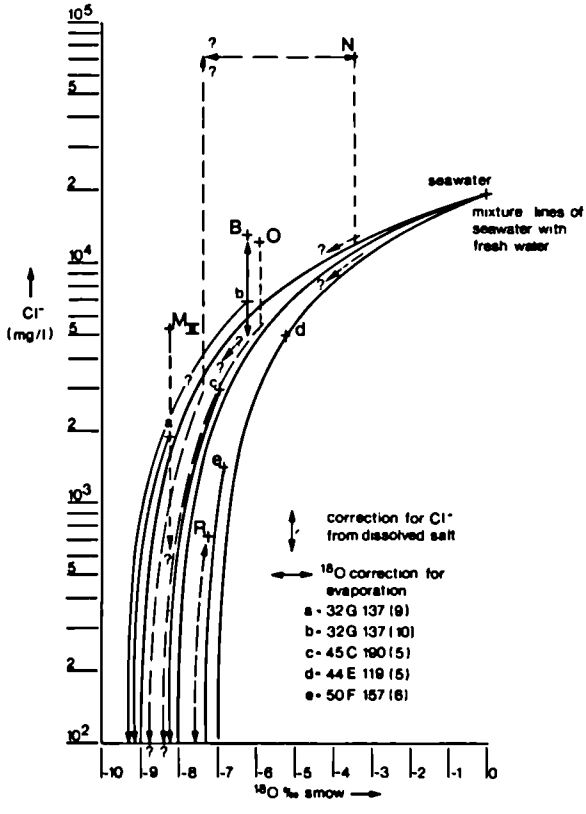

fig. 9 Plot of Cl vs. ^{18}O.

piezometric contour lines running parallel to the infiltration boundary and then slowly changing to lines lying parallel with the coast line of the North Sea. The amounts of water moving through the deep aquifers are limited by the low transmissivity. Because the available data pertain only to the peripheral parts of the basin, a numerical model was set up for estimation of the deep flow systems. For a cross-section running from the Twenthe region to the North Sea (see fig. 2) we constructed a model with the bedded salt as base. The length is 150 km, starting at the outcrop of the Mesozoic. For this first appoximation the hydrological units are treated as homogeneous. The boundary conditions taken for the model are as follows. The sea-level and the piezometric head of the Quaternary system (fig. 2) serve as upper boundary conditions. The lower boundary (rock-salt) is impermeable, as are the front and back sides of the model. Calculation with the computer code METROPOL (12) yielded flow- velocity values of up to about 0.1 m/a in the aquifer adjacent to the bedded salt. The

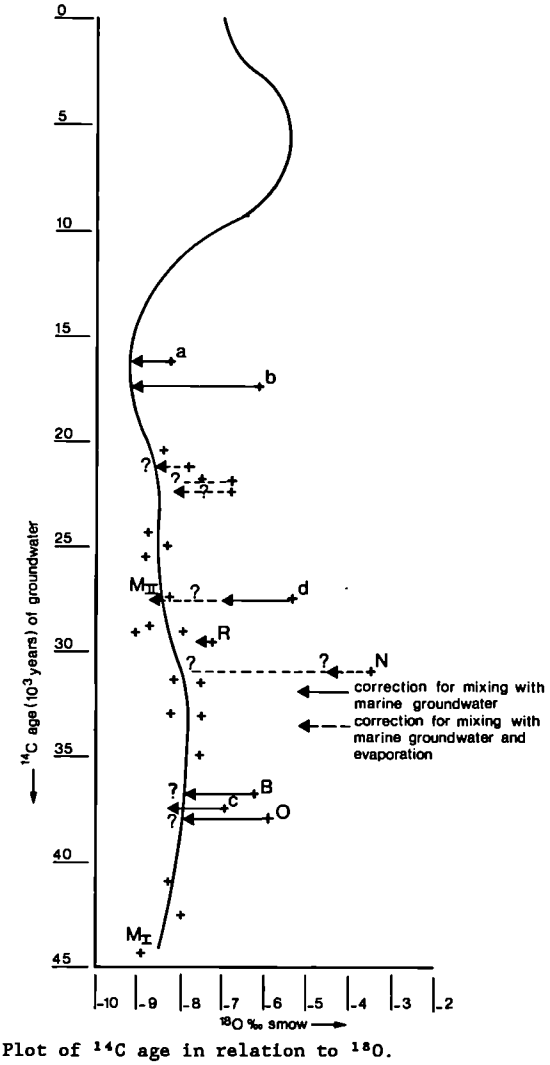

fig. 10 Plot of ^{14}C age in relation to ^{18}O.

highest velocities occur in the shallow system and the deepest systems. The results obtained with the model show that the flow follows mainly horizontal pathways. The model confirms the possibility of the existence of a flow system in the deepest parts of the Basin which is fed by infiltration close to its boundaries (see fig. 11).

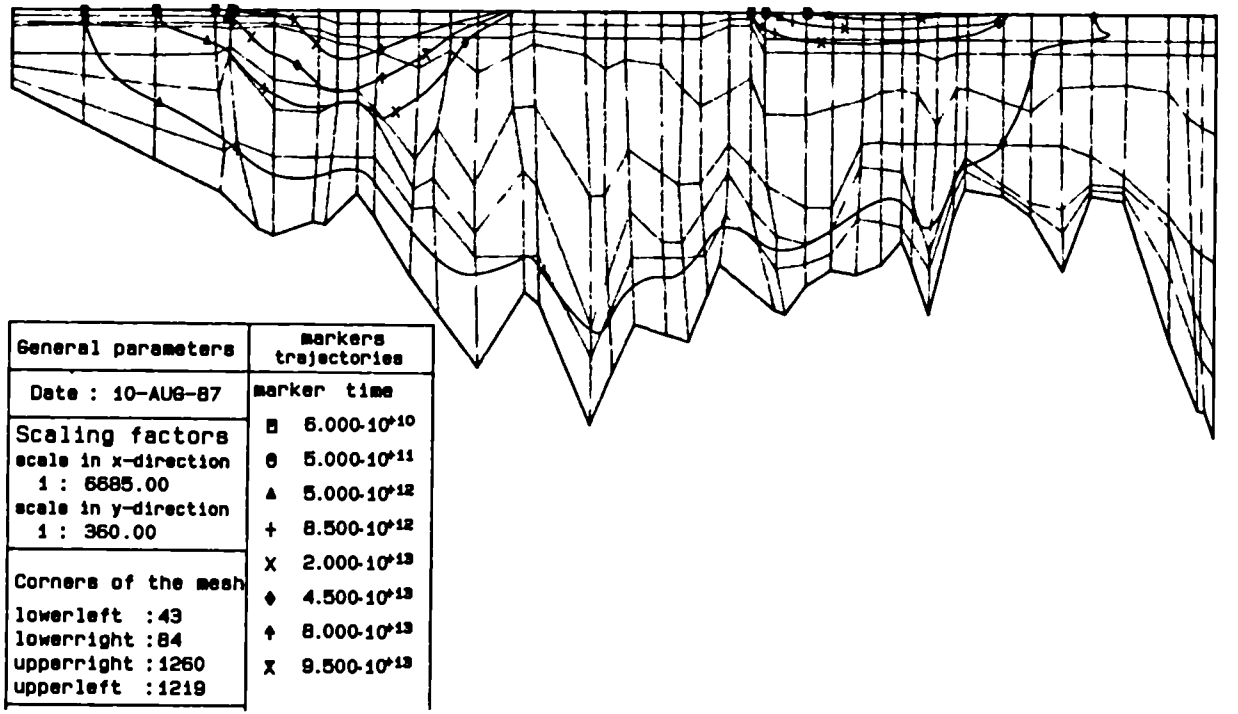

fig. 11 Model of a S - N cross-section through the NE Netherlands with trajectories starting from surface.

According to the model, the deep flow is determined mainly by topography on a larger scale than that of the Plio-Pleistocene groundwater system. The geological factors governing this deep flow in The Netherlands and adjacient areas are the height of the infiltration areas of the deep aquifers, the fault systems, and the extent of the aquifers. Locally, diapirism of salt can disturb this deep flow system. Breaks in the covering clay close to diapirs sometimes allow upward or downward flow. Depending on the head differences relative to the Plio-Pleistocene aquifer locally, e.g. in Reusel, water penetrates into the deep aquifer and mixes with the water originating from the outcrop area.

5. Conclusions

Interpretation of the findings of hydrological research in deep boreholes under study has led to the following conclusions:

- In one of the locations (Nieuweschans) the quality of the groundwater is determined by dissolution of rock-salt from diapiric salt.
- In another location (Broekhuizenvorst) strong indications were obtained for the presence of dissolved evaporites originating from Zechstein deposits to the east.
- The Br/Cl ratio seems to be a useful parameter for the identification of rock-salt dissolution.
- All of the investigated wells have a measurable ^{14}C content, which implies that the groundwater belongs to a hydrological cycle.
- ^{18}O isotope analyses corrected for evaporation effects offer a basis for estimation of the relative share taken by meteoric water in the investigated groundwater.
- Because boreholes elsewhere were not available, only flow in deep aquifers, within a zone of some tens of kilometres along the basin boundary could be established.

In view of the results obtained in these studies and with numerical models, it is concluded that there is reasonable agreement between the conductivity given by calibrated numerical models and isotope interpretation. Furthermore, although in general the deep flow can be expected to continue horizontally, as indicated by a large-scale model, infiltration by more recent water is possible locally in disturbed zones. For example this is the case close to salt diapirs.

REFERENCES

1. ZIEGLER, P.A., 1982. Geological atlas of Western and Central Europe. Shell Int. Petroleum Maatschappij B.V.
2. GLASBERGEN, P., 1985. The origin of groundwater in Carboniferous and Devonian aquifers at Maastricht, Geologie en Mijnbouw 64: 123-129.
3. BLESS, M.J.M. ET AL., 1981. Preliminary report on Lower Tertiary-Upper Cretaceous, and Dinantian-Famennian rocks in the boreholes Heugem-1/1a and Kastanjelaan-2 (Maastricht, The Netherlands). Mededelingen Rijks Geologische Dienst 35-15: 333-415.
4. SMAN, H.T., 1985. Een regionaal gehydrologisch modelonderzoek van de Centrale Slenk van Noord-Brabant. Rapport 840438003. Rijksinstituut voor Volksgezondheid en Milieuhygiene, Leidschedam.
5. FLINK, J., 1985. De verspreiding van arseen in het grondwater in Zuidelijk Noord-Brabant. Rapport 840348004. Rijksinstituut voor Volksgezondheid en Milieuhygiene, Leidschedam.

6. ROOIJEN, P. VAN, P. KLOSTERMANN, J.W.CHR. DOPPERT, C.K. RESCHER, J.W. VERBEEK, B.C. SLIGGERS, P. GLASBERGEN, 1984. Stratigraphy and tectonics in the Peel-Venlo area as indicated by Tertiary sediments in the Broekhuizenvorst and Gelderen T1 boreholes. Mededelingen Rijks Geologische Dienst 38-1: 1-27.
7. MICHEL, G., 1963. Untersuchungen über die Tiefenlage der Grenze Süsswasser-Salzwasser in nördlichen Rheinland und anschliessenden Teilen Westfalens, zugleich ein Beitrag zur Hydrogeologie und Chemie des tiefen Grundwassers. Forschungsber. d. Land. Nordrhein-Westfalen 1239, 123 p.
8. GLASBERGEN, P., 1981. Extreme salt concentrations in deep aquifers in The Netherlands. The Science of the total Environment 21: 251-259.
9. HERBERT, H.-J., W. SANDER, D. PANZER, 1986. Results of the geochemical survey programme accompanying the flooding of the potash salt mine Hope in Northern Germany. Solution Mining research Institute Autumn Meeting 1986, Amsterdam.
10. FRAPE, S.K. AND P. FRITZ, 1984. Water-rock interaction and chemistry of groundwaters from the Canadian Shield. Geochimica et Cosmochimica Acta 48:1617-1627.
11. GLASBERGEN, P., W.G. MOOK, 1982. Natuurlijke isotopen als hulpmiddel bij regionaal geohydrologisch onderzoek in de provincie Groningen. H_2O 15: 682-686, 704.
12. SAUTER, F., 1987. METROPOL, a three-dimensional model for groundwater flow and transport of pollutants; users manual, mathematical description. Report 728514002, National Institute of Public Health and Environmental Hygiene, Bilthoven.

NATURAL MINERAL ANALOGUES FROM A HYDROTHERMALLY ALTERED GRANITE

D.C. GREEN and V.A. GUTHRIE

Cambridgeshire College of Arts and Technology
and
Geology Department, University of Tasmania

Summary

Uranium, thorium and R.E.E. concentrations and distribution from a deep drill hole within the Coles Bay granite are being investigated using fission-track micromapping and electron microprobe analytical techniques, amongst others, in an attempt to provide a natural analogue of potential far field radionuclide movement. For example, uranium occurs in three mineralogical locales: 1. as background in quartz, fresh biotite and feldspars; 2. in resistate accessory minerals which contribute the greatest concentration of uranium, and 3. as minerals formed during hydrothermal alteration. Alteration minerals are dominated by Fe carbonates and oxides and Ti oxides (? anatase and secondary sphene), with chlorite and clays (phengite and sericite). The fission track distribution is mostly non-uniform and may be affected by further alteration indicating the dominant mechanism for fixation of uranium as adsorption and ionic exchange. These minerals are found replacing biotite or infilling fractures throughout the rock. Of these distributions, uranium associated with secondary minerals provides the most appropriate far-field analogue. Preliminary leach tests indicate preferential adsorption of 239-Pu from 239-Pu doped SYNROC onto these secondary alteration phases.

1.1 Introduction

A fully cored, 1008m deep vertical drill hole in the Coles Bay granite, an alkali feldspar granitoid on the east coast of Tasmania, Australia, permits a detailed mineralogical study of a typical high heat productivity granite with U, Th contents above 20 ppm. This pluton lies within a Devonian tin province and shows all gradations between a pale pink, porphyritic alkali granite with fresh biotite and a bright red granite with patches of pale green phengite. The nature of the alteration, fracture pattern and distinctive red colour suggest that this body is typical of granites that have suffered late stage hydrothermal alteration. In the core there are also small intervals of

fine grained, pink, phyric granite that appear to intrude the main body as shallowly dipping sheets. The phyric granites contain fresh muscovite (only slightly phengitic), are enriched in Rb and Y but depleted in Ba, Sr, Zr. Fluorite, tourmaline and siderite are common accessory minerals in the fine grained granite.

The drill site was selected on the basis of a γ-ray survey (Collins, Wyatt and Yeates, 1981) by the Bureau of Mineral Resources and the Geological Survey of Tasmania to identify areas of high K, U, Th activity. In general, these areas of heat-producing elements coincide with areas of tin/tungsten mineralisation in plutonic rocks. Regional gravity data suggests that the granite at Coles Bay extends to a depth of at least 5 km. Granite outcrops make up most of the Freycinet Peninsula, particularly on the seaward side of a major north--south fault, approximately parallel to the eastern coastline of Tasmania.

The hole was drilled by the Department of Mines, Tasmania, in 1982-83, with a Longyear 44 rig using NQ series wireline diamond core bits. Core recovery was essentially 100% and the 47.6 mm diameter core is stored at the Department of Mines store, Rosny Park, Tasmania.

1.2 Petrology

The altered biotite granite pluton at Coles Bay is one of the voluminous Devonian granitoids that intrude the Ordovician to Devonian quartzwackes and mudstones of the Mathinna Beds in N.E. Tasmania. The plutons range in composition from biotite-hornblende granodiorite to alkali (two mica) granites and form a major tin province (e.g. Groves et al., 1977). Similar rocks of the Blue Tier Batholith, to the north of Coles Bay, have been studied extensively in recent years and there is broad agreement that the Devonian granitoids of Tasmania were derived by melting of a variable protolith of Proterozoic rocks at different crustal levels and that within pluton variations were emphasised by fractional crystallisation, assimilation or restite unmixing (McCarthy and Groves, 1979; Cocker, 1982;, McClenaghan and Williams, 1982; and Higgins et al., 1985). The association of tin mineralisation with volatile and alkali-rich fluids (greisens) and the presence of an overlap between magmatic and post-magmatic, sub-solidus processes is remarked upon by most recent workers.

Over 80% of the core is of medium to coarse grained biotite granite, sometimes markedly porphyritic in K-feldspar with megacrysts up to 30 mm in length but more commonly with both K-feldspar and quartz phenocrysts in a coarsely equigranular texture. The colour varies from grey to bright red in colour. Fresh biotite is more abundant in grey granite and pink-red, clouded K-feldspar is associated with deterioration of the biotite and the development of a green, turbid colouration in the plagioclase (albite) of the groundmass in the 'pink' granites.

The other main rock type is a fine-medium grained equigranular microgranite with a saccharoidal texture. This is well developed between depths of 415 m and 480 m and between 536 m and 580 m where both the upper and lower contacts are gradational, and between 660.3 m and 679 m, and 708.5 to 724.3 m where the upper contacts are distinct but the lower contacts remain gradational. In the core, this rock type

occurs as sub-horizontal sheets. Examples of the boundary between the two major petrographic types are seen in road cuttings near the Coles Bay fishing wharf.

In thin-section, the K-feldspar is a microcline microperthite; fresh biotite is a red-brown siderophyllite but this is commonly replaced in the pink granites by green phengite or, more rarely, by chlorite. Anhedral plagioclase (albite) is almost invariably altered to some extent. Increased intensity of alteration is marked by an increase in the proportion of secondary phases as well as increased cloudiness in the K-feldspar megacrysts. Secondary phases include sericite/phengite, pale coloured biotite, carbonates, topaz, chlorite, tourmaline, fluorite, sphene, and quartz.

Samples of the Coles Bay granite dated by Rb-Sr and K-Ar techniques give ages of about 380 Ma. However, Cocker (1982) demonstrates evidence for open system behaviour in both whole rock and mineral isochrons, commenting "that the alteration and Rb-Sr metasomatism must have occurred within a short time of magmatic crystallisation for the preservation of linear isochrons".

In surface exposures and at the Coles Bay quarry, many authors have commented upon the gradational nature of the alteration where intensity of alteration ('reddening') is related to proximity to major joints and faults. This pattern of alteration is strongly evident in the core samples. It is clear that separation of a hydrothermal fluid has overlapped the formation of master joint systems in the cooling pluton.

1.3 Mineralogy

Fission track micromapping reveals that some of the primary U has undergone secondary redistribution into (a) brookite and "secondary sphenes" and (b) into microcracks filled with carbonates, Fe-Mn oxy-hydroxides and clay minerals. Three main distributions are evident (Guthrie and Kleeman, 1986);

1. Background U located within major rock forming phases such as quartz, fresh biotite and feldspars (see CB 869). The uranium appears to be associated with alteration minerals within these phases rather than in the crystal lattices of the minerals themselves. These concentrations constitute a minor contribution to total uranium content.
2. Resistate U contributes the greatest concentration of uranium, and is located within resistate accessory minerals. This uranium is usually uniformly distributed throughout the individual mineral grains and appears to be unaffected by any hydrothermal alteration, indicating its primary concentration within the crystal lattice (Fowler, 1981; Speer et al., 1981). The major contributing minerals are monazite $(Ce,La,Th)PO_4$, xenotime YPO_4, zircon $Zr(SiO_4)$, apatite $Ca_5(PO_4)_3(OH,F,Cl)$, ilmenite $FeTiO_3$, rutile TiO_2, pyrite FeS, polycrase and various other unidentified submicroscopic uranium/thorium-bearing minerals (see CB 869).
3. Secondary U located within alteration and secondary minerals formed during hydrothermal alteration also contributes significantly to total uranium within the granite. These are dominated by Fe carbonates and oxides and Ti oxides (? anatase and secondary sphene), with chlorite and clays (phengite and sericite) providing major contributions. The fission-track distribution is mostly non-uniform

and affected by further alteration indicating the dominant mechanisms for fixation or uranium as adsorption and ionic exchange (Bajo et al., 1983). These minerals are mostly found replacing biotite (see CB 963, CB 235), or infilling fractures throughout the rock (see CB 669).

Of these distributions, uranium associated with secondary minerals provides the most appropriate mineralogical analogue of radioactive waste disposal in the far field environment. Electron microprobe analyses of iron-rich secondary phases are of carbonates (Mn-bearing siderite) rather than oxides (e.g. hematite). These phases also commonly coexist with calcite (see CB 650).

The lack of uniform uranium distributions associated with these iron-rich phases and a tendency towards increased concentrations of U at the grain margins (see CB 423), indicates that the uranium may be held by adsorption and ionic exchange to the iron, or by complexing with $[CO_3]^{2-}$ ions (Tieh et al., 1980; Speer et al., 1981). This is particularly prevalent where the uranium distribution reflects the random occurrence of fracture infilling materials (see CB 423).

It is difficult to determine the nature of Ti oxide phase which appears to form as an alteration product of secondary sphene after biotite. Microscopically, it occurs as blue, weakly pleochroic euhedral crystals suggestive of anatase (see CB 270), or in poorly defined aggregations, possibly brookite (see CB 119). Fe is present in both 'anatase' and 'brookite' and some Ca (as a possible relict of the sphene) is also present.

The fission-track distribution relating to this Ti oxide phase indicates that it preferentially concentrates uranium (see CB 119, CB 270), and the patchy occurrences suggest adsorption as the mechanism for uranium fixation.

Other fracture infilling minerals which display patchy fission track registrations include phengite, sericite and chlorite (see CB 669). The phengite/sericite phase is often Fe-rich, and the associated chlorite is relatively Mg poor and Fe rich. The sorptive capacity of both these phases is well known (Zhmodik, et al., 1980) and is assumed to control uranium fixation.

1.4 Leach tests

Leach tests are being carried out on 10mm x 2mm granite discs in contact with SYNROC, and a SYNROC control sample held under MCC-1 test conditions at 70°C for seven days. Currently only alpha-particle mobility is being studied through 239-Pu-doped SYNROC. The activity of the leachate from each sample is measured using alpha-spectrometry and the degree of activity adsorbed onto the face of the granite discs is measured using the alpha-track etch technique.

Preliminary results indicate a loss of 239-Pu from SYNROC into solution (Levins and Smart, 1984), and adsorption of some of this activity by the granite discs. This adsorption is evident in the decreased activity of the leachate solution from the granite samples (compared to the SYNROC control sample), and high alpha track counts on the track detector from the granite face. Further experiments indicate higher activity on the granite face in proximity (<1mm) to SYNROC than on the face affected only by the circulating solutions.

The track etch technique also shows non-uniform distribution of alpha-particle activity on the granite face such as clusters, stars and

stringers. This may indicate preferential adsorption by individual mineral phases including secondary and alteration minerals. However, further experiments are necessary to confirm this conclusion.

1.5 Conclusions

Late stage (deuteric) alteration of the Coles Bay granite results in an enhanced capacity for uranium (and possibly 239-Pu) fixation. An increased sorption capacity for actinides combined with the low permeability of such hydrothermally altered granites, suggests that deep burial of radioactive waste within engineered barriers in such rocks may provide the reducing conditions, extremely slow groundwater movement and mechanical stability for effective retardation of radionuclide migration towards the surface. However, where minerals on joint planes are exposed to substantial chemical weathering near the surface, and to groundwater movement at depth, less stable interstitial adsorption sites permit removal of actinides readily and are, therefore, not an effective barrier.

REFERENCES

1. BAJO, C., RYBACK, L., and WEIBEL, M. (1983). Extraction of uranium and thorium from Swiss granites and their microdistribution, 2. Microdistribution of uranium and thorium. Chem. Geol., 39: 299-318.
2. COCKER, J.D. (1982) Rb-Sr geochronology and Sr isotopic composition of Devonian granitoids, eastern Tasmania. J. Geol. Soc. Aust. 29, 139-157.
3. COLLINS, P.L.F., WYATT, B.W. and YEATES, A.N. (1981). A gamma-ray spectrometer and magnetic susceptibility survey of Tasmanian granitoids. Unpub. Rept Dept Mines Tasm. 1981/41.
4. FOWLER, M.B., (1981). U content, distribution and migration in the Glendessary syenite, Inverness-shire. Mineral. Mag., 44: 443-448.
5. GROVES, D.I., COCKER, J.D. and JENNINGS, D.J. (1977). The Blue Tier Batholith. Bull. Geol. Surv. Tasm. 55, 171pp.
6. GUTHRIE, V.A. and KLEEMAN, J.D. (1986). Changing uranium distributions during weathering of granite. Chem. Geol., 54: 113-126.
7. HIGGINS, N.C., SOLOMON, M. and VARNE, R. (1985). The genesis of the Blue Tier Batholith, northeastern Tasmania, Australia. Lithos, 18, 129-149.
8. LEVINS, D.M. and SMART, R. St. C. (1984). Effects of acidification and complexation from radiolytic reactions on leach rates of SYNROC C and nuclear waste glass. Nature, 309: 776-778.
9. McCARTHY, T.S. and GROVES, D.I. (1979). The Blue Tier Batholith, northeastern Tasmania. Contrib. Mineral. Petrol. 71, 193-209.
10. McCLENAGHAN, M.P. and WILLIAMS, P.R. (1982). Distribution and characterisation of granitoid intrusions in the Blue Tier area. Pap. Geol. Surv. Tasm. 4, 32 pp.

11. SPEER, J.A., SOLBERG, T.N., and BECKER, S.W. (1981). Petrography of the uranium bearing minerals of the Liberty Hill Pluton, South Carolina: Phase assemblages and migration of uranium in granitoid rocks. Econ. Geol., 76: 2162-2175.
12. TIEH, T.T., LEDGER, E.B., and ROWE, M.W. (1980). Release of uranium from granitic rocks during in situ weathering and initial erosion (central Texas). Chem. Geol., 29: 227-248.
13. ZHMODIK, S.M., MIRONOV, A.G. and NEMIROVSKAYA, N.A. (1980). Uranium distribution in iron hydroxides from weathered mantle, as shown by α-radiography. Dokl. Acad. Sci. U.S.S.R., Earth Sci. Sect., 250 (6): 219-222.

A quantitative approach to exchange phenomena between low temperature hydrothermal solutions and granitic rocks: Methodology and preliminary studies in the Entraygues granite

P. Peaudecerf[+], A.M. Chapuis[°], M. Jébrak[+], B. Lemière[+], J.F. Sureau[+] and P.L. Blanc[°]

[+] BRGM (F) [°] CEA-IPSN (F)

The choice of a model analogue of a radioactive waste repository requires precise definition of the phenomena to be studied. The main problem to be solved by this approach is the development of low enthalpy geothermal systems near the repository, which would be likely to facilitate the migration of radionuclides towards the surface. A study has thus been undertaken on fossil geothermal systems in order to determine the various characteristics of migration of the elements analogous to the radionuclides (U, Th, REE, Sc, Sr).

While, in respect of the great number of possible geological parameters, the selected site should be as simple as possible, it should nevertheless meet a number of criteria regarded as essential for the purposes of the investigation:

1) A granitic setting.

2) A hydrothermal system including a low temperature phase, that was installed a considerable time after the end of the plutonic events.

3) Good quality outcrops with considerable lateral and vertical extent so that observations can be made on rocks unaffected by supergene alteration.

4) The presence of uraniferous minerals.

5) A light tectonism, preferably extensional, without significant cataclasis.

There are few sites in Western Europe that meet all these criteria. Consideration of possible sites in France showed that most have been affected either by significant cataclasis or by supergene alteration that has destroyed the hydrothermal parageneses. However, one site, at Foumbillou in the Lot valley, has been found to meet all the criteria.

The Foumbillou mineral occurrence is a metre-thick vein of chalcedonic quartz with traces of galena, marcasite, pyrite, baryte and uraniferous minerals. Zones of alteration one to five meters thick on both sides of the vein show variations in the behaviour of the elements according to the mode of circulation of the fossil hydrothermal fluids. The paper will give the first results of work in progress: recognition of the fluids forming the system, geometry of the exchanges and first implications for the storage studies.

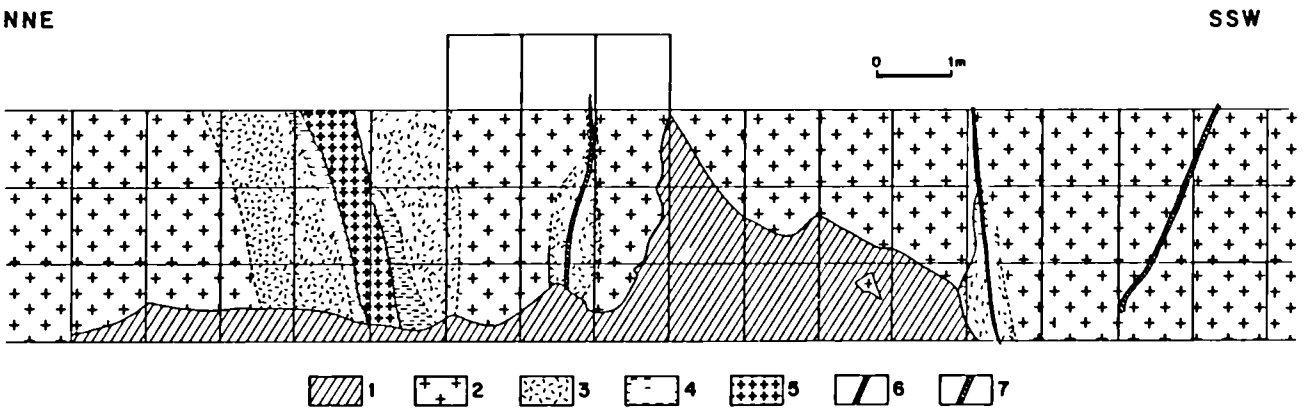

Cross-section through the Foumbillou mineralized system:

1. Loose earth
2. Porphyritic monzogranite
3. More or less developed pervasive weathering, muscovitization and chloritization of biotite
4. Mylonitization and argillation
5. Silica-bearing mylonitic zone with sulphur minerals, main vein
6. Dark silica vein
7. Pyrite - barite - illite vein

ENVIRONMENTAL TRACERS FOR VALIDATING PREDICTIVE MODELS*

J. PATYN, P. DEL MARMOL and M. MONSECOUR
Centre d'Etudes de l'Energie Nucléaire (CEN/SCK)

Summary

Since 1974 the Belgian Nuclear Research Establishment (SCK/CEN) at Mol has been studying the suitability of the Boom clay formation as a potential host formation to evacuate radioactive wastes.

In this context several models have been developed concerning the regional hydrology and migration patterns in the clay. The current research to validate these models by studying the environmental isotopes in both the Boom clay formation and the contiguous aquifers, is presented in this paper.

1.1. Introduction

Since more than a decade SCK/CEN has been studying, on its own site, the suitability of the Boom clay as a potential host formation for the disposal of conditioned high level and long-lived radioactive wastes from the Belgian nuclear power production.

As a support for the performance and long term safety assessments and for the general site reconnaissance in this project, a regional hydrological research programme has been developed to identify and to model the overall deep groundwater flow system around the Mol site. Extensive groundwater sampling as well on a regional scale as in an underground research facility within the Boom clay is performed in view of validating a hydrodynamic model by hydrochemical and tracer studies.

1.2. Hydrogeological research programme

A hydrogeological investigation in the region around Mol, covering an area of about 2,500 km² has been focused on getting a precise picture of the groundwater flow system and the geological structure.

* Study performed in the framework of contracts granted by the Commission of European Communities and by NIRAS/ONDRAF, as part of the current SCK/CEN R&D-programme on radioactive waste disposal into argillaceous formations.

The regular gently dipping layered sequence of alternating confining formations and sandy aquifers was confirmed by numerous borings in the area.

Throughout the whole studied area (Fig. 1), 132 hydrological observation wells have been installed, which allow the monitoring of the piezometric heights for the aquifers. These wells allow also a geochemical sampling of the different water bearing strata, and appropriate procedures have been developed to get these samples as representative as possible.

Because of their importance for the identification of the groundwater flow, the observation wells have also been used to determine the hydrodynamic characteristics of the confined aquifers. Mainly slug tests and single well pumping tests have been performed, and although such methods offer results with lower accuracy, the main interest for a regional study was given to the spatial variability of these parameters, rather than to accurate tests which yield only punctual information.

In the neogene aquifer overlying the Boom clay, the overall transmissivity has been calculated by a simple inverse model, that has been used to analyse the natural fluctuations of the water level in the observation wells. Transmissivity values obtained from this approach match very well with those calculated from classical tests in the aquifer.

On the basis of geological and hydrogeological observations, the regional aquifer system has been conceived as a multilayered system consisting of three main aquifers : the water table aquifer of the neogene sands, the confined rupelian aquifer underlying the Boom clay and the bruxellian sands, separated from the former aquifer by the bartonian clay. In the model it is assumed that a Darcyan porous-medium flow occurs in the confining formations which allow a vertical connection between the aquifers.

The behaviour of the system has been simulated by means of the NEWSAM-model, developed by Ecole Nationale Supérieure des Mines de Paris. These simulations allow to reproduce very well the observed hydraulic heads, and, as a result, the general flow scheme of Fig. 2 has been obtained to describe the whole aquifer system. The natural flow in the aquifers is determined by the drain potentials in the outcrop areas, and is directed from east to west. In the eastern part of the studied region, analysis of the regional groundwater flow indicates a downward movement through the Boom clay, whereas in the western part calculations point out that leakage flow is directed upward.

However the fact that a model simulates the observed hydraulic data does not necessarily imply that the model is correct, since in most groundwater systems there exist sufficient degrees of freedom, so that one unique solution can hardly be determined. Therefore additional information emerging from hydrochemistry and isotope hydrology has been used for validating the model concept.

1.3. Natural tracers for the verification of the model

Hydrochemistry and isotope hydrology can provide information on type, origin, age and history of groundwater. Origin deals with location, period and processes of recharge, while history deals essentially with mixing and salinization processes and flow path.

The most commonly used isotopes for this purpose are those which are a constituent of the water molecules (^{18}O, ^{2}H, ^{3}H) and other environmental isotopes (^{14}C, ^{13}C, ...) which occur in dissolved compounds.

In the studied area, ^{14}C-activities were measured in the aquifers above and below the Boom clay, and the measured activities have been linked with the data emerging from the hydrodynamic model. It was found that ^{14}C activities could not be explained solely by horizontal flow originating from the outcrop area, nor by alternative model concepts that assume a hydraulic contact between the neogene and rupelian aquifer in the eastern part of the region. On the other hand calculations show that measured activities match well with leakage velocities derived from the hydrodynamic model, if an effective porosity of about 1 %, and an hydraulic conductivity of 10^{-10} m/s.

Groundwaters have also been analysed for major and trace elements and for stable isotopes. As far as the hydrochemical behaviour of the system is concerned, preliminary analyses have been made on the characterisation of the various groundwater types and the TDS-content. In a first stage, methods have been looked for that could allow for an easy discrimination of distinct water types. By representing the overall chemical composition of the groundwaters in a Piper trilinear diagram, it has been concluded that most of the groundwater above the Boom clay belongs to the calcium carbonate type, while groundwaters below the Boom clay are to be classified as sodium carbonate or sodium chloride water types.

The TDS-content has been determined on samples from the wells installed in the rupelian aquifer, which are geographically located along an E-W profile and thus are essentially parallel to the E-W groundwater flow. This flow line has been selected because these wells might be indicative for a relation between the flow system and the hydrochemistry. Although the groundwater in the rupelian aquifer is known to flow from east to west, and one would expect an increasing TDS-value along the same direction, TDS-content is decreasing along the flow direction (Fig. 3). This phenomenon could be explained by mixing with fresh water, leaking through the Boom clay, but on the other hand secondary slightly soluble compounds in the rupelian aquifer cannot be ruled out. Therefore, research is still going on to see whether formation of secondary minerals is likely to happen or not.

1.4. Local research

If there really exists a convective groundwater movement in the Boom clay, the convincing arguments should be given by the composition of the interstitial clay water.

For that purpose more than 20 piezometers consisting of sintered metal screens have been installed in the vicinity of the underground research facility at various depths and along various inclinations. These piezometers are mainly used to collect representative interstitial water samples under strict anaerobic conditions for accurate chemical analyses, ^{14}C-measurement and U/Th isotopic ratio determinations ; they allow also to monitor the hydrostatic pressure around the underground facility and to derive values for hydraulic conductivity.

Earlier samples analysed for ^{14}C revealed a detectable activity, indicating apparent ages of the water of the order of 30,000 years. Nevertheless, these results need further confirmation as obtained values are very close to the detection limit of the method used. Therefore, the interstitial clay water tapped from the installed piezometers are being analysed for ^{14}C-activities to verify whether a downward age gradient can be found or not ; in the same way, the behaviour of other trace elements (B, U) is investigated.

REFERENCES

1. BAETSLE, L.H., BONNE, A. and DEJONGHE, P. (1986). The Hades demonstration project for radwaste disposal in deep clay. Int. Conf. on Radioactive Waste Management. Winnipeg, Sept. 7-11, 1986
2. PATYN, J. (1985). Contribution à la recherche hydrogéologique liée à l'évacuation de déchets radioactifs dans une formation argileuse. Ph. D. Dissertation. CIG, Ecole des Mines de Paris, 1985
3. del MARMOL, P. et al. (1986). Groundwater dating by C-14 in the vicinity of a potential clay repository for radioactive waste disposal. ENC-conference, June 1-6, Geneva, 1986

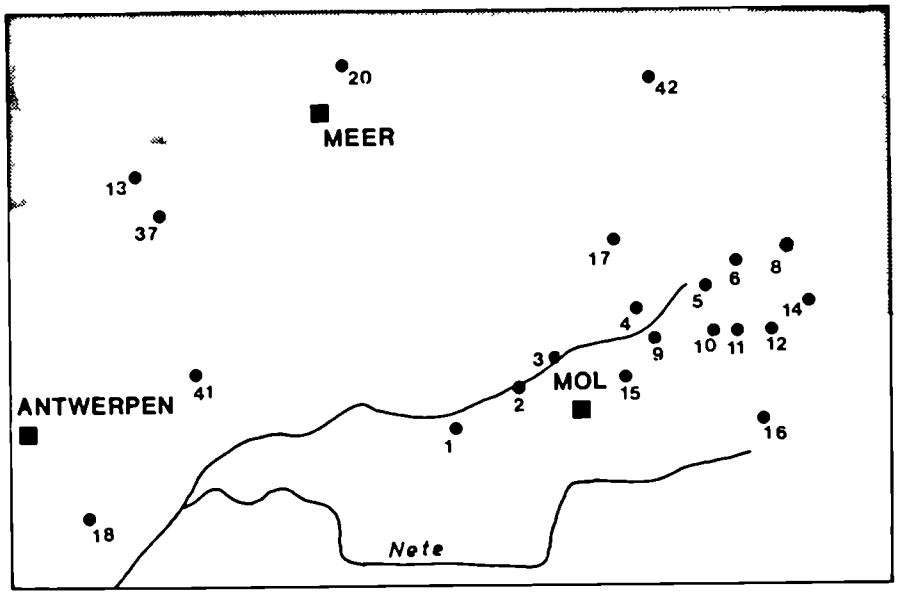

FIG. 1 : LOCALISATION OF OBSERVATION WELLS

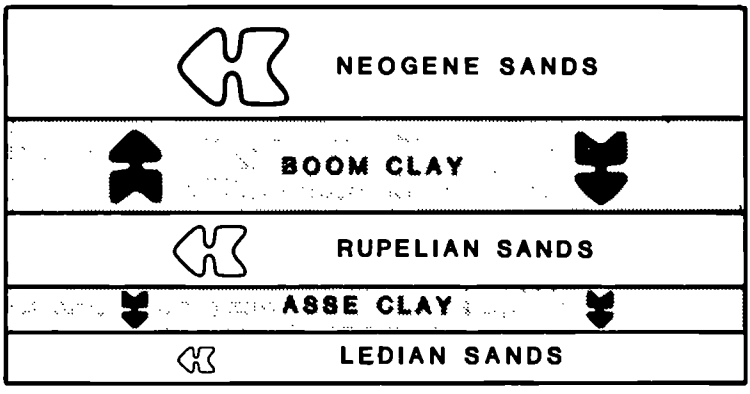

FIG. 2 : GENERAL FLOW SCHEME FOR MULTILAYERED AQUIFER SYSTEM

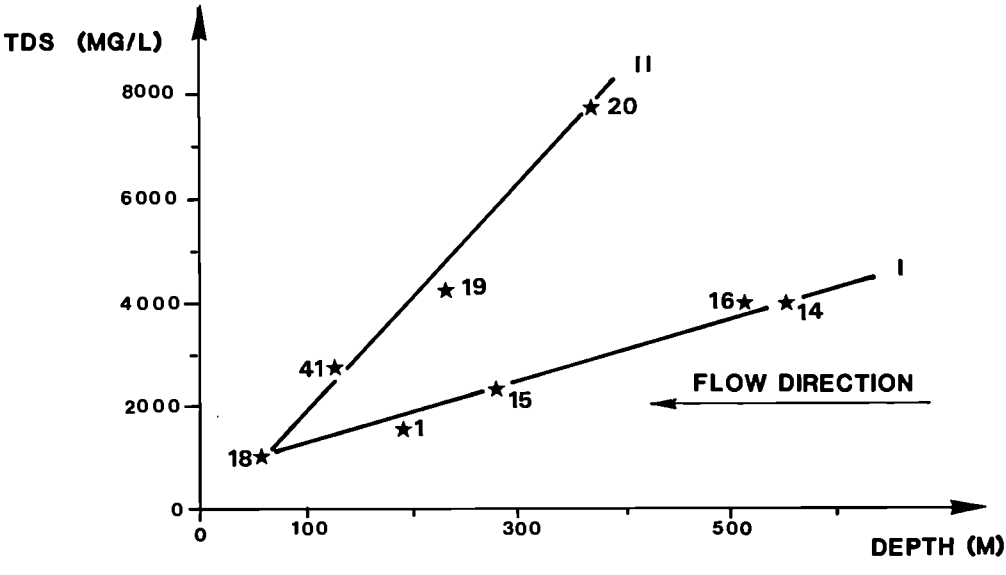

FIG. 3 EVOLUTION TDS-CONTENT RUPELIAN AQUIFER

HYDROTHERMAL ALTERATION IN THE AURIAT GRANITE (MASSIF CENTRAL, FRANCE): ANALOGY WITH A RADWASTE DISPOSAL

JC. PARNEIX, M.T. MENAGER, L. TROTIGNON, JC. PETIT
SESD/LECALT, CEN-FAR, BP 6, 92265 Fontenay-Aux-Roses Cedex, FRANCE

I. INTRODUCTION

Hydrothermal systems in granites offer the opportunity of estimating the possible effects of fluid circulations in an intragranitic nuclear waste repository. Indeed, information on both the alteration of primary minerals as well as its link to fissure density, and remobilisation of trace elements such as actinides and rare earths are of prime importance for assessing the efficiency of granite as a geological barrier from both the tectonic, petrol gic and geochemical viewpoints (CEA report, 1981).

In order to answer some of these questions, we have investigated the hydrothermal alteration of the Auriat granite (Massif Central, France) where a fossil geothermal system of short duration has been active 270 MY ago. This batholite has been chosen because it is located in a quite well known geological area and because an exceptionally long drill-core (1000 m) was available. A double analogy appears possible between such a natural system and a radwaste disposal : first the circulation of fluids induced by some geological heat source, its associated alteration phenomena and the consequences of the heat period (≈ 1000 yrs) in a repository; second a comparison between the migration behaviours of radiotoxic nuclides and their chemical analogue elements.

The Auriat granite is localised in the northwestern part of the Massif Central. Its setting has been dated at 324 MY by the U Pb method applied to monazite grains (GEBAUER et al., 1981). This granite is a part of several granitic massifs intruded in the Massif Central at the end of the upper visean. It is in contact with older metamorphic units such as carboniferous gneisses to the north and silurian or ordovician micashists to the south (AUTRAN, 1980). The Auriat batholite has a surface area of approximately 80 km^2.

II. EXPERIMENTAL METHODS

Fourty samples were collected along the drill-core, peculiarly at depths where fissures and their altered borders were clearly visible. Thin sections were prepared systematically. As alteration takes place at varying scales from cm-sized fissures down to sub µm-sized ones, a specific experimental approach has been developed which is described in detail elsewhere (PARNEIX and PETIT, 1987 . Our procedure combines techniques which give textural, morphological, crystallographical and chemical information on very small quantities of matter studied inside fissures or on their borders. Indeed, we used optical and scanning electron

microscopies, energy dispersive X-ray and electron microprobe analysis as well as a micropicking technique followed by step-scan X-ray diffraction initially elaborated by BEAUFORT et al. (1983) which allows the crystallographic identification of micro quantities of matter (0.001 mg). The micro-mapping of uranium was performed with the fission track method ; the microdistribution of thorium and rare earth elements was obtained by means of the Energy Dispersive X-ray device attached to the scanning electron microscope. Finally, modeling of the various alteration parageneses was achieved with the EQ 3/6 computer code written by WOLERY (1979). This code allows both the calculation of element speciations in solution and reaction paths for dissolving minerals and precipitating new phases.

III. RESULTS AND DISCUSSIONS

The investigation of the Auriat geothermal system allows to infer very useful data for assessing the retention capacity of granite as a geological barrier in a nuclear waste repository. Indeed, information on the anisotropy of the fissure network, the nature of secondary parageneses, the intensity of alteration as well as the mobilisation of selected analogue elements (U, Th and REE) can be obtained. In addition, the modeling of water-rock interactions by means of EQ 3/6 gives rough estimates of the alteration time necessary to produce the observed parageneses and the variations of rock porosity with increasing degree of alteration. We will now discuss in detail each of these topics.

1. Anisotropy of the fissure network

It is already well known that fissures in granite are very heterogeneously distributed at all scales. Their orientation and density depend on the tectonic constraints to which the batholite has been subjected during its setting and during posterior regional events. Accordingly, the Auriat fissure network is extremely anisotropically distributed and consists of two main types of fissures : the first one is constituted of µm-sized to cm-sized subvertical fissures which intersect both the unaltered parts of the granite and those affected by a pervasive chloritisation of biotites. The second one consists of sporadically distributed subhorizontal fissures with a size ranging from about 10 µm to one cm. These fissures intersect all other ones and are therefore posterior to the first type. The density of both types of fissures remains constant all along the 1000 m-drill core. Therefore, the variations observed in the nature and intensity of hydrothermal alteration are independent of the geometric characteristics of the rock and are to be correlated only with the physico-chemistry of water/rock interactions. This fissure network has been studied by the CEA/BRGM (CEA report, 1981) and correlations with the regional tectonic have indeed been found. We will not describe in greater details this fissure network, mainly because only two drill-cores are available in this granite, which is clearly not sufficient to fully characterise the fissure distribution at the batholite scale. Nevertheless, it is worth underlying again that fissures, which will potentially conduct fluids from the repository toward the biosphere will likely be extremely heterogeneously distributed in most rocks of this type.

2. Secondary parageneses

Our petrographic observations show that biotite and plagioclase are the two most altered primary constituents of granite. We have evidenced three main steps of hydrothermal alteration from which clues about the

range of temperatures f mineral crystallisations can be inferred :

- the pervasive chloritisati n f biotites, which is the first step, leads t the transf rmation of primary biotites into chlorite type I , rth se and a titanium oxide. It is ubiquitous al ng the drill-core, except around 230-290 m and 8 -1 0 m. This mineralogical reacti n occurs at the sites of biotites with no change in the Mg Mg + Fe ratio and, m re broadly, with no external input f matter except water PARNEIX, 1987 . This phenomen n is due to an unknown heat source and cannot be correlated to a precise geol gical event. It is usually considered (TURPIN, 1984 , based on 180 160 data, that the fluid resp nsible for this transf rmati n has a meteoric origin and impregnates the micro-fissuration of the rock. The temperatures estimated by this author for this phen menon 45 -350 C , are largely greater than th se expected in a nuclear waste repository < 2 0°C and hence we will n t consider this type of alteration in our analogic approach.

- The hydr thermal alterati n in subvertical veins occurs next, and leads to two different parageneses according to the nature of the initial rock :
  - the unaltered granite gives schematically a K-feldspar-epidote-chlorite type II) - sphene-fluorite assemblage between 800-1000 m. Around these K-Feldspar veins, the alteration extends to a few millimeters in defining three zones : i. in the first one, close to the vein, chlorite completely replaces biotite in association with sphene, epid te and sometimes flu rite ; ii. in the second one, biotite is only partially chl ritised and associated minerals are similar ; iii. in the third one, which constitutes a transition with the unaltered rock, crystals of epidote are bserved. Between 230 and 290 m K-feldspar is associated with chlorate, pyrite, fluorite, a chlorite-smectite interstratified (corrensite type) and calcite. The balance of the chemical reactions associated with these transformations imply the input of silica, potassium and carbonic gas in the system, likely brought by the fluid PARNEIX, 1987).

  - The pre-chl ritised granite mainly leads to an illite-dolomite-hematite associati n. X-ray diffracti n sh ws that these veins also contain a disordered smectite-illite interstratified with 60 % smectitic layers. Between 400 and 800 m, quartz, pyrite and chalcopyrite are also associated to illite. In addition, in the upper parts of the drill-core, dioctahedral phyll silicates occur instead of illite, namely a disordered illite-smectite interstratified with 20 % smectic layers (146 to 219 m) with dolomite in the middle of veins. Chlorites type I) are also transformed into kaolinite, a disordered illite-smectite interstratified with 60 % smectitic layers, ankerite and d lomite. Finally, between 172 m and the surface, a dioctahedral chlorite replaces the illite-smectite interstratified. This transformation where the ISII-type illite-smectite interstratified has been considered as illite implies the input in the system of silicon, potassium, protons and carbonic gas PARNEIX, 1987). Around these veins an alteration zone 10 to 40 mm-wide is noted in which the Ca-rich parts of plagi clase are transformed into two superimposed interstratified minerals, namely one of the ISII-type reflecting a temperature range 16 -22 C and an IS one formed at a lower temperature ~ 100 -130 C. Around veins, the

fraction of smectitic layers varies from 5 to 8 % for the first type and from 60 to 40 % for the second one towards the bulk unaltered rock. These features have been interpreted by PARNEIX (1987) as reflecting the superposition of two temperature gradients linked to the cooling history of the geothermal system.

The K-containing minerals present in these subvertical veins have been dated in collaboration with Montigny (IPG, Strasbourg) on four samples (368, 396, 311 and 960 m) by the K-Ar method at ≃ 270 MY, i.e roughly ≃ 50 MY after the setting of the batholite. Therefore, this alteration has not been induced during its cooling. Rather, PARNEIX (1987) has attributed the functioning of a geothermal system at Auriat to the thermal flux linked to the injection of lamprophyres which, reportedly (FRIEDRICH, 1984), have intruded the granites of this region in the range 240-290 MY. Indeed, LEROY and HOLLIGER (1984) have dated the pitchblende-pyrite mineralisation of the adjacent St SYLVESTRE massif by the U-Pb method at 276 MY and correlated the U-mobilisation to the injection of observable lamprophyres.

Relatively precise estimates of temperatures can be deduced from the observed parageneses. In fact, a decreasing temperature gradient ≃ 150°C/km from the bottom to the top of the drill-core can be inferred from our observations : a chlorite epidote-sphene assemblage, similar to the propylitic alteration, is indicative of a temperature range 350-250°C (LOWELL and GUILBERT, 1970). Illite proves a temperature range 300-200°C (VELDE, 1985), whereas corrensite is formed between 200-280°C (HENLEY and ELLIS, 1983) and the illite-smectite (20 %) interstratified between 140-180°C (SHRODON and EBERL, 1984).

The alteration in subhorizontal veins is the last hydrothermal event to which the Auriat granite has been subjected. The corresponding parageneses are superimposed on all types of previously developed alterations. These veins, sporadically distributed along the drill-core are mainly composed of carbonates, namely ankerite and siderite. Accordingly, the writing of the corresponding chemical reaction necessitates a huge amount of carbonic gas brought by fluids. Around these veins, the alteration zone of a width ≃ 100 µm, shows kaolinite and ankerite replacing chlorite whereas siderite substitute pyrite. In addition, biotites are replaced by a disordered illite-smectite interstratified with 60 % smectitic layers; plagioclases can be moderately altered into kaolinite and an illite-smectite interstratified with 65 % smectitic layers. This type of alteration is likely associated with a low temperature (≃ 60°C).

The description of the various parageneses that occurred during water/rock interactions in the range 400-25°C is extremely interesting for understanding the processes of granite alteration but cannot be straighforwardly extrapolated to a repository until the fluid composition is determined. Modeling with EQ 3/6 has been performed at different temperatures on both the unaltered granite (300°C and 200°C corresponding to 800 and 200 m, respectively) and the previously chloritised one (200°C). We have chosen a composition of the fluid typical of average granitic waters (table 1, from BROOKINS, 1984). As observed, only two mineral couples were assumed to dissolve, namely biolite-plagioclase in the unaltered rock and chlorite-plagioclase in the pre-altered one. The lack of thermodynamic data in EQ 3/6 for solid solutions have pushed us to some simplification of the dissolution process. For plagioclase, where the Ca-rich is consistently the most altered part, and as sodium is not

incorporated in any new phase, we have used the anorthite end-member in our dissolution modeling, although oligoclase is present at Auriat. Similarly, biotite has been m deled by the annite and phlogopite end-members. In our computer runs, we let EQ 6 choose, the stable mineral assemblages at each temperature between the 25 phases actually formed at Auriat. Unfortunatly titanium compounds could not be simulated as our data base is incomplete as regards these minerals. Completion of this data base is in progress.

Our main results (table 2 indicate a reasonably good agreement between our simulations and the parageneses actually observed inside veins. Some minor discrepancies are however noted, which are discussed elsewhere (PARNEIX, 1987).

Two important implications for the analogy with a nuclear waste repository can be drawn from these simulations :

i. EQ 3/6 has proved to be an efficient code for simulating water/rock interactions in a complex natural system. It gives us confidence in applying it to the prediction of secondary phases susceptible to occur in a repository during the interaction fluids technological barriers rock.

ii. The parageneses observed at Auriat for temperatures $\leq$ 200°C are to be expected in the far field of a nuclear waste disposal where the effect of technological barrier dissolution on the composition of fluids should be negligeable. Hence, when trying to assess the retention capacity of the geological barrier sorption or mineralisation of radionuclides, variations of porosity, etc...) this type of minerals should be considered (see 3). Provided that the necessary thermodynamic data are available for specific minerals, it could also be used for the prediction of parageneses in the near field where the dissolution of technological barriers probably affect dramatically the composition of fluids. In particular, a marked improvement of the data base will likely have to be made, for example for iron and boron compounds originating fr m the corrosion of canisters and from the dissolution of nuclear glasses, respectively.

iii. The time of alteration expected to produce a given secondary paragenesis can also be simulated with EQ 3 6 and gives some hints on the duration of the geothermal system. To achieve this goal, we let the code dissolve anorthite and biotite, which again are the least corrosion-resistant primary minerals of granite. Their molar proportions were chosen on the basis of our petrographic data on the Auriat granite ; their respective kinetics of dissolution were taken from the literature. The kinetics of anorthite used was the value proposed by FLEER (1982) at 25°C (5.6×10^{-13} mole $cm^{-2}.s-1$) and extrapolated at 300°C, assuming an activation energy similar to that measured for quartz by RIMSTIDT and BARNES (198). This estimate leads to a value ~ 10^{-7} $mole.cm^{-2}.s-1$, also used for biotite for which, unfortunately, no reliable experimental data are available. Assuming that a fissure can be simulated by an elongated parallelepiped with a mean width ~ 0.3 mm, its length was calculated for having a volume of contained solution of one liter (this constraint is imposed by the code). The reacting surface area was estimated as the fraction of the fissure surface occupied by anorthite and biotite, thus defining a surface area upon volume ratio, then injected into EQ 3/6.

Species	Concentration (mole/l)
Na^+	7.57×10^{-3}
K^+	2.56×10^{-4}
Ca^{2+}	2.48×10^{-4}
Mg^{2+}	4.09×10^{-7}
SiO_{2aq}	1.21×10^{-4}
CO_3^{--}	5.57×10^{-6}
Cl^-	7.98×10^{-3}
SO_4^{--}	6.66×10^{-19}
HCO_3^-	7.46×10^{-5}
HS^-	1.96×10^{-4}
pH	9.03
Eh (V)	- 0.47
$Logf O_2$	- 76.8

Table 1 : Composition at 30°C of the granitic water used in our EQ 3/6 simulations (from (BROOKINS, 1984).

TYPE OF ROCK	TEMPERATURE (°C)	PARAGENESES	
		NATURAL SYSTEM	EQ 3/6 SIMULATION
UNALTERED GRANITE	300	K-Feldspar - Epidote - Chlorite - Ca-Saponite (± sphene and fluorite)	K-Feldspar - Chlorite - Epidote - Saponite Ca
	200	K-Feldspar - Pyrite - Fluorite - corrensite - calcite - chlorite	K-Feldspar - Chlorite - Pyrite - Calcite
CHLORITISED GRANITE	200	Illite - Dolomite - Hematite	Illite - Dolomite - Hematite

Table 2 : Comparison between the parageneses simulated by EQ 3/6 and those observed in subvertical fissures at Auriat.

Our results show first a good agreement with observed parageneses corresponding to the propylitic-like alteration (see above) and second that the system reaches equilibrium after an incredibly short period of time ; indeed the solution appears saturated for anorthite after only a few seconds. The whole quantity of anorthite actually destroyed in the alteration zone around fissures would then be dissolved in an estimated time of 36 min. Even if one assumes errors in the determination of simulation parameters (dissolution kinetics, water/rock ratio, evolution of affinity during dissolution, etc...) by several orders of magnitude, it remains that the formation of alteration parageneses actually observed is an extremely quick phenomenon compared to other time spans characteristic of geological phenomena. Therefore, PARNEIX (1987) has concluded that the Auriat geothermal system has probably functioned via a great number of hot water pulses of very short durations similarly to geysers. As regards the implication of such a finding for a repository, we expect that both the decrease of porosity and the increase in the retention capacity of the rock due to secondary minerals will occur rather quickly after the start of fluid circulation.

3. INTENSITY OF ALTERATION

Alteration is relevant to the efficiency of the geological barrier in a disposal because it affects two major characteristics of the rock, namely its mineral constituents and, through volumic changes associated with mineralogical transformations, its porosity. For assessing the variations of the retention capacity due to alteration, it is necessary to identify, for given water rock conditions, the nature and quantities of each secondary comp nent susceptible either to sorb or incorporate radiotoxic nuclides, and to evaluate the rock permeability. The study of a natural geothermal system can greatly help making this estimate. Indeed, our observations at Auriat leads to the following comments :

i. alteration is ubiquitous in all open spaces at all scales (fractures, fissures, grain boundaries, etc...), reflecting the circulation of fluids. All pore spaces in altered zones are usually totally filled with secondary products. For instance, intragranular fluid inclusions are remnants of a flow of solutions down to a µm-scale. Contrary to fractures or fissures down to a millimetric size, which should be quite easy to quantify, the density of micropores and its contribution to the overall mass transfer, is very difficult to estimate and is a subject of current research (SIMMONS and CARUSO, 1983). However, one should note that dissolution/recristallisation processes often induce a decrease of porosity and therefore of the rock permeability (VAUGHAN et al, 1986) which is reportedly attributed to the precipitation of secondary products inside fissures. One can conclude that circulation of fluids is not necessarily detrimental to the safety of the repository on long time spans.

ii. alteration around fissures appears to be limited to a width of a few millimeters up to about one centimeter. Indeed, we have shown the existence of an empirical linear relation (figure 1) between the ratio : width of alteration upon thickness of fissures (A L) and the temperature of the fluid inferred from the mineral assemblage present within the fissure. For instance, a maximum temperature ≃ 150°C in a repository would lead to an A L ratio ≃ 5 with a rock similar to the Auriat granite, i.e. an alteration zone ≃ 5 mm-wide around millimetric veins. Of course, the intensity of alteration around veins is rock specific and strongly depends in particular on its texture. PARNEIX (1987) has demonstrated that the intensity of alteration around fissures at Auriat has been likely restricted by the diffusion of water through the rock rather than by thermal conductivity. This very small width of alteration also suggest that, for the composition of circulating fluids at Auriat, the contribution of the microporosity to the mass transfer should have been relatively limited. It should be stressed that, f r solutions strongly undersaturated with quartz and in very peculiar geochemical conditions (CATHELINEAU, 1987), alteration can occur on much large scales, such as during the episyenitisation of granites. However, for a given granitic site, the intensity of alteration to be expected could be deduced from establishing such an A L = f(T) relation for ancient geothermal alterations.

iii. The quantities of each secondary mineral and the variations of porosity due to alteration can be estimated at each temperature with the following procedure. First the modal and chemical composition of the rock must be known as well as the chemical composition of the fluid with which it will interact. The porosity has to be evaluated, for instance by means of Hg-porosimeter measurements or image analysis

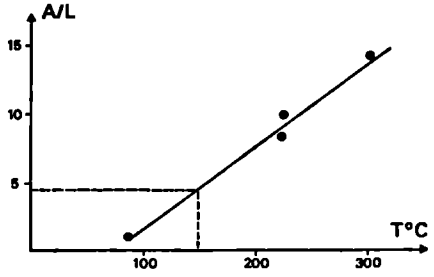

Figure 1 : Empirical relation between the ratio width of alteration upon thickness of fissure (A/L) and the temperature of the fluid in the Auriat granite.

Temperature (°C)	Nature and Mass (kg) of minerals		K_d (m^3/kg)		
			Cs	Sr	U
60	Dolomite	0.69	0.007	-	-
	Ca-Montronite	1.09	0.388	0.187	0.325
	I/S 90 %	2.74	0.545	0.150	0.531
	Rutile	0.07	-	-	-
	Quartz	5.64	0.001	0.001	0
	K-Feldspar	4.04	0.009	0.002	-
	Albite	4.20	0.009	0.004	-
	Muscovite	0.72	0.015	0.005	0.459
140	Chlorite(Ripidolite)	3.60	0.129	0.002	0.524
	Hematite	0.85	0.002	0.004	-
	Calcite	2.01	0.007	-	0.007
	I/S 20 %	10.38	0.400	0.080	0.524
	Rutile	0.29	-	-	-
	Quartz	22.57	0.001	0.001	0
	K-Feldspar	16.16	0.009	0.002	-
	Albite	16.82	0.009	0.004	-
	Muscovite	2.90	0.015	0.005	0.459

Table 3 : Nature and mass of minerals implied in the complete alteration at 60°C and 140°C of the 1 m^3 of granite (see text) and corresponding sorption capacities for Cs, Sr and U.

Radioelement (concentration in fluid)	Temperature (°C)	Estimated variation of porosity (%)	Mass of radioelement fixed by 1 m^3 of granite (mole)
Cs (10^{-5} Mole/l)	60	- 9	2.06×10^{-2}
	140	- 23	4.93×10^{-2}
Sr (10^{-5} Mole/l)	60	- 9	6.4×10^{-3}
	140	- 23	9.76×10^{-3}
U (10^{-7} Mole/l)	60	- 9	2.08×10^{-4}
	140	- 23	8.6×10^{-4}

Table 4 : Estimated decrease in porosity and sorbed quantities of Cs, Sr and U on 1 m^3 of granite at 60°C and 140°C.

on resin-in ected samples. In particular the fraction due to fissures of sufficient width 0.01 to 1 mm) to efficiently contribute dissolution must be estimated. The amount of rock subjected to a given temperature can be estimated from the thermal flux of wastes disposed in the repository and geometric parameters. For each temperature and given chemical rea tions, EQ 3 6 then allows to predict the stable mineral assemblages, the quantities of dissolved primary minerals and of each new phase. By substraction of the corresponding weighted sum of specific volumes, a variation of porosity can then be deduced. Finally, sorption data and crystallochemical data from the literature permit a rough estimate of radionuclide fixation for each secondary phase and hence the assessment of the retention capacity of the altered rock.

Such a procedure has been applied by PARNEIX (1987) to the Auriat granite. One can deduce from these results summarised in table 3 and 4, that, in the water rock conditions simulated, the alteration of granite leads to the formation of much more sorbing phases than primary minerals and a significant decrease of porosity. Henceforth, hydrothermal alteration should be beneficial for the retention capacity of the rock.

4. MOBILISATION OF U, TH, AND REE

We have also started an investigation of the microdistribution of uranium, thorium and rare earths as well as their mobilisation during the different stages of hydrothermal alteration described in the preceding sections. These elements are currently considered as possible chemical analogues of transuranic elements (CHAPMAN and SMELLIE, 1986) : for instance LRRE(III) for Pu(III), Am(III) and Cm(III), U and Th for the various species of Np, Th(IV) for Pu(IV), U(IV) for Pu(IV) and U(VI) for Pu(V). Our preliminary results, which could have interesting implications for the migration of actinides in a repository, are the following :

i. The range of concentrations in uranium, thorium and light rare earths (La) are 13-30 ppm, 10-20 ppm and 10-40 ppm respectively. In the Auriat granite, the main accessory minerals are uraninite, monazite, zircon, apatite, thorite, and scarce allanite. These minerals are relevant to the migration of actinides in a repository from two viewpoints : firstly, some of them are susceptible to dissolve during hydrothermal alteration and to release their U, Th and REE constituents ; all these elements could compete with transuranic elements for sorption or mineralisation in secondary phases. An oversimplified evaluation pinpoints the potential importance of this phenomenon. Let consider a 1 mm-wide fissure which would be altered at 150°C on a thickness ≃ 5 mm (see 3). If one assume that all U, Th and REE incorporated in accessory minerals present in this alteration zone are leached towards the fissure, we can easily calculate that concentrations ≃ 1000 ppm of these elements could be released in the fluid. Of course, the geochemistry of these elements in natural systems is much more complex : accessory minerals are very selectively dissolved (for instance zircon is peculiarly corrosion-resistant) depending on both their dissolution kinetic constants and the chemistry of fluids. For instance, a study by CATHELINEAU (1987) on U, Th and REE mobility during alteration of granitoids shows the major role of phosphate concentrations in solution on the rate of monazite destabilisation. The speciation of released elements could also markedly limit their mobile fraction in solution. Secondly, some of these accessory

minerals can also precipitate as alteration products and could therefore help us estimate the quantities of radionuclides susceptible to be trapped in their lattices during their crystallisations.

ii. the micro-mapping of U and micro-analysis of Th and REE give very few information on transport mechanisms through the rock. However, our observations show that an important fraction of these released elements is incorporated in secondary phases closely associated with partly altered primary minerals (figure 2). We therefore suggest that mass transfers in the Auriat granite occurred on very small distances for at least a fraction of the amount released of these elements. This conclusion agrees with that of PARNEIX (1987) for the transfer of major elements during hydrothermal alteration of this massif.

iii. our results also indicate that released U, Th and REE atoms are trapped in a great variety of secondary phases. As expected, they are in part associated with phyllosilicates but a noticeable fraction is also incorporated into titanium and iron oxides, coffinite, sphene, epidote, carbonates (siderite) and REE carbonates etc.. (figure 3). In many occurrences, U, Th and REE are not substituted as trace elements into secondary minerals but rather are major constituents of these phases. Hence, when estimating the amounts of these elements susceptible to be immobilised during their transport by alteration products one should absolutely consider these minor phases. It is worth noting that the modeling we intend to perform in a next step of our work will likely by hampered by a lack of thermodynamic data for some of these components.

IV CONCLUSION

Several interesting conclusions can be drawn from the analogical study of a fossil geothermal system at Auriat and a nuclear waste disposal in granites. Firstly, we have observed that circulation of fluids in such a rock proceeds through an extremely anisotropic network of μm to m-sized fissures. The ubiquity of the hydrothermal alteration in all pore spaces with sizes $\geq$ 0.01 mm is also a noticeable feature. Secondly, we have identified in detail the alteration parageneses which are likely to form upon circulation of fluids for temperatures < 200°C to be found in a repository. These mineral assemblages are mainly constituted of various phyllosilicates, carbonates plus numerous minor phases which incorporate an important fraction of released U, Th and REE atoms. Our investigation pinpoints the major role that geochemical codes such as EQ 3/6 can play in modeling hydrothermal alterations in natural systems and in predicting the possible evolution of a repository with time. We feel now confident in using it for trying to identify the secondary phases which could form with solutions of peculiar compositions originating from the repository.

Finally, this investigation strongly suggests that the circulation of fluids through an intragranitic repository leads to a complex mixture of beneficial and detrimental phenomena which must be properly studied to assess the safety of the disposal. Indeed, we have shown that alteration induces both the precipitation of secondary phases of increased sorbing capacities and a decrease of the rock porosity. This would a priori limit mass transfers through the geological barrier. On the other hand, the circulation of fluids is well-known to be the most likely means of destruction for technological barriers such as nuclear glasses and for radionuclide transport. But, we have also shown that the competition for retention between actinides and their natural analogue counterparts is a

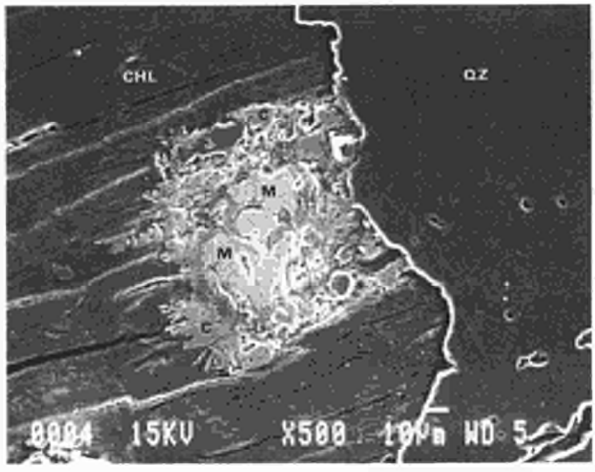

Figure 2 : SEM micrograph on a monazite (M) included into a chlorite (CHL), partly altered and replaced on its boundary by REE and Th-rich carbonates (C), (Qz quartz).

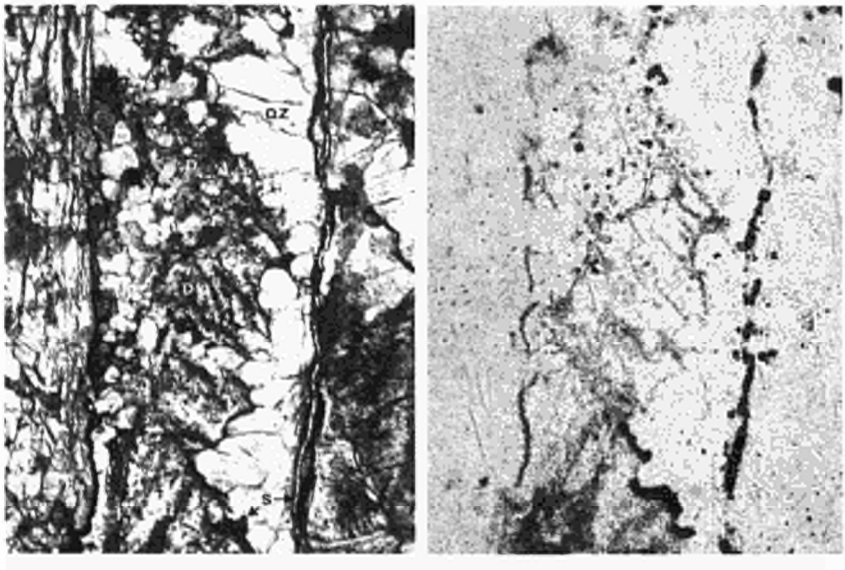

Figure 3 : Microdistribution of uranium by the fission track method (right), in the alteration phases of a subvertical fissure (left) of the Auriat granite observed by optical microscopy in the transmission mode (X 250), (Qz quartz, S siderite, D dolomite).

phenomenon which needs to be quantitatively taken into account. Clearly, this last point necessitates further investigation. Finally, we suggest that, apart from all other considerations already discussed in the literature, the most appropriate granites would be low U-Th-REE- containing ones in which, in addition, these elements should be incorporated in particularly corrosion-resistant accessory minerals.

BIBLIOGRAPHY

[1] AUTRAN A. (1980). La zone interne de l'orogénèse varisque en France de l'Ouest, excursion extraordinaire de la Soc. Geol. de France (Mai 1979) Bull. Soc. Geol. France, 7, 21.

[2] BEAUFORT D., DUDOIGNON P, PROUST D., PARNEIX JC., MEUNIER A. (1983). Microdrilling in thin sections: a useful method for the identification of clay minerals in situ. Clay Minerals, 18, 219-222.

[3] BROOKINS D.G. (1984). Geochemical aspects of radioactive waste disposal. Ed. Springer Verlag, 347p.

[4] CATHELINEAU M. (1987). Les interactions entre fluides et roches : thermométrie et modélisation. Exemple d'un système géothermique actif (Los Azufres, Mexique) et d'altérations fossiles dans la chaîne varisque. Thèse de doctorat d'Etat INPL, NANCY, 515p.

[5] CATHELINEAU M. (1987). U-Th-REE mobility during albitization and quartz dissolution in granitoïds : evidence from South-East French Massif Central. Bull. Mineral., 110, In press.

[6] CEA-Report (1981). Investigation par forages profonds du granite d'Auriat. Rapport CSDR 81/03.

[7] CHAPMAN N.A. and SMELLIE J.A.T. (1986). Natural analogues to the conditions around a final repository for high-level radioactive waste. Chem. Geol., 55, 388p.

[8] FLEER V.N. (1982). The dissolution kinetics of anorthite ($CaAl_2Si_2O_8$) and synthetic strontium feldspar ($SrAl_2Si_2O_8$) in aqueous solutions below 100°C : with applications to the geological disposal of radioactive nuclear wastes. Ph.D Thesis, Penn. State Univ., University Park (USA).

[9] FRIEDRICH M. (1984). Le complexe granitique hyperalumineux de St Sylvestre, Nord-Ouest du Massif Central français. Geol. Geochim. Uranium, Mém. Nancy, 1984, 5, 361p.

[10] GEBAUER D, BERNARD-GRIFFITHS J. and GRUNENFELDER M. (1981). U-Pb zircon and monazite dating of the mafic ultramafic complex and its country rocks. Example : Sauviat sur Vige, French Central Massif. Contrib. Mineral. Petrol., 76, 292-300.

[11] LEROY J. and HOLLIGER P. (1984). Mineralogical, chemical and isotopic (U-Pb Method) studies of hercynian uraniferous mineralisations (Margnac and Fanay mines, Limousin, France). Chem. Geol., 45, 121-134.

[12] LOWELL J.D. and GUILBERT J.M. (1970). Lateral and vertical alteration - mineralization zoning in porphyry ore deposits. Econ. Geol., 65, 4, 373-408.

[13] PARNEIX J.C. (1987). Mécanismes d'altération hydrothermale des granites. Implications pour le stockage des déchets nucléaires. Thèse de doctorat d'Etat, Université P et M. Curie, A paraître.

[14] PARNEIX J.C. and PETIT J.C. (1987). Hydrothermal alteration in Auriat granite (Massif Central, France) : Mineralogy and geochemistry of an old geothermal system. Geochim. Cosmochim. Acta, in press.

[15] RIMSTIDT J.D. and BARNES H.L. (1980). The kinetics of silica - water reaction. Geochim. Cosmochim. Acta, 44, 1683-1699.
[16] SIMMONS G. and CARUSO L. (1983). Microcracks and radioactive waste disposal. Mat. Res. Soc. Symp. Proc., 15, Ed Brookings D.G. North-Holland Publishing, 331-338.
[17] SHRODON J. and EBERL D.D. (1984). Illite in micas : Reviews in mineralogy, Bailey ed., 13, 495-544.
[18] TURPIN L. (1984). Altérations hydrothermales et caractérisation isotopique (O-H-C) des minéraux et des fluides dans le massif uranifère de St Sylvestre. Extension à d'autres gisements intragranitiques d'uranium français. Geol. Geochim. Uranium, Mem. NANCY, 1984, 6, 290p.
[19] VAUGHAN P.J., MOORE D.E., MORROW C.A. and BYERLEE J.D. (1986) Role of cracks in progressive permeability reduction during flow of heated aqueous fluids through granite. J. Geophy. Res., 91, B7, 7517-7530.
[20] VELDE B. (1985). Electron microprobe analysis of clay minerals. Clay Minerals, 19, 243-247.
[21] WOLERY T.J. (1979). Calculation of chemical equilibria between aqueous solution and minerals : the EQ 3/6 software package. U.C.L.L report n° 52558, 41p.

Natural Analogue Study of Tono Sandstone Type Uranium Deposit in Japan

C. Sato, Y. Ochiai and S. Takeda
Waste Management and Raw Material Devision
Power Reactor and Nuclear Fuel Development Corporation (PNC)

Summary

Sandstone type uranium deposit, located in Tono area, central part of Japan, has been recognized as a potentially useful analogue of geological isolation of radioactive wastes in Japan. The uranium deposit occurs as the stratiform which is less than 150 m in depth and below the water table. The studied area is not far from inhabitant. Preliminary study has been undertaken on migration of natural uranium series nuclides and on hydrogeochemistry in Tsukiyoshi ore body. The radioactive disequilibrium study of drill core shows that the equilibrium has been almost kept within the ore body. The hydrogeochemical study has revealed that there are three types of groundwater classified in correspondence with the stratigraphy and high-alkaline, fluorine-riched groundwater is confined into paleoweathered basement granite and permeable beds in the ore horizon.
The aim of this study is to reveal the geological, geochemical and hydrogical conditions which is favorable to keep uranium series nuclides undisturbed for a certain period of time, and to prove the feasibility of underground disposal of radioactive wastes in Japan where geological environment is complicated and unstable.

1. Introduction

Japanese island arch is a part of the circum-Pacific mobile belt and not considered to have geological stability as the area such as Precamblian shield. However, geological isolation of high level radioactive waste has been recognized to be basically feasible in Japan by means of a combination of engineered and natural barriers. Occurrence of uranium deposit as natural analogue is thought to support the verification of geological isolation system.

Uranium deposits including small bodies in Japan, most of which are sandstone-type hosted in Tertiary system overlying cretaceous granites, have been reviewed from the point of natural analogue. As a result, Tono deposit was chosen as the most favorable one for the following reasons, (1) it is the only unmined deposit with minable ore grade, (2) it has a size which is roughly equivalent to that of the repository, (3) it is possible to investigate the influence of fault and groundwater on nuclide migration and (4) many information is already available(1),(2),(3),(4),(5).

A boundary between oxidized and reduced zone which is common in roll

front type deposit is not observed in this deposit. A reducing environment may have been dominant during and after the deposition. It is particularly important in natural analogue atudy to investigate the geological, geochemical and hydrogical conditions which is favorable to keep uranium series nuclides undisturbed. Product of this study also make a contribution to site characterization as well as to validation of model for performance assessment.

Preliminary study was carried out on mainly nuclides distribution and hydrogeochemistry in Tsukiyoshi ore body of Tono deposit in order to discuss the availability of natural analogue study in thia deposit.

2. Geological Outline

Tono area is located in 350 km southwest of Tokyo. In this area, sedimentary rocks of Miocene age overlie uncomformably cretaceous granites(Fig. 1). The remarkable structual feature of uranium occurrence is paleochannel control on the plane of unconformity. The most favorable zone in the channel for uranium mineralization is in the lower part of tertiary fluvial sediment of Toki Group which is composed of arkosic sandstone, taffaceous sandstone, carbonaceous mudstone and conglomerate. The depth of uranium occurrence is less than 150 m (Fig.2,3).

The deposit is classified into sandstone type. Most of uranium is characteristically accompanied with zeolite, clay minerals, carbonaceous matter et al (2). Very small amount of uraninite and coffinite are observed.

Tono uranium deposit consists of four ore bodies namely Tsukiyoshi, Misano, Utozaka and Jorinji. Tsukiyoshi ore body is roughly 3400 m by 500 m in size with thickness of 1 to 3 m. There is a reverse fault named Tsukiyoshi Fault,E-W, 60-70°S, with a throw of 35 m,which cuts the ore body. Shaft and gallery for exploration have been constructed in the middle part of the ore body. Present natural analogue study is undertaken within Tsukiyoshi ore body.

3. Distribution of Natural Uranium Nuclides

The preliminary studies was made for ore samples which were taken from the gallery and drill core within the ore body.

3.1 Sample and Location

(i) Samples in the gallery

The samples were collected in the exploration gallery, and their locations are shown in Fig.3,4. The redistribution of radionuclides after construction of the gallery is assumed for samples(No.1-10) taken from the surface of the gallery. Sample No.11, in the outside of the ore body, is a radioactive anomaly accompanied with a fragment of carbonized wood.

(ii) Drill core samples

Drill core samples were taken from the uranium mineralized zone and its neighbours at upstream and midstream in channel structures of the ore body. The locations of the drill holes, SN-2 and AI-12, are shown in Fig.3.

3.2 Mineralogy

The mineralogy of samples in the gallery are shown in Table-I. The samples within ore zone mainly consist of quartz, plagioclase, kaolinite, montmorillonite, calcite and heulandite. Low amount of iron oxides as limonite are also present. In a few samples(No.5,6,7), secondary uranium minerals as andersonite and zippeite are observed which may have mineralized due to oxidation after construction of the gallery. Sample No.11 contains a

large quantity of sulfate minerals as jarosite and gypsum in addition to montmorillonite, kaolinite and carbonized wood. Autoradiography and radioluxograpy show uranium does not exist in carbonized wood but in clay minerals in this particular sample.

Except for small amount of pyrite, the mineral composition of the drill core samples is similar to that of the gallery samples No.1-4.

3.3 Natural Uranium Series Disequilibrium

(i) Samples from the gallery

Assey of U-238, U-234 and Th-230 were carried out by alpha spectrometry. Ra-226 and Pb-210 were nondestructively analysed by high pure germanium detector. In the gamma-ray measurement, samle was kept in sealed container for three weeks and U-238 was calculated from the 63 keV gamma ray of the short lived daughter Th-234.

The results of assay are presented in Table-I together with the uranium contents. The relative activities of U-238, U-234 and Th-230 are plotted in ternary diagram Fig.5 (6). According to their radioactive disequilibrium states, the following geochemical processes which cause redistributions of uranium series nuclides can be infered.

No.1: U-238, U-234 and Th-230 are almost in radioactive equilibrium. This means that the age is older than at least a million years. On the other hand radium is slightly leached out by reduced groundwater fairly recently.

No.2,4,10,11: Uranium, preferentially U-234, and radium is partially leached out probably by oxidized groundwater. While long lived daughter Th-230 which is almost immobile is present in excess state.

No.3,5,6,7,8,9: Accumlation of uranium occurred fairly recently by secondary inflow of uranium, in which excess of U-234 was contained by alpha recoil process.

(ii) Drill core samples

The U-234/U-238 and Th-230/U-234 activity ratios are shown in Fig.6. together with uranium content and geologic colum. There are no significant fractionations between these nuclides in the two drill cores from upstream and midstream of the channel structure of Tsukiyoshi ore body. However, the results of SN-2 cores suggest partial uranium leaching had occurred just above unconformity.

3.4 Selective Phase Separation

Sequential extraction techniques were applied to identify the phases of uranium series nuclides in ore. The following five fractions were separated as identicable phases: exchangeable, bond to carbonates, bond to iron oxides, bond to organic matter and resudial (7). Leaching procedures and reagents are summarized in Table-II, and the results obtained on samples from the gallery are shown in Fig.7. A large portion of uranium is associated with carbonates and iron oxides, even though total of iron and carbonate is less than 6 percent in weight for all of the samples.

Complementary measurements as alpha spectrum and X-ray diffraction are not yet performed on the individual leachates and on the residuals following each extraction.

4. Hydrogeochemistry

Uranium in Tono deposit could be originated from the basement granites and transported by circulated groundwater through permeable host rock. The uranium deposit is assumed to be enriched by repetitions of leaching- and fixing cycle between host rock and groundwater (3). The present ore horizon lies below water table and mostly in aquiclude.

The general stratigraphy of Tono area is composed of Toki Group, Mizunami G., and Seto G. in ascending order. Groundwater samples were collected from each geological group for chemical analysis (Table-III, Fig.3.).

There is a significant increase in pH, bicarbonate, sodium and fluorine in correspondence with the stratigraphical depth. The groundwater in Toki Group where uranium is deposited is classified chemically as Na-HCO_3 type. The high level of these ions seems to be caused by long term interaction between water and the minerals in host rock (4). The results of tritium analysis suggest that the groundwater is stagnate for more than 50 years. However, the groundwater in Toki Group doesn't contain higher level of uranium in contrast to higher bicarbonate content. The uranium concentration is almost as same as that of surface water.

These results suggest that the groundwater in ore horizon is stagnate for a long time and the hydrogeochemical environment is reducing.

5. Conclusions and Future Studies

The results of preliminary study are summarized as follows:

(1) A quite minor disequilibrium of uranium series nuclides is observed in the ore body.
(2) A large portion of uranium exist in the three fractions of carbonate, iron oxides and exchangeables.
(3) Three types of groundwater is identified in correspondence with the stratigraphy of Tono area.
(4) The groundwater of ore zone is characterized by high content of bicarbonate, sodium and fluorine ion against the low content of uranium and tritium ion.

These results suggest that this natural analogue study is available to reveal the favorable environment for the repository and to demonstrate the feasibility of the geological isolation as well as to understand the nuclides migration by groundwater.

Therefore, the future studies should include the following subjects to contribute the assessment of radioactive waste repository sites:

(1) Detailed study on nuclides distribution within and around the ore body.
(2) Detailed geological and mineralogical study with a emphasis on uranium occurrence.
(3) Investigation on colloid formation and transport.
(4) Further study on hydrogeology and hydrogeochemistry including development of in-situ measurement technique.
(5) Validation of developed model for nuclide migration.

The authers wish to thank Prof. Dr. T. Nakanishi of Kanazawa University and Dr. T. Murano and Dr. M. Yamakawa of Power Reactor and Nuclear Fuel Development Corporation for valusble suggestion.

References

(1) Sakanoue,M. et al, Geochem. Jour. 2, (1968) 71-86
(2) Katayama,N., Hirono,S. and Hirono,S., IAEA-SM-183/11, (1974) 437-452
(3) Doi,K., Hirono,S. and Sakamaki,Y., Econ. Geol. 70,(4), (1975) 628-646
(4) Sakamaki,Y., IAEA-TECDOC-328, (1985) 135-154
(5) Yanagisawa,M., Sci. Papers Coll.Faculty of Science,Kanazawa Univ.(1983)
(6) Rosholt,J.N., Uranium Series Disequilibrium Applications to Environmental Problems, Claredon Press, Oxford, (1982) 167-180
(7) Tissier,A. et al, Anal. Chem. 51,(7),(1979) 844-850

Table-I. Activity ratios, uranium concentrations and minerals in the samples from the gallery

Sample NO	$^{234}U/^{238}U$	$^{230}Th/^{234}U$	$^{226}Ra/^{230}Th$	$^{210}Pb/^{226}Ra$	U_3O_8 %	Main Minenals (*)
1	1.01	1.01	0.95	1.09	0.175	Qz , Pl , Kao , Cal
2	0.84	1.87	0.90	1.02	0.100	Qz . Pl , Kao , Zeo
3	1.04	0.94	0.85	0.95	0.031	Qz . Pl , Mont , Cal
4	0.84	1.94	1.05	0.92	0.121	Qz . Pl , Mont
5	1.01	0.80	1.07	1.00	0.166	Qz Pl , Kao , Zeo , Cal
6	1.19	0.75	1.01	1.11	0.091	Qz . Pl , Zeo , Kao
7	1.11	0.84	1.02	1.05	0.063	Qz . Pl , Zeo
8	1.00	0.75	1.29	1.08	0.097	Qz . Pl , Cal
9	1.01	0.72	1.22	1.03	0.060	Qz . Pl , Mont , Kao
10	0.94	1.12	0.87	1.03	0.067	Qz . Pl , Mont , Kao , Zeo , Cal
11	0.96	4.94	0.86	1.05	0.200	Mont , Kao , Fel , Jar , Gyp

(*) Qz : Quartz , Pl : Plagioclase , Kao : Kaolinite , Mont:Montmorillonite
Cal : Calcite , Zeo : Zeolite (Heulandite) , Fel : Feldspar
Jar : Jarosite , Gyp : Gypsum

Table-II. Sequential extraction procedures for selective phase separation

Fraction	Extractant	Condition
1.Exchangeable	1M NaOAc 10ml (PH 8.7)	Room Temperature Occacional Agitation 24H
2.Bond to Carbonates	1M NaOAc+HOAc 10ml (PH 5.0)	Room Temperature Occacional Agitation 24H
3.Bond to Fe Oxides	0.04M $NH_2OH \cdot HCl$ +25%HOAc 0 ml	90℃,6H Occasional Agitation
4.Bond to Organic Matter	(1)30%H_2O_2 5ml +0.02MHNO_3 3ml (2)30%H_2O_2 3ml (3)3.2M NH_4OAc+20%NH_3, 5ml	(1) 85℃,6H Occasional Agitation (2) 85℃,2H Occasional Agitation (3) Room Temperature Occasional Agitation
5.Bond to Silicates	(1)HF 10ml+$HClO_4$ 3ml (2)6M HCl	(1) Digestion (2) Disolution

Initial Weight of Sample : 1g

Table-III. Hydrogeochemical composition of waters around Tsukiyoshi ore body

Samples (*)	Resistivity	pH	HCO_3	Cl	SO_4	F	Na	K	Ca	Mg	Total Fe	U	^3H	No. of Samples
	(ohm-cm)		(ppm)	(ppm)	(ppm)	(ppm)	(ppm)	(ppm)	(ppm)	(ppm)	(ppm)	(ppb)	(pCi/l)	
Surface water	3000	6.5	10	3	7	0.2	<1	1	5	1	0.3	0.1	35	3
Ground-water in Seto Group	4000	6.0	20	4	10	0.1	2	2	3	1	0.1	0.2	35	1
Ground-water in Mizunami G.	4500	7.2	60	5	10	0.1	18	4	20	0.5	<0.1	<0.1	-	2
Ground-water in Toki G.	5000	8.6	90	1	1	3	35	0.3	5	0.1	0.1	0.1	<3	5

(*) See Fig.3

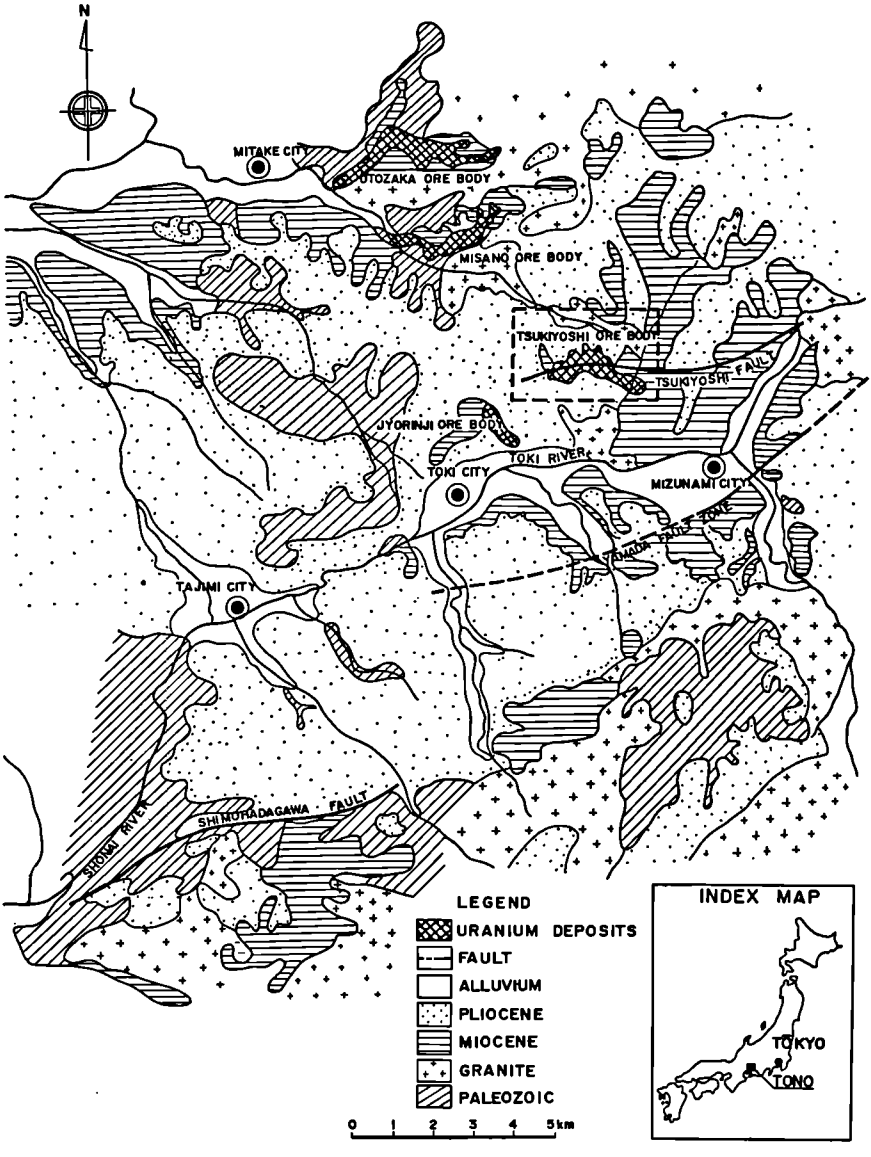

Fig. 1. Shematic geologic map aruond Tono area and the location of Tono uranium deposit.

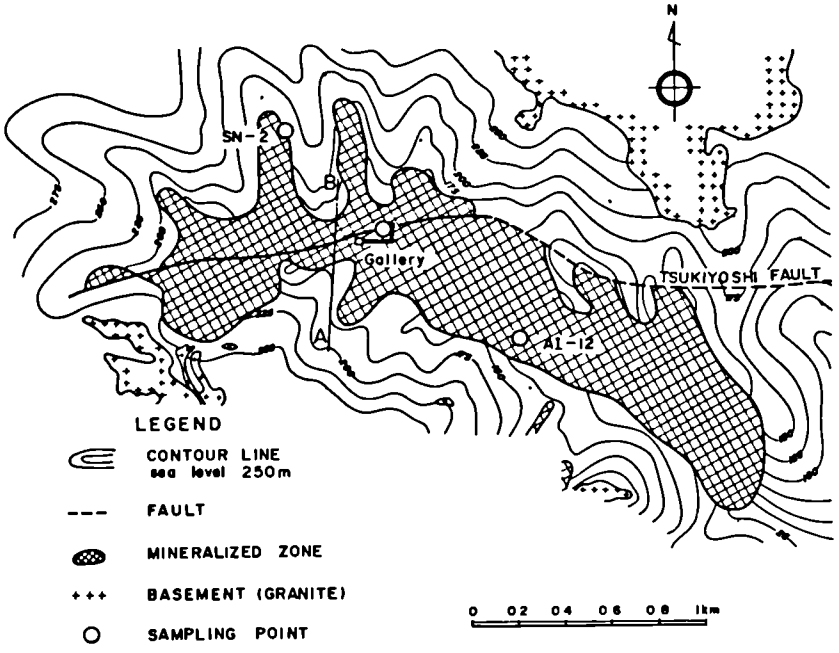

Fig. 2. Underground contour map of the plane of unconformity above the basement of Tsukiyoshi area and sampling locations in Tsukiyoshi ore body.

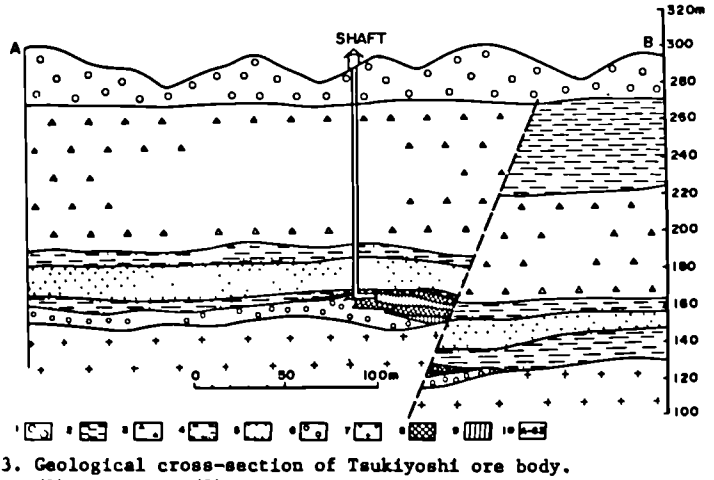

Fig. 3. Geological cross-section of Tsukiyoshi ore body.
(1)Seto Group,(2)upper members of Mizunami Group,(3)lower members of Mizunami G.,(4)sandstones and shales in Toki Group,(5)cabonaceous in Toki G.,(6)conglomerates in Toki G.,(7)basement granite,(8)low-grade ores,(9)high-grade ores.

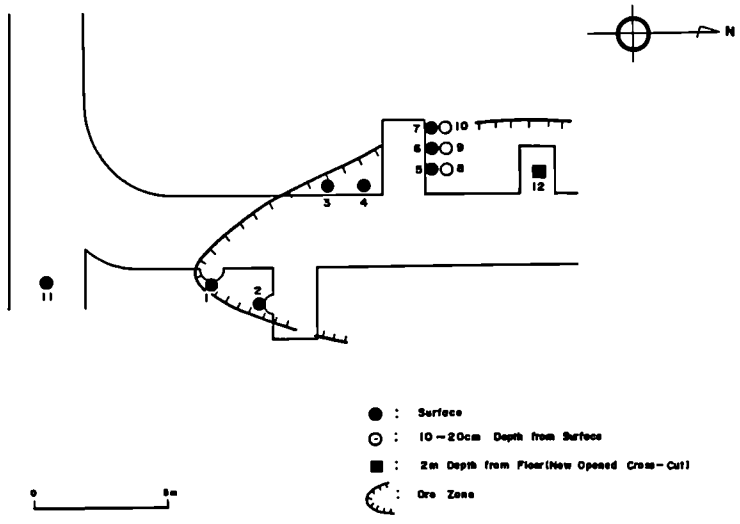

Fig. 4. Locations of the samples collected from gallery of Tsukiyoshi ore body.

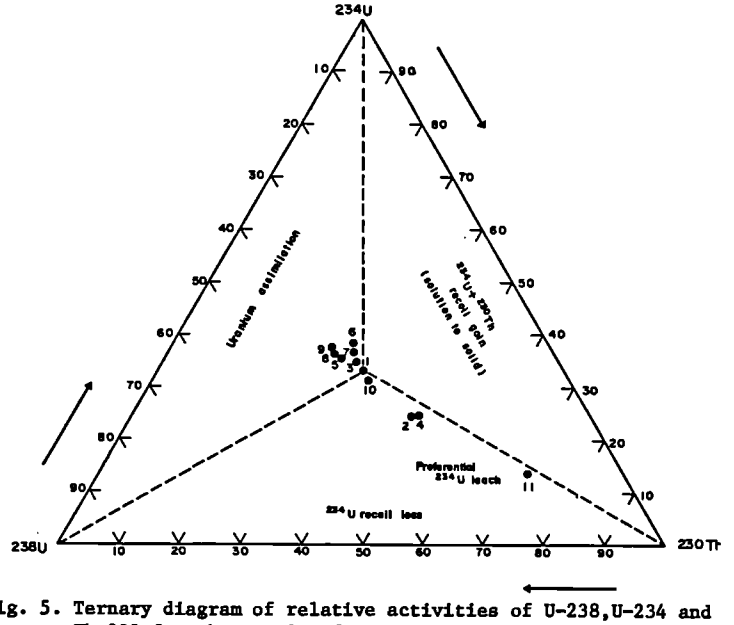

Fig. 5. Ternary diagram of relative activities of U-238,U-234 and Th-230 for the samples from the gallery.

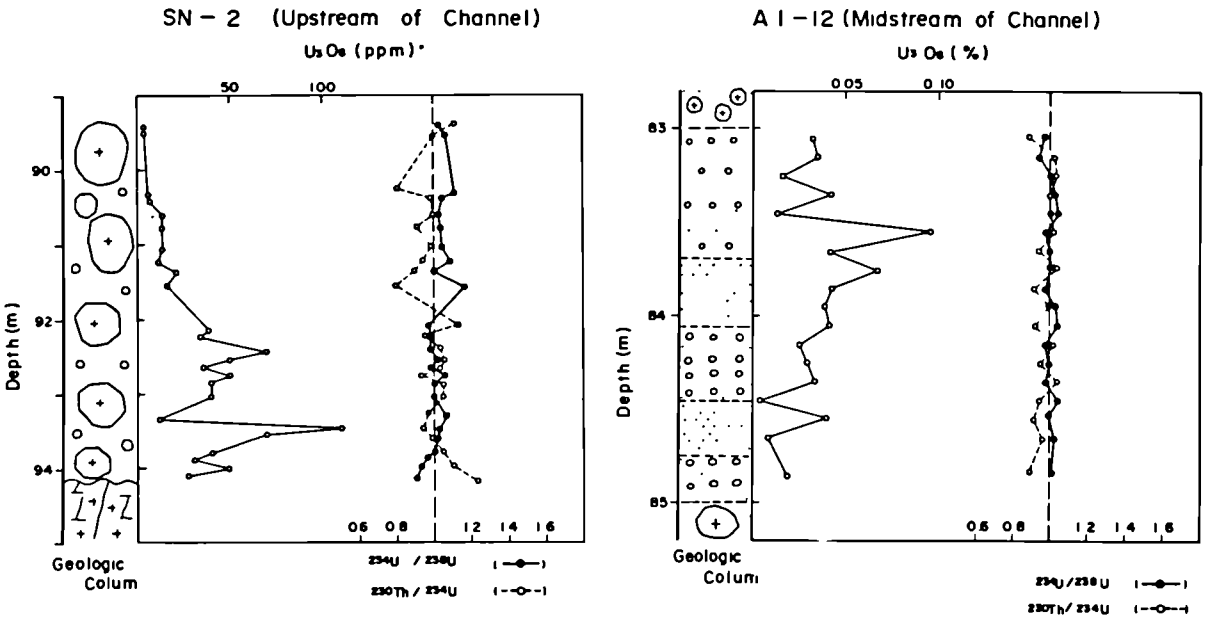

Fig. 6. Variation with depth of activity ratios and uranium concentrations for drill core samples from the upstream and midstream of Tsukiyoshi ore body.

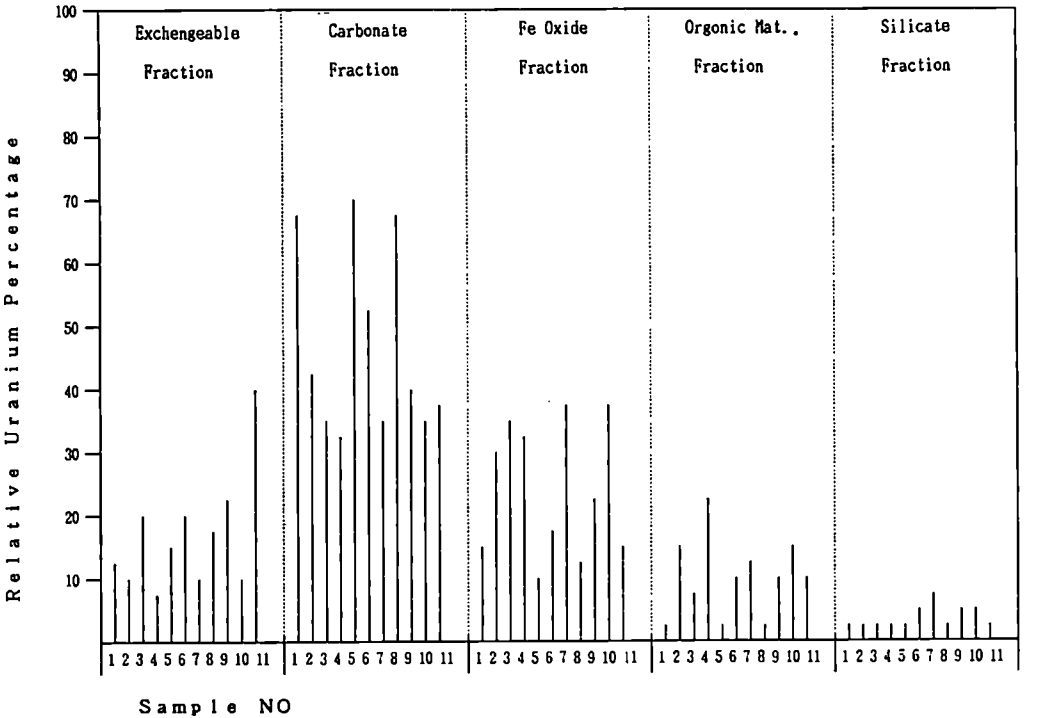

Fig. 7. Relative percentage of uranium in selectively extracted phase for samples in the gallery.

NATURAL ANALOGUE STUDIES AT GRIMSEL, SOUTHERN SWITZERLAND

W R Alexander, R D Scott, A B MacKenzie
(SURRC, East Kilbride, Scotland) and
I G McKinley (E.I.R., WÜrenlingen, Switzerland)

Abstract

As an analogue to processes affecting radionuclide migration in a crystalline rock waste repository, the distribution of natural decay series radionuclides and rare earth elements has been examined in two contrasting rock drillcore sections from NAGRA's underground test laboratory in Grimsel, southern Switzerland. The results indicate that mechanical damage to rocks associated with water-bearing fractures in the crystalline rock repository may subsequently result in sites suitable for the retardation of migrating radionuclides.

1. Introduction

This project was conceived principally to relate to previous analogue studies carried out by NAGRA (Switzerland) and SKB (Sweden) which were initiated as part of the assessment of the concept of disposal of nuclear fuel waste in a crystalline rock repository (1). In particular, this work, carried out in conjunction with the Mineralogisch-petrographisches Institut, Universitat Bern, focuses on the use of parent-daughter disequilibria in natural decay series radionuclides as an analogue to processes affecting radionuclide transport in water-conducting fractures in the bedrock. Such fractures have been identified by NAGRA and SKB as sites of potential radionuclide retardation through processes such as sorption and migration into the water-saturated rock matrix adjacent to the fracture(2).

Recent studies have shown that naturally occurring U radionuclides may be mobilised by rock-water interactions in the vicinity of these fractures (3, 4). It has been suggested (3) that enhanced porosity and mineralogical alteration around a fracture due to hydrothermal activity are important prerequisites for the penetration of radionuclides from the fracture system into the associated rock.

Here we present new information from two rock drillcores from NAGRA's underground test laboratory in Grimsel, southern Switzerland which were examined to elucidate the process of formation of fluorescent secondary U phases which have appeared in numerous places on the laboratory tunnel walls since excavation. The results indicate that,along with hydrothermally induced alteration, mechanical damage to the rocks associated with a fracture (or tunnel) can also significantly improve the ability of that rock to immobilise radionuclides.

2. Sample Description

The two cores (WT121 and WT119.5E) discussed here were drilled in 1986 from the WT drift in NAGRA's underground test laboratory (Felslabor), which was excavated in 1979 in the Grimsel granitoid body of the Aare Massif, southern Switzerland (a map of the Felslabor is presented by C Degueldre in volume 1 of these proceedings). Core WT121 was taken from a site of active

deposition of secondary uranium minerals onto the tunnel walls whereas core WT119.5E, from an unmineralised area some 1-2m away, represents a control. Subsequent sub-sampling and petrographic description of the material was carried out by the Mineralogisch-petrographisches Institut, Universitat Bern.

The rocks are generally representative of the Grimsel granite-granodiorite as described in previous studies (3, 5). In hand specimen they are light to mid-grey, medium to coarse-grained, slightly gneissose, mineralogically homogenous and unaltered. Major constituents are quartz, k-feldspar > plagioclase, biotite > muscovite, hornblende and epidote with accessory sphene, orthite, apatite, zircon, calcite and magnetite. Weak alteration of feldspars to sericite and biotite to chlorite is discernable in thin section. The area around the control core, WT119.5E, is dry; that is to say that the rock in this area of the tunnel does not conduct appreciable quanitities of water whereas in the area of the mineralised core, WT121, there is a limited flow of water associated with the rock (probably no more than capillary flow: 6).

3. Methods

For U-series measurements samples of the powdered granite were spiked with ^{232}U in equilibrium with ^{228}Th and then digested with aqua regia and hydrofluoric acid in a vented microwave oven (7, 8). Insoluble material was further digested in a Parr microwave-transparent high-pressure digestion bomb (9). U and Th were recovered from the combined leachings by anion-exchange techniques (10) and were then electro deposited onto stainless steel discs for α-spectrometry measurements with Si surface barrier detectors. The precision of the results is $\pm$ 4% for the $^{234}U/^{238}U$ activity ratios and $\pm$ 7% for the $^{230}Th/^{234}U$ activity ratio.

^{226}Ra analyses were carried out by direct counting of the 609-keV peak in the γ-spectrum of ^{226}Ra decay products in a sub-sample of the untreated powdered granite. It should be stressed that this peak, produced by ^{214}Bi decay, can only be used if it is assumed that ^{222}Rn does not escape to any significant extent from the sample

REE, Fe, Co, Cs and Mn analyses were carried out on 0.2g of untreated, powdered granite using instrumental neutron activation analyses (INAA) (11, 12).

The fluorescent secondary U minerals present on the tunnel walls were collected from two sites: one sample, from the access tunnel to the Oberhasli Power Station Company's Grimsel I Hydropower Station (a common access tunnel shared with the Felslabor), is assumed to be some thirty years old and consists of the uranium carbonates grimselite and schroeckingerite (13). The other sample, from within three metres of the site of core WT121 in the WT drift, is only three years old (because the tunnel walls were washed three years ago so removing the water soluble U-carbonates) and consists of an amorphous U-carbonate. These secondary phases were washed off the rock surface with dilute HCl, filtered through 0.45 µm pore-diameter filters dried down and weighed. Once re-dissolved in dilute HCl and spike added, U was co-precipitated with an Fe carrier, the Fe subsequently re-dissolved and exchanged with ether. The U series measurements were then carried out as detailed above.

4. Results

4.1 core WT121

The distribution of U and its daughter decay products are displayed in

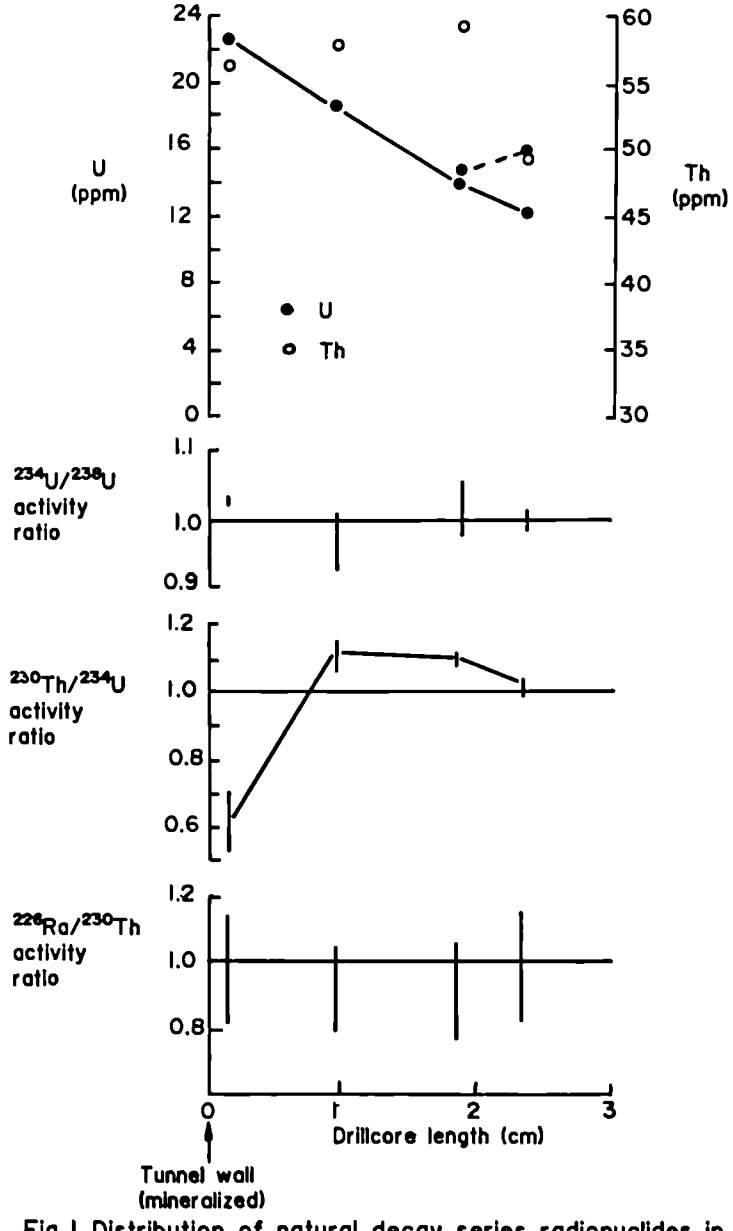

Fig 1 Distribution of natural decay series radionuclides in core WT121

TABLE 1 Natural Decay Series Results for Core WT121 ($dpmg^{-1}$ unless stated)

Sample	Distance from rock Surface (cm)	U (ppm)	Th (ppm)	Th/U	^{238}U	^{234}U	$^{234}U/^{238}U$	^{230}Th	$^{230}Th/^{234}U$	^{226}Ra	$^{226}Ra/^{230}Th$	^{232}Th
A	0.15	22.42 ± 0.15	56.14 ± 0.45	2.5	16.48 ± 0.11	16.98 ± 0.11	1.03 ± 0.01	10.49 ± 0.09	0.62 ± 0.09	10.32 ± 1.82	0.98 ± 0.18	13.56 ± 0.11
B	0.95	18.54 ± 0.24	57.96 ± 0.81	3.1	13.63 ± 0.04	13.23 ± 0.07	0.97 ± 0.04	14.68 ± 0.07	1.11 ± 0.04	13.44 ± 1.96	0.92 ± 0.13	14.00 ± 0.07
C	1.85	14.77 ± 0.27	59.20 ± 0.70	4.0	10.86 ± 0.09	11.13 ± 0.09	1.02 ± 0.04	12.25 ± 0.15	1.10 + 0.02	11.10 ± 1.64	0.91 ± 0.14	14.30 ± 0.17
		14.01 ± 0.18	-	-	10.30 ± 0.08	10.95 ± 0.08	1.06 ± 0.04	-	-	-	-	-
D	2.35	12.44 ± 0.07	-	-	9.15 ± 0.05	9.19 ± 0.06	1.00 ± 0.01	-	-	-	-	-
		16.17 ± 0.09	49.60 ± 0.61	3.1	11.89 ± 0.06	12.00 ± 0.06	1.01 ± 0.02	12.21 ± 0.12	1.02 ± 0.02	11.64 ± 1.68	0.98 ± 0.17	11.98 ± 0.11

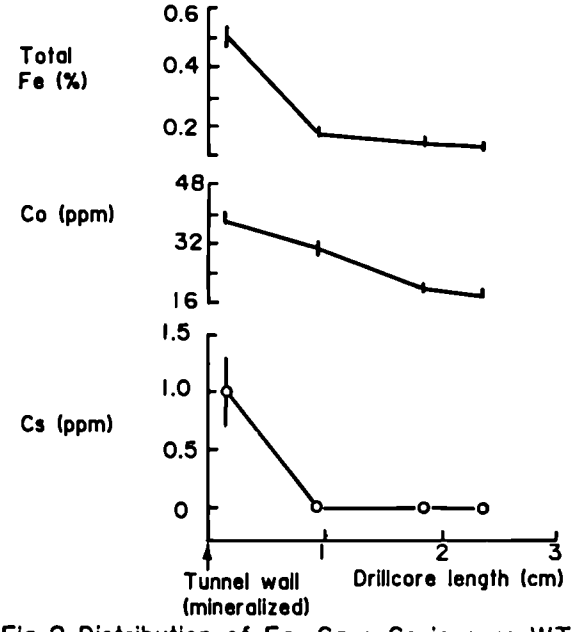

Fig 2 Distribution of Fe, Ca + Cs in core WT 121

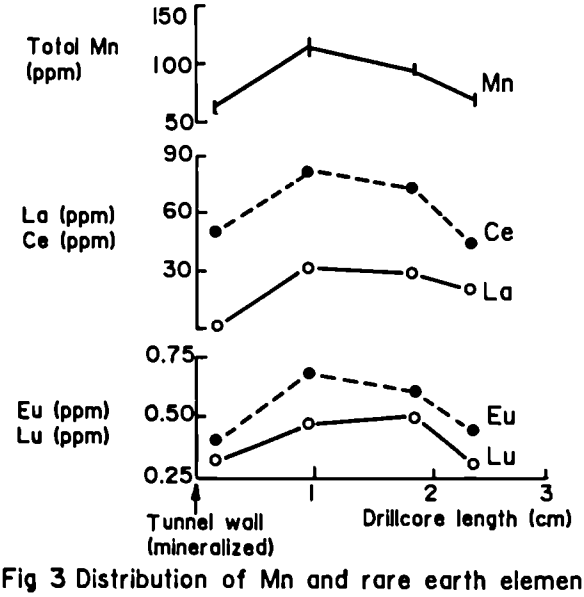

Fig 3 Distribution of Mn and rare earth elements (La, Ce, Nu and Lu) in core WT121

figure 1 and tabulated in table 1. Fe, Co and Cs are displayed in figure 2 while, Mn and the rare earth elements (only La, Ce, Eu and Lu are displayed in this report but they are representative of the others) are shown in figure 3. Other elements analysed but not detailed here include Na, K, Ba, Sc, Nd, Sm, Hf and Ta(14).

There is a marked increase in the U content of the rock along the core, rising from 12.44ppm at 2.4cm from the tunnel wall to 22.42ppm immediately below the tunnel surface whereas Th increases slightly from 56.14ppm in the first sample to 59.20ppm by 1.8cm before falling to 49.60 ppm by 2.4cm. Two samples of the secondary U phases from the tunnel walls were analysed and have U contents of 5% (30 year old sample) and 1.5% (3 year old sample). There is no obvious relationship between U and Th in the whole rock suggesting the presence of distinct U-rich phases and Th-rich phases. In samples of Grimsel granite from within 1 km of the sample site the main U and Th bearing minerals have been identified as allanite, thorite, zircon, apatite and occasionally polycrase (15).

The $^{234}U/^{238}U$ activity ratios and the $^{226}Ra/^{230}Th$ activity ratios both indicate equilibrium (fig 1). The $^{230}Th/^{234}U$ activity ratios clearly deviate markedly from unity, rising from near unity at 2.4 cm to 1.1 at 1 cm before dropping rapidly to 0.6 immediately behind the tunnel wall. Assuming the immobility of Th under normal groundwater conditions (16), the high activity ratios at 1-2cm in the core indicate loss of ^{234}U in this zone of the rock followed by deposition at or near the tunnel wall inducing the very low $^{230}Th/^{234}U$ activity ratio of 0.6. The secondary U carbonates from the tunnel wall have $^{234}U/^{238}U$ activity ratios of unity, clearly indicating a non-fractioned U supply from the rockwater and so implying that ^{238}U is equally removed in the 1-2 cm zone of this core.

Fe, Co and Cs (fig 2) behave in a similar manner to U with highest levels at the tunnel wall and sharp decreases in concentration with distance into the rock. Along with the clear remobilisation of these particular elements it should also be noted that there has been a significant loss of Fe and Cs from the system with the maximum levels of 0.4% Fe and 1.0ppm Cs in core WT121 which contrasts with the corresponding levels of 1.16%Fe and 1.5ppm Cs in the control core WT119.5E. Co, on the other hand, is greatly enriched in the mineralised core with a maximum concentration of 37.9ppm compared with only 1.8ppm in core WT119.5E.

Mn and REE's display a distribution like that of Th (cf figs 1 and 3). Because this grouping of elements is associated with differing phases in the granite (eg Eu with feldspars, Ce with biotite, Mn with epidote, Th with zircon etc), it is likely that the patterns merely reflect the original mineralogical inhomogeneity of the granite.

4.2 core WT119.5E

The distribution of U and its daughter decay products are illustrated in figure 4 and listed in Table II. Fe, Co and Cs are shown in figure 5 while Mn and the REE's are displayed in figure 6.

In contrast to core WT121 there is no obvious trend in the U distribution in the rock although the Th content does decrease with distance along the core. While the concentrations of U and Th (4.94 - 6.17 ppm and 17.55 - 32.83 ppm respectively) are lower than in core WT121 they are similar to previous analyses of the Grimsel granite (3, 14, 15).

The relatively invariant patterns in the Fe, Co and Cs data (fig 5) and the Mn, La and Lu data (fig 6) are taken to be a reflection of the original mineralogy of the granite and, indeed, are not dissimilar to previous results for Grimsel granites (3, 14, 15). The high Eu level at 5 cm suggests an area enriched in feldspars with the low Ce concentration

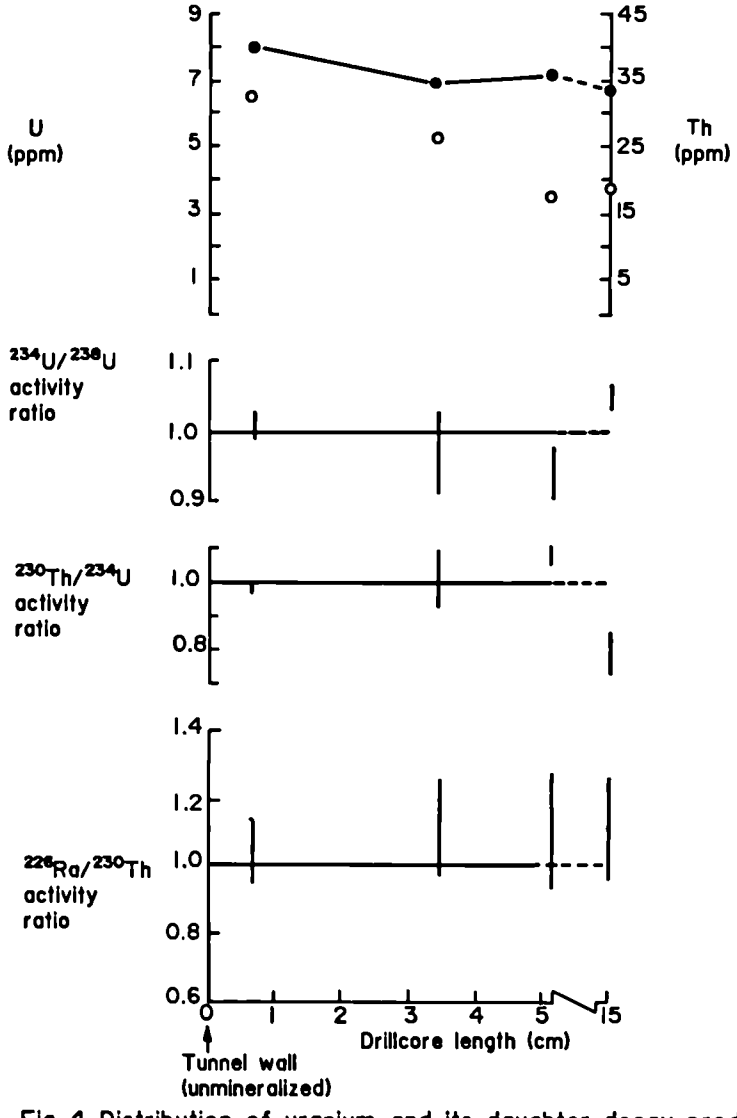

Fig 4 Distribution of uranium and its daughter decay products, thorium, total iron and total manganese in core WT119.5E

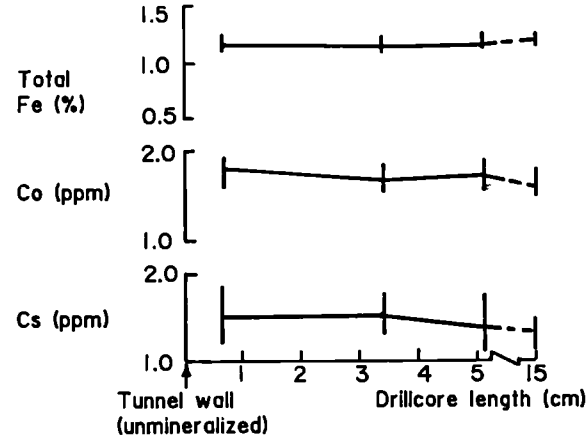

Fig 5 Distribution of Fe, Co and Cs in core WTII9.5E

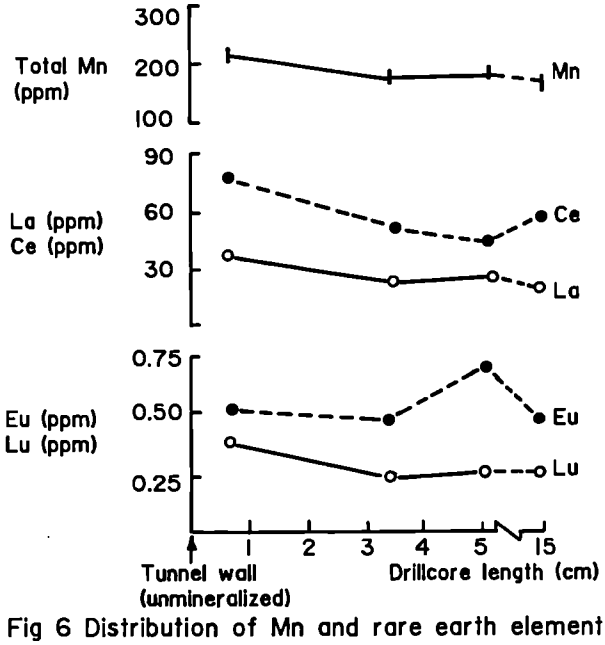

Fig 6 Distribution of Mn and rare earth elements (La, Ce, Eu and Lu) in core WTII9.5E

TABLE II Natural Decay Series Results for Core WT119.5E ($dpmg^{-1}$ unless stated)

Sample	Distance from rock Surface (cm)	U (ppm)	Th (ppm)	Th/U	^{238}U	^{234}U	$^{234}U/^{238}U$	^{230}Th	$^{230}Th/^{234}U$	^{226}Ra	^{226}Ra ^{230}Th	^{232}Th
A	0.65	7.98 ± 0.07	32.83 ± 0.25	4.1	5.87 ± 0.05	5.86 ± 0.05	1.00 ± 0.02	5.83 ± 0.05	0.99 ± 0.02	6.00 ± 0.57	1.03 ± 0.11	7.93 ± 0.06
B	3.4	6.83 ± 0.22	25.83 ± 0.22	3.8	5.02 ± 0.06	4.85 ± 0.06	0.97 ± 0.06	4.92 ± 0.06	1.01 ± 0.08	5.46 ± 0.65	1.11 ± 0.14	6.24 ± 0.05
		6.83 ± 0.11	-	-	5.02 ± 0.08	4.82 ± 0.06	0.96 ± 0.05	-	-	-	-	-
C	5.1	6.02 ± 0.45	17.55 ± 0.35	2.9	4.43 ± 0.35	4.35 ± 0.33	0.98 ± 0.14	4.72 ± 0.09	1.08 ± 0.03	4.96 ± 0.47	1.05 ± 0.12	4.24 ± 0.09
		7.10 ± 0.13	-	-	5.22 ± 0.04	5.60 ± 0.05	0.93 ± 0.04	-	-	-	-	-
D	15.0	6.72 ± 0.05	18.67 ± 0.41	2.8	4.94 ± 0.04	5.20 ± 0.04	1.05 ± 0.02	4.10 ± 0.08	0.79 ± 0.02	4.51 ± 0.56	1.10 ± 0.16	4.51 ± 0.10

in the same area reflecting a concomitant decrease in biotite.

Overall the trends in the data are explicable in terms of mineralogical inhomogeneity in the granite and this is allied to the fact that the $^{234}U/^{238}U$, $^{230}Th/^{234}U$ and $^{226}Ra/^{230}Th$ activity ratios show secular equilibrium indicating a lack of remobilisation of the U-series decay products within the last 1Myr. It seems likely then thet the rock represented by this core has experienced no rock-water reactions during recent geological time.

5. Discussion

Clearly the rock associated with the mineralised surfaces in the laboratory tunnels (represented here by core WT121) is quite distinct from that of the 'average' Grimsel granite/granodiorite (represented by core WT119.5E). As well as displaying anomalously elevated U and Th (and Co) levels with associated low Fe and Cs concentrations, this rock is water conducting. The high natural decay series concentrations imply an initial U enrichment in a strongly reducing area of the granite with associated removal of redox sensitive Fe and Cs by leaching of the easily reduced accessory and/or secondary phases in the whole rock.

It is difficult to ascertain the time of the original U enrichment due to the secondary remobilisation which affects most of core WT121. However, there is evidence that the trend of the $^{230}Th/^{234}U$ activity ratios is towards unity by 2-3 cm into the rock (fig 1). While thia needs to be checked by a longer drillcore, it may be an indication that outside the 0-2 cm deep zone of present U remobilisation there has been no rock-water interaction in the last 1-3 Myr. The mechanism of U enrichment is similarly unclear although the relatively unaltered state of the rock (14) and the lack of appreciable loss of L.REE's in comparison to H.REE's (fig 3) indicates that it is unlikely that hydrothermal activity waa involved(17,18).

What is obvious both from the appearance of the fluorescent secondary U phases on the tunnel walls of the laboratory and from the data presented in figs 1 and 2 is that there has been and continues to be remobilisation of at least part of the 'excess' U. The construction of the tunnels for the underground laboratory has caused the U remobilisation by introducing (atmospheric) oxygen into the rock-water system. Oxidation of the U from the IV to VI state releases available U to solution and, at the same time, the increased oxygen concentration precipitates reduced Fe and Cs from the water so producing a maximum in the whole rock just below the surface of the tunnel wall. Such a system has frequently been reported in, for example, sandstone roll-front deposits (19 - 21). Co is probably associated with the Fe-oxyhydroxides (22, 23). A minimum amount of drilling fluid (oxygenated lake water) was used during the boring of the tunnel (24) but it is conceivable that at least some of the water flowing from the mineralised zone originates from this period. Analyses of water collected from the site of core WT121 are being carried out as a check on this but this should not change the above scenario for U remobilisation appreciably.

According to recent models (24, 25) of diffusional penetration of oxygen into reducing rock matrices, the above described redox front would be expected to penetrate the rock to a depth of less than 1 mm since tunnel construction. However, the distributions of U, Fe and Cs in core WT121 indicate that the redox front has penetrated at least 2 cm into the granite here. This is of great significance to radwaste disposal modelling becauae this is an indication that it is possible to produce a large reaction zone for radionuclide fixation around a tunnel or fissure in a crystalline rock simply by mechanical damage produced by tunnelling and faulting. This will rapidly increase the penetration of oxidising agents (mainly O_2 and H_2O_2 in

a repository tunnel (2^6), O_2 around a fissure (3) into the reducing rock so greatly increasing the amount of reductants (such as ferrous iron) involved in the reaction. This in turn increases the redox front readily available for fixation of U and other redox sensitive radionuclides such as Np, Tc and, in some circumstances, Pu and consequently greatly alters models (eg 26) on the release rates of radionuclides from spent fuel in a waste repository.

6. Summary

Examination of a natural analogue to processes affecting radionuclide migration in water conducting fractures has identified a significant weakness in present models describing the retention of radionuclides released from a waste repository. It appears that the mechanical alteration of rocks associated with a fissure (or repository tunnel) can greatly increase the depth of penetration of oxidising agents into the rock and so greatly increase the ability of reductants such as ferrous iron to fix such redox sensitive radionuclides as U, Np and Tc.

References

1. N.A. Chapman, I.G. McKinley and J.A.T. Smellie, (1984). NAGRA Technical Report 84-41, Baden, Switzerland.
2. J. Hadermann and F. Roesel, (1985). NAGRA Technical Report 85-40, Baden, Switzerland.
3. J.A.T. Smellie, A.B. Mackenzie and R.D. Scott, (1986). Chem. Geol. 55 pp. 233-254.
4. M. Gascoyne and H.P. Schwarcz, (1986). Chem. Geol. 59 pp 75-85.
5. H.A. Stalder, (1964). Schweizerische mineralogische and petrographische Mitteilungen, 44/1 pp. 187-398.
6. P. Baretschi, pers. comm.
7. R.A. Nadkarni, (1984). Anal. Chem. 56 pp. 2233-2237.
8. P.J. Lamothe, T.L. Fries and J.C. Consul, (1986). Anal. Chem. 58 pp. 1881-1886.
9. Parr (1986). Parr Inst. C^{09}, Illinois, USA.
10. M.P. Bacon and J.N. Rosholt (1982). Geochim. Cosmochim. Acta, 46 pp. 651-666.
11. A.B. Mackenzie, R.D. Scott, I.G. McKinley and J.M. West (1983). IGS London, Rep No FLPU 83-6 pp. 48.
12. A.B. Mackenzie, P. Bowden and J.A. Kinnaird, (1984). J. Radioanaly. Chem. 82, pp. 341-352.
13. H. Dollinger, pers. comm.
14. W.R. Alexander, A.B. Mackenzie and R.D. Scott 81987). NAGRA Technical Report 87-08, Baden, Switzerland (in prep).
15. C. Bajo (1980). PhD thesis, Federal Inst. of Tech. Zurich, No 6738.
16. D. Langmuir and J.S. Herman (1980). Geochim. Cosmochim. Acta 44 pp. 1753-1766.
17. D.H.M. Alderton, J.A. Pearce and P.J. Potts (1980). Earth Planet. Sci. Lett. 49, pp. 149-165.
18. L. Griffault, M. Jebrak, B. Lemiere, P. Piantone and J.F. Sureau. (1987). Natural Analogues in Radioactive Waste Disposal, Brussels 28-30th April, 1987. Preprint of Symposium Proceedings Vol 1.
19. J.K. Osmond and J.B. Cowart (1982). Uranium Series Disequilibrium: Applications to Environmental Problems. eds. M Ivanovich and R S Harmon Clarendon Press, Oxford.

20. S. Colley and J. Thomson (1985). Geochim. Cosmochim. Acta 49, pp. 2339-2348.
21. D.G. Brookins (1987). Natural Analogues in Radioactive Waste Disposal, Preprint of Symposium Proceedings, Brussels. 28th-30th April, 1987. ed. B. Come C.E.C. Programme on Radwaste Management.
22. M.H. Kurbatov, G.B.Wood and J.D. Kurbatov (1951). J. Phys. Chem. 55 pp. 1170-1182.
23. T.P. O'Conner and D.R. Kester 81975). Geochim. Cosmochim. Acta 39 pp. 1531-1543.
24. U. Frick, pers. comm.
25. I. Neretnieks (1983). Nucl. Technol. 62, pp. 110-115.
26. I. Neretnieks (1986). Chem. Geol. 55, pp. 175-188.
27. I. Neretnieks (1984). Scientific Basis for Nuclear Waste Management Vol 7. eds. G. L. McVay, Elsevier, Amsterdam. pp. 1009-1002.

DISPLAYS - SLIDE SHOW

DISPLAYS

Alligator Rivers, Australia (AAEC)

Cigar Lake, Saskatchewan (AECL)

Investigations in Italian clays (ENEA)

"Interactions between thorium and humic compounds in surface waters" (I. KUCHER, N. MIEKELEY, PUC, BRAZIL)

Loch Lomond and other British sites (BGS)

The MOL site, Belgium (CEN/SCK)

Poços de Caldas, Brazil (J. SMELLIE et al.)

US Natural analogue sites (co-ordinator: D. BROOKINS)

SLIDE SHOW

Some results of the Poços de Caldas project

(H. SCHORSCHER, University São Paulo, Brazil)

LIST OF PARTICIPANTS

Dr. P.L. AIREY
IAEA
P.O. Box 100

A - 1400 VIENNA

Mr. W.R. ALEXANDER
Scottish Universities Research and Reactor Center
East Kilbride

UK - GLASGOW G75 0QU

Mr. M. Di ANDRETTA
ENEA
CRE CASACCIA
Casella Postale 2400

I - 00100 ROMA

Mr. J. ASTUDILLO PASTOR
ENRESA
Paseo de la Castellana 135

E - 28046 MADRID

Dr. P.F. BAERTSCHI
NAGRA
Parkstrasse 23

CH - 5401 BADEN

Mr. P.L. BLANC
CEA-IPSN-DPT
CEN-FAR
B.P. 6

F - 92260 FONTENAY-AUX-ROSES

Mr. W. BODE
GSF-IFT
Theodor-Heuss Strasse 4

D - 3300 BRAUNSCHWEIG

Dr. D. BROOKINS
The University of New Mexico
Department of Geology
ALBUQUERQUE, NM 87131

U.S.A.

Mr. G. BUCKAU
Technische Universität München
Institut Für Radiochemie

D - 8046 GARCHING

Mr. N. CADELLI
Commission of the European Communities
DG XII/D/2

Mr. S. CARLYLE
OCDE - AEN
38, boulevard Suchet

F - 75016 PARIS

Dr. N.A. CHAPMAN
BGS
Nickerhill, Keyworth

UK - NOTTINGHAM NG12 5GG

Dr. D. CLARK
GSF-IFT
Theodor-Heuss Strasse 4

D - 3300 BRAUNSCHWEIG

Mr. B. COME
Commission of the European Communities
DG XII/D/2

Dr. J.J. CRAMER
AECL - WNRE
PINAWA, MANITOBA ROE 1LO

CANADA

Dr. D.B. CURTIS
Los Alamos National Laboratory
INC7, MSJ 514, P.O. Box 1663
LOS ALAMOS, NM 87545

U.S.A.

Mr. DA CONCEICAO SEVERO
Lab. Nacional de Engenharia e Tecnologia Industrial
E.N. 10,2685 SACAVEM

PORTUGAL

Mr. M. D'ALESSANDRO
JRC Ispra

I - 21020 VARESE

Mr. J.P.L. DEARLOVE
Theoretical Physics Division
AERE Harwell

UK - OXFORDSHIRE OX11 ORA

Dr. C. DEGUELDRE
EIR

CH - 5303 WUERENLINGEN

Mr. G. DE MARSILY
Ecole des Mines - CIG
35, rue St-Honoré

F - 77305 FONTAINEBLEAU

Dr. P. DUERDEN
Australian Atomic Energy Commission
Private Mail Bag
Sutherland
NEW SOUTH WALES 2232

AUSTRALIA

Dr. E.M. DURRANCE
University of Exeter
Dpt. of Geology

UK - EXETER EX4 4QE

Mr. W.A. ELDERS
Institute of Geophysics and Planetary Physics
University of California
RIVERSIDE, CALIFORNIA 92521
U.S.A.

Mr. P. ESCALIER DES ORRES
CEA-IPSN-DAS-SAED
CEN-FAR
B.P. 6

F - 92260 FONTENAY-AUX-ROSES

Dr. F. GIRARDI
JRC Ispra

I - 21020 VARESE

Dr. N.T. HARRISON
Department of the Environment
Romney House
43 Marsham Street

UK - LONDON SW1 3PY

Mr. H.S. FEARN
NRPB

UK - DIDCOT, OXON, OX11 ORQ

Dr. P. GLASBERGEN
RIVM
P.O. Box 1

NL - 3720 BA BILTHOVEN

Dr. M.J. HEATH
Geological Consultant
Hillcrest, Church Coombe

UK - REDRUTH, CORNWALL, TR16 6RT

Dr. U. FRICK
NAGRA
Parkstrasse 23

CH - 5401 BADEN

Dr. D.C. GREEN
Cambridge College of
Arts and Technology
East Road

UK - CAMBRIDGE, CB1 1PT

Dr. K.H. HELLMUTH
Finnish Centre for Radiation
and Nuclear Safety
P.O. Box 268

SF - 00101 HELSINKI

Mr. M. FRIEDRICH
CREGU
BP 23

F - 54501 VANDOEUVRE-LEZ-NANCY

Dr. M.C. HAEGG
National Institute of
Radiation Protection
P.O. Box 60204

S - 10401 STOCKHOLM

Mr. P.N.J. HENRION
SCK/CEN
Boeretang 200

B - 2400 MOL

Dr. M. GASCOYNE
Applied Geoscience Branch
AECL - WNRE
PINAWA, MANITOBA ROE 1LO

CANADA

Mr. B. HAIJTINK
Commission of the European
Communities
DG XII/D/2

Dr. F. HERZOG
Swiss Federal Institute
for Reactor Research
EIR

CH - 5303 WUERENLINGEN

Dr. A.K. GAUTSCHI
NAGRA
Parkstrasse 23

CH - 5401 BADEN

Dr. ROLF O. HALLBERG
Department of Geology
University of Stockholm

S - 10691 STOCKHOLM

Dr. B. HOFMANN
Mineralogy - Petrology Inst.
University of Bern
Baltzerstrasse 1

CH - 3012 BERN

Dr. F. GERA
ISMES
Via dei Crocifari 44

I - 00187 ROMA

Mr. T. HANAI
PNC Paris Office
4-8, rue Sainte-Anne

F - 75001 PARIS

Dr. P.J. HOOKER
British Geological Survey
Nickerhill

UK - KEYWORTH, NOTT. NG12 5GG

Dr. H. GIES
GSF-IFT
Theodor-Heuss Strasse 4

D - 3300 BRAUNSCHWEIG

Dr. C.J. HARDY
Australian Atomic
Energy Commission
Private Mail Bag
SUTHERLAND, NSW 2232
AUSTRALIA

Mr. K. HUBENTHAL
BMFT
Heinemannstrasse 2
D - 5300 BONN

Mr. E. ILLUKKA
Finnish Centre for Radiation and Nuclear Safety
P.O. Box 268

SF - 00101 HELSINKI

Mr. J. LARUE
GRS
Schwertnergasse 1

D - 5000 KOLN

Dr. I. MCKINLEY
EIR

CH - 5303 WUERENLINGEN

Dr. M. IVANOVICH
AERE Harwell
Nuclear Physics Division

UK - DIDCOT, OXON OX11 ORA

Mr. E. LEDOUX
Ecole des Mines - CIG
35, rue St-Honoré

F - 77305 FONTAINEBLEAU CEDEX

Ms. M.T. MENAGER
CEA-DRDD-LECALT
CEN-FAR
B.P. 6

F - 92260 FONTENAY-AUX-ROSES

Mr. Ph. JACQUIER
CEA-IPSN-DAS-SAED
CEN-FAR
B.P. 6

F - 92260 FONTENAY-AUX-ROSES

Dr. D. LEVER
UKAEA Harwell
Theoretical Physics Division

UK - DIDCOT, OXON OX11 ORA

Dr. N. MIEKELEY
Dept. of Chemistry
P.U.C.
RIO DE JANEIRO

BRAZIL

Dr. F. KARLSSON
SKB
P.O. Box 5864

S - 10248 STOCKHOLM

Mr. I.A. LINDBERG
Geological Survey of Finland
Nuclear Waste Disposal Research
Kivimiehentie 1

SF - 02150 ESPOO

Dr. H. NAKAMURA
HLW Management Lab.
JAERI TOKAIMURA
NAKAGUN IBARAKIKEN

JAPAN

Mr. Y. KATO
Nuclear Fuel Division
Atomic Energy Bureau
Science & Technology Agency
2-2-1 KASUMIGASEKI
CHIYODA-KU, TOKYO

JAPAN

Dr. P. LINSALATA
New York University
Medical Centre
TUXEDO, N.Y. 10987

U.S.A.

Mr. I. NERETNIEKS
Royal Institute of Technology
Department of Chemical Engineering

S - 10044 STOCKHOLM

Dr. J.I. KIM
Technische Universität München
Institut für Radiochemie

D - 8046 GARCHING

Dr. G. LONGWORTH
AERE-Harwell
Uranium Series Disequilibrium Section

UK - DIDCOT, OXON, OX11 ORA

Mr. OCHIAI
Power Reactor & Nuclear Fuel Development Corp.
Waste Isolation Office
9-13 1-Choume Akasaka
MINATOKU, TOKYO 107

JAPAN

Dr. Linda KOVACH
US Nuclear Regulatory Commission, NL 005
WASHINGTON DC 20555

U.S.A.

Dr. W. LUTZE
Hahn-Meitner Institut
Postfach 390128

D - 1000 BERLIN 39

Mr. S. ORLOWSKI
Commission of the European Communities
DG XII/D/2

Mr. Ph. LALIEUX
ONDRAF-NIRAS
Bd du Régent, 54, bte 5

B - 1000 BRUXELLES

Mr. A.B. MACKENZIE
Scottish Universities Research and Reactor Centre
East Kilbride

UK - GLASGOW G75 0QU

Mr. P. OUSTRIERE
ANDRA
31-33 rue de la Fédération

F - 75752 PARIS CEDEX 15

Dr. T. PAPP
SKB
Box 5864

S - 10248 STOCKHOLM

Mr. J. PATIJN
CEN/SCK
Boeretang 200

B - 2400 MOL

Mr. P. PEAUDECERF
BRGM-STO
BP 6009

F - 45060 ORLEANS CEDEX

Prof. E. PENNA-FRANCA
Institute of Biophysics - UFRJ
ILHA DO FUNDAO
RIO DE JANEIRO

BRAZIL

Mr. J.C. PETIT
CEA-DRDD-LECALT
Centre d'Etudes Nucléaires
B.P. 6

F - 92260 FONTENAY-AUX-ROSES

Mr. P. PITKAENEN
Technical Research Center
of Finland
Betonimiehenkuva 1

SF - 02150 ESPOO

Mr. V. POLISCUK
Waste Management Division
Atomic Energy Control Board
P.O. Box 1046, 270 Albert St.
OTTAWA, ONTARIO K1P5S9

CANADA

Dr. C. POLIZZANO
ENEA
CRE Casaccia
Casella Postale 2400
I - 00100 ROMA

Mr. B. POTY
CREGU
BP 23

F - 54501 VANDOEUVRE-LEZ-NANCY

Mr. K. RASILAINEN
Technical Research Center
of Finland
Nuclear Engineering Lab.
P.O. Box 169

SF - 00181 HELSINKI

Dr. D. READ
W.S. ATKINS & PARTNERS
Longcross Court
Newport Road

UK - CARDIFF CF2 1AD

Ms. C. ROSS
British Geological Survey
Nicker Hill

UK - KEYWORTH, NOTT. NG12 5GG

Dr. F.P. SARGENT
AECL - GACB - WNRE
PINAWA, MANITOBA ROE 1LO

CANADA

Mr. H. SCHORSCHER
USP-IG-DPM
Cx.P 20899
CEP-01489 SAO PAULO SP

BRAZIL

Mr. G. SCHWARZ
GRS
Schwertnergasse 1

D - 5000 KOLN

Dr. R.D. SCOTT
SURRC
East Kilbride

UK - GLASGOW G75 0QU

Mr. M. SHEA
Battelle/OWTD
7000 S. ADAMS St.
WILLOWBROOK, IL 60521

U.S.A.

Dr. B. SKYTTE JENSEN
Risø N.L.
P.O. Box 49

DK - 4000 ROSKILDE

Mr. J. SMELLIE
SGAB
P.O. Box 1424

S - 75144 UPPSALA

Mr. R. SOUBEYRAN
Ecole des Mines - CIG
35, rue St-Honoré

F - 77305 FONTAINEBLEAU CEDEX

Mr. A.D. STALIOS
CEN/SCK
Material Physics Dpt.
Boeretang 200

B - 2400 MOL

Dr. J.F. SUREAU
BRGM - GMX
B.P. 6009

F - 45060 ORLEANS CEDEX

Mr. A. TALLOS GONZALEZ
Junta de Energia Nuclear
(CIEMAT)
Avenida Complutense 22

E - 28040 MADRID

Dr. J. TAYLOR
Elektrowatt Engineering
Services (UK) Ltd.
GRANDFORD HOUSE, 16 Carfax

UK - HORSHAM, SUSSEX RH12 1UP

Mr. VALKIAINEN
Technical Research Center
of Finland
Reactor Laboratory
Otakaari 3 A

SF - 02150 ESPOO

Mr. P. VAN ISEGHEM
CEN/SCK
Boeretang 200

B - 2400 MOL

Dr. A. VAN LUIK
Battelle Pacific Northwest
Laboratory, P.O. Box 999
RICHLAND, WASHINGTON 99352

U.S.A.

Dr. A. VELA
Consejo de Seguridad Nuclear
Sor Angela de la Cruz 3

E - 28020 MADRID

Mr. P. VENET
Commission of the European
Communities
DG XII/D/1

Dr. I.F. VOVK
Division of Nuclear
Fuel Cycle
IAEA
P.O. Box 100

A - 1400 VIENNA

Mr. N. WABER
Mineralogy - Petrology Inst.
University of Bern
Baltzestrasse 1

CH - 3012 BERN

Dr. L. WERME
SKB
Box 5864

S - 10248 STOCKHOLM

Dr. Z.H. ZHOU
The University of
Western Ontario
Dpt. of Geology
Biological & Geological Bldg.
LONDON, ONTARIO N6A 5B7

CANADA

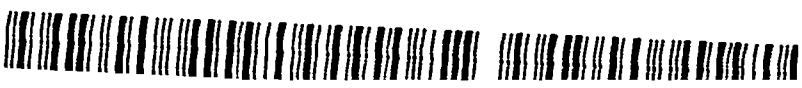

Radioactive Waste Management Series

Incineration of Radioactive Waste

The Offshore Disposal of Radioactive Waste by Drilled Emplacement: A Feasibility Study

Ocean Disposal of Radioactive Waste by Penetrator Emplacement

Leaching of Low and Medium Level Waste Packages under Disposal Conditions

Reliability of Sub-seabed Disposal Operations for High Level Waste

Denitration of Radioactive Liquid Waste

Direct Disposal of Spent Nuclear Fuel

Natural Analogues in Radioactive Waste Disposal

ISBN 0 86010 929 1 (series)

ISBN 1-85333-105-8 (volume)